

Stony Brook University



OFFICIAL COPY

The official electronic file of this thesis or dissertation is maintained by the University Libraries on behalf of The Graduate School at Stony Brook University.

© All Rights Reserved by Author.

Discovery of Neoteric Antibacterial Agents Targeting the Cell Division Protein FtsZ

A Dissertation Presented

by

Divya Awasthi

to

The Graduate School

in Partial Fulfillment of the

Requirements

for the Degree of

Doctor of Philosophy

in

Chemistry

Stony Brook University

August 2014

Stony Brook University

The Graduate School

Divya Awasthi

We, the dissertation committee for the above candidate for the
Doctor of Philosophy degree, hereby recommend
acceptance of this dissertation.

Professor Iwao Ojima
Department of Chemistry

Professor Robert Kerber
Department of Chemistry

Professor Dale Drueckhammer
Department of Chemistry

Takushi Kaneko, Ph.D.
Senior Project Leader, TB Alliance
Visiting Professor, Institute of Chemical Biology and Drug
Discovery, Stony Brook, Stony Brook, NY

This dissertation is accepted by the Graduate School

Charles Taber
Dean of the Graduate School

Abstract of the Dissertation

Discovery of Neoteric Antibacterial Agents Targeting the Cell Division Protein FtsZ

by

Divya Awasthi

Doctor of Philosophy

in

Chemistry

Stony Brook University

2014

FtsZ protein, which bears limited sequence homology to tubulin in eukaryotic cells, is involved in bacterial cell division. Interference with the assembly/disassembly dynamics of this protein affects the cell division processes, leading to inhibition of septation. Our laboratory has synthesized libraries of novel 2,5,6- and 2,5,7-trisubstituted benzimidazoles to target this vital cell division protein for antibacterial drug discovery. Specifically, we have identified >200 compounds possessing activity against the infectious bacterial pathogen, *Mycobacterium tuberculosis* (*Mtb*). These compounds exhibit excellent activity against drug-sensitive and drug-resistant *Mtb* strains along with displaying potency against *Mtb* grown under hypoxic conditions. In addition, these compounds inhibit *Mtb* FtsZ polymerization while enhancing its GTPase activity which was ascertained via light scattering assays, GTPase assays and Transmission electron microscopy (TEM) imaging studies. Extensive optimization studies on the initial lead compound **SB-P3G2** possessing a 6-diethylamino group has led us to a series of 6-dimethylamino substituted benzimidazoles with superior *in vitro* activity against *Mtb* (MIC 0.06 – 0.63 µg/mL). In the murine acute model of TB infection, a representative compound from this series, **SB-P17G-A38**, when dosed orally or intraperitoneally, dramatically reduced the bacterial load in the lung by 6 Log₁₀ CFU and 5 Log₁₀ CFU in the spleen. These results are very exciting since treatment with **SB-P17G-A38** essentially eliminated all live bacteria from the spleen of the infected mice. Furthermore, the trisubstituted benzimidazole libraries have been screened against other bacterial pathogens like *F. tularensis*, *Y. pestis* and *B. thailandensis*, to successfully identify

several hit compounds active at MIC \leq 5 μ g/mL. This elucidates the broad spectrum potency of these compounds.

We have also synthesized non-cytotoxic taxanes which selectively inhibit *Mtb* cell growth (MIC 1.25-2.5 μ M). The target of the lead taxanes, **SB-RA-2001** and **SB-RA-5001**, has been validated as *Mtb* FtsZ via TEM imaging.

To expand on the benzimidazole scaffold, a series of 2,5,6-trisubstituted benzoxazoles have also been synthesized and evaluated for anti-tubercular activity. This series of compounds although in a nascent stage, offers a new pharmacophores for the discovery of antibacterial agents.

Table of Contents

| | |
|----------------------------|-----|
| List of Figures..... | x |
| List of Schemes..... | xii |
| List of Tables..... | xiv |
| List of Abbreviations..... | xvi |

Chapter 1

FtsZ: A Novel Target for Antibacterial Drug Discovery

| | |
|-----------------------------------------------------------------------|----|
| 1.1. Introduction..... | 2 |
| 1.2. FtsZ as a target for antitubercular drug discovery | 6 |
| 1.2.1. 2-Alkoxy-carbonylaminopyridines and 2-carbamoylpteridine | 7 |
| 1.2.2. Taxanes | 8 |
| 1.2.3. Trisubstituted benzimidazoles | 10 |
| 1.3. References..... | 11 |

Chapter 2

Synthesis and Optimization of Novel Trisubstituted Benzimidazoles

| | |
|-----------------------------------------------------------------------------------|----|
| 2.1. Introduction..... | 20 |
| 2.1.1. The road leading to trisubstituted benzimidazoles as a pharmacophore | 21 |
| 2.1.1.1. Albendazole and thiabendazole..... | 21 |
| 2.1.1.2. 2-Alkoxy-carbonylaminopyridines and 2-carbamoylpteridine | 22 |
| 2.1.1.3. Trisubstituted benzimidazole as a pharmacophore | 22 |
| 2.2. Results and Discussion | 23 |
| 2.2.1. Synthesis of 2,5,6-trisubstituted benzimidazole library | 23 |

| | | |
|----------|----------------------------------------------------------------------------------------------|----|
| 2.2.2. | Optimization of 2,5,6-trisubstituted benzimidazoles..... | 26 |
| 2.2.3. | Optimization of 2,5,6-trisubstituted benzimidazoles based on metabolite identification | 33 |
| 2.2.3.1. | Metabolites of SB-P3G2 | 33 |
| 2.2.3.2. | Metabolite identification of lead 5-position benzamido compounds | 39 |
| 2.2.4. | Significance of 2-cyclohexyl group..... | 41 |
| 2.2.5. | Synthesis of substituted 5-position benzylamino group | 42 |
| 2.2.6. | Salt formation of SB-P3G2 and SB-P17G-A38 | 44 |
| 2.2.7. | New trisubstituted benzimidazoles with unknown MIC | 45 |
| 2.3. | Conclusion | 46 |
| 2.4. | Experimental Section | 46 |
| 2.5. | References..... | 81 |

Chapter 3

Target Validation and *In vivo-In vitro* Evaluation of Novel Benzimidazole-Based Anti-tubercular Agents

| | | |
|--------|--------------------------------------------------------------|----|
| 3.1. | FtsZ as a novel target for antibacterial drug discovery..... | 87 |
| 3.2. | Results and Discussion | 89 |
| 3.2.1. | <i>Mtb</i> FtsZ Polymerization Inhibitory Assay..... | 89 |
| 3.2.2. | <i>Mtb</i> FtsZ GTPase Assay..... | 90 |
| 3.2.3. | Transmission Electron Microscopy (TEM) analysis..... | 91 |

| | | |
|--------|---------------------------------------------------------------------------|-----|
| 3.2.4. | Photo-affinity labeling..... | 95 |
| 3.2.5. | <i>In vivo</i> and <i>in vitro</i> evaluation of lead benzimidazoles..... | 96 |
| 3.2.6. | ADME profiling of lead compounds..... | 100 |
| 3.3. | Conclusion | 101 |
| 3.4. | Experimental Section..... | 102 |
| 3.5. | References..... | 107 |

Chapter 4

Discovery of Trisubstituted Benzimidazoles Against *F. tularensis*

| | | |
|--------|---------------------------------------------------------|-----|
| 4.1. | Introduction..... | 112 |
| 4.2. | Results and Discussion | 114 |
| 4.2.1. | Re-synthesis of hits against <i>F. tularensis</i> | 114 |
| 4.2.2. | Preliminary target validation studies | 116 |
| 4.3. | Conclusion | 117 |
| 4.4. | Experimental Section..... | 118 |
| 4.5. | References..... | 123 |

Chapter 5

Synthesis and Optimization of Novel Trisubstituted Benzoxazoles

| | | |
|--------|------------------------------------------------------------------|-----|
| 5.1. | Investigating trisubstituted benzoxazole scaffold..... | 126 |
| 5.2. | Results and Discussion | 127 |
| 5.2.1. | Synthesis of trisubstituted benzoxazoles | 127 |
| 5.2.2. | Benzoxazole analogues of SB-P8B2 and SB-P8B4 | 135 |

| | | |
|--------|-----------------------------------------------------------------------|-----|
| 5.2.3. | Benzoxazole analogues of SB-P6B10 and SB-P17G-A20 | 136 |
| 5.2.4. | Accurate MIC of synthesized benzoxazoles..... | 137 |
| 5.3. | Conclusion | 138 |
| 5.4. | Experimental Section | 138 |
| 5.5. | References..... | 149 |

Chapter 6

Target Validation Studies with **SB-RA-2001** and **SB-RA-5001**

| | | |
|--------|------------------------------------------------------------|-----|
| 6.1. | Introduction..... | 151 |
| 6.2. | Results and Discussion | 153 |
| 6.2.1. | Synthesis of C-13 side chain precursors..... | 154 |
| 6.2.2. | Synthesis of SB-RA-5001 and SB-RA-2001 | 157 |
| 6.2.3. | <i>In vitro</i> evaluation of SB-RA-2001 | 158 |
| 6.2.4. | TEM Imaging with SB-RA-5001 | 160 |
| 6.3. | Conclusion | 161 |
| 6.4. | Experimental Section | 161 |
| 6.5. | References..... | 168 |

Bibliography

| | |
|----------------|-----|
| Chapter 1..... | 170 |
| Chapter 2..... | 177 |
| Chapter 3..... | 181 |

| | |
|----------------|-----|
| Chapter 4..... | 184 |
| Chapter 5..... | 186 |
| Chapter 6..... | 187 |

Appendices

| | |
|-----------------------------|-----|
| A1. Appendix Chapter 2..... | 190 |
| A2. Appendix Chapter 3..... | 336 |
| A3. Appendix Chapter 4..... | 346 |
| A4. Appendix Chapter 5..... | 356 |
| A5. Appendix Chapter 6..... | 415 |

List of Figures

Chapter 1

| | |
|---------------------------------------------------------------------|---|
| Figure 1.1. Current antitubercular drugs..... | 3 |
| Figure 1.2. Polymerization-depolymerization dynamics of FtsZ..... | 4 |
| Figure 1.3. Z-ring regulatory system. | 6 |
| Figure 1.4. Antitubercular compounds developed at SRI..... | 8 |
| Figure 1.5. <i>Mtb</i> FtsZ inhibitors: Taxane-based compounds..... | 9 |

Chapter 2

| | |
|-------------------------------------------------------------------------------------------------|----|
| Figure 2.1. Graphic presentation of the Z-ring formation and cell division..... | 20 |
| Figure 2.2. Known tubulin inhibitors targeting FtsZ..... | 21 |
| Figure 2.3. MIC values of the eight hit 2,5,6-trisubstituted benzimidazoles..... | 23 |
| Figure 2.4. FtsZ polymerization inhibition monitored via light scattering..... | 23 |
| Figure 2.5. Cell based assay results of library..... | 24 |
| Figure 2.6. Structure of hit compounds at cut off values of MIC ≤ 5 $\mu\text{g/mL}$ | 25 |
| Figure 2.7. Proposed optimization of 2,5,6-trisubstituted benzimidazoles..... | 26 |
| Figure 2.8. Metabolite formed in mouse/human microsome..... | 34 |
| Figure 2.9. Metabolite identification of SB-P17G-A16 | 39 |

Chapter 3

| | |
|-------------------------------------------------------------------------------------------------------------------------------------------------------|----|
| Figure 3.1. Proposed conformational change induced in FtsZ dimer..... | 88 |
| Figure 3.2. Dose dependent inhibition of <i>Mtb</i> FtsZ polymerization by SB-P17G-C2 (A), SB-P17G-C12 (B) and SB-P20G3 (C)..... | 90 |
| Figure 3.3. Enhancement of GTPase activity of FtsZ by SB-P3G2 and SB-P3G5 | 91 |
| Figure 3.4. Transmission electron microscope (TEM) images of FtsZ..... | 92 |
| Figure 3.5. Transmission Electron Microscopy (TEM) Images of FtsZ..... | 93 |
| Figure 3.6. TEM Images of FtsZ..... | 94 |
| Figure 3.7. TEM Imaging..... | 95 |
| Figure 3.8. Structures of lead benzimidazoles..... | 97 |
| Figure 3.9. Time dose curve..... | 97 |

| | |
|---------------------------------------------------------------------------|----|
| Figure 3.10. <i>In vivo</i> studies in murine model of TB infection | 99 |
|---------------------------------------------------------------------------|----|

Chapter 4

| | |
|-------------------------------------------------------------------------------------------------------------------------------------------|-----|
| Figure 4.1. Structures of 2,5,6-trisubstituted benzimidazoles against <i>F. tularensis</i> at 1 µg/mL with > 90 % growth inhibition | 113 |
| Figure 4.2. Structures of 2,5,7-trisubstituted benzimidazoles against <i>F. tularensis</i> at 1 µg/mL with > 90 % growth inhibition | 113 |
| Figure 4.3. Structures of hit benzimidazoles against <i>F. tularensis</i> with 40-50 % growth inhibition 0.2 µg/mL..... | 114 |
| Figure 4.4. TEM Images of <i>F. tul</i> FtsZ..... | 116 |
| Figure 4.5. TEM Images of <i>F. tul</i> FtsZ..... | 117 |

Chapter 5

| | |
|-----------------------------------------------------------------------------|-----|
| Figure 5.1. Lead benzimidazole with potent antibacterial activity..... | 126 |
| Figure 5.2. Proposed benzoxazoles to be synthesized | 126 |
| Figure 5.3. Benzoxazole synthesis employed by Peng <i>et al.</i> | 127 |
| Figure 5.4. Thionyl chloride catalyzed cyclization..... | 128 |
| Figure 5.5. Benzoxazole synthesis employed by Kuroyanagi <i>et al.</i> | 130 |

Chapter 6

| | |
|-----------------------------------------------------------------------------------------------------------------------------------------------|-----|
| Figure 6.1. GTP binding site in FtsZ | 151 |
| Figure 6.2. Lead taxanes identified by RT-PCR assay | 152 |
| Figure 6.3. Hit TRA and C-seco baccatin analogues..... | 153 |
| Figure 6.4. Electron micrograph of <i>Mtb</i> cells before (A) and after treatment with SB-RA-20018 (B) and SB-RA-5001 (C)..... | 153 |
| Figure 6.5. Photoaffinity labeled analogues of lead taxanes-based anti-TB compounds | 154 |
| Figure 6.6. TEM imaging with SB-RA-2001 | 159 |
| Figure 6.7. <i>Bacillus subtilis</i> 168 cells treated with SB-RA-2001 | 160 |
| Figure 6.8. TEM Images of FtsZ with SB-RA-5001 | 161 |

List of Schemes

Chapter 2

| | |
|----------------------------------------------------------------------------------------------------------------------------------------|----|
| Scheme 2.1. Synthesis of 2,5,6-trisubstituted benzimidazoles | 24 |
| Scheme 2.2. Synthesis of 5-position functionalized trisubstituted benzimidazoles | 26 |
| Scheme 2.3. Nucleophilic aromatic substitution of 6-chlorobenzimidazole | 34 |
| Scheme 2.4. Synthesis of 5-amino-2-cyclohexyl-6-N-ethylamino-1 <i>H</i> -benzo[<i>d</i>]imidazole | 38 |
| Scheme 2.5. Failed synthesis of 5-amino-2-cyclohexyl-6- <i>N</i> -ethylamino-1 <i>H</i> -benzo[<i>d</i>]imidazole | 38 |
| Scheme 2.6. Metabolite synthesis | 38 |
| Scheme 2.7. Synthesis of 2-(4,4-difluorocyclohexyl) analogues | 40 |
| Scheme 2.8. Synthesis of 2-cyclohexyl-5-(4-methoxybenzamido)-6- <i>N</i> -methylamino-1 <i>H</i> - benzo[<i>d</i>]imidazole | 41 |
| Scheme 2.9. Synthesis of 2-modified 6-dimethylamino-1 <i>H</i> -benzo[<i>d</i>]imidazole | 42 |
| Scheme 2.10. Synthesis of 5-position <i>N</i> -benzylamino group | 42 |
| Scheme 2.11. Fumaric acid salt preparation | 45 |

Chapter 3

| | |
|-----------------------------------------------------------------|----|
| Scheme 3.1. Synthesis of photo-affinity labeled analogues | 96 |
|-----------------------------------------------------------------|----|

Chapter 4

| | |
|-----------------------------------------------------------------------|-----|
| Scheme 4.1. Synthesis of hit 2,5,6 trisubstituted benzimidazole | 114 |
| Scheme 4.2. Synthesis of hit 2,5,7 trisubstituted benzimidazole | 115 |

Chapter 5

| | |
|---------------------------------------------------------------------------------------------------------------|-----|
| Scheme 5.1. Reaction to synthesize trisubstituted benzoxazole | 127 |
| Scheme 5.2. Reduction-cyclization of 1-cyclohexylcarbonyloxy-2,4-dinitro-5- diethylaminobenzene | 128 |
| Scheme 5.3. Indium triflate as a Lewis acid for 2-aromatic or 2-heteroaromatic benzoxazole synthesis | 129 |
| Scheme 5.4. Optimization of synthesis of trisubstituted benzoxazoles | 130 |
| Scheme 5.5. Optimized synthesis of 2,5,6-trisubstituted benzoxazoles | 134 |

| | |
|---------------------------------------------------------------------------|-----|
| Scheme 5.6. Synthesis of benzoxazole analogues of hit benzimidazoles..... | 136 |
| Scheme 5.7. Synthesis of benzoxazole analogues of hit benzimidazoles..... | 137 |

Chapter 6

| | |
|---------------------------------------------------------------------------------------------|-----|
| Scheme 6.1. Synthesis of C-13 side chain precursor | 155 |
| Scheme 6.2. Synthesis of photoaffinity labeled analogues of C-13 side chain precursors..... | 156 |
| Scheme 6.3. Synthesis of (<i>E</i>)-3-(naphthalen-2-yl)acrylic acid..... | 156 |
| Scheme 6.4. Synthesis of SB-RA-5001 | 157 |
| Scheme 6.5. Synthesis of SB-RA-2001 | 158 |

List of Tables

Chapter 1

| | |
|----------------------------------------------------------------------------------------------------------------|---|
| Table 1.1. Antimicrobial activities of taxanes against drug-sensitive and multidrug-resistant <i>Mtb</i> | 9 |
|----------------------------------------------------------------------------------------------------------------|---|

Chapter 2

| | |
|------------------------------------------------------------------------------------------------------------------------------------------------------------------------------------------------------------------------|----|
| Table 2.1. Antibacterial activity of 5-carbamate benzimidazoles against <i>Mtb</i> H37Rv strain (MIC, $\mu\text{g/mL}$), their cytotoxicity (IC_{50} , $\mu\text{g/mL}$), and microsomal instability | 27 |
| Table 2.2. Antibacterial activity of 5-urea benzimidazoles against <i>Mtb</i> H37Rv strain (MIC, $\mu\text{g/mL}$) and their cytotoxicity (IC_{50} , $\mu\text{g/mL}$) | 28 |
| Table 2.3. Antibacterial activity of 5-benzamido benzimidazoles against <i>Mtb</i> H37Rv strain (MIC, $\mu\text{g/mL}$) and their cytotoxicity (IC_{50} , $\mu\text{g/mL}$) | 29 |
| Table 2.4. Microsomal instability of representative 5-benzamido compounds | 30 |
| Table 2.5. Antibacterial activity of 5-benzamido benzimidazoles against <i>Mtb</i> H37Rv strain (MIC, $\mu\text{g/mL}$) and their cytotoxicity (IC_{50} , $\mu\text{g/mL}$) | 31 |
| Table 2.6. Antibacterial activity against <i>Mtb</i> H37Rv strain (MIC, $\mu\text{g/mL}$), their cytotoxicity (IC_{50} , $\mu\text{g/mL}$) and microsomal instability | 33 |
| Table 2.7. Nucleophilic aromatic substitution of 2,4-dinitro-5-fluoroaniline | 35 |
| Table 2.8. Synthesis of <i>N</i> -Benzyl- <i>N</i> -ethylamine | 36 |
| Table 2.9. Synthesis of metabolite M10 | 39 |
| Table 2.10. Reaction condition optimization | 43 |
| Table 2.11. Optimization of 5-benzamido reduction | 44 |
| Table 2.12. New trisubstituted benzimidazoles to be evaluated against <i>Mtb</i> H37Rv | 46 |

Chapter 3

| | |
|---------------------------------------------------------------------------------------------------------|-----|
| Table 3.1. Antibacterial activity (MIC $\mu\text{g/mL}$) against clinical isolates of <i>Mtb</i> | 100 |
| Table 3.2. ADME profiling of SB-P17G-A33 , SB-P17G-A38 and SB-P17G-A42 | 101 |

Chapter 5

| | |
|--------------------------------------------------------------------------------------|-----|
| Table 5.1. Optimization of nucleophilic aromatic substitution | 131 |
| Table 5.2. Nucleophilic aromatic substitution of 5-position chloro with amines | 132 |

| | |
|------------------------------------------------------------------------------------------------------|-----|
| Table 5.3. Nucleophilic aromatic substitution of 5-chloro-6-nitro-2- <i>p</i> -tolylbenzoxazole..... | 133 |
| Table 5.4. Failed synthesis of benzoxazole | 135 |
| Table 5.5. Accurate MIC of trisubstituted benzoxazole against <i>Mtb</i> H37Rv | 138 |

List of Abbreviations

| | |
|----------------------|-------------------------------------------------|
| 10-DAB | 10-Deacetylbaccatin III |
| ADME | Absorption, distribution, metabolism, excretion |
| AIDS | Acquired immune deficiency syndrome |
| ATP | Adenosine triphosphate |
| <i>B. subtilis</i> | <i>Bacillus subtilis</i> |
| BSA | Bovine serum albumin |
| CA-MRSA | Community acquired MRSA |
| CDC | Center for disease control and prevention |
| CFU | Colony forming unit |
| C NMR | Carbon nuclear magnetic resonance |
| CYP3A4 | CytochromeP3A4 |
| DAPI | 4',6-diamidino-2-phenylindole |
| DCC | <i>N,N'</i> -Dicyclohexylcarbodiimide |
| DCU | Dicyclohexylurea |
| DDQ | 2,3-Dichloro-5,6-dicyano-1,4-benzoquinone |
| DIPEA | diisopropylethylamine |
| DMAP | Dimethylaminopyridine |
| DMF | Dimethylformamide |
| DMSO | Dimethylsulfoxide |
| DNA | Deoxyribonucleic acid |
| <i>E. coli</i> | <i>Escherichia coli</i> |
| EDC | 1-Ethyl-3-(3-dimethylaminopropyl)carbodiimide |
| EPR | Enhanced permeability and retention |
| EtOAc | Ethyl acetate |
| <i>F. tularensis</i> | <i>Fransicella tularensis</i> |
| <i>F. tul</i> | <i>Fransicella tularensis</i> |

| | |
|------------------|---------------------------------------------|
| FAB | Fast atom bombardment |
| FDA | Food & drug administration |
| FtsZ | Filamentous temperature-sensitive protein Z |
| GDP | Guanosine diphosphate |
| GKO | Gamma interferon knockout |
| GTPase | Guanosine triphosphatase |
| GTP | Guanosine triphosphate |
| HCl | Hydrochloric acid |
| hERG | human Ether-à-go-go-Related Gene |
| Hex | Hexanes |
| H NMR | Proton nuclear magnetic resonance |
| HPLC | High performance liquid chromatography |
| HRMS | High resolution mass spectrometry |
| HSA | Human serum albumin |
| HTP | High throughput |
| IC ₅₀ | Half maximal inhibitory concentration |
| ID ₅₀ | Median infectious dose |
| INH | Isoniazid |
| IP | Intraperitoneally |
| IPTG | Isopropyl β-D-1-thiogalactopyranoside |
| ITC | Isothermal titration calorimetry |
| LB | Lysogeny broth |
| LD ₅₀ | Median lethal dose |
| mp | Melting point |
| MABA | Microplate alamar blue assay |
| MDR | Multidrug resistant |
| MDR-TB | Multi-drug resistant tuberculosis |

| | |
|--------------------|--------------------------------------------------------------------------------------------------------|
| MES | 2-(<i>N</i> -morpholino)ethanesulfonic acid |
| MIC | Minimum inhibitory concentration |
| Mid | Midazolam |
| MRSA | Methicillin-resistant staphylococcus aureus |
| <i>M. smeg</i> | <i>Mycobacterium smegmatis</i> |
| <i>Mtb</i> | <i>Mycobacterium tuberculosis</i> |
| NHS | <i>N</i> -hydroxysuccinimide |
| NIAID | National institute of allergy and infectious diseases |
| OD | Optical density |
| OTBA | 3-{5-[4-Oxo-2-thioxo-3-(3-trifluoromethylphenyl)-thiazolidin-5-ylidenemethyl]-furan-2-yl}-benzoic acid |
| PAL | Photoaffinity-labeling |
| PBS | Phosphate buffer saline |
| PCR | Polymerase chain reaction |
| P-gp | P-glycoprotein |
| Ph ₃ P | Triphenylphosphine |
| Ph ₃ PO | Triphenylphosphine oxide |
| Pi | Inorganic phosphate |
| PK | Pharmacokinetics |
| PMSF | Phenylmethylsulfonyl fluoride |
| PO | Oral administration |
| RNA | Ribonucleic acid |
| rt | Room temperature |
| <i>S. aureus</i> | <i>Staphylococcus aureus</i> |
| SAR | Structure-activity relationship |
| SEM | Scanning electron microscopy |
| SI | Selectivity index |

| | |
|------------------|---------------------------------------|
| SRI | Southern research institute |
| TB | Tuberculosis |
| TBZ | Thiabendazole |
| TEM | Transmission electron microscopy |
| TEA | Triethylamine |
| Temp | Temperature |
| TES chloride | Triethylsilyl chloride |
| Testo | Testosterone |
| TFA | Trifluoroacetic acid |
| THF | Tetrahydrofuran |
| TLC | Thin layer chromatography |
| TRAs | Taxane reversal agents |
| VRE | Vancomycin-resistant enterococci |
| WHO | World Health Organization |
| XDR-TB | Extremely drug-resistant tuberculosis |
| <i>Y. pestis</i> | <i>Yersinia pestis</i> |

Acknowledgments

Six years ago, I set myself on a path to create something that mattered. As part of that quest, I left my home and family and moved to the United States to pursue my Ph.D. All I had was a desire to immerse myself in projects that compel me to challenge status quo, are dynamic, and surround me with extremely talented individuals. This journey would have been fruitless, if not entirely impossible, without the support and good cheer of my brilliant team of advisors, and colleagues.

Thus far, my thirst for knowledge has guided me to career choices that have broadened my knowledge, challenged my boundaries, and established my path to success. My next logical step is to pursue a postdoctoral position. I am ready to share my knowledge with others and be inspired by their experiences. I am ready to move forward, to embrace new opportunities, and to meet new challenges. I would be ill prepared for this adventure if I didn't have the support of my advisor Professor Ojima. His guidance and demand for excellence pushed me to work hard and to never give up. He has taught me to not settle for mediocrity and always aim high. Professor Ojima is a great mentor who recognizes the potential in his students and drives them to work hard. I profoundly appreciate his encouragement, leadership, motivation and applaud his dedication to research.

My interactions with Professor Kerber, Professor Scharer, Professor Drueckhammer, and Professor Tonge have always been insightful and I appreciate the advice and recommendations they gave to me throughout my Ph.D. The incredible chemistry department faculty at Stony Brook University has made me a better chemist. Dr. James Marecek and Francis Picart deserve a special thanks for all the NMR support they have provided along the years and Dr. Bela Ruzsicska for MS support.

I have been fortunate to work with amazing collaborators at Colorado State University and Sanofi-Aventis. Specially, Dr. Susan E. Knudson who performed MIC determination of the several 100 compounds I sent to her and performed *in vivo* evaluations, and Dr. Richard Slayden for his valuable contribution and suggestions. Our team leader at Sanofi, Dr. Laurent Goullieux gave me a taste of how a pharmaceutical company functions and I got a glimpse of the drug discovery pipeline. Dr. Laurent Goullieux, Dr. H el ene Vermet and the other team members have made significant contributions which has allowed us to make great headway in our project.

I sincerely thank my fellow peers and Ojima group lab member who have made my Ph.D. experience memorable. A special thanks to Ilaria Zanardi, my mentor and friend, who guided me, made fun of me, and taught me during my first year in the lab. I am especially thankful for my wonderful friends who have tolerated my incessant complaining and random but frequent outbursts. They have been supportive and patient with me and I appreciate their friendship.

A special thanks to Mrs. Yoko Ojima for her kindness and hospitality. She is a great host and a very warm person. I want to thank Mrs. Patricia Marinaccio for all her support and always offering her shoulder to cry on and Mrs. Roxanne Brockner was the chatting sessions.

Finally I want to express my deepest gratitude to my family, for their unconditional love, support, and understanding.

“There’s nothing that makes you more insane than family. Or more happy. Or more exasperated. Or more... secure.” Jim butcher

I would like to end with a quote from Robin Williams

“You’re only given a little spark of madness. You mustn’t lose it.”

Chapter 1

FtsZ: A Novel Target for Antibacterial Drug Discovery

Table of Contents

| | |
|------------------------------------------------------------------------------|----|
| Chapter 1 | 1 |
| 1.1. Introduction | 2 |
| 1.2. FtsZ as a target for antitubercular drug discovery | 6 |
| 1.2.1. 2-Alkoxy-carbonylaminopyridines and 2-carbamoylpteridine | 7 |
| 1.2.2. Taxanes | 8 |
| 1.2.3. Trisubstituted benzimidazoles | 10 |
| 1.3. References | 11 |

1.1. Introduction

Tuberculosis (TB) was responsible for 1.3 million deaths in 2012, which was second only to HIV/AIDS related fatalities among all infectious diseases.^{1,2} TB is caused by *Mycobacterium tuberculosis* (*Mtb*) and is highly contagious when airborne.³ It has been estimated that 90% of people who are exposed to or infected with this pathogen have latent-TB, which has a 10% chance of progressing to an active-TB diseased state.^{4, 5} Recent statistics from the World Health Organization (WHO) report an estimated 8.6 million new TB cases globally in 2012.^{3, 6} Among these cases, 13% were HIV-positive individuals with 320,000 deaths, which demonstrates the ability of the bacteria to target immunocompromised patients.^{3, 6} It has also been reported that worldwide 3.6% of the new cases and 20% of the previously reported cases of TB were caused by *Mtb* strains resistant to isoniazid and rifampicin and were therefore, classified as Multi drug resistant TB (MDR-TB).^{3, 6} MDR-TB resistant to at least one of the three injectable “second-line” antibiotics and fluoroquinolones is classified as extensively drug resistant-TB (XDR-TB). About 9.6% of MDR-TB cases have been classified as XDR-TB by WHO and 92 countries have reported at least one case of XDR-TB.^{3, 6}

Despite extensive research, the drugs used to treat tuberculosis infection are still limited to the classical antibacterial drugs that target cell wall biosynthesis, nucleic acid synthesis, protein synthesis, etc. (**Figure 1.1**).⁷ Only recently, after a gap of 40 years, a new TB drug -Bedaquiline- has been approved for treatment of MDR-TB.^{8, 9} Widespread bacterial resistance to existing therapeutics for bacterial infections has been a key hurdle for the complete treatment of this disease therefore, in order to compete with the adaptive genetic machinery of bacteria, there is an imperative need to identify novel therapeutic targets. In this respect, FtsZ, an essential bacterial cytokinesis protein, is a highly promising therapeutic target since, the disruption of cell division would lead to the inhibition/arrest of bacterial infection.^{10, 11}

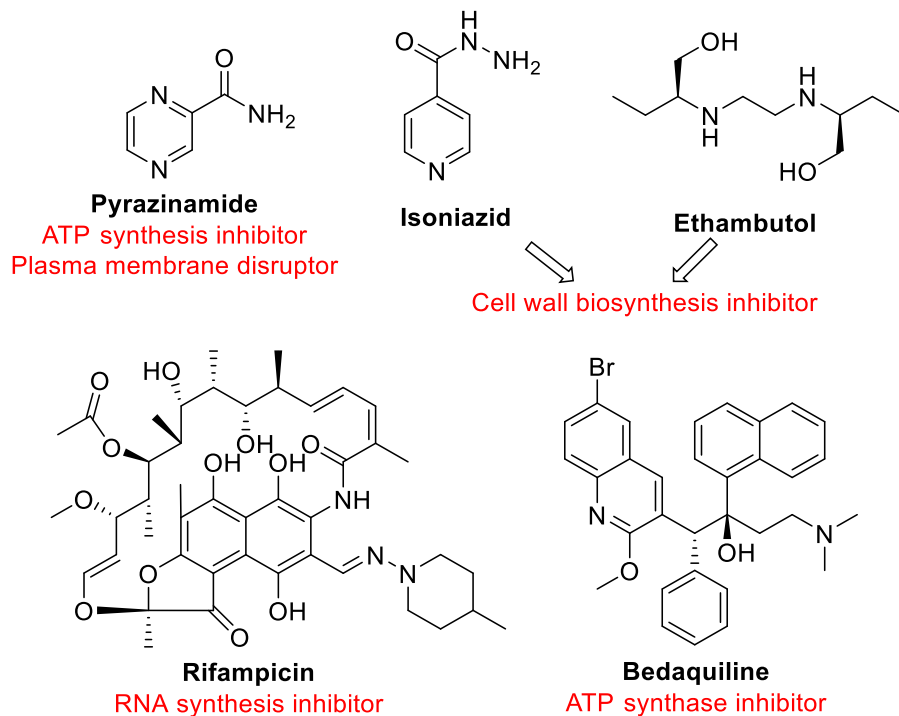


Figure 1.1. Current antitubercular drugs

Filamentous temperature-sensitive protein Z (FtsZ), an essential bacterial cytokinesis protein, is a highly promising therapeutic target, the disruption of which leads to the inhibition/arrest of bacterial infection.^{10, 11} In the presence of guanosine triphosphate (GTP), FtsZ undergoes self-assembly bi-directionally at the center of the cell to form a highly dynamic structure known as the “Z-ring” (**Figure 1.2**).¹²⁻²⁰ FtsZ, a prokaryotic homolog of tubulin, is a GTPase and its GTPase activity is dependent on the protein concentration and is stimulated by self-association in a manner similar to tubulin.^{17, 18, 21, 22} The GTP binding ‘signature’ sequence found in all 152 sequences of α -, β -, and γ -tubulins has also been observed in FtsZ proteins from 11 bacterial species. Additionally, Mukherjee *et al.* have established significant sequence similarity over the first 260 amino acids of tubulin and 220 amino acids of FtsZ.²³ The alignment includes 16 amino acids that are identical in all the tubulins and FtsZ sequences they compared and includes 50-90 amino acids with convincing sequence similarity.²³

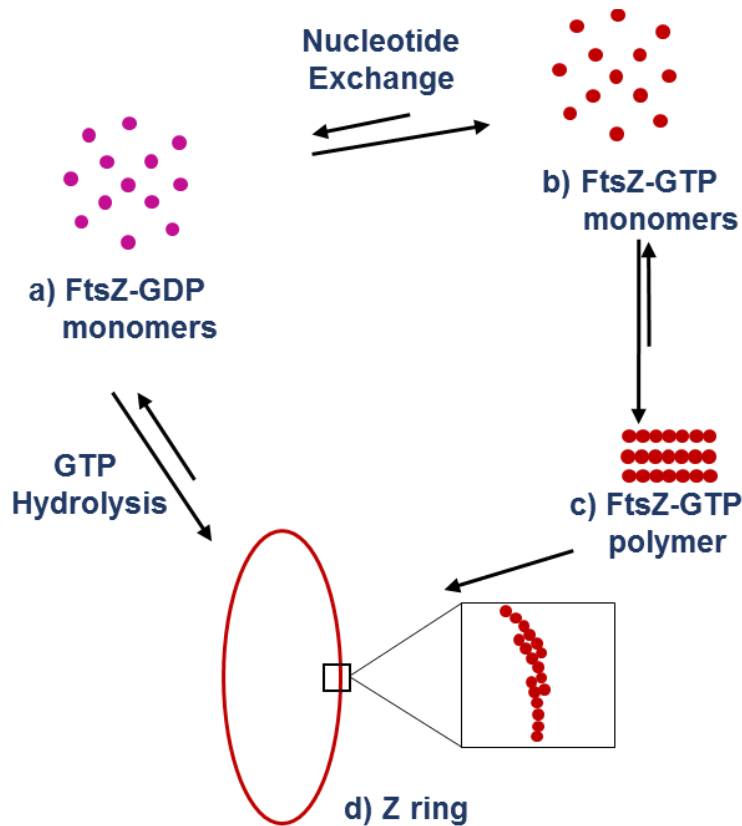


Figure 1.2. Polymerization-depolymerization dynamics of FtsZ

(A, B) Nucleotide exchange between GDP-bound FtsZ and GTP-bound FtsZ with rapid equilibrium, favoring GTP-bound FtsZ (C) Polymerization begins and long-straight protofilaments starts to form after a critical concentration of GTP-bound FtsZ is achieved. (D) Lateral interactions between short overlapping protofilaments lead to Z ring formation. Hydrolysis of GTP to GDP leads to instability of Z ring and its subsequent depolymerization.

FtsZ polymerization to form the Z ring is a key event in bacterial cell division. During cell division, following the recruitment of several other cell division proteins, Z-ring contraction occurs, resulting in septum formation and eventually cell division.⁴ Although the structure of the Z-ring formed *in vivo* is not well understood, it has been suggested that its architecture might consist of a large number of short, overlapping protofilament rather than a continuous ring²⁴ where each protofilament is composed of FtsZ subunits stacked head to tail with GTP sandwiched between two FtsZ subunits.²⁵⁻²⁷ The integrity of the Z ring is maintained by polymerization of FtsZ and its associated GTPase activity. Romberg and Mitchison showed that *in vitro* GTP-bound FtsZ polymerizes into straight polymers.^{28, 29} Following GTP hydrolysis, polymers bound to GDP favored curved conformation as opposed to straight polymers.³⁰ It has been proposed that GTP hydrolysis generates a force during septation where nucleotide-dependent transitions from straight

to a curved polymer can transmit mechanical work to the membrane leading to constriction of the Z-ring.^{24, 30} However, the ability of certain FtsZ mutants to divide in spite of undetectable GTPase activity suggests that FtsZ's GTPase activity is not the source of power during contraction of the septum but is probably important for symmetrical invagination.^{31, 32} Additionally, experiments with liposomes (tubular membrane) and observation of curved and straight protofilaments indicate that protofilament bending is more likely a plausible mechanism for producing the contraction force.^{24, 33} It is believed that the curved conformation of the protofilaments itself cannot pull the membrane to complete scission.³⁴ It has been suggested that the final step of scission can be completed by membrane fluctuations.³⁴ The remodeling of the cell wall, which starts from the membrane invagination, may become a positive force pushing the septum toward closure, leading to the final scission.³⁴⁻³⁶

FtsZ is the first protein to localize to the division site in bacteria and the Z ring marks the site of cell division. In *E. coli* and *B. subtilis* two regulatory systems, the Min system and the nucleoid occlusion (NO) system, play an important role in influencing the placement of the Z ring (**Figure 1.3**). The Min system is composed of MinC, MinD, and MinE which are the product of the *minB* operon.³⁷ MinC/MinD block septation at potential division sites (cell poles or mid-cell) while MinE counteracts their effect in a topological specific manner to ensure cell septation occurs only at midcell during the cell division cycle. Specifically, MinC once activated by MinD, acts as the division block while MinE most likely prevents this activation of MinC offsetting its inhibitory effect.³⁸ In *B. subtilis*, DivIVA instead of MinE, is the topological regulator which is recruited to the division site in a FtsZ-dependent manner and restricts MinC and MinD at the cell poles.³⁹⁻⁴¹ Consequently in both organisms the MinCD concentration is highest in the polar regions of the cell, blocking Z ring formation at the poles.

The premature formation of the Z ring over the nucleoid or chromosomes is prevented by the NO system. SImA in *E. coli*⁴²⁻⁴⁵ and Noc in *B. subtilis*,^{46, 47} two non-homologous proteins, bind to the chromosome, which occupies a midcell location during the late stages of replication and segregation. As segregation progresses, the concentration of NO drops at midcell, allowing the Z ring to form.⁴⁸

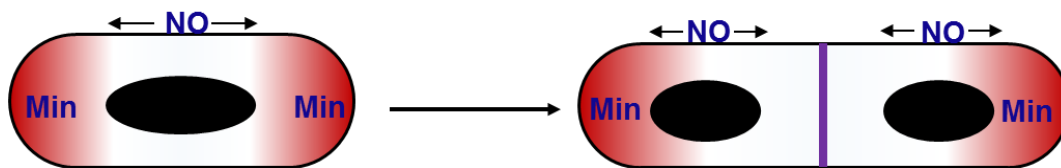


Figure 1.3. Z-ring regulatory system

Min system and NO system ensure Z ring formation occurs only at midcell and not the poles. Min system forms a gradient with high concentration at the poles while NO occupies the central region. Chromosome segregation and separation causes a reprieve in NO concentration at midcell allowing Z ring formation at this site.

Recently, Rodrigues *et al.* have shown that *B. subtilis* cells are able to form correctly positioned Z ring, although less efficiently, even in the complete absence of both the Min system and Noc system.⁴⁹ Additionally, FtsZ over production could counter this inefficiency significantly and increase the proportion of midcell Z rings.⁴⁹ Their work indicates that in *B. subtilis*, Min and NO ensure the formation of the Z ring at midcell at the correct time during the cell cycle versus the previous hypothesis that they identify the midcell as the correct division site. Some other factors control the positioning of the Z ring. Moriya *et al.* propose a “ready-set-go” model in which the midcell becomes increasingly ‘potentiated’ for Z ring formation as initiation of DNA replication is progressively completed.⁵⁰ As the cell progresses in the initiation phase of replication, an accumulation of positive factors contributes to this ‘Potentiation’ of midcell Z ring formation.⁵⁰

It is worth mentioning that while many of the proteins involved in chromosomal segregation and cell division are conserved across the bacterial taxa, others appear limited to Gram-negative or Gram-positive bacteria. Analysis of the *Mtb* genome sequence revealed that many of the genes that encode proteins involved in regulation of septum formation and cell division are not annotated.⁹ The regulatory proteins including the Min and NO systems described above have not been identified in *Mtb* thus far.

1.2. FtsZ as a target for antitubercular drug discovery

FtsZ has emerged as a promising target for antibacterial drug discovery efforts to identify pathogen specific as well as broad-spectrum agents.^{51, 52} Several classes of compounds, including but not limited to, OTBA,⁵³ 2-alkoxycarbonylaminopyridines,⁵⁴ 2-carbamoylpteridine,⁵⁵ taxanes,⁵⁶ benzimidazoles,⁵⁷ GTP analogues,^{58, 59} benzo[c]phenanthridines,^{60, 61} isoquinolines,⁶²⁻⁶⁴

PC190723,^{65, 66} Zantrins,⁶⁷ and chrysophaentins⁶⁸ have been identified as potent agents targeting FtsZ. Against *Mtb* FtsZ, taxanes⁵⁶ and benzimidazoles⁵⁷ developed in the Ojima lab have emerged as promising leads in the last several years after the pioneering work by the Southern Research Institute group.^{54, 55, 62, 69}

1.2.1. 2-Alkoxy-carbonylaminopyridines and 2-carbamoylpteridine

White *et al.* screened a series of 2-alkoxy-carbonylaminopyridines developed as tubulin inhibitors against *Mtb* to identify SRI-3072 and SRI-7614 (**Figure 1.4**) as potential *Mtb* FtsZ inhibitors.⁵⁴ It was found that SRI-3072 was highly specific to *Mtb* FtsZ with a selectivity index (SI = IC₅₀/MIC) of 42 and did not inhibit tubulin polymerization at 100 µM concentration, while SRI-7614 (SI >32) inhibited tubulin polymerization as well (ID₅₀ = 4 µM). Treatment of *Mtb* FtsZ with 100 µM of SRI-3072 led to 20 % inhibition of GTP hydrolysis. SRI-3072 also exhibited moderate activity against a range of Gram-positive bacteria, including drug-resistant strains. As an optimization of SRI-3072, 2-carbamoylpteridine analogues of SRI-3072 were also synthesized and assayed against *Mtb* H37Ra. Analogue 1 (**Figure 1.4**) was found to possess 8-fold better MIC than the parent compound but was inactive *in vivo*.^{55, 69} Additionally, optimized analogue 2 when dosed at 10 mg/kg in the short term GKO model of TB infection reduced the bacterial load in the lung by 0.83 Log₁₀CFU but failed to show potency in the spleen (0.5 Log₁₀CFU).⁶⁹ Unfortunately, these compounds are not being pursued any further due to the significant toxicity observed in the animal model.⁶⁹

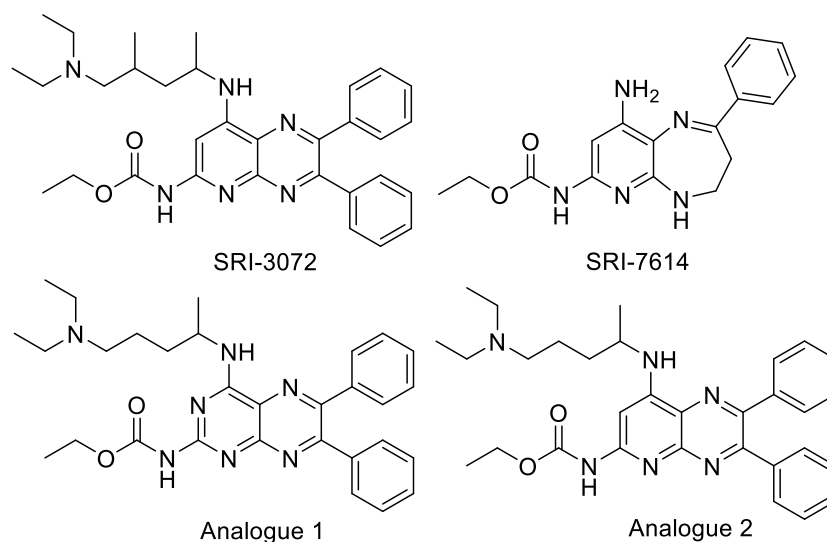


Figure 1.4. Antitubercular compounds developed at SRI

1.2.2. Taxanes

As FtsZ and tubulin have close functional homology,⁷⁰⁻⁷² compounds that are known to inhibit or stabilize tubulin/microtubules can serve as a good starting point for the development of novel antibacterial agents.^{51, 52, 57, 73, 74} After modifications, these tubulin inhibitors can be made specific to target FtsZ with no appreciable cytotoxicity to eukaryotic cells. Based on this premise, the taxane based compounds designed in the Ojima research group by Huang *et al.* were screened for their antibacterial activity against *Mtb* H37Rv in collaboration with Dr. Kirikae.⁵⁶ Real time (RT) PCR-based assay was employed to screen a library of 120 taxanes belonging to two classes: taxol-like compounds which stabilize microtubules⁷⁵⁻⁷⁷ and non-cytotoxic taxane-multidrug resistance (MDR) reversal agents (TRAs)⁷⁸⁻⁸⁴ which inhibit the efflux pumps of ATP-binding cassette (ABC) transporters such as P-glycoprotein (P-gp). Several of these exhibited significant anti-TB activity.⁵⁶ From the MIC values and cytotoxicity assay, **SB-T-0032** and **SB-RA-2001** (Figure) were selected for further studies. SB-RA series of taxanes bearing a (*E*)-3-(naphtha-2-yl)acryloyl (2-NpCH=CHCO) group at the C-13 position exhibited MIC between 2.5-5 μ M against drug-sensitive and drug-resistant *Mtb* strains. A new library of taxanes based on the above SB-RA series was therefore prepared by modification of 10-deacetylbaccatin III (DAB). These **SB-RA-2001** analogues were found to exhibit higher specificity to FtsZ than microtubules and have the same level of anti-TB activity to that of **SB-T-0032** (Table 1.1).

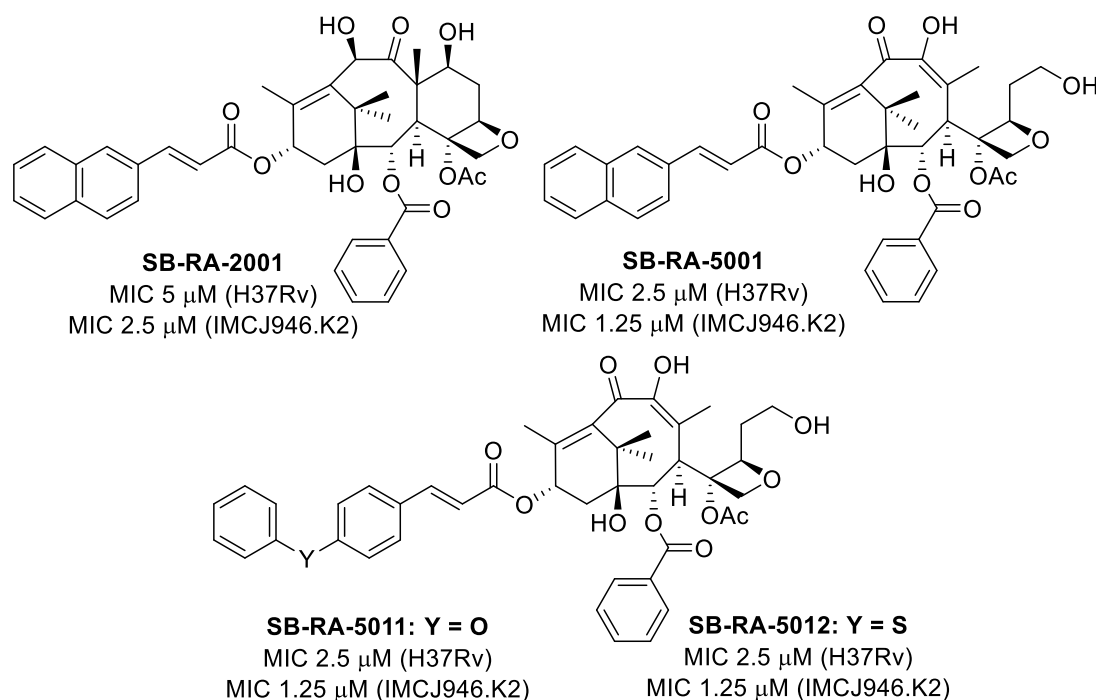


Figure 1.5. *Mtb* FtsZ inhibitors: Taxane-based compounds

Table 1.1. Antimicrobial activities of taxanes against drug-sensitive and multidrug-resistant *Mtb*^a

| Taxane | <i>Mtb</i> MIC (μM) | | Cytotoxicity (IC ₅₀ , μM) | |
|----------------|----------------------------------|------------|--------------------------------------------------|-------|
| | H37Rv | IMCJ946.K2 | MCF7 | A549 |
| Paclitaxel | 40 | 40 | 0.019 | 0.028 |
| SB-T-0032 | 5 | 1.25 | 0.65 | 0.65 |
| SB-RA-2001 | 5 | 2.5 | 4.5 | 15.7 |
| SB-RA-5001 | 2.5 | 1.25 | >80 | >80 |
| SB-RA-5001MeO6 | 2.5 | 2.5 | >80 | >80 |
| SB-RA-5011 | 2.5 | 1.25 | >80 | >80 |
| SB-RA-5012 | 2.5 | 1.25 | >80 | >80 |

^a*M. tuberculosis* IMCJ946.K2 is resistant to nine drugs including INH, RIF, EMB, streptomycin, kanamycin, ethionamid, *p*-aminosalicylic acid, cycloserine and enviomycin. MCF7 and A549 cells: human breast and non-small cell lung cancer cell lines, respectively. Adapted from Ref. 56.

Another class of taxane analogues with C-seco-baccatin skeleton, the anti-angiogenic taxoid (IDN5390),^{85, 86} have also been observed to be less cytotoxic than paclitaxel. Therefore, C-seco analogues of **SB-RA-2001** have been studied and were found to possess anti-TB activity (MIC 1.25-2.5 μ M) against drug-sensitive and drug-resistant *Mtb* strains without appreciable cytotoxicity (IC₅₀ > 80 μ M) (**Table 1.1**).

1.2.3. Trisubstituted benzimidazoles

The Ojima research group has explored the trisubstituted benzimidazole scaffold to develop novel antibacterial agents. Initially, a library of 349 trisubstituted benzimidazoles were synthesized and screened against *Mtb* H37Rv.⁵⁷ From the initial 26 hits, 9 compounds showed activity at 0.56-6.1 μ g/mL, based on the more accurate Alamar blue assay.⁵⁷ Target validation studies and extensive SAR studies have been carried out and are discussed in detail in this dissertation.

1.3. References

1. World Health Organization, Tuberculosis: data and country profiles. <http://www.who.int/tb/country/en/>.
2. Gandhi, N. R.; Moll, A.; Sturm, A. W.; Pawinski, R.; Govender, T.; Lalloo, U.; Zeller, K.; Andrews, J.; Friedland, G., Extensively drug-resistant tuberculosis as a cause of death in patients co-infected with tuberculosis and HIV in a rural area of South Africa. *Lancet* **2006**, *368*, 1575-80
3. Bloom, B. R.; Murray, C. J., Tuberculosis: commentary on a reemergent killer. *Science* **1992**, *257*, 1055-64
4. Errington, J.; Daniel, R. A.; Scheffers, D.-J., Cytokinesis in bacteria. *Microbiol. Mol. Biol. Rev.* **2003**, *67*, 52-65
5. Raviglione, M. C., Issues facing TB control (7). Multiple drug-resistant tuberculosis. *Scott Med J* **2000**, *45*, 52-5; discussion 56
6. World Health Organization, Tuberculosis: Data and Country Profiles. Available at http://www.who.int/tb/publications/global_report/gtbr13_executive_summary.pdf?ua=1.
7. Miller, J. R.; Waldrop, G. L., Discovery of novel antibacterials. *Expert Opin. Drug Discovery* **2010**, *5*, 145-154
8. Diacon, A. H.; Pym, A.; Grobusch, M.; Patientia, R.; Rustomjee, R.; Page-Shipp, L.; Pistorius, C.; Krause, R.; Bogoshi, M.; Churchyard, G.; Venter, A.; Allen, J.; Palomino, J. C.; De Marez, T.; van Heeswijk, R. P.; Lounis, N.; Meyvisch, P.; Verbeeck, J.; Parys, W.; de Beule, K.; Andries, K.; Mc Neeley, D. F., The diarylquinoline TMC207 for multidrug-resistant tuberculosis. *N Engl J Med* **2009**, *360*, 2397-405
9. Slayden, R. A.; Knudson, D. L.; Belisle, J. T., Identification of cell cycle regulators in *Mycobacterium tuberculosis* by inhibition of septum formation and global transcriptional analysis. *Microbiology* **2006**, *152*, 1789-1797
10. Vollmer, W., The prokaryotic cytoskeleton: A putative target for inhibitors and antibiotics? *Appl. Microbiol. Biotechnol.* **2006**, *73*, 37-47
11. Margalit, D. N.; Romberg, L.; Mets, R. B.; Hebert, A. M.; Mitchison, T. J.; Kirschner, M. W.; RayChaudhuri, D., Targeting cell division: Small-molecule inhibitors of FtsZ GTPase perturb cytokinetic ring assembly and induce bacterial lethality. *Proc. Natl. Acad. Sci. U. S. A.* **2004**, *101*, 11821-11826

12. Ben-Yehuda, S.; Losick, R., Asymmetric cell division in *B. subtilis* involves a spiral-like intermediate of the cytokinetic protein FtsZ. *Cell* **2002**, *109*, 257-266
13. Goehring, N. W.; Beckwith, J., Diverse paths to midcell: assembly of the bacterial cell division machinery. *Curr. Biol.* **2005**, *15*, R514-R526
14. Leung, A. K. W.; White, E. L.; Ross, L. J.; Reynolds, R. C.; DeVito, J. A.; Borhani, D. W., Structure of *Mycobacterium tuberculosis* FtsZ Reveals Unexpected, G Protein-like Conformational Switches. *J. Mol. Biol.* **2004**, *342*, 953-970
15. Moller-Jensen, J.; Loewe, J., Increasing complexity of the bacterial cytoskeleton. *Curr. Opin. Cell Biol.* **2005**, *17*, 75-81
16. Thanedar, S.; Margolin, W., FtsZ Exhibits Rapid Movement and Oscillation Waves in Helix-like Patterns in *Escherichia coli*. *Curr. Biol.* **2004**, *14*, 1167-1173
17. de Boer, P.; Crossley, R.; Rothfield, L., The essential bacterial cell-division protein FtsZ is a GTPase. *Nature* **1992**, *359*, 254-6
18. RayChaudhuri, D.; Park, J. T., *Escherichia coli* cell-division gene *ftsZ* encodes a novel GTP-binding protein. *Nature* **1992**, *359*, 251-4
19. Adams, D. W.; Errington, J., Bacterial cell division: assembly, maintenance and disassembly of the Z ring. *Nat. Rev. Microbiol.* **2009**, *7*, 642-653
20. Erickson Harold, P.; Anderson David, E.; Osawa, M., FtsZ in bacterial cytokinesis: cytoskeleton and force generator all in one. *Microbiol. Mol. Biol. Rev.* **2010**, *74*, 504-28
21. Mukherjee, A.; Dai, K.; Lutkenhaus, J., *Escherichia coli* cell division protein FtsZ is a guanine nucleotide binding protein. *Proc. Natl. Acad. Sci. U. S. A.* **1993**, *90*, 1053-1057
22. Erickson, H. P.; O'Brien, E. T., Microtubule Dynamic Instability and GTP Hydrolysis. *Annu. Rev. Biophys. Biomol. Struct.* **1992**, *21*, 145-166
23. Mukherjee, A.; Lutkenhaus, J., Guanine nucleotide-dependent assembly of FtsZ into filaments. *J. Bacteriol.* **1994**, *176*, 2754-8
24. Li, Z.; Trimble, M. J.; Brun, Y. V.; Jensen, G. J., The structure of FtsZ filaments in vivo suggests a force-generating role in cell division. *Embo J.* **2007**, *26*, 4694-4708
25. Caplan, M. R.; Erickson, H. P., Apparent Cooperative Assembly of the Bacterial Cell Division Protein FtsZ Demonstrated by Isothermal Titration Calorimetry. *J. Biol. Chem.* **2003**, *278*, 13784-13788

26. Chen, Y.; Bjornson, K.; Redick, S. D.; Erickson, H. P., A rapid fluorescence assay for FtsZ assembly indicates cooperative assembly with a dimer nucleus. *Biophys. J.* **2005**, *88*, 505-514
27. Romberg, L.; Simon, M.; Erickson, H. P., Polymerization of FtsZ, a bacterial homolog of tubulin. Is assembly cooperative? *J. Biol. Chem.* **2001**, *276*, 11743-11753
28. Huecas, S.; Andreu, J. M., Polymerization of nucleotide-free, GDP- and GTP-bound cell division protein FtsZ: GDP makes the difference. *FEBS Lett.* **2004**, *569*, 43-48
29. Romberg, L.; Mitchison, T. J., Rate-Limiting Guanosine 5'-Triphosphate Hydrolysis during Nucleotide Turnover by FtsZ, a Prokaryotic Tubulin Homologue Involved in Bacterial Cell Division. *Biochemistry* **2004**, *43*, 282-288
30. Lu, C.; Reedy, M.; Erickson, H. P., Straight and curved conformations of FtsZ are regulated by GTP hydrolysis. *J. Bacteriol.* **2000**, *182*, 164-170
31. Mukherjee, A.; Saez, C.; Lutkenhaus, J., Assembly of an FtsZ mutant deficient in GTPase activity has implications for FtsZ assembly and the role of the Z ring in cell division. *J. Bacteriol.* **2001**, *183*, 7190-7197
32. Oliva, M. A.; Trambaiolo, D.; Loewe, J., Structural Insights into the Conformational Variability of FtsZ. *J. Mol. Biol.* **2007**, *373*, 1229-1242
33. Osawa, M.; Anderson, D. E.; Erickson, H. P., Reconstitution of Contractile FtsZ Rings in Liposomes. *Science* **2008**, *320*, 792-794
34. Erickson Harold, P.; Anderson David, E.; Osawa, M., FtsZ in bacterial cytokinesis: cytoskeleton and force generator all in one. *Microbiol Molecul. Biol. Rev.* **2010**, *74*, 504-28
35. Yanagisawa, M.; Imai, M.; Taniguchi, T., Shape Deformation of Ternary Vesicles Coupled with Phase Separation. *Phys. Rev. Lett.* **2008**, *100*, 148102/1-148102/4
36. Zhu, T. F.; Szostak, J. W., Coupled Growth and Division of Model protocell membranes. *J. Am. Chem. Soc.* **2009**, *131*, 5705-5713
37. de Boer, P. A. J.; Crossley, R. E.; Rothfield, L. I., A division inhibitor and a topological specificity factor coded for by the minicell locus determine proper placement of the division septum in *E. coli*. *Cell* **1989**, *56*, 641-649
38. De Boer, P. A. J.; Crossley, R. E.; Rothfield, L. I., Roles of MinC and MinD in the site-specific septation block mediated by the MinCDE system of *Escherichia coli*. *J. Bacteriol.* **1992**, *174*, 63-70

39. Edwards, D. H.; Errington, J., The Bacillus subtilis DivIVA protein targets to the division septum and controls the site specificity of cell division. *Mol Microbiol.* **1997**, *24*, 905-15
40. Marston, A. L.; Thomaidis, H. B.; Edwards, D. H.; Sharpe, M. E.; Errington, J., Polar localization of the MinD protein of Bacillus subtilis and its role in selection of the mid-cell division site. *Genes Dev.* **1998**, *12*, 3419-30
41. Marston, A. L.; Errington, J., Selection of the midcell division site in Bacillus subtilis through MinD-dependent polar localization and activation of MinC. *Mol Microbiol.* **1999**, *33*, 84-96
42. Bernhardt, T. G.; de Boer, P. A. J., SlmA, a Nucleoid-Associated, FtsZ Binding Protein Required for Blocking Septal Ring Assembly over Chromosomes in E. coli. *Molecular Cell* **2005**, *18*, 555-564
43. Tonthat, N. K.; Milam, S. L.; Chinnam, N.; Whitfill, T.; Margolin, W.; Schumacher, M. A., SlmA forms a higher-order structure on DNA that inhibits cytokinetic Z-ring formation over the nucleoid. *Proc. Natl. Acad. Sci. U. S. A.* **2013**, *110*, 10586-10591
44. Tonthat, N. K.; Arold, S. T.; Pickering, B. F.; Van Dyke, M. W.; Liang, S.; Lu, Y.; Beuria, T. K.; Margolin, W.; Schumacher, M. A., Molecular mechanism by which the nucleoid occlusion factor, SlmA, keeps cytokinesis in check. *The EMBO Journal* **2011**, *30*, 154-164
45. Cho, H.; McManus, H. R.; Dove, S. L.; Bernhardt, T. G., Nucleoid occlusion factor SlmA is a DNA-activated FtsZ polymerization antagonist. *Proc. Natl. Acad. Sci. U. S. A.* **2011**, *108*, 3773-3778
46. Wu, L. J.; Errington, J., Coordination of cell division and chromosome segregation by a nucleoid occlusion protein in Bacillus subtilis. *Cell.* **2004**, *117*, 917-25
47. Wu, L. J.; Errington, J., Nucleoid occlusion and bacterial cell division. *Nat. Rev. Microbiol.* **2011**, *10*, 8-12
48. Monahan, L. G.; Liew, A. T. F.; Bottomley, A. L.; Harry, E. J., Division site positioning in bacteria: one size does not fit all. *Front. Microbiol.* **2014**, *5*,
49. Rodrigues, C. D. A.; Harry, E. J., The Min System and Nucleoid Occlusion Are Not Required for Identifying the Division Site in Bacillus subtilis but Ensure Its Efficient Utilization. *PLoS Genet* **2012**, *8*, e1002561
50. Moriya, S.; Rashid, R. A.; Rodrigues, C. D. A.; Harry, E. J., Influence of the nucleoid and the early stages of DNA replication on positioning the division site in Bacillus subtilis. *Mol. Microbiol.* **2010**, *76*, 634-647

51. Awasthi, D.; Kumar, K.; Ojima, I., Therapeutic potential of FtsZ inhibition: a patent perspective. *Expert Opin. Ther. Pat.* **2011**, *21*, 657-679
52. Kumar, K.; Awasthi, D.; Berger, W. T.; Tonge, P. J.; Slayden, R. A.; Ojima, I., Discovery of anti-TB agents that target the cell-division protein FtsZ. *Future Med. Chem.* **2010**, *2*, 1305-1323
53. Beuria, T. K.; Singh, P.; Surolia, A.; Panda, D., Promoting assembly and bundling of FtsZ as a strategy to inhibit bacterial cell division: A new approach for developing novel antibacterial drugs. *Biochem. J.* **2009**, *423*, 61-69
54. White, E. L.; Suling, W. J.; Ross, L. J.; Seitz, L. E.; Reynolds, R. C., 2-Alkoxy-carbonylaminopyridines: inhibitors of Mycobacterium tuberculosis FtsZ. *J. Antimicrob. Chemother.* **2002**, *50*, 111-114
55. Reynolds, R. C.; Srivastava, S.; Ross, L. J.; Suling, W. J.; White, E. L., A new 2-carbamoyl pteridine that inhibits mycobacterial FtsZ. *Bioorg. Med. Chem. Lett.* **2004**, *14*, 3161-3164
56. Huang, Q.; Kirikae, F.; Kirikae, T.; Pepe, A.; Amin, A.; Respicio, L.; Slayden, R. A.; Tonge, P. J.; Ojima, I., Targeting FtsZ for Antituberculosis Drug Discovery: Noncytotoxic Taxanes as Novel Antituberculosis Agents. *J. Med. Chem.* **2006**, *49*, 463-466
57. Kumar, K.; Awasthi, D.; Lee, S.-Y.; Zanardi, I.; Ruzsicska, B.; Knudson, S.; Tonge, P. J.; Slayden, R. A.; Ojima, I., Novel Trisubstituted Benzimidazoles, Targeting Mtb FtsZ, as a New Class of Antitubercular Agents. *J. Med. Chem.* **2011**, *54*, 374-381
58. Laeppchen, T.; Hartog, A. F.; Pinas, V. A.; Koomen, G.-J.; Den Blaauwen, T., GTP Analogue Inhibits Polymerization and GTPase Activity of the Bacterial Protein FtsZ without Affecting Its Eukaryotic Homologue Tubulin. *Biochemistry* **2005**, *44*, 7879-7884
59. Paradis-Bleau, C.; Beaumont, M.; Sanschagrín, F.; Voyer, N.; Levesque, R. C., Parallel solid synthesis of inhibitors of the essential cell division FtsZ enzyme as a new potential class of antibacterials. *Bioorg. Med. Chem.* **2007**, *15*, 1330-1340
60. Parhi, A.; Kelley, C.; Kaul, M.; Pilch, D. S.; LaVoie, E. J., Antibacterial activity of substituted 5-methylbenzo[c]phenanthridinium derivatives. *Bioorg. Med. Chem. Lett.* **2012**, *22*, 7080-7083
61. Beuria, T. K.; Santra, M. K.; Panda, D., Sanguinarine Blocks Cytokinesis in Bacteria by Inhibiting FtsZ Assembly and Bundling. *Biochemistry* **2005**, *44*, 16584-16593

62. Mathew, B.; Ross, L.; Reynolds, R. C., A novel quinoline derivative that inhibits mycobacterial FtsZ. *Tuberculosis* **2013**, *93*, 398-400
63. Kelley, C.; Zhang, Y.; Parhi, A.; Kaul, M.; Pilch, D. S.; LaVoie, E. J., 3-Phenyl substituted 6,7-dimethoxyisoquinoline derivatives as FtsZ-targeting antibacterial agents. *Bioorg. Med. Chem.* **2012**, *20*, 7012-7029
64. Parhi, A.; Lu, S.; Kelley, C.; Kaul, M.; Pilch, D. S.; LaVoie, E. J., Antibacterial activity of substituted dibenzo[a,g]quinolizin-7-ium derivatives. *Bioorg. Med. Chem. Lett.* **2012**, *22*, 6962-6966
65. Haydon, D. J.; Stokes, N. R.; Ure, R.; Galbraith, G.; Bennett, J. M.; Brown, D. R.; Baker, P. J.; Barynin, V. V.; Rice, D. W.; Sedelnikova, S. E.; Heal, J. R.; Sheridan, J. M.; Aiwale, S. T.; Chauhan, P. K.; Srivastava, A.; Taneja, A.; Collins, I.; Errington, J.; Czaplowski, L. G., An Inhibitor of FtsZ with Potent and Selective Anti-Staphylococcal Activity. *Science* **2008**, *321*, 1673-1675
66. Haydon, D. J.; Bennett, J. M.; Brown, D.; Collins, I.; Galbraith, G.; Lancett, P.; Macdonald, R.; Stokes, N. R.; Chauhan, P. K.; Sutariya, J. K.; Nayal, N.; Srivastava, A.; Beanland, J.; Hall, R.; Henstock, V.; Noula, C.; Rockley, C.; Czaplowski, L., Creating an antibacterial with in vivo efficacy: synthesis and characterization of potent inhibitors of the bacterial cell division protein FtsZ with improved pharmaceutical properties. *J. Med. Chem.* **2010**, *53*, 3927-3936
67. Margalit, D. N.; Romberg, L.; Mets, R. B.; Hebert, A. M.; Mitchison, T. J.; Kirschner, M. W.; RayChaudhuri, D., Targeting cell division: Small-molecule inhibitors of FtsZ GTPase perturb cytokinetic ring assembly and induce bacterial lethality. [Erratum to document cited in CA141:271048]. *Proc. Natl. Acad. Sci. U. S. A.* **2004**, *101*, 13969
68. Plaza, A.; Keffer, J. L.; Bifulco, G.; Lloyd, J. R.; Bewley, C. A., Chrysopaentins A-H, antibacterial bisdiarylbutene macrocycles that inhibit the bacterial cell division protein FtsZ. *J. Am. Chem. Soc.* **2010**, *132*, 9069-9077
69. Mathew, B.; Srivastava, S.; Ross, L. J.; Suling, W. J.; White, E. L.; Woolhiser, L. K.; Lenaerts, A. J.; Reynolds, R. C., Novel pyridopyrazine and pyrimidothiazine derivatives as FtsZ inhibitors. *Bioorg. Med. Chem.* **2011**, *19*, 7120-7128

70. Erickson, H. P.; Taylor, D. W.; Taylor, K. A.; Bramhill, D., Bacterial cell division protein FtsZ assembles into protofilament sheets and minirings, structural homologs of tubulin polymers. *Proc. Natl. Acad. Sci. USA* **1996**, *93*, 519-23
71. Lowe, J.; Amos, L. A., Crystal structure of the bacterial cell-division protein FtsZ. *Nature* **1998**, *391*, 203-6
72. Lowe, J.; Amos, L. A., Tubulin-like protofilaments in Ca²⁺-induced FtsZ sheets. *Embo J.* **1999**, *18*, 2364-71
73. Lappchen, T.; Hartog Aloysius, F.; Pinas Victorine, A.; Koomen, G.-J.; den Blaauwen, T., GTP analogue inhibits polymerization and GTPase activity of the bacterial protein FtsZ without affecting its eukaryotic homologue tubulin. *Biochemistry* **2005**, *44*, 7879-84
74. Huang, Q.; Tonge Peter, J.; Slayden Richard, A.; Kirikae, T.; Ojima, I., FtsZ: a novel target for tuberculosis drug discovery. *Curr. Top. Med. Chem.* **2007**, *7*, 527-43
75. Georg, G. I.; Chen, T. T.; Ojima, I.; Wyas, D. M.; Editors, *Taxane Anticancer Agents: Basic Science and Current Status. ACS Symp. Ser.* 1995; Vol. 583, p 353.
76. Kingston, D. G. I.; Jagtap, P. G.; Yuan, H.; Samala, L., The chemistry of taxol and related taxoids. *Prog. Chem. Org. Nat. Prod.* **2002**, *84*, 53-225
77. Ojima, I.; Kuduk, S. D.; Chakravarty, S., Recent advances in the medicinal chemistry of taxoid anticancer agents. *Adv. Med. Chem.* **1999**, *4*, 69-124
78. Brooks, T. A.; Kennedy, D. R.; Gruol, D. J.; Ojima, I.; Baer, M. R.; Bernacki, R. J., Structure-activity analysis of taxane-based broad-spectrum multidrug resistance modulators. *Anticancer Res.* **2004**, *24*, 409-415
79. Brooks Tracy, A.; Minderman, H.; O'Loughlin Kieran, L.; Pera, P.; Ojima, I.; Baer Maria, R.; Bernacki Ralph, J.; Brooks, T., Taxane-based reversal agents modulate drug resistance mediated by P-glycoprotein, multidrug resistance protein, and breast cancer resistance protein. *Mol. Cancer Ther.* **2003**, *2*, 1195-205
80. Minderman, H.; Brooks, T. A.; O'Loughlin, K. L.; Ojima, I.; Bernacki, R. J.; Baer, M. R., Broad-spectrum modulation of ATP-binding cassette transport proteins by the taxane derivatives ortataxel (IDN-5109, BAY 59-8862) and tRA96023. *Cancer Chemother. Pharmacol.* **2004**, *53*, 363-369
81. Ojima, I.; Borella, C. P.; Wu, X.; Bounaud, P.-Y.; Oderda, C. F.; Sturm, M.; Miller, M. L.; Chakravarty, S.; Chen, J.; Huang, Q.; Pera, P.; Brooks, T. A.; Baer, M. R.; Bernacki, R. J.,

- Design, Synthesis and Structure-Activity Relationships of Novel Taxane-Based Multidrug Resistance Reversal Agents. *J. Med. Chem.* **2005**, *48*, 2218-2228
82. Ojima, I.; Bounaud, P.-Y.; Bernacki, R. J., New weapons in the fight against cancer. *Chemtech* **1998**, *28*, 31-36
83. Ojima, I.; Bounaud, P.-Y.; Bernacki, R. J., Designing taxanes to treat multidrug-resistant tumors. *Mod. Drug Discovery* **1999**, *2*, 45,47-48,51-52
84. Ojima, I.; Bounaud, P.-Y.; Oderda, C. F., Recent strategies for the treatment of multi-drug resistance in cancer cells. *Expert Opin. Ther. Pat.* **1998**, *8*, 1587-1598
85. Appendino, G.; Danieli, B.; Jakupovic, J.; Belloro, E.; Scambia, G.; Bombardelli, E., The chemistry and occurrence of taxane derivatives. XXX. Synthesis and evaluation of C-seco paclitaxel analogs. *Tetrahedron Lett.* **1997**, *38*, 4273-4276
86. Taraboletti, G.; Micheletti, G.; Rieppi, M.; Poli, M.; Turatto, M.; Rossi, C.; Borsotti, P.; Roccabianca, P.; Scanziani, E.; Nicoletti, M. I.; Bombardelli, E.; Morazzoni, P.; Riva, A.; Giavazzi, R., Antiangiogenic and antitumor activity of IDN 5390, a new taxane derivative. *Clin. Cancer Res.* **2002**, *8*, 1182-1188

Chapter 2

Synthesis and Optimization of Novel Trisubstituted Benzimidazoles

Table of Contents

| | |
|----------------------------------------------------------------------------------------------------|----|
| Chapter 2 | 19 |
| 2.1. Introduction..... | 20 |
| 2.1.1. The road leading to trisubstituted benzimidazoles as a pharmacophore | 21 |
| 2.1.1.1. Albendazole and thiabendazole | 21 |
| 2.1.1.2. 2-Alkoxy-carbonylaminopyridines and 2-carbamoylpteridine | 22 |
| 2.1.1.3. Trisubstituted benzimidazole as a pharmacophore | 22 |
| 2.2. Results and Discussion..... | 23 |
| 2.2.1. Synthesis of 2,5,6-trisubstituted benzimidazole library | 23 |
| 2.2.2. Optimization of 2,5,6-trisubstituted benzimidazoles..... | 26 |
| 2.2.3. Optimization of 2,5,6-trisubstituted benzimidazoles based on metabolite identification..... | 33 |
| 2.2.3.1. Metabolites of SB-P3G2..... | 33 |
| 2.2.3.2. Metabolite identification of lead 5-position benzamido compounds | 39 |
| 2.2.4. Significance of 2-cyclohexyl group | 41 |
| 2.2.5. Synthesis of substituted 5-position benzylamino group | 42 |
| 2.2.6. Salt formation of SB-P3G2 and SB-P17G-A38..... | 45 |
| 2.2.7. New trisubstituted benzimidazoles with unknown MIC..... | 45 |
| 2.3. Conclusion | 46 |
| 2.4. Experimental Section..... | 47 |
| 2.5. References..... | 82 |

2.1. Introduction

FtsZ, an essential bacterial cytokinesis protein, is a highly promising therapeutic target since, the disruption of cell division would lead to the inhibition/arrest of bacterial infection.^{1, 2} In the presence of guanosine triphosphate (GTP), FtsZ undergoes self-assembly bi-directionally at the center of the cell to form a highly dynamic structure known as the “Z-ring” (**Figure 2.1**).³⁻¹¹ During cell division, following the recruitment of several other cell division proteins, Z-ring contraction occurs, resulting in septum formation and eventually cell division.¹² Accordingly, the inhibition of proper FtsZ assembly would block septum formation and then cell division, which should lead to bacterial growth inhibition and cell death.^{1, 13-17} FtsZ offers a significant potential advantage over traditional targets as it is a highly conserved protein in prokaryotes. Thus, in addition to being pathogen specific, FtsZ inhibitors may be developed as broad-spectrum antibacterial agents for the treatment of a variety of bacterial infections.¹⁸ Since FtsZ is an essential and conserved protein for bacterial cell division, it is believed that escaping the FtsZ-targeted compounds by mutating the protein may be demanding for the bacteria.^{19, 20} Recently, Haydon *et al.* have isolated staphylococcal strains resistant to anti-FtsZ compounds with relatively low frequency reiterating the difficulty in developing resistance.²¹ This suggests that resistance mechanisms against compounds developed for FtsZ inhibition may not be widespread in nature.²⁰

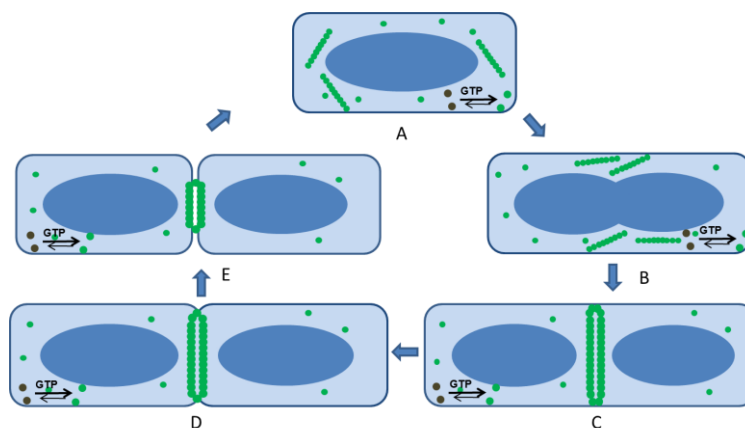


Figure 2.1. Graphic presentation of the Z-ring formation and cell division

(A) Bacterial cell before the beginning of cell division with FtsZ protofilaments scattered in the cell and undergoing continuous nucleotide exchange, favoring GTP-bound FtsZ (B) cell elongation and chromosome segregation, localization of FtsZ protofilaments at the mid cell. (C) Formation of the Z-ring: the ‘steady-state turnover’- GTP hydrolysis competes continuously with protofilament growth during polymerization. (D &E) Formation of septum and subsequent constriction of the Z-ring followed by membrane fluctuation to bring about cell division. Adapted from Ref. 22.

FtsZ inhibitors have been actively investigated for pathogen specific as well as broad-spectrum antibacterial drug discovery.^{14, 22} Several classes of compounds have been identified as promising leads for antibacterial drug development, including OTBA,²³ 2-alkoxycarbonylamino pyridines,²⁴ 2-carbamoyl pteridine,²⁵ taxanes,¹³ benzimidazoles,²⁶ GTP analogues,^{27, 28} benzo[c]phenanthridines,^{29, 30} isoquinolines,³¹⁻³³ PC190723,^{21, 34} Zantrins,³⁵ and chrysopaentins³⁶. However, against *Mtb* FtsZ, only taxanes¹³ and benzimidazoles²⁶ developed in the Ojima lab have emerged as promising leads in the last several years after the pioneering work by the Southern Research Institute group.^{24, 25, 31, 37}

2.1.1. The road leading to trisubstituted benzimidazoles as a pharmacophore

2.1.1.1. Albendazole and thiabendazole

Albendazole and thiabendazole are known tubulin polymerization inhibitors which bind to the colchicine-binding site of tubulin (**Figure 2.2**). To test their effect on the *ftsZ* gene product *Sarcina et al.* treated cyanobacterial and bacterial cultures with thiabendazole and observed cell elongation.³⁸ In addition, they also observed increased amount of DNA, in DAPI-DNA-stained thiabendazole-treated *Synechococcus* 7942 cells, which indicated that DNA replication still occurred in the presence of thiabendazole. Independently, Slayden *et al.* studied the cell morphology and transcriptional response of *Mtb* cells treated with albendazole and thiabendazole and observed cell filamentation and up-regulation of genes encoding for septum formation.³⁹ These results suggested that thiabendazole and albendazole interfered and delayed *Mtb* cytokinesis.

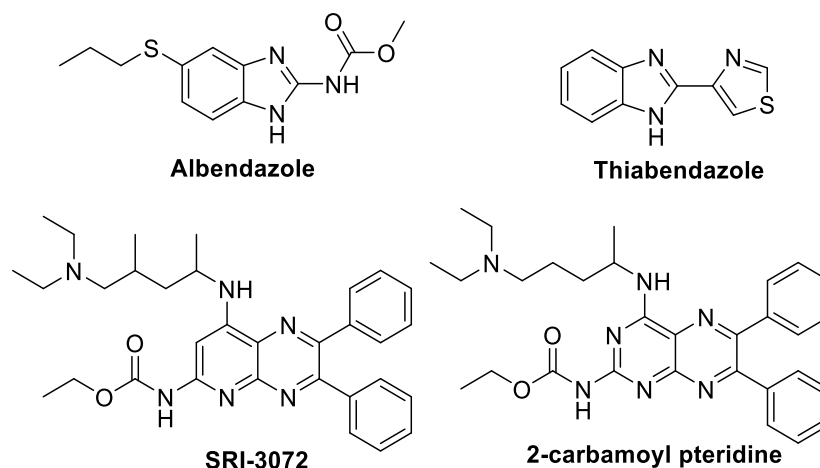


Figure 2.2. Known tubulin inhibitors targeting FtsZ

2.1.1.2. 2-Alkoxy-carbonylaminopyridines and 2-carbamoylpteridine

SRI-3072 was identified as an antibacterial agent from the screening of a series of 2-alkoxy-carbonylaminopyridines and 2-alkoxy-carbonylaminopyrimidines which were initially designed as tubulin inhibitors by Southern Research Institute (SRI). Since tubulin and FtsZ share the same GTP binding motif and have sequence similarity (<20 %), the effect of SRI-3072 on inhibition of tubulin polymerization was evaluated.²⁴ It was found that SRI-3072 was highly specific to *Mtb* FtsZ with a selectivity index (SI = IC₅₀/MIC) of 42 and did not inhibit tubulin polymerization at 100 μM concentration. Treatment of *Mtb* FtsZ with 100 μM of SRI-3072 led to 20 % inhibition of GTP hydrolysis. SRI-3072 also exhibited moderate activity against a range of Gram-positive bacteria, including drug-resistant strains. As an optimization of SRI-3072, 2-carbamoylpteridine analogues of SRI-3072 were also synthesized and assayed against *Mtb* H37Ra. Analogue 4 (**Figure 2.2**) was found to possess 8-fold better MIC than the parent compound.²⁵

2.1.1.3. Trisubstituted benzimidazole as a pharmacophore

Recognizing the potential of the benzimidazole pharmacophore common to both albendazole and thiabendazole, and combining the SAR developed by SRI, the Ojima Research group pursued the trisubstituted benzimidazole scaffold to develop novel antibacterial agents. Initially, a library of 349 trisubstituted benzimidazoles, specifically 2,5,6- and 2,5,7-trisubstituted benzimidazoles (**Figure 2.3**), were synthesized employing polymer-assisted solution phase synthesis.²⁶ From an initial screen performed against *Mtb* H37Rv strain, 26 compounds were identified that inhibited *Mtb* cell growth with MIC values ≤ 5 μg/mL, in triplicates. Furthermore, among the 26 hits, 9 compounds showed potency at 0.56-6.1 μg/mL, based on the more accurate Alamar blue assay. The target of these novel trisubstituted benzimidazoles was confirmed by light scattering assay. The experiment showed a marked decrease in the polymerization of FtsZ on addition of the hit compounds and a complete shut-down of polymerization was observed at concentrations as low as 20 μM of inhibitor, confirming FtsZ as the drug target (**Figure 2.4**).²⁶ Also from the preliminary structure-activity relationship studies the cyclohexyl group at the C-2 position, diethylamino group at the C-6 position and alkyl carbamates or benzamides at the C-5 position were identified as crucial substituents for inhibitory activity.

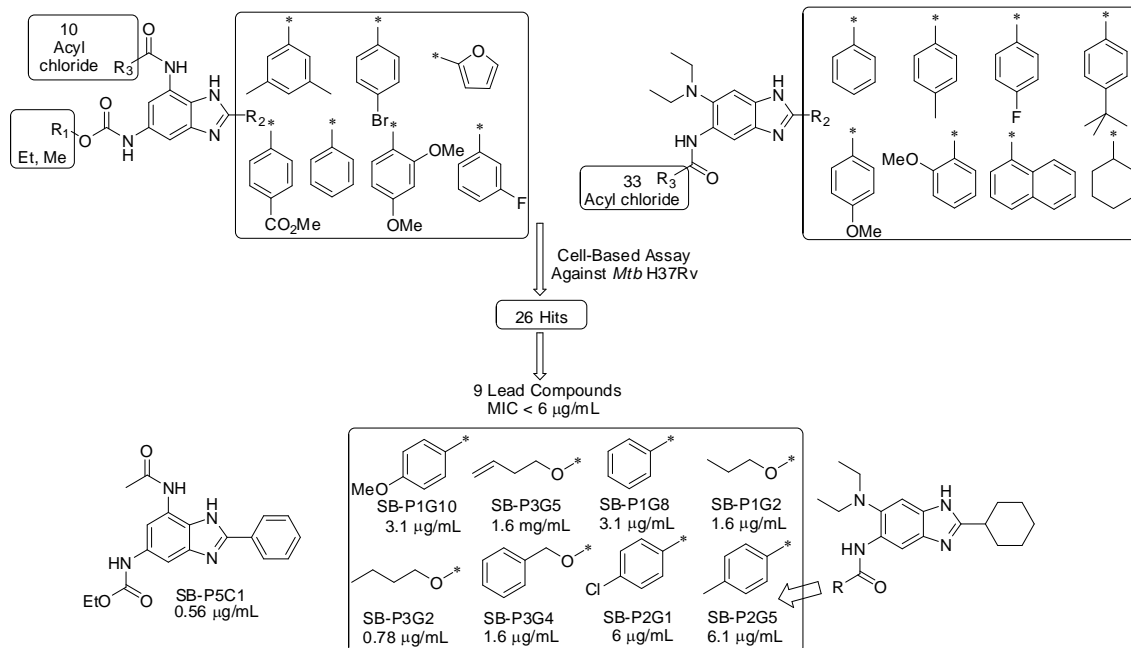


Figure 2.3. MIC values of the eight hit 2,5,6-trisubstituted benzimidazoles ²⁶

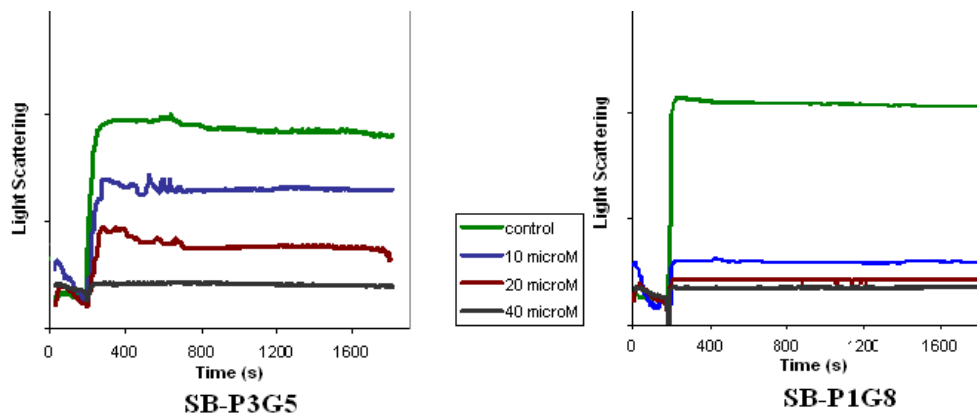


Figure 2.4. FtsZ polymerization inhibition monitored via light scattering
Adapted from Ref. 26

Continuing on with this work and to better understand the SAR, new libraries of trisubstituted benzimidazoles were synthesized and evaluated for antitubercular activity.

2.2. Results and Discussion

2.2.1. Synthesis of 2,5,6-trisubstituted benzimidazole library

As mentioned above, based on SAR studies the importance of cyclohexyl ring at the C-2 position, diethylamino group at the C-6 position, and alkyl carbamates or benzamides at the C-5 position has been recognized. Keeping the cyclohexyl ring fixed at the C-2 position, a library of

238 compounds with various diethylamino group congeners at the C-6 position was synthesized. A preliminary screening against H37Rv strains using micro broth dilution method and Alamar blue assay identified two compounds, **SB-P8B2** and **SB-P8B4**, with MIC <0.5µg/mL (**Figure 2.5**).²⁶

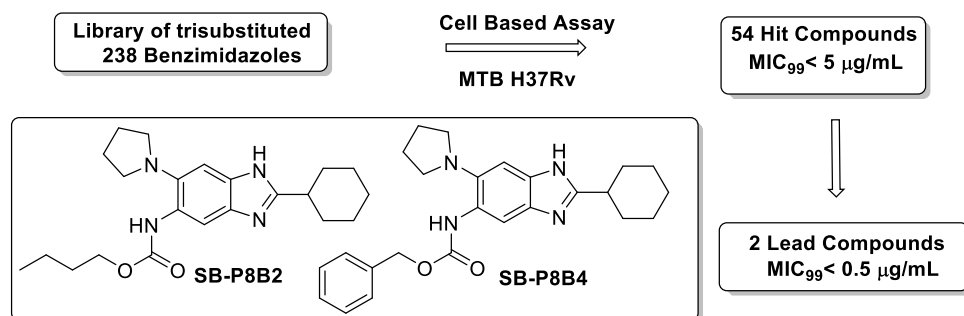
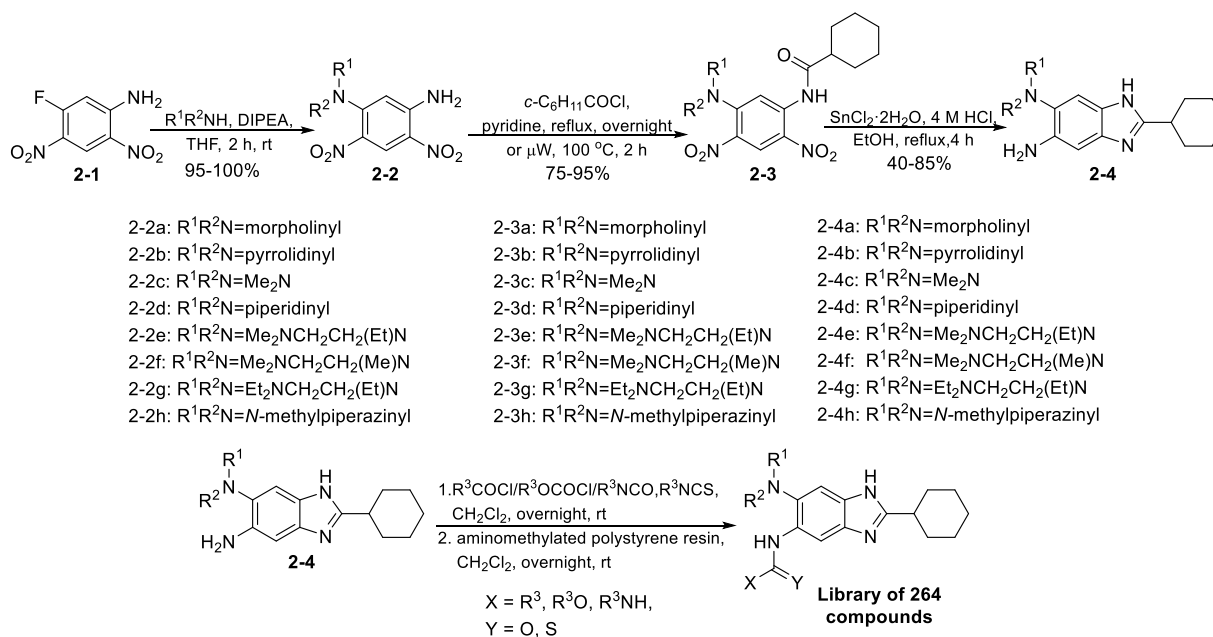


Figure 2.5. Cell based assay results of library²⁶

To have an in-house duplicate of this library, the intermediates were re-synthesized as shown in the general scheme below (**Scheme 2.1**).²⁶ Additionally, new libraries of 6-diethylamino mimics were synthesized using the same intermediates to expand our database and develop an extensive SAR profile. The intermediate with a 6-*N,N*-dimethylamino group was used for the first time in this library and has now been found to afford the most potent antitubercular compounds up to now.



Scheme 2.1. Synthesis of 2,5,6-trisubstituted benzimidazoles^{26, 40}

The aromatic nucleophilic substitution of commercially available 2,4-dinitro-5-fluoroaniline with various amines afforded 5-dialkylaminodinitroanilines **2-2(a-h)** in 95-100% yields. The acylation of **2-2(a-h)** with cyclohexanecarbonyl chloride gave the corresponding *N*-acylanilines **2-3(a-h)** in 75-95% yields. One-pot reduction and cyclization in the presence of stannous chloride dihydrate and 4 M hydrochloric acid gave 5-aminobenzimidazoles **2-4(a-h)** in 40-85% yields. Intermediates **2-4a**, **2-4b**, **2-4(d-h)** were used to re-synthesize previously designed libraries (Plates 6, 7, and 8). For the synthesis of the new library, the intermediates **2-4(a-h)** were dissolved in methylene chloride and transferred to 96-well plates. A series of different acyl chlorides, alkyl chloroformates, sulfonyl chlorides, isocyanates and/or isothiocyanates were used to afford a new library of 264 compounds (Plates 18,19 and 21). The synthesized library was screened in triplicates in a 96-well format (single point assay) against *Mtb* H37Rv by our collaborator at CSU to identify 15 compounds active at a cut off value of MIC ≤ 5 $\mu\text{g/mL}$ (**Figure 2.7**). Since the compounds in the plates are not purified before the preliminary screening against *Mtb*, the hit compound identified at MIC ≤ 5 $\mu\text{g/mL}$ are resynthesized, tested for purity and re-evaluated against *Mtb* H37Rv to determine accurate MIC values. Resynthesis and accurate MIC determination are discussed in the following sections.

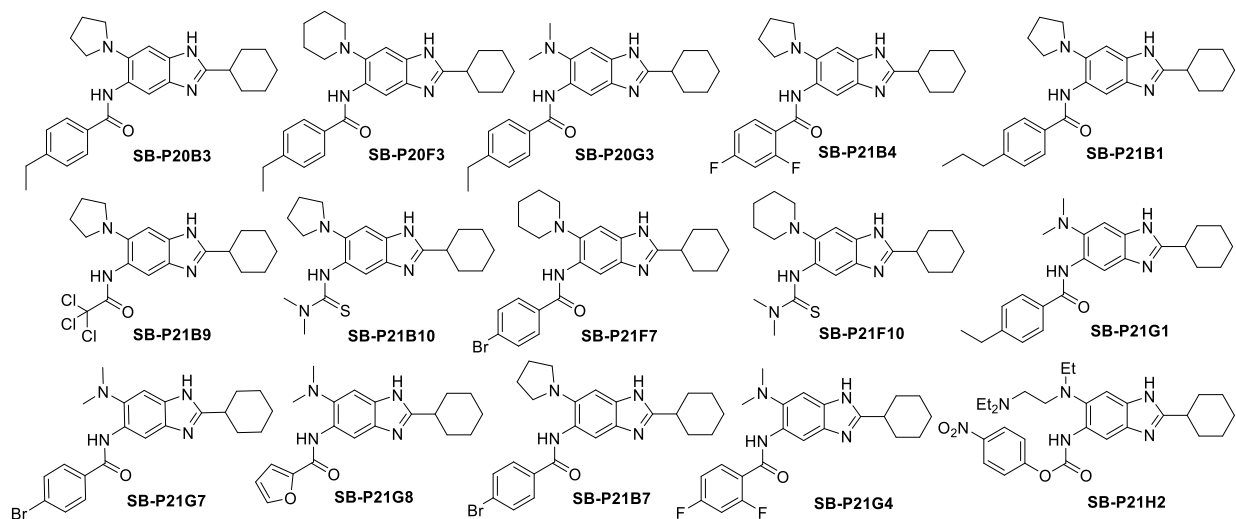


Figure 2.6. Structure of hit compounds at cut off values of MIC ≤ 5 $\mu\text{g/mL}$

2.2.2. Optimization of 2,5,6-trisubstituted benzimidazoles

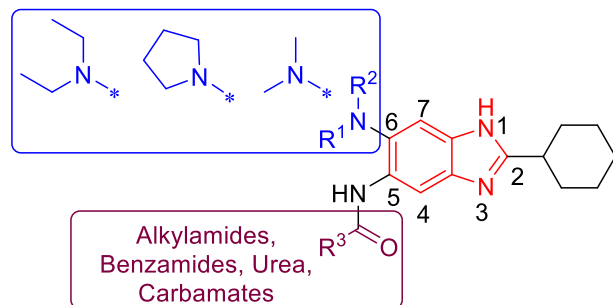
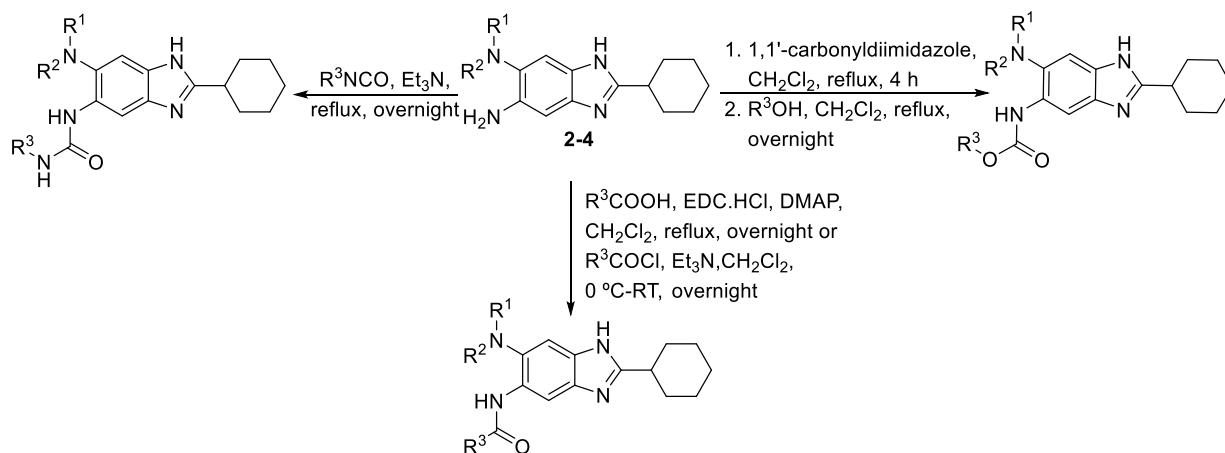


Figure 2.7. Proposed optimization of 2,5,6-trisubstituted benzimidazoles ⁴⁰

Previously identified lead compounds **SB-P3G2** and **SB-P8B2** have been found to be bactericidal and also active against non-replicating *Mtb* grown under low oxygen conditions.^{40, 41} The latter result is particularly exciting since it indicates that these compounds have potential to be effective against latent TB infection. Furthermore, **SB-P3G2** has exhibited good efficacy *in vivo* in the standard acute infection model using immune incompetent GKO mice.⁴¹ Since **SB-P3G2** and **SB-P8B2** have shown very promising antibacterial activities *in vitro* and *in vivo*, we started optimization of these leads through systematic structural modifications at the 5 and 6 positions, keeping the cyclohexyl group at the 2 position intact as shown in **Figure 2.7**. The general procedure outlined in **Scheme 2.2** was followed for synthesis.⁴⁰



Scheme 2.2. Synthesis of 5-position functionalized trisubstituted benzimidazoles ⁴⁰

Based on the early lead compounds, **SB-P3G2** and **SB-P8B2**, which possess a butylcarbamate group at the 5-position, 6-dimethylamino analogue with the same substituent was

synthesized. Fortuitously, this compound (**SB-P17G-C2**) was 13 times more active than **SB-P3G2**. Additional carbamate analogues of **SB-P17G-C2** were synthesized and observed to be potent antitubercular agents with MIC ranging from 0.06-0.63 $\mu\text{g/mL}$.⁴⁰ To assess the potential *in vivo* pharmacokinetics (PK), stability of these very potent molecules were evaluated in the presence of human and mouse plasma by our collaborator at Sanofi-Aventis. **SB-P17G-C2** was found to be stable in human plasma with 6.1% hydrolysis after 4 h incubation, but it was very unstable in mouse plasma undergoing 87.6% hydrolysis after a 4 h incubation. To assess the extent of metabolic conversion, **SB-P17G-C2** was evaluated using a microsomal stability assay. **SB-P17G-C2** was found to be highly labile with 90% and 96% degradation in the presence of human and mouse liver microsomes, respectively.⁴² All the other carbamates followed the same trend (**Table 2.1**).

Table 2.1. Antibacterial activity of 5-carbamate benzimidazoles against *Mtb* H37Rv strain (MIC, $\mu\text{g/mL}$), their cytotoxicity (IC_{50} , $\mu\text{g/mL}$), and microsomal instability

| Compound | R ¹ R ² N | R ³ O | <i>Mtb</i> H37Rv MIC | Vero Cytotoxicity | Microsomal Metabolism* Human | Microsomal Metabolism* Mouse |
|-------------|---------------------------------|------------------|-------------------------|----------------------|---------------------------------|---------------------------------|
| SB-P3G2 | | | 0.63 | >100 | 78% | 98% |
| SB-P17G-C2 | | | 0.06 | >100 | 97% | 99% |
| SB-P17G-C4 | | | 0.16 | >100 | 74% | 99% |
| SB-P17G-C8 | | | 0.31 | >100 | 86% | 98% |
| SB-P17G-C12 | | | 0.63 | >100 | N.D. | N.D. |

*values indicate percentage of compound metabolized in the microsomes
MIC and cytotoxicity were determined at CSU; Microsomal metabolism were assessed at Sanofi-Aventis
Adapted from Ref. 40

Since a urea moiety might be a potential isostere of the carbamate substituent, we examined the effect of urea moieties at the 5 position, on the antibacterial activity. As **Table 2.2**

shows, the introduction of a urea group to the 5 position in place of a carbamate group was detrimental to the potency. Compound **SB-P17G-U2** with a 5-dimethylamino group retained good potency but it wasn't comparable to **SB-P17G-C2** and was therefore not tested for plasma/metabolic stability.

Carbamates at the 5-position exhibit poor plasma and metabolic stability in humans/mice, and their urea isosteres display significantly lower activity against *Mtb* therefore, optimization of the 5-position became necessary. Of the 15 hits identified from the previously synthesized library of 264 compounds, 12 compounds were substituted 5-benzamides. In addition, **SB-P1G8** with 5-benzamide synthesized by previous group member had been shown to target *Mtb* FtsZ via light scattering assay, and therefore logic demanded we optimize 5-position by synthesizing a library of 5-benzamides.

Table 2.2. Antibacterial activity of 5-urea benzimidazoles against *Mtb* H37Rv strain (MIC, $\mu\text{g/mL}$) and their cytotoxicity (IC_{50} , $\mu\text{g/mL}$)

| Compound | R ¹ R ² N | R ³ NH | <i>Mtb</i> H37Rv MIC | Vero Cytotoxicity |
|------------|---------------------------------|-------------------|-------------------------|----------------------|
| SB-P1G-U2 | | | >100 | >100 |
| SB-P1G-U4 | | | >100 | >100 |
| SB-P1G-U6 | | | >100 | >100 |
| SB-P8B-U2 | | | 25.0 | >100 |
| SB-P8B-U4 | | | 25.0 | >100 |
| SB-P8B-U6 | | | 100 | >100 |
| SB-P17G-U2 | | | 6.25 | >100 |

MIC and cytotoxicity were determined at CSU. Adapted from Ref. 40

The 5-position benzamides synthesized from 6-diethylamino and 6-pyrrolidinyl benzimidazoles were tested against *Mtb* and **SB-P7B2** was the most potent amongst them with an MIC of 1.56 $\mu\text{g/mL}$ (**Table 2.3**). On the other hand, the 6-dimethylamino analogue of **SB-P7B2** was active at 0.31 $\mu\text{g/mL}$. Since the 5-position benzamides obtained from 5-amino-2-cyclohexyl-6-dimethylaminobenzimidazole were the most active, a small library of benzamides maintaining the 6-dimethylamino group was synthesized (**Table 2.5**).

Table 2.3. Antibacterial activity of 5-benzamido benzimidazoles against *Mtb* H37Rv strain (MIC, $\mu\text{g/mL}$) and their cytotoxicity (IC_{50} , $\mu\text{g/mL}$)

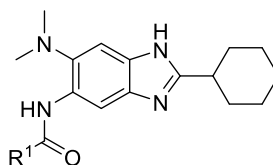
| Compound | R ¹ R ² N | R ³ | <i>Mtb</i> H37Rv MIC | Vero Cytotoxicity |
|----------|---------------------------------|----------------|----------------------|-------------------|
| SB-P2G5 | | | 12.5 | >100 |
| SB-P2G1 | | | 6.0 | >100 |
| SB-P6B8 | | | 6.25 | >100 |
| SB-P6B10 | | | 6.25 | >100 |
| SB-P7B5 | | | 3.13 | >100 |
| SB-P7B2 | | | 1.56 | >100 |
| SB-P7B11 | | | 12.5 | >100 |

MIC and cytotoxicity were determined at CSU. Adapted from Ref. 40

SB-P17G-A15, **SB-P17G-A16**, and **SB-P17G-A20**⁴² with benzamido, *p*-methoxybenzamido, and *p*-trifluoromethoxybenzamido group respectively, were the first three compounds to be synthesized and tested for their stability in plasma and microsomes. **SB-P17G-A20** was found to be stable in human and mouse plasma with only 0.1% and 24.4% hydrolysis, respectively, after a 4 h incubation.⁴² **SB-P17G-A16** and **SB-P17G-A20** exhibited only moderate

lability in the presence of liver microsomes with both showing only 39% conversion in human liver microsomes, and 49% and 45% conversion in mouse liver microsomes, respectively. However, **SB-P17G-A15** without *p*-substitution on the benzamido group was readily metabolized indicating the importance of this substitution, which is exemplified by the trend followed by *p*-alkylbenzamides. The *p*-alkylbenzamides (methyl, ethyl, *n*-propyl, *tert*-butyl) showed similar antibacterial activities and stability profiles among them, but were less stable than **SB-P17G-A20** (Table 2.4).

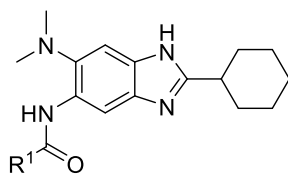
Table 2.4. Microsomal instability of representative 5-benzamido compounds



| Compound | R ¹ | Microsomal Stability* | |
|-------------|----------------|-----------------------|-------|
| | | Human | Mouse |
| SB-P17G-A15 | | 97% | 97% |
| SB-P17G-A28 | | 61% | 81% |
| SB-P20G3 | | 55% | 70% |
| SB-P21G1 | | 56% | 41% |
| SB-P17G-A23 | | 55% | 54% |
| SB-P17G-A20 | | 39% | 45% |
| SB-P17G-A16 | | 39% | 49% |

*values indicate percentage of compound metabolized in the microsomes; Microsomal metabolism were assessed at Sanofi-Aventis. Adapted from Ref. 40 and Ref. 42

Table 2.5. Antibacterial activity of 5-benzamido benzimidazoles against *Mtb* H37Rv strain (MIC, $\mu\text{g/mL}$) and their cytotoxicity (IC_{50} , $\mu\text{g/mL}$)



| Compound | R ¹ | <i>Mtb</i> H37Rv MIC | Vero Cytotoxicity | Compound | R ¹ | <i>Mtb</i> H37Rv MIC | Vero Cytotoxicity |
|-------------|----------------|----------------------|-------------------|-------------|----------------|----------------------|-------------------|
| SB-P17G-A15 | | 1.56 | >100 | SB-P17G-A16 | | 0.31 | >100 |
| SB-P17G-A19 | | 0.31 | >100 | SB-P17G-A25 | | 6.25 | >100 |
| SB-P17G-A20 | | 0.16 | >100 | SB-P17G-A29 | | 0.63 | >100 |
| SB-P17G-A40 | | 0.31 | >100 | SB-P17G-A27 | | 12.5 | >100 |
| SB-P17G-A43 | | 1.25 | >100 | SB-P17G-A36 | | >50 | >100 |
| SB-P17G-A28 | | 0.31 | >100 | SB-P17G-A37 | | >50 | >100 |
| SB-P20G3 | | 0.16 | >100 | SB-P17G-A35 | | 6.25 | >100 |
| SB-P21G1 | | 0.63 | >100 | SB-P17G-A10 | | 0.63 | >100 |
| SB-P17G-A23 | | 1.56 | >100 | SB-P17G-A39 | | 6.25 | >100 |
| SB-P17G-A30 | | 5.0 | >100 | SB-P17G-A41 | | <0.78 | >100 |
| SB-P21G8 | | 6.25 | >100 | SB-P17G-A22 | | >100 | >100 |
| SB-P21G7 | | 0.31 | >100 | SB-P17G-A31 | | >10 | >100 |
| SB-P17G-A7 | | 3.13 | >100 | SB-P17G-A26 | | >100 | >100 |
| SB-P17G-A24 | | 0.63 | >100 | | | | |
| SB-P21G4 | | 0.31 | >100 | | | | |

MIC and cytotoxicity were determined at CSU. Adapted from Ref. 40

To further study the effect of *o,m,p*-substituents several analogues with 6-dimethylamino group were synthesized. Trifluoromethylthiobenzamido and 3-trifluoromethoxybenzamido analogues of **SB-P17G-A20** were synthesized and the switch from trifluoromethoxy to trifluorothiomethyl although harmless for potency was detrimental to the microsomal stability; 95% and 45% metabolism in human and mouse, respectively. **SB-P17G-A25** with *o*-methoxybenzamido group was less potent than **SB-P17G-A16** against *Mtb* but the *o,m*-dimethoxybenzamido compound was equally potent and showed improved microsomal stability. All different combinations of dimethoxybenzamides were synthesized, but no general trend in their antibacterial activity was observed. The *o*-hydroxy-*m*-methoxy compound was also synthesized (**SB-P17G-A39**) but unlike **SB-P17G-A29**, it was active at 6.25 µg/mL. Surprisingly, 2,4,6-trimethoxybenzamide (**SB-P17G-A41**) was active at <0.78 µg/mL, and was stable in human (27% metabolized) and mouse (47% metabolized) microsomes.

The major metabolite identified from the microsomal stability assay for all the 5-position benzamides was the result of hydrolysis at the 5-position. Therefore, several *o*-substituted benzamides were synthesized to increase the steric bulk at the 5-position to inhibit this hydrolysis. The 2,6-dichlorobenzamide unfortunately wasn't active against *Mtb* implying that the *o*-substituents can't be too bulky if we want to retain the antibacterial activity. **SB-P21G4** with *o*-fluoro substituent was active at 0.31 µg/mL and was reasonably stable in human (55%) and mouse (64%) microsomes. Therefore, 2,6-difluoro-4-methoxybenzamido, 2,3-difluoro-4-trifluoromethylbenzamido, 2-fluoro-4-trifluoromethylbenzamido, and 2-fluoro-4-trifluoromethoxybenzamido, at 5-position of the benzimidazole were synthesized. 4-Trifluoromethylbenzamide, was also synthesized for comparison with **SB-P17G-A20** (Table 2.6). All these new compounds were reasonably stable in the microsomal stability assay and potent against *Mtb*. The improved stability can be attributed to the hydrogen bonding between the ortho fluorine and the amide nitrogen. **SB-P17G-A33**, **A38** and **A42** have been advanced to the standard acute infection model using immune incompetent GKO mice.

Table 2.6. Antibacterial activity against *Mtb* H37Rv strain (MIC, $\mu\text{g/mL}$), their cytotoxicity (IC_{50} , $\mu\text{g/mL}$) and microsomal instability

| Compound | R ¹ | <i>Mtb</i> H37Rv MIC | Vero Cytotoxicity | Microsomal Metabolism* Human | Microsomal Metabolism* Mouse |
|-------------|----------------|-------------------------|----------------------|---------------------------------|---------------------------------|
| SB-P17G-A32 | | 0.16 | >100 | 25% | 44% |
| SB-P17G-A42 | | 0.16 | >100 | 12% | 13% |
| SB-P17G-A38 | | 0.16 | >100 | 13% | 4% |
| SB-P17G-A33 | | 0.62 | >100 | 5% | 17% |
| SB-P17G-A34 | | 1.56 | >100 | 23% | 46% |

*values indicate percentage of compound metabolized in the microsomes; MIC and cytotoxicity were determined at CSU; Microsomal metabolism were assessed at Sanofi-Aventis

2.2.3. Optimization of 2,5,6-trisubstituted benzimidazoles based on metabolite identification

2.2.3.1. Metabolites of SB-P3G2

As mentioned previously, **SB-P3G2**, the parent lead compound is readily metabolized in mouse/human microsomes, which demanded the identification of the metabolites formed via LC-MS/MS studies. Our collaborators at Sanofi-Aventis identified the hydrolysis of the carbamate to yield 5-amino-2-cyclohexyl-6-*N,N*-diethylaminobenzimidazole (**M5**) as the major culprit for instability and also observed de-ethylation of the 6-diethylamino group (**Figure 2.8**). Additionally, **M5** once formed, could cyclize to form **M2** as well. Efforts were directed towards the synthesis of the de-ethylated metabolite formed from **SB-P3G2** to ascertain if this molecule is active against *Mtb*.

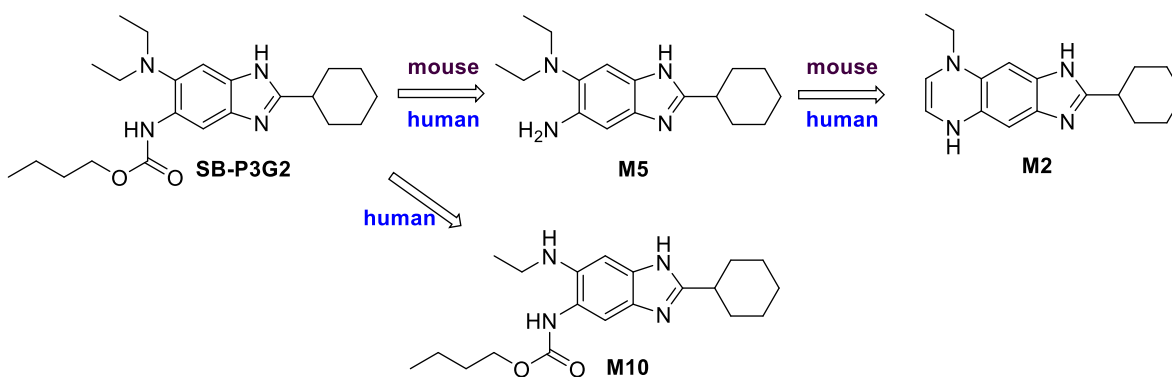
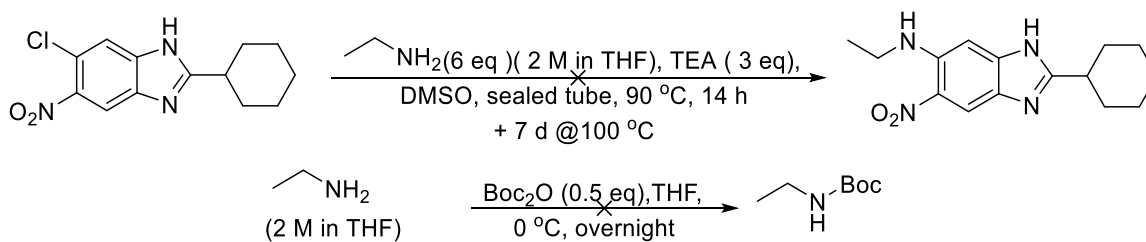
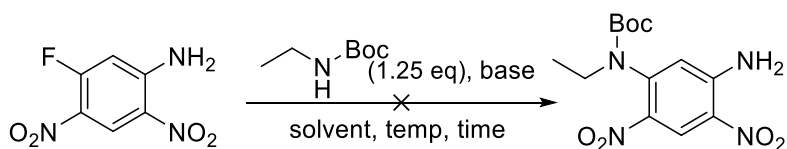


Figure 2.8. Metabolite formed in mouse/human microsomes

The previously synthesized 6-chloro-2-cyclohexyl-5-nitrobenzimidazole was treated with ethylamine under harsh conditions without any successful conversion to 2-cyclohexyl-6-ethylamino-5-nitrobenzimidazole (**Scheme 2.3**). Next, *tert*-butyloxycarbonyl protected ethylamine was synthesized and nucleophilic aromatic substitution of commercially available 2,4-dinitro-5-fluoroaniline under various conditions was attempted (**Table 2.7**). The reaction did not proceed due to the de-activating effect of the boc-group on nitrogen of the substituted ethylamine.



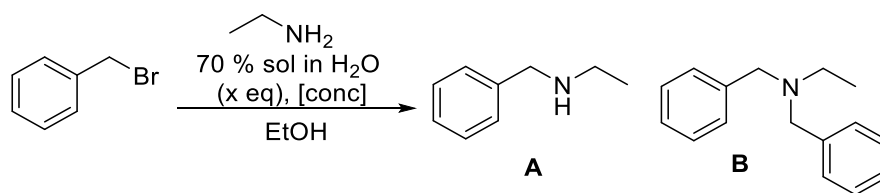
Scheme 2.3. Nucleophilic aromatic substitution of 6-chlorobenzimidazole

Table 2.7. Nucleophilic aromatic substitution of 2,4-dinitro-5-fluoroaniline

| Base | Solvent | Temp, Time | Result |
|---------------------------------------------|---------|------------------------|------------|
| DIPEA (1.25 eq) | THF | rt, 14 h 60 °C, 8 h | No product |
| Cs ₂ CO ₃ (2.2 eq) | DMF | rt, 14 h | No product |
| DIPEA (1.2 eq) | THF | 60 °C, 3h μW | No product |

Since *N*-benzyl-*N*-ethylamine will not be deactivated, literature procedure was followed to synthesize this molecule (**Table 2.8**). Several attempts to synthesize the mono-benzylated amine failed.⁴³ The dibenzylated product was always formed instead, and the reaction conditions could not be manipulated to obtain the mono-benzylated product. Diluting the reaction mixture as well as lowering the reaction temperature was ineffective. Dropwise addition of the reagent was also not advantageous.

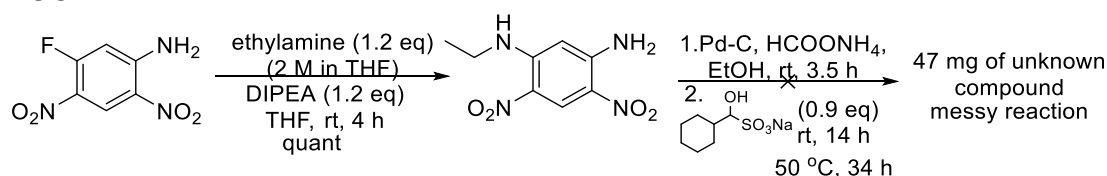
Table 2.8. Synthesis of *N*-Benzyl-*N*-ethylamine



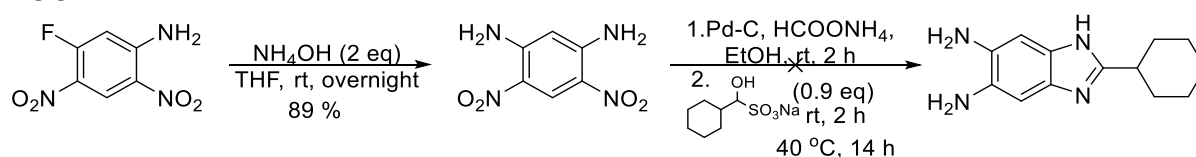
| Benzyl Bromide [conc] | Ethylamine 70 % sol in H₂O (x eq), [conc] | Temp | Result |
|------------------------------|-------------------------------------------------------------|-------------|---------------|
| [1.2] | 2 eq [2.4] | 0 °C - rt | B |
| [0.2] | 10 eq [4] | 0 °C - rt | B |
| [0.08] | 10 eq [2] | 0 °C - rt | B |

Alternatively, four different routes were employed to synthesize the metabolite. Route 1 involved conversion of 2,4-dinitro-5-fluoroaniline to 5-ethylamino-2,4-dinitroaniline followed by reduction of the two nitro groups to amino group and cyclization with the bisulfite salt of cyclohexanecarboxaldehyde. The final reaction was messy and the benzimidazole could not be isolated from the mixture. Route 2 started with substitution of 5-fluoro with 5-amino group using ammonium hydroxide solution. This was followed by reduction catalyzed by 10 wt.% Pd-C and ammoniumformate, and treatment with the bisulfite salt of cyclohexanecarboxaldehyde for cyclization to give the benzimidazole. The reaction was unsuccessful and led to the formation of an unidentified product. In route 3, 1,3-diamino-4,6-dinitrobenzene was treated with cyclohexanecarboxylic acid to form 1-(cyclohexanecarboxamido)-5-amino-2,4-dinitrobenzene. The crude product was subjected to stannous (II) chloride catalyzed reduction, and aqueous hydrochloric acid (HCl) catalyzed cyclization. Yet again, no product was obtained. Fortunately, route 4 successfully yielded 5-amino-2-cyclohexyl-6-(*N*-ethylamino)-1*H*-benzo[*d*]imidazole in 68% yield (**Scheme 2.4**).

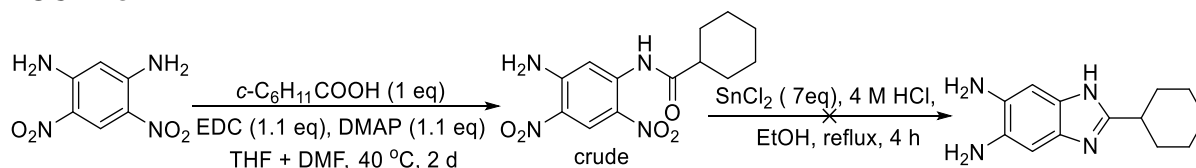
ROUTE 1



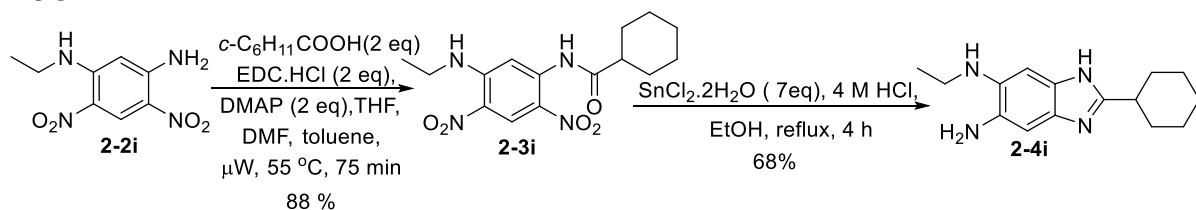
ROUTE 2



ROUTE 3

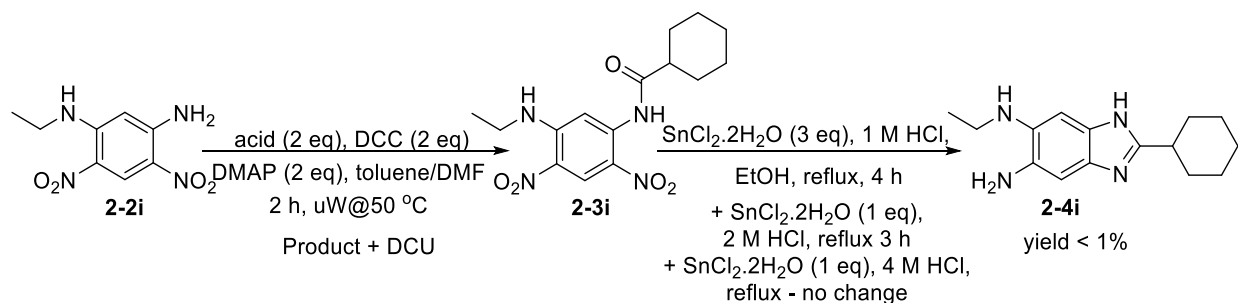


ROUTE 4



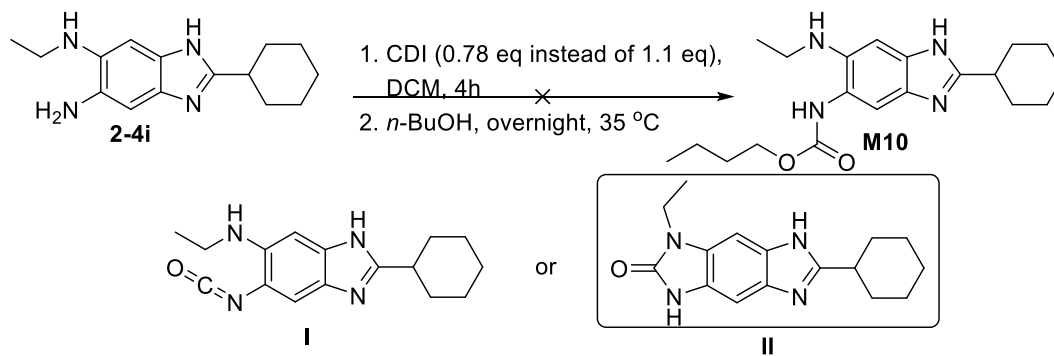
Scheme 2.4. Synthesis of 5-amino-2-cyclohexyl-6-N-ethylamino-1H-benzo[d]imidazole

The first step was treating 2,4-dinitro-5-fluoroaniline with ethylamine. The aromatic nucleophilic substitution proceeded smoothly, and was followed by EDC.HCl/DMAP coupling to form 1-cyclohexanecarboxamido-5-N-ethylamino-2,4-dinitrobenzene. This was subjected to reduction-cyclization to obtain the final intermediate 5-amino-2-cyclohexyl-6-N-ethylamino-1H-benzo[d]imidazole. The same procedure was tried with a change in step two, where DCC/DMAP was used instead of EDC.HCl/DMAP, but removal of DCU was challenging and this resulted in poor yield in the subsequent reduction-cyclization step (**Scheme 2.5**).



Scheme 2.5. Failed synthesis of 5-amino-2-cyclohexyl-6-N-ethylamino-1H-benzo[d]imidazole

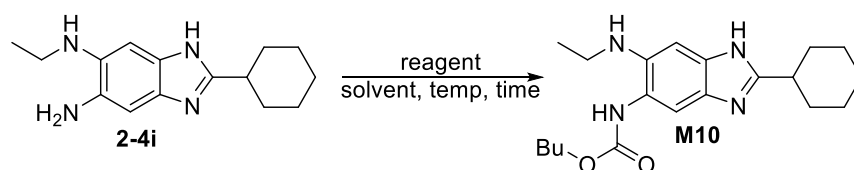
Synthesis of the carbamate was difficult (**Scheme 2.6**). The first step was conversion of 5-amino to isocyanate followed by addition of *n*-butanol to form the carbamate. The reaction did not proceed as expected and product **II** was formed by nucleophilic attack at the carbonyl group of the isocyanate by the 6-ethylamino group.

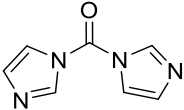
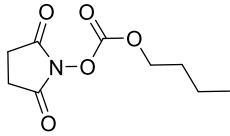


Scheme 2.6. Metabolite synthesis

In a second attempt, instead of dichloromethane, butanol was used as the solvent in the hope that once the isocyanate is formed, the alcohol attacks the electrophilic carbonyl before the intramolecular amine attack. Even this reaction did not yield the desired product and the TLC was very messy. Finally, the intermediate was treated with *N*-hydroxysuccinimide ester of butyl chloroformate but this reaction showed 6 spots on TLC (**Table 2.9**).

Table 2.9. Synthesis of metabolite M10



| Reagent | Solvent | Time | Temp | Result |
|-----------------------------------------------------------------------------------------------|-------------------|------|-----------|-----------|
|  (1.1 eq) | <i>n</i> -butanol | 14 h | 35 °C | Messy TLC |
|  (0.9 eq) | DCM | 14 h | 0 °C - rt | Messy TLC |

The synthesis of the de-ethylated metabolite (**M10**) has been unsuccessful so far, and is not being pursued any further.

2.2.3.2. Metabolite identification of lead 5-position benzamido compounds

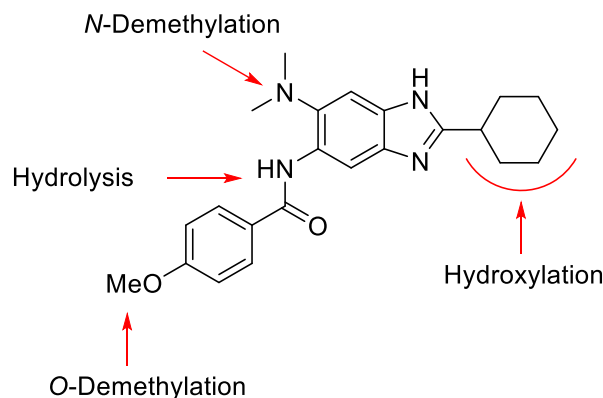
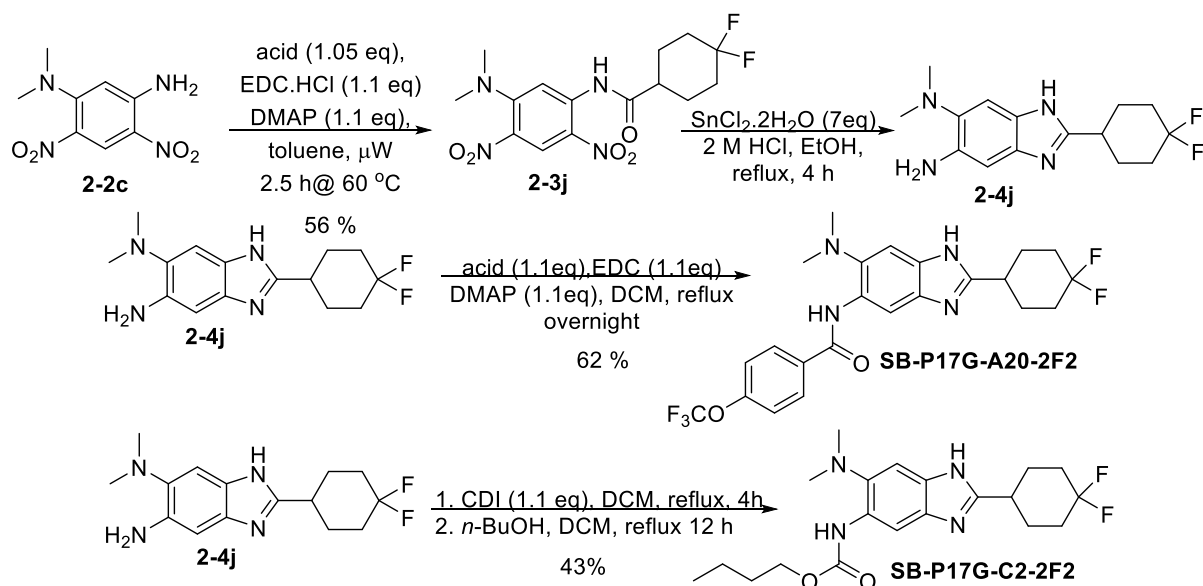


Figure 2.9. Metabolite identification of SB-P17G-A16

Metabolic stability studies performed by our collaborators at Sanofi-Aventis on **SB-P17G-A16** and **SB-P17G-A20** in human and mouse microsomes confirmed that some amount of hydroxylation of the 2-position cyclohexyl group is observed (**Figure 2.9**). 4,4-Difluorocyclohexyl analogue of **SB-P17G-A20** was therefore synthesized. Since 4,4-difluorocyclohexane-1-carbonyl chloride isn't commercially available, the corresponding acid

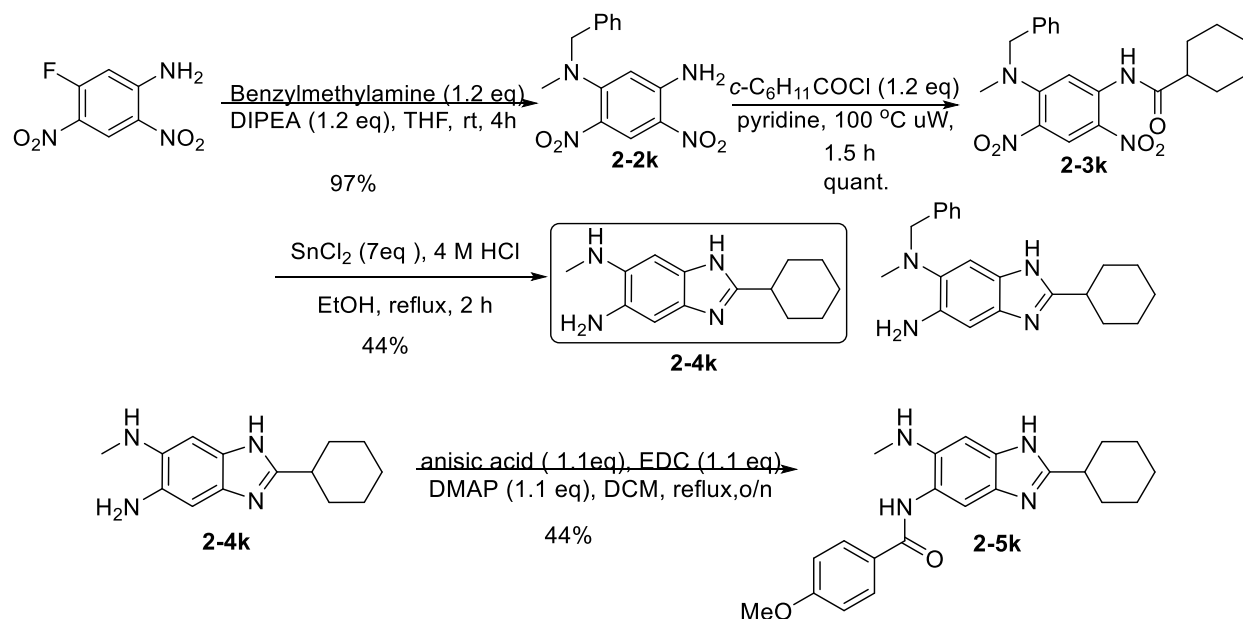
was used. 2,4-Dinitro-5-*N,N*-dimethylaminoaniline is very deactivated due to the electron withdrawing nitro groups therefore, microwave reactor was employed for the coupling reaction followed by reduction and cyclization in the presence of stannous chloride dihydrate to yield the benzimidazole. The 5-position amine was coupled with 4-trifluoromethoxybenzoic acid to yield the difluorocyclohexyl analogue of **SB-P17G-A20** (**Scheme 2.7**). This molecule was active with MIC value of 1.25 $\mu\text{g/mL}$ and was surprisingly very stable in the microsomal stability assay; 9% metabolism in human microsomes, 0% hydrolysis in mouse microsome. Since carbamates at 5 position are more potent than benzamides, the 4,4-difluorocyclohexyl analogue of **SB-P17G-C2** was also synthesized to test the stability while maintaining the activity of the compound. Although this molecule retained antibacterial activity (0.63 $\mu\text{g/mL}$), it was rapidly metabolized in human (80%)/mouse (94%) microsomes.



Scheme 2.7. Synthesis of 2-(4,4-difluorocyclohexyl) analogues

De-methylation of the 6-position dimethylamino group was also identified as one of the metabolites of **SB-P17G-A16** and **SB-P17G-A20**. Efforts were directed towards synthesizing this molecule (**Scheme 2.8**). Commercially available 2,4-dinitro-5-fluoroaniline was treated with benzylmethylamine to obtain 5-(*N*-benzyl-*N*-methylamino)-2,4-dinitroaniline which was acylated with cyclohexanecarbonyl chloride. In the presence of stannous chloride and aqueous hydrochloric acid, reduction of the two nitro groups and cyclization to obtain the benzimidazole proceeded to yield 5-amino-2-cyclohexyl-6-*N*-methylamino-1*H*-benzo[*d*]imidazole instead of 5-

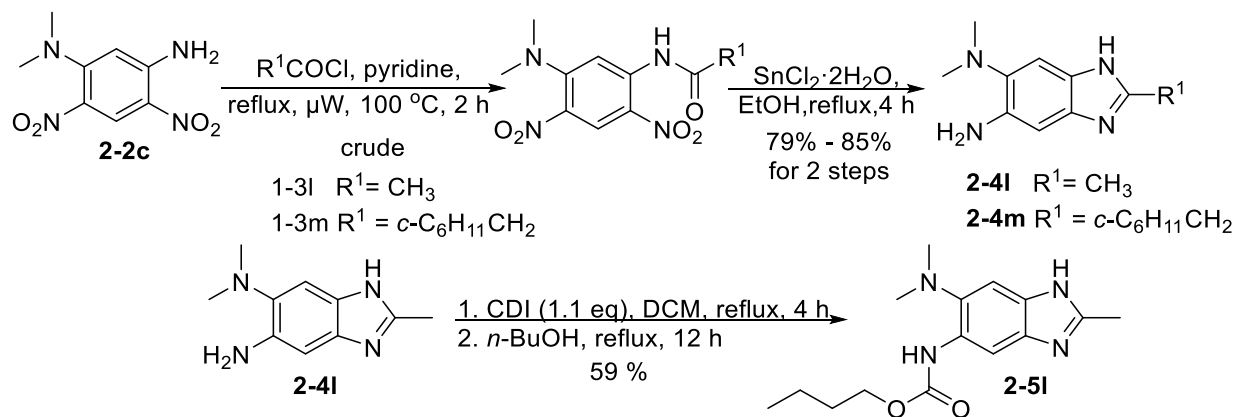
amino-2-cyclohexyl-6-(*N*-benzyl-*N*-methylamino)-1*H*-benzo[*d*]imidazole. Unfortunately, the benzyl group was removed in this step. The reaction of this intermediate with anisic acid yielded the 6-monomethylamino analogue of **SB-P17G-A16** in poor yield. The accurate MIC and stability of this compound have not been evaluated yet.



Scheme 2.8. Synthesis of 2-cyclohexyl-5-(4-methoxybenzamido)-6-*N*-methylamino-1*H*-benzo[*d*]imidazole

2.2.4. Significance of 2-cyclohexyl group

So far, 6-dimethylamino benzimidazole analogues with cyclohexyl group at 2-position have been synthesized and tested for antitubercular activity. To ascertain the importance of this group, 2-methyl analogue of **SB-P17G-C2** was synthesized (**Scheme 2.9**). Based on MIC determination, 2-methyl substituted analogue of **SB-P17G-C2** (MIC = 25 $\mu\text{g/mL}$) was not potent, confirming that the cyclohexyl group at 2-position is essential for activity.

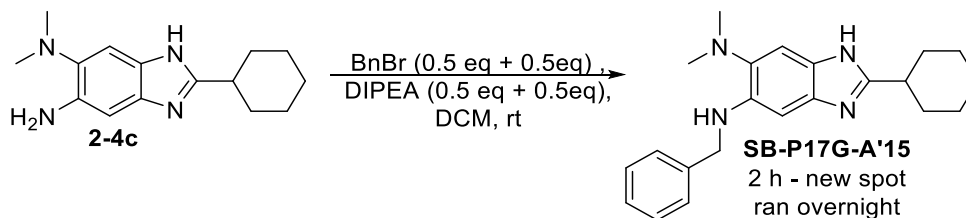


Scheme 2.9. Synthesis of 2-modified 6-dimethylamino-1H-benzo[d]imidazole

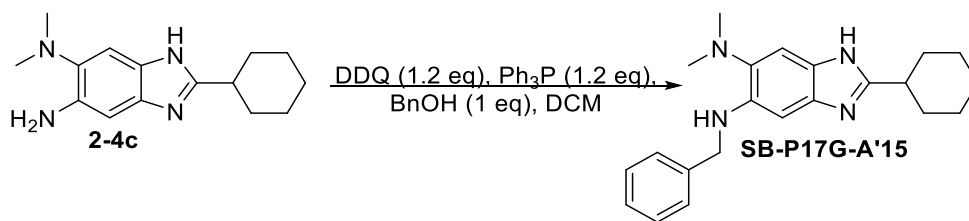
The 2-(cyclohexylmethyl) substituted 6-dimethylamino-1H-benzo[d]imidazole was also synthesized and will be used to synthesize analogues of **SB-P17G-A20** and other lead compounds.

2.2.5. Synthesis of substituted 5-position benzylamino group

As described previously, although the 5-position benzamides are more stable than the carbamates *in vivo*, there is still scope for improvement. To discover stable 5-position analogues, attempts were made to synthesize amines as shown below. To synthesize 5-benzylamino-2-cyclohexyl-6-dimethylamino-1H-benzo[d]imidazole, the 5-amino intermediate was treated with benzyl bromide but after two flash columns very little pure product was obtained. Mostly disubstitution was observed. Procedure published by Iranpoor *et al.* was also tried but no product was observed.⁴⁴ As shown in **Table 2.10**, running the reaction for longer time or at higher temperature didn't help.



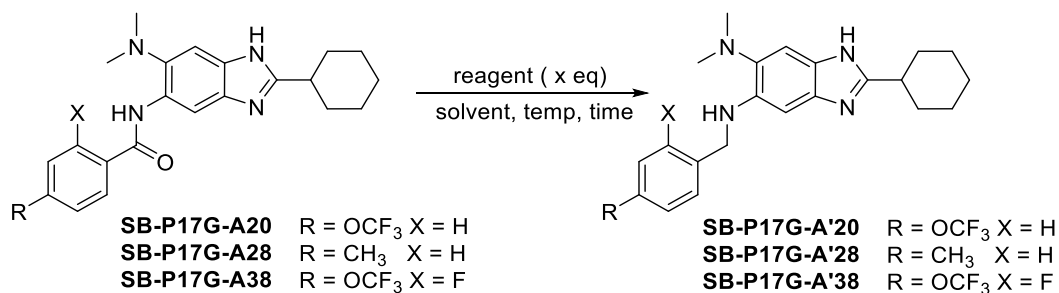
Scheme 2.10. Synthesis of 5-position N-benzylamino group

Table 2.10. Reaction condition optimization

| Time | Temp | Reaction |
|--------|--------|------------------|
| 2 mins | rt | No product |
| 3 h | rt | No product |
| 24 h | reflux | V little product |

Furthermore, attempts were also made to synthesize the 5-position amines via reduction of the amide group using borane. Reduction with a solution of borane in tetrahydrofuran was very slow and required 36 h, after which product was obtained following column chromatography, but the yield was low and purification was problematic. A solution of borane stabilized with dimethyl sulfide in toluene was also tried, but in this case no product formation was observed at room temperature after 4 h (**Table 2.11**). Under reflux conditions product formation was observed, but complete removal of borane was difficult. Most likely, boron formed a complex with the nitrogens in the molecule and therefore broad peaks were observed in NMR. Alternatively, the reaction with BH₃.THF was re-tried in a sealed tube, without any success. Surprisingly, the reaction progressed under reflux conditions, but harsh conditions were required to remove any complexed boron. Stirring the reaction mixture in 1 M sodium hydroxide followed by further treatment with excess DABCO succeeded in affording the product, although in poor yield. When **SB-P17G-A38** was used, the reaction was refluxed for 16 h, and for workup the reaction was quenched with saturated solution of NaHCO₃ and treated with excess DABCO under reflux condition for 16 h. This successfully removed the complexed borane and the product was obtained in 75% yield.

Table 2.11. Optimization of 5-benzamido reduction

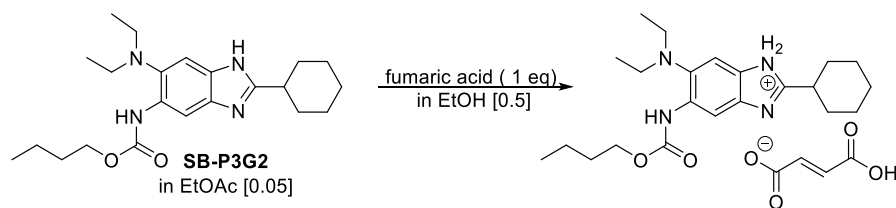


| SM | Reagent | Solvent | Temp | Time | Workup | Result |
|-------------|------------------------------------------------------------|---------------|--------------------------|------|------------------------------------------------------------|---------------------------------|
| SB-P17G-A20 | BH ₃ .THF (1 M) 10 eq | THF | rt | 36 h | quenched with NaHCO ₃ | Dirty product, Poor yield |
| SB-P17G-A20 | BH ₃ .SMe ₂ (2 M in toluene) 1 eq | toluene | reflux | 4 h | quenched with NaHCO ₃ | No product |
| SB-P17G-A20 | BH ₃ .SMe ₂ (2 M in toluene) 1 eq | toluene | reflux | 16 h | reflux with NaHCO ₃ for 3 h | little product |
| SB-P17G-A20 | BH ₃ .THF (1 M) (excess) | no solvent | rt sealed tube | 72 h | quenched with piperidine | SM |
| SB-P17G-A28 | BH ₃ .THF (1 M) (excess) | no solvent | 66 °C, sealed tube | 12 h | quenched with 1 M NaOH | SM |
| SB-P17G-A28 | BH ₃ .THF (1 M) (excess) | no solvent | 66 °C, reflux | 24 h | quenched with 1 M NaOH, stirred with DABCO | Product, poor yield |
| SB-P17G-A38 | BH ₃ .THF (1 M) (excess) | no solvent | 66 °C, reflux | 16 h | quenched with 1 M NaOH +excess DABCO. Reflux 16 h | Product, 75% yield |

So far only **5-N-benzylamino-2-cyclohexyl-6-N,N-dimethylamino-1H-benzo[d]imidazole (SB-P17G-A'15)** has been tested against *Mtb* H37Rv and was found to be active at an MIC value of 0.78 µg/mL.

2.2.6. Salt formation of SB-P3G2 and SB-P17G-A38

Formulation studies on our lead compound **SB-P3G2** has shown that it has poor solubility and crashes out in PBS. Therefore, efforts were made to improve the solubility by making salt of **SB-P3G2**. All attempts made towards synthesis of the succinic acid salt of **SB-P3G2** and **SB-P8B2** were unsuccessful. Fumaric acid salt could be successfully synthesized. **SB-P3G2** was dissolved in minimum amount of cold ethyl acetate and a solution of fumaric acid in ethanol or methanol was added to it. Since no precipitation was observed on addition of diethyl ether, the solvent was removed on the rotary evaporator and hot ethyl acetate plus few drops of ethanol were added to re-dissolve everything. On cooling the desired salt precipitated out. The salt was characterized by ^1H NMR. Even though the salt wasn't soluble in ethanol:PBS (1:1) at a concentration of 40 mg/mL, in solutol:ethanol (1:1) at the same concentration, the solution could withstand 6 times dilution with PBS. Similarly, the fumaric acid salt of **SB-P17G-A38** was prepared.



2.2.7. New trisubstituted benzimidazoles with unknown MIC

In addition to the extensive library of compounds discussed above to identify potent antitubercular compounds, **Table 2.12** summaries the more recently synthesized compounds which have not been evaluated yet.

Table 2.12. New trisubstituted benzimidazoles to be evaluated against *Mtb* H37Rv

| Compound | R ¹ R ² N | R ³ |
|-------------|---------------------------------|----------------|
| SB-P6C-A50 | | |
| SB-P17G-A50 | | |
| SB-P17G-A47 | | |
| SB-P17G-A51 | | |
| SB-P17G-A52 | | |
| SB-P17G-A53 | | |

2.3. Conclusion

Building on our early lead compounds **SB-P3G2** and **SB-P8B2**, extensive SAR study on 2-cyclohexyl-5,6-disubstituted benzimidazoles for their antibacterial activities against *Mtb* H37Rv strain was performed. It has been observed that the nature of the 6-amino group exerts remarkable effects on the antibacterial activity. Specifically, a small dimethylamino group at the 6-position dramatically increases the potency. SAR study has led us to the discovery of **SB-P17G-C2** with exceptional potency (MIC 0.06 $\mu\text{g}/\text{mL}$), which bears a butoxycarbonylamino group at the 5 position and a dimethylamino group at the 6 position. Due to poor metabolic stability in human/mice liver microsomes, **SB-P17G-C2** is not active in the murine model of TB infection. A series of 5-benzamido compounds based on **SB-P17G-C2** have been found to be potent against *Mtb* while exhibiting reasonable stability in human/mice microsome. **SB-P17G-A38**, which is the current lead, has been moved forward for an extensive preclinical evaluation of its pharmacological properties, and has been evaluated for its *in vivo* efficacy (discussed in **Chapter 3**).

Further optimization studies to identify more potent compounds with improved stability is currently underway in our laboratory. In this vein, compounds discussed in **Table 2.12** will be evaluated against *Mtb*. Of particular interest is **SB-P17G-A52** since the influence of two trifluoromethyl groups on the 5 position benzamide has not been evaluated yet. Although the compound is expected to be lipophilic because of the fluorines, the metabolic stability is predicted to improve. The substituted 5-benzylamino compounds, **SB-P17G-A'15**, **SB-P17G-A'20**, **SB-P17G-A'28**, and **SB-P17G-A'38**, are also of interest since metabolism due to hydrolysis of the 5 position amide will not be observed. **SB-P17G-A'15** was active at an MIC value of 0.78 $\mu\text{g/mL}$ and therefore the other analogues as well are likely to be potent against *Mtb*.

2.4. Experimental Section

Methods. ^1H and ^{13}C NMR spectra were measured on a Bruker or Varian 300, 400 or 500 MHz NMR spectrometer. Melting points were measured on a Thomas Hoover Capillary melting point apparatus and are uncorrected. TLC was performed on silica coated aluminum sheets (thickness 200 μm) or alumina coated (thickness 200 μm) aluminum sheets supplied by Sorbent Technologies and column chromatography was carried out on Siliaflash® P60 silica gel, 40-63 μm (230-400 mesh) supplied by Silicycle. Aluminum oxide, activated, neutral, Brockmann Grade I, 58 Å, was supplied by Alfa Aesar. High-resolution mass spectra were obtained from the Mass Spectrometry Laboratory, University of Illinois at Urbana-Champaign, Urbana, IL. Purity of synthesized compounds was determined by a Shimadzu LC-2010A HT series HPLC assembly or Agilent 1100 series HPLC assembly. Four analytical conditions were used and noted as a part of the characterization data for synthesized compounds. HPLC (1): Adsorbosphere Silica 5 μ , 250 \times 4.6 mm column, isopropanol and hexanes, flow rate of 1 mL/min, t = 0-40 min, gradient of 5-50% isopropanol. HPLC (2): Adsorbosphere Silica 5 μ , 250 \times 4.6 mm column, isopropanol and hexanes, flow rate of 1.0 mL/min, t = 0-20 min, gradient of 5-50% isopropanol. HPLC (3): Kinetex PFP, 2.6 μm , 4.6 mm \times 100 mm column, methanol and water, flow rate of 0.3 mL/min, t = 0-30 min, gradient of 40-95% MeOH. HPLC (4): Kinetex PFP, 2.6 μm , 4.6 mm \times 100 mm column, solvent A of water/acetonitrile 95:5 (25 mM ammonium acetate, pH 6.5), solvent B of water/acetonitrile, 5:95 (25mM ammonium acetate, pH

6.5), temperature of 25 °C, flow rate of 1.0 mL/min, t = 0-15 min, gradient of 20-95% solvent B. Measurements were made at 254 nm and 303 nm.

Materials. Solvents (HPLC grade or better), and all the other chemicals were purchased from Fisher Scientific Co. (Pittsburgh, PA). The chemicals were purchased from Aldrich Co., Synquest Inc. and Sigma. Tetrahydrofuran (THF) was freshly distilled from sodium metal and benzophenone. Dichloromethane was also distilled immediately prior to use under nitrogen from calcium hydride.

Synthesis of 2,5,6-trisubstituted benzimidazole library

Synthesis of 5-*N,N*-dimethylamino-2,4-dinitroaniline (2-2c): To a solution of 2,4-dinitro-5-fluoroaniline (2 g, 9.95 mmol) and DIPEA (2.01 mL, 11.94 mmol) in THF (30 mL) was added a solution of 2 M dimethylamine in methanol (5.97 mL, 11.94 mmol), dissolved in THF (30 mL), dropwise. The mixture was stirred at room temperature for 4 h. The reaction mixture was diluted with dichloromethane, washed with water three times and dried over anhydrous magnesium sulfate. The solvent was evaporated to afford 5-*N,N*-dimethylamino-2,4-dinitroaniline as a yellow solid; mp 164-165 °C (2.22 g, quant. yield): ¹H NMR (300 MHz, CDCl₃) δ 2.94 (br. s, 6 H), 6.01 (br. s, 1 H), 6.41 (br. s, 2H), 8.8 (br. s, 1 H); ¹³C NMR (101 MHz, CDCl₃) δ 42.5 100.7, 123.6, 128.8, 130.5, 147.9, 150.7; HRMS (ESI) *m/z* calcd for C₈H₁₀N₄O₄ H⁺: 227.0775, Found: 227.0778 (Δ = 1.4 ppm).

Same procedure was used for the synthesis of **2-(2a-h)**.

5-Morpholino-2,4-dinitroaniline (2-2a): Yellow solid (93% yield); mp 194-195 °C; ¹H NMR (400 MHz, acetone-d₆) δ 3.11 (t, 4 H, *J* = 4.8 Hz), 3.77 (t, 4 H, *J* = 4.8 Hz), 6.60 (s, 1 H), 7.54 (br. s, 2 H), 8.78 (s, 1 H); ¹³C NMR (101 MHz, acetone-d₆) δ 52.04, 66.93, 105.5, 125.2, 128.7, 131.9, 150.3, 151.9; MS (ESI) *m/z* 260 (M+1)⁺.

2,4-Dinitro-5-(pyrrolidin-1-yl)aniline (2-2b): Yellow solid (quantitative yield); mp 169-171 °C; ¹H NMR (500 MHz, CDCl₃) δ 2.0 (m, 4 H), 3.27 (m, 4 H), 5.91 (s, 1 H), 6.30 (br. s, NH), 8.71 (s, 1 H); ¹³C NMR (125 MHz, CDCl₃) δ 25.63, 50.96, 98.26, 122.8, 127.9, 130.1, 146.7, 147.2. MS (ESI) *m/z* 255.1 (M+1)⁺.

2,4-Dinitro-5-(piperidin-1-yl)aniline (2-2d): Yellow solid (98% yield); mp 115-116 °C; ¹H NMR (400 MHz, acetone-d₆) δ 1.64 (m, 6 H), 3.08 (t, 4 H, *J* = 4.8 Hz), 6.51 (s, 1 H), 7.43 (br. s, 2 H), 8.69 (s, 1 H); ¹³C NMR (101 MHz, acetone-d₆) δ 24.64, 26.27, 52.72, 104.81, 124.6, 128.5, 131.9, 150.2, 152.2; MS (ESI) *m/z* 267.1 (M+1)⁺.

3-(*N',N'*-Dimethyl-*N*-ethylethylenediamino)-4,6-dinitroaniline (2-2e): Yellow solid (88% yield); mp 83-85 °C; ¹H NMR (400 MHz, acetone-d₆) δ 1.18 (t, 3 H, *J* = 7.0 Hz), 2.16 (s, 6 H), 2.48 (t, 2 H, *J* = 7.2 Hz), 3.29 (m, 4 H), 6.56 (s, 1 H), 7.41 (br. s, 2 H), 8.60 (s, 1 H); ¹³C NMR (101 MHz, acetone-d₆) δ 12.67, 45.93, 47.45, 50.54, 57.33, 104.5, 124.0, 128.2, 132.4, 149.8, 150.3; MS (ESI) *m/z* 298.1 (M+1)⁺.

3-(*N',N',N*-Trimethylethylenediamino)-4,6-dinitroaniline (2-2f): Yellow solid (93% yield); mp 134-135 °C; ¹H NMR (400 MHz, acetone-d₆) δ 2.16 (s, 6 H), 2.55 (t, 2 H, *J* = 6.4 Hz), 2.93 (s, 3 H), 3.28 (t, 2 H, *J* = 6.9 Hz), 6.48 (s, 1 H), 7.37 (br. s, 2 H), 8.62 (s, 1 H); ¹³C NMR (101 MHz, acetone-d₆) δ 40.17, 45.89, 53.17, 57.13, 102.7, 123.9, 128.5, 131.5, 149.7, 151.1; MS (ESI) *m/z* 284.1 (M+1)⁺.

3-(*N',N',N*-Triethylethylenediamino)-4,6-dinitroaniline (2-2g): Brown oil (99% yield); ¹H NMR (300 MHz, CDCl₃) δ 0.99 (t, 6 H, *J* = 7.2 Hz), 1.20 (t, 3 H, *J* = 7.2 Hz), 2.50 (q, 4 H, *J* = 7.2 Hz), 2.60 (t, 2 H, *J* = 7.5 Hz), 3.25 (m, 4 H), 6.17 (s, 1 H), 6.37 (br. s, 2 H), 8.75 (s, 1 H). ¹³C NMR (101 MHz, acetone-d₆) δ 12.54, 12.74, 47.51, 48.05, 51.20, 51.40, 104.6, 124.1, 128.2, 132.5, 149.7, 150.3; Mass (ESI) *m/z* 326.2 (M+1)⁺.

5-(4-Methylpiperazin-1-yl)-2,4-dinitroaniline (2-2h): Yellow solid (98% yield); mp 148-150 °C; ¹H NMR (400 MHz, acetone-d₆) δ 2.26 (s, 3 H), 2.50 (t, 4 H, *J* = 4.8 Hz), 3.11 (t, 4 H, *J* = 4.8 Hz), 6.56 (s, 1 H), 7.50 (br. s, 2 H), 8.79 (s, 1 H); ¹³C NMR (101 MHz, acetone-d₆) δ 46.28, 51.55, 55.25, 105.4, 124.9, 128.6, 132.0, 150.2, 151.8; MS (ESI) *m/z* 282.1 (M+1)⁺.

Synthesis of 1-cyclohexanecarboxamido-5-*N,N*-dimethylamino-2,4-dinitrobenzene (2-3c): A solution of 5-*N,N*-dimethylamino-2,4-dinitroaniline (2.22 g, 9.8 mmol) and cyclohexanecarbonyl chloride (1.5 mL, 10.78 mmol) in pyridine (12 mL) was refluxed overnight. The reaction mixture was concentrated on a rotary evaporator to obtain a yellow residue. The residue was washed with methanol to obtain the product 1-cyclohexanecarboxamido-5-(*N,N*-dimethylamino)-2,4-dinitrobenzene as yellow solid (2.96 g,

90% yield); mp 148-149 °C; ¹H NMR (300 MHz, CDCl₃) δ 1.21-1.43 (m, 3 H), 1.67-1.79 (m, 1 H), 1.80-1.94 (m, 2 H), 1.97-2.09 (m, 2 H), 2.32-2.45 (m, 1 H), 3.06 (s, 6 H), 8.60 (s, 1 H), 8.85 (s, 1 H), 11.00 (s, 1 H); ¹³C NMR (101 MHz, CDCl₃) δ 25.5, 25.6, 29.4, 42.5, 47.3, 106.1, 125.0, 127.4, 131.3, 138.7, 150.1, 175.9; HRMS (ESI) *m/z* calcd for C₁₅H₂₀N₄O₅H⁺: 337.1507, Found: 337.1511 (Δ = 1.3 ppm).

Same procedure was used for the synthesis of **2-(3a-h)**.

1-Cyclohexanecarboxamido-2,4-dinitro-5-*N*-morpholinobenzene (2-3a): Yellow solid (93% yield); mp 160-161 °C; ¹H NMR (300 MHz, CDCl₃) δ 1.23-1.54 (m, 4 H), 1.74 (m, 2 H), 1.84-2.04 (m, 4 H), 2.37 (m, 1 H), 3.28 (t, 4 H, *J* = 4.5 Hz), 3.85 (t, 4 H, *J* = 4.5 Hz), 8.64 (s, 1 H), 8.87 (s, 1 H); ¹³C NMR (101 MHz, CDCl₃) δ 25.43, 28.76, 29.36, 47.28, 50.97, 66.09, 108.7, 126.6, 127.1, 132.9, 139.5, 150.4, 176.0; MS (ESI) *m/z* 379.2 (M+1)⁺.

1-Cyclohexanecarboxamido-2,4-dinitro-5-(pyrrolidin-1-yl)benzene (2-3b): Yellow solid (83 % yield); mp 181-182 °C; ¹H NMR (500 MHz, CDCl₃) δ 1.6-1.3 (m, 7 H), 1.73 (m, 1 H), 1.87 (m, 2 H), 2.02 (m, 6 H), 2.37 (m, 1 H), 3.37 (m, 4 H), 8.46 (s, 1 H), 8.71 (s, 1 H), 10.95 (s, 1 H); ¹³C NMR (125 MHz, CDCl₃) δ 25.43, 25.46, 25.52, 29.33, 47.21, 51.26, 104.8, 124.2, 126.8, 130.8, 138.2, 146.5, 175.8. MS (ESI) *m/z* 363.1 (M+1)⁺.

1-Cyclohexanecarboxamido-2,4-dinitro-5-(piperidin-1-yl)benzene (2-3d): Yellow solid (96% yield); mp 154-155 °C; ¹H NMR (400 MHz, CDCl₃) δ 1.30 (m, 3 H), 1.47 (m, 2 H), 1.69 (m, 7 H), 1.82 (m, 2 H), 2.00 (m, 2 H), 2.38 (m, 1 H), 3.22 (t, 4 H, *J* = 4.2 Hz), 8.57 (s, 1 H), 8.77 (s, 1 H), 10.96 (s, 1 H); ¹³C NMR (101 MHz, CDCl₃) δ 25.52, 25.24, 25.36, 29.26, 47.15, 51.88, 108.3, 125.5, 127.2, 132.4, 139.1, 150.5, 175.80; MS (ESI) *m/z* 377.1 (M+1)⁺.

1-Cyclohexanecarboxamido-2,4-dinitro-5-*N,N'*-dimethyl-*N*-ethylethylenediaminobenzene (2-3e): Yellow solid (50% yield); mp 212-213 °C; ¹H NMR (400 MHz, CDCl₃) δ 1.23 (t, 3 H, *J* = 7.2 Hz), 1.35 (m, 2 H), 1.51 (m, 2 H), 1.68 (m, 1 H), 1.82 (m, 2 H), 1.98 (m, 2 H), 2.22 (s, 6 H), 2.36 (m, 1 H), 2.54 (t, 2 H, *J* = 7.2 Hz), 3.40 (m, 4 H), 8.64 (s, 1 H), 8.73 (s, 1 H), 10.93 (s, 1 H); ¹³C NMR (101 MHz, CDCl₃) δ 12.35, 25.47, 25.53, 29.38, 45.52, 47.32, 50.05, 56.09, 108.0, 125.2, 126.9, 132.9, 138.7, 149.2, 175.8; MS (ESI) *m/z* 408.3 (M+1)⁺.

1-Cyclohexanecarboxamido-2,4-dinitro-5-*N',N',N'*-trimethylethylenediaminobenzene (2-3f):

Yellow solid (83% yield); mp 160-161 °C; ¹H NMR (300 MHz, CDCl₃) δ 1.19-1.33 (m, 3 H), 1.47 (m, 2 H, *J* = 12.4 Hz), 1.67 (m, 1 H), 1.82 (m, 2 H), 1.97 (m, 2 H), 2.22 (s, 6 H), 2.37 (m, 1 H), 2.67 (t, 2 H, *J* = 6.8 Hz), 2.96 (s, 3 H), 3.5 (t, 2 H, *J* = 6.8 Hz), 8.58 (s, 1 H), 8.71 (s, 1 H), 10.90 (s, 1 H); ¹³C NMR (101 MHz, CDCl₃) δ 25.39, 25.47, 29.29, 40.52, 45.5, 47.22, 52.48, 55.79, 106.6, 124.9, 127.1, 131.7, 138.6, 149.7, 175.6; MS (ESI) *m/z* 394.2 (M+1)⁺.

1-Cyclohexanecarboxamido-2,4-dinitro-5-*N,N',N'*-triethylethylenediaminobenzene (2-3g):

Yellow oil (94% yield); ¹H NMR (400 MHz, CDCl₃) δ 1.01 (t, 6 H, *J* = 7.2 Hz), 1.24 (t, 3 H, *J* = 7.2 Hz), 1.37-1.72 (m, 5 H), 1.99 (m, 2 H), 2.35 (m, 1 H), 2.61 (q, 4 H, *J* = 6.8 Hz), 2.74 (t, 2 H, *J* = 7.6 Hz), 3.38 (q, 2 H, *J* = 6.8 Hz), 3.45 (t, 2 H, *J* = 6.8 Hz), 8.62 (s, 1 H), 8.71 (s, 1 H), 10.93 (s, 1 H); ¹³C NMR (101 MHz, CDCl₃) δ 10.72, 12.25, 25.52, 25.86, 29.3, 43.86, 46.6, 47.28, 47.56, 49.35, 49.58, 107.9, 125.3, 126.9, 132.9, 138.7, 149.1, 175.7, 180.6; MS (ESI) *m/z* 436.2 (M+1)⁺.

1-Cyclohexanecarboxamido-5-(4-methylpiperazin-1-yl)-2,4-dinitrobenzene (2-3h):

Yellow solid (74% yield); mp 90-92 °C; ¹H NMR (400 MHz, CDCl₃) δ 1.23-1.39 (m, 3 H), 1.50 (m, 2 H, *J* = 12.4 Hz), 1.70 (d, 1 H, *J* = 12 Hz), 1.83 (m, 2 H, *J* = 12 Hz), 2.04 (m, 2 H, *J* = 12 Hz), 2.37 (m, 4 H), 2.58 (t, 4 H, *J* = 4.5 Hz), 3.33 (t, 4 H, *J* = 4.5 Hz), 8.62 (s, 1 H), 8.85 (s, 1 H), 10.91 (s, 1 H); ¹³C NMR (101 MHz, CDCl₃) δ 25.44, 29.36, 45.76, 47.28, 50.52, 54.15, 108.7, 126.2, 127.2, 132.8, 139.4, 150.2, 175.9. MS (ESI) *m/z* 392.1 (M+1)⁺.

Synthesis of 5-amino-2-cyclohexyl-6-*N,N*-dimethylamino-1*H*-benzo[*d*]imidazole (2-4c): To a solution of 1-cyclohexanecarboxamido-5-*N,N*-dimethylamino-2,4-dinitrobenzene (2.96 g, 8.8 mmol) in ethanol (100 mL) was added solid stannous chloride dihydrate (11.64 g, 61.6 mmol). Concentrated hydrochloric acid (50 mL) was added to the reaction mixture such that the final concentration of HCl was 4 M in the reaction flask. The reaction mixture was refluxed for 4 h. Upon completion, the reaction mixture was basified with 30% sodium hydroxide solution. Excess stannous chloride formed a soluble salt in excess base. The desired product was extracted with dichloromethane and purified by flash chromatography on alumina using ethyl acetate as eluent to afford the product as a light brown solid (1.56 g, 69% yield); mp 135-137 °C: ¹H NMR (300 MHz, CDCl₃) δ 1.14-1.46 (m, 4 H), 1.54-1.86 (m, 5 H), 1.99-2.17 (m, 2 H), 2.64 (s, 6 H), 2.73-2.87 (m, 1 H), 6.81 (s, 5 H), 7.26 (s, 1 H); ¹³C NMR (101 MHz, CDCl₃) δ 26.0, 26.2, 32.2,

38.8, 44.8, 98.9, 106.7, 133.1, 134.5, 138.0, 138.3, 158.2; HRMS (ESI) m/z calcd for $C_{15}H_{22}N_4H^+$: 259.1917, Found: 259.1914 ($\Delta = -1.2$ ppm).

Same procedure was used for the synthesis of **2-(4a-h)**.

5-Amino-2-cyclohexyl-6-(morpholino)-1H-benzo[d]imidazole (2-4a): Brown solid (79% yield); mp 124-125 °C; 1H NMR (400 MHz, $CDCl_3$) δ 1.23-1.39 (m, 4 H), 1.59-1.84 (m, 5 H), 2.10 (m, 2 H), 2.82 (m, 1 H), 2.89 (t, 4 H, $J = 4.5$ Hz), 3.85 (t, 4 H, $J = 4.5$ Hz), 6.83 (s, 1 H), 7.26 (s, 1 H), 10.94 (s, 1 H); ^{13}C NMR (101 MHz, $CDCl_3$) δ 25.80, 29.58, 31.78, 38.30, 45.63, 52.33, 67.66, 98.19, 107.4, 136.3, 138.1, 157.3; HRMS (FAB) m/z calcd for $C_{17}H_{24}N_4OH^+$: 301.2028, Found: 301.2022 ($\Delta = -2.0$ ppm).

5-Amino-2-cyclohexyl-6-(pyrrolidin-1-yl)-1H-benzo[d]imidazole (2-4b): Off white solid (50% yield); mp 138-140 °C; 1H NMR (300 MHz, $CDCl_3$) δ 1.29-1.12 (m, 3 H), 1.5-1.79 (m, 5 H), 1.85 (broad s, 4 H), 2.07 (m, 2 H), 2.81 (m, 1 H), 2.97 (q, 4 H, $J = 5.4$ Hz), 6.80 (s, 1 H), 7.23 (s, 1 H); ^{13}C NMR (101 MHz, $CDCl_3$) δ 23.97, 25.78, 26.01, 31.94, 38.48, 51.92, 98.81, 106.1, 132.9, 133.8, 134.78, 138.28, 157.53, HRMS (FAB) m/z calcd for $C_{17}H_{24}N_4H^+$: 285.2072, Found: 285.2079 ($\Delta = -2.5$ ppm).

5-Amino-2-cyclohexyl-6-(piperidinyl)-1H-benzo[d]imidazole (2-4d): Pale brown solid (82% yield); mp >200 °C; 1H NMR (400 MHz, $CDCl_3$) δ 1.24 (m, 4 H), 1.65 (m, 8 H), 1.77 (m, 2 H), 2.07 (m, 2 H), 2.84 (broad m, 5 H), 6.89 (s, 1 H), 7.22 (s, 1 H); ^{13}C NMR (101 MHz, $CDCl_3$) δ 24.15, 25.72, 26.01, 26.89, 32.00, 38.58, 53.58, 98.57, 107.0, 132.8, 134.3, 137.8, 138.0, 157.97; HRMS (FAB) m/z calcd for $C_{18}H_{26}N_4H^+$: 299.2236, Found: 299.2229 ($\Delta = -2.3$ ppm).

5-Amino-2-cyclohexyl-6-(*N,N'*-dimethyl-*N*-ethylethylenediamino)-1H-benzo[d]imidazole (2-4e): Pale brown solid (74% yield); mp turned black at 120 °C; 1H NMR (400 MHz, $CDCl_3$) δ 0.89 (t, 3 H, $J = 7.2$ Hz), 1.12-1.29 (m, 3 H), 1.56-1.74 (m, 5 H), 2.01 (m, 2 H), 2.12 (s, 6 H), 2.28 (t, 2 H, $J = 6.8$ Hz), 2.73 (m, 1 H), 2.84 (q, 2 H, $J = 6.8$ Hz), 2.97 (t, 2 H, $J = 6.8$ Hz), 6.72 (s, 1 H), 7.23 (s, 1 H); ^{13}C NMR (101 MHz, $CDCl_3$) δ 12.48, 25.68, 25.95, 31.85, 38.50, 45.54, 49.91, 52.99, 57.43, 63.38, 98.01, 110.3, 133.5, 133.9, 134.6, 140.4, 158.1; HRMS (FAB) m/z calcd for $C_{19}H_{31}N_5H^+$: 330.2658, Found: 330.2649 ($\Delta = -2.7$ ppm).

5-Amino-2-cyclohexyl-6-(*N',N',N*-trimethylethylenediamino)-1*H*-benzo[*d*]imidazole (2-4f):

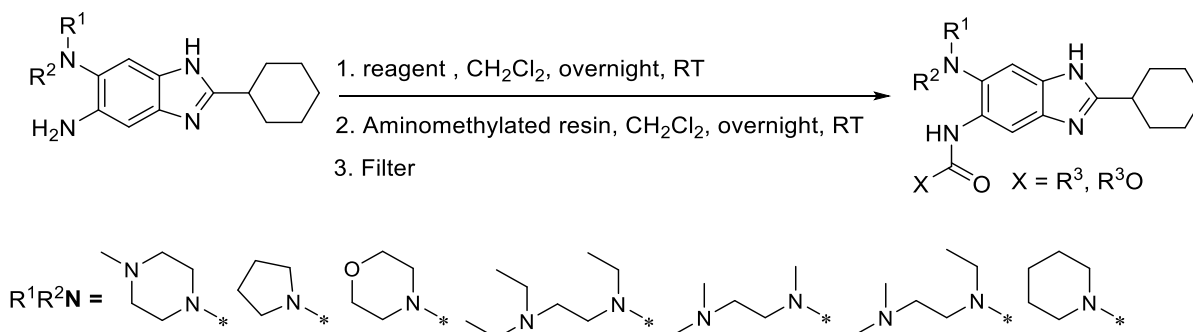
Pale brown solid (59% yield); mp: turned black at 120 °C; ¹H NMR (400 MHz, CDCl₃) δ 1.25 (m, 3 H), 1.60-1.76 (m, 5 H), 2.04 (m, 2 H), 2.24 (s, 6 H), 2.42 (t, 2 H, *J* = 6.4 Hz), 2.59 (s, 3 H), 2.80 (m, 1 H), 2.92 (t, 2 H, *J* = 6.4 Hz), 6.75 (s, 1 H), 7.22 (s, 1 H); ¹³C NMR (101 MHz, CDCl₃) δ 25.71, 25.97, 31.89, 38.42, 42.96, 45.45, 54.74, 57.36, 98.20, 108.3, 132.6, 134.2, 136.7, 139.1, 157.8; HRMS (FAB) *m/z* calcd for C₁₈H₂₉N₅H⁺: 316.2501, Found: 316.2498 (Δ = -0.9 ppm).

5-Amino-2-cyclohexyl-6-(*N',N',N*-triethylethylenediamino)-1*H*-benzo[*d*]imidazole (2-4g):

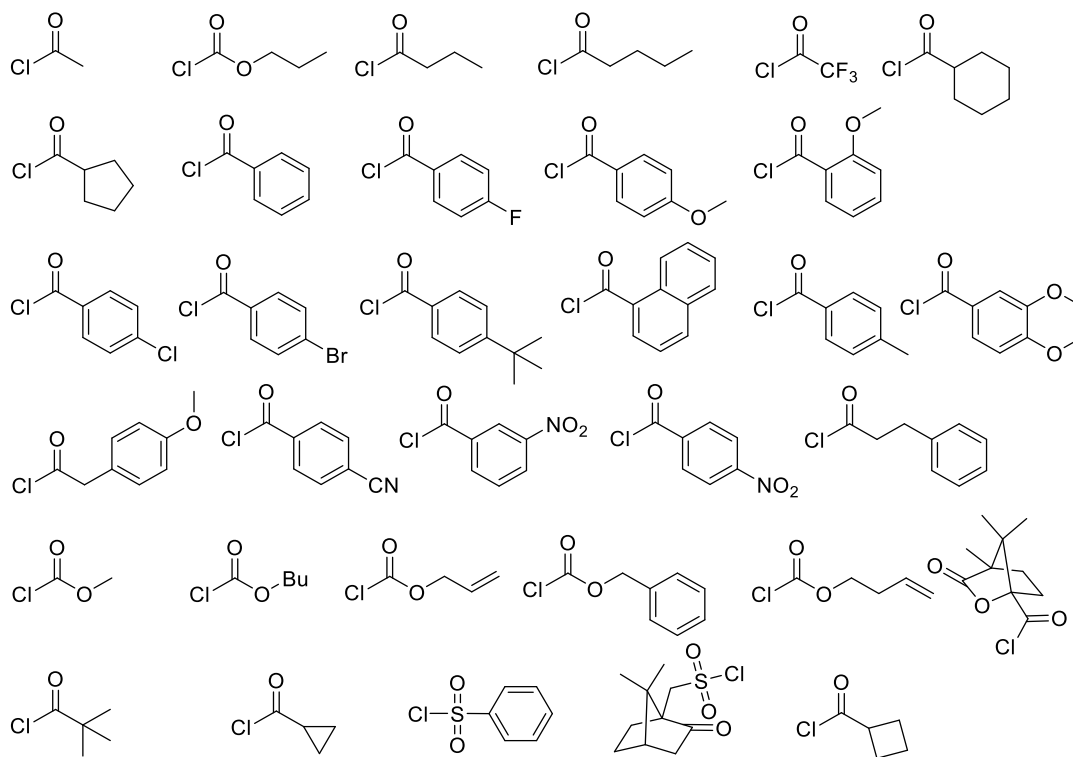
Pale brown solid (81% yield); mp turned black at 120 °C; ¹H NMR (300 MHz, CDCl₃) δ 0.95 (t, 9 H, *J* = 7.2 Hz), 1.20-1.35 (m, 5 H), 1.59-1.81 (m, 6 H), 2.05 (m, 2 H), 2.42 (m, 6 H), 2.79 (m, 1 H), 2.90 (m, 2 H, *J* = 6.9 Hz), 2.98 (t, 2 H, *J* = 6.9 Hz), 6.78 (s, 1 H), 7.27 (s, 1 H); ¹³C NMR (101 MHz, CDCl₃) δ 11.28, 12.33, 25.43, 25.51, 25.81, 31.75, 38.38, 46.94, 49.08, 51.01, 52.98, 98.05, 109.8, 133.0, 133.9, 140.1, 158.0; HRMS (FAB) *m/z* calcd for C₂₁H₃₅N₅H⁺: 358.2971, Found: 358.2975 (Δ = 1.1 ppm).

5-Amino-2-cyclohexyl-6-(4-methylpiperazinyl)-1*H*-benzo[*d*]imidazole (2-4h):

Brown solid (82% yield); mp 143-145 °C; ¹H NMR (400 MHz, CDCl₃) δ 1.25 (m, 3 H), 1.61 (m, 3 H), 1.75 (m, 2 H), 2.02 (m, 2 H), 2.31 (s, 3 H), 2.50 (br. m, 4 H), 2.78 (m, 1 H), 2.86 (br. s, 4 H), 6.74 (s, 1 H), 7.16 (s, 1 H); ¹³C NMR (101 MHz, CDCl₃) δ 25.70, 25.95, 30.50, 31.87, 38.47, 46.01, 51.78, 55.85, 98.89, 106.9, 132.5, 134.7, 136.4, 137.7, 158.0; HRMS (FAB) *m/z* calcd for C₁₈H₂₇N₅H⁺: 314.2345, Found: 314.2348 (Δ = 1.0 ppm).

Re-Synthesis of the library of 2,5,6-trisubstituted benzimidazoles (Plate 6,7, 8)

List of reagents

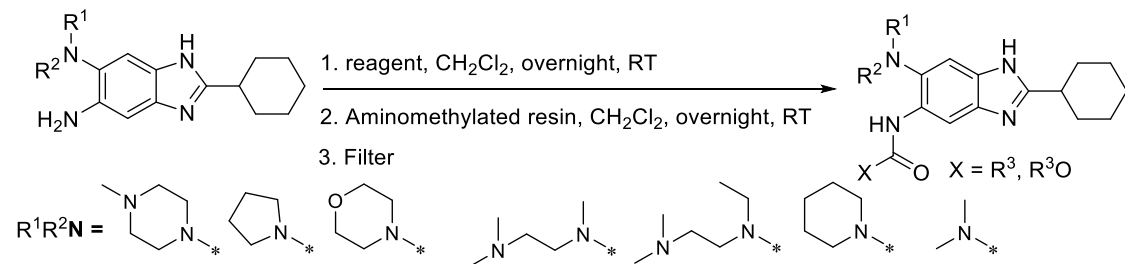


The intermediates **2-4a**, **2-4b**, **2-4d~2-4h** (0.01 mmol), thus synthesized, were dissolved in dichloromethane and transferred into 96 well plates, and to these wells were added 33 different acyl chlorides/sulfonyl chlorides (1.1 eq.) or alkyl chloroformates (1 eq) and reacted overnight on a shaker. Acyl chlorides/sulfonyl chlorides and alkyl chloroformates used for the library synthesis are shown in Figure S1. Aminomethylated polystyrene resin EHL (200-400 mesh), 2 % DVB (10 eq) was added to scavenge excess or unreacted acyl chlorides or alkyl chloroformates. After reacting on a shaker overnight, the resin was filtered to provide the library of 2,5,6-trisubstituted benzimidazoles. The library of compounds was dissolved in dichloromethane and divide into two such that each well now had half the concentration of final compound (equivalent to 0.05 mmol of starting material).

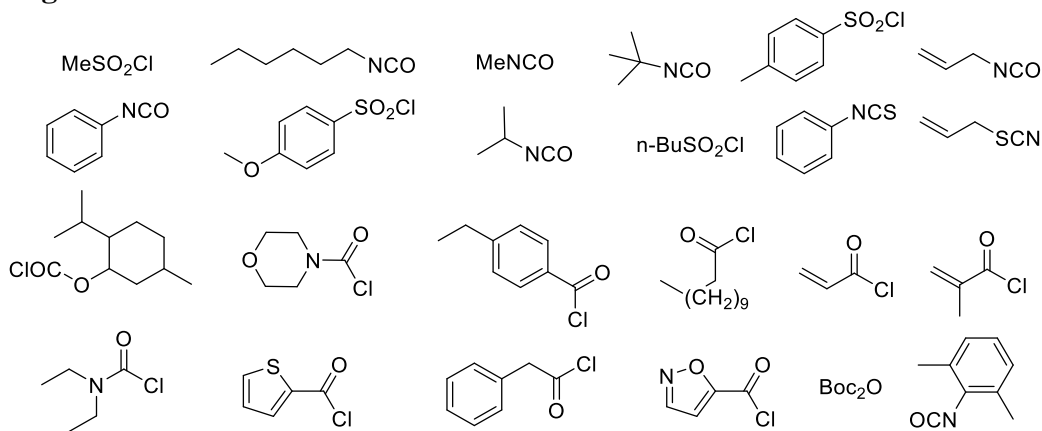
Same procedure was used to synthesize the libraries described below.

Synthesis of the library of 2,5,6-trisubstituted benzimidazoles (Plates 17, 18, 21)

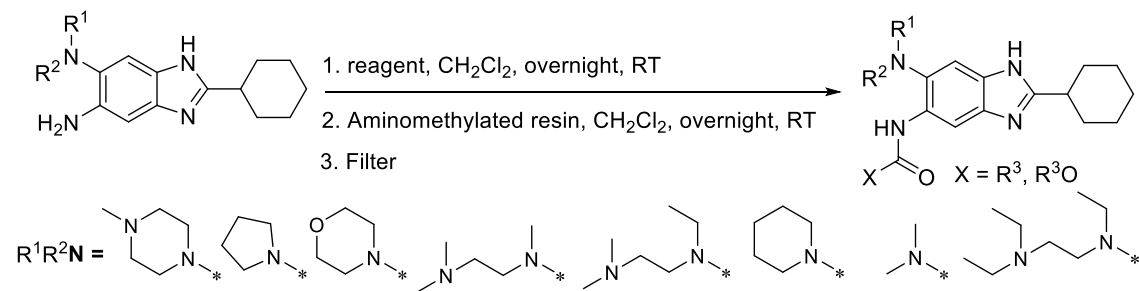
Intermediates and reagents used for Plate 17 and 18



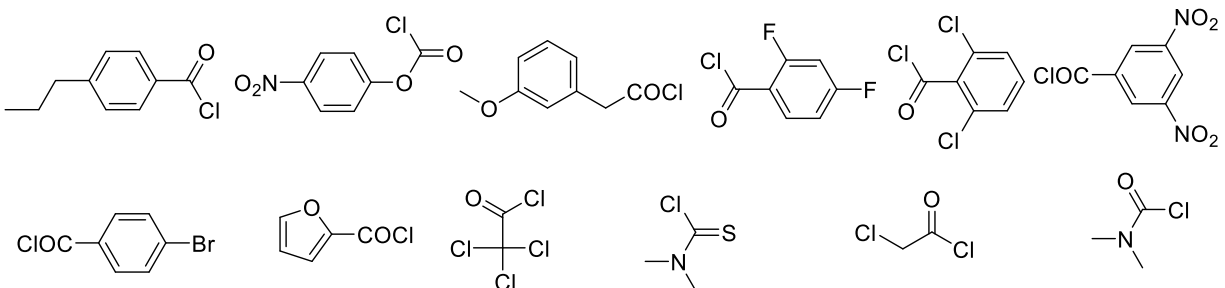
List of reagents



Intermediates and reagents used for Plate 21



List of reagents



Synthesis of 2,5,6-trisubstituted benzimidazoles with 5-position carbamate

5-Butyloxycarbonylamino-2-cyclohexyl-6-*N,N*-dimethylamino-1*H*-benzo[*d*]imidazole (SB-P17G-C2): A solution of **2-4c** (100 mg, 0.39 mmol) and 1,1'-carbonyldiimidazole (69 mg, 0.43 mmol) in dichloromethane (2 mL) was stirred under reflux conditions for 4 hours. After all the starting material had disappeared, *n*-butanol (71 μ L, 0.77 mmol) was added and the reaction was refluxed for additional 12 hours. After the completion of the reaction, the reaction mixture was concentrated. The crude was purified by flash chromatography on silica gel (gradient: 30-70% ethyl acetate /hexanes) to give **SB-P17G-C2** as a white solid (111 mg, 79% yield); mp 182-183 °C; ¹H NMR (300 MHz, CDCl₃) δ 0.97 (t, *J* = 7.28 Hz, 3 H), 1.23-1.51 (m, 6 H), 1.55-1.78 (m, 5 H), 1.79-1.91 (m, 2 H), 2.10 (d, *J* = 12.91 Hz, 2 H), 2.64 (s, 6 H), 2.76-2.92 (m, 1 H), 4.20 (t, *J* = 6.73 Hz, 2 H), 7.55 (br. s, 1 H), 8.20 (br. s, 2 H), 9.20 (br. s, 1 H); ¹³C NMR (101 MHz, CDCl₃) δ 14.0, 19.3, 26.0, 26.2, 31.3, 32.0, 38.6, 45.8, 65.2, 100.9, 109.5, 129.8, 132.1, 136.6, 139.1, 154.4, 159.0; HRMS (FAB) *m/z* calcd for C₂₀H₃₀N₄O₂H⁺: 359.2442, Found: 359.2443 (Δ = 0.4 ppm); HPLC (1): *t* = 8.9 min, purity > 99%.

The same procedure was followed for the synthesis of **SB-P17G-C4**, **SB-P17G-C8** and **SB-P17G-C12**

5-Benzyloxycarbonylamino-2-cyclohexyl-6-*N,N*-dimethylamino-1*H*-benzo[*d*]imidazole (SB-P17G-C4): White solid (82% yield); mp 145-146 °C; ¹H NMR (300 MHz, CDCl₃) δ 1.15-1.40 (m, 3 H), 1.45-1.87 (m, 5 H), 2.03 (d, *J* = 11.73 Hz, 2 H), 2.60 (s, 6 H), 2.74-2.92 (m, 1 H), 5.23 (s, 2 H), 7.28-7.60 (m, 6 H), 8.14-8.42 (m, 2 H), 10.23 (br. s, 1 H); ¹³C NMR (126 MHz, CDCl₃) δ 21.8, 25.9, 26.1, 31.80, 31.84, 38.3, 38.3, 45.8, 67.1, 100.9, 109.5, 128.5, 128.8, 129.9, 131.6, 136.0, 136.4, 139.4, 153.9, 158.9, 175.9; HRMS (FAB) *m/z* calcd for C₂₃H₂₈N₄O₂H⁺: 393.2285, Found: 393.2290 (Δ = 1.3 ppm); HPLC (1): *t* = 9.0 min, purity > 99%.

2-Cyclohexyl-5-ethoxyethoxycarbonylamino-6-*N,N*-dimethylamino-1*H*-benzo[*d*]imidazole (SB-P17G-C8): White solid (86% yield); mp 158-159 °C; ¹H NMR (500 MHz, CDCl₃) δ 1.20-1.44 (m, 7 H), 1.62 (qd, *J* = 12.31, 3.05 Hz, 2 H), 1.72 (d, *J* = 12.82 Hz, 1 H), 1.83 (d, *J* = 13.12 Hz, 2 H), 2.09 (d, *J* = 12.51 Hz, 2 H), 2.61 (s, 6 H), 2.77-2.93 (m, 1 H), 3.58 (q, *J* = 5.00 Hz, 2 H), 3.71 (t, *J* = 5.00 Hz, 2 H), 4.36 (t, *J* = 5.00 Hz, 2 H), 7.51 (br. s, 1 H), 8.07-8.48 (m, 2 H),

9.40 (br. s, 1 H); ^{13}C NMR (126 MHz, CDCl_3) δ 15.3, 26.0, 26.2, 29.9, 32.0, 38.6, 45.9, 64.4, 66.9, 69.0, 99.5, 111.1, 129.7, 139.0, 154.0, 159.0; HRMS (FAB) m/z calcd for $\text{C}_{20}\text{H}_{30}\text{N}_4\text{O}_3\text{H}^+$: 375.2391, Found: 375.2410 ($\Delta = 5.1$ ppm); HPLC (1): $t = 12.7$ min, purity > 99%.

2-Cyclohexyl-5-trifluoroethoxycarbonylamino-6-*N,N*-dimethylamino-1*H*-

benzo[*d*]imidazole (SB-P17G-C12): White solid (70% yield); mp 190-191°C; ^1H NMR (400 MHz, CDCl_3) δ 1.05-1.43 (m, 4 H), 1.50-1.91 (m, 5 H), 1.96-2.21 (m, 2 H), 2.61 (s, 6 H), 2.83-2.89 (m, 1 H), 4.56 (q, $J = 8.53$ Hz, 2 H), 7.45 (s, 1 H), 8.19 (s, 1 H), 8.41 (s, 1 H); ^{13}C NMR (101 MHz, CDCl_3) δ 14.3, 22.8, 25.9, 26.2, 32.1, 38.8, 45.8, 60.4, 60.7, 61.1, 61.5, 101.8, 109.7, 119.2, 121.9, 124.7, 127.5, 128.6, 139.1, 151.8, 159.8; HRMS (FAB) m/z calcd for $\text{C}_{18}\text{H}_{23}\text{F}_3\text{N}_4\text{O}_2\text{H}^+$: 385.1846, Found: 385.1851 ($\Delta = 1.3$ ppm); HPLC (1): $t = 9.1$ min, purity > 99%.

Synthesis of 2,5,6-trisubstituted benzimidazoles with 5-position ureas

2-Cyclohexyl-5-(3-propylurea)-6-pyrrolidinyl-1*H*-benzo[*d*]imidazole (SB-P6B-U6):

To a solution of **2-4b** (100 mg, 0.35 mmol) in dichloromethane (DCM) (3 mL), was added *n*-propylisocyanate (32.9 mg, 0.39 mmol) and triethylamine (0.39 mmol). The reaction was refluxed for 14 h and then diluted with ethyl acetate, transferred to a separatory funnel and washed with water, saturated sodium bicarbonate solution, and brine. The organic layer was dried over magnesium sulfate and concentrated using rotary evaporator. The crude product was purified by flash chromatography (column was packed with DCM, 2% methanol was used steadily increasing to 5% methanol) to obtain the product as a white solid (80% yield); mp 231-232 °C; ^1H NMR (400 MHz, Methanol- d_4) δ 0.95 (t, $J = 7.2$ Hz, 3 H), 1.26-1.69 (m, 8 H), 1.75-1.78 (m, 1 H), 1.84-1.88 (m, 2 H), 1.92-2.11 (m, 6 H), 2.83 (m, 1 H), 3.04 (s, 4 H), 3.16 (t, $J = 7.03$ Hz, 2 H), 7.24 (s, 1 H), 7.92 (s, 1 H); ^{13}C NMR (126 MHz, Methanol- d_4) δ 11.9, 24.6, 25.5, 27.1, 27.4, 33.0, 40.0, 42.9, 53.9, 106.3, 107.1, 130.9, 134.5, 136.5, 139.2, 159.2, 160.5; HRMS (FAB) m/z calcd for $\text{C}_{21}\text{H}_{31}\text{N}_5\text{OH}^+$: 370.2601, Found: 370.2611 ($\Delta = 2.6$ ppm); HPLC (1): $t = 17.7$ min, purity > 99%.

Same procedure was followed for the synthesis of the other urea analogues

5-(4-Butylurea)-2-cyclohexyl-6-*N,N*-diethylamino-1*H*-benzo[*d*]imidazole (SB-P1G-U2):

White solid (70% yield); mp 197-198 °C; ^1H NMR (500 MHz, Methanol- d_4) δ 0.95-1.10 (m, 9

H), 1.36-1.66 (m, 7 H), 1.67-1.79 (m, 2 H), 1.80-1.90 (m, 1 H), 1.90-2.01 (m, 2 H), 2.14 (d, $J = 13.73$ Hz, 2 H), 2.93 (m, 1 H), 3.06 (quin, $J = 7.20$ Hz, 4 H), 3.29 (q, $J = 7.20$ Hz, 2 H), 7.42 (d, $J = 7.02$ Hz, 1 H), 8.27 (d, $J = 7.63$ Hz, 2 H); ^{13}C NMR (126 MHz, Methanol- d_4) δ 13.0, 13.01, 14.3, 21.3, 27.1, 27.4, 33.0, 33.5, 40.0, 40.7, 51.7, 103.2, 111.3, 135.3, 135.9, 136.2, 158.7, 160.7; HRMS (FAB) m/z calcd for $\text{C}_{22}\text{H}_{35}\text{N}_5\text{OH}^+$: 386.2914, Found: 386.2911 ($\Delta = -0.9$ ppm); HPLC (1): $t = 12.7$ min, purity > 99%.

5-(Benzylurea)-2-cyclohexyl-6-*N,N*-diethylamino-1*H*-benzo[*d*]imidazole (SB-P1G-U4):

White solid (94% yield); mp 198-199 °C; ^1H NMR (400 MHz, Methanol- d_4) δ 0.90 (t, $J = 7.15$ Hz, 6 H), 1.23-1.52 (m, 4 H), 1.57-1.70 (m, 2 H), 1.77 (d, $J = 14.31$ Hz, 1 H), 1.86 (d, $J = 13.05$ Hz, 2 H), 1.98-2.12 (m, 2 H), 2.84-2.87 (m, 1 H), 2.95 (q, $J = 7.00$ Hz, 4 H), 4.34-4.45 (m, 2 H), 7.19-7.26 (m, 1 H), 7.28-7.39 (m, 5 H), 8.22 (s, 1 H); ^{13}C NMR (101 MHz, Methanol- d_4) δ 13.0, 27.1, 27.3, 33.0, 40.0, 44.8, 51.6, 103.4, 111.3, 128.2, 128.4, 129.7, 135.1, 136.0, 136.3, 141.3, 158.5, 160.8; HRMS (FAB) m/z calcd for $\text{C}_{25}\text{H}_{33}\text{N}_5\text{OH}^+$: 420.2758, Found: 420.2761 ($\Delta = 0.7$ ppm); HPLC (1): $t = 13.4$ min, purity > 99%.

2-Cyclohexyl-6-*N,N*-diethylamino-5-(3-propylurea)-1*H*-benzo[*d*]imidazole (SB-P1G-U6):

White solid (87% yield); mp 216-217 °C; ^1H NMR (400 MHz, Methanol- d_4) δ 0.87-1.01 (m, 9 H), 1.23-1.50 (m, 4 H), 1.51-1.70 (m, 4 H), 1.71-1.79 (m, 1 H), 1.85 (dt, $J = 13.18, 3.33$ Hz, 2 H), 2.05 (d, $J = 13.40$ Hz, 2 H), 2.84-2.88 (m, 1 H), 2.96 (q, $J = 7.2$ Hz, 4 H), 3.16 (t, $J = 7.20$ Hz, 2 H), 7.33 (s, 1 H), 8.20 (s, 1 H); ^{13}C NMR (101 MHz, Methanol- d_4) δ 11.9, 13.0, 24.5, 27.1, 27.4, 33.0, 40.0, 42.8, 51.6, 103.2, 111.3, 135.3, 136.0, 136.2, 158.7, 160.7; HRMS (FAB) m/z calcd for $\text{C}_{21}\text{H}_{33}\text{N}_5\text{OH}^+$: 372.2758, Found: 372.2754 ($\Delta = -1.0$ ppm); HPLC (1): $t = 12.6$ min, purity > 99%.

5-(4-Butylurea)-2-cyclohexyl-6-pyrrolidinyl-1*H*-benzo[*d*]imidazole (SB-P6B-U2):

White solid (96% yield); mp 206-207 °C; ^1H NMR (400 MHz, Methanol- d_4) δ 0.95 (t, $J = 7.2$ Hz, 3 H), 1.26-1.55 (m, 7 H), 1.56-1.70 (m, 2 H), 1.71-1.82 (m, 1 H), 1.82-1.91 (m, 2 H), 1.91-2.11 (m, 6 H), 2.79-2.87 (m, 1 H), 3.03 (br. s, 4 H), 3.20 (t, $J = 7.2$ Hz, 2 H), 7.24 (s, 1 H), 7.94 (s, 1 H); ^{13}C NMR (101 MHz, Methanol- d_4) δ 14.3, 21.2, 27.12, 25.5, 27.3, 33.0, 33.5, 39.9, 40.8, 53.9, 106.3, 107.1, 131.0, 134.4, 136.4, 139.3, 159.2, 160.4; HRMS (FAB) m/z calcd for $\text{C}_{22}\text{H}_{33}\text{N}_5\text{OH}^+$: 384.2758, Found: 384.2755 ($\Delta = -0.8$ ppm); HPLC (1): $t = 14.2$ min, purity > 99%.

5-(4-Benzylurea)-2-cyclohexyl-6-pyrrolidinyl-1H-benzo[d]imidazole (SB-P6B-U4): White solid (91% yield); mp 225-226 °C; ¹H NMR (500 MHz, Methanol-d₄) δ 1.26-1.49 (m, 3 H), 1.56-1.68 (m, 2 H), 1.71-1.79 (m, 1 H), 1.80-1.89 (m, 2 H), 1.92 (br. s, 4 H), 1.98-2.10 (m, 2 H), 2.80-2.85 (m, 1 H), 3.01 (br. s, 4 H), 4.39 (s, 2 H), 7.18-7.26 (m, 2 H), 7.26-7.37 (m, 4 H), 7.96 (s, 1 H); ¹³C NMR (126 MHz, Methanol-d₄) δ 25.5, 27.1, 27.3, 33.0, 39.9, 44.8, 53.8, 106.2, 107.4, 128.2, 128.4, 129.7, 130.7, 134.4, 136.5, 139.4, 141.3, 159.1, 160.5; HRMS (FAB) *m/z* calcd for C₂₅H₃₁N₅OH⁺: 418.2601, Found: 418.2604 (Δ = 0.6 ppm); HPLC (1): t = 14.5 min, purity > 99%.

5-(4-Butylurea)-2-cyclohexyl-6-N,N-dimethylamino-1H-benzo[d]imidazole (SB-P17G-U2): White solid (74% yield); mp 185-186 °C; ¹H NMR (400 MHz, Methanol-d₄) δ 1.71 (t, *J* = 7.28 Hz, 3 H), 1.98-2.27 (m, 7 H), 2.30-2.44 (m, 2 H), 2.49 (d, *J* = 12.30 Hz, 1 H), 2.54-2.65 (m, 2 H), 2.73-2.85 (m, 2 H), 3.38 (s, 6 H), 3.57 (m, 1 H), 3.89 (q, *J* = 6.53 Hz, 2 H), 4.15 (br. s, 1 H), 7.80 (br. s, 1 H), 8.05 (br. s, 1 H), 8.83 (br. s, 1 H), 8.97 (s, 1 H), 12.54 (br. s, 1 H); ¹³C NMR (126 MHz, Methanol-d₄) δ 14.3, 21.2, 27.0, 27.3, 32.9, 33.5, 39.7, 40.7, 45.8, 104.3, 107.7, 132.3, 134.3, 135.0, 141.4, 158.8, 160.1; HRMS (FAB) *m/z* calcd for C₂₀H₃₁N₅OH⁺: 358.2601, Found: 358.2609 (Δ = 2.1 ppm); HPLC (1): t = 15.3 min, purity > 99%.

Synthesis of 2,5,6-trisubstituted benzimidazoles with 5-position benzamido group

The following compounds were synthesized using EDC/DMAP coupling reaction.

5-Benzamido-2-cyclohexyl-6-N,N-dimethylamino-1H-benzo[d]imidazole (SB-P17G-A15): To a solution of **2-4c** (70 mg, 0.27 mmol) in 2 mL of dichloromethane was added the hydrochloric acid salt of 1-ethyl-3-(3-dimethylaminopropyl) carbodiimide (57.5 mg, 0.3 mmol) (EDC) and benzoic acid (36.4 mg, 0.30 mmol). 4-Dimethylaminopyridine (DMAP) (36.4 mg, 0.30 mmol) was added to the above reaction mixture which was refluxed overnight. After completion of the reaction as per TLC, the reaction mixture was diluted with dichloromethane, transferred to a separatory funnel, and the organic layer was washed with water, sodium bicarbonate, and brine. The organic layer was dried over magnesium sulfate, filtered, and concentrated using rotary evaporator. The crude product was purified by flash chromatography (column was packed with hexane, 30% ethyl acetate was used with gradual increase to 50% ethyl acetate) to obtain the product as a white solid (83 mg, 85% yield); mp 158-159 °C; ¹H NMR

(300 MHz, CDCl₃) δ 1.07-1.19 (m, 3 H), 1.54-1.71 (m, 5 H), 1.97-2.03 (m, 2 H, $J = 12.9$ Hz), 2.74 (s, 6 H), 2.85 (m, 1 H), 7.58 (m, 3 H), 7.67 (s, 1 H), 7.95 (d, 1 H, $J = 6.6$ Hz), 8.91 (s, 1 H), 9.88 (s, 1 H); ¹³C NMR (126 MHz, CDCl₃) δ 25.9, 26.1, 29.9, 32.0, 38.6, 46.2, 101.8, 110.9, 127.2, 129.0, 129.2, 131.4, 132.0, 135.8, 139.4, 139.9, 160.1, 165.7; HRMS (FAB) m/z calcd for C₂₂H₂₆N₄OH⁺: 363.2179, Found: 363.2190 ($\Delta = 2.9$ ppm); HPLC (1): $t = 11.0$ min, purity > 99%.

5-Benzamido-2-cyclohexyl-6-pyrrolinyl-1H-benzo[d]imidazole (SB-P6B8): White solid (76% yield); mp 197-198 °C; ¹H NMR (500 MHz, CDCl₃) δ 1.04-1.35 (m, 4 H), 1.51-1.68 (m, 3 H), 1.74 (dt, $J = 13.20, 3.32$ Hz, 2 H), 1.92-2.11 (m, 6 H), 2.75 (m, 1 H), 3.07 (br. s, 4 H), 7.46-7.71 (m, 4 H), 7.95 (d, $J = 8.80$ Hz, 2 H), 8.86 (s, 1 H), 9.91 (br. s, 1 H), 10.45 (br. s, 1 H); ¹³C NMR (126 MHz, CDCl₃) δ 24.6, 25.9, 26.2, 32.0, 38.7, 54.2, 101.8, 111.1, 127.1, 129.2, 129.9, 131.9, 135.7, 136.0, 159.8, 165.3; HRMS (FAB) m/z calcd for C₂₄H₂₈N₄OH⁺: 389.2336, Found: 389.2349 ($\Delta = 3.4$ ppm); HPLC (1): $t = 8.1$ min, purity > 99%.

5-(4-Bromobenzamido)-2-cyclohexyl-6-pyrrolidinyl-1H-benzo[d]imidazole (SB-P7B2): White solid (76% yield); mp 215-216 °C; ¹H NMR (500 MHz, DMSO-d₆) δ 1.19-1.45 (m, 3 H), 1.58 (qd, $J = 12.21$ Hz, 3.05 Hz, 2 H), 1.64-1.74 (m, 1 H), 1.79 (dt, $J = 12.89, 3.17$ Hz, 2 H), 1.88 (br. s, 4 H), 2.00 (d, $J = 10.68$ Hz, 2 H), 2.72-2.86 (m, 1 H), 3.06 (br. s, 4 H), 7.16 (br. s, 1 H), 7.68-7.86 (m, 3 H), 7.91 (d, $J = 8.24$ Hz, 2 H), 9.82 (s, 4 H), 11.90 (br. s, 1 H); ¹³C NMR (101 MHz, DMSO-d₆ at 55 °C) δ 24.1, 25.2, 25.4, 31.0, 37.5, 51.9, 124.9, 125.8, 128.9, 131.4, 134.0, 138.3, 158.6, 163.4; HRMS (FAB) m/z calcd for C₂₄H₂₇BrN₄OH⁺: 467.1441, Found: 467.1443 ($\Delta = 0.4$ ppm); HPLC (2): $t = 9.6$ min, purity > 98%.

2-Cyclohexyl-5-(4-trifluoromethoxybenzamido)-6-N,N-dimethylamino-1H-benzo[d]imidazole (SB-P17G-A20): White solid (70% yield); mp 210-211 °C; ¹H NMR (400 MHz, CDCl₃) δ 1.08-1.31 (m, 3 H), 1.53-1.70 (m, 3 H), 1.70-1.81 (m, 2 H), 1.99-2.09 (m, 2 H), 2.69-2.83 (m, 7 H), 7.35-7.42 (m, 2 H), 7.60 (s, 1 H), 7.97-8.04 (m, 2 H), 8.81 (s, 1 H), 9.90 (s, 1 H); ¹³C NMR (101 MHz, CDCl₃) δ 25.68, 25.93, 31.78, 38.47, 45.95, 119.08, 121.00, 121.01, 128.85, 128.91, 133.95, 139.43, 151.64, 159.68, 163.91; HRMS (FAB) m/z calcd for C₂₃H₂₅F₃N₄O₂H⁺: 447.2002, Found: 447.2007 ($\Delta = 1.0$ ppm); HPLC (1): $t = 10.3$ min, purity > 99%.

2-Cyclohexyl-5-(4-difluoromethoxybenzamido)-6-*N,N*-dimethylamino-1*H*-

benzo[*d*]imidazole (SB-P17G-A19): White solid (65% yield); mp 183-185 °C; ¹H NMR (500 MHz, CDCl₃) δ 1.06 - 1.24 (m, 3 H), 1.50 - 1.66 (m, 3 H), 1.71 (d, *J* = 12.82 Hz, 2 H), 2.00 (d, *J* = 12.21 Hz, 2 H), 2.50 - 2.94 (m, 7 H), 6.39 - 6.84 (m, 0 H), 7.28 (d, *J* = 8.54 Hz, 2 H), 7.59 (br. s, 1 H), 7.99 (d, *J* = 8.54 Hz, 2 H), 8.84 (s, 1 H), 9.90 (br. s, 1 H), 10.82 (br. s, 1 H); ¹³C NMR (126 MHz, CDCl₃) δ 14.3, 25.9, 26.1, 31.8, 32.0, 34.9, 38.7, 46.1, 101.8, 110.9, 113.5, 115.6, 117.7, 119.7, 128.9, 129.1, 132.7, 139.5, 153.8, 160.1, 164.4; HRMS (FAB) *m/z* calcd for C₂₃H₂₆F₂N₄O₂H⁺: 429.2097, Found: 429.2100 (Δ = 0.8 ppm); HPLC (1): *t* = 12.8 min, purity > 99%.

2-Cyclohexyl-5-(4-trifluoromethylthiobenzamido)-6-*N,N*-dimethylamino-1*H*-

benzo[*d*]imidazole (SB-P17G-A40): Brown solid (56% yield); mp 209-210 °C; ¹H NMR (300 MHz, CDCl₃) δ 0.98 - 1.29 (m, 3 H), 1.47 - 1.83 (m, 5 H), 2.01 (d, *J* = 11.73 Hz, 2 H), 2.74 (s, 7 H), 7.62 (br. s., 1 H), 7.85 (d, *J* = 7.82 Hz, 2 H), 8.02 (d, *J* = 8.20 Hz, 2 H), 8.87 (s, 1 H), 10.04 (br. s., 3 H), 11.00 (br. s, 1 H); ¹³C NMR (101 MHz, CDCl₃) δ 25.9, 26.1, 32.0, 38.7, 46.2, 101.6, 111.2, 128.1, 128.6, 128.9, 131.1, 131.3, 136.6, 137.9, 139.6, 160.0, 164.1; HRMS (FAB) *m/z* calcd for C₂₃H₂₅F₃N₄OSH⁺: 463.1774, Found: 463.1776 (Δ = 0.4 ppm).

2-Cyclohexyl-5-(3-trifluoromethoxybenzamido)-6-*N,N*-dimethylamino-1*H*-

benzo[*d*]imidazole (SB-P17G-A43): Yellow solid (77 % yield); mp 165-166 °C; ¹H NMR (400 MHz, CDCl₃) δ 1.04 - 1.21 (m, 3 H), 1.51 - 1.73 (m, 5 H), 1.99 (d, *J* = 11.80 Hz, 2 H), 2.63 - 2.81 (m, 7 H), 7.42 (d, *J* = 8.28 Hz, 1 H), 7.51 - 7.66 (m, 2 H), 7.78 - 7.92 (m, 2 H), 8.83 (s, 1 H), 9.96 (br. s., 1 H); ¹³C NMR (101 MHz, CDCl₃) δ 25.8, 26.0, 31.9, 38.7, 46.0, 102.3, 110.4, 119.3, 119.9, 121.9, 124.1, 125.0, 128.6, 130.6, 137.8, 139.5, 149.8, 149.9, 160.4, 163.8, 195.4; HRMS (FAB) *m/z* calcd for C₂₃H₂₅F₃N₄O₂H⁺: 447.2002, Found: 447.2000 (Δ = -0.4 ppm).

2-Cyclohexyl-6-*N,N*-dimethylamino-5-(4-methylbenzamido)-1*H*-benzo[*d*]imidazole (SB-

P17G-A28): White solid (76% yield); mp 179-180 °C; ¹H NMR (500 MHz, CDCl₃) δ 1.05-1.27 (m, 3 H), 1.50-1.77 (m, 5 H), 1.99 (d, *J* = 12.51 Hz, 2 H), 2.46 (s, 3 H), 2.66-2.78 (m, 7 H), 7.35 (d, *J* = 8.24 Hz, 2 H), 7.61 (s, 1 H), 7.87 (d, *J* = 8.24 Hz, 2 H), 8.89 (s, 1 H), 9.90 (s, 1 H), 10.65 (br. s, 1 H); ¹³C NMR (126 MHz, CDCl₃) δ 21.7, 25.9, 26.2, 32.0, 38.6, 46.1, 101.7, 110.9, 127.2, 129.2, 129.8, 131.3, 133.0, 139.4, 139.8, 142.5, 159.9, 165.7; HRMS (FAB) *m/z* calcd for

$C_{23}H_{28}N_4OH^+$: 377.2336, Found: 377.2349 ($\Delta = 3.5$ ppm); HPLC (1): $t = 10.6$ min, purity > 99%.

2-Cyclohexyl-5-(4-ethylbenzamido)-6-*N,N*-dimethylamino-1*H*-benzo[*d*]imidazole (SB-P20G3): White solid (72% yield); mp 177-178 °C; 1H NMR (400 MHz, $CDCl_3$) δ 1.03-1.23 (m, 3 H), 1.30 (t, $J = 7.65$ Hz, 3 H), 1.50-1.63 (m, 3 H), 1.68 (d, $J = 7.28$ Hz, 2 H), 1.97 (d, $J = 11.80$ Hz, 2 H), 2.60-2.87 (m, 9 H), 7.38 (d, $J = 8.03$ Hz, 2 H), 7.61 (br. s, 1 H), 7.90 (d, $J = 8.03$ Hz, 2 H), 8.93 (d, $J = 5.02$ Hz, 1 H), 9.93 (br. s, 3 H); ^{13}C NMR (101 MHz, $CDCl_3$) δ 15.6, 25.9, 26.1, 29.1, 32.0, 38.6, 46.1, 101.8, 110.8, 127.3, 128.7, 129.1, 129.2, 131.5, 133.3, 139.3, 139.8, 148.7, 160.0, 160.1, 165.8; HRMS (FAB) m/z calcd for $C_{24}H_{30}N_4OH^+$: 391.2492, Found: 391.2500 ($\Delta = 1.9$ ppm); HPLC (1): $t = 9.9$ min, purity > 99%.

5-(4-Bromobenzamido)-2-cyclohexyl-6-*N,N*-dimethylamino-1*H*-benzo[*d*]imidazole (SB-P21G7): Yellow solid (78% yield); mp 207-208 °C; 1H NMR (500 MHz, Methanol- d_4) δ 0.80-1.02 (m, 1 H), 1.16-2.21 (m, 13 H), 2.54-3.00 (m, 7 H), 7.44 (s, 1 H), 7.60-7.98 (m, 4 H), 8.46 (s, 1 H); ^{13}C NMR (126 MHz, Methanol- d_4) δ 27.1, 27.3, 31.9, 33.0, 40.0, 46.1, 65.6, 106.9, 108.2, 127.6, 129.9, 130.0, 133.4, 135.5, 142.3, 161.6, 166.2; HRMS (FAB) m/z calcd for $C_{22}H_{25}BrN_4OH^+$: 441.1285, Found: 441.1287 ($\Delta = 0.6$ ppm); HPLC (1): $t = 9.9$ min, purity > 99%.

5-(3-Bromobenzamido)-2-cyclohexyl-6-*N,N*-dimethylamino-1*H*-benzo[*d*]imidazole (SB-P17G-A7): Yellow solid (59% yield); mp 148-149 °C; 1H NMR (500 MHz, Methanol- d_4) δ 1.28-1.38 (m, 1 H), 1.40-1.52 (m, 2 H), 1.57-1.93 (m, 5 H), 2.06 (d, $J = 11.60$ Hz, 2 H), 2.65-2.80 (m, 6 H), 2.80-2.93 (m, 1 H), 7.38-7.49 (m, 2 H), 7.66-7.76 (m, 1 H), 7.80-7.91 (m, 1 H), 8.02-8.13 (m, 1 H), 8.43 (s, 1 H); ^{13}C NMR (126 MHz, Methanol- d_4) δ 27.10, 27.31, 32.9, 39.95, 46.06, 106.96, 108.03, 124.08, 126.62, 129.75, 131.56, 131.91, 135.21, 135.95, 137.36, 138.51, 138.53, 142.33, 142.36, 161.53, 161.55, 165.48, 165.54; HRMS (FAB) m/z calcd for $C_{22}H_{25}BrN_4OH^+$: 441.1285, Found: 441.1288 ($\Delta = 0.8$ ppm); HPLC (1): $t = 10.5$ min, purity > 99%.

2-Cyclohexyl-5-(2,3-dimethoxybenzamido)-6-*N,N*-dimethylamino-1*H*-benzo[*d*]imidazole (SB-P17G-A29): White solid (84 % yield); mp 135-136 °C; 1H NMR (500 MHz, $CDCl_3$) δ 0.98 - 1.20 (m, 3 H), 1.50 - 1.69 (m, 5 H), 1.96 (d, $J = 11.90$ Hz, 2 H), 2.67 - 2.75 (m, 7 H), 3.96 (s, 6 H), 6.99 (d, $J = 8.54$ Hz, 1 H), 7.50 (dd, $J = 8.24, 1.83$ Hz, 1 H), 7.54 - 7.62 (m, 2 H), 8.85 (s, 1

H), 9.85 (s, 1 H); ^{13}C NMR (126 MHz, CDCl_3) δ 25.8, 26.1, 31.9, 38.7, 46.0, 56.2, 56.3, 102.2, 110.1, 110.8, 110.9, 119.7, 128.2, 129.1, 131.9, 138.7, 139.4, 149.4, 152.2, 159.9, 165.2; HRMS (FAB) m/z calcd for $\text{C}_{25}\text{H}_{32}\text{N}_4\text{O}_4\text{H}^+$: 423.2391, Found: 423.2395 ($\Delta = 0.9$ ppm)

2-Cyclohexyl-5-(2,4-dimethoxybenzamido)-6-*N,N*-dimethylamino-1*H*-benzo[*d*]imidazole

(SB-P17G-A27): White solid (76 % yield); mp 163-164 °C; ^1H NMR (400 MHz, CDCl_3) δ 0.92 - 1.21 (m, 3 H), 1.41 - 1.70 (m, 5 H), 1.94 (d, $J = 11.54$ Hz, 2 H), 2.72 (br. s., 7 H), 3.89 (s, 3 H), 4.05 (s, 3 H), 6.58 (br. s, 1 H), 6.67 (d, $J = 8.03$ Hz, 1 H), 7.53 (s, 1 H), 8.35 (d, $J = 8.53$ Hz, 1 H), 9.03 (s, 1 H), 11.30 (br. s, 1 H); ^{13}C NMR (101 MHz, CDCl_3) δ 25.7, 26.1, 31.9, 38.6, 45.9, 55.8, 55.9, 98.8, 103.0, 105.7, 109.8, 115.5, 130.2, 131.5, 134.2, 139.9, 159.1, 159.7, 163.6, 163.9; HRMS (FAB) m/z calcd for $\text{C}_{25}\text{H}_{32}\text{N}_4\text{O}_4\text{H}^+$: 423.2391, Found: 423.2391 ($\Delta = 0.0$ ppm)

2-Cyclohexyl-5-(2,5-dimethoxybenzamido)-6-*N,N*-dimethylamino-1*H*-benzo[*d*]imidazole

(SB-P17G-A36): White solid (85% yield); mp 242-243 °C; ^1H NMR (500 MHz, CDCl_3) δ 1.01 - 1.25 (m, 3 H), 1.51 - 1.63 (m, 3 H), 1.70 (d, $J = 13.12$ Hz, 2 H), 2.00 (d, $J = 12.21$ Hz, 2 H), 2.62 - 2.85 (m, 7 H), 3.86 (s, 3 H), 4.05 (s, 3 H), 6.95 - 7.15 (m, 2 H), 7.55 (br. s, 1 H), 7.94 (d, $J = 3.05$ Hz, 1 H), 9.00 (s, 1 H), 10.31 (br. s, 1 H), 11.50 (br. s, 1 H); ^{13}C NMR (126 MHz, CDCl_3) δ 25.8, 26.1, 32.0, 38.7, 46.0, 56.1, 56.5, 102.5, 110.5, 113.2, 116.0, 119.7, 123.1, 130.2, 131.2, 140.0, 152.0, 154.2, 159.7, 163.3; HRMS (FAB) m/z calcd for $\text{C}_{24}\text{H}_{30}\text{N}_4\text{O}_3\text{H}^+$: 423.2391, Found: 423.2391 ($\Delta = 0.0$ ppm)

2-Cyclohexyl-5-(2,6-dimethoxybenzamido)-6-*N,N*-dimethylamino-1*H*-benzo[*d*]imidazole

(SB-P17G-A37): White solid (55% yield); mp 244-245 °C; ^1H NMR (500 MHz, CDCl_3) δ 1.01 - 1.19 (m, 3 H), 1.42 - 1.72 (m, 5 H), 1.92 (d, $J = 11.90$ Hz, 2 H), 2.46 - 2.58 (m, 1 H), 2.66 (s, 6 H), 3.80 (s, 6 H), 6.67 (d, $J = 8.24$ Hz, 2 H), 7.38 (t, $J = 8.39$ Hz, 2 H), 7.54 (br. s, 2 H), 8.99 (s, 1 H), 9.12 (br. s, 1 H), 11.53 (br. s, 1 H); ^{13}C NMR (126 MHz, CDCl_3) δ 26.0, 26.3, 31.8, 38.6, 45.9, 56.1, 102.9, 104.3, 110.0, 116.9, 128.9, 131.1, 131.7, 139.1, 139.7, 157.7, 160.0, 164.0; HRMS (FAB) m/z calcd for $\text{C}_{24}\text{H}_{30}\text{N}_4\text{O}_3\text{H}^+$: 423.2391, Found: 423.2390 ($\Delta = -0.2$ ppm)

2-Cyclohexyl-5-(3,4-dimethoxybenzamido)-6-*N,N*-dimethylamino-1*H*-benzo[*d*]imidazole

(SB-P17G-A35): White solid (79 % yield); mp 156-157 °C; ^1H NMR (500 MHz, CDCl_3) δ 0.95 - 1.16 (m, 3 H), 1.43 - 1.71 (m, 5 H), 1.92 (d, $J = 10.68$ Hz, 2 H), 2.67 (br. s, 7 H), 3.93 (br. s, 6 H), 6.96 (d, $J = 7.63$ Hz, 1 H), 7.45 - 7.54 (m, 2 H), 7.58 (br. s, 1 H), 8.83 (br. s., 1 H), 9.84 (br.

s, 1 H); ^{13}C NMR (126 MHz, CDCl_3) δ 25.7, 26.0, 31.8, 38.6, 45.9, 56.1, 56.2, 102.3, 109.9, 110.6, 110.7, 119.6, 128.1, 128.9, 132.0, 138.8, 139.2, 149.3, 152.1, 160.1, 165.1; HRMS (FAB) m/z calcd for $\text{C}_{25}\text{H}_{32}\text{N}_4\text{O}_4\text{H}^+$: 423.2391, Found: 423.2386 ($\Delta = -1.2$ ppm)

2-Cyclohexyl-5-(3,5-methoxybenzamido)-6-*N,N*-dimethylamino-1*H*-benzo[*d*]imidazole (SB-P17G-A10): White solid (82% yield); mp 219-220 °C; ^1H NMR (500 MHz, CDCl_3) δ 1.00 - 1.20 (m, 3 H), 1.49 - 1.71 (m, 5 H), 1.95 (d, $J = 11.60$ Hz, 2 H), 2.65 - 2.76 (m, 7 H), 3.86 (s, 6 H), 6.65 (t, $J = 2.14$ Hz, 1 H), 7.08 (d, $J = 2.14$ Hz, 2 H), 7.56 (br. s, 1 H), 8.90 (s, 1 H), 9.86 (br. s, 1 H); ^{13}C NMR (126 MHz, CDCl_3) δ 25.8, 26.1, 32.0, 38.7, 46.0, 55.7, 101.9, 103.5, 105.2, 110.7, 128.8, 131.5, 138.0, 139.4, 139.7, 160.2, 161.3, 165.6; HRMS (FAB) m/z calcd for $\text{C}_{25}\text{H}_{32}\text{N}_4\text{O}_4\text{H}^+$: 423.2391, Found: 423.2391 ($\Delta = 0.0$ ppm)

2-Cyclohexyl-5-(2-hydroxy-3-methoxybenzamido)-6-*N,N*-dimethylamino-1*H*-benzo[*d*]imidazole (SB-P17G-A39): Brown solid (40% yield); mp 215-216 °C; ^1H NMR (500 MHz, CDCl_3) δ 1.13 - 1.31 (m, 3 H), 1.51 - 1.66 (m, 3 H), 1.68 - 1.79 (m, 2 H), 2.03 (d, $J = 11.60$ Hz, 2 H), 2.65 (s, 6 H), 2.75 - 2.85 (m, 1 H), 3.86 (s, 3 H), 6.84 (t, $J = 8.09$ Hz, 1 H), 6.96 (d, $J = 7.93$ Hz, 1 H), 7.17 - 7.24 (m, 1 H), 7.50 (s, 1 H), 8.61 (s, 1 H), 10.14 (br. s, 1 H), 12.02 (br. s, 1 H); ^{13}C NMR (126 MHz, CDCl_3) δ 25.9, 26.2, 32.0, 38.6, 46.1, 56.4, 102.9, 110.0, 115.0, 116.2, 117.8, 118.8, 128.7, 132.0, 138.5, 140.0, 149.4, 151.6, 159.8, 167.5; HRMS (FAB) m/z calcd for $\text{C}_{23}\text{H}_{28}\text{N}_4\text{O}_3\text{H}^+$: 409.2234, Found: 409.2231 ($\Delta = -0.7$ ppm).

2-Cyclohexyl-5-(2,4,6-trimethoxybenzamido)-6-*N,N*-dimethylamino-1*H*-benzo[*d*]imidazole (SB-P17G-A41): White solid (44% yield); mp 212-213 °C; ^1H NMR (400 MHz, acetone- d_6) δ 1.18 - 1.46 (m, 3 H), 1.54 - 1.74 (m, 3 H), 1.79 (dt, $J = 12.86, 3.11$ Hz, 2 H), 2.06 - 2.10 (m, 2 H), 2.66 (s, 6 H), 2.77 - 2.84 (m, 1 H), 3.82 (s, 6 H), 3.88 (s, 3 H), 6.33 (s, 2 H), 7.42 (s, 1 H), 8.79 (s, 1 H); ^{13}C NMR (101 MHz, acetone- d_6) δ 26.8, 26.8, 32.5, 39.3, 46.0, 55.9, 56.3, 91.8, 111.1, 111.1, 130.4, 130.6, 139.6, 159.5, 159.8, 163.3, 163.5; HRMS (FAB) m/z calcd for $\text{C}_{25}\text{H}_{32}\text{N}_4\text{O}_4\text{H}^+$: 453.2496, Found: 453.2499 ($\Delta = 0.7$ ppm).

2-Cyclohexyl-5-(4-trifluoromethylbenzamido)-6-*N,N*-dimethylamino-1*H*-benzo[*d*]imidazole (SB-P17G-A32): Yellow solid (79 % yield); mp 196-197 °C; ^1H NMR (400 MHz, CDCl_3) δ 1.09 - 1.26 (m, 3 H), 1.52 - 1.79 (m, 5 H), 2.04 (d, $J = 12.05$ Hz, 2 H), 2.63 - 2.89 (m, 7 H), 7.61 (br. s, 1 H), 7.82 (d, $J = 8.03$ Hz, 2 H), 8.07 (d, $J = 8.03$ Hz, 2 H), 8.83 (s, 1 H), 9.97 (br. s, 1 H); ^{13}C

NMR (101 MHz, CDCl₃) δ 25.9, 26.1, 32.0, 38.7, 46.2, 102.1, 110.9, 122.5, 125.2, 126.2, 126.2, 127.6, 128.9, 133.5, 133.8, 139.1, 139.6, 160.1, 164.2; HRMS (FAB) m/z calcd for C₂₃H₂₅F₃N₄OH⁺: 431.2053, Found: 431.2055 (Δ = 0.5 ppm).

2-Cyclohexyl-5-(2-fluoro-4-trifluoromethylbenzamido)-6-*N,N*-dimethylamino-1*H*-

benzo[*d*]imidazole (SB-P17G-A42): Yellow solid (58% yield); mp 190-191 °C; ¹H NMR (400 MHz, CDCl₃) δ 1.07 - 1.35 (m, 3 H), 1.54 - 1.84 (m, 5 H), 1.96 - 2.16 (m, 2 H), 2.60 - 2.89 (m, 7 H), 7.44 - 7.78 (m, 3 H), 8.33 (t, J = 7.78 Hz, 1 H), 8.85 (br. s, 1 H), 10.44 (br. s, 2 H); ¹³C NMR (101 MHz, CDCl₃) δ 25.9, 26.1, 32.0, 38.8, 46.0, 102.2, 111.1, 114.1, 114.4, 121.6, 122.0, 124.3, 125.9, 126.0, 129.2, 131.1, 133.1, 135.2, 135.5, 139.8, 140.2, 158.7, 160.1, 161.2; HRMS (FAB) m/z calcd for C₂₃H₂₄F₄N₄OH⁺: 449.1959, Found: 449.1955 (Δ = -0.9 ppm).

2-Cyclohexyl-5-(2-fluoro-4-trifluoromethoxybenzamido)-6-*N,N*-dimethylamino-1*H*-

benzo[*d*]imidazole (SB-P17G-A38): Yellow solid (82% yield); mp 204-205 °C; ¹H NMR (500 MHz, Methanol-*d*₄) δ 1.47 (d, J = 12.82 Hz, 3 H), 1.66 (dd, J = 12.36, 3.20 Hz, 2 H), 1.75 - 1.82 (m, 1 H), 1.89 (d, J = 13.43 Hz, 2 H), 2.03 - 2.13 (m, 2 H), 2.73 (s, 6 H), 2.82 - 2.95 (m, 1 H), 7.25 - 7.39 (m, 2 H), 7.46 (br. s, 1 H), 8.12 - 8.25 (m, 1 H), 8.64 (s, 1 H); ¹³C NMR (126 MHz, Methanol-*d*₄) δ 27.1, 27.3, 33.0, 40.0, 46.2, 104.1, 110.5, 110.7, 118.3, 118.7, 120.8, 122.4, 122.5, 122.8, 124.9, 130.4, 134.5, 134.5, 141.8, 153.4, 153.5, 160.9, 161.6, 161.6, 162.9; HRMS (FAB) m/z calcd for C₂₃H₂₄F₄N₄O₂H⁺: 465.1908, Found: 465.1919 (Δ = 2.4 ppm).

2-Cyclohexyl-5-(2,3-difluoro-4-trifluoromethylbenzamido)-6-*N,N*-dimethylamino-1*H*-

benzo[*d*]imidazole (SB-P17G-A33): Yellow solid (84% yield); mp 191-192 °C; ¹H NMR (500 MHz, CDCl₃) δ 1.16 - 1.32 (m, 3 H), 1.59 - 1.89 (m, 5 H), 2.12 - 2.23 (m, 2 H), 2.64 (br. s, 6 H), 3.15 (br. s, 1 H), 7.47 - 7.54 (m, 1 H), 7.64 (br. s, 1 H), 7.92 (br. s, 1 H), 8.84 (br. s, 1 H), 10.13 (br. s, 1 H), 10.40 (br. s, 1 H); ¹³C NMR (126 MHz, CDCl₃) δ 25.5, 25.9, 31.6, 37.9, 45.6, 104.6, 107.7, 118.4, 120.6, 122.1, 122.5, 122.6, 122.7, 122.8, 123.1, 123.1, 123.3, 123.3, 123.4, 124.9, 126.3, 127.5, 130.6, 131.1, 132.5, 141.5, 147.4, 147.5, 147.9, 148.0, 149.6, 149.9, 150.1, 158.6, 159.1; HRMS (FAB) m/z calcd for C₂₃H₂₃F₅N₄OH⁺: 467.1865, Found: 467.1866 (Δ = 0.2 ppm).

2-Cyclohexyl-5-(2,6-difluoro-4-methoxybenzamido)-6-*N,N*-dimethylamino-1*H*-

benzo[*d*]imidazole (SB-P17G-A34): Light brown solid (53 % yield); mp 198-199 °C; ¹H NMR (500 MHz, CDCl₃) δ 1.12 - 1.26 (m, 3 H), 1.50 - 1.75 (m, 5 H), 2.01 (d, J = 11.90 Hz, 2 H), 2.60

- 2.80 (m, 7 H), 3.86 (s, 3 H), 6.59 (d, $J = 9.77$ Hz, 2 H), 7.58 (br. s., 1 H), 8.90 (s, 1 H), 9.62 (br. s, 1 H); ^{13}C NMR (126 MHz, CDCl_3) δ 25.9, 26.3, 31.9, 38.7, 46.1, 56.3, 98.8, 99.0, 102.6, 107.6, 107.8, 107.9, 110.5, 128.8, 131.7, 139.3, 139.8, 158.5, 160.2, 160.3, 160.4, 162.3, 162.4, 162.5, 162.6, 162.7; HRMS (FAB) m/z calcd for $\text{C}_{23}\text{H}_{26}\text{F}_2\text{N}_4\text{O}_2\text{H}^+$: 429.2097, Found: 429.2098 ($\Delta = 0.2$ ppm).

The following compounds were synthesized using the corresponding acyl chloride.

2-Cyclohexyl-5-(4-methoxybenzamido)-6-*N,N*-dimethylamino-1*H*-benzo[*d*]imidazole (SB-P17G-A16): To a solution of **2-4c** (100 mg, 0.39 mmol) in dichloromethane (2 mL) was added triethylamine (60 μL , 0.43 mmol). To this, 4-methoxybenzoyl chloride (53.3 μL , 0.39 mmol) was added drop wise at 0 $^\circ\text{C}$ and reacted at room temperature. After completion of the reaction, the reaction mixture was diluted with ethyl acetate and transferred to a separatory funnel. The organic layer was washed with saturated aqueous sodium bicarbonate solution, followed by water, and brine. The organic layer was dried over magnesium sulfate, filtered and concentrated. The crude product was purified by flash chromatography on silica gel (gradient: 30-70% ethyl acetate /hexanes) to obtain the product which was then treated with activated charcoal to yield the product as a white solid (130 mg, 86% yield); mp 201-202 $^\circ\text{C}$; ^1H NMR (400 MHz, CDCl_3) δ 0.97 - 1.26 (m, 3 H), 1.46 - 1.76 (m, 5 H), 1.96 (d, $J = 12.05$ Hz, 2 H), 2.63 - 2.82 (m, 7 H), 3.88 (s, 3 H), 7.04 (d, $J = 8.53$ Hz, 2 H), 7.56 (br. s, 1 H), 7.95 (d, $J = 8.53$ Hz, 2 H), 8.89 (s, 1 H), **9.85** (br. s, 1 H), 11.28 (br. s, 1 H); ^{13}C NMR (101 MHz, CDCl_3) δ 25.8, 26.1, 32.0, 38.7, 46.1, 55.7, 101.9, 110.6, 114.3, 127.9, 129.0, 129.0, 131.6, 139.3, 160.1, 162.6, 165.2; HRMS (FAB) m/z calcd for $\text{C}_{23}\text{H}_{28}\text{N}_4\text{O}_2\text{H}^+$: 393.2285, Found: 393.2285 ($\Delta = 0.0$ ppm); HPLC (1): $t = 13.2$ min, purity > 99%.

2-Cyclohexyl-6-*N,N*-diethylamino-5-(4-methylbenzamido)-1*H*-benzo[*d*]imidazole (SB-P2G5): White solid (65% yield); mp 183-184 $^\circ\text{C}$; ^1H NMR (300 MHz, CDCl_3) δ 0.97 (t, 6 H, $J = 6$ Hz), 1.20-1.30 (m, 3 H), 1.58-1.78 (m, 5 H), 2.06-2.08 (m, 2 H), 2.45 (s, 3 H), 2.76-2.77 (m, 1 H), 3.03 (q, 4 H, $J = 7.2$ Hz), 7.34 (d, 2 H, $J = 8.4$ Hz) 7.59 (s, 1 H), 7.87 (d, 2 H, $J = 8.1$ Hz), 8.91 (s, 1 H), 10.31 (s, 1 H); ^{13}C NMR (101 MHz, CDCl_3) δ 13.09, 21.48, 25.63, 25.92, 31.72, 38.40, 50.75, 100.9, 113.1, 126.8, 129.6, 131.8, 132.7, 135.0, 139.4, 142.1, 159.8, 165.1; HRMS

(FAB) m/z calcd for $C_{25}H_{32}N_4OH^+$: 405.2649, Found: 405.2654 ($\Delta = 1.2$ ppm); HPLC (4): $t = 10.1$ min, purity > 99%.

5-Chlorobenzamido-2-cyclohexyl-6-*N,N*-diethylamino-1*H*-benzo[*d*]imidazole (SB-P2G1):

White solid (64% yield); mp 216-217 °C (turned brown); 1H NMR (400 MHz, $CDCl_3$) δ 0.96 (t, $J = 7.2$ Hz, 6 H), 1.21-1.32 (m, 2 H), 1.59-1.81 (m, 5 H), 2.08 (m, 2 H), 2.79 (m, 1 H), 3.02 (m, $J = 7$ Hz, 4 H), 7.50 (d, $J = 6.8$ Hz, 2 H), 7.58 (s, 1 H), 7.88 (d, $J = 8.8$ Hz, 2 H), 8.82 (s, 1 H), 10.31 (s, 1 H); ^{13}C NMR (126 MHz, $CDCl_3$) δ 13.12, 25.75, 25.97, 29.69, 31.76, 38.47, 50.78, 100.5, 113.6, 128.3, 129.1, 131.3, 131.8, 133.9, 135.2, 137.9, 139.6, 159.5, 163.7; HRMS (FAB) m/z calcd for $C_{24}H_{29}N_4OClH^+$: 425.2108. Found: 425.2108 ($\Delta = -0.0$ ppm). HPLC (2): $t = 10.5$ min, purity > 99%.

2-Cyclohexyl-5-(4-methoxybenzamido)-6-pyrrolydiny-1*H*-benzo[*d*]imidazole (SB-P6B10):

White solid (56% yield); mp 195-196 °C; 1H NMR (400 MHz, $CDCl_3$) δ 1.08-1.35 (m, 5 H), 1.52-1.69 (m, 3 H), 1.70-1.80 (m, 2 H), 1.96-2.10 (m, 6 H), 2.76 (m, 1 H), 3.06 (br. s, 4 H), 3.90 (s, 3 H), 7.03 (d, $J = 8.8$ Hz, 2 H), 7.57 (br. s, 1 H), 7.91 (d, $J = 8.8$ Hz, 2 H), 8.80 (s, 1 H), 9.77 (br. s, 1 H); ^{13}C NMR (101 MHz, $CDCl_3$) δ 24.6, 25.9, 26.2, 32.0, 38.7, 54.1, 55.7, 100.2, 114.4, 128.0, 128.9, 130.1, 136.0, 159.7, 162.6, 164.9; HRMS (FAB) m/z calcd for $C_{25}H_{30}N_4O_2H^+$: 419.2442, Found: 419.2450 ($\Delta = 2.0$ ppm); HPLC (2): $t = 12.8$ min, purity > 98%.

2-Cyclohexyl-5-(4-methylbenzamido)-6-pyrrolodiny-1*H*-benzo[*d*]imidazole (SB-P7B5):

White solid (40% yield); mp 179-180 °C; 1H NMR (500 MHz, $CDCl_3$) δ 1.00-1.37 (m, 4 H), 1.49-1.65 (m, 3 H), 1.71 (dt, $J = 13.05, 3.40$ Hz, 2 H), 1.92-2.09 (m, 6 H), 2.45 (s, 3 H), 2.73 (m, 1 H), 3.05 (br. s, 4 H), 7.34 (d, $J = 8.24$ Hz, 2 H), 7.58 (br. s, 1 H), 7.85 (d, $J = 8.20$ Hz, 2 H), 8.86 (s, 1 H), 9.85 (br. s, 1 H), 10.70 (br. s, 1 H); ^{13}C NMR (126 MHz, $CDCl_3$) δ 21.7, 24.6, 25.9, 26.2, 32.0, 38.7, 54.1, 101.9, 110.9, 127.1, 129.8, 129.9, 130.1, 131.3, 132.9, 136.0, 139.9, 142.4, 159.9, 165.4; HRMS (FAB) m/z calcd for $C_{25}H_{30}N_4OH^+$: 403.2492, Found: 403.2496 ($\Delta = 0.9$ ppm); HPLC (2): $t = 9.1$ min, purity > 98%.

2-Cyclohexyl-5-(3-phenylpropanamido)-6-pyrrolidiny-1*H*-benzo[*d*]imidazole (SB-P7B11):

White solid (97% yield); mp 146-147 °C; 1H NMR (500 MHz, $CDCl_3$) δ 1.16-1.40 (m, 4 H), 1.57-1.73 (m, 3 H), 1.80 (dt, $J = 13.05, 3.40$ Hz, 2 H), 1.84-1.94 (m, 4 H), 2.09 (d, $J = 12.90$ Hz, 2 H), 2.76 (t, $J = 7.40$ Hz, 2 H), 2.80-2.92 (m, 5 H), 3.11 (t, $J = 7.40$ Hz, 2 H), 7.15-7.34 (m, 5

H), 7.47 (s, 1 H), 8.58 (s, 1 H), 8.75 (br. s, 1 H); ^{13}C NMR (126 MHz, CDCl_3) δ 24.5, 26.0, 26.2, 29.9, 32.0, 32.2, 38.7, 40.5, 53.7, 103.2, 109.3, 126.6, 128.5, 128.8, 129.4, 131.6, 136.0, 138.5, 140.6, 159.6, 170.4; HRMS (FAB) m/z calcd for $\text{C}_{26}\text{H}_{32}\text{N}_4\text{OH}^+$: 417.2649, Found: 417.2654 ($\Delta = 1.2$ ppm); HPLC (2): $t = 11.3$ min, purity > 98%.

2-Cyclohexyl-6-*N,N*-dimethylamino-5-(4-propylbenzamido)-1*H*-benzo[*d*]imidazole (SB-P21G1): White solid (75% yield); mp 190-191°C; ^1H NMR (400 MHz, CDCl_3) δ 0.98 (t, $J = 7.40$ Hz, 3 H), 1.03-1.36 (m, 4 H), 1.48-1.77 (m, 8 H), 1.94 (d, $J = 13.30$ Hz, 2 H), 2.62-2.80 (m, 9 H), 7.36 (d, $J = 8.28$ Hz, 2 H), 7.61 (s, 1 H), 7.91 (d, $J = 8.03$ Hz, 2 H), 8.94 (s, 1 H), 9.95 (s, 1 H), 11.15 (br. s, 1 H); ^{13}C NMR (101 MHz, CDCl_3) δ 14.0, 24.5, 25.8, 26.1, 32.0, 38.1, 38.6, 46.1, 101.8, 110.8, 127.2, 129.0, 129.3, 131.5, 133.2, 139.3, 139.8, 147.2, 160.2, 165.8; HRMS (FAB) m/z calcd for $\text{C}_{25}\text{H}_{32}\text{N}_4\text{OH}^+$: 405.2649, Found: 405.2651 ($\Delta = 0.5$ ppm); HPLC (1): $t = 8.0$ min, purity > 99%.

5-(4-*tert*-Butylbenzamido)-2-cyclohexyl-6-*N,N*-dimethylamino-1*H*-benzo[*d*]imidazole (SB-P17G-A23): White solid (74% yield); mp 222-223 °C; ^1H NMR (500 MHz, CDCl_3) δ 0.96-1.20 (m, 4 H), 1.39 (s, 9 H), 1.49-1.72 (m, 5 H), 1.96 (d, $J = 12.21$ Hz, 2 H), 2.74 (s, 7 H), 7.58 (d, $J = 8.24$ Hz, 3 H), 7.93 (d, $J = 8.54$ Hz, 2 H), 8.97 (s, 1 H), 9.98 (s, 1 H), 11.00 (s, 1 H); ^{13}C NMR (126 MHz, CDCl_3) δ 25.8, 26.1, 31.4, 32.0, 35.2, 38.6, 46.2, 101.7, 110.9, 126.2, 127.1, 129.2, 133.0, 139.3, 139.8, 155.5, 160.1, 165.8; HRMS (FAB) m/z calcd for $\text{C}_{26}\text{H}_{34}\text{N}_4\text{OH}^+$: 419.2805, Found: 419.2809 ($\Delta = 0.9$ ppm); HPLC (1): $t = 9.0$ min, purity > 99%.

2-Cyclohexyl-6-*N,N*-dimethylamino-5-(thiophene-2-carboxamido)-1*H*-benzo[*d*]imidazole (SB-P17G-A30): White solid (75% yield); mp 139-140 °C; ^1H NMR (500 MHz, CDCl_3) δ 1.00-1.08 (m, 1 H), 1.11-1.24 (m, 2 H), 1.51-1.61 (m, 3 H), 1.63-1.69 (m, 2 H), 1.97 (d, $J = 11.90$ Hz, 2 H), 2.12 (s, 1 H), 2.69 (s, 6 H), 2.77-2.84 (m, 1 H), 7.16 (dd, $J = 4.88, 3.66$ Hz, 1 H), 7.56 (d, $J = 1.00$ Hz, 2 H), 7.67 (dd, $J = 3.66, 0.61$ Hz, 1 H), 8.72 (s, 1 H), 9.75 (s, 1 H), 10.20 (br. s, 1 H); ^{13}C NMR (126 MHz, CDCl_3) δ 22.2, 25.7, 26.1, 31.8, 38.5, 45.9, 102.6, 109.7, 128.2, 128.4, 128.7, 130.8, 131.7, 137.9, 139.5, 140.1, 160.1, 160.1, 175.3; HRMS (FAB) m/z calcd for $\text{C}_{20}\text{H}_{23}\text{N}_4\text{OSH}^+$: 369.1744, Found: 369.1742 ($\Delta = -0.4$ ppm); HPLC (1): $t = 11.8$ min, purity > 98%.

2-Cyclohexyl-5-(furan-2-carboxamido)-6-*N,N*-dimethylamino-1*H*-benzo[*d*]imidazole (SB-P21G8): White solid (71% yield); mp 214-215 °C; ¹H NMR (400 MHz, CDCl₃) δ 1.10-1.37 (m, 3 H), 1.55-1.84 (m, 5 H), 2.06 (d, *J* = 14.81 Hz, 2 H), 2.67-2.88 (m, 7 H), 6.56-6.66 (m, *J* = 3.60, 1.90 Hz, 1 H), 7.22-7.32 (m, 1 H), 7.52-7.68 (m, 2 H), 8.79 (s, 1 H), 9.98 (s, 1 H), 10.59 (s, 1 H); ¹³C NMR (101 MHz, CDCl₃) δ 25.9, 26.2, 32.0, 38.7, 46.0, 101.8, 110.8, 112.6, 114.9, 128.6, 131.2, 139.6, 139.9, 144.7, 148.8, 156.4, 159.9; HRMS (FAB) *m/z* calcd for C₂₀H₂₄N₄O₂H⁺: 353.1972, Found: 353.1982 (Δ = 2.8 ppm); HPLC (1): *t* = 11.6 min, purity > 99%.

2-Cyclohexyl-5-(4-fluorobenzamido)-6-*N,N*-dimethylamino-1*H*-benzo[*d*]imidazole (SB-P17G-A24): White solid (70% yield); mp 196-197 °C; ¹H NMR (500 MHz, Methanol-*d*₄) δ 2.00-2.26 (m, 3 H), 2.34-2.45 (m, 2 H), 2.46-2.55 (m, 1 H), 2.60 (dt, *J* = 12.97, 3.28 Hz, 2 H), 2.81 (d, *J* = 13.12 Hz, 2 H), 3.48 (s, 6 H), 3.58-3.67 (m, 1 H), 8.20 (t, *J* = 8.85 Hz, 2 H), 8.82 (dd, *J* = 8.85, 5.49 Hz, 2 H), 9.07 (br. s, 1 H), 10.50 (br. s, 1 H), 12.80 (s, 1 H); ¹³C NMR (126 MHz, Methanol-*d*₄) δ 35.1, 35.2, 40.9, 47.3, 54.9, 111.6, 112.1, 119.5, 121.1, 125.3, 125.5, 136.7, 137.5, 139.2, 139.3, 140.3, 141.1, 141.1, 149.3, 150.7, 168.8, 172.7, 174.7; HRMS (FAB) *m/z* calcd for C₂₂H₂₅FN₄OH⁺: 381.2085, Found: 381.2088 (Δ = 0.7 ppm); HPLC (1): *t* = 11.4 min, purity > 99%.

2-Cyclohexyl-5-(2,4-difluorobenzamido)-6-*N,N*-dimethylamino-1*H*-benzo[*d*]imidazole (SB-P21G4): White solid (70% yield); mp 212-213 °C; ¹H NMR (400 MHz, Methanol-*d*₄) δ 1.29-1.55 (m, 3 H), 1.58-1.94 (m, 5 H), 2.07 (d, *J* = 12.05 Hz, 2 H), 2.72 (s, 6 H), 2.81-2.95 (m, 1 H), 7.10-7.24 (m, 2 H), 7.45 (s, 1 H), 8.06-8.21 (m, 1 H), 8.63 (s, 1 H); ¹³C NMR (101 MHz, Methanol-*d*₄) δ 27.12, 27.34, 30.81, 32.98, 40.00 46.16, 105.42, 105.69, 105.71, 105.97, 106.17, 108.39, 113.54, 113.57, 113.76, 113.78, 119.94, 119.97, 120.05, 120.09, 130.57, 134.62, 134.65, 134.72, 134.76, 141.75, 161.04, 161.16, 161.54, 161.90, 161.94, 163.53, 163.65, 165.26, 165.39, 167.79; HRMS (FAB) *m/z* calcd for C₂₂H₂₄F₂N₄OH⁺: 399.1991, Found: 399.1988 (Δ = -0.7 ppm); HPLC (1): *t* = 8.9 min, purity > 99%.

2-Cyclohexyl-5-(2-methoxybenzamido)-6-*N,N*-dimethylamino-1*H*-benzo[*d*]imidazole (SB-P17G-A25): White solid (60% yield); mp = 179-180 °C; ¹H NMR (500 MHz, CDCl₃) δ 0.94 - 1.14 (m, 3 H), 1.46 - 1.66 (m, 5 H), 1.94 (d, *J* = 11.90 Hz, 2 H), 2.62 - 2.80 (m, 7 H), 4.08 (s, 3 H), 7.08 (d, *J* = 8.24 Hz, 1 H), 7.16 (t, *J* = 7.48 Hz, 1 H), 7.47 - 7.61 (m, 2 H), 8.39 (dd, *J* = 7.78, 1.68 Hz, 1 H), 9.06 (s, 1 H), 11.42 (br. s, 1 H); ¹³C NMR (126 MHz, CDCl₃) δ 25.8, 26.1, 31.9,

38.7, 46.0, 55.9, 102.9, 110.3, 111.6, 121.6, 122.5, 129.9, 131.5, 132.5, 133.3, 139.5, 139.8, 157.7, 160.0, 163.7. HRMS (FAB) m/z calcd for $C_{23}H_{28}N_4O_2H^+$: 393.2285, Found: 393.2288 ($\Delta = 0.8$ ppm).

2-Cyclohexyl-5-(2,6-dichlorobenzamido)-6-*N,N*-dimethylamino-1*H*-benzo[*d*]imidazole (SB-P17G-A22): White solid (86% yield); mp 195-196 °C; 1H NMR (500 MHz, DMSO- d_6) δ 1.22 - 1.31 (m, 1 H), 1.33 - 1.44 (m, 2 H), 1.58 (qd, $J = 12.21, 3.05$ Hz, 2 H), 1.66 - 1.72 (m, 1 H), 1.79 (dt, $J = 12.89, 3.17$ Hz, 2 H), 2.00 (d, $J = 11.29$ Hz, 2 H), 2.62 (s, 6 H), 2.77 - 2.86 (m, 1 H), 7.29 (br. s, 1 H), 7.43 - 7.50 (m, 1 H), 7.51 - 7.57 (m, 2 H), 8.20 (br. s, 1 H), 9.77 (s, 1 H), 11.98 (br. s, 1 H); ^{13}C NMR (126 MHz, DMSO- d_6) δ 25.5, 25.6, 31.3, 37.7, 45.0, 103.7, 109.3, 126.9, 128.1, 131.1, 131.3, 136.7, 140.4, 159.3, 162.2; HRMS (FAB) m/z calcd for $C_{22}H_{24}Cl_2N_4OH^+$: 431.1400, Found: 431.1402 ($\Delta = 0.5$ ppm).

5-Cyclobutylamido-2-cyclohexyl-6-*N,N*-dimethylamino-1*H*-benzo[*d*]imidazole (SB-P17G-A31): White solid (68 % yield); mp 210-211 °C; 1H NMR (400 MHz, $CDCl_3$) δ 1.12 - 1.37 (m, 3 H), 1.53 - 1.83 (m, 5 H), 1.85 - 2.12 (m, 4 H), 2.23 - 2.48 (m, 4 H), 2.61 (br. s, 6 H), 2.80 (t, $J = 11.29$ Hz, 1 H), 3.30 (t, $J = 8.41$ Hz, 1 H), 7.46 (br. s, 1 H), 8.58 (s, 1 H), 8.85 (br. s, 1 H); ^{13}C NMR (101 MHz, $CDCl_3$) δ 18.2, 25.8, 26.0, 26.2, 31.9, 38.7, 41.5, 45.7, 102.5, 109.8, 128.6, 131.6, 139.1, 159.9, 173.3; HRMS (FAB) m/z calcd for $C_{20}H_{28}N_4OH^+$: 341.2336, Found: 341.2345 ($\Delta = 2.6$ ppm).

2-Cyclohexyl-5-[2-(4-methoxyphenyl)acetamido]-6-*N,N*-dimethylamino-1*H*-benzo[*d*]imidazole (SB-P17G-A26): White solid (88% yield); mp 167-168 °C; 1H NMR (400 MHz, $CDCl_3$) δ 1.17-1.42 (m, 3 H), 1.55-1.77 (m, 3 H), 1.83 (d, $J = 12.80$ Hz, 2 H), 2.12 (d, $J = 12.05$ Hz, 2 H), 2.34 (s, 6 H), 2.79-3.00 (m, 1 H), 3.78 (s, 2 H), 3.83 (s, 3 H), 6.95 (d, $J = 8.28$ Hz, 6 H), 7.28 (s, 2 H), 7.44 (s, 1 H), 8.63 (s, 1 H), 9.00 (s, 1 H); ^{13}C NMR (101 MHz, $CDCl_3$) δ 26.0, 26.2, 31.9, 38.7, 44.8, 45.5, 55.6, 101.8, 109.9, 114.0, 114.7, 126.7, 129.3, 130.5, 131.0, 139.5, 159.4, 159.5, 169.9; HRMS (FAB) m/z calcd for $C_{24}H_{30}N_4O_2H^+$: 407.2442, Found: 407.2246 ($\Delta = 1.1$ ppm); HPLC (1): $t = 13.4$ min, purity > 99%.

Synthesis of metabolites of SB-P3G2

5-*N*-ethylamino-2,4-dinitroaniline (2-2i): To a solution of 2,4-dinitro-5-fluoroaniline (200 mg, 0.99 mmol) and DIPEA (209 μ L, 12 mmol) in THF (3 mL) was added drop wise a solution of 2 M ethylamine in THF (0.6 mL, 1.2 mmol), diluted in THF (3 mL). The mixture was stirred at room temperature for 4 h. After removal of THF on rotary evaporator, the reaction mixture was diluted with dichloromethane, washed with water three times, dried over anhydrous magnesium sulfate and filtered. The solvent was evaporated to afford 5-*N*-ethylamino-2,4-dinitroaniline as a yellow solid (222 mg, quant. yield); mp = 209-210 °C; ^1H NMR (400 MHz, acetone- d_6) δ 1.33 (t, J = 7.15 Hz, 3 H), 3.37 (quin, J = 6.65 Hz, 2 H), 6.23 (s, 1 H), 7.40 (br. s., 2 H), 8.10 (br. s., 1 H), 9.02 (s, 1 H); ^{13}C NMR (101 MHz, acetone- d_6) δ 14.3, 38.8, 96.0, 96.1, 129.4, 149.2, 151.0, 151.1; MS (ESI) m/z 227.1 ($\text{M}+1$) $^+$.

Route 1: To a solution of 5-*N*-ethylamino-2,4-dinitroaniline (206 mg, 0.91 mmol) in ethanol (15 mL), was added ammonium formate (1.3 g) and 10 wt% Pd/C (115 mg). The mixture maintained under nitrogen, was stirred at room temperature for 1 h. After completion of reaction, the Pd/C catalyst and excess ammonium formate was filtered off over celite. The filtrate was washed with 5 mL of EtOH, and the solution was treated with the sodium bisulfite adduct (177 mg, 0.82 mmol) of the cyclohexanecarboxaldehyde, at 0 °C. After 14 h at room temperature under nitrogen, the reaction didn't progress and was heated at 50 °C for 34 h. The reaction mixture was concentrated to dryness using rotary evaporator. The residue was purified by chromatography on alumina gel to obtain an unknown compound.

Route 2: 4,6-Dinitrobenzene-1,3-diamine: A solution of 2,4-dinitro-5-fluoroaniline (225 mg, 1.12 mmol), ammonium hydroxide (0.8 mL, 2.24 mmol) in THF (8 mL) was stirred at room temperature. After 4 h, the solvent was removed on a rotary evaporator and the product was obtained by filtering the residue and washing it with water to obtain the product as a yellow solid (197 mg, 89%). ^1H NMR (300 MHz, Methanol- d_4) δ 6.13 (s, 1 H), 9.05 (s, 1 H).

Route 3: 4,6-dinitrobenzene-1,3-diamine was treated with the sodium bisulfite adduct of the cyclohexanecarboxaldehyde as described above but 5,6-diamino-2-cyclohexyl-1*H*-benzo[*d*]imidazole was not obtained.

Route 4: 1-Cyclohexanecarboxamido-2,4-dinitro-5-ethylaminobenzene (2-3i): To a solution of **5-N-ethylamino-2,4-dinitroaniline** (102 mg, 0.45 mmol) in toluene (0.5 mL), tetrahydrofuran (1 mL) and dimethylformamide (0.3 mL) was added 1-ethyl-3-(3-dimethylaminopropyl) carbodiimide (172.5 mg, 0.93 mmol) (EDC.HCl) and cyclohexanecarboxylic acid (116 mg, 0.93 mmol). 4-Dimethylaminopyridine (DMAP) (110 mg, 0.90 mmol) was added to the above reaction mixture, and the reaction was irradiated in the microwave reactor at 55 °C for 75 mins. After completion of the reaction as per TLC, the reaction mixture was diluted with ethyl acetate, transferred to a separatory funnel and the organic layer was washed with water, aqueous sodium bicarbonate and brine. The organic layer was dried over magnesium sulfate, filtered, and concentrated using rotary evaporator. The crude product was purified by silica gel flash chromatography (column was packed with hexane, 30% ethyl acetate was used with gradual increase to 50% ethyl acetate) to obtain the product as a yellow solid (133 mg, 88% yield). mp 145-148 °C, ¹H NMR (300 MHz, CDCl₃) δ 1.33 - 1.80 (m, 9 H), 1.81 - 1.93 (m, 2 H), 2.03 (d, *J* = 12.36 Hz, 2 H), 2.39 (tt, *J* = 11.43, 3.54 Hz, 1 H), 3.36 - 3.61 (m, 2 H), 8.32 - 8.60 (m, 2 H), 9.26 (s, 1 H), 11.02 (br. s., 1 H); MS (ESI) *m/z* 335.1 (M-1).

5-Amino-2-cyclohexyl-6-N-ethylamino-1H-benzo[d]imidazole (2-4i): To a solution of 1-cyclohexanecarboxamido-5-N-ethylamino-2,4-dinitrobenzene (133 mg, 0.40 mmol) in ethanol (6 mL) was added solid stannous chloride dihydrate (625 mg, 2.77 mmol). Concentrated hydrochloric acid (3 mL) was added to the reaction mixture such that the final concentration of HCl was 4 M in the reaction flask. The reaction mixture was refluxed for 6 h. Upon completion, the reaction mixture was basified with 30% sodium hydroxide solution. Excess stannous chloride formed a soluble salt in excess base. The desired product was extracted with dichloromethane and purified by flash chromatography on alumina using ethyl acetate as eluent to afford the product as a dark brown solid (69 mg, 68% yield); ¹H NMR (300 MHz, CDCl₃) δ 1.09 - 1.44 (m, 8 H), 1.54 - 1.89 (m, 6 H), 1.97 - 2.24 (m, 2 H), 2.76 - 2.98 (m, 1 H), 3.09 (q, *J* = 7.14 Hz, 2 H), 6.79 (s, 1 H), 6.92 (s, 1 H)

A solution of **5-amino-2-cyclohexyl-6-N-ethylamino-1H-benzo[d]imidazole** (69 mg, 0.27 mmol) and 1,1'-carbonyldiimidazole (34 mg, 0.21 mmol) in dichloromethane (2 mL) was stirred under reflux conditions for 4 hours. After all the starting material had disappeared, *n*-butanol (35 μL, 0.38 mmol) was added and the reaction was refluxed for an additional 12 h.

After the completion of the reaction, the reaction mixture was concentrated. The crude was purified by flash chromatography on silica gel (spiked with TEA, gradient: 1-5% methanol/ethyl acetate) to give 41 mg of a compound identified as **6-Cyclohexyl-3-ethyl-3,5-dihydrobenzo[1,2-d:4,5-d']diimidazol-2(1H)-one**: ^1H NMR (300 MHz, Methanol- d_4) δ 1.23 - 1.54 (m, 7 H), 1.57 - 1.95 (m, 5 H), 2.08 (d, J = 11.26 Hz, 2 H), 2.82 - 2.94 (m, 1 H), 3.96 (q, J = 7.14 Hz, 2 H), 7.18 (overlapping s, 2 H).

Synthesis of 4,4-difluorocyclohexyl analogues of SB-P17G-A20 and SB-P17G-C2.

5-Amino-2-(4,4-difluorocyclohexyl)-6-*N,N*-dimethylamino-1*H*-benzo[*d*]imidazole (2-4j/SB-P17G-2F2): A solution of **2-2c** (408 mg, 1.78 mmol), hydrochloride salt of 1-ethyl-3-(3-dimethylaminopropyl) carbodiimide (359 mg, 1.87 mmol) (EDC.HCl), 4,4-difluorocyclohexane-1-carboxylic acid (306.3 mg, 1.87 mmol), and 4-dimethylaminopyridine (DMAP) (229 mg, 1.87 mmol) in toluene (5 mL) was irradiated in the microwave reactor at 60 °C for 2.5 h. After completion of the reaction as per TLC, the reaction mixture was diluted with ethyl acetate, transferred to a separatory funnel and the organic layer was washed with water, aqueous sodium bicarbonate and brine. The organic layer was dried over magnesium sulfate, filtered, and concentrated using rotary evaporator. The crude product (377 mg) was refluxed in EtOH (50 mL) with $\text{SnCl}_2 \cdot 2\text{H}_2\text{O}$ (1.6 g, 7.09 mmol), 12 M HCl (10 mL) for 4 h. Upon completion, the reaction mixture was basified with 30% sodium hydroxide solution. Excess stannous chloride formed a soluble salt in excess base. The desired product was extracted with dichloromethane and purified by flash chromatography on alumina using ethyl acetate as eluent to afford the product as a beige solid; mp = 159-161 °C; ^1H NMR (400 MHz, CDCl_3) δ 1.59 - 1.86 (m, 2 H), 1.93 - 2.20 (m, 6 H), 2.63 (s, 6 H), 2.89 (t, J = 11.17 Hz, 1 H), 6.78 (s, 1 H), 7.23 (s, 1 H); ^{13}C NMR (101 MHz, CDCl_3) δ 28.0, 28.1, 33.0, 33.3, 33.5, 36.4, 44.7, 98.7, 107.0, 120.5, 122.9, 125.3, 133.1, 134.3, 138.6, 138.8, 155.1; MS (ESI) m/z 295.1 ($\text{M}+1$) $^+$.

2-(4,4-Difluorocyclohexyl-5-(4-trifluoromethoxybenzamido)-6-*N,N*-dimethylamino-1*H*-benzo[*d*]imidazole (SB-P17G-A20-2F2): It was synthesized following procedure described for **SB-P17G-A15**. Beige solid (62 % yield); mp = 217-218 °C; ^1H NMR (500 MHz, CDCl_3) δ 1.60 - 1.82 (m, 2 H), 1.90 - 2.26 (m, 6 H), 2.75 (s, 6 H), 2.80 - 2.99 (m, 1 H), 7.31 - 7.47 (m, J = 8.24 Hz, 2 H), 7.63 (br. s, 1 H), 8.00 (d, J = 9.46 Hz, 1 H), 8.82 (s, 1 H), 9.92 (br. s, 1 H), 10.64 (br.

s., 1 H); ^{13}C NMR (126 MHz, CDCl_3) δ 27.9, 27.9, 33.0, 33.2, 33.4, 36.4, 46.1, 101.8, 111.2, 121.2, 129.0, 129.2, 131.3, 134.0, 139.9, 152.0, 157.3, 164.4; HRMS (FAB) m/z calcd for $\text{C}_{23}\text{H}_{23}\text{F}_5\text{N}_4\text{O}_2\text{H}^+$: 483.1814, Found: 483.1816 ($\Delta = 0.4$ ppm).

5-Butoxycarbonylamino-2-(4,4-difluorocyclohexyl)-6-*N,N*-dimethylamino-1*H*-benzo[*d*]imidazole (SB-P17G-C2-2F2): A solution of 5-amino-2-cyclohexyl-6-(*N,N*-dimethylamino)-1*H*-benzo[*d*]imidazole (50 mg, 0.17 mmol) and 1,1'-carbonyldiimidazole (31 mg, 0.19 mmol) in dichloromethane (2 mL) was stirred under reflux conditions for 4 hours. After all the starting material had disappeared, *n*-butanol (35 μL , 0.34 mmol) was added, and the reaction was refluxed for an additional 12 h. After the completion of the reaction, the reaction mixture was concentrated. The crude was purified by flash chromatography on silica gel (gradient: 30-70% ethyl acetate /hexanes) to obtain product as a white solid (35 mg, 43% yield); mp 154-155 $^\circ\text{C}$; ^1H NMR (300 MHz, CDCl_3) δ 0.97 (t, $J = 7.36$ Hz, 3 H), 1.35 - 1.54 (m, 2 H), 1.60 - 2.31 (m, 11 H), 2.65 (s, 6 H), 2.97 (br. s, 1 H), 4.20 (t, $J = 6.71$ Hz, 2 H), 7.48 (br. s, 1 H), 8.06 - 8.35 (m, 2 H); ^{13}C NMR (101 MHz, CDCl_3) δ 14.0, 19.3, 27.9, 28.0, 29.9, 31.3, 33.0, 33.3, 33.5, 36.4, 45.8, 65.2, 130.1, 139.4, 154.5, 156.2; HRMS (FAB) m/z calcd for $\text{C}_{20}\text{H}_{28}\text{F}_2\text{N}_4\text{O}_2\text{H}^+$: 395.2253, Found: 395.2258 ($\Delta = 1.3$ ppm).

Synthesis of *N*-demethylated analogues of SB-P17G-A16

5-*N*-Benzyl-*N*-methyl-2,4-dinitroaniline (2-2k): Yellow solid (97% yield); mp = 164-165 $^\circ\text{C}$; ^1H NMR (400 MHz, acetone- d_6) δ 2.83 (s, 3 H), 4.48 (s, 2 H), 6.49 (s, 1 H), 7.24 - 7.48 (m, 7 H), 8.69 (s, 1 H); ^{13}C NMR (101 MHz, acetone- d_6) δ 40.8, 58.4, 103.6, 128.4, 128.5, 128.6, 129.5, 137.4, 149.7, 149.8, 151.2; MS (ESI) m/z 303.0 ($\text{M}+1$) $^+$.

5-Amino-2-cyclohexyl-6-*N*-methylamino-1*H*-benzo[*d*]imidazole (2-4k): Black solid (44% yield); ^1H NMR (300 MHz, CDCl_3) δ 1.28 - 1.44 (m, 3 H), 1.48 - 1.92 (m, 7 H), 1.99 - 2.13 (m, 2 H), 2.74 - 2.90 (m, 4 H), 6.77 (s, 1 H), 6.91 (s, 1 H); MS (ESI) m/z 245.1 ($\text{M}+1$) $^+$.

2-Cyclohexyl-5-(4-methoxybenzamido)-6-*N*-methylamino-1*H*-benzo[*d*]imidazole (2-5k): White solid (44% yield); mp > 240 $^\circ\text{C}$; ^1H NMR (500 MHz, CDCl_3) δ 1.36 - 1.55 (m, 3 H), 1.65 - 1.83 (m, 3 H), 1.87 - 1.96 (m, 2 H), 2.07 - 2.14 (m, 2 H), 2.89 - 3.00 (m, 1 H), 7.13 (d, $J = 8.85$ Hz, 2 H), 7.56 (s, 1 H), 7.67 - 7.78 (m, 3 H); ^{13}C NMR (126 MHz, Methanol- d_4) δ 27.2, 27.4,

32.4, 33.0, 40.3, 56.1, 114.9, 115.5, 123.4, 130.9, 132.2, 135.3, 140.3, 155.8, 162.2, 162.8; HRMS (FAB) m/z calcd for $C_{22}H_{26}N_4O_2H^+$: 379.2129, Found 379.2133 ($\Delta = 1.1$ ppm).

Synthesis of 2-methyl and 2-cyclohexylmethyl analogue SB-P17G-C2

5-Amino-2-methyl-6-*N,N*-dimethylamino-1*H*-benzo[*d*]imidazole (2-4l): A solution of 5-*N,N*-dimethylamino-2,4-dinitroaniline (302 mg, 1.34 mmol) and acetyl chloride (115.4 mg, 1.47 mmol) in pyridine (2 mL) was irradiated at 100 °C in the microwave for 1 h. Additional 0.5 eq of acetyl chloride was added and reaction mixture was heated for 1 h to push reaction to completion. The crude product was isolated by removing solvent on the rotary evaporator, re-dissolved in ethyl acetate and transferred to the separatory funnel. The organic layer was washed with copper sulfate solution, brine, dried over magnesium sulfate, filtered, and concentrated. The crude material was refluxed with stannous chloride dihydrate (1.93 g, 8.53 mmol) in ethanol (30 mL) for 4 h. The reaction was monitored by FIA analysis and following completion of reaction the solvent was removed on the rotary evaporator. The reaction mixture was basified with excess aqueous sodium hydroxide. The aqueous layer was extracted with dichloromethane. The combined organic layer was dried over magnesium sulfate, and concentrated. The product was isolated as a black solid (201 mg, 87% yield). 1H NMR (500 MHz, $CDCl_3$) δ 2.08 - 3.05 (m, 9 H), 6.79 (br. s, 1 H), 7.18 (br. s, 1 H); ^{13}C NMR (126 MHz, $CDCl_3$) δ 14.6, 44.7, 98.8, 106.1, 132.9, 134.7, 138.0, 138.3, 150.0; MS (ESI) m/z 191.1 ($M+1$) $^+$.

1-(Cyclohexylmethylcarboxamido)-5-*N,N*-dimethylamino-2,4-dinitrobenzene (2-3m): mp 132-134 °C; 1H NMR (400 MHz, $CDCl_3$) δ 0.97 - 1.38 (m, 5 H), 1.62 - 1.81 (m, 5 H), 1.82 - 1.97 (m, 1 H), 2.37 (d, $J = 7.03$ Hz, 2 H), 3.05 (s, 6 H), 8.57 (s, 1 H), 8.82 (s, 1 H), 10.88 (br. s, 1 H); ^{13}C NMR (101 MHz, $CDCl_3$) δ 26.2, 26.2, 33.2, 35.5, 42.7, 47.1, 106.2, 125.1, 127.7, 131.6, 138.7, 150.4, 172.5; MS (ESI) m/z 351.1 ($M+1$) $^+$.

5-Amino-2-cyclohexylmethyl-6-*N,N*-dimethylamino-1*H*-benzo[*d*]imidazole (2-4m): Beige solid (85% yield over 2 steps); mp 130-132 °C; 1H NMR (400 MHz, $CDCl_3$) δ 0.82 - 1.21 (m, 5 H), 1.54 - 1.72 (m, 5 H), 1.74 - 1.88 (m, $J = 14.52, 7.31, 3.51, 3.51$ Hz, 1 H), 2.49 - 2.86 (m, 8 H), 6.81 (s, 1 H), 7.24 (s, 1 H); ^{13}C NMR (101 MHz, $CDCl_3$) δ 26.2, 26.4, 33.4, 37.1, 38.0, 44.8, 98.6, 106.7, 132.9, 134.2, 138.4, 138.5, 152.7; HRMS (FAB) m/z calcd for $C_{16}H_{24}N_4H^+$: 273.2074, Found 273.2069 ($\Delta = -1.8$ ppm).

5-Butyloxycarbonylamino-2-methyl-6-*N,N*-dimethylamino-1*H*-benzo[*d*]imidazole (2-5I): A solution of 5-amino-2-methyl-6-*N,N*-dimethylamino-1*H*-benzo[*d*]imidazole (45 mg, 0.24 mmol) and 1,1'-carbonyldiimidazole (42 mg, 0.26 mmol) in dichloromethane (2 mL) was stirred under reflux conditions for 4 hours. After all the starting material had disappeared, *n*-butanol (71 μ L, 0.77 mmol) was added and the reaction was refluxed for an additional 12 h. After the completion of the reaction, the reaction mixture was concentrated. The crude was purified by flash chromatography on silica gel (gradient: 30-70% ethyl acetate /hexanes) to give the product as a white solid (41 mg, 59% yield). mp =156-157 °C; ¹H NMR (500 MHz, CDCl₃) δ 0.96 (t, *J* = 7.32 Hz, 3 H), 1.38 - 1.50 (m, 2 H), 1.69 (quin, *J* = 7.17 Hz, 2 H), 2.57 (s, 3 H), 2.64 (s, 6 H), 4.20 (t, *J* = 6.71 Hz, 2 H), 7.42 (s, 1 H), 8.19 (br. s, 1 H), 8.24 (br. s, 1 H); ¹³C NMR (126 MHz, CDCl₃) δ 14.0, 15.2, 19.3, 31.3, 45.8, 65.2, 100.8, 109.2, 129.6, 133.0, 137.4, 138.9, 151.1, 154.4; HRMS (FAB) *m/z* calcd for C₁₅H₂₂N₄O₂H⁺: 291.1816, Found 291.1814 (Δ = -0.7 ppm).

Synthesis of 5-*N*-benzylamino-2-cyclohexyl-6-*N,N*-dimethylamino-1*H*-benzo[*d*]imidazole (SB-P17G-A'15): To a solution of 5-amino-2-cyclohexyl-6-(*N,N*-dimethylamino)-1*H*-benzo[*d*]imidazole (108 mg, 0.42 mmol) in dichloromethane (2 mL) was added benzyl bromide (71.5 mg, 0.42 mmol) dropwise at 0 °C and reacted at room temperature. After completion of the reaction, the reaction mixture was diluted with ethyl acetate and transferred to a separatory funnel. The organic layer was washed with saturated sodium bicarbonate solution, followed by water, and brine. The organic layer was dried over magnesium sulfate. The crude product was purified by flash chromatography on silica gel (gradient: 30-70% ethyl acetate/hexanes) to obtain the slightly impure product (27 mg) which was then recrystallized from methanol and water. mp = 79-80 °C; ¹H NMR (300 MHz, CDCl₃) δ 1.20 - 1.35 (m, 3 H), 1.49 - 1.76 (m, 5 H), 1.99 (d, *J* = 10.80 Hz, 2 H), 2.51 - 2.80 (m, 7 H), 4.27 (s, 2 H), 6.51 (s, 1 H), 7.05 - 7.39 (m, 7 H); ¹³C NMR (126 MHz, CDCl₃) δ 25.9, 26.1, 29.9, 31.9, 38.1, 44.9, 49.0, 93.5, 107.1, 127.2, 127.5, 128.8, 138.7, 140.0, 141.0, 156.1; HRMS (FAB) *m/z* calcd for C₂₂H₂₈N₄H⁺: 349.2387, Found 349.2390 (Δ = 0.9 ppm).

Synthesis of 2-cyclohexyl-5-(*N*-4-trifluoromethoxybenzylamino)-6-(*N,N*-dimethylamino)-1*H*-benzo[*d*]imidazole (SB-P17G-A'20): Reaction mixture containing 2-cyclohexyl-5-(4-trifluoromethoxybenzamido)-6-(*N,N*-dimethylamino)-1*H*-benzo[*d*]imidazole (54 mg, 0.12 mmol), 1 M BH₃.THF (3.7 mL), and tetrahydrofuran (1.8 mL) was stirred at room

temperature for 36 h. The reaction was diluted with ethyl acetate, sodium bicarbonate was added and the reaction was transferred to a separatory funnel. The organic layer was washed with saturated sodium bicarbonate solution, water and brine. The organic layer was dried over magnesium sulfate and concentrated on a rotary evaporator followed by column chromatography. Poor separation was observed therefore all column fractions were combined and treated with excess sodium bicarbonate. After 24 h, the reaction was worked up as before and alumina gel chromatography yielded product as an off white solid. (20 mg, 38% yield); mp 101-103 °C; ¹H NMR (500 MHz, CDCl₃) δ 1.23 - 1.35 (m, 3 H), 1.52 - 1.64 (m, 2 H), 1.69 (d, *J* = 12.51 Hz, 1 H), 1.78 (d, *J* = 13.12 Hz, 2 H), 2.04 (d, *J* = 11.60 Hz, 2 H), 2.66 (s, 6 H), 2.73 - 2.84 (m, 1 H), 4.32 (s, 2 H), 6.53 (s, 1 H), 7.14 (d, *J* = 7.93 Hz, 2 H), 7.28 - 7.42 (m, 3 H); ¹³C NMR (126 MHz, CDCl₃) δ 26.0, 26.2, 32.1, 38.5, 45.0, 48.3, 94.1, 107.3, 121.2, 128.6, 131.5, 133.9, 138.1, 139.0, 140.2, 148.3, 157.0; HRMS (ESI) *m/z* calcd for C₂₃H₂₇F₃N₄OH⁺: 433.2210, Found: 433.2214 (Δ = -0.87 ppm).

Synthesis of 2-cyclohexyl-5-(*N*-4-methylbenzylamino)-6-(*N,N*-dimethylamino)-1*H*-benzo[*d*]imidazole (SB-P17G-A'28): Reaction mixture containing 2-cyclohexyl-5-(4-methylbenzamido)-6-(*N,N*-dimethylamino)-1*H*-benzo[*d*]imidazole (50 mg, 0.133 mmol), 1 M BH₃.THF (1.1 mL) was refluxed. After 24 h the reaction mixture was cooled to 0 °C and 1 M NaOH was added to it. The reaction mixture was stirred at rt for 14 h. The reaction mixture was transferred to a separatory funnel, diluted with ethyl acetate and the organic layer was washed with saturated sodium bicarbonate solution, water and brine. The organic layer was dried over magnesium sulfate and concentrated on a rotary evaporator followed by alumina gel column chromatography (gradient: 1% MeOH/DCM to 6% MeOH/DCM). NMR spectrum of compound showed broad peaks indicating presence of boron impurities and was therefore treated with excess 1,4-diazabicyclo[2.2.2]octane (DABCO) in toluene. After 24 h, the reaction was worked up as before to obtain product as a pale yellow solid. (18 mg); mp 155-156 °C; ¹H NMR (500 MHz, CDCl₃) δ 1.31 - 1.45 (m, 3 H), 1.56 - 1.73 (m, 3 H), 1.77 - 1.87 (m, 2 H), 2.07 (d, *J* = 10.07 Hz, 2 H), 2.34 (s, 3 H), 2.66 (s, 6 H), 2.74 - 2.89 (m, 1 H), 4.30 (s, 2 H), 5.24 (br. s, 1 H), 6.58 (br. s, 1 H), 7.14 (d, *J* = 7.93 Hz, 2 H), 7.27 (d, *J* = 7.93 Hz, 2 H), 7.32 (br. s, 1 H); ¹³C NMR (126 MHz, CDCl₃) δ 21.3, 26.0, 26.2, 32.1, 38.4, 45.0, 48.8, 93.5, 107.6, 127.5, 129.4,

129.6, 133.2, 136.7, 137.0, 138.3, 140.8, 156.4; HRMS (FAB) m/z calcd for $C_{23}H_{30}N_4H^+$: 363.2543, Found 363.2545 ($\Delta = 0.6$ ppm).

2-Cyclohexyl-5-(*N*-(2-fluoro-4-trifluoromethoxybenzylamino)-6-(*N,N*-dimethylamino)-1*H*-benzo[*d*]imidazole (SB-P17G-A'38): Yellow solid (75% yield); mp 86-88 °C; 1H NMR (400 MHz, $CDCl_3$) δ 1.20 - 1.36 (m, 3 H), 1.51 - 1.73 (m, 3 H), 1.79 (d, $J = 13.05$ Hz, 2 H), 2.05 (d, $J = 11.54$ Hz, 2 H), 2.66 (s, 6 H), 2.74 - 2.88 (m, 1 H), 4.39 (s, 2 H), 6.55 (s, 1 H), 6.87 - 7.00 (m, 2 H), 7.31 (s, 1 H), 7.36 (t, $J = 8.53$ Hz, 1 H); ^{13}C NMR (101 MHz, $CDCl_3$) δ 26.0, 26.2, 32.1, 38.5, 42.0, 42.1, 45.1, 94.0, 107.5, 108.8, 109.1, 116.7, 116.8, 119.2, 121.8, 124.4, 125.9, 126.0, 129.9, 130.0, 131.7, 131.8, 133.9, 134.0, 138.2, 139.9, 148.6, 148.7, 157.1, 159.4, 161.9; HRMS (ESI) m/z calcd for $C_{23}H_{26}F_4N_4OH^+$: 451.2116, Found: 451.2118 ($\Delta = -0.57$ ppm).

Salt of fumaric acid salts of SB-P3G2 and SB-P17G-A38

SB-P3G2-Fum salt: To a solution of **SB-P3G2** (85 mg, 0.21 mmol) in ethyl acetate (4 mL) was added fumaric acid (24 mg, 0.21 mmol) dissolved in ethanol (0.5 mL). Ether (12 mL) was added to the above solution and the mixture was chilled on ice. No precipitation was observed. All solvent was removed on a rotary evaporator and the residue was re-dissolved in minimum amount of hot ethyl acetate. On cooling the salt precipitated out. mp 150 °C. 1H NMR (400 MHz, Methanol- d_4) δ 0.87 - 1.05 (m, 9 H), 1.31 - 1.56 (m, 5 H), 1.61 - 1.74 (m, 4 H), 1.78 (m, 1 H), 1.84 - 1.98 (m, 2 H), 2.13 (d, $J = 11.54$ Hz, 2 H), 2.88 - 3.18 (m, 5 H), 4.18 (t, $J = 6.65$ Hz, 2 H), 6.74 (s, 2 H), 7.53 (s, 1 H), 8.31 (s, 1 H); ^{13}C NMR (101 MHz, Methanol- d_4) δ 13.1, 14.2, 20.3, 26.7, 26.9, 32.3, 38.7, 51.3, 66.3, 102.9, 110.4, 131.1, 132.4, 135.6, 135.9, 138.7, 155.5, 159.7, 170.0.

SB-P17G-A38-Fumaric acid salt: mp 223-224 °C; 1H NMR (500 MHz, Methanol- d_4) δ 1.33 - 1.42 (m, 1 H), 1.44 - 1.55 (m, 2 H), 1.68 (dd, $J = 12.36, 3.20$ Hz, 2 H), 1.76 - 1.84 (m, 1 H), 1.91 (dt, $J = 13.35, 3.09$ Hz, 2 H), 2.13 (d, $J = 11.60$ Hz, 2 H), 2.75 (s, 6 H), 2.95 - 3.08 (m, 1 H), 7.26 - 7.42 (m, 2 H), 7.53 (s, 1 H), 8.20 (t, $J = 9.00$ Hz, 1 H), 8.74 (s, 1 H); ^{13}C NMR (126 MHz, Methanol- d_4) δ 26.9, 27.1, 32.5, 39.2, 45.9, 106.0, 107.8, 110.5, 110.7, 118.4, 120.8, 122.1, 122.2, 122.8, 124.9, 131.9, 132.9, 133.8, 134.5, 134.6, 135.7, 143.4, 153.5, 153.6, 160.5, 161.0, 161.8, 161.8, 163.0, 169.4.

Synthesis of compounds with unknown MIC

SB-P6C-A50 and **SB-P17G-A50** were synthesized following the procedure described for **SB-P17G-A16**. **SB-P17G-A47**, **SB-P17G-A51**, **SB-P17G-A53** were synthesized following the procedure described for **SB-P17G-A15**.

2-Cyclohexyl-5-(5-nitrofur-2-carboxamido)-6-morpholino-1H-benzo[d]imidazole (SB-P6C-A50): Yellow solid (98% yield); mp >240 °C; ¹H NMR (500 MHz, DMSO-d₆) δ 1.19 - 1.31 (m, 1 H), 1.32 - 1.44 (m, 2 H), 1.51 - 1.63 (m, 2 H), 1.69 (d, *J* = 12.51 Hz, 1 H), 1.74 - 1.86 (m, 2 H), 1.99 (d, *J* = 10.99 Hz, 2 H), 2.71 - 2.95 (m, 5 H), 3.88 (br. s., 4 H), 7.53 (d, *J* = 3.66 Hz, 2 H), 7.83 (d, *J* = 3.97 Hz, 1 H), 8.40 (s, 1 H), 10.22 (br. s, 1 H), 12.14 (br. s, 1 H); ¹³C NMR (126 MHz, DMSO-d₆) δ 25.5, 25.6, 31.3, 37.7, 53.0, 67.0, 101.1, 111.6, 113.9, 116.4, 127.2, 131.2, 137.1, 139.7, 148.1, 151.2, 153.2, 159.8; HRMS (FAB) *m/z* calcd for C₂₂H₂₅N₅O₅H⁺: 440.1928, Found 440.1937 (Δ = 2.0 ppm).

2-Cyclohexyl-5-(5-nitrofur-2-carboxamido)-6-*N,N*-dimethylamino-1H-benzo[d]imidazole (SB-P17G-A50): Yellow solid (88% yield); mp = turned black > 225 °C; ¹H NMR (400 MHz, Methanol-d₄) δ 1.31 - 1.53 (m, 3 H), 1.57 - 1.72 (m, 2 H), 1.78 (d, *J* = 12.55 Hz, 1 H), 1.88 (d, *J* = 12.80 Hz, 2 H), 2.07 (d, *J* = 11.80 Hz, 2 H), 2.77 (s, 6 H), 2.81 - 2.92 (m, *J* = 11.92, 11.92 Hz, 1 H), 7.32-7.34 (m, 1 H), 7.45 (s, 1 H), 7.47 - 7.53 (m, 1 H), 8.48 (s, 1 H); ¹³C NMR (101 MHz, Methanol-d₄) δ 27.1, 27.3, 32.9, 40.0, 46.1, 106.2, 108.3, 113.6, 117.3, 129.2, 135.4, 137.3, 141.9, 149.6, 153.2, 155.6, 161.8; HRMS (FAB) *m/z* calcd for C₂₀H₂₃N₅O₄H⁺: 398.1823, Found: 398.1821 (Δ = -0.5 ppm).

2-Cyclohexyl-5-(2,2-difluorobenzo[d][1,3]dioxole-4-carboxamido)-6-*N,N*-dimethylamino-1H-benzo[d]imidazole (SB-P17G-A47): Yellow solid (77% yield); mp = 245-246 °C; ¹H NMR (400 MHz, CDCl₃) δ 1.13 - 1.31 (m, 3 H), 1.51 - 1.80 (m, 5 H), 1.98 - 2.12 (m, 2 H), 2.60 - 2.91 (m, 7 H), 7.60 (br. s, 1 H), 7.92 (br. s, 1 H), 8.88 (br. s, 1 H), 10.57 (br. s, 2 H); ¹³C NMR (101 MHz, CDCl₃) δ 25.9, 26.2, 32.0, 38.8, 45.9, 101.9, 111.4, 112.8, 118.4, 124.3, 124.8, 129.0, 129.6, 131.6, 134.2, 139.7, 141.0, 144.1, 159.7, 160.0; HRMS (FAB) *m/z* calcd for C₂₃H₂₄F₂N₄O₃H⁺: 443.1889, Found: 443.1899 (Δ = 2.3 ppm).

2-Cyclohexyl-6-(*N,N*-dimethylamino)-5-(6-trifluoromethylnicotinamido)-1*H*-

benzo[*d*]imidazole (SB-P17G-A51): Yellow solid (78% yield); mp = 220-221 °C; ¹H NMR (500 MHz, CDCl₃) δ 1.22 - 1.39 (m, 3 H), 1.54 - 1.76 (m, 3 H), 1.82 (d, *J* = 11.90 Hz, 2 H), 2.11 (d, *J* = 11.29 Hz, 2 H), 2.64 - 2.89 (m, 7 H), 7.62 (br. s., 1 H), 7.87 (d, *J* = 7.93 Hz, 1 H), 8.46 (d, *J* = 7.32 Hz, 1 H), 8.73 (br. s., 1 H), 9.25 (br. s., 1 H), 10.07 (br. s., 2 H) ¹³C NMR (126 MHz, CDCl₃) δ 26.0, 26.2, 32.0, 38.7, 46.2, 101.5, 111.4, 120.3, 120.9, 122.5, 128.8, 131.0, 133.9, 137.1, 139.6, 140.2, 148.2, 150.4, 150.7, 160.0, 161.7; HRMS (FAB) *m/z* calcd for C₂₂H₂₄F₃N₅OH⁺: 432.2006, Found: 432.2007 (Δ = 0.2 ppm).

2-Cyclohexyl-6-*N,N*-dimethylamino-5-[2,3,5,6-tetrafluoro-4-(trifluoromethyl)benzamido]-

1*H*-benzo[*d*]imidazole (SB-P17G-A53): Yellow solid (30 % yield); mp = 204-205 °C; ¹H NMR (400 MHz, Methanol-*d*₄) δ 1.32 - 1.55 (m, 3 H), 1.60 - 1.73 (m, 2 H), 1.79 (d, *J* = 12.55 Hz, 1 H), 1.83 - 1.94 (m, 2 H), 2.08 (d, *J* = 11.54 Hz, 2 H), 2.70 (s, 6 H), 2.82 - 2.95 (m, 1 H), 7.42 (s, 1 H), 8.38 (s, 1 H); ¹³C NMR (101 MHz, Methanol-*d*₄) δ 27.1, 27.3, 33.0, 40.0, 45.9, 107.6, 108.3, 128.9, 135.3, 137.9, 143.1, 144.3, 146.9, 156.9, 161.9; HRMS (FAB) *m/z* calcd for C₂₃H₂₁F₇N₄OH⁺: 503.1676, Found: 503.1665 (Δ = -2.2 ppm).

2-Cyclohexyl-6-*N,N*-dimethylamino-5-[6-fluoro-2,4-(trifluoromethyl)benzamido]-

1*H*-benzo[*d*]imidazole (SB-P17G-A52): A solution of 6-fluoro-2,4-(trifluoromethyl)benzoic acid (139 mg, 0.5 mmol), oxalyl chloride (65 μL, 0.75 mmol), dimethylformamide (few drops) in dichloromethane (2 mL) was stirred overnight at room temperature to obtain the corresponding acyl chloride (crude). To this was added **2-4c** (130 mg, 0.5 mmol) and triethylamine (210 μL, 1.5 mmol). The reaction was stirred at room temperature for 14 h. After completion, the reaction mixture was transferred to a separatory funnel, diluted with ethyl acetate and washed with sat. sodium bicarbonate solution, water and brine. The organic layer was dried over magnesium sulfate, filtered and concentrated on a rotary evaporator followed by silica gel column chromatography (gradient: 1:1 ethyl acetate/hexanes) to obtain the product as a yellow solid (198 mg, 77% yield over two steps); mp = 233-234 °C; ¹H NMR (500 MHz, Methanol-*d*₄) δ 1.29 - 1.49 (m, 3 H), 1.59 - 1.70 (m, 2 H), 1.72 - 1.80 (m, 1 H), 1.86 (dt, *J* = 12.97, 2.98 Hz, 2 H), 2.02 - 2.12 (m, 2 H), 2.66 (s, 6 H), 2.82 - 2.91 (m, 1 H), 7.40 (s, 1 H), 7.93 - 8.02 (m, 2 H), 8.38 (s, 1 H); ¹³C NMR (126 MHz, Methanol-*d*₄) δ 27.1, 27.3, 32.9, 40.0, 45.9, 107.6, 108.2, 118.9, 119.1, 120.7, 120.7, 122.9, 123.0, 123.0, 123.0, 125.1, 125.2, 127.3, 127.4, 129.3, 129.6,

129.8, 131.2, 131.2, 131.4, 131.5, 131.7, 131.7, 132.0, 132.0, 134.3, 134.4, 134.6, 134.6, 134.9, 134.9, 135.1, 137.8, 143.1, 159.9, 161.5, 161.8, 161.9; HRMS (FAB) m/z calcd for $C_{24}H_{23}F_7N_4OH^+$: 517.1833, Found: 517.1843 ($\Delta = -1.9$ ppm).

Evaluation of oxidative metabolic lability in mouse/human liver microsomes⁴²

Lability studies for the compounds were performed by our collaborators at Sanofi-Aventis as described below for **SB-P17G-A20**. Microsomal fractions were prepared in the Drug Disposition Domain at DSAR Montpellier (371 rue du Pr. J. Blayac, 34184 Montpellier Cedex 04, France). SB-P17G-A20 at 5 μ M concentration was incubated with microsomal proteins (human or mouse, 1 mg/mL) in an incubation buffer containing phosphate 0.1 M, pH 7.4 and 1 mM NADPH as cofactor for cytochrome P-450 (CYP). The flavin-containing monooxygenases (FMO)-dependent reactions were run in the presence of bovine serum albumin (BSA, 0.1%) for the duration of 0 and 20 min (with or without microsomal proteins and/or cofactors). Enzyme activity was stopped with one volume of acetonitrile containing the internal standard, dextromethorphan. Following protein precipitation with acetonitrile and their removal by centrifugation, supernatant fluids were analyzed by LC/MS-MS.

Chromatographic conditions for LC analysis for SB-P17G-A20: 5 μ L of the sample was injected to Hypersil Gold Thermo C18 (50 mm \times 2.1 mm, 1.9 μ m), Solvent A: ammonium acetate (0.08 g)/formic acid (2 mL)/HPLC water up to 1000 mL. Solvent B: ammonium acetate (0.08 g)/formic acid (2 mL)/methanol (200 mL)/acetonitrile up to 1000 mL, flow rate of 0.5 mL/min, $t = 0$ –3 min, gradient of 10–100% of B. Retention time for **SB-P17G-A20** was 1.52 min.

MS/MS condition used for detection: Thermo Finnigan TSQ Quantum Ultra instrument, ESI positive ion ionization mode. Each compound is studied in duplicates. Results are expressed in percentage of lability (or total metabolism).

Total metabolism = $[1 - (UC_1 \text{ Peak Area}) / (UC_2 \text{ Peak Area})] \times 100$.

UC_n = Unchanged compound in condition n ; $n = 1$: incubation in the presence of NADPH cofactor after $T = 20$ min; $n = 2$: incubation without cofactor at $T = 0$ min

2.5. References

1. Vollmer, W., The prokaryotic cytoskeleton: A putative target for inhibitors and antibiotics? *Appl. Microbiol. Biotechnol.* **2006**, *73*, 37-47
2. Margalit, D. N.; Romberg, L.; Mets, R. B.; Hebert, A. M.; Mitchison, T. J.; Kirschner, M. W.; RayChaudhuri, D., Targeting cell division: Small-molecule inhibitors of FtsZ GTPase perturb cytokinetic ring assembly and induce bacterial lethality. *Proc. Natl. Acad. Sci. U. S. A.* **2004**, *101*, 11821-11826
3. Ben-Yehuda, S.; Losick, R., Asymmetric cell division in *B. subtilis* involves a spiral-like intermediate of the cytokinetic protein FtsZ. *Cell* **2002**, *109*, 257-266
4. Goehring, N. W.; Beckwith, J., Diverse paths to midcell: assembly of the bacterial cell division machinery. *Curr. Biol.* **2005**, *15*, R514-R526
5. Leung, A. K. W.; White, E. L.; Ross, L. J.; Reynolds, R. C.; DeVito, J. A.; Borhani, D. W., Structure of *Mycobacterium tuberculosis* FtsZ Reveals Unexpected, G Protein-like Conformational Switches. *J. Mol. Biol.* **2004**, *342*, 953-970
6. Moller-Jensen, J.; Loewe, J., Increasing complexity of the bacterial cytoskeleton. *Curr. Opin. Cell Biol.* **2005**, *17*, 75-81
7. Thanedar, S.; Margolin, W., FtsZ Exhibits Rapid Movement and Oscillation Waves in Helix-like Patterns in *Escherichia coli*. *Curr. Biol.* **2004**, *14*, 1167-1173
8. de Boer, P.; Crossley, R.; Rothfield, L., The essential bacterial cell-division protein FtsZ is a GTPase. *Nature* **1992**, *359*, 254-6
9. RayChaudhuri, D.; Park, J. T., *Escherichia coli* cell-division gene *ftsZ* encodes a novel GTP-binding protein. *Nature* **1992**, *359*, 251-4
10. Adams, D. W.; Errington, J., Bacterial cell division: assembly, maintenance and disassembly of the Z ring. *Nat. Rev. Microbiol.* **2009**, *7*, 642-653
11. Erickson Harold, P.; Anderson David, E.; Osawa, M., FtsZ in bacterial cytokinesis: cytoskeleton and force generator all in one. *Microbiol. Mol. Biol. Rev.* **2010**, *74*, 504-28
12. Errington, J.; Daniel, R. A.; Scheffers, D.-J., Cytokinesis in bacteria. *Microbiol. Mol. Biol. Rev.* **2003**, *67*, 52-65
13. Huang, Q.; Kirikae, F.; Kirikae, T.; Pepe, A.; Amin, A.; Respicio, L.; Slayden, R. A.; Tonge, P. J.; Ojima, I., Targeting FtsZ for Antituberculosis Drug Discovery: Noncytotoxic Taxanes as Novel Antituberculosis Agents. *J. Med. Chem.* **2006**, *49*, 463-466

14. Kumar, K.; Awasthi, D.; Berger, W. T.; Tonge, P. J.; Slayden, R. A.; Ojima, I., Discovery of anti-TB agents that target the cell-division protein FtsZ. *Future Med. Chem.* **2010**, *2*, 1305-1323
15. Respicio, L.; Nair, P. A.; Huang, Q.; Burcu, A. B.; Tracz, S.; Truglio, J. J.; Kisker, C.; Raleigh, D. P.; Ojima, I.; Knudson, D. L.; Tonge, P. J.; Slayden, R. A., Characterizing Septum Inhibition in Mycobacterium tuberculosis for Novel Drug Discovery. *Tuberculosis* **2008**, *88*, 420-429
16. Slayden, R. A.; Knudson, D. L.; Belisle, J. T., Identification of cell cycle regulators in Mycobacterium tuberculosis by inhibition of septum formation and global transcriptional analysis. *Microbiology* **2006**, *152*, 1789-1797
17. Huang, Q.; Tonge Peter, J.; Slayden Richard, A.; Kirikae, T.; Ojima, I., FtsZ: a novel target for tuberculosis drug discovery. *Curr. Top. Med. Chem.* **2007**, *7*, 527-43
18. Lock, R. L.; Harry, E. J., Cell-division inhibitors: new insights for future antibiotics. *Nat. Rev. Drug Discovery* **2008**, *7*, 324-338
19. Margolin, W., Themes and variations in prokaryotic cell division. *FEMS Microbiol. Rev.* **2000**, *24*, 531-548
20. Rothfield, L.; Justice, S.; Garcia-Lara, J., Bacterial cell division. *Annu. Rev. Genet.* **1999**, *33*, 423-448
21. Haydon, D. J.; Stokes, N. R.; Ure, R.; Galbraith, G.; Bennett, J. M.; Brown, D. R.; Baker, P. J.; Barynin, V. V.; Rice, D. W.; Sedelnikova, S. E.; Heal, J. R.; Sheridan, J. M.; Aiwale, S. T.; Chauhan, P. K.; Srivastava, A.; Taneja, A.; Collins, I.; Errington, J.; Czaplewski, L. G., An Inhibitor of FtsZ with Potent and Selective Anti-Staphylococcal Activity. *Science* **2008**, *321*, 1673-1675
22. Awasthi, D.; Kumar, K.; Ojima, I., Therapeutic potential of FtsZ inhibition: a patent perspective. *Expert Opin. Ther. Pat.* **2011**, *21*, 657-679
23. Beuria, T. K.; Singh, P.; Surolia, A.; Panda, D., Promoting assembly and bundling of FtsZ as a strategy to inhibit bacterial cell division: A new approach for developing novel antibacterial drugs. *Biochem. J.* **2009**, *423*, 61-69
24. White, E. L.; Suling, W. J.; Ross, L. J.; Seitz, L. E.; Reynolds, R. C., 2-Alkoxy-carbonylaminopyridines: inhibitors of Mycobacterium tuberculosis FtsZ. *J. Antimicrob. Chemother.* **2002**, *50*, 111-114

25. Reynolds, R. C.; Srivastava, S.; Ross, L. J.; Suling, W. J.; White, E. L., A new 2-carbamoyl pteridine that inhibits mycobacterial FtsZ. *Bioorg. Med. Chem. Lett.* **2004**, *14*, 3161-3164
26. Kumar, K.; Awasthi, D.; Lee, S.-Y.; Zanardi, I.; Ruzsicska, B.; Knudson, S.; Tonge, P. J.; Slayden, R. A.; Ojima, I., Novel Trisubstituted Benzimidazoles, Targeting Mtb FtsZ, as a New Class of Antitubercular Agents. *J. Med. Chem.* **2011**, *54*, 374-381
27. Laeppchen, T.; Hartog, A. F.; Pinas, V. A.; Koomen, G.-J.; Den Blaauwen, T., GTP Analogue Inhibits Polymerization and GTPase Activity of the Bacterial Protein FtsZ without Affecting Its Eukaryotic Homologue Tubulin. *Biochemistry* **2005**, *44*, 7879-7884
28. Paradis-Bleau, C.; Beaumont, M.; Sanschagrin, F.; Voyer, N.; Levesque, R. C., Parallel solid synthesis of inhibitors of the essential cell division FtsZ enzyme as a new potential class of antibacterials. *Bioorg. Med. Chem.* **2007**, *15*, 1330-1340
29. Parhi, A.; Kelley, C.; Kaul, M.; Pilch, D. S.; LaVoie, E. J., Antibacterial activity of substituted 5-methylbenzo[c]phenanthridinium derivatives. *Bioorg. Med. Chem. Lett.* **2012**, *22*, 7080-7083
30. Beuria, T. K.; Santra, M. K.; Panda, D., Sanguinarine Blocks Cytokinesis in Bacteria by Inhibiting FtsZ Assembly and Bundling. *Biochemistry* **2005**, *44*, 16584-16593
31. Mathew, B.; Ross, L.; Reynolds, R. C., A novel quinoline derivative that inhibits mycobacterial FtsZ. *Tuberculosis* **2013**, *93*, 398-400
32. Kelley, C.; Zhang, Y.; Parhi, A.; Kaul, M.; Pilch, D. S.; LaVoie, E. J., 3-Phenyl substituted 6,7-dimethoxyisoquinoline derivatives as FtsZ-targeting antibacterial agents. *Bioorg. Med. Chem.* **2012**, *20*, 7012-7029
33. Parhi, A.; Lu, S.; Kelley, C.; Kaul, M.; Pilch, D. S.; LaVoie, E. J., Antibacterial activity of substituted dibenzo[a,g]quinolizin-7-ium derivatives. *Bioorg. Med. Chem. Lett.* **2012**, *22*, 6962-6966
34. Haydon, D. J.; Bennett, J. M.; Brown, D.; Collins, I.; Galbraith, G.; Lancett, P.; Macdonald, R.; Stokes, N. R.; Chauhan, P. K.; Sutariya, J. K.; Nayal, N.; Srivastava, A.; Beanland, J.; Hall, R.; Henstock, V.; Noula, C.; Rockley, C.; Czaplewski, L., Creating an antibacterial with in vivo efficacy: synthesis and characterization of potent inhibitors of the bacterial cell division protein FtsZ with improved pharmaceutical properties. *J. Med. Chem.* **2010**, *53*, 3927-3936

35. Margalit, D. N.; Romberg, L.; Mets, R. B.; Hebert, A. M.; Mitchison, T. J.; Kirschner, M. W.; RayChaudhuri, D., Targeting cell division: Small-molecule inhibitors of FtsZ GTPase perturb cytokinetic ring assembly and induce bacterial lethality. [Erratum to document cited in CA141:271048]. *Proc. Natl. Acad. Sci. U. S. A.* **2004**, *101*, 13969
36. Plaza, A.; Keffer, J. L.; Bifulco, G.; Lloyd, J. R.; Bewley, C. A., Chrysopaentins A-H, antibacterial bisdiarylbutene macrocycles that inhibit the bacterial cell division protein FtsZ. *J. Am. Chem. Soc.* **2010**, *132*, 9069-9077
37. Mathew, B.; Srivastava, S.; Ross, L. J.; Suling, W. J.; White, E. L.; Woolhiser, L. K.; Lenaerts, A. J.; Reynolds, R. C., Novel pyridopyrazine and pyrimidothiazine derivatives as FtsZ inhibitors. *Bioorg. Med. Chem.* **2011**, *19*, 7120-7128
38. Sarcina, M.; Mullineaux, C. W., Effects of tubulin assembly inhibitors on cell division in prokaryotes in vivo. *FEMS Microbiol. Lett.* **2000**, *191*, 25-29
39. Slayden, R. A.; Knudson, D. L.; Belisle, J. T., Identification of cell cycle regulators in *Mycobacterium tuberculosis* by inhibition of septum formation and global transcriptional analysis. *Microbiology* **2006**, *152*, 1789-1797
40. Awasthi, D.; Kumar, K.; Knudson, S. E.; Slayden, R. A.; Ojima, I., SAR Studies on Trisubstituted Benzimidazoles as Inhibitors of Mtb FtsZ for the Development of Novel Antitubercular Agents. *J. Med. Chem.* **2013**, *56*, 9756-9770
41. Knudson, S. E.; Kumar, K.; Awasthi, D.; Ojima, I.; Slayden, R. A., Potency of benzimidazoles and in vitro activity–efficacy relationship against *Mycobacteria tuberculosis*. *Tuberculosis* **2014**, *94*, 271-276
42. Knudson, S. E.; Awasthi, D.; Kumar, K.; Ojima, I.; Slayden, R. A., A Trisubstituted benzimidazole cell division inhibitor with efficacy against *Mycobacteria tuberculosis*. *PLoS ONE* **2014**, *9*, e93953 (2014)
43. Yoakim, C.; Ogilvie, W. W.; Cameron, D. R.; Chabot, C.; Guse, I.; Hache, B.; Naud, J.; O'Meara, J. A.; Plante, R.; Deziel, R., Î²-Lactam Derivatives as Inhibitors of Human Cytomegalovirus Protease. *J. Med. Chem.* **1998**, *41*, 2882-2891
44. Iranpoor, N.; Firouzabadi, H.; Nowrouzi, N.; Khalili, D., Selective mono- and di-N-alkylation of aromatic amines with alcohols and acylation of aromatic amines using Ph₃P/DDQ. *Tetrahedron* **2009**, *65*, 3893-3899

Chapter 3

Target Validation and *In vivo-In vitro* Evaluation of Novel Benzimidazole-Based Anti-tubercular Agents

Table of Contents

| | |
|----------------------------------------------------------------------------------|-----|
| Chapter 3 | 86 |
| 3.1. FtsZ as a novel target for antibacterial drug discovery | 87 |
| 3.2. Results and Discussion..... | 89 |
| 3.2.1. <i>Mtb</i> FtsZ Polymerization Inhibitory Assay | 89 |
| 3.2.2. <i>Mtb</i> FtsZ GTPase Assay | 90 |
| 3.2.3. Transmission Electron Microscopy (TEM) analysis | 91 |
| 3.2.4. Photo-affinity labeling | 95 |
| 3.2.5. <i>In vivo</i> and <i>in vitro</i> evaluation of lead benzimidazoles..... | 96 |
| 3.2.6. ADME profiling of lead compounds | 100 |
| 3.3. Conclusion | 101 |
| 3.4. Experimental Section..... | 102 |
| 3.5. References..... | 107 |

3.1. FtsZ as a novel target for antibacterial drug discovery

FtsZ is an essential protein involved in bacterial cell division. FtsZ polymerization is believed to initiate from a single point on the inner surface of the cell membrane and it rapidly extends bi-directionally to form an arc and then a closed ring called the Z-ring.^{1,2,3,4,5} FtsZ polymerization is GTP dependent and the resultant Z-ring is dynamic in nature with a rapid turnover since, a large number of FtsZ monomers are present in the cytoplasm of the dividing cell.⁶ The septation process is initiated by unknown signals which, then initiates the contraction of the Z ring and its de-polymerization.

Three crystal structures of *Mtb* FtsZ complexed to citrate (PDB 1rq2), GDP (PDB 1rq7) and GTP- γ -S (PDB 1rlu) have been determined to shed some light into the polymerization of FtsZ.³ It is still not known whether FtsZ monomers polymerize longitudinally or laterally. Leung *et al.* have proposed that the two *Mtb* FtsZ subunits associate laterally unlike tubulin subunits which associate longitudinally.³ They have proposed a spiral filament model for FtsZ based on the presence of a secondary structural switch in subunit A (H2 residues 41-50) and subunit B. They observed that in subunit A, H2 adopts α -helical conformation whereas in subunit B it adopts a β -stranded conformation.

More recently Li *et al.* have reported a structure of *Mtb* FtsZ bound to GDP in which the subunits are arranged in a head-to-tail manner, and display a curved conformational state.⁷ They identified Leu268 as a key residue involved in the hydrophobic inter-subunit interaction which on mutation from L269E failed to polymerize *in vitro*. They have proposed a “hinge-opening” motion pivoted around the interface of the *Mtb*-FtsZ-GDP dimer. The T3 loop which interacts extensively with the T7 loop of the top FtsZ subunit adopts a compact state (Tension or T state) when bound to GTP and switches to a relaxed conformation (R state) when bound to GDP. The switch of the T3 loop from T to R state triggered by the hydrolysis of GTP and release of the γ -phosphate weakens the T3-T7 interaction driving the hinge-opening event around the pivot point leading to the curved conformational state of the FtsZ polymer. According to their studies, the straight to curved transition of FtsZ protofilament may provide enough energy for Z-ring constriction and supports the “hydrolyze and bend” model proposed by Erickson *et al.*⁸

Figure 3.1 displays the conformational changes *Mtb* FtsZ undergoes following GTP hydrolysis. The T3 loop is in the T state when FtsZ monomer binds GTP. GTP bound FtsZs interact longitudinally to form a dimer in which the T3 loop on one monomer interacts extensively with T7 loop of the other monomer. Following GTP hydrolysis and release of the γ -phosphate, the T3 loop adopts the R state leading to a bend centered on L269 which gives the curved longitudinal dimer.⁷

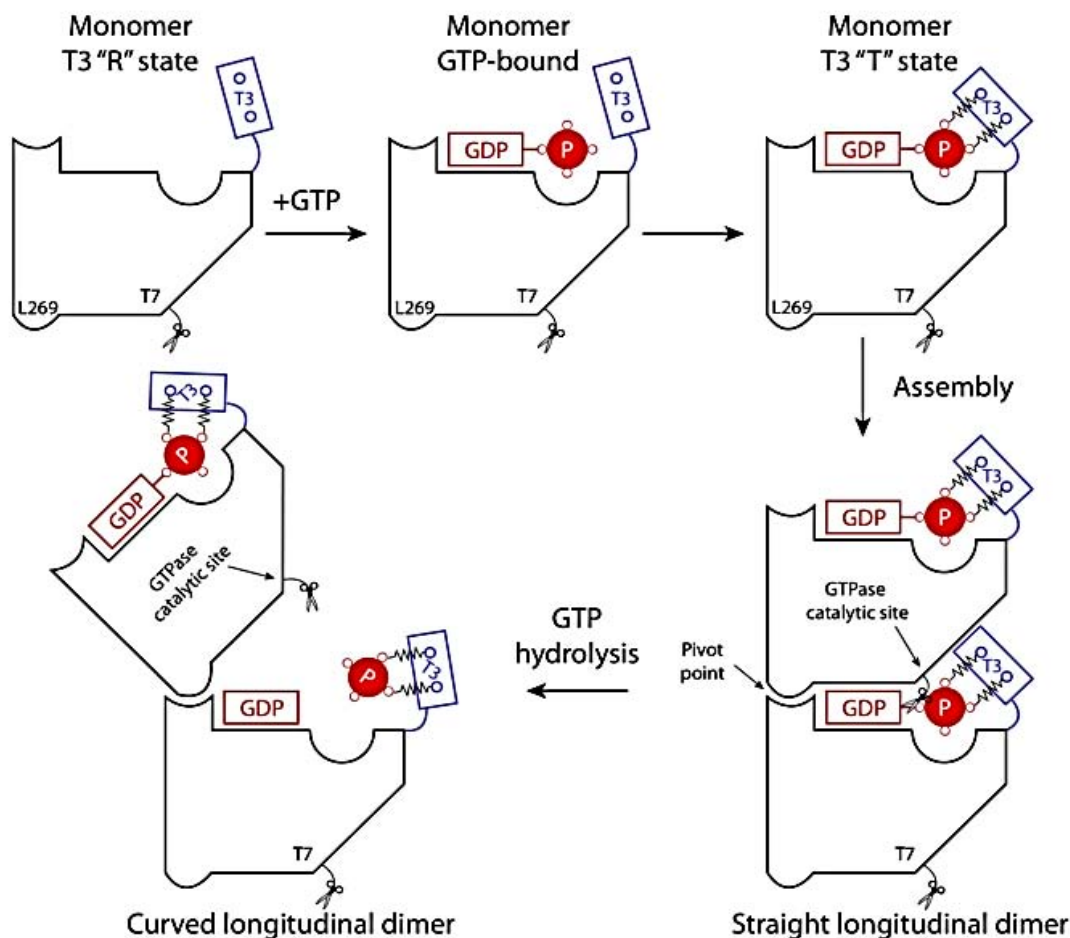


Figure 3.1. Proposed conformational change induced in FtsZ dimer
Adapted from Ref. 8

Although FtsZ functioning and dynamics are not completely understood, it is actively being investigated as a drug target. So far, compounds targeting FtsZ can be divided into two groups; a) FtsZ polymer stabilizing agents and b) inhibitor of FtsZ polymerization.^{9, 10} Several classes of compounds have been identified as promising leads for antibacterial drug development, including OTBA,¹¹ 2-alkoxycarbonylaminopyridines,¹² 2-carbamoylpteridine,¹³ taxanes,¹⁴

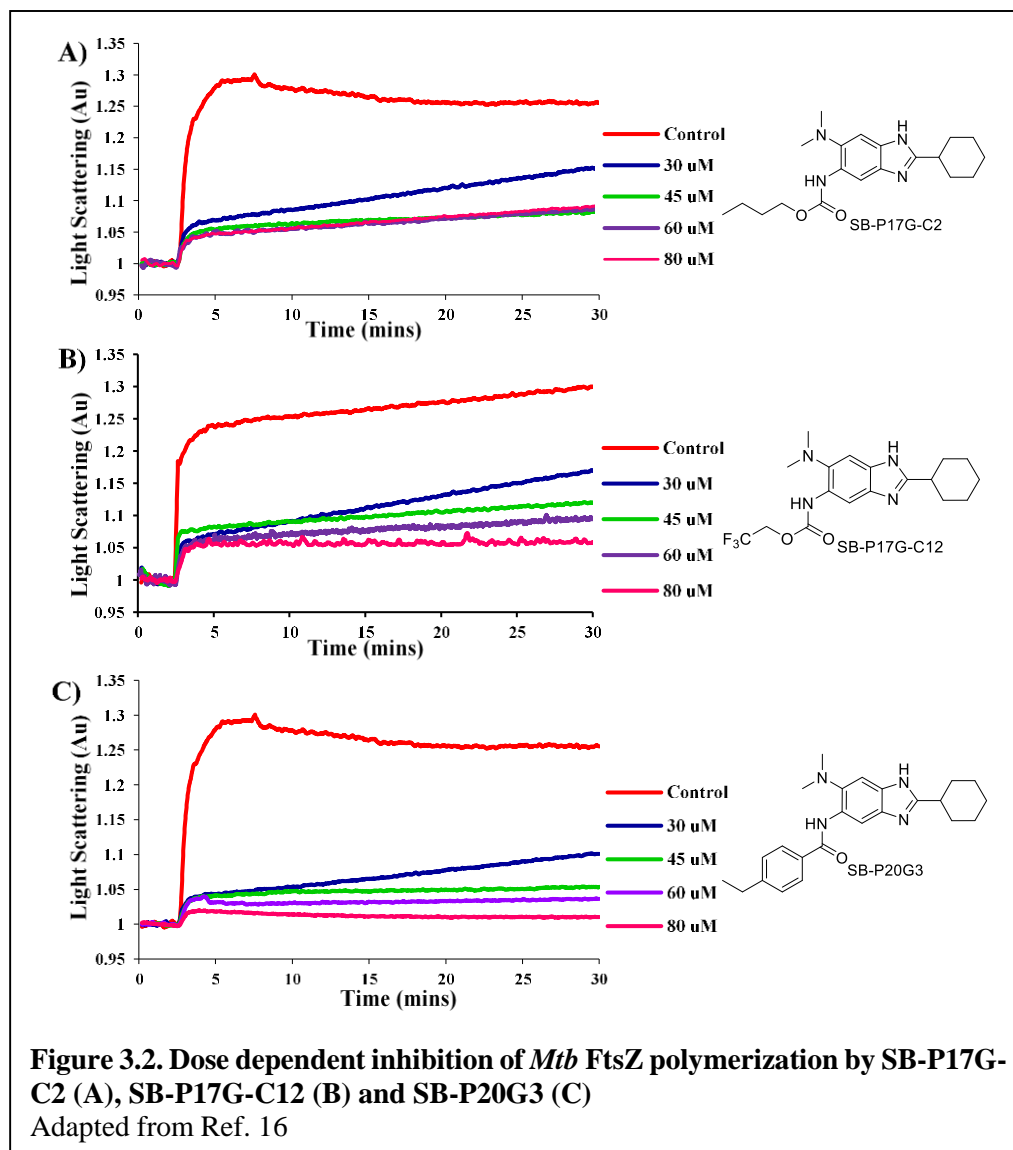
benzimidazoles,¹⁵⁻¹⁷ GTP analogs,^{18, 19} benzo[c]phenanthridines,^{20, 21} isoquinolines,²²⁻²⁴ PC190723,^{25, 26} Zantrins,²⁷ and chrysophaentins²⁸. Against *Mtb* FtsZ, only taxanes¹⁴ and benzimidazoles¹⁵⁻¹⁷ developed in the Ojima lab have emerged as promising leads in the last several years after the pioneering work by the Southern Research Institute group.^{12, 13, 22, 29}

To prove the hypothesis that our potent and efficacious trisubstituted benzimidazoles inhibit *Mtb* FtsZ, the protein was expressed in *E. coli* and the effect of the compounds on the protein was evaluated by a) Light scattering assay b) GTPase assay and c) TEM imaging. In addition, the ADME profiles of the lead compounds were evaluated. The most promising compounds were assessed in the animal model of TB infection.

3.2. Results and Discussion

3.2.1. *Mtb* FtsZ Polymerization Inhibitory Assay

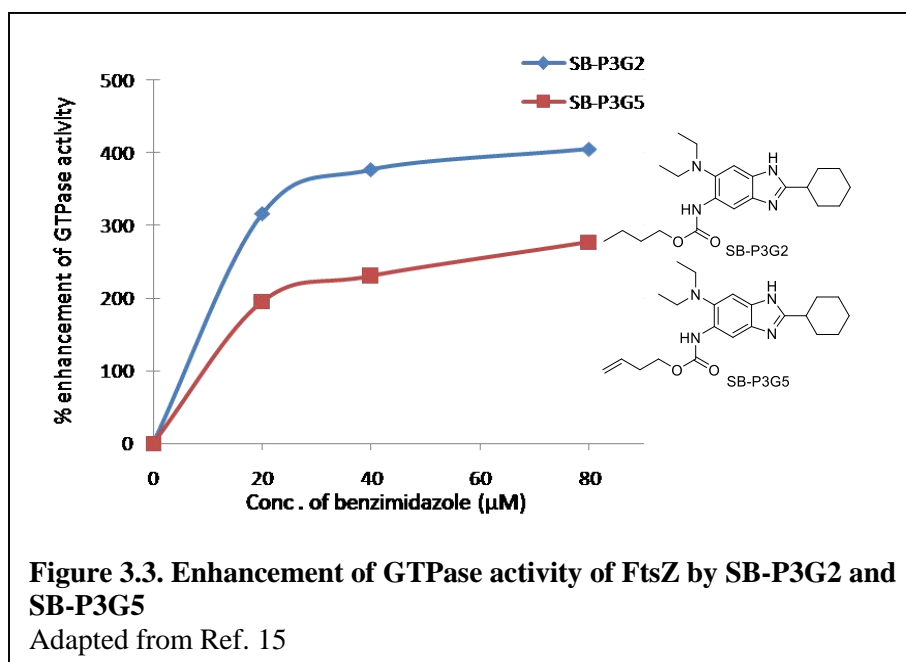
The parent lead compounds **SB-P3G2**, **SB-P3G5**, and **SB-P1G8** have been shown to inhibit the polymerization of *Mtb* FtsZ *in vitro*, in a dose dependent manner. To confirm that the new series of compounds also target *Mtb* FtsZ, the most potent compound, **SB-P17G-C2**, was selected for the light scattering assay.^{15, 16, 30} In addition, compounds **SB-P17G-C12**, and **SB-P20G3** with MIC of 0.63 µg/mL and 0.16 µg/mL, respectively, were also tested. As **Figure 3.2** shows, **SB-P17G-C2**, **SB-P17G-C12** and **SB-P20G3** inhibit the assembly of *Mtb* FtsZ in a dose dependent manner. Since the extent of light scattering correlates to the extent of FtsZ polymerization/aggregation, reduction in light scattering in presence of the compounds demonstrates their inhibitory effect on *Mtb* FtsZ assembly.



3.2.2. *Mtb* FtsZ GTPase Assay

The assembly and disassembly of FtsZ protein has been shown to be GTP dependent. Since FtsZ has GTPase activity, the Malachite Green assay³¹ was performed to monitor the amount of inorganic phosphate (Pi) released upon treatment of *Mtb* FtsZ with two lead compounds, **SB-P3G2** and **SB-P3G5**. On treatment of *Mtb* FtsZ with these two compounds, an enhancement in GTPase activity was observed (**Figure 3.3**).¹⁵ This unique behavior is analogous to the effect that curcumin exhibited on recombinant *E. coli* FtsZ.²⁸ Enhancement in the GTPase activity together with the fact that these compounds inhibit polymerization of *Mtb* FtsZ leads us to conclude that the increased GTPase activity causes the instability of *Mtb* FtsZ polymer. As a result of the instability,

Mtb FtsZ is unable to polymerize normally, leading to the efficient inhibition of the formation of sizable *Mtb* FtsZ polymers and filaments.



3.2.3. Transmission Electron Microscopy (TEM) analysis

To investigate the effect of the hit compounds on polymerization of the FtsZ protein, transmission electron microscopy (TEM) imaging of the treated and untreated *Mtb* FtsZ protein was carried out. The experiment has been performed several times with the potent trisubstituted benzimidazoles.

TEM imaging with SB-P3G2:¹⁵ *Mtb* FtsZ (5 μM) polymerized in the presence of GTP (25 μM), was diluted 5 times with polymerization buffer and immediately transferred onto a carbon coated copper-mesh grid for TEM imaging. *Mtb* FtsZ protein treated with GTP and 40/80 μM **SB-P3G2** were visualized (**Figure 3.4**). The protein treated with colchicine, which is known to inhibit FtsZ polymerization, was used as a reference in this set of experiments (**Figure 3.4F, G**). As anticipated, there was a considerable reduction in the extent of FtsZ protofilament formation upon treatment with **SB-P3G2** compared to the control experiment. At 40 μM **SB-P3G2**, the density of *Mtb* FtsZ protofilaments was substantially reduced (**Figure 3.4B, C**). Furthermore, the protofilaments were short and very thin. At 80 μM, the formation of protofilaments was drastically reduced and only numerous tiny aggregates were formed (**Figure 3.4D, E**). In sharp contrast, the

Mtb FtsZ protein treated with a high concentration (200 μ M) of colchicine showed decreased and thinner protofilaments (**Figure 3.4G, H**) but with more or less similar morphology compared with that of GTP-initiated polymerization and protofilaments (**Figure 3.4A, B**). These results clearly indicate the highly efficient inhibition of *Mtb* FtsZ assembly by **SB-P3G2** in a dose-dependent manner with a novel mechanism of action.

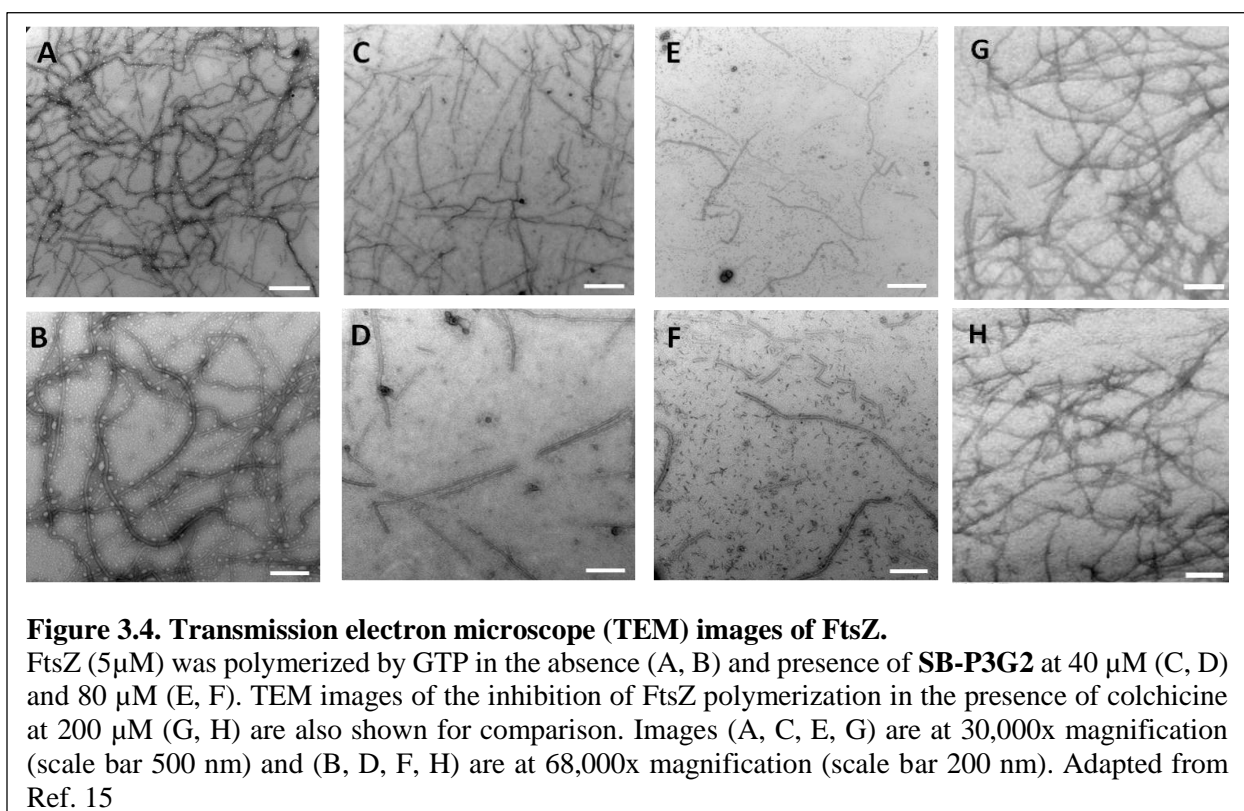


Figure 3.4. Transmission electron microscope (TEM) images of FtsZ.

FtsZ (5 μ M) was polymerized by GTP in the absence (A, B) and presence of **SB-P3G2** at 40 μ M (C, D) and 80 μ M (E, F). TEM images of the inhibition of FtsZ polymerization in the presence of colchicine at 200 μ M (G, H) are also shown for comparison. Images (A, C, E, G) are at 30,000x magnification (scale bar 500 nm) and (B, D, F, H) are at 68,000x magnification (scale bar 200 nm). Adapted from Ref. 15

TEM Imaging with SB-P17G-C2 and SB-P17G-A20: As the optimization of the lead benzimidazoles progressed, more potent compounds were identified and TEM imaging was performed with several of the new leads to confirm their target. To visualize the effect of the most active compounds, **SB-P17G-C2** and **SB-P17G-A20**, TEM imaging was performed. At 40 μ M treatment for both the drugs the polymers formed were short and thin when compared to control. At 80 μ M treatment with **SB-P17G-C2**, the effect was more apparent but for **SB-P17G-A20** surprisingly, very few regions of the grid showed any polymers (**Figure 3.5**).³² Mostly the grid was empty implying that the drug is very effective. To optimize the experiment, next time the grids were prepared by diluting the sample 2 times versus 5 times before loading on the grid.

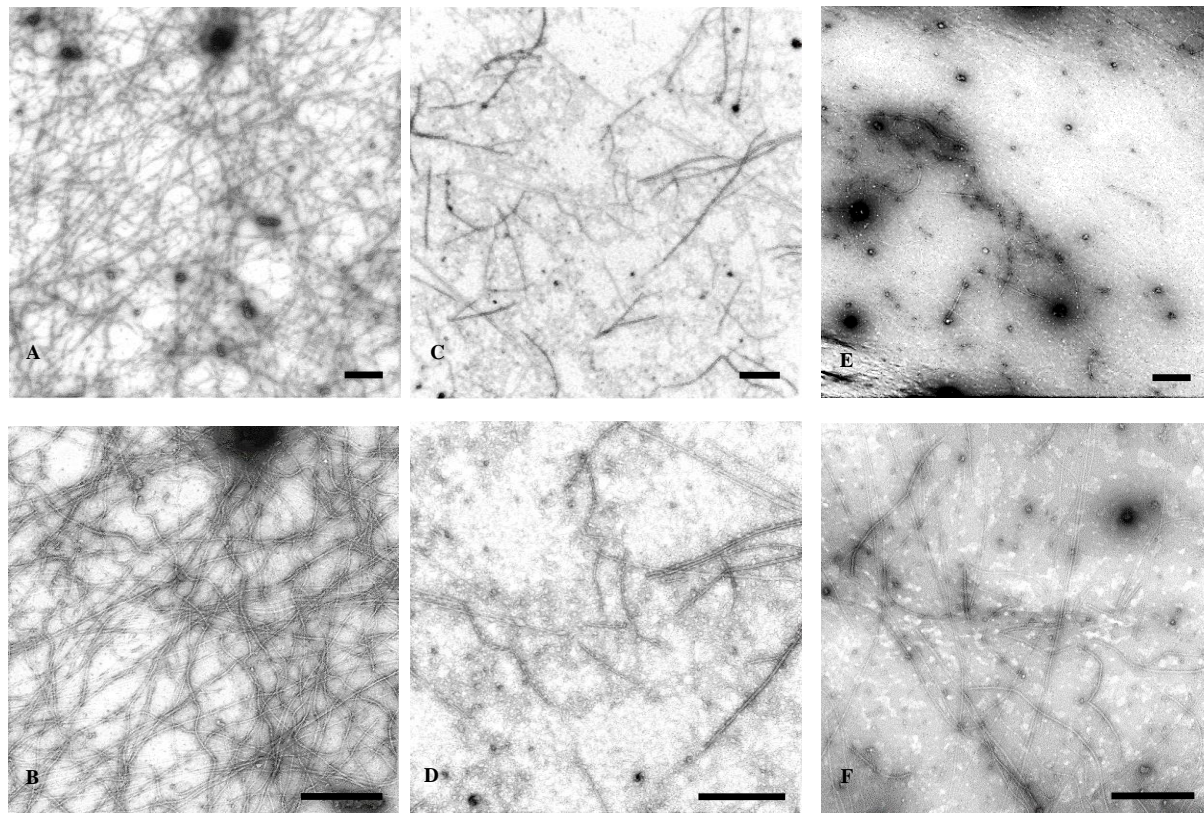
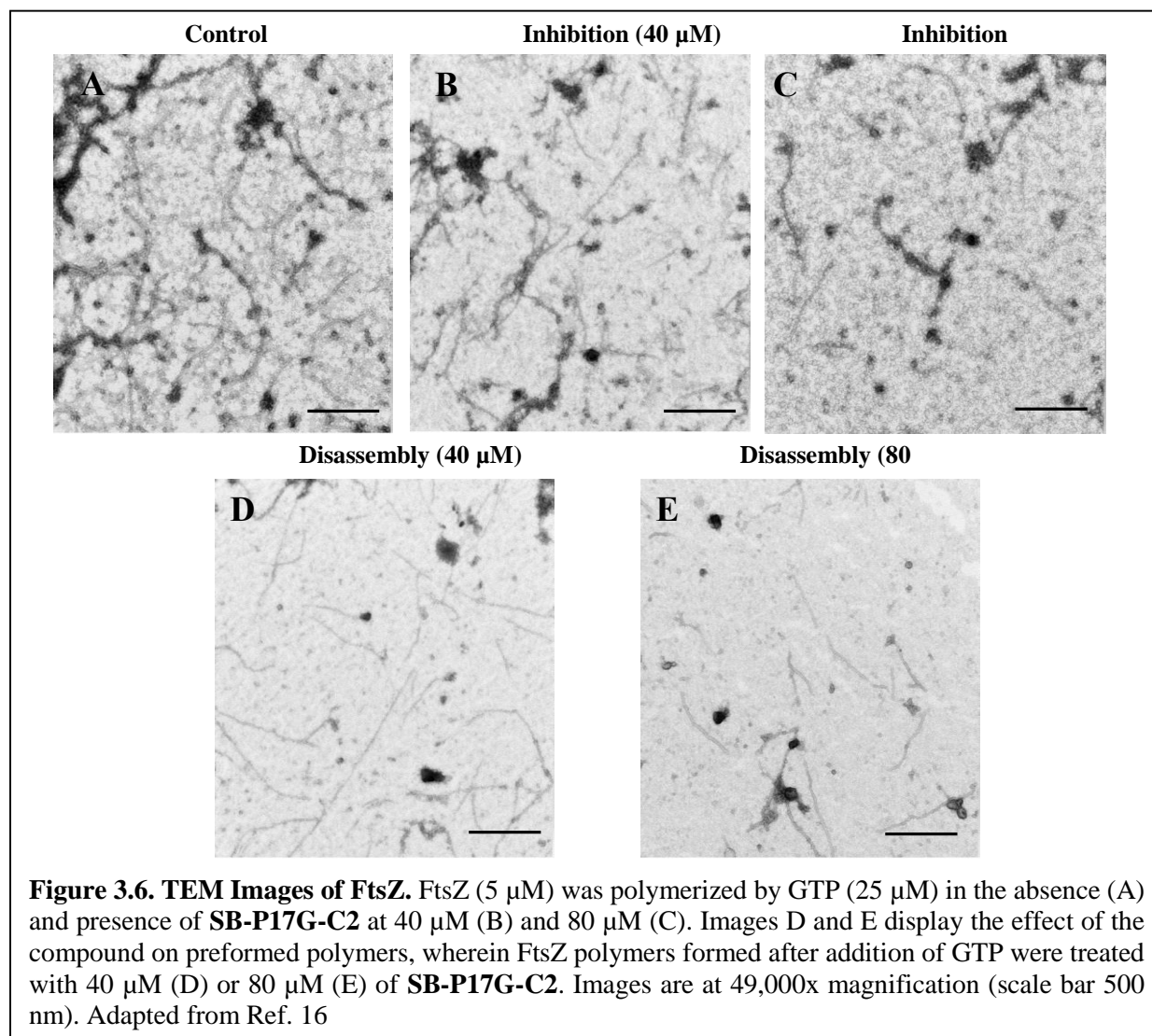
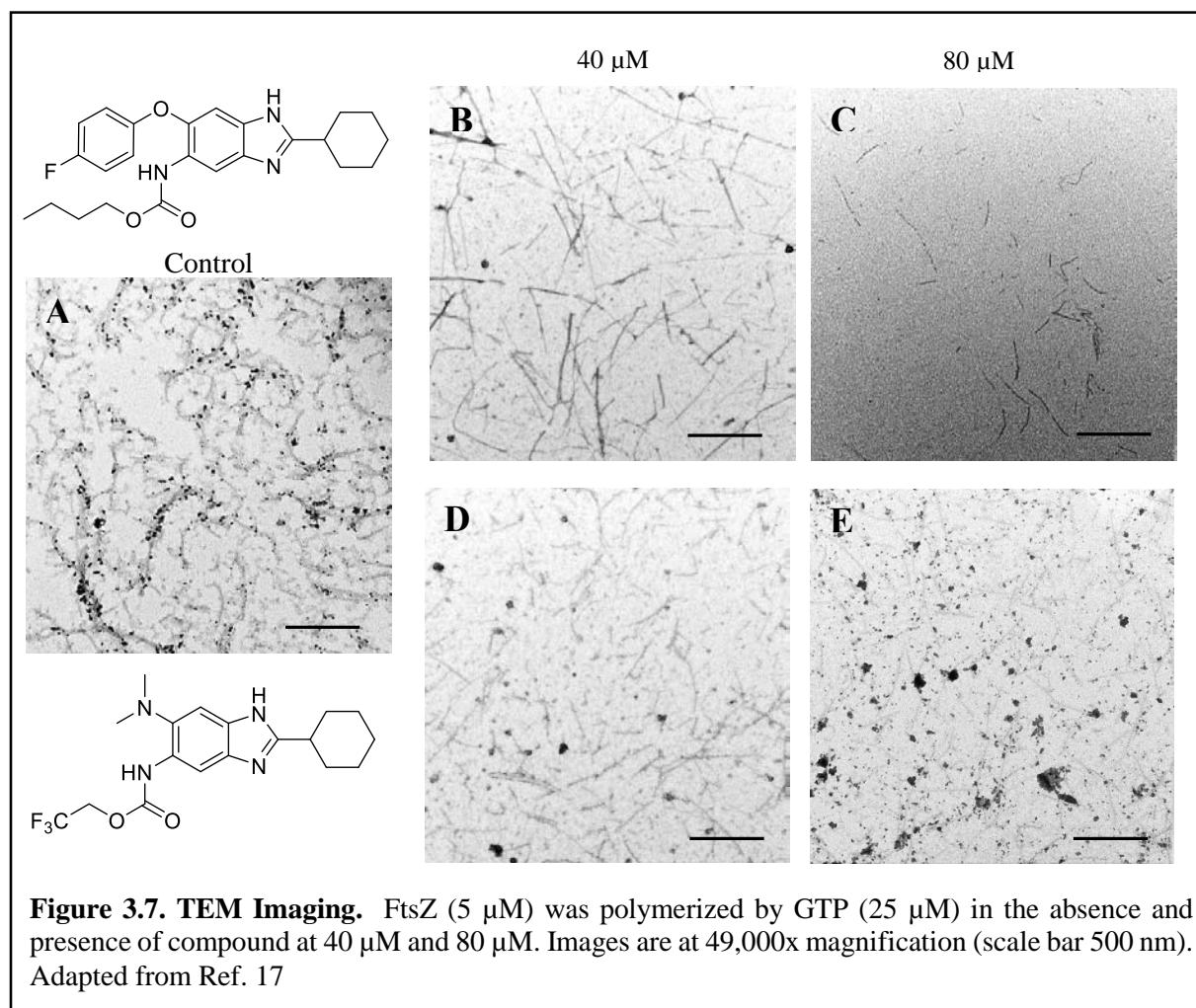


Figure 3.5. Transmission Electron Microscopy (TEM) Images of FtsZ. FtsZ (5 μ M) was polymerized by GTP (25 μ M) in the absence (A, B) and presence of **SB-P17G-A20** at 40 μ M (C, D) and 80 μ M (E, F). Images A, C and E are 23000x magnification and B, D, F are at 49,000x magnification (scale bar 500 nm).

Disassembly of *Mtb* FtsZ Polymers with SB-P17G-C2:¹⁶ *Mtb* FtsZ (5 μ M) was incubated with 40 μ M or 80 μ M of **SB-P17G-C2** followed by addition of GTP (25 μ M) to initiate polymerization. The grids were prepared by diluting sample 2 times versus 5 times based on previous experiment. The TEM images of *Mtb* FtsZ treated with 40 μ M clearly showed reduction in the density and population of FtsZ polymers, protofilaments and aggregates when compared to the untreated protein polymers (**Figure 3.6A, B**). The effect was more apparent at 80 μ M treatment (**Figure 3.6C**). In addition to inhibiting the assembly of *Mtb* FtsZ in the presence of GTP, **SB-P17G-C2** was also capable of disrupting the formed FtsZ polymers and aggregates as shown by images D and E. *Mtb* FtsZ (5 μ M) was polymerized by adding GTP (25 μ M) and then treated with 40 μ M or 80 μ M of **SB-P17G-C2**. The polymerized protein was depolymerized/disassembled after the addition of **SB-P17G-C2**. These results clearly indicate that **SB-P17G-C2** interacts with *Mtb* FtsZ and deters its normal GTP initiated polymerization.



TEM Imaging with SB-P26D2¹⁷ and SB-P17G-C12: TEM imaging of *Mtb* FtsZ is also useful to validate the molecular target of lead compounds.¹⁵ *Mtb* FtsZ (5 μ M) was incubated with 40 μ M or 80 μ M of **SB-P26D2** (Figure 3.7B, C)¹⁷ and **SB-P17G-C12** (Figure 3.7D, E) followed by addition of GTP (25 μ M) to initiate polymerization. The TEM images of *Mtb* FtsZ treated with 40 μ M clearly show reduction in the density and population of FtsZ polymers, protofilaments and aggregates when compared to the untreated protein polymers (Figure 3.7A). The effect is more apparent at 80 μ M treatment (Figure 3.7C, E).

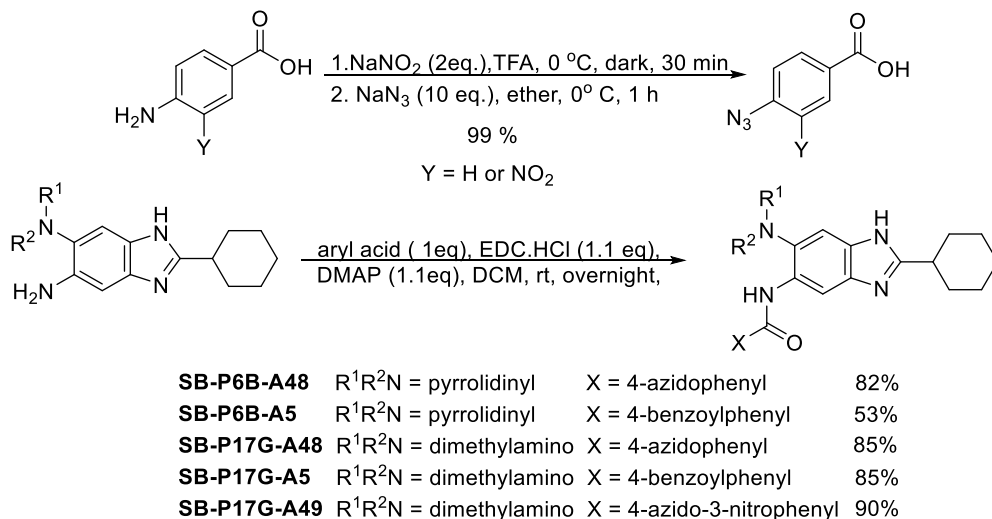


3.2.4. Photo-affinity labeling

We have synthesized very potent anti-tubercular compounds targeting the cell division protein FtsZ but the binding site of this series of compounds has not been identified so far. Photo-affinity labeling studies is one technique that can be employed to determine the binding site. This will allow the design of more efficacious trisubstituted benzimidazoles. In this vein, the synthesis of photo affinity labeled analogues of the lead benzimidazoles was initiated.

The synthesis of photoaffinity analogue with a *p*-azido group with respect to the 5 position benzamido group was carried out starting with diazotization of 4-aminobenzoic acid and subsequent nucleophilic substitution by azido group to form *p*-azidobenzoic acid in 99% yield. The acid was used to obtain 4-azido analogues of **SB-P6B8** and **SB-P17G-A15** using EDC/DMAP

coupling reaction. 4-Benzoylbenzoic acid is commercially available and the *p*-benzoyl analogues were also synthesized in the same manner.



Scheme 3.1. Synthesis of photo-affinity labeled analogues

The wavelength required to photolyze the azido group is <360 nm which induces protein degradation. Therefore, the 3-nitro-4-azidobenzamido analogue was also synthesized since a nitro group increases the wavelength required for optimal photolysis. The acid was synthesized from commercially available 4-amino-3-nitrobenzoic acid as previously described for 4-azidobenzoic acid and was coupled to the appropriate intermediate to obtain **SB-P17G-A49**.

The MIC values of these analogues will be determined against *Mtb* and the most potent molecule will be used in the photo-affinity labeling studies.

3.2.5. *In vivo* and *in vitro* evaluation of lead benzimidazoles

To evaluate the efficacy of the lead compounds (**Figure 3.8**) in animal model of TB infection, our collaborators at Colorado State University performed various studies. *Mtb* cell growth was monitored in the presence of different concentrations of our lead benzimidazoles, **SB-P3G2**, **SB-P8B2**, **SB-P17G-C2**, **SB-P17G-A16**, and **SB-P17G-A20**. Inhibition of bacterial cell growth was dose dependent and inhibition was observed at concentrations higher than 0.68 and 0.31 µg/mL for **SB-P3G2** and **SB-P8B2**, respectively. Similar results were observed for the other compounds at concentrations higher than the MIC value of the compounds.

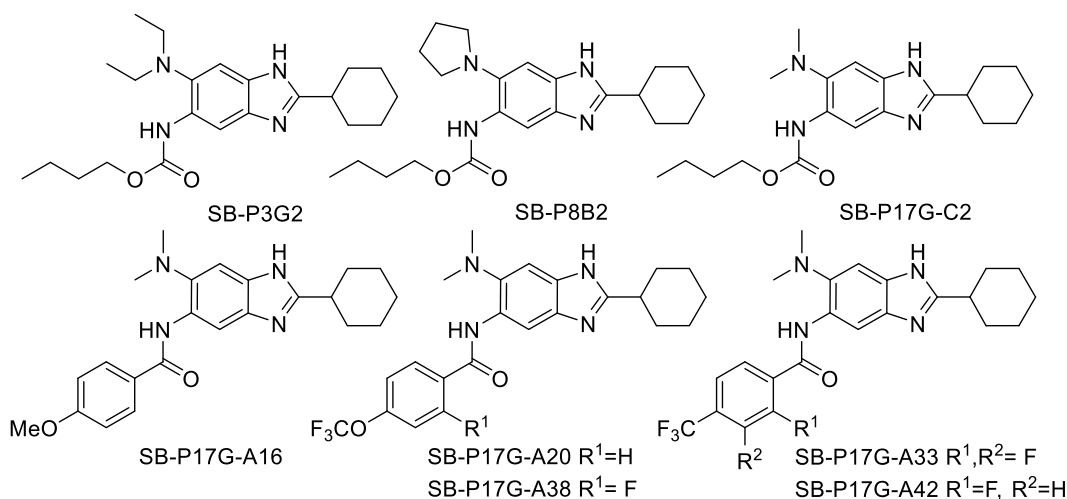


Figure 3.8. Structures of lead benzimidazoles

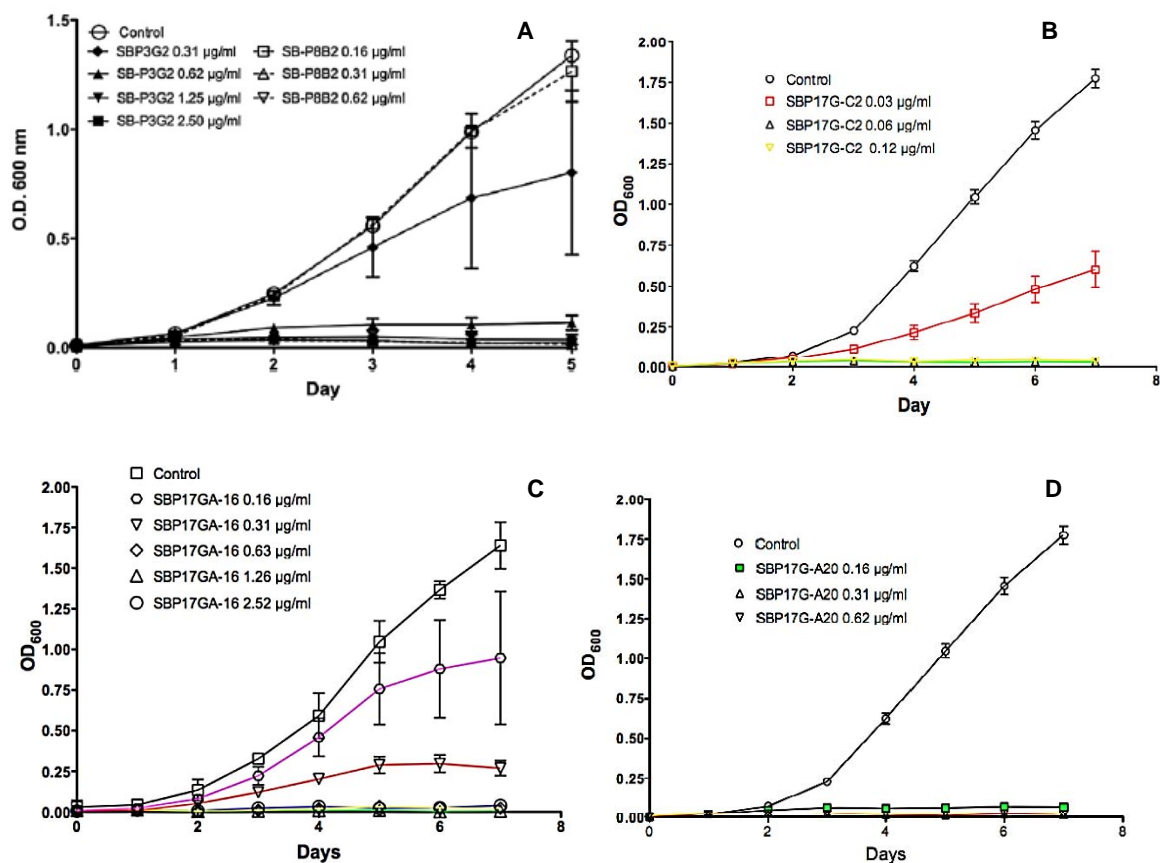


Figure 3.9. Time dose curve. Bacterial growth was assessed in the presence of different concentrations of (A) SBP3G2, (B) SB-P17G-C2, (C) SB-P17G-A16 and (D) SB-P17G-A20 by optical density. Adapted from Ref. 32 and Ref. 33

The most potent compounds were progressed to *in vivo* testing in the rapid mouse model of active tuberculosis infection. **SB-P3G2** when dosed IP at 150 mg/kg for 9 consecutive days to immune incompetent GKO mice reduced the bacterial load of *Mtb* H37Rv by $0.71 \pm 0.17 \log_{10}$ CFU in the lungs and $0.41 \pm 0.36 \log_{10}$ CFU in spleen.³³ Isoniazid reduced the bacterial load by $1.8 \log_{10}$ CFU in the lung and below the level of detection in the spleen. In the second dissemination model of infection using immune competent C57BL/6 mice, **SB-P3G2** reduced the bacterial load of *Mtb* Erdman in the spleen by \log_{10} CFU 1.6 ± 0.49 . Isoniazid reduced the bacterial load in the lung and spleen below detectable levels. In the different animal models tested, **SB-P3G2** always showed some level of detectable efficacy. Together, these animal studies showed that **SB-P3G2** had efficacy against an acute infection and could prevent dissemination to secondary sites.³³

Unlike **SB-P3G2**, **SB-P17G-C2** was not effective *in vivo* even though it has 13 fold better MIC value against *Mtb*. The lack of *in vivo* efficacy can be attributed to the poor metabolic stability of **SB-P17G-C2**. **SB-P17G-C2** was found to be stable in human plasma with 6.1% hydrolysis after 4 h of incubation but it was very unstable in mouse plasma undergoing 87.6% hydrolysis after 4 h incubation. To assess the extent of metabolic conversion, **SB-P17G-C2** was evaluated using a microsomal stability assay. It was found to be highly labile with 90% and 96% degradation in the presence of human and mouse liver microsomes, respectively. All the other carbamates followed the same trend.

In contrast, **SB-P17G-A16**, **SB-P17G-A20** and the more advanced lead compounds **SB-P17G-A33**, **SB-P17G-A38**, and **SB-P17G-A42** with a C-5 position benzamide displayed improved metabolic stability. In the TB murine acute model of infection, **SB-P17G-A20** resulted in reduction in bacterial load in the lungs and spleen by $1.73 \pm 0.24 \log_{10}$ CFU and $2.68 \pm \log_{10}$ CFU, respectively, when delivered at 50 mg/kg by (IP) twice daily (b.i.d).³² In addition to being effective via IP dosing, **SB-P17G-A38** and **SB-P17G-A42**, when dosed orally, successfully reduced the bacterial load in the lungs by 6 and 5.4 \log_{10} CFU, respectively. In the spleen, the observed reduction was 6.2 \log_{10} CFU for both the compounds. These results are very exciting since treatment with the two compounds essentially eliminated all live bacteria from the spleen of the infected mice. These highly promising results reveal the tremendous potential of our benzimidazoles as next-generation antibacterial agents.

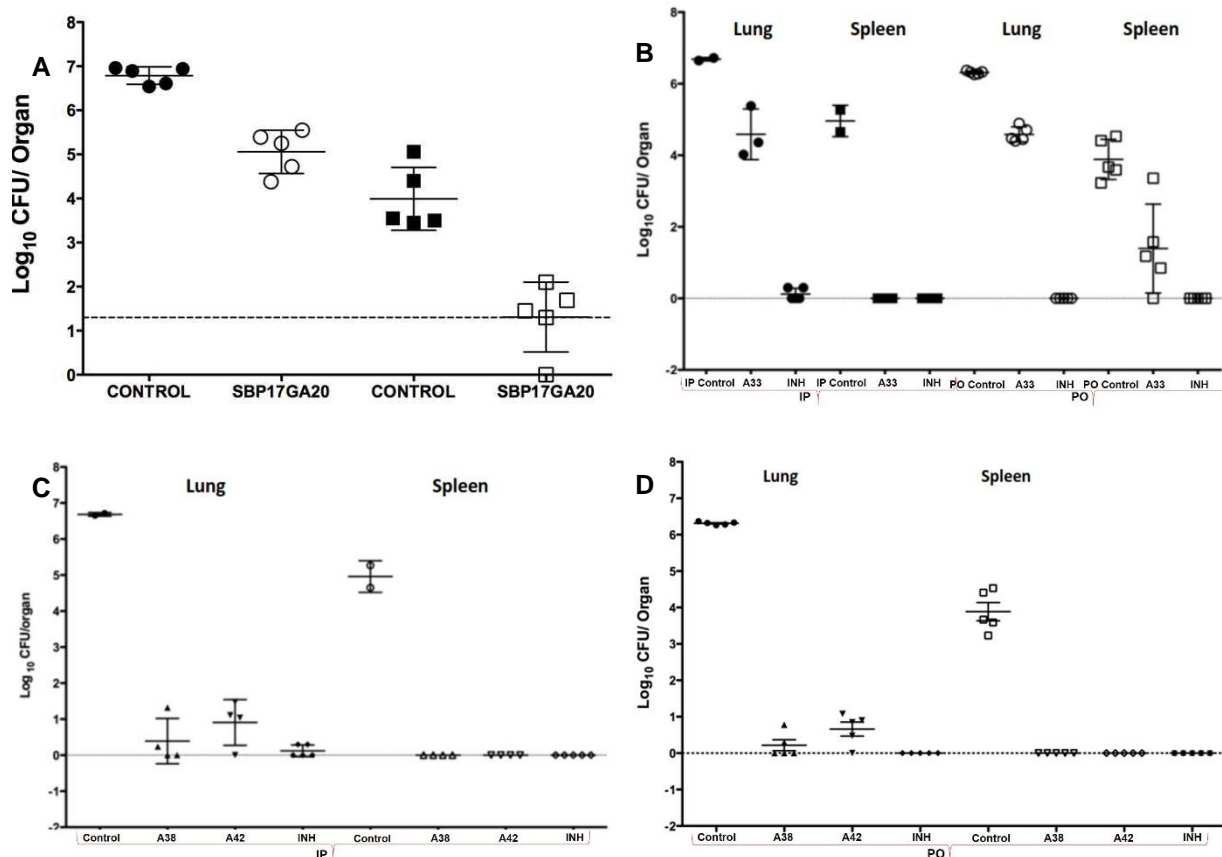


Figure 3.10. *In vivo* studies in murine model of TB infection. (A) SB-P17G-A20 dosed IP at 50 mg/kg twice daily in the murine model of TB infection (B) SB-P17G-A33 dosed IP and PO (C) IP dosing of SB-P17G-A38 and SB-P17G-A42 (D) PO dosing of SB-P17G-A38 and SB-P17G-A42. Adapted from Ref. 32 and Ref. 33

The potent lead compound **SB-P8B2** was also tested in combination with rifampicin against *Mtb* cells and was 8 times more potent in its presence, while the activity of rifampicin was doubled.³³ Σ FIC, which is defined as the sum of the FICs (MIC of a drug in combination/MIC of that drug alone) for all the drugs tested in the combination, was 0.63 for **SB-P8B2**-rifampicin combination. Drugs are considered synergistic when the Σ FIC is less than 0.5 and antagonistic when the Σ FIC is greater than 4 and in this case the value lies within the range implying that two drugs aren't synergistic nor antagonistic with respect to each other.

Antibacterial potency of the lead compounds was also evaluated against clinical isolates of *Mtb* exhibiting different resistance profiles. As expected, the benzimidazole didn't discriminate between the *Mtb* strains (**Table 3.1**).^{16, 32, 33} The unbiased ability of these compounds to kill drug-resistant strains of *Mtb* demonstrates the significance of FtsZ as a drug target to develop new

generation anti-TB drugs. It is also worthy of note that **SB-P3G2**, **SB-P8B2** and **SB-P17G-A20** exhibited substantial activity against non-replicating *Mtb* cells at 10-30 $\mu\text{g/mL}$ concentration (94-99% inhibition) in the low oxygen recovery assay (LORA)^{32, 33}. The results strongly suggest that these FtsZ inhibitors not only blocks Z-ring formation, but also affect the maintenance of the *Mtb* cells and will potentially be active against latent TB.

Table 3.1. Antibacterial activity (MIC $\mu\text{g/mL}$) against clinical isolates of *Mtb*

| Compound | <i>Mtb</i> strains | | | |
|--------------------|--------------------|--------|-------|------|
| | H37Rv | NHN382 | TN587 | W210 |
| INH | 0.013 | 0.25 | 0.25 | 0.01 |
| SB-P3G2 | 0.63 | 1.25 | 1.25 | 1.25 |
| SB-P17G-C2 | 0.06 | 0.06 | 0.13 | 0.06 |
| SB-P20G3 | 0.16 | 0.16 | 0.16 | 0.16 |
| SB-P17G-A20 | 0.16 | 0.16 | 0.16 | 0.16 |
| SB-P17G-A19 | 0.31 | 0.31 | 0.63 | 0.31 |
| SB-P21G7 | 0.31 | 0.31 | 0.31 | 0.31 |
| SB-P17G-A24 | 0.63 | 0.63 | 0.63 | 0.63 |
| SB-P17G-A16 | 0.63 | 0.63 | 0.63 | 0.63 |

MIC values were determination at CSU. Adapted from Ref. 15 and Ref. 16

3.2.6. ADME profiling of lead compounds

Our collaborators at Sanofi-Aventis have performed extensive ADME profiling of our lead compounds. **Table 3.2** summarizes the results for **SB-P17G-A33**, **SB-P17G-A38** and **SB-P17G-A42**. In the presence of human/mouse serum, all three compounds have lower IC₈₀ values against *Mtb* cells than in the absence of serum. In the Caco-2 permeability assay, all three compounds show desirable permeability indicating they can be absorbed through the intestinal wall. They are cleared at a reasonable rate by the hepatic system with 55%, 54% and 55% contribution from CYP3A4 for **SB-P17G-A33**, **SB-P17G-A38**, and **SB-P17G-A42**, respectively. Fortunately these compounds do not inhibit CYP3A4 in the presence of Midazolam (Mid) and Testosterone (Testo) but in their absence **SB-P17G-A38** and **SB-P17G-A42** inhibited the enzyme at 10 μM and 9 μM , respectively. Also they are not potent inducers of the cytochrome family namely, CYP1A2, 2B6, and 3A. The key hurdle these molecules need to clear is their hERG inhibition and a clean ion channel panel profile (Na^+ , K^+ , Ca^{2+}). Preliminary Purkinje fiber results indicate that **SB-P17G-A38** inhibits the Na^+ and K^+ channels which might lead to arrhythmia.

Table 3.2. ADME profiling of SB-P17G-A33, SB-P17G-A38 and SB-P17G-A42

| OK/manageable/ Issue | SB-P17G-A33 | SB-P17G-A38 | SB-P17G-A42 |
|--------------------------------------------------------------------|--------------------|--------------------|--------------------|
| <i>Mtb</i> activity: IC ₈₀ ± h / m serum | 0.05 / 1.4 / 2.9 | 0.07 / 2 / 7.5 | 0.07 / 0.57 / 1.7 |
| Caco2 (P _{tot} / recovery %) | 78 (59%) | 82 (64%) | 273 (55%) |
| Hep. clearance Cl _{int} (mL/h/10 ⁶ hep) h/m | 0.097 / 0.108 | 0.058 / 0.049 | 0.103 / pending |
| CYP3A4 contribution | 55% | 54% | 55% |
| CYP3A4 inhibition +Mid or Testosterone | >30µM | >30µM | >30µM |
| CYP3A4 (Time dependent inhibition) | >40µM | 10 µM (-8.3%) | 9 µM (-7.6%) |
| CYP1A2/2B6/3A induction % | 0 / 4 / 6 | 30 / 18 / 12 | 0 / 2 / 4 |
| hERG inhibition % @ 1/10 µM (IC ₅₀) | 54 / 93 (0.95 µM) | 83 / 94 (0.24 µM) | 75 / 99 |

This work was performed by our collaborators at Sanofi-Aventis

SB-P17G-A38 and its congeners although very potent in the murine model of TB infection still require more fine-tuning before they can be progressed further as drug candidates.

3.3. Conclusion

The trisubstituted benzimidazoles, **SB-P17G-A38** and **SB-P17G-A42** have been shown to be worthy contenders with isoniazid in the murine model of TB. Especially, when dosed orally (PO), these molecules reduced the bacterial load in the spleen by the same level as isoniazid. ADME profile of **SB-P17G-A38**, our current lead compound, is very promising although hERG inhibition is a major concern that needs to be addressed. Along with being efficacious *in vivo*, the target of our lead compounds has been validated as FtsZ via Polymerization assay, GTPase assay and TEM imaging. **SB-P17G-C2**, the most potent compound against *Mtb* cells, along with others has been shown to inhibit the extent of FtsZ polymerization while enhancing its GTPase activity. Along with preventing FtsZ polymerization *in vitro*, these molecules can also disassemble preformed polymers. This series of compounds deservedly warrants further studies.

3.4. Experimental Section

Methods. ^1H and ^{13}C NMR spectra were measured on a Bruker or Varian 300, 400 or 500 MHz NMR spectrometer. Melting points were measured on a Thomas Hoover Capillary melting point apparatus and are uncorrected. TLC was performed on silica coated aluminum sheets (thickness 200 μm) or alumina coated (thickness 200 μm) aluminum sheets supplied by Sorbent Technologies and column chromatography was carried out on Siliaflash® P60 silica gel, 40-63 μm (230-400 mesh) supplied by Silicycle. Aluminum oxide, activated, neutral, Brockmann Grade I, 58 Å, was supplied by Alfa Aesar.

Light scattering assays were performed using a PTI-QM4 spectrofluorimeter. FEI Tecnai12 BioTwinG transmission electron microscope with an AMT XR-60 CCD digital camera system was used to acquire transmission electron microscopy images.

Materials. BL21(DE3) cells, His-Bind protein purification resin and the buffers were purchased from Novagen. Bradford kit for protein concentration determination was purchased from Sigma. Buffer salts (reagent grade or better), solvents (HPLC grade or better), and all the other chemicals were purchased from Fisher Scientific Co. (Pittsburgh, PA). The chemicals were purchased from Aldrich Co., Synquest Inc. and Sigma and purified before use by standard methods. Tetrahydrofuran (THF) was freshly distilled from sodium metal and benzophenone. Dichloromethane was also distilled immediately prior to use under nitrogen from calcium hydride.

Synthesis of 5-(4-azidobenzamido)-2-cyclohexyl-6-pyrrolidinyl-1H-benzo[d]imidazole (SB-P6B-A48): 4-Aminobenzoic acid (500 mg, 3.64 mmol) dissolved in TFA (12 mL) was diazotized in the dark at 0 °C with NaNO_2 (500 mg, 7.24 mmol). After stirring for 30 minutes, sodium azide (2.37 g, 36.4 mmol) was slowly added to the reaction mixture over a period of 5 minutes. After an additional 15 minutes, diethyl ether (10 mL) was added and the entire mixture was stirred for 1 hour. The reaction mixture was washed with excess water, extracted with diethyl ether (three times), dried over magnesium sulfate, and filtered. Removal of excess TFA as an azeotrope with benzene gave 4-azidobenzoic acid as a white powder (586 mg, 99% yield) with MP 182-184 °C (lit. mp 185 °C).

To a solution of 5-amino-2-cyclohexyl-6-(pyrrolidin-1-yl)-1H-benzo[d]imidazole (100 mg, 0.35 mmol) in 2 mL of dichloromethane added 1-ethyl-3-(3-dimethylaminopropyl)

carbodiimide (1.1 eq) (EDC) and acid (1.1 eq). 4-Dimethylaminopyridine (DMAP) (1.1 eq) was added to the above reaction mixture and the reaction was stirred overnight at room temperature. After completion of the reaction as per TLC, the reaction mixture was diluted with dichloromethane followed by the addition of triethylamine. The reaction mixture was transferred to a separatory funnel and the organic layer was washed with water, sodium bicarbonate and finally brine. The organic layer was dried over magnesium sulfate and concentrated using rotary evaporator. The crude product was purified by flash chromatography (column was packed with hexane, 20% ethyl acetate was used steadily increasing to 50% ethyl acetate) to obtain the product as a light yellow solid (123 mg, 81% yield). Mp turned black ≥ 200 °C; ^1H NMR (500 MHz, CDCl_3) δ 1.17 - 1.38 (m, 3 H), 1.50 - 1.85 (m, 5 H), 1.89 - 2.16 (m, 6 H), 2.67 - 2.87 (m, 1 H), 2.94 - 3.15 (m, 4 H), 7.12 (d, $J = 7.93$ Hz, 1 H), 7.59 (br. s, 1 H), 7.94 (t, $J = 7.32$ Hz, 1 H), 8.75 (s, 1 H), 9.82 (br. s, 2 H); ^{13}C NMR (126 MHz, CDCl_3) δ 24.7, 26.0, 26.2, 32.0, 38.7, 54.2, 101.6, 111.3, 119.6, 128.8, 130.0, 132.1, 136.1, 143.8, 159.6, 164.1. This compound is literature unknown and new.

5-(4-Azidobenzamido)-2-cyclohexyl-6-*N,N*-dimethylamino-1*H*-benzo[*d*]imidazole (SB-P17G-A48): Light brown solid (85% yield); mp 166-167 °C; ^1H NMR (400 MHz, DMSO-d_6) δ 1.25 - 1.47 (m, 3 H), 1.53 - 1.82 (m, 5 H), 2.00 (d, $J = 10.29$ Hz, 2 H), 2.67 (s, 6 H), 2.75 - 2.89 (m, 1 H), 7.29 (d, $J = 8.53$ Hz, 2 H), 7.40 (br. s, 1 H), 7.98 (d, $J = 8.53$ Hz, 2 H), 8.28 (br. s, 1 H), 9.71 (br. s, 1 H), 12.00 (br. s, 1 H); ^{13}C NMR (101 MHz, DMSO-d_6) δ 25.5, 25.6, 31.3, 37.7, 45.2, 102.5, 110.0, 119.4, 127.6, 128.9, 131.4, 139.6, 142.7, 159.1, 163.1. This compound is literature unknown and new.

5-(4-Azido-3-nitrobenzamido)-2-cyclohexyl-6-*N,N*-dimethylamino-1*H*-benzo[*d*]imidazole (SB-P17G-A49): Orange solid (90% yield); turned black ≥ 165 °C; ^1H NMR (500 MHz, CDCl_3) δ 1.27 - 1.46 (m, 3 H), 1.60 - 1.88 (m, 5 H), 2.13 (d, $J = 10.68$ Hz, 2 H), 2.66 - 2.99 (m, 7 H), 7.39 - 8.22 (m, 4 H), 8.67 (br. s, 1 H), 9.91 (br. s, 1 H); ^{13}C NMR (126 MHz, CDCl_3) δ 26.0, 26.2, 32.0, 38.7, 46.2, 102.2, 110.7, 112.7, 114.5, 119.2, 128.8, 131.4, 139.7, 152.6, 159.9, 162.2. This compound is literature unknown and new.

5-(4-Benzoylbenzamido)-2-cyclohexyl-6-pyrrolidinyl-1*H*-benzo[*d*]imidazole (SB-P6B-A5): Yellow solid (53% yield); mp 236 -237 °C; ^1H NMR (500 MHz, DMSO-d_6) δ 1.20 - 1.45 (m, 3 H), 1.59 (q, $J = 11.19$ Hz, 2 H), 1.69 (d, $J = 11.29$ Hz, 1 H), 1.79 (d, $J = 11.60$ Hz, 2 H), 1.90 (br.

s, 4 H), 2.00 (d, $J = 11.29$ Hz, 2 H), 2.81 (t, $J = 10.68$ Hz, 1 H), 3.09 (br. s, 4 H), 7.19 (br. s, 1 H), 7.55 - 7.65 (m, 2 H), 7.66 - 8.03 (m, 6 H), 8.12 (d, $J = 7.02$ Hz, 2 H), 9.95 (br. s, 1 H); ^{13}C NMR (126 MHz, DMSO- d_6) δ 24.4, 25.5, 25.6, 31.3, 37.7, 52.0, 79.0, 125.3, 127.4, 128.7, 129.7, 129.9, 133.1, 136.7, 138.1, 139.1, 139.4, 158.9, 163.8, 195.4; HRMS (FAB) m/z calcd for $\text{C}_{31}\text{H}_{32}\text{N}_4\text{O}_2\text{H}^+$: 493.2598, Found: 493.2596 ($\Delta = -0.4$ ppm). This compound is literature unknown and new.

5-(4-Benzoylbenzamido)-2-cyclohexyl-6-*N,N*-dimethylamino-1*H*-benzo[*d*]imidazole (SB-P17G-A5): Yellow solid (72% yield); mp >240 °C; ^1H NMR (500 MHz, DMSO- d_6) δ 1.20 - 1.44 (m, 3 H), 1.53 - 1.86 (m, 5 H), 1.95 - 2.09 (m, 2 H), 2.68 (s, 6 H), 2.76 - 2.88 (m, 1 H), 7.14 - 7.53 (m, 1 H), 7.59 (t, $J = 7.63$ Hz, 2 H), 7.71 (t, $J = 7.48$ Hz, 1 H), 7.76 - 7.84 (m, 2 H), 7.85 - 7.93 (m, $J = 7.93$ Hz, 2 H), 8.03 - 8.18 (m, $J = 7.93$ Hz, 2 H), 8.21 - 8.43 (m, 1 H), 9.63 - 9.98 (m, 1 H), 12.05 (br. s, 1 H); ^{13}C NMR (126 MHz, DMSO- d_6) δ 25.5, 25.6, 31.3, 37.7, 45.3, 102.1, 102.5, 110.0, 111.4, 127.2, 127.8, 128.7, 129.7, 130.0, 130.8, 133.1, 136.6, 138.2, 139.4, 139.7, 159.3, 163.3, 195.3; HRMS (FAB) m/z calcd for $\text{C}_{29}\text{H}_{30}\text{N}_4\text{O}_2\text{H}^+$: 467.2442, Found: 467.2443 ($\Delta = 0.2$ ppm). This compound is literature unknown and new.

***Mtb* FtsZ Protein Preparation.**^{15, 16} Preparation 1) pET 15b vector plasmid (1.5 μL and 3 μL) was transformed into 100 μL of BL21(DE3) pLys cells. The transformed cells were plated onto LB plates, containing 100 $\mu\text{g}/\text{mL}$ ampicillin. The antibiotic concentration was kept the same for the following steps. The plates were incubated overnight at 37 °C. The colonies were picked and grown in 10 mL of LB media at 37 °C at 250 rpm shake rate. The inoculum was transferred to 1 L of LB media in a 4 L flask and grown to an OD of 0.4 at A600. Then, 1 mM IPTG was added to induce protein expression overnight at 32 °C at 250 rpm shake rate. Next day the cells were harvested at 5K rpm for 30 min and re-suspended in approximately 20-30 mL binding buffer (300 mM NaCl, 50 mM NaH_2PO_4 , 10 mM imidazole, pH = 8). The re-suspended cells were lysed using ultra-sonicator. The lysate was centrifuged in an ultracentrifuge at 33K rpm for 90 min. The supernatant was filtered and loaded onto Ni^{2+} -NTA column washed with 50 mL of binding buffer and eluted using a gradient of binding buffer with 50-250 mM imidazole. The eluted protein was immediately loaded onto a G-25 size exclusion chromatography column, pre-equilibrated with the polymerization buffer (50 mM MES, 5mM MgCl_2 , 50 mM KCl, pH 6.5). The protein fractions were concentrated and stored at -80 °C for further use. Since the number of aromatic residues in *Mtb* FtsZ protein are low (Tyr: 1, Trp: 0), it is not reliable to follow concentration of protein by

scanning at A280. The concentration of protein was therefore ascertained using the BCA kit from Sigma.

Preparation 2) *E. coli* expression plasmid encoding the *ftsZ* gene (pET 15b vector) was transformed into 100 μ L of BL21(DE3) cells. The transformed cells were plated onto LB plates, containing 100 μ g/mL ampicillin. The antibiotic concentration was kept the same for the following steps. The plates were incubated overnight at 37 °C. The colonies were picked and grown in 10 mL of LB media at 37 °C at 250 rpm shake rate. The inoculum was transferred to 1 L of LB media in a 4 L flask and grown to an OD of 0.6 at A600. Then, 1 mM IPTG was added to induce protein expression overnight at 25 °C at 250 rpm shake rate. Next day the cells were harvested at 4,225 \times *g* for 15 min and re-suspended in approximately 20-30 mL binding buffer (500 mM NaCl, 20 mM sodium phosphate, pH 7.8). The re-suspended cells were lysed using cell disruptor. The lysate was centrifuged in an ultracentrifuge at 126,603 \times *g*, 4 °C for 90 min. The supernatant was filtered and loaded onto Ni²⁺-NTA column washed with 50 mL of binding buffer and eluted using a gradient of binding buffer with 30-500 mM imidazole. The eluted protein was first dialyzed against the polymerization buffer (50 mM MES, 5mM MgCl₂, 50 mM KCl, pH 6.5) and then polymerization buffer containing 10% v/v glycerol. Alternatively, the eluted protein was dialyzed against buffer containing 50 mM Tris, 5mM MgCl₂, 50 mM KCl, pH 7.2 followed by buffer containing 10% v/v glycerol. The protein after dialysis was concentrated and stored at -80 °C for further use. Since the number of aromatic residues in *Mtb* FtsZ protein are low (Tyr: 1, Trp: 0), it is not reliable to follow concentration of protein by scanning at A280. The concentration of protein was therefore ascertained using the Bradford kit from Sigma.

Polymerization Assay.^{15, 16, 30} Protein obtained from preparation 2 was used for this assay. FtsZ (15 μ M) was equilibrated in polymerization buffer (50 mM MES, 100 mM KCl, 5 mM MgCl₂, pH 6.5) at 25 °C. Polymerization was measured by light scattering using a PTI-QM4 spectrofluorimeter set at 400 nm excitation/emission, 2 nm slit width, 860 V). Polymerization was initiated with 50 μ M GTP and monitored for up to 30 minutes. Compound stock solutions were prepared in DMSO and incubated with *Mtb* FtsZ prior to initiation of polymerization with GTP. The percentage of DMSO was maintained at 2% for all experiments.

GTPase Activity.^{15, 31} Protein obtained from preparation 1 was used for this assay. The amount of inorganic phosphate (Pi) released during the assembly of FtsZ was measured using a standard Malachite Green/ammonium molybdate assay.³² Briefly, FtsZ protein (10 μ M) was

incubated without or with a benzimidazole at different concentrations (0, 20, 40, and 80 μM) in polymerization buffer (50 mM MES, 5 mM MgCl_2 , 50 mM KCl, pH 6.5) at room temperature for 15 min. Then, 50 μM GTP was added to the reaction mixture and incubated at 37 $^\circ\text{C}$ to start the hydrolysis reaction. After 30 min of incubation, Malachite Green reagent (20% v/v) was added to the reaction mixtures to quench the reaction. The reaction mixtures were centrifuged at 13K rpm for 90 s to remove the protein debris. The samples (100 μL) were transferred to a 96-well plate, and the absorbance of each well was measured at 620 nm. The background absorbance was subtracted from all the readings. A phosphate standard curve was prepared using phosphate standard provided with a Malachite Green assay kit (Sensolyte). All the solutions were prepared in polymerization buffer.

Transmission Electron Microscopy (TEM) Analysis.^{15, 16} Protein obtained from preparation 2 was used for this assay. Stock solution of **SB-P17G-C2** was prepared in ethanol. *Mtb* FtsZ (5 μM) was incubated with 40 or 80 μM of **SB-P17G-C2** in the polymerization buffer (50 mM MES, 5 mM MgCl_2 , 100 mM KCl, pH 6.5) for 15 min on ice. To each solution was added GTP to the final concentration of 25 μM . The resulting solution was incubated at 37 $^\circ\text{C}$ for 30 min. The incubated solution was diluted 2 times with the polymerization buffer and immediately transferred to carbon coated 300 mesh formvar copper grid and negatively stained with 1% uranyl acetate. To visualize the effect of **SB-P17G-C2** on preformed polymers, *Mtb* FtsZ (5 μM) was allowed to polymerize at 37 $^\circ\text{C}$ in the presence of GTP (25 μM) for 30 mins. **SB-P17G-C2** (40 μM or 80 μM) was added to the polymerized protein and incubated for additional 5 min. The resulting solution was diluted 2 times with the polymerization buffer and immediately transferred to carbon coated 300 mesh formvar copper grid and negatively stained with 1% uranyl acetate. The samples were viewed at the Microscopy Imaging Center at Stony Brook University, with a FEI Tecnai12 BioTwinG transmission electron microscope at 80 kV. Digital images were acquired with an AMT XR-60 CCD digital camera system.

3.5. References

1. Ben-Yehuda, S.; Losick, R., Asymmetric cell division in *B. subtilis* involves a spiral-like intermediate of the cytokinetic protein FtsZ. *Cell (Cambridge, MA, U. S.)* **2002**, *109*, 257-266
2. Goehring, N. W.; Beckwith, J., Diverse paths to midcell: assembly of the bacterial cell division machinery. *Curr. Biol.* **2005**, *15*, R514-R526
3. Leung, A. K. W.; White, E. L.; Ross, L. J.; Reynolds, R. C.; DeVito, J. A.; Borhani, D. W., Structure of Mycobacterium tuberculosis FtsZ Reveals Unexpected, G Protein-like Conformational Switches. *J. Mol. Biol.* **2004**, *342*, 953-970
4. Moller-Jensen, J.; Loewe, J., Increasing complexity of the bacterial cytoskeleton. *Curr. Opin. Cell Biol.* **2005**, *17*, 75-81
5. Thanedar, S.; Margolin, W., FtsZ Exhibits Rapid Movement and Oscillation Waves in Helix-like Patterns in Escherichia coli. *Curr. Biol.* **2004**, *14*, 1167-1173
6. Pelham, R. J.; Chang, F., Actin dynamics in the contractile ring during cytokinesis in fission yeast. *Nature* **2002**, *419*, 82-86
7. Li, Y.; Hsin, J.; Zhao, L.; Cheng, Y.; Shang, W.; Huang, K. C.; Wang, H.-W.; Ye, S., FtsZ Protofilaments Use a Hinge-Opening Mechanism for Constrictive Force Generation. *Science* **2013**, *341*, 392-395
8. Erickson, H. P.; Taylor, D. W.; Taylor, K. A.; Bramhill, D., Bacterial cell division protein FtsZ assembles into protofilament sheets and minirings, structural homologs of tubulin polymers. *Proc. Natl. Acad. Sci. U. S. A.* **1996**, *93*, 519-23
9. Awasthi, D.; Kumar, K.; Ojima, I., Therapeutic potential of FtsZ inhibition: a patent perspective. *Expert Opin. Ther. Pat.* **2011**, *21*, 657-679
10. Kumar, K.; Awasthi, D.; Berger, W. T.; Tonge, P. J.; Slayden, R. A.; Ojima, I., Discovery of anti-TB agents that target the cell-division protein FtsZ. *Future Med. Chem.* **2010**, *2*, 1305-1323
11. Beuria, T. K.; Singh, P.; Surolia, A.; Panda, D., Promoting assembly and bundling of FtsZ as a strategy to inhibit bacterial cell division: A new approach for developing novel antibacterial drugs. *Biochem. J.* **2009**, *423*, 61-69
12. White, E. L.; Suling, W. J.; Ross, L. J.; Seitz, L. E.; Reynolds, R. C., 2-Alkoxy-carbonylaminopyridines: inhibitors of Mycobacterium tuberculosis FtsZ. *J. Antimicrob. Chemother.* **2002**, *50*, 111-114

13. Reynolds, R. C.; Srivastava, S.; Ross, L. J.; Suling, W. J.; White, E. L., A new 2-carbamoyl pteridine that inhibits mycobacterial FtsZ. *Bioorg. Med. Chem. Lett.* **2004**, *14*, 3161-3164
14. Huang, Q.; Kirikae, F.; Kirikae, T.; Pepe, A.; Amin, A.; Respicio, L.; Slayden, R. A.; Tonge, P. J.; Ojima, I., Targeting FtsZ for Antituberculosis Drug Discovery: Noncytotoxic Taxanes as Novel Antituberculosis Agents. *J. Med. Chem.* **2006**, *49*, 463-466
15. Kumar, K.; Awasthi, D.; Lee, S.-Y.; Zanardi, I.; Ruzsicska, B.; Knudson, S.; Tonge, P. J.; Slayden, R. A.; Ojima, I., Novel Trisubstituted Benzimidazoles, Targeting Mtb FtsZ, as a New Class of Antitubercular Agents. *J. Med. Chem.* **2011**, *54*, 374-381
16. Awasthi, D.; Kumar, K.; Knudson, S. E.; Slayden, R. A.; Ojima, I., SAR Studies on Trisubstituted Benzimidazoles as Inhibitors of Mtb FtsZ for the Development of Novel Antitubercular Agents. *J. Med. Chem.* **2013**, *56*, 9756-9770
17. Park, B.; Awasthi, D.; Chowdhury, S. R.; Melief, E. H.; Kumar, K.; Knudson, S. E.; Slayden, R. A.; Ojima, I., Design, synthesis and evaluation of novel 2,5,6-trisubstituted benzimidazoles targeting FtsZ as antitubercular agents. *Bioorg. Med. Chem.* **2014**, *22*, 2602-2612
18. Laeppchen, T.; Hartog, A. F.; Pinas, V. A.; Koomen, G.-J.; Den Blaauwen, T., GTP Analogue Inhibits Polymerization and GTPase Activity of the Bacterial Protein FtsZ without Affecting Its Eukaryotic Homologue Tubulin. *Biochemistry* **2005**, *44*, 7879-7884
19. Paradis-Bleau, C.; Beaumont, M.; Sanschagrín, F.; Voyer, N.; Levesque, R. C., Parallel solid synthesis of inhibitors of the essential cell division FtsZ enzyme as a new potential class of antibacterials. *Bioorg. Med. Chem.* **2007**, *15*, 1330-1340
20. Parhi, A.; Kelley, C.; Kaul, M.; Pilch, D. S.; LaVoie, E. J., Antibacterial activity of substituted 5-methylbenzo[c]phenanthridinium derivatives. *Bioorg. Med. Chem. Lett.* **2012**, *22*, 7080-7083
21. Beuria, T. K.; Santra, M. K.; Panda, D., Sanguinarine Blocks Cytokinesis in Bacteria by Inhibiting FtsZ Assembly and Bundling. *Biochemistry* **2005**, *44*, 16584-16593
22. Mathew, B.; Ross, L.; Reynolds, R. C., A novel quinoline derivative that inhibits mycobacterial FtsZ. *Tuberculosis* **2013**, *93*, 398-400
23. Kelley, C.; Zhang, Y.; Parhi, A.; Kaul, M.; Pilch, D. S.; LaVoie, E. J., 3-Phenyl substituted 6,7-dimethoxyisoquinoline derivatives as FtsZ-targeting antibacterial agents. *Bioorg. Med. Chem.* **2012**, *20*, 7012-7029

24. Parhi, A.; Lu, S.; Kelley, C.; Kaul, M.; Pilch, D. S.; LaVoie, E. J., Antibacterial activity of substituted dibenzo[a,g]quinolizin-7-ium derivatives. *Bioorg. Med. Chem. Lett.* **2012**, *22*, 6962-6966
25. Haydon, D. J.; Stokes, N. R.; Ure, R.; Galbraith, G.; Bennett, J. M.; Brown, D. R.; Baker, P. J.; Barynin, V. V.; Rice, D. W.; Sedelnikova, S. E.; Heal, J. R.; Sheridan, J. M.; Aiwale, S. T.; Chauhan, P. K.; Srivastava, A.; Taneja, A.; Collins, I.; Errington, J.; Czaplowski, L. G., An Inhibitor of FtsZ with Potent and Selective Anti-Staphylococcal Activity. *Science* **2008**, *321*, 1673-1675
26. Haydon, D. J.; Bennett, J. M.; Brown, D.; Collins, I.; Galbraith, G.; Lancett, P.; Macdonald, R.; Stokes, N. R.; Chauhan, P. K.; Sutariya, J. K.; Nayal, N.; Srivastava, A.; Beanland, J.; Hall, R.; Henstock, V.; Noula, C.; Rockley, C.; Czaplowski, L., Creating an antibacterial with in vivo efficacy: synthesis and characterization of potent inhibitors of the bacterial cell division protein FtsZ with improved pharmaceutical properties. *J. Med. Chem.* **2010**, *53*, 3927-3936
27. Margalit, D. N.; Romberg, L.; Mets, R. B.; Hebert, A. M.; Mitchison, T. J.; Kirschner, M. W.; RayChaudhuri, D., Targeting cell division: Small-molecule inhibitors of FtsZ GTPase perturb cytokinetic ring assembly and induce bacterial lethality. [Erratum to document cited in CA141:271048]. *Proc. Natl. Acad. Sci. U. S. A.* **2004**, *101*, 13969
28. Plaza, A.; Keffer, J. L.; Bifulco, G.; Lloyd, J. R.; Bewley, C. A., Chrysopaentins A-H, antibacterial bisdiarylbutene macrocycles that inhibit the bacterial cell division protein FtsZ. *J. Am. Chem. Soc.* **2010**, *132*, 9069-9077
29. Mathew, B.; Srivastava, S.; Ross, L. J.; Suling, W. J.; White, E. L.; Woolhiser, L. K.; Lenaerts, A. J.; Reynolds, R. C., Novel pyridopyrazine and pyrimidothiazine derivatives as FtsZ inhibitors. *Bioorg. Med. Chem.* **2011**, *19*, 7120-7128
30. White, E. L.; Ross, L. J.; Reynolds, R. C.; Seitz, L. E.; Moore, G. D.; Borhani, D. W., Slow Polymerization of *Mycobacterium tuberculosis* FtsZ. *J. Bacteriol.* **2000**, *182*, 4028 -4034
31. Geladopoulos, T. P.; Sotiroudis, T. G.; Evangelopoulos, A. E., A malachite green colorimetric assay for protein phosphatase activity. *Anal. Biochem.* **1991**, *192*, 112-116
32. Knudson, S. E.; Awasthi, D.; Kumar, K.; Ojima, I.; Slayden, R. A., A Trisubstituted benzimidazole cell division inhibitor with efficacy against *Mycobacteria tuberculosis*. *PLoS ONE* **2014**, *9*, e93953 (2014)

33. Knudson, S. E.; Kumar, K.; Awasthi, D.; Ojima, I.; Slayden, R. A., Potency of benzimidazoles and in vitro activity–efficacy relationship against Mycobacteria tuberculosis. *Tuberculosis* **2014**, *94*, 271-276

Chapter 4

Discovery of Trisubstituted Benzimidazoles Against *F. tularensis*

Table of Contents

| | |
|----------------------------------------------------------------|-----|
| Chapter 4 | 111 |
| 4.1. Introduction..... | 112 |
| 4.2. Results and Discussion..... | 114 |
| 4.2.1. Re-synthesis of hits against <i>F. tularensis</i> | 114 |
| 4.2.2. Preliminary target validation studies | 116 |
| 4.3. Conclusion | 117 |
| 4.4. Experimental Section..... | 118 |
| 4.5. References..... | 123 |

4.1. Introduction

Bacterial infections due to pathogens such as methicillin-resistant *Staphylococcus aureus* (MRSA),¹ vancomycin-resistant *enterococci* (VRE),² *F. tularensis*,³ *Y. pestis*⁴ and others have re-emerged as major health concerns throughout the world. Amongst them, *F. tularensis*, a gram negative bacteria, has attracted widespread attention as a potential bioterrorism weapon.⁵ The bacteria reside in rabbits or rodents but can infect humans through vectors such as mosquitos and fleas causing tularemia.^{5,6} The symptoms of tularemia include fever, ulcers, dyspnea, and others.^{5,7} Primarily, the bacteria infect macrophages of the host organism where it multiplies and later invades the lungs, spleen, liver, and kidneys.^{5,8} Among the four known subspecies of *F. tularensis*, Type A is the most virulent and is associated with the most lethal pulmonary infections.⁹ It is highly virulent as it can cause a fatal infection on exposure to doses as low as 10 colony forming units.^{10,11} Due to its high infectivity that enables airborne transmission, difficult diagnosis, and a very low infection dose, *F. tularensis* has been classified as category A list of select agents by NIAID.^{5,8} According to studies done in 1970, the WHO predicted that the release of 50 kg of *F. tularensis* in air over a city with a population of 5 million would result in 250,000 cases of disease.¹²

Treatment against this pathogen still relies on the traditional antibacterial drugs which target cell wall biosynthesis, nucleic acid synthesis, protein synthesis, etc.¹³ The infection is largely treated by antibiotics like aminoglycosides, streptomycin, tetracycline, chloramphenicol, and quinolones.^{14,15} However, these antibiotics have either shown high toxicity or a high relapse rate.^{5,16} Since we have successfully identified potent antitubercular compounds targeting *Mtb* FtsZ, our extensive library of benzimidazoles was screened against *F. tularensis* LVS.¹⁷⁻¹⁹

Preliminary screening performed at CSU against *F. tularensis* LVS strain using the “Microplate Alamar Blue assay (MABA)” in a 96-well format (single point assay in triplicates) identified 11 compounds from the 2,5,6-trisubstituted benzimidazole library (**Figure 4.1**) and 6 compounds from the 2,5,7-trisubstituted benzimidazole library exhibiting greater than 90 % growth inhibition at 1 µg/mL (**Figure 4.2**). Additionally, 7 compounds exhibited 40-50 % growth inhibition at 0.2 µg/mL (**Figure 4.3**).¹⁹

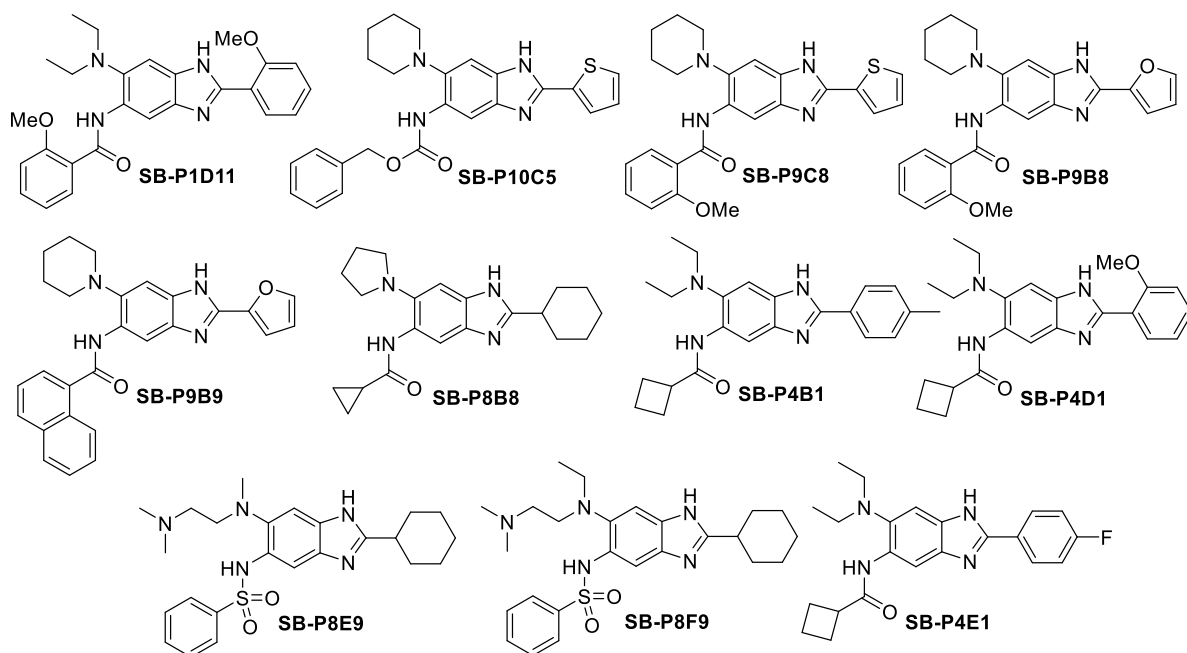


Figure 4.1. Structures of 2,5,6-trisubstituted benzimidazoles against *F. tularensis* at 1 $\mu\text{g}/\text{mL}$ with > 90 % growth inhibition¹⁹

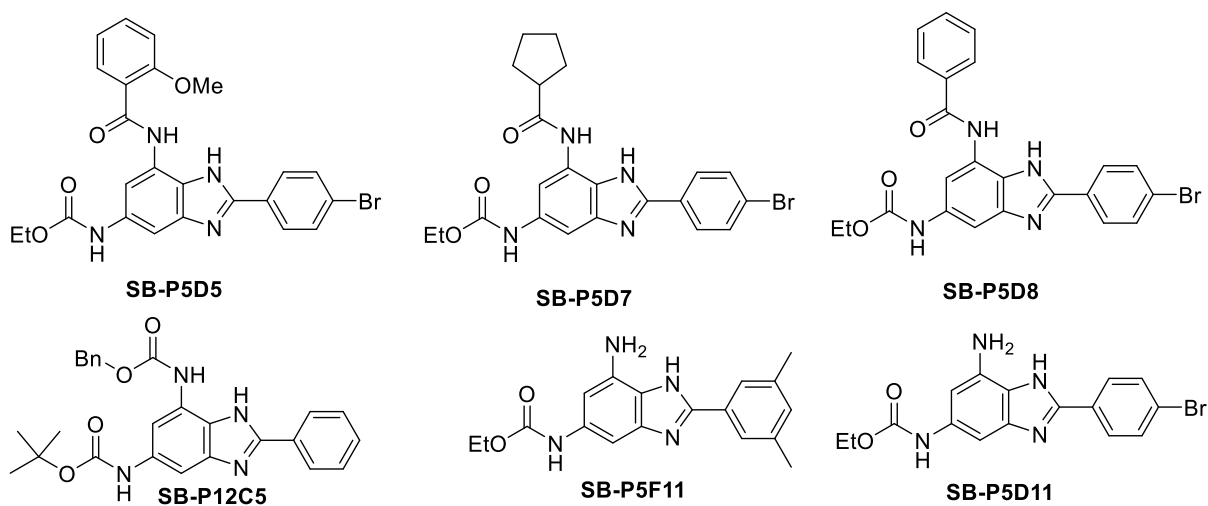


Figure 4.2. Structures of 2,5,7-trisubstituted benzimidazoles against *F. tularensis* at 1 $\mu\text{g}/\text{mL}$ with > 90 % growth inhibition¹⁹

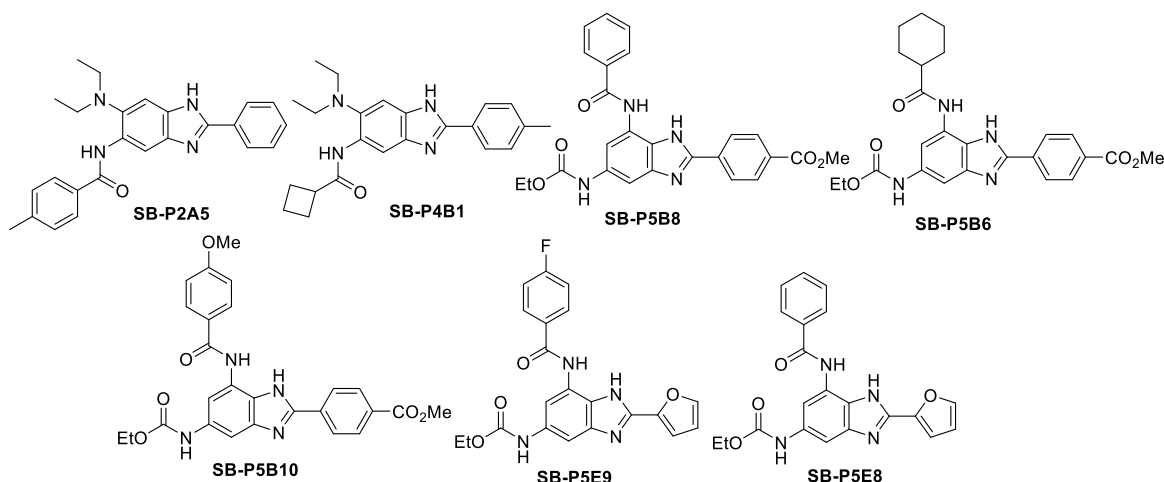


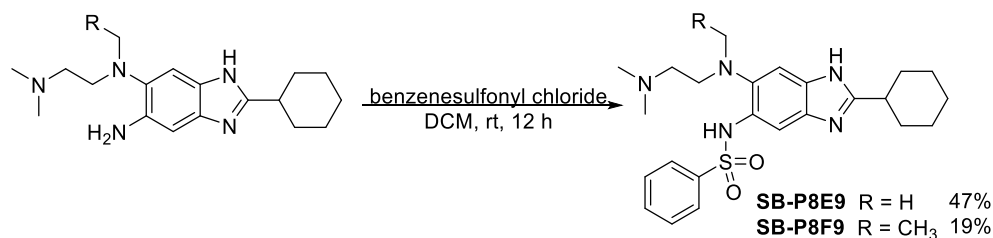
Figure 4.3. Structures of hit benzimidazoles against *F. tularensis* with 40-50 % growth inhibition 0.2 $\mu\text{g}/\text{mL}$ ¹⁹

To determine the accurate MIC values of the compounds against the bacteria, the molecules were resynthesized.

4.2. Results and Discussion

4.2.1. Re-synthesis of hits against *F. tularensis*

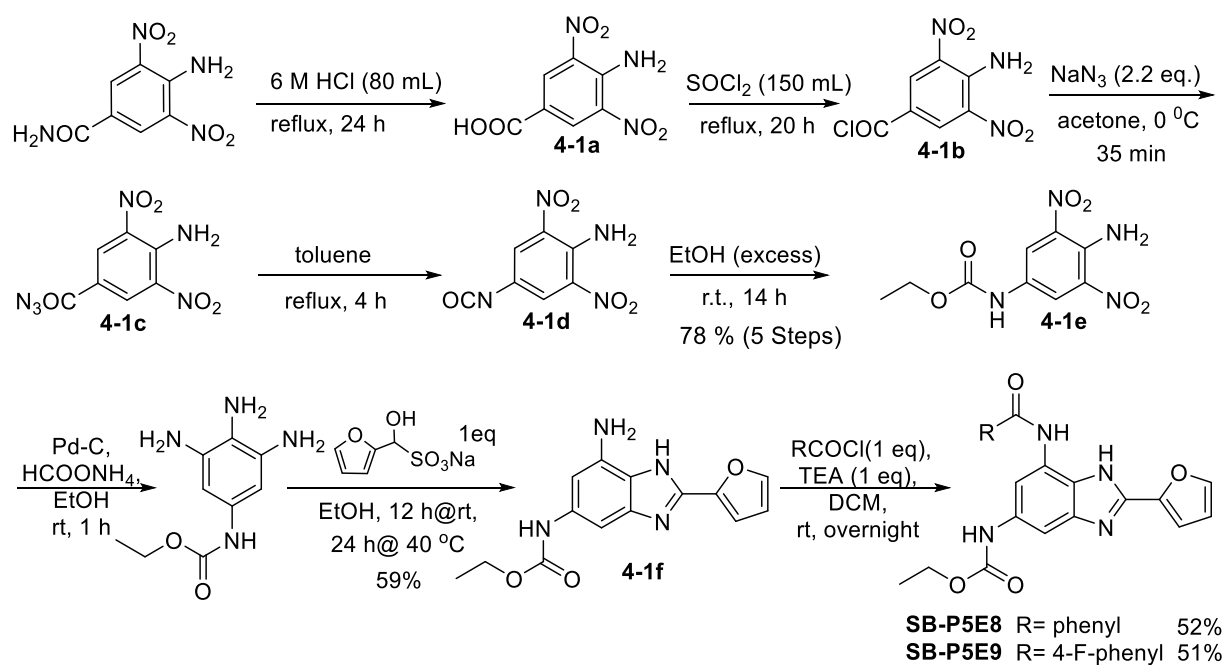
To synthesize **SB-P8B8**, the previously prepared intermediate **2-4b** was treated with cyclopropanecarboxylic acid to obtain the desired product. **SB-P8E9** and **SB-P8F9** were synthesized by treating the appropriate intermediate with benzenesulfonyl chloride (**Scheme 4.1**).



Scheme 4.1. Synthesis of hit 2,5,6-trisubstituted benzimidazole¹⁹

SB-P5E8 and **SB-P5E9** were synthesized from the common intermediate as described below (**Scheme 4.2**).¹⁹ The first step of the reaction sequence was the hydrolysis of 4-amino-3,5-dinitrobenzamide in the presence of concentrated hydrochloric acid followed by the conversion of the acid **4-1a** to the corresponding acid chloride **4-1b**. The acid chloride was treated with sodium azide at low temperature, since it is explosive, to give the acyl azide **4-1c**. This underwent the Curtius re-arrangement on refluxing in toluene to generate the isocyanate intermediate **4-1d** which

was treated with ethanol to obtain the desired carbamate intermediate **4-1e** in 78% yield (5 steps). The intermediate **4-1e** was subjected to reduction with ammonium formate in the presence of 10 wt% Pd-C. The reaction was found to be very sensitive to trace amount of water in ethanol. The diamino intermediate was treated with the bisulfite adduct of furan-2-carbaldehyde to give the desired 2,5,7-trisubstituted benzimidazole intermediate in 59% yield. The final hit compounds 7-benzamido-5-ethoxycarbonylamino-2-(1-furyl)-1*H*-benzo[*d*]imidazole (**SB-P5E8**) and 7-(4-fluorobenzamido-5-ethoxycarbonylamino-2-(1-furyl)-1*H*-benzo[*d*]imidazole (**SB-P5E9**) were synthesized by benzylation of the 7-amino group of the benzimidazole intermediate with the appropriate benzoyl chloride. The final benzylation reaction was observed to be low yielding. In addition the purification of the final compounds was difficult (**Scheme 4.2**).

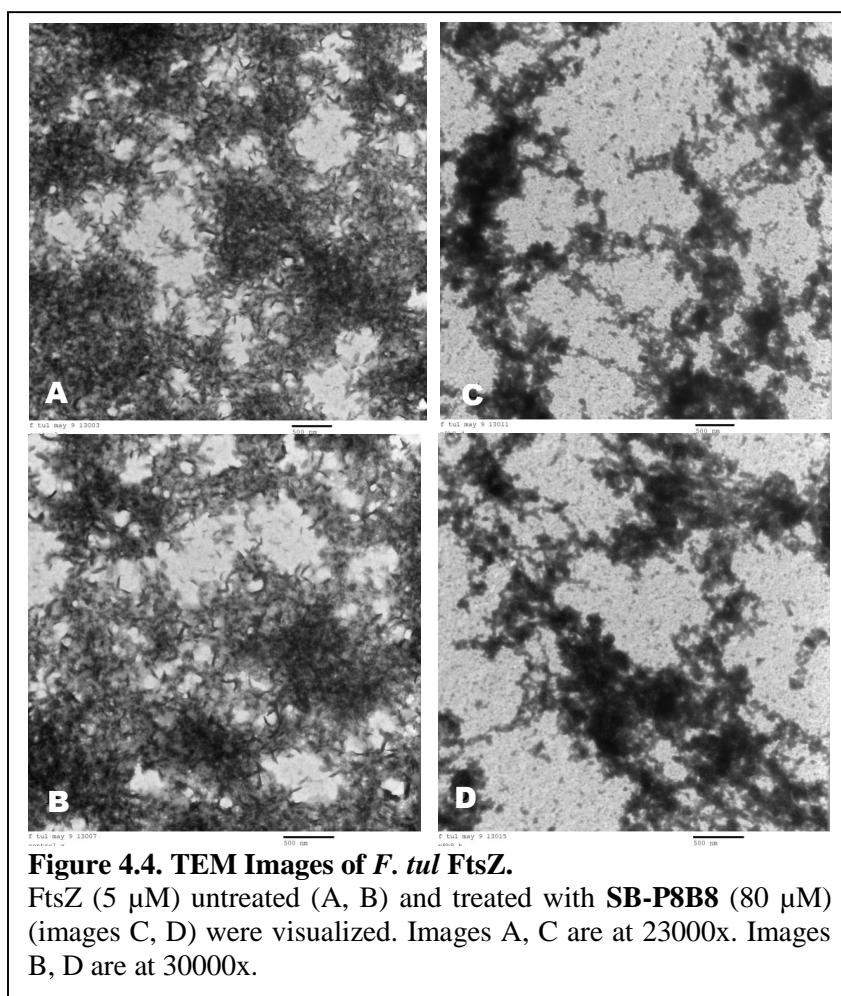


Scheme 4.2. Synthesis of hit 2,5,7 trisubstituted benzimidazole¹⁹

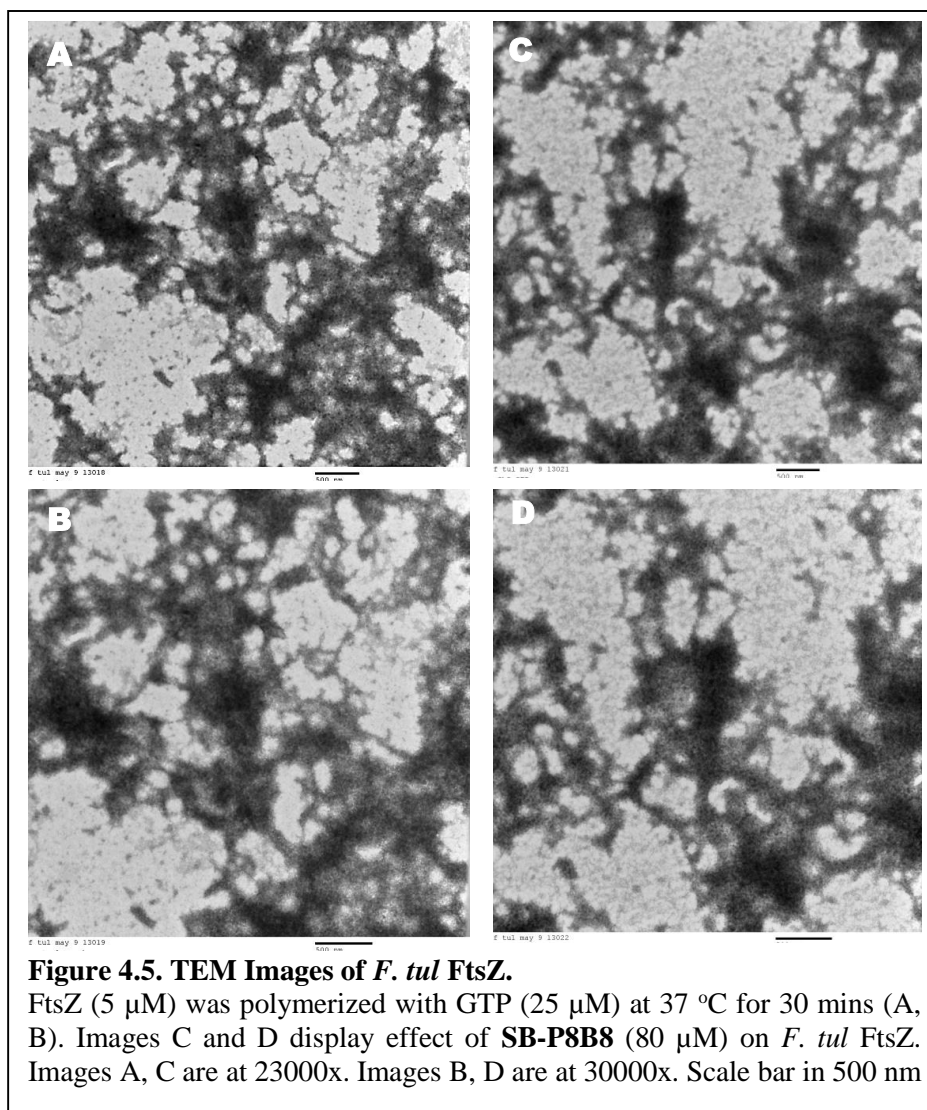
The accurate MIC values of the 5 re-synthesized compounds were determined against *F. tularensis* LVS.¹⁹ The 5-benzenesulfonamides, **SB-P8E8** and **SB-P8E9**, were not active with MIC > 30 µg/mL. **SB-P8B8** was active with an MIC₉₀ value of 2.1 µg/mL while **SB-P5E9** and **SB-P5E8** were active at 2.8 and 3.8 µg/mL, respectively.

4.2.2. Preliminary target validation studies

Expression and purification of *F. tul* FtsZ protein has been posing problems in our laboratory. The protein tends to form aggregates, and this was confirmed by TEM analysis. It was hypothesized that treating protein with a benzimidazole inhibitor might help break up the aggregates. **SB-P8B8** active against *F.tul* LVS at MIC₉₀ = 2.1 µg/mL was selected and *F.tul* FtsZ (5 µM) was incubated without or with 80 µM of **SB-P8B8** for 15 mins on ice and then grids were prepared for visualization. Some amount of de-aggregation was observed for treated protein (**Figure 4.4.**).



Furthermore, the effect of the compound was also tested following addition of GTP. FtsZ (5 µM) was incubated with 80 µM of **SB-P8B8** followed by addition of GTP (25 µM) to initiate polymerization. The compound treated protein once again was less crowded in comparison to the untreated protein (**Figure 4.5**), although the effect was not as pronounced.



4.3. Conclusion

In summary, libraries of trisubstituted benzimidazoles were screened against *F. tularensis* LVS strain to identify novel antibacterial compounds. Three of the identified 2,5,6- and 2 of the 2,5,7-trisubstituted benzimidazoles were resynthesized and evaluated against the bacteria. Additionally, preliminary target validation against *F. tul* FtsZ was unsuccessful since the protein is prone to aggregation. Further optimization of protein expression and purification are currently underway in our laboratory.

4.4. Experimental Section

Methods. ^1H and ^{13}C NMR spectra were measured on a Bruker or Varian 300, 400 or 500 MHz NMR spectrometer. Melting points were measured on a Thomas Hoover Capillary melting point apparatus and are uncorrected. TLC was performed on silica coated aluminum sheets (thickness 200 μm) or alumina coated (thickness 200 μm) aluminum sheets supplied by Sorbent Technologies and column chromatography was carried out on Siliaflash® P60 silica gel, 40-63 μm (230-400 mesh) supplied by Silicycle. Aluminum oxide, activated, neutral, Brockmann Grade I, 58 Å, was supplied by Alfa Aesar.

FEI Tecnai12 BioTwinG transmission electron microscope with an AMT XR-60 CCD digital camera system was used to acquire transmission electron microscopy images.

Materials. The chemicals were purchased from Aldrich Co., Synquest Inc. and Sigma and purified before use by standard methods. Tetrahydrofuran (THF) was freshly distilled from sodium metal and benzophenone. Dichloromethane was also distilled immediately prior to use under nitrogen from calcium hydride.

Synthesis of SB-P8B8: To a solution of **2-4b** (100 mg, 0.35 mmol) in 2 mL of dichloromethane was added 1-ethyl-3-(3-dimethylaminopropyl) carbodiimide (1.1 eq) (EDC) and cyclopentanecarboxylic acid (1.1 eq). 4-Dimethylaminopyridine (DMAP) (1.1 eq) was added to the above reaction mixture, and the reaction was stirred overnight at room temperature. After completion of the reaction as per TLC, the reaction mixture was diluted with dichloromethane followed by the addition of triethylamine. The reaction mixture was transferred to a separatory funnel and the organic layer was washed with water, aqueous sodium bicarbonate and brine. The organic layer was dried over magnesium sulfate, filtered and concentrated using rotary evaporator. The crude product was purified by flash chromatography (column was packed with hexane, 20% ethyl acetate was used steadily increasing to 40% ethyl acetate) to obtain the product as an off-white solid (90 mg, 73% yield). Light brown solid; mp 165-166 °C; ^1H NMR (400 MHz, CDCl_3) δ 0.80 - 0.93 (m, 4 H), 1.08 - 1.15 (m, 2 H), 1.20 - 1.39 (m, 6 H), 1.50 - 1.73 (m, 5 H), 1.74 - 1.84 (m, 2 H), 1.89 - 2.03 (m, 6 H), 2.70 - 2.82 (m, 1 H), 2.99 (br. s, 4 H), 7.46 (s, 1 H), 8.44 (s, 1 H), 8.93 (s, 1 H); ^{13}C NMR (101 MHz, CDCl_3) δ 8.0, 16.4, 24.6, 26.0, 26.3, 31.9, 38.6, 53.8, 103.0,

109.6, 129.5, 131.4, 136.0, 138.6, 159.7, 172.0; HRMS (ESI) m/z calcd for $C_{21}H_{28}N_4OH^+$: 353.2336, Found: 353,2341 ($\Delta = -1.4$ ppm).

Synthesis of 5-benzenesulfonamido-2-cyclohexyl-6-(*N',N'*-dimethyl-*N*-ethylethylenediamino)-1*H*-benzo[*d*]imidazole (SB-P8F9): To a solution of **2-4e** (115 mg, 0.39 mmol) in dichloromethane (5 mL) was added benzenesulfonyl chloride dropwise at room temperature. After the addition, the mixture was stirred at room temperature overnight. After the completion of the reaction, the reaction mixture was washed with a saturated solution of sodium bicarbonate. The organic layer was separated and dried over anhydrous magnesium sulfate, filtered and concentrated under reduced pressure. The crude product was purified by flash chromatography to obtain product as a white solid; 19% yield; mp 187-188 °C; 1H NMR (400 MHz, Methanol- d_4) δ 0.60 (t, $J = 7.15$ Hz, 3 H), 1.35 - 1.52 (m, 3 H), 1.63 (qd, $J = 12.38, 3.01$ Hz, 3 H), 1.72 - 1.81 (m, 1 H), 1.87 (dt, $J = 12.86, 3.11$ Hz, 2 H), 2.00 - 2.10 (m, 2 H), 2.35 (t, $J = 5.77$ Hz, 2 H), 2.39 (s, 6 H), 2.74 (q, $J = 7.03$ Hz, 2 H), 2.80 - 2.94 (m, 3 H), 7.29 (s, 1 H), 7.36 - 7.44 (m, 2 H), 7.46 - 7.52 (m, 1 H), 7.68 - 7.79 (m, 3 H); ^{13}C NMR (101 MHz, Methanol- d_4) δ 13.4, 27.1, 27.3, 32.9, 40.0, 45.1, 50.8, 55.2, 57.8, 107.4, 111.1, 128.2, 130.1, 133.1, 133.6, 139.6, 142.4, 161.8; HRMS (ESI) m/z calcd for $C_{25}H_{35}N_5O_2SH^+$: 470.2590, Found: 470.2590 ($\Delta = 0.0$ ppm).

Same procedure was followed for the synthesis of **5-benzenesulfonamido-2-cyclohexyl-6-(*N',N',N*-trimethylethylenediamino)-1*H*-benzo[*d*]imidazole (SB-P8E9):** White solid; 47 % yield; mp >200 °C; 1H NMR (400 MHz, Methanol- d_4) δ 1.34 - 1.51 (m, 3 H), 1.54 - 1.68 (m, 2 H), 1.76 (d, $J = 12.30$ Hz, 1 H), 1.86 (d, $J = 13.05$ Hz, 2 H), 2.04 (d, $J = 11.80$ Hz, 2 H), 2.54 (s, 3 H), 2.83 - 2.95 (m, 7 H), 3.27 (d, $J = 5.02$ Hz, 2 H), 3.32 (d, $J = 7.03$ Hz, 2 H), 7.39 (d, $J = 13.30$ Hz, 2 H), 7.52 (t, $J = 7.65$ Hz, 2 H), 7.60 (t, $J = 7.40$ Hz, 1 H), 7.86 (d, $J = 7.53$ Hz, 2 H); ^{13}C NMR (101 MHz, Methanol- d_4) δ 27.0, 27.1, 32.7, 39.6, 44.1, 44.9, 52.2, 56.6, 109.0, 109.4, 128.5, 130.1, 130.4, 134.4, 135.8, 136.4, 141.4, 142.6, 162.0; HRMS (ESI) m/z calcd for $C_{24}H_{33}N_5O_2SH^+$: 456.2430, Found: 456.2433 ($\Delta = -0.7$ ppm).

Synthesis of 4-ethoxycarbonylamino-2,6-dinitrobenzene (4-1e): A suspension of 4-amino-3,5-dinitrobenzamide (3 g, 13.27 mmol) in 6 N HCl (80 mL) was refluxed overnight. The following day, the reaction mixture was cooled down and the precipitate was filtered to afford a yellow solid, which was dissolved in 150 mL of thionyl chloride, and refluxed overnight. After removal of thionyl chloride by distillation, the crude acid chloride was immediately dissolved in

40 mL of acetone in an ice bath. A solution of sodium azide (1.89 g, 29.18 mmol) dissolved in 8 mL of ice water was added drop-wise. After 30 min at 0°C, 12 mL of ice water was added to the reaction mixture and the extraction was performed with CH₂Cl₂. The organic layer was dried over MgSO₄, and concentrated on the rotary evaporator. The obtained acyl azide was dissolved in toluene and refluxed for 4 h to form the corresponding isocyanate. After the reaction mixture cooled down, excess anhydrous EtOH was added and reaction was stirred overnight at room temperature. The reaction mixture was concentrated and purified by flash chromatography on silica gel (hexanes/EtOAc 1/8 to 1.5/3.5) to afford 4-ethoxycarbonylamino-2,6-dinitrobenzene as a bright red solid (mp 163-165 °C, 2.9 g, 78% yield): ¹H NMR (300 MHz, CDCl₃) δ 8.64 (s, 2 H), 6.59 (br. s, 1 H), 4.26 (q, 2 H, *J* = 6.9 Hz), 1.33 (t, 3 H, *J* = 6.9 Hz); ¹³C NMR (100 MHz, Methanol-d₄) δ 15.00, 62.53, 125.2, 127.9, 136.3, 139.0, 156.1; HRMS (FAB) *m/z* calcd for C₉H₁₀N₄O₆H⁺: 271.0677, Found: 271.0679 (Δ = -0.7 ppm).

Synthesis of 7-amino-5-ethoxycarbonylamino-2-(1-furyl)-1H-benzo[*d*]imidazole (4-1f): To a suspension of 4-ethoxycarbonylamino-2,6-dinitrobenzene (500 mg, 1.85 mmol) in ethanol (64 mL), were added ammonium formate (2.74 g) and 10 wt% Pd/C (245 mg). The mixture, maintained under nitrogen, was stirred at room temperature for 1 h. After completion of the reaction, a solution of sodium bisulfite adduct (223 mg, 1.035 mmol) of the 2-furaldehyde in water (1 mL) was added to the reaction flask. To push the reaction to completion after stirring for 12 h at room temperature under nitrogen, the reaction mixture was heated at 40 °C for 24 h. The reaction mixture was then concentrated to dryness by rotary evaporator. Dichloromethane was added to the residue and filtered over celite to remove the catalyst. The organic layer was transferred to a separatory funnel, washed with water, and brine. The organic layer was dried over magnesium sulfate, filtered and concentrated. The resultant residue was purified by chromatography on silica gel to afford the desired product as a brown solid (314 mg, 59 % yield): dark brown solid; mp 124-126°C; ¹H NMR (300MHz, Methanol-d₄) δ 1.27 (t, *J* = 7.2 Hz, 3 H), 4.15 (q, *J* = 7.2 Hz, 2 H), 6.56 (d, *J* = 22.4 Hz, 2 H), 7.03 (m, 1 H), 7.14 (s, 1 H), 7.62 (s, 1 H); ¹³C NMR (100 MHz, Methanol-d₄) δ 15.09, 61.90, 93.55, 100.91, 110.61, 113.14, 137.33, 139.17, 143.47, 145.24, 146.82, 156.41; HRMS (FAB) *m/z* calcd for C₁₄H₁₄N₄O₃H⁺: 287.1143, Found: 287.1144 (Δ = -0.3 ppm).

Synthesis of 7-benzamido-5-ethoxycarbonylamino-2-(1-furyl)-1H-benzo[d]imidazole (SB-P5E8): 7-Amino-5-ethoxycarbonylamino-2-(1-furyl)-1H-benzo[d]imidazole (**4-1f**) (100 mg, 0.38 mmol) was dissolved in dichloromethane and triethylamine (53.5 μ L, 0.38 mmol) was added to the solution. To this, benzoyl chloride (49.2 μ L, 0.42 mmol) was added dropwise while on ice and reacted overnight at room temperature. After completion of the reaction as per TLC, the reaction mixture was diluted with ethyl acetate and transferred to a separatory funnel. The organic layer was washed with saturated sodium bicarbonate solution, followed by water, and brine. The organic layer was dried over magnesium sulfate, filtered and concentrated on a rotary evaporator. The crude product was purified by flash chromatography to obtain the product which was then treated with activated charcoal to obtain a final yield of 52 % yield (78 mg). Light brown solid; mp turned black at 140 $^{\circ}$ C; 1 H NMR (400 MHz, CDCl₃) δ 1.26 (t, J = 7.15 Hz, 3 H), 4.18 (q, J = 7.03 Hz, 2 H), 6.43 (br. s, 1 H), 6.90 - 7.09 (m, 1 H), 7.27 - 7.81 (m, 6 H), 7.97 (d, J = 7.53 Hz, 2 H), 9.14 (br. s, 1 H); 13 C NMR (101 MHz, CDCl₃) δ 14.7, 61.5, 106.2, 110.9, 112.4, 127.7, 128.8, 132.2, 134.5, 143.1, 144.1, 145.0, 154.8, 166.5; HRMS (ESI) m/z calcd for C₂₁H₁₈N₄O₄H⁺: 391.1401, Found: 391.1406 (Δ = -1.3 ppm).

Same procedure was followed for the synthesis of **7-(4-fluorobenzamido)-5-ethoxycarbonylamino-2-(1-furyl)-1H-benzo[d]imidazole (SB-P5E9):** Light brown solid; 51 % yield; mp turned black at 140 $^{\circ}$ C; 1 H NMR (400 MHz, CDCl₃) δ 1.24 (t, J = 7.03 Hz, 3 H), 4.16 (q, J = 6.78 Hz, 2 H), 6.41 (br. s, 1 H), 6.96 - 7.17 (m, 3 H), 7.28 - 7.72 (m, 3 H), 7.90 - 7.99 (m, 2 H), 9.11 (br. s, 1 H); 13 C NMR (101 MHz, CDCl₃) δ 14.7, 61.5, 106.6, 110.8, 112.4, 115.7, 116.0, 130.0, 130.1, 130.7, 134.4, 143.2, 144.1, 145.0, 154.8, 163.9, 165.4, 166.4; HRMS (ESI) m/z calcd for C₂₁H₁₇FN₄O₄H⁺: 409.1316, Found: 409.1312 (Δ = 1.0 ppm).

Transmission Electron Microscopy (TEM) Analysis: Protein prepared by Dr. Eduard Melief was used for this assay. Stock solution of **SB-P8B8** was prepared in ethanol. FtsZ (5 μ M) was incubated with 80 μ M of **SB-P8B8** in the polymerization buffer (50 mM MES, 5mM MgCl₂, 100 mM KCl, pH 6.5) for 15 min on ice. The resulting solution was diluted 2 times with the polymerization buffer and immediately transferred to carbon coated 300 mesh formvar copper grid and negatively stained with 1% uranyl acetate. Alternatively, FtsZ (5 μ M) was incubated with 80 μ M of **SB-P8B8** in the polymerization buffer (50 mM MES, 5mM MgCl₂, 100 mM KCl, pH 6.5) for 15 min on ice. To each solution was added GTP to the final concentration of 25 μ M. The

resulting solution was incubated at 37 °C for 30 min. The incubated solution was diluted 2 times with the polymerization buffer and immediately transferred to carbon coated 300 mesh formvar copper grid and negatively stained with 1% uranyl acetate. The samples were viewed at the Microscopy Imaging Center at Stony Brook University, with a FEI Tecnai12 BioTwinG transmission electron microscope at 80 kV. Digital images were acquired with an AMT XR-60 CCD digital camera system.

4.5. References

1. Gould, I. M.; David, M. Z.; Esposito, S.; Garau, J.; Lina, G.; Mazzei, T.; Peters, G., New insights into meticillin-resistant *Staphylococcus aureus* (MRSA) pathogenesis, treatment and resistance. *Int. J. Antimicrob. Agents* **2012**, *39*, 96-104
2. Wang, J.-L.; Hsueh, P.-R., Therapeutic options for infections due to vancomycin-resistant enterococci. *Expert Opin. Pharmacother.* **2009**, *10*, 785-796
3. McLendon, M. K.; Apicella, M. A.; Allen, L.-A. H., *Francisella tularensis*: taxonomy, genetics, and immunopathogenesis of a potential agent of biowarfare. *Annu. Rev. Microbiol.* **2006**, *60*, 167-185
4. Feodorova, V. A.; Corbel, M. J., Prospects for new plague vaccines. *Expert Rev. Vaccines* **2009**, *8*, 1721-1738
5. Oyston, P. C. F.; Sjoestedt, A.; Titball, R. W., Tularemia: bioterrorism defence renews interest in *Francisella tularensis*. *Nature Reviews Microbiology* **2004**, *2*, 967-978
6. Ryan, K. J.; Ray, C. G., *Sherris Medical Microbiology: An Introduction to Infectious Diseases*. McGraw Hill: 2004; p 488-490.
7. Evans, M. E.; Gregory, D. W.; Schaffner, W.; McGee, Z. A. *Tularemia: a 30-year experience with 88 cases*; United States FIELD Citation:., 1985; pp 251-69.
8. Dennis, D. T.; Inglesby, T. V.; Henderson, D. A.; Bartlett, J. G.; Ascher, M. S.; Eitzen, E.; Fine, A. D.; Friedlander, A. M.; Hauer, J.; Layton, M.; Lillibridge, S. R.; McDade, J. E.; Osterholm, M. T.; O'Toole, T.; Parker, G.; Perl, T. M.; Russell, P. K.; Tonat, K., Tularemia as a biological weapon: medical and public health management. *Jama* **2001**, *285*, 2763-73
9. Larsson, P.; Oyston, P. C. F.; Chain, P.; Chu, M. C.; Duffield, M.; Fuxelius, H.-H.; Garcia, E.; Haelltorp, G.; Johansson, D.; Isherwood, K. E.; Karp, P. D.; Larsson, E.; Liu, Y.; Michell, S.; Prior, J.; Prior, R.; Malfatti, S.; Sjoestedt, A.; Svensson, K.; Thompson, N.; Vergez, L.; Wagg, J. K.; Wren, B. W.; Lindler, L. E.; Andersson, S. G. E.; Forsman, M.; Titball, R. W., The complete genome sequence of *Francisella tularensis*, the causative agent of tularemia. *Nat. Genet.* **2004**, *37*, 153-159
10. Saslaw, S.; Eigelsbach, H. T.; Wilson, H. E.; Prior, J. A.; Carhart, S., Tularemia vaccine study. I. Intracutaneous challenge. *Arch Intern Med* **1961**, *107*, 689-701
11. Saslaw, S.; Eigelsbach, H. T.; Prior, J. A.; Wilson, H. E.; Carhart, S., Tularemia vaccine study. II. Respiratory challenge. *Arch Intern Med* **1961**, *107*, 702-14

12. Health Aspects of Chemical and Biological Weapons. *World Health Organization* **1970**,
13. Miller, J. R.; Waldrop, G. L., Discovery of novel antibacterials. *Expert Opin. Drug Discovery* **2010** *5*, 145-154
14. World Health Organization, Tuberculosis: Data and Country Profiles. Available at http://www.who.int/tb/publications/global_report/gtbr13_executive_summary.pdf?ua=1.
15. Enderlin, G.; Morales, L.; Jacobs, R. F.; Cross, J. T., Streptomycin and alternative agents for the treatment of tularemia: review of the literature. *Clinical infectious diseases an official publication of the Infectious Diseases Society of America* **1994**, *19*, 42-7
16. Ikaheimo, I.; Syrjala, H.; Karhukorpi, J.; Schildt, R.; Koskela, M., In vitro antibiotic susceptibility of *Francisella tularensis* isolated from humans and animals. *J. Antimicrob. Chemother.* **2000**, *46*, 287-290
17. Awasthi, D.; Kumar, K.; Knudson, S. E.; Slayden, R. A.; Ojima, I., SAR Studies on Trisubstituted Benzimidazoles as Inhibitors of Mtb FtsZ for the Development of Novel Antitubercular Agents. *J. Med. Chem.* **2013**, *56*, 9756-9770
18. Kumar, K.; Awasthi, D.; Lee, S.-Y.; Zanardi, I.; Ruzsicska, B.; Knudson, S.; Tonge, P. J.; Slayden, R. A.; Ojima, I., Novel Trisubstituted Benzimidazoles, Targeting Mtb FtsZ, as a New Class of Antitubercular Agents. *J. Med. Chem.* **2011**, *54*, 374-381
19. Kumar, K.; Awasthi, D.; Lee, S.-Y.; Cummings, J. E.; Knudson, S. E.; Slayden, R. A.; Ojima, I., Benzimidazole-based antibacterial agents against *Francisella tularensis*. *Bioorg. Med. Chem.* **2013**, *21*, 3318-26

Chapter 5

Synthesis and Optimization of Novel Trisubstituted Benzoxazoles

Table of Contents

| | |
|----------------------------------------------------------------|-----|
| Chapter 5 | 125 |
| 5.1. Investigating trisubstituted benzoxazole scaffold | 126 |
| 5.2. Results and Discussion..... | 127 |
| 5.2.1. Synthesis of trisubstituted benzoxazoles..... | 127 |
| 5.2.2. Benzoxazole analogues of SB-P8B2 and SB-P8B4..... | 135 |
| 5.2.3. Benzoxazole analogues of SB-P6B10 and SB-P17G-A20 | 136 |
| 5.2.4. Accurate MIC of synthesized benzoxazoles | 137 |
| 5.3. Conclusion | 138 |
| 5.4. Experimental Section..... | 138 |
| 5.5. References | 149 |

5.1. Investigating trisubstituted benzoxazole scaffold

In an effort to expand our existing library and to diversify the substrate scaffold, the synthesis of trisubstituted benzoxazoles was initiated. We started with the 2,5,6-trisubstituted benzoxazoles since this pattern on the benzimidazole scaffold has been well explored in our laboratory and has led to the identification of potent antibacterial agents. Although several published methods are available for the synthesis of benzoxazoles, the desired 5-dialkylamino-6-aminobenzoxazoles with different 2-position substituents have not been synthesized thus far. Additionally, they have not been explored as antibacterial agents targeting the cell division protein FtsZ.

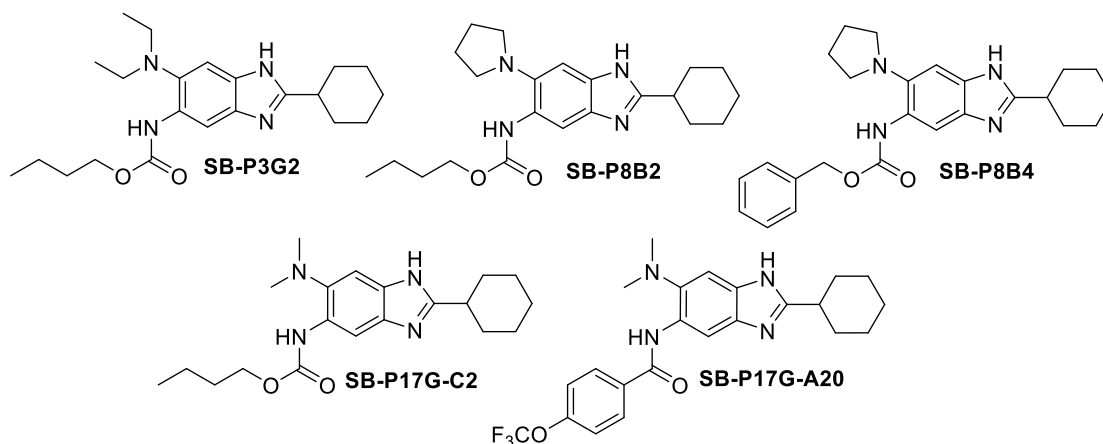


Figure 5.1. Lead benzimidazole with potent antibacterial activity ^{1,2}

Analogues of the lead compounds from the benzimidazole series namely, **SB-P3G2**, **SB-P8B2**, **SB-P8B4**, **SB-P17G-C2** and **SB-P17G-A20**, served as the initial target molecules (**Figure 5.1**).^{1,2} To identify new antibacterial agents and to develop a preliminary SAR, exploration of the 2-position was also planned. **Figure 5.2** elaborates a representative set of trisubstituted benzoxazoles to be synthesized.

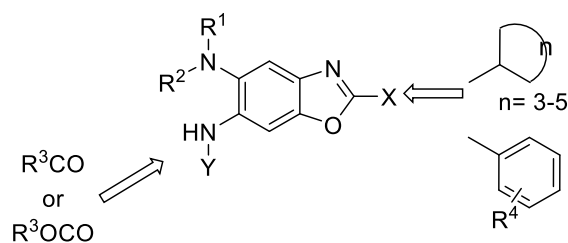


Figure 5.2. Proposed benzoxazoles to be synthesized

5.2. Results and Discussion

5.2.1. Synthesis of trisubstituted benzoxazoles

Peng *et al.* have described a method for direct base-promoted intramolecular *o*-arylation of *o*-haloanilides to afford benzoxazoles (**Figure 5.3**).³ According to the proposed mechanism the reaction proceeds via benzyne mechanism. Following this procedure, intermediate **5-1b** synthesized by benzoylation of **5-1a**, was treated with anhydrous potassium carbonate in dimethyl sulfoxide at 140 °C. Unfortunately after 2 days under the reaction conditions no product formation was observed. Since the reaction proceeds via benzyne mechanism, the electron withdrawing nitro group may have reduced the reactivity of the substrate. To this end, the nitro group was reduced to the amine in the presence of stannous chloride, and the substrate was subjected again to the reaction conditions. After 3 h in the microwave reactor at 140 °C, followed by purification via column chromatography two major spots were isolated. The mass spectra of the two major spots was observed to be MS (ESI) m/z 356 (M+1)⁺ and MS (ESI) m/z 279 (M+1)⁺, respectively and the ¹H NMR was inconclusive.

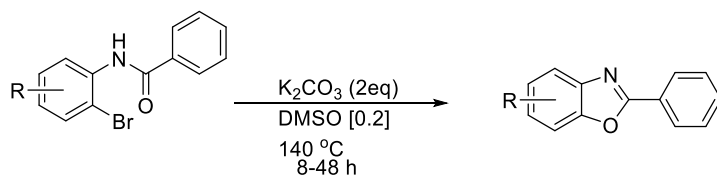
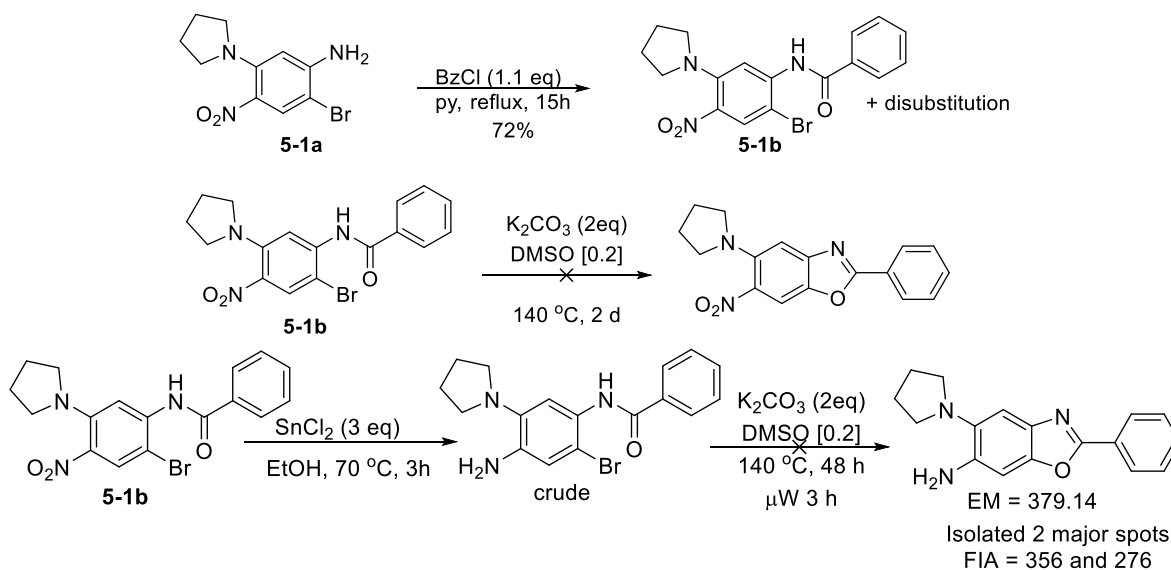


Figure 5.3. Benzoxazole synthesis employed by Peng *et al.*³



Scheme 5.1. Reaction to synthesize trisubstituted benzoxazole³

Next, the procedure adopted by Muller *et al.* was attempted (**Figure 5.4**).⁴ Starting from 1-cyclohexylcarbonyloxy-5-diethylamino-2,4-dinitrobenzene (**5-1c**), the substrate was treated with 7 equivalents of stannous chloride for 6 h followed by treatment of the crude material with thionyl chloride and pyridine in benzene (**Scheme 5.2**). The reaction was monitored by mass spectroscopy and no mass peak corresponding to the product was observed. The reaction was performed again with the intention of isolating the reduced product first and then subjecting it to the next step. To this end, the dinitro substrate (**5-1c**) was treated with 10 equivalents of stannous chloride for 26 h. The reaction was followed by mass spectroscopy and an additional 3 equivalent of stannous chloride was added to the reaction mixture. Mass spectroscopic analysis showed a peak of MS (ESI) m/z 302 (M+1)⁺ which is 3.21 units less than that of the product.

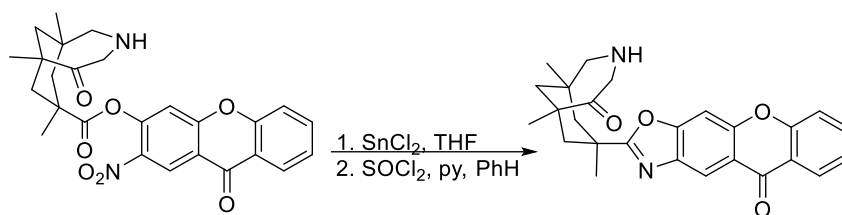
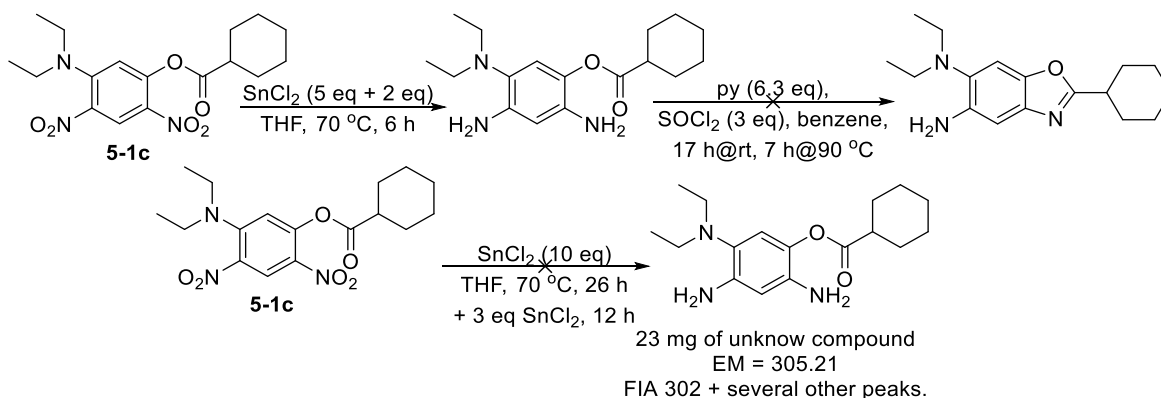
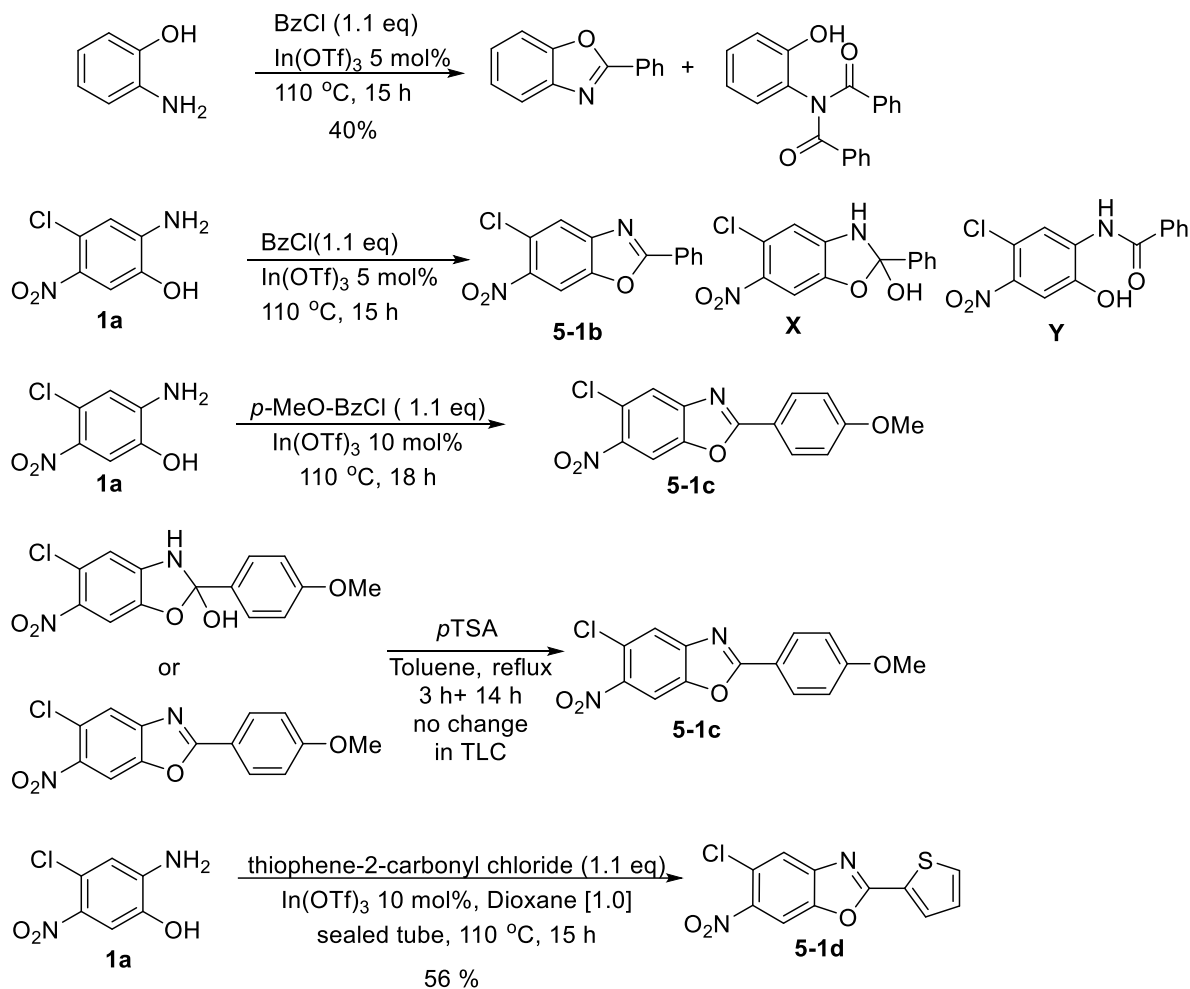


Figure 5.4. Thionyl chloride catalyzed cyclization⁴



Scheme 5.2. Reduction-cyclization of 1-cyclohexylcarbonyloxy-2,4-dinitro-5-diethylaminobenzene⁴

Since the above two methods did not give fruitful results alternative methods were tested. In the presence of $\text{In}(\text{OTf})_3$, *o*-aminophenol and aromatic carbonyl chlorides have been shown to cyclize under neat conditions to yield benzoxazoles.⁵



Scheme 5.3. Indium triflate as a Lewis acid for 2-aromatic or 2-heteroaromatic benzoxazole synthesis⁵

The method was employed to successfully obtain 2-phenylbenzoxazole in 40% yield from commercially available 2-aminophenol but a lot of disubstituted phenol was obtained as by-product (**Scheme 5.3**). The same reaction was carried out with 2-amino-4-chloro-5-nitrophenol and benzoyl chloride in which case the exact structure of the compound could not be ascertained. The mass spectrum displayed MS (ESI) m/z 293 ($M+1$)⁺ whereas the exact mass of the product is 274.01. The +18 peak implies that the cyclization may not have gone to completion and possibly resulted in the formation of **X** or **Y** (**Scheme 5.3**). On increasing the catalyst loading to 10% In(OTf)₃ and increasing the reaction time to 18 hours with *p*-methoxybenzoyl chloride, the desired product was obtained. Although the FIA still showed the +18 peak, formation of the benzoxazole was confirmed by treating the product with dehydrating agent, *p*TSA. There was no change in R_f on TLC and ¹H NMR confirmed the formation of the desired benzoxazole, which was purified by

recrystallization to obtain product in 53% yield. To synthesize 5-chloro-6-nitro-2-(thiophen-2-yl)benzoxazole, indium triflate (10 mol%) and dioxane (solvent) were used, and the yield was only 56%.

A different procedure followed by Kuroyanagi *et al.* was also examined (**Figure 5.5**).⁶ In the first step (**Scheme 5.4**), substituted aminophenol was treated with acyl chloride in the presence of diisopropylethylamine as a base to obtain the *N*-acylated product. Acid catalyzed cyclization yielded the desired benzoxazole. When the reaction was performed with cyclohexanecarbonyl chloride, a lot of di-acylated intermediate was recovered as by-product after acid catalyzed cyclization. In the next optimization, the equivalence of the carbonyl chloride was reduced, and the reaction proceeded smoothly to yield the desired product in 70% yield.

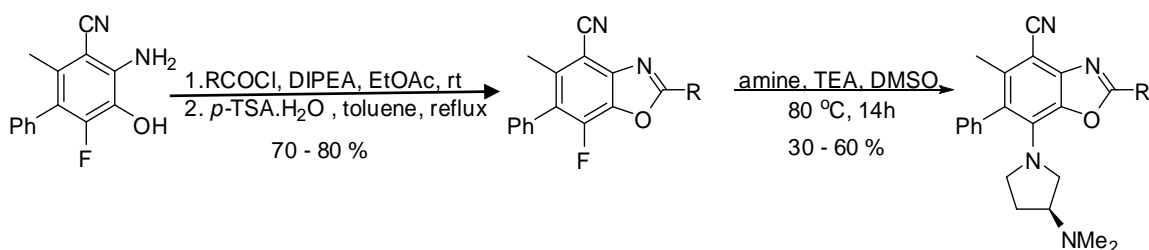
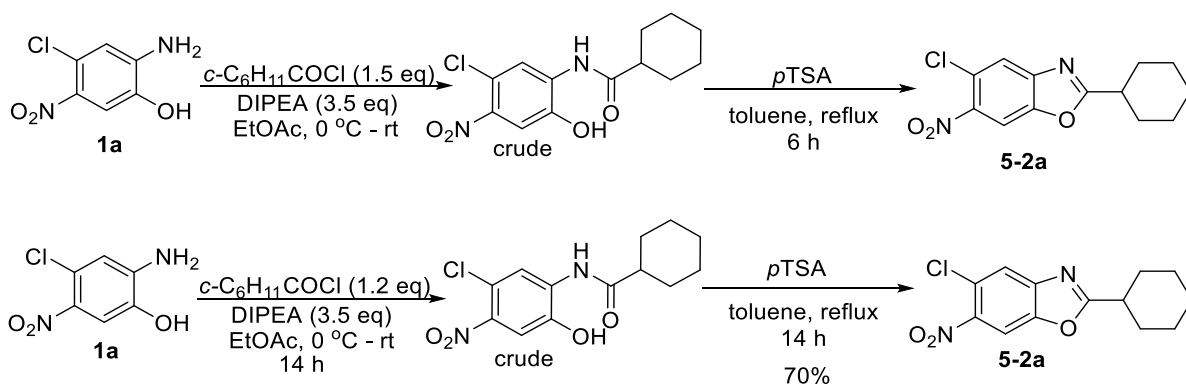
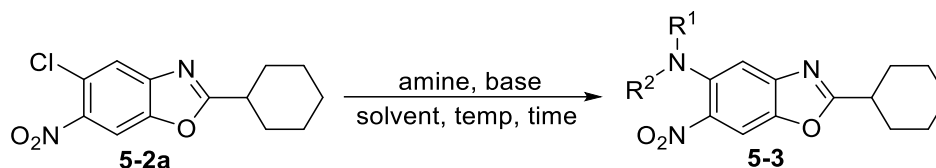


Figure 5.5. Benzoxazole synthesis employed by Kuroyanagi *et al.*⁶



Scheme 5.4. Optimization of synthesis of trisubstituted benzoxazoles

The next step was to substitute the chloro group of 5-chloro-2-cyclohexyl-6-nitrobenzoxazole with different amines. Various reaction conditions as summarized in **Table 5.1** were attempted.

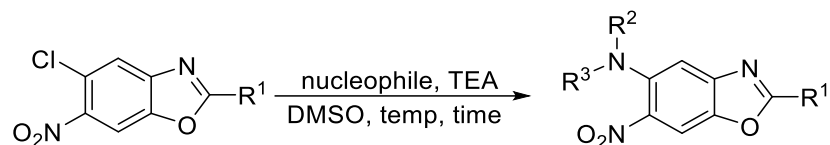
Table 5.1. Optimization of nucleophilic aromatic substitution

| Amine | Base | Solvent | Temp | Time | Result |
|------------------------------|------------------------------------------|---------|--------------------------------------------------|-----------------------|--------------------------|
| Pyrrolidine 2 eq | TEA 2.15 eq | DMSO | 80 °C | 12 h | SM:P = 1:1.7 |
| Pyrrolidine 1.5 eq | NaH ^a 1.5 eq | THF | rt | 24 h | Mostly SM |
| Pyrrolidine 2.5 eq + 1 eq | K ₂ CO ₃ 2.5 eq | DMF | 85 °C | 24 h | P<10% yield Messy rxn |
| Diethylamine 2.5 eq | K ₂ CO ₃ 2.5 eq | DMF | 80 °C, sealed tube 80 °C, μW 120 °C, μW | 12 h 1h 30 mins | Messy rxn |
| N-methylpiperazine 2.5 eq | K ₂ CO ₃ 2.5 eq | DMSO | 120 °C, sealed tube | 24 h | No product |

^a Pyrrolidine was stirred with NaH for 40 mins and then the intermediate was added

Since triethylamine and dimethyl sulfoxide worked the best, the same reaction was performed at 90 °C in the microwave reactor. After 10 h, product was obtained in 76% conversion yield. When piperidine was used as base, the product was only obtained in 50% conversion yield under microwave conditions and 69% conversion yield when conventional heating was used in a sealed tube. The procedure for this nucleophilic aromatic substitution is yet to be standardized. As **Table 5.2** shows, the reaction conditions had to be altered for the different 2-position modified benzoxazoles and was not reproducible.

Table 5.2. Nucleophilic aromatic substitution of 5-position chloro with amines

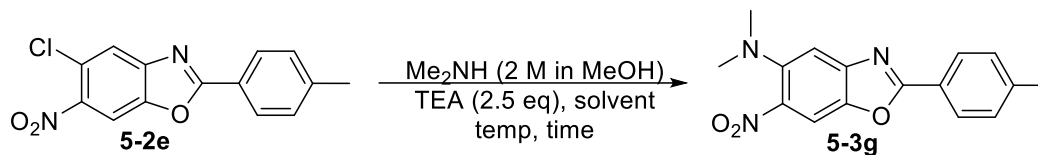


| R¹ | Nucleophile | TEA (eq) | Temp | Time | Conversion Yield |
|------------------------------|------------------------------|-----------------|---------------------------|-------------------|-------------------------|
| 2-cyclohexyl | pyrrolidine 2 eq + 1 eq | 2.15 + 1 | 90 °C, μ W | 10 h | 76% |
| | pyrrolidine 2.5 eq | 2.5 | 80 °C, sealed tube | 48 h | 76% |
| | piperidine 2 eq | 2.15 | 80 °C, μ W 100 °C, | 2 h 3 h | 50% |
| | piperidine 2 eq | 2.15 | 100 °C sealed tube | 14 h | 69% |
| | dimethylamine 2.5 eq | 2.5 | 90 °C sealed tube | 72 h | 75% |
| 2-(<i>p</i> -methoxyphenyl) | pyrrolidine 2 eq + 0.5 eq | 2.15 + 0.5 | 80 °C, sealed tube | 14 h + 18 h | crude |
| 2-phenyl | pyrrolidine 2 eq | 2.15 | 80 °C, sealed tube | 15 h | 59% |
| 2-cyclopentyl | pyrrolidine 2.5 eq | 2.5 | 80 °C, sealed tube | 48 h | 58% |
| 2-cyclobutyl | dimethylamine 2.5 eq | 2.5 | 90 °C sealed tube | 48 h | 63% |
| 2-(pentan-3-yl) | dimethylamine 2.5 eq | 2.5 | 90 °C sealed tube | 48 h | 100% (solvent heavy) |

Dimethyl sulfoxide could not be used as solvent to substitute the chlorine of 5-chloro-6-nitro-2-*p*-tolylbenzoxazole because of poor solubility of the intermediate. Increasing the reaction temperature to 100 °C and increasing the reaction time did not improve the conversion. Changing the solvent to toluene and heating the reaction at 90 °C for 2 d in a sealed tube or employing

microwave irradiation also gave poor conversion. After three separate attempts at synthesizing the compound, only 74 mg of 5-*N,N*-dimethylamino-6-nitro-2-tolylbenzoxazole was obtained.

Table 5.3. Nucleophilic aromatic substitution of 5-chloro-6-nitro-2-*p*-tolylbenzoxazole

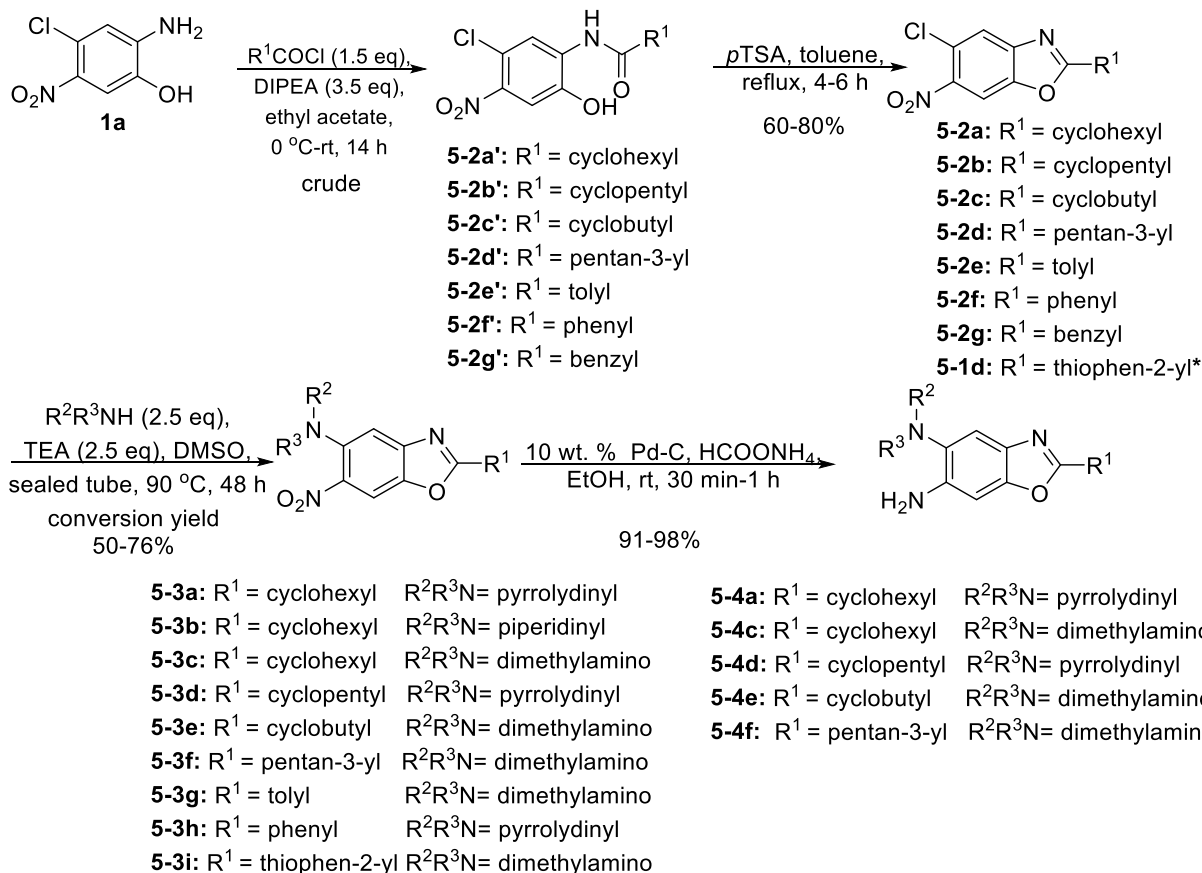


| Me₂NH (2 M in MeOH) | TEA | Solvent | Vessel | Temp | Time | Result^a |
|-------------------------------------------|------------|----------------|---------------|-------------|-------------|---------------------------|
| 2.5 eq | 2.5 eq | DMSO | Sealed tube | 90 °C | 2 d | Low |
| + 1 eq | | | | 100 °C | 1 d | conversion |
| 2.5 eq | 2.5 eq | toluene | Sealed tube | 90 °C | 2 d | Low conversion |
| 2.5 eq | 2.5 eq | toluene | μW | 90 °C | 4 h | Low conversion |

^a combined all the fraction to obtain 74 mg of product

The reduction of 6-position nitro to amine proceeded smoothly with 10 wt.% Pd-C and ammonium formate.

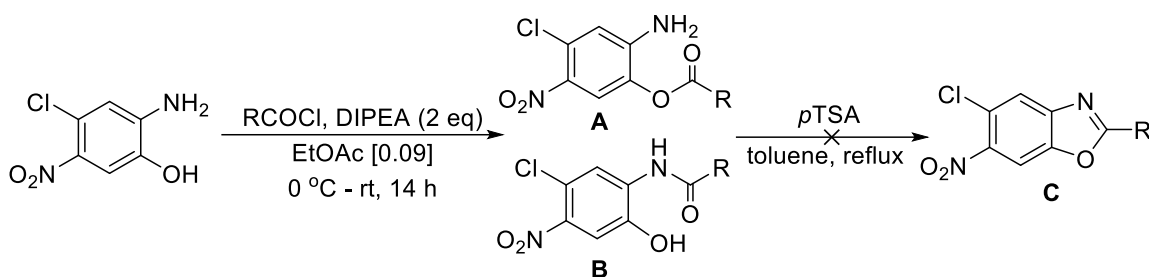
The general scheme for the synthesis of trisubstituted benzoxazole developed thus far is summarized below (**Scheme 5.5**). 5-Chloro-6-nitro-2-(thiophen-2-yl)benzo[*d*]oxazole (**5-1d**) was synthesized using indium triflate as describe in **Scheme 5.3**.

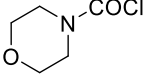
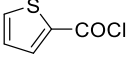
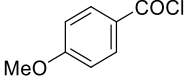


Scheme 5.5. Optimized synthesis of 2,5,6-trisubstituted benzoxazoles

***5-1d** was synthesized from **1a** via In(OTf)₃ catalyzed cyclization.

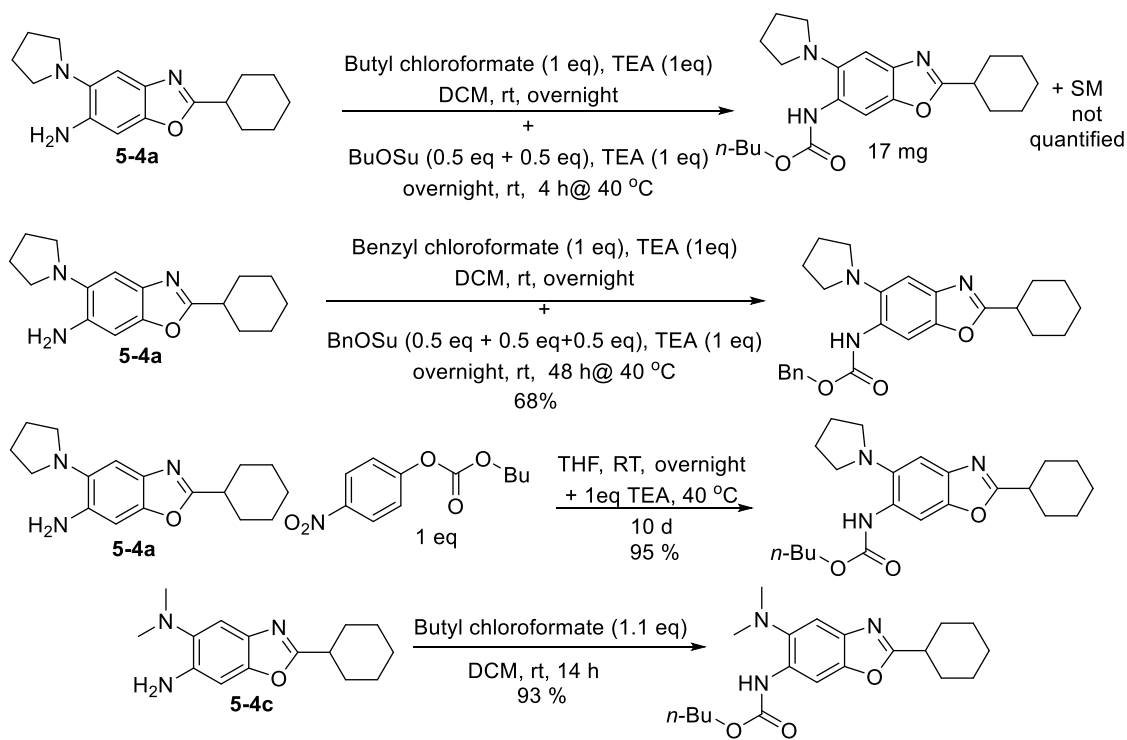
It is worth noting that the developed methodology did not work when morpholino-4-carbonyl chloride or thiophene-2-carbonyl chloride was used in the first step. For morpholine-4-carbonyl chloride, the first attempt at *N*-acylation failed, but the second attempt with 2.5 equivalence of morpholine-4-carbonyl chloride progressed to yield the *O*-acylated aniline instead of the desired *N*-acylated compound, which didn't cyclize in the presence of *p*TSA. Similarly for thiophene-2-carbonyl chloride and 4-methoxybenzoyl chloride the *O*-acylated aniline was obtained which didn't convert to the desired benzoxazole. Since In(OTf)₃ has been shown to promote cyclization by Wang *et al.*, 10 mol % was used on the ester under solvent free conditions in a sealed tube at 110 °C for 14 h, but these conditions also failed (**Table 5.4**).

Table 5.4. Failed synthesis of benzoxazole

| RCOCl | DIPEA | A/B | C |
|----------------------------------------------------------------------------------------------|----------------|------------|--------------|
|  2.5 eq | 2.0 eq | A | Not observed |
|  1.0 eq | 2.0 eq | A | Not observed |
|  1.0 eq | 3.5 eq | A | Not observed |

5.2.2. Benzoxazole analogues of SB-P8B2 and SB-P8B4

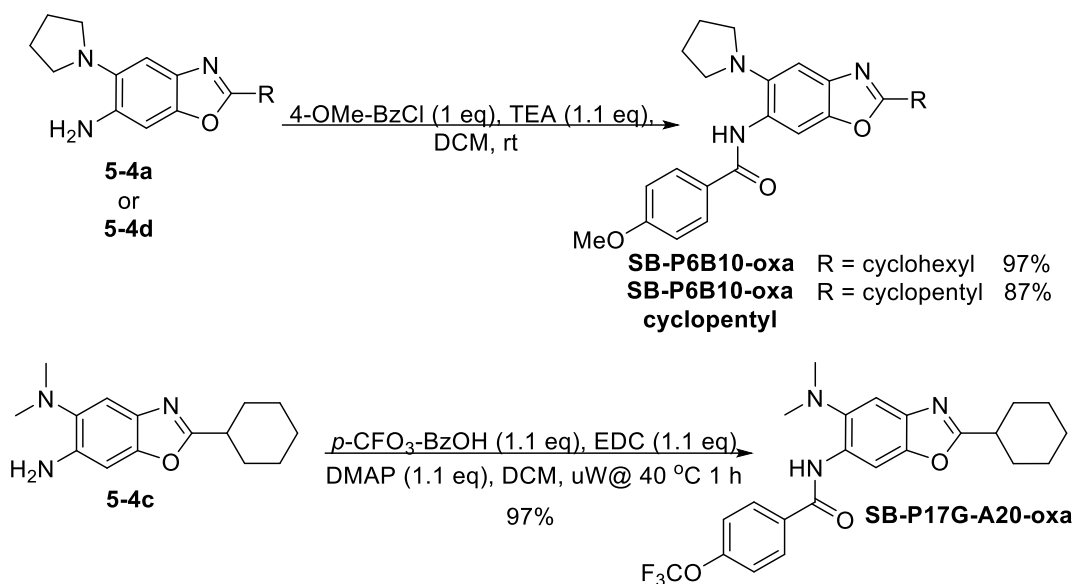
2-Cyclohexyl-5-pyrrolidinyl-6-nitro-1*H*-benzoxazole was treated with *n*-butyl chloroformate and triethylamine as the base. After 12 h at room temperature very little conversion was observed. To push the reaction, the activated succinimide ester of *n*-butyl chloroformate (BuOSu) was added and the reaction was heated for 4 hours at $40\text{ }^\circ\text{C}$, which also didn't improve the conversion. Similar result was observed when using benzylOSu ester (BnOSu). Another attempt at functionalizing the 6-amino group with butyl 4-nitrophenyl carbonate gave 95 % yield of the desired product but required 10 days for completion. Surprisingly, when 6-amino-2-cyclohexyl-5-(*N,N*-dimethylamino)benzoxazole was treated with *n*-butyl chloroformate, the reaction proceeded smoothly to yield the product in 93% yield.



Scheme 5.6. Synthesis of benzoxazole analogues of hit benzimidazoles

5.2.3. Benzoxazole analogues of SB-P6B10 and SB-P17G-A20

Previously synthesized 6-amino-2-cyclohexyl-5-(pyrrolidin-1-yl)benzoxazole and 6-amino-2-cyclopentyl-5-(pyrrolidin-1-yl)benzoxazole were treated with 4-methoxybenzoyl chloride to obtain 6-(4-methoxybenzamido)-2-cyclohexyl-5-(pyrrolidin-1-yl)benzoxazole and 6-(4-methoxybenzamido)-2-cyclopentyl-5-(pyrrolidin-1-yl)benzoxazole in 97% and 87% yield respectively (**Scheme 5.7**).



Scheme 5.7. Synthesis of benzoxazole analogues of hit benzimidazoles

Additionally the benzoxazole analogue of **SB-P17G-A20** was synthesized to evaluate the hERG activity of the molecule. In comparison to **SB-P17G-A20**, the benzoxazole is significantly less potent against *Mtb* but the hERG activity is reduced implying that switching from imidazole to oxazole influences the undesirable hERG activation.

5.2.4. Accurate MIC of synthesized benzoxazoles

Table 5.5 shows the accurate MIC values of the synthesized benzoxazoles. The benzoxazole analogues were not as active as the corresponding hit benzimidazole compounds. Extensive SAR profiling is necessary to identify molecules with potent antibacterial activity.

Table 5.5. Accurate MIC of trisubstituted benzoxazole against *Mtb* H37Rv

| Compound | R ² R ³ N | R ¹ | R ⁴ | MIC (μg/mL) H37Rv |
|-------------------------|---------------------------------|----------------|----------------|----------------------|
| SB-P6B-oxa | | | H | 50 |
| SB-P8B2-oxa | | | | 6.25 |
| SB-P8B4-oxa | | | | 6.25 |
| SB-P17G-C2-oxa | | | | n.d. |
| SB-P6B10-oxa | | | | >100 |
| SB-P6B10-oxacyclopentyl | | | | >100 |
| SB-P17G-A20-oxa | | | | 6.25 |

MIC values were determined at CSU

5.3. Conclusion

The trisubstituted benzoxazoles are in a nascent stage of drug discovery. Target validation studies on FtsZ and extensive SAR studies are required to develop this series of compounds as novel antibacterial agents. Similar to the benzimidazole series of compounds, libraries of trisubstituted benzoxazoles will be synthesized and evaluated against *Mtb* and other pathogenic bacteria such as *MRSA*, *F. tularensis*, *Y. pestis* etc. Also, different substitution patterns on the benzoxazole scaffold will be explored in due course.

5.4. Experimental Section

Methods. ¹H and ¹³C NMR spectra were measured on a Bruker or Varian 300, 400, or 500 MHz NMR spectrometer. Melting points were measured on a Thomas Hoover Capillary melting

point apparatus and are uncorrected. TLC was performed on silica coated aluminum sheets (thickness 200 μm) or alumina coated (thickness 200 μm) aluminum sheets supplied by Sorbent Technologies and column chromatography was carried out on Siliaflash® P60 silica gel, 40-63 μm (230-400 mesh) supplied by Silicycle. Aluminum oxide, activated, neutral, Brockmann Grade I, 58 Å, was supplied by Alfa Aesar.

Materials. The chemicals were purchased from Aldrich Co., Synquest Inc. and Sigma and purified before use by standard methods. Tetrahydrofuran (THF) was freshly distilled from sodium metal and benzophenone. Dichloromethane was also distilled immediately prior to use under nitrogen from calcium hydride.

Synthesis of 5-chloro-2-(4-methoxyphenyl)-6-nitrobenzo[*d*]oxazole (5-1c): 2-Amino-4-chloro-5-nitrophenol (100 mg, 0.53 mmol) and 4-methoxybenzoyl chloride (99.5 mg, 0.583 mmol) were placed in a sealed tube containing $\text{In}(\text{OTf})_3$ (30 mg, 10 mol%). The reaction mixture was heated to 110 °C for 18 h. After cooling, the reaction mixture was treated with a dilute solution of NaOH (1 M). The solution was extracted with ethyl acetate (3×5.0 mL), the organic layer was dried over magnesium sulfate and concentrated with a rotary evaporator. The product was recrystallized from the crude residue using ethyl acetate/hexanes and obtained as an orange solid. (160 mg, 90% yield). ^1H NMR (300 MHz, CDCl_3) δ 3.92 (s, 3 H), 7.06 (d, $J = 8.79$ Hz, 2 H), 7.84 (s, 1 H), 8.15 (s, 1 H), 8.17 - 8.29 (m, 2 H). This compound is literature unknown and new.

Same procedure was followed for the synthesis of **5-1b** except 5 mol% of $\text{In}(\text{OTf})_3$ was used.

5-Chloro-6-nitro-2-phenylbenzo[*d*]oxazole (5-1b): ^1H NMR (300 MHz, Methanol- d_4) δ 7.23 (s, 1 H), 7.49 - 7.65 (m, 3 H), 7.94 - 8.03 (m, 2 H), 8.45 (s, 1 H). This compound is literature unknown and new.

5-Chloro-6-nitro-2-(thiophen-2-yl)benzo[*d*]oxazole (5-1d): same procedure as described for **1c** was used except dioxane was used as solvent. Light orange solid (56% yield); mp 207-208 °C; ^1H NMR (500 MHz, acetone- d_6) δ 7.37 (dd, $J = 4.88, 3.66$ Hz, 1 H), 7.98 - 8.05 (m, 2 H), 8.09 (dd, $J = 3.66, 1.22$ Hz, 1 H), 8.44 (s, 1 H); ^{13}C NMR (126 MHz, acetone- d_6) δ 109.7, 121.8, 122.5, 123.5, 128.7, 130.0, 133.3, 134.4, 146.8, 149.3, 164.5. MS (ESI) m/z 280.9 ($\text{M}+1$) $^+$. This compound is literature unknown and new.

Synthesis of 5-chloro-2-cyclohexyl-6-nitrobenzo[d]oxazole (5-2a):

Cyclohexanecarbonyl chloride (1.2 eq) was added dropwise to a solution of 2-amino-4-chloro-5-nitrophenol (2.00 g, 10.6 mmol) and *N,N*-diisopropylethylamine (3.5 eq) in ethyl acetate (120 mL) at 0 °C, and then the mixture was stirred at room temperature for 14 h. The reaction mixture was diluted with ethyl acetate, transferred to a separatory funnel, and the organic layer was washed with brine, dried over Mg₂SO₄, filtered, and concentrated. A solution of the residue and *p*-toluenesulfonic acid monohydrate (50 mg) in toluene (70 mL) was stirred at reflux for 6 h. The mixture was concentrated and the residue was diluted with ethyl acetate. The organic layer was washed with brine, dried over Mg₂SO₄, filtered, and concentrated. The residue was purified by silica gel flash chromatography (ethyl acetate/hexane = 1/10) to afford a light yellow solid (2.074 g, 70% yield over two steps). mp 84-85 °C; ¹H NMR (400 MHz, CDCl₃) δ 1.27 - 1.49 (m, 3 H), 1.63 - 1.79 (m, 3 H), 1.81 - 1.94 (m, 2 H), 2.12 - 2.21 (m, 2 H), 3.00 (tt, *J* = 11.26, 3.54 Hz, 1 H), 7.79 (s, 1 H), 8.05 (s, 1 H); ¹³C NMR (101 MHz, CDCl₃) δ 25.6, 25.7, 30.4, 38.3, 108.7, 122.2, 123.4, 144.5, 145.4, 148.2, 176.0; MS (ESI) *m/z* 281.1 (M+1)⁺. This compound is literature unknown and new.

The same procedure was followed for the synthesis of **5-2(b-g)**.

5-Chloro-2-cyclopentyl-6-nitrobenzo[d]oxazole (5-2b): Light yellow solid (84% yield); mp 60-61 °C; ¹H NMR (400 MHz, CDCl₃) δ 1.64 - 1.92 (m, 4 H), 1.92 - 2.09 (m, 2 H), 2.18 (td, *J* = 12.49, 7.91 Hz, 2 H), 3.41 (quin, *J* = 8.09 Hz, 1 H), 7.76 (s, 1 H), 8.03 (s, 1 H); ¹³C NMR (101 MHz, CDCl₃) δ 25.9, 31.6, 39.2, 108.6, 122.1, 123.4, 144.4, 145.4, 148.4, 176.5. MS (ESI) *m/z* 267.0 (M+1)⁺. This compound is literature unknown and new.

5-Chloro-2-cyclobutyl-6-nitrobenzo[d]oxazole (5-2c): Light yellow solid (60 % yield); mp 64-65 °C; ¹H NMR (500 MHz, CDCl₃) δ 2.04 - 2.23 (m, 2 H), 2.45 - 2.60 (m, 4 H), 3.83 (quind, *J* = 8.54, 0.92 Hz, 1 H), 7.80 (s, 10 H), 8.06 (s, 1 H); ¹³C NMR (126 MHz, CDCl₃) δ 19.0, 27.2, 33.6, 108.7, 122.2, 123.6, 144.6, 145.5, 148.4, 175.1. MS (ESI) *m/z* 252.9 (M+1)⁺. This compound is literature unknown and new.

5-Chloro-2-(penta-3-yl)-6-nitrobenzo[d]oxazole (5-2d): Light yellow solid (86 % yield); mp 44-45 °C; ¹H NMR (500 MHz, CDCl₃) δ 0.83 (t, *J* = 7.32 Hz, 6 H), 1.70 - 1.86 (m, 4 H), 2.86 (tt, *J* = 8.39, 5.80 Hz, 1 H), 7.72 (s, 1 H), 8.00 (s, 1 H); ¹³C NMR (126 MHz, CDCl₃) δ 11.7, 26.0, 43.6,

108.5, 122.0, 123.1, 144.3, 145.1, 148.2, 175.6. MS (ESI) m/z 269.0 (M+1)⁺. This compound is literature unknown and new.

5-Chloro-6-nitro-2-*p*-tolylbenzo[*d*]oxazole (5-2e): Beige solid (70% yield); mp 208-209 °C; ¹H NMR (500 MHz, CDCl₃) δ 2.47 (s, 3 H), 7.37 (d, *J* = 8.24 Hz, 2 H), 7.85 (s, 1 H), 8.08 - 8.19 (m, 3 H); ¹³C NMR (126 MHz, CDCl₃) δ 22.0, 108.8, 122.3, 123.0, 124.1, 128.5, 130.2, 144.3, 144.5, 146.3, 148.3, 168.4. MS (ESI) m/z 289.0 (M+1)⁺. This compound is literature unknown and new.

5-Chloro-6-nitro-2-phenylbenzo[*d*]oxazole (5-2f): Dirty white solid (60 % yield); mp 197-198 °C; ¹H NMR (400 MHz, CDCl₃) δ 7.51 - 7.75 (m, 3 H), 7.89 (br. s., 1 H), 8.08 - 8.51 (m, 3 H); ¹³C NMR (101 MHz, CDCl₃) δ 108.9, 122.5, 124.1, 125.8, 128.5, 129.4, 133.3, 144.8, 146.1, 148.4, 168.1; MS (ESI) m/z 275.0 (M+1)⁺. This compound is literature unknown and new.

5-Chloro-2-benzyl-6-nitrobenzo[*d*]oxazole (5-2g): Light yellow solid (76% yield); mp 101-102 °C; ¹H NMR (500 MHz, CDCl₃) δ 4.32 (s, 2 H), 7.29 - 7.40 (m, 5 H), 7.82 (s, 1 H), 8.03 (s, 1 H); ¹³C NMR (126 MHz, CDCl₃) δ 35.5, 108.8, 122.5, 123.6, 128.0, 129.2, 129.2, 133.6, 144.8, 145.3, 148.6, 170.8. MS (ESI) m/z 289.0 (M+1)⁺. This compound is literature unknown and new.

Synthesis of 2-cyclohexyl-6-nitro-5-(pyrrolidin-1-yl)benzo[*d*]oxazole (5-3a): 5-Chloro-2-cyclohexyl-6-nitrobenzoxazole (400 mg, 1.43 mmol), pyrrolidine (2.5 eq), triethylamine (2.5 eq) and dimethyl sulfoxide were placed in a sealed tube and heated at 90 °C for 48 h. The reaction mixture was diluted with ethyl acetate and transferred to a separatory funnel. The organic layer was washed with water (3 times) brine, dried over magnesium sulfate and concentrated. The residue was purified by silica gel chromatography to afford the orange colored product in 76% (314 mg) conversion yield. mp 78-79 °C; ¹H NMR (500 MHz, CDCl₃) δ 1.26 - 1.49 (m, 4 H), 1.61 - 1.79 (m, 3 H), 1.86 (m, 2 H), 1.93 - 2.04 (m, 4 H), 2.09 - 2.19 (m, 2 H), 2.93 (tt, *J* = 11.29, 3.66 Hz, 1 H), 3.14 - 3.25 (m, 4 H), 7.16 (s, 1 H), 7.90 (s, 1 H); ¹³C NMR (126 MHz, CDCl₃) δ 25.7, 25.9, 26.0, 30.5, 38.3, 51.1, 104.8, 108.4, 135.1, 141.5, 142.1, 146.3, 175.3. MS (ESI) m/z 316.1 (M+1)⁺. This compound is literature unknown and new.

The same procedure was followed for the synthesis of **5-3(a,b,d,h)**

2-Cyclohexyl-6-nitro-5-(piperidin-1-yl)benzo[d]oxazole (5-3b): Orange solid (69% conversion yield); mp 110-111 °C; ¹H NMR (500 MHz, CDCl₃) δ 1.23 - 1.45 (m, 3 H), 1.47 - 1.58 (m, 2 H), 1.58 - 1.75 (m, 7 H), 1.82 (dt, *J* = 13.28, 3.43 Hz, 2 H), 2.04 - 2.18 (m, 2 H), 2.83 - 2.99 (m, 5 H), 7.41 (s, 1 H), 7.87 (s, 1 H); ¹³C NMR (126 MHz, CDCl₃) δ 24.1, 25.6, 25.8, 26.3, 30.4, 38.1, 54.5, 107.9, 111.9, 141.8, 144.7, 145.4, 145.8, 174.8. MS (ESI) *m/z* 330.1 (M+1)⁺. This compound is literature unknown and new.

2-Cyclopentyl-6-nitro-5-(pyrrolidin-1-yl)benzo[d]oxazole (5-3d): Orange oil (58% yield); ¹H NMR (500 MHz, CDCl₃) δ 1.64 - 1.76 (m, 2 H), 1.76 - 1.90 (m, 2 H), 1.92 - 2.04 (m, 6 H), 2.07 - 2.17 (m, 2 H), 3.10 - 3.23 (m, 4 H), 3.32 (quin, *J* = 8.09 Hz, 1 H), 7.12 (s, 1 H), 7.86 (s, 1 H); ¹³C NMR (126 MHz, CDCl₃) δ 25.8, 25.9, 31.5, 39.2, 51.1, 104.6, 108.3, 135.0, 141.7, 142.0, 146.3, 175.6. MS (ESI) *m/z* 302.1 (M+1)⁺. This compound is literature unknown and new.

6-Nitro-2-phenyl-5-(pyrrolidin-1-yl)benzo[d]oxazole (5-3h): Orange solid (59% conversion yield); mp 163-165 °C; ¹H NMR (400 MHz, CDCl₃) δ 1.93 - 2.10 (m, 4 H), 3.16 - 3.29 (m, 4 H), 7.23 (s, 1 H), 7.47 - 7.63 (m, 3 H), 8.00 (s, 1 H), 8.23 (d, *J* = 6.78 Hz, 2 H); ¹³C NMR (101 MHz, CDCl₃) δ 26.0, 51.2, 104.9, 108.7, 126.6, 128.3, 129.2, 132.6, 135.5, 141.7, 142.4, 146.9, 167.4. MS (ESI) *m/z* 310.0 (M+1)⁺. This compound is literature unknown and new.

Synthesis of 2-cyclohexyl-5-*N,N*-dimethylamino-6-nitrobenzo[d]oxazole (5-3c): 5-Chloro-2-cyclohexyl-6-nitrobenzoxazole (500 mg, 1.78 mmol), dimethylamine (2.5 eq from 2 M solution in MeOH), triethylamine (2.5 eq) and dimethyl sulfoxide were placed in a sealed tube and heated at 90 °C for 48 h. The reaction mixture was diluted with ethyl acetate and transferred to a separatory funnel. The organic layer was washed with water (3 times) brine, dried over magnesium sulfate and concentrated. The residue was purified by silica gel chromatography to afford the product as an orange solid in 75% conversion yield. mp 115-116 °C; ¹H NMR (400 MHz, CDCl₃) δ 1.21 - 1.50 (m, 3 H), 1.61 - 1.76 (m, 3 H), 1.81 - 1.89 (m, 2 H), 2.10 - 2.17 (m, 2 H), 2.84 (s, 6 H), 2.88 - 3.01 (m, 1 H), 7.33 (s, 1 H), 7.92 (s, 1 H); ¹³C NMR (101 MHz, CDCl₃) δ 25.6, 25.8, 30.4, 38.2, 44.0, 108.5, 109.2, 138.9, 143.6, 145.5, 145.9, 175.2. MS (ESI) *m/z* 290.0 (M+1)⁺. This compound is literature unknown and new.

The same procedure was followed for the synthesis of **5-3(e-f)**

5-*N,N*-Dimethylamino-6-nitro-2-cyclobutylbenzo[*d*]oxazole (5-3e): Orange oil; ¹H NMR (500 MHz, CDCl₃) δ 2.01 - 2.21 (m, 2 H), 2.42 - 2.57 (m, 4 H), 2.85 (s, 6 H), 3.72 - 3.81 (m, 1 H), 7.33 (s, 1 H), 7.92 (s, 1 H); ¹³C NMR (126 MHz, CDCl₃) δ 19.0, 27.2, 33.7, 43.9, 108.6, 109.1, 138.9, 143.7, 145.6, 146.0, 174.3. MS (ESI) *m/z* 262.0 (M+1)⁺. This compound is literature unknown and new.

5-*N,N*-Dimethylamino-6-nitro-2-(pentan-3-yl)benzo[*d*]oxazole (5-3f): Orange oil; ¹H NMR (500 MHz, CDCl₃) δ 0.91 (t, *J* = 7.48 Hz, 6 H), 1.76 - 1.93 (m, 4 H), 2.79 - 2.92 (m, 7 H), 7.36 (s, 1 H), 7.95 (s, 1 H); ¹³C NMR (126 MHz, CDCl₃) δ 12.0, 26.3, 43.8, 44.0, 108.6, 109.2, 139.0, 143.7, 145.6, 145.8, 175.0. MS (ESI) *m/z* 278.0 (M+1)⁺. This compound is literature unknown and new.

Synthesis of 5-*N,N*-dimethylamino-6-nitro-2-tolylbenzo[*d*]oxazole (5-3g): To synthesize **5-3g** different conditions were employed. Trial 1: 5-Chloro-6-nitro-2-*p*-tolylbenzoxazole (506 mg, 1.75 mmol), dimethylamine (2.5 eq from 2 M solution in MeOH), triethylamine (2.5 eq), and dimethyl sulfoxide (5 mL) were placed in a sealed tube and heated at 90 °C for 48 h. No conversion was observed therefore 1 eq of dimethylamine was added and the temperature was increased to 100 °C without any success. Trial 2: 5-Chloro-6-nitro-2-*p*-tolylbenzoxazole (116 mg, 0.4 mmol), dimethylamine (2.5 eq from 2 M solution in MeOH), triethylamine (2.5 eq), and toluene (1 mL) were placed in a sealed tube and heated at 90 °C for 48 h. Very little conversion was observed. Trail 3: 5-Chloro-6-nitro-2-*p*-tolylbenzoxazole (238 mg, 0.83 mmol), dimethylamine (2.5 eq from 2 M solution in MeOH), triethylamine (2.5 eq), and toluene (2 mL) were placed in a vial and irradiated at 90 °C for 4 h. The fractions from the 3 trials were combined, diluted with ethyl acetate and transferred to a separatory funnel. The organic layer was washed with water (3 times) brine, dried over magnesium sulfate, filtered, and concentrated. The residue was purified by silica gel chromatography to afford 74 mg of the product. Orange solid; mp 175-176 °C; ¹H NMR (500 MHz, CDCl₃) δ 2.44 (s, 3 H), 2.88 (s, 6 H), 7.32 (d, *J* = 8.24 Hz, 2 H), 7.37 (s, 1 H), 8.00 (s, 1 H), 8.09 (d, *J* = 8.24 Hz, 2 H); ¹³C NMR (126 MHz, CDCl₃) δ 21.9, 43.8, 108.8, 108.9, 123.6, 128.2, 130.0, 138.7, 143.5, 143.5, 145.9, 146.8, 167.6. MS (ESI) *m/z* 298.0 (M+1)⁺. This compound is literature unknown and new.

5-*N,N*-Dimethylamino-6-nitro-2-(thiophen-2-yl)benzo[*d*]oxazole (5-3i): Orange solid (67% conversion yield); mp 126-127 °C; ¹H NMR (500 MHz, CDCl₃) δ 2.89 (s, 6 H), 7.22 (dd, *J* = 4.88,

3.66 Hz, 1 H), 7.37 (s, 1 H), 7.64 (dd, $J = 5.04, 1.07$ Hz, 1 H), 7.95 (dd, $J = 3.66, 1.22$ Hz, 1 H), 8.02 (s, 1 H); ^{13}C NMR (126 MHz, CDCl_3) δ 43.8, 108.8, 108.8, 128.8, 128.9, 131.6, 132.1, 138.6, 143.3, 146.1, 146.7, 163.3. MS (ESI) m/z 290.0 ($\text{M}+1$)⁺. This compound is literature unknown and new.

Synthesis of 6-amino-2-cyclohexyl-5-(pyrrolidin-1-yl)benzo[d]oxazole (5-4a). To a suspension of 2-cyclohexyl-6-nitro-5-(pyrrolidin-1-yl)benzoxazole (314 mg, 0.99 mmol) in ethanol (30 mL), were added ammonium formate (1.55 g) and 10 wt.% Pd-C (143 mg). The mixture, maintained under nitrogen, was stirred at room temperature for 30 minutes. After completion of reaction, the reaction was concentrated on the rotary evaporator. Ethyl acetate was added and the Pd-C catalyst and excess ammonium formate was filtered off over celite. The filtrate was transferred to a separatory funnel and the organic layer was washed with water, brine, dried over magnesium sulfate and concentrated. The product was obtained as a brown solid in 91% yield without requiring any further purification. mp 119-120 °C; ^1H NMR (400 MHz, CDCl_3) δ 1.23 - 1.47 (m, 3 H), 1.58 - 1.76 (m, 3 H), 1.78 - 1.88 (m, 2 H), 1.88 - 1.99 (m, 4 H), 2.07 - 2.19 (m, 2 H), 2.86 (tt, $J = 11.29, 3.64$ Hz, 1 H), 3.01 (br. s., 4 H), 4.09 (br. s., 2 H), 6.83 (s, 1 H), 7.33 (s, 1 H); ^{13}C NMR (101 MHz, CDCl_3) δ 24.2, 25.9, 26.1, 30.8, 38.0, 52.1, 96.2, 110.0, 133.4, 135.6, 140.5, 148.0, 168.4; HRMS (ESI) m/z calcd for $\text{C}_{17}\text{H}_{23}\text{N}_3\text{OH}^+$: 286.1914, Found: 286.1913 ($\Delta = 0.19$ ppm). This compound is literature unknown and new.

6-Amino-2-cyclohexyl-5-(*N,N*-dimethylamino)benzo[d]oxazole (5-4c): Light brown (95% yield); mp 75-76 °C; ^1H NMR (400 MHz, CDCl_3) δ 1.23 - 1.43 (m, 3 H), 1.55 - 1.73 (m, 3 H), 1.75 - 1.88 (m, 2 H), 2.09 (d, $J = 12.05$ Hz, 2 H), 2.63 (s, 6 H), 2.77 - 2.90 (m, 1 H), 4.16 (br. s., 2 H), 6.78 (s, 1 H), 7.32 (s, 1 H); ^{13}C NMR (101 MHz, CDCl_3) δ 25.8, 25.9, 30.7, 37.9, 44.5, 95.9, 110.4, 133.2, 138.7, 140.1, 148.1, 168.3; HRMS (ESI) m/z calcd for $\text{C}_{15}\text{H}_{21}\text{N}_3\text{OH}^+$: 260.1757, Found: 260.1756 ($\Delta = 0.46$ ppm). This compound is literature unknown and new.

6-Amino-2-cyclopentyl-5-(pyrrolidin-1-yl)benzo[d]oxazole (5-4d): Light brown (77% yield); mp 54-55 °C; ^1H NMR (400 MHz, CDCl_3) δ 1.60 - 1.85 (m, 4 H), 1.86 - 2.02 (m, 6 H), 2.03 - 2.15 (m, 2 H), 2.90 - 3.08 (m, 4 H), 3.27 (quin, $J = 8.03$ Hz, 1 H), 4.09 (br. s., 2 H), 6.80 (s, 1 H), 7.30 (s, 1 H); ^{13}C NMR (101 MHz, CDCl_3) δ 24.1, 25.7, 31.5, 38.9, 52.0, 96.1, 109.8, 133.3, 135.4,

140.4, 148.1, 168.4; HRMS (ESI) m/z calcd for $C_{16}H_{21}N_3OH^+$: 272.1757, Found: 272.1755 ($\Delta = 0.78$ ppm). This compound is literature unknown and new.

6-Amino-2-cyclobutyl-5-(*N,N*-dimethylamino)benzo[*d*]oxazole (5-4e): Dark brown solid (98% yield); mp 105-107 °C; 1H NMR (400 MHz, $CDCl_3$) δ 1.94 - 2.16 (m, 2 H), 2.34 - 2.55 (m, 4 H), 2.65 (s, 6 H), 3.69 (quin, $J = 8.53$ Hz, 1 H), 4.17 (br. s, 2 H), 6.80 (s, 1 H), 7.32 (s, 1 H); ^{13}C NMR (101 MHz, $CDCl_3$) δ 18.9, 27.3, 33.6, 44.6, 96.0, 110.4, 133.4, 138.9, 140.2, 148.4, 167.4; HRMS (ESI) m/z calcd for $C_{13}H_{17}N_3OH^+$: 232.1444, Found: 232.1441 ($\Delta = 1.57$ ppm). This compound is literature unknown and new.

6-Amino-5-(*N,N*-dimethylamino)-2-(pentan-3-yl)benzo[*d*]oxazole (5-4f): Viscous oil; 1H NMR (400 MHz, $CDCl_3$) δ 0.83 (t, $J = 7.40$ Hz, 6 H), 1.61 - 1.86 (m, 4 H), 2.55 - 2.61 (m, 6 H), 2.66 - 2.80 (m, 1 H), 4.17 (br. s, 2 H), 6.76 (s, 1 H), 7.28 (s, 1 H); ^{13}C NMR (101 MHz, $CDCl_3$) δ 11.8, 26.3, 43.3, 44.3, 95.8, 110.2, 133.0, 138.6, 140.1, 148.1, 167.5; HRMS (ESI) m/z calcd for $C_{14}H_{21}N_3OH^+$: 248.1757, Found: 248.1751 ($\Delta = 2.39$ ppm). This compound is literature unknown and new.

Synthesis of 6-butoxycarbonylamino-2-cyclohexyl-5-(pyrrolidin-1-yl)benzo[*d*]oxazole (SB-P8B2-oxa) (Route A): To a solution of 6-amino-2-cyclohexyl-5-(pyrrolidin-1-yl)benzoxazole (54 mg, 0.189 mmol) in dichloromethane were added triethylamine (1 eq) and butyl chloroformate (1 eq). The mixture was stirred overnight at room temperature. TLC after 24 h showed poor conversion therefore butyl OSu ester was added 0.5 eq + 0.5 eq at a time. Triethylamine (1 eq) was also added and the reaction was stirred for an additional 24 h followed by heating at 40 °C for 2 h. The reaction was stopped and the reaction mixture was concentrated on a rotary evaporator. The crude mixture was loaded on silica column packed with hexanes. The product eluted at 1:4 ethyl acetate/hexane. Starting material was recovered but not quantified. Yield 17 mg. The final compound is literature unknown and new.

The same procedure was followed for the synthesis of **6-benzyloxycarbonylamino-2-cyclohexyl-5-(pyrrolidin-1-yl)benzo[*d*]oxazole (SB-P8B4-oxa)** with the additional modifications mentioned in the scheme. 68% yield (54 mg); mp 99-100 °C; 1H NMR (500 MHz, $CDCl_3$) δ 1.29 - 1.47 (m, 4 H), 1.58 - 1.79 (m, 5 H), 1.80 - 1.90 (m, 2 H), 1.96 (br. s., 4 H), 2.14 (d, $J = 10.68$ Hz, 2 H), 2.85 - 3.08 (m, 5 H), 5.24 (s, 2 H), 7.31 - 7.55 (m, 6 H), 8.11 (br. s., 1 H),

8.31 (br. s., 1 H); ^{13}C NMR (126 MHz, CDCl_3) δ 24.6, 25.8, 26.0, 29.9, 30.7, 38.1, 53.8, 67.1, 100.5, 111.3, 128.6, 128.6, 128.8, 131.9, 136.4, 136.5, 137.0, 148.1, 153.7, 170.6; HRMS (ESI) m/z calcd for $\text{C}_{25}\text{H}_{29}\text{N}_3\text{O}_3\text{H}^+$: 420.2282, Found: 420.2284 ($\Delta = 0.5$ ppm). This compound is literature unknown and new.

Synthesis of 6-butoxycarbonylamino-2-cyclohexyl-5-(pyrrolidin-1-yl)benzo[d]oxazole (SB-P8B2-oxa) (Route B): To a solution of 6-amino-2-cyclohexyl-5-(pyrrolidin-1-yl)benzoxazole (87 mg, 0.305 mmol) in tetrahydrofuran (3 mL), butyl 4-nitrophenyl carbonate (72.9 mg, 0.305 mmol) was added. The mixture was stirred overnight at 60 °C. TLC after 24 h showed poor conversion therefore triethylamine (1 eq) was added and the reaction was run for 10 days. The reaction was stopped and the reaction mixture was concentrated on a rotary evaporator. The crude mixture was dissolved in ethyl acetate and transferred to a separatory funnel. The organic layer was washed with sodium bicarbonate solution, water and brine. The organic layer was collected, dried over magnesium sulfate, filtered and concentrated. The crude material was loaded on silica column packed with hexanes. The product eluted at 1:10 ethyl acetate/hexane. 95% yield (112 mg). mp 68-69 °C; ^1H NMR (400 MHz, CDCl_3) δ 0.94 (t, $J = 7.40$ Hz, 3 H), 1.15 - 1.48 (m, 7 H), 1.59 - 1.74 (m, 5 H), 1.77 - 1.86 (m, 2 H), 1.91 - 2.01 (m, 4 H), 2.08 - 2.17 (m, 2 H), 2.82 - 3.04 (m, 5 H), 4.17 (t, $J = 6.78$ Hz, 2 H), 7.44 (s, 1 H), 7.95 (br. s., 1 H), 8.24 (br. s., 1 H); ^{13}C NMR (101 MHz, CDCl_3) δ 13.9, 19.2, 24.5, 25.7, 25.9, 30.6, 31.2, 38.0, 53.6, 65.2, 100.4, 111.0, 131.9, 136.1, 136.9, 148.0, 154.0, 170.3; HRMS (ESI) m/z calcd for $\text{C}_{22}\text{H}_{31}\text{N}_3\text{O}_3\text{H}^+$: 386.2438, Found: 386.2438 ($\Delta = 0$ ppm). This compound is literature unknown and new.

Synthesis of 6-butoxycarbonylamino-2-cyclohexyl-5-(*N,N*-dimethylamino)benzo[d]oxazole (SB-P17G-C2-oxa): To a solution of 6-amino-2-cyclohexyl-5-(*N,N*-dimethylamino)benzoxazole (31 mg, 0.12 mmol) in dichloromethane was added butyl chloroformate (1 eq). The mixture was stirred overnight at room temperature. TLC after 16 h showed conversion therefore, the reaction was stopped, and the reaction mixture was concentrated on a rotary evaporator. The crude mixture was loaded on silica column packed with hexanes. The product was obtained as a pale brown solid (40 mg, 93% yield). Mp 55-57 °C; ^1H NMR (500 MHz, CDCl_3) δ 0.96 (t, $J = 7.32$ Hz, 3 H), 1.26 - 1.51 (m, 6 H), 1.58 - 1.76 (m, 6 H), 1.79 - 1.87 (m, $J = 13.00, 3.40, 3.40$ Hz, 2 H), 2.08 - 2.19 (m, 2 H), 2.56 - 2.72 (m, 6 H), 2.85 - 2.94 (m, $J = 11.30, 11.30, 3.70, 3.70$ Hz, 1 H), 4.19 (t, $J = 6.71$ Hz, 2 H), 7.47 (s, 1 H), 8.15 (s, 1 H), 8.29 (br. s., 1 H);

^{13}C NMR (126 MHz, CDCl_3) δ 14.0, 19.3, 25.8, 26.0, 30.7, 31.2, 38.0, 45.7, 65.2, 100.1, 111.3, 131.5, 136.0, 139.9, 148.3, 154.0, 170.4; HRMS (ESI) m/z calcd for $\text{C}_{20}\text{H}_{29}\text{N}_3\text{O}_3\text{H}^+$: 360.2282, Found: 360.2275 ($\Delta = -1.9$ ppm). This compound is literature unknown and new.

Synthesis of 6-(4-methoxybenzamido)-2-cyclohexyl-5-(pyrrolidin-1-yl)benzo[d]oxazole (SB-P6B10-oxa): To a solution of 2-cyclohexyl-6-nitro-5-(pyrrolidin-1-yl)benzoxazole (52 mg, 0.18 mmol) in dichloromethane (1 mL) was added triethylamine (25 μL , 0.2 mmol). To this, 4-methoxybenzoyl chloride (25 μL , 0.18 mmol) was added dropwise at 0 $^\circ\text{C}$ and reacted at room temperature. After completion of the reaction, the reaction mixture was diluted with ethyl acetate and transferred to a separatory funnel. The organic layer was washed with saturated sodium bicarbonate solution, followed by water and finally brine. The organic layer was dried over magnesium sulfate, filtered and concentrated. The crude product was purified by flash chromatography on silica gel (gradient: 0-30% ethyl acetate /hexanes) to obtain the product which was then treated with activated charcoal to yield the product as a white solid in 97% yield. mp 148-149 $^\circ\text{C}$; ^1H NMR (400 MHz, CDCl_3) δ 1.28 - 1.49 (m, 3 H), 1.63 - 1.78 (m, 3 H), 1.81 - 1.91 (m, 2 H), 1.98 - 2.07 (m, 4 H), 2.09 - 2.24 (m, 2 H), 2.87 - 3.00 (m, 1 H), 3.00 - 3.13 (m, 4 H), 3.88 (s, 3 H), 7.00 (d, $J = 8.78$ Hz, 2 H), 7.54 (s, 1 H), 7.87 (d, $J = 8.78$ Hz, 2 H), 8.74 (s, 1 H), 9.59 (s, 1 H); ^{13}C NMR (101 MHz, CDCl_3) δ 24.6, 25.8, 26.0, 30.7, 38.1, 53.9, 55.7, 101.8, 111.3, 114.3, 127.6, 128.9, 132.1, 137.0, 137.4, 148.1, 162.6, 164.5, 170.9; HRMS (ESI) m/z calcd for $\text{C}_{25}\text{H}_{29}\text{N}_3\text{O}_3\text{H}^+$: 420.2282, Found: 420.2285 ($\Delta = 0.7$ ppm). This compound is literature unknown and new.

Same procedure was followed for the synthesis of **6-(4-methoxybenzamido)-2-cyclopentyl-5-(pyrrolidin-1-yl)benzo[d]oxazole** to obtain product in 87 % yield. mp 123-125 $^\circ\text{C}$; ^1H NMR (400 MHz, CDCl_3) δ 1.55 - 1.78 (m, 2 H), 1.78 - 1.90 (m, 2 H), 1.97 - 2.07 (m, 6 H), 2.09 - 2.26 (m, 2 H), 2.99 - 3.11 (m, 4 H), 3.36 (t, $J = 8.03$ Hz, 1 H), 3.84 - 3.93 (m, 3 H), 7.00 (d, $J = 2.00$ Hz, 8 H), 7.52 (s, 1 H), 7.87 (d, $J = 8.78$ Hz, 2 H), 8.74 (s, 1 H), 9.59 (s, 1 H); ^{13}C NMR (101 MHz, CDCl_3) δ 24.6, 25.9, 31.6, 39.1, 53.9, 55.7, 101.8, 111.2, 114.3, 127.6, 128.9, 132.1, 137.4, 148.3, 162.6, 164.5, 171.1; HRMS (ESI) m/z calcd for $\text{C}_{24}\text{H}_{27}\text{N}_3\text{O}_3\text{H}^+$: 406.2125, Found: 406.2134 ($\Delta = 2.2$ ppm). This compound is literature unknown and new.

Synthesis of 2-cyclohexyl-6-(4-trifluoromethoxybenzamido)-5-(*N,N*-dimethylamino)benzo[*d*]oxazole (SB-P17G-A20-oxa): A solution of 6-amino-2-cyclohexyl-5-(*N,N*-dimethylamino)benzoxazole (52 mg, 0.2 mmol), DMAP (27 mg, 0.22 mmol), EDC.HCl (42 mg, 0.22 mmol), 4-trifluoromethoxybenzoic acid (46 mg, 0.22 mmol) in dichloromethane (1 mL) was irradiated in the microwave reactor at 40 °C for 1 h. TLC confirmed completion of reaction. The mixture was diluted with ethyl acetate, transferred to a separatory funnel and washed with water, saturated solution of sodium bicarbonate and brine. The organic layer was dried over magnesium sulfate, filtered and concentrated on a rotary evaporator. The crude mixture was purified via silica gel chromatography (1:4 ethyl acetate/hexanes) and the product was obtained as a white solid (86 mg, 97% yield). mp 97-98 °C; ¹H NMR (400 MHz, CDCl₃) δ 1.27 - 1.53 (m, 3 H), 1.59 - 1.93 (m, 5 H), 2.15 (d, *J* = 11.04 Hz, 2 H), 2.72 (br. s, 6 H), 2.85 - 3.06 (m, 1 H), 7.34 (d, *J* = 7.53 Hz, 2 H), 7.55 (br. s, 1 H), 7.96 (d, *J* = 7.53 Hz, 2 H), 8.75 (br. s, 1 H), 9.72 (br. s, 1 H); ¹³C NMR (101 MHz, CDCl₃) δ 25.8, 25.9, 30.7, 38.1, 45.9, 101.8, 111.4, 119.2, 121.0, 121.8, 129.1, 131.1, 133.8, 137.3, 140.7, 148.2, 151.8, 163.7, 171.1; HRMS (ESI) *m/z* calcd for C₂₃H₂₄F₃N₃O₃H⁺: 448.1843, Found: 448.1838 (Δ = -1.1 ppm). This compound is literature unknown and new.

5.5. References

1. Awasthi, D.; Kumar, K.; Knudson, S. E.; Slayden, R. A.; Ojima, I., SAR Studies on Trisubstituted Benzimidazoles as Inhibitors of Mtb FtsZ for the Development of Novel Antitubercular Agents. *J. Med. Chem.* **2013**, *56*, 9756-9770
2. Kumar, K.; Awasthi, D.; Lee, S.-Y.; Zanardi, I.; Ruzsicska, B.; Knudson, S.; Tonge, P. J.; Slayden, R. A.; Ojima, I., Novel Trisubstituted Benzimidazoles, Targeting Mtb FtsZ, as a New Class of Antitubercular Agents. *J. Med. Chem.* **2011**, *54*, 374-381
3. Peng, J.; Zong, C.; Ye, M.; Chen, T.; Gao, D.; Wang, Y.; Chen, C., Direct transition-metal-free intramolecular C-O bond formation: synthesis of benzoxazole derivatives. *Org. Biomol. Chem.* **2011**, *9*, 1225-1230
4. Muller, C.; Bauer, A.; Bach, T., Light-driven enantioselective organocatalysis. *Angew Chem Int Ed Engl* **2009**, *48*, 6640-2
5. Wang, B.; Zhang, Y.; Li, P.; Wang, L., An efficient and practical synthesis of benzoxazoles from acyl chlorides and 2-aminophenols catalyzed by Lewis acid In(OTf)₃ under solvent-free reaction conditions. *Chin. J. Chem.* **2010**, *28*, 1697-1703
6. Kuroyanagi, J.-i.; Kanai, K.; Sugimoto, Y.; Horiuchi, T.; Achiwa, I.; Takeshita, H.; Kawakami, K., 1,3-Benzoxazole-4-carbonitrile as a novel antifungal scaffold of β -1,6-glucan synthesis inhibitors. *Bioorg. Med. Chem.* **2010**, *18*, 7593-7606

Chapter 6

Target Validation Studies with SB-RA-2001 and SB-RA-5001

Table of Contents

| | |
|-------------------------------------------------------|-----|
| Chapter 6 | 150 |
| 6.1. Introduction..... | 151 |
| 6.2. Results and Discussion..... | 153 |
| 6.2.1. Synthesis of C-13 side chain precursors | 154 |
| 6.2.2. Synthesis of SB-RA-5001 and SB-RA-2001..... | 157 |
| 6.2.3. <i>In vitro</i> evaluation of SB-RA-2001 | 158 |
| 6.2.4. TEM Imaging with SB-RA-5001 | 160 |
| 6.3. Conclusion | 161 |
| 6.4. Experimental Section..... | 161 |
| 6.5. References..... | 168 |

6.1. Introduction

Mtb FtsZ is made up of two subunits namely A and B. The GTP binding site is present on subunit A and consists of T1-T6 loops which form a Rossmann fold.^{1,2} This feature is common with $\alpha\beta$ -tubulin and FtsZ from other species such as *M. jannaschii*.^{1,2}

Three crystal structures of *Mtb*-FtsZ complexed to citrate (PDB 1rq2), GDP (PDB 1rq7) and GTP- γ -S (PDB 1rlu) have been determined to shed some light into the polymerization of FtsZ.³ Leung *et al.* have proposed that the two *Mtb* FtsZ subunits associate laterally unlike tubulin subunits which associate longitudinally.³ They have proposed a spiral filament model for FtsZ based on the presence of a secondary structural switch in subunit A (H2 residues 41-50) and subunit B. They observed that in subunit A H2 adopts α -helical conformation whereas in subunit B it adopts a β -stranded conformation.

Figure 6.1 shows the GTP binding site in subunit A (blue). The red ribbon is subunit B. The β 2 strand of subunit B hydrogen bonds to β 3 strand of subunit A in anti-parallel fashion to form the link between the two subunits.

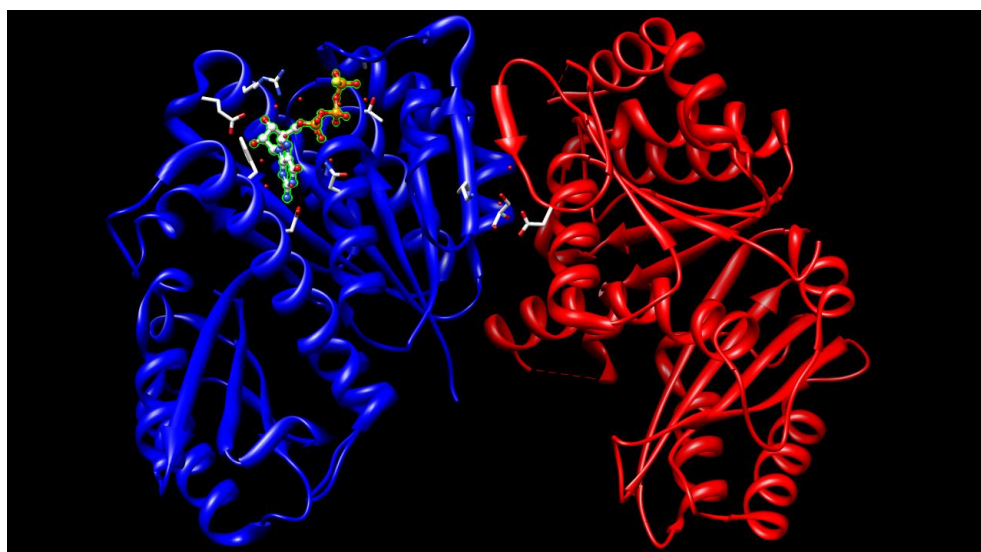


Figure 6.1. GTP binding site in FtsZ

Adapted from Ref. 3

As mentioned previously, the Rossmann fold formed in subunit A between T1-T6 loops is a feature common to both tubulin and FtsZ.^{1,2} Both tubulin and FtsZ have limited sequence similarity of about 10-18% and therefore, compounds which inhibit tubulin can serve as a good starting point for identifying compounds inhibiting FtsZ.⁴ Based on this rationale a library of

taxanes synthesized by Huang *et al.* was screened for anti-bacterial activity by Dr. Kirikae.⁵ Real time (RT) PCR-based assay was employed to screen a library of 120 taxanes belonging to two classes: taxol-like compounds which stabilize microtubules⁶⁻⁸ and non-cytotoxic taxane-multidrug resistance (MDR) reversal agents (TRAs)⁹⁻¹⁵ which inhibit the efflux pumps of ATP-binding cassette (ABC) transporters such as P-glycoprotein (P-gp). Several of these exhibited significant anti-TB activity.⁵ From the MIC values and cytotoxicity assay, **SB-T-0032** and **SB-RA-2001** (**Figure 6.2**) were selected for further studies. SB-RA series of taxanes bearing a (*E*)-3-(naphtha-2-yl)acryloyl (2-NpCH=CHCO) group at the C-13 position exhibited MIC between 2.5-5 μ M against drug-sensitive and drug-resistant *Mtb* strains. A new library of taxanes based on the above SB-RA series was therefore prepared by modification of 10-deacetybaccatin III (DAB). These **SB-RA-2001** analogues were found to exhibit higher specificity to FtsZ than microtubules and have the same level of anti-TB activity to that of **SB-T-0032**.

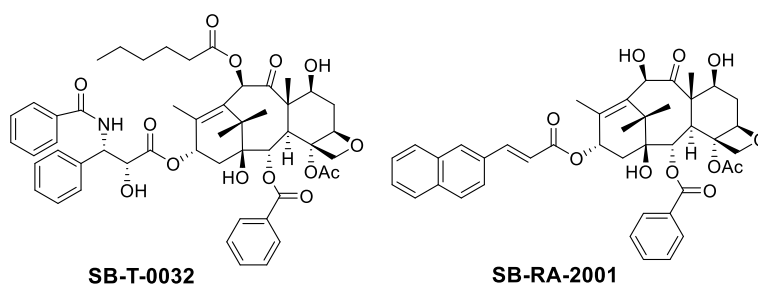


Figure 6.2. Lead taxanes identified by RT-PCR assay

Another class of taxane analogues with C-seco-baccatin skeleton, the anti-angiogenic taxoid (IDN5390),^{16, 17} have also been observed to be less cytotoxic than paclitaxel. Therefore, C-seco analogues of **SB-RA-2001** have been studied and were found to possess anti-TB activity (MIC 1.25-2.5 μ M) against drug-sensitive and drug-resistant *Mtb* strains without appreciable cytotoxicity ($IC_{50} > 80 \mu$ M). The scanning electron microscopy (SEM) images of *Mtb* cells treated with two compounds (**Figure 6.4**) belonging to this series of taxanes is shown in **Figure 6.3**. These images with **SB-RA-20018** and **SB-RA-5001** clearly show substantial elongation and filamentation, a phenotypic response to FtsZ inactivation (**Figure 6.4**).⁵

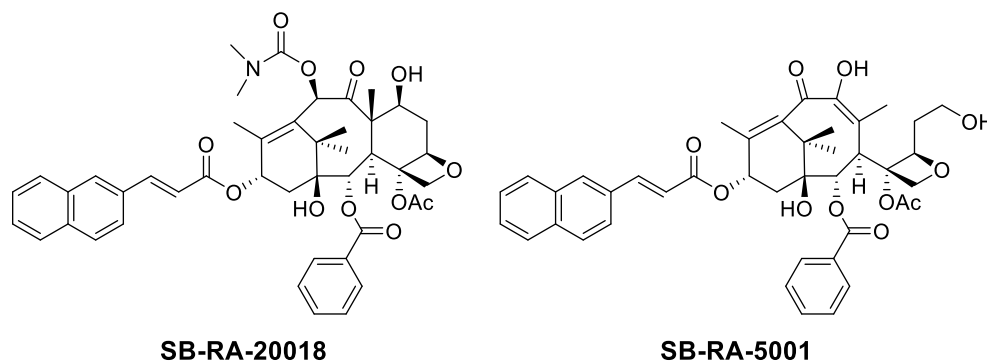
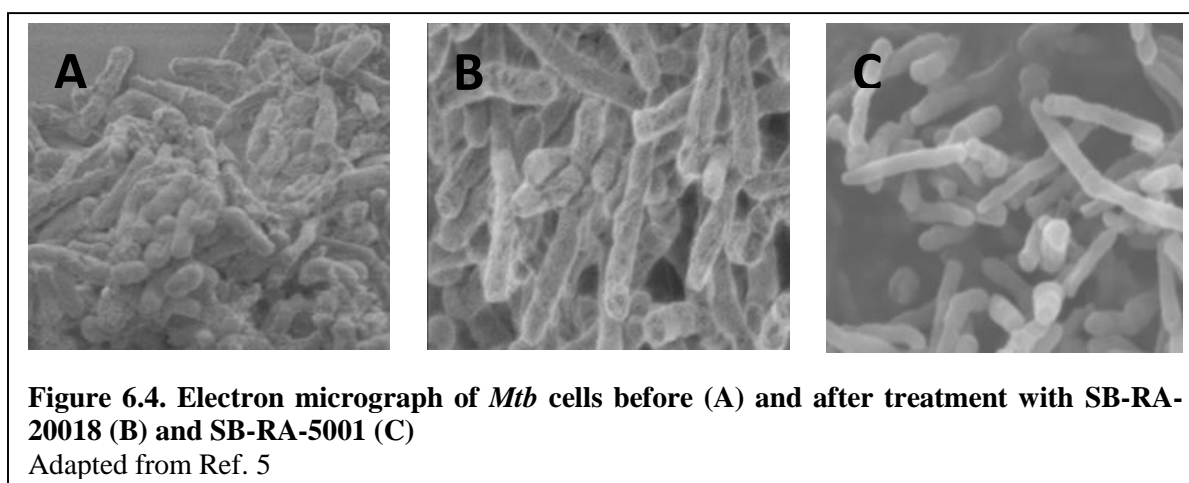


Figure 6.3. Hit TRA and C-seco baccatin analogues⁵



6.2. Results and Discussion

Cell elongation and filamentation of *Mtb* cells treated with the taxanes is an indirect confirmation of FtsZ as the target of these molecules. Transmission electron microscopy (TEM) of *Mtb* FtsZ protein in the presence of the taxanes would help visualize the direct impact of the compounds. To this end, **SB-RA-2001** and **SB-RA-5001** were selected for TEM studies. The two molecules were synthesized following published procedures developed in the Ojima lab.⁵ Side chain precursors required for the synthesis of analogues of **SB-RA-5011** and **SB-RA-5012** with a photo-reactive benzophenone group were also synthesized. These molecules can be used to ascertain the binding site of these taxanes on *Mtb* FtsZ via photo-affinity labeling studies.

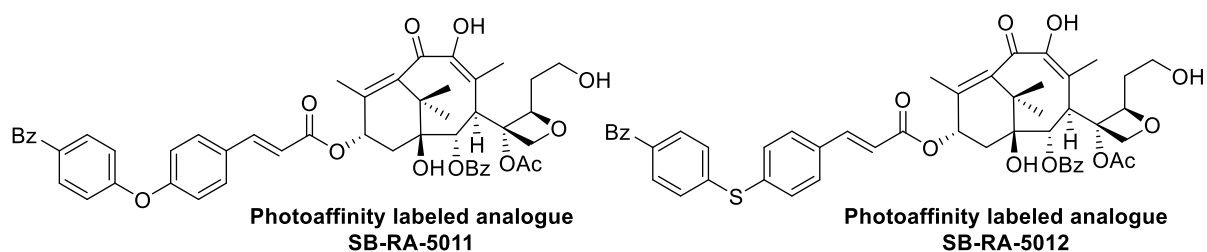
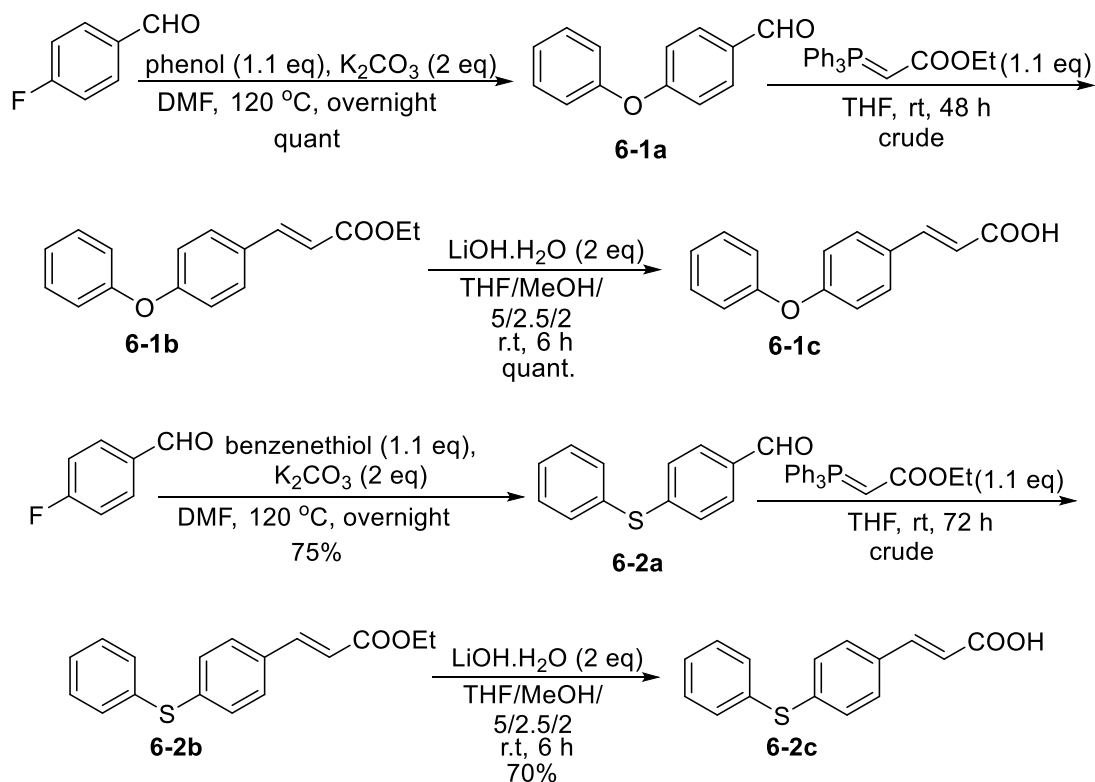


Figure 6.5. Photoaffinity labeled analogues of lead taxanes-based anti-TB compounds

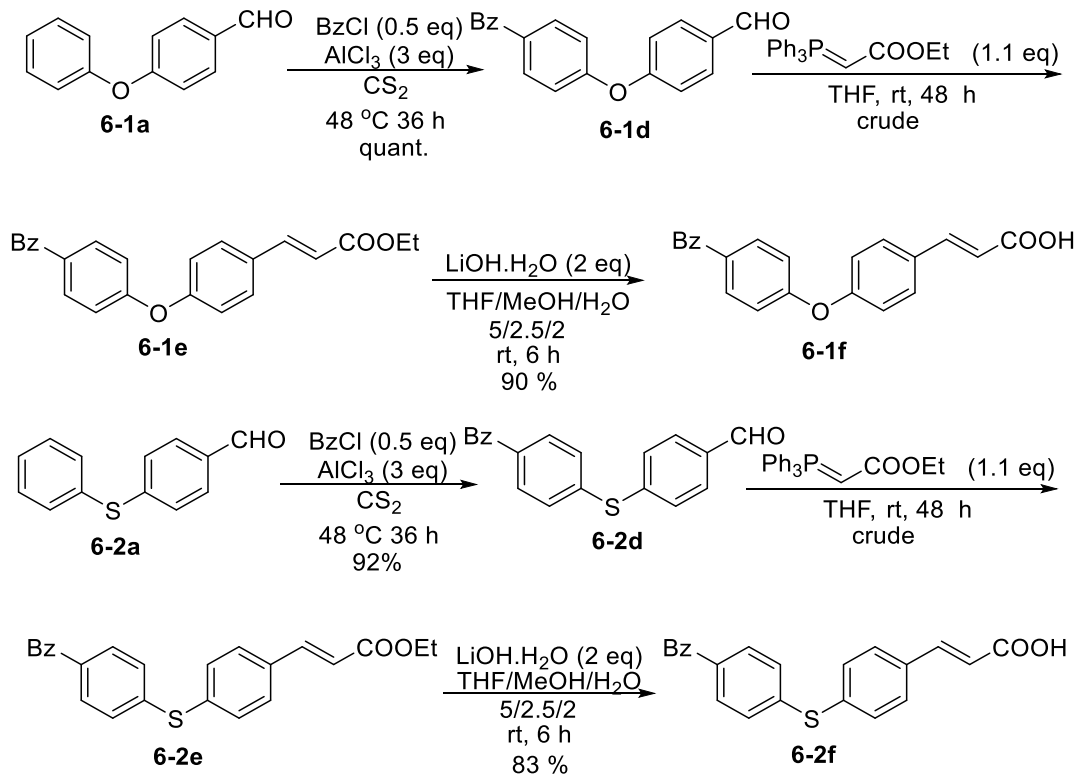
6.2.1. Synthesis of C-13 side chain precursors

The first step towards synthesizing the taxane-based anti-TB compounds was to obtain the side chains which will ultimately be coupled to the C-13 position of the C-seco skeleton (**Scheme 6.1**). To form the biphenyl ether linkage, phenol was treated with *p*-halobenzaldehyde. The reaction was tried with two benzaldehydes. When *p*-bromobenzaldehyde was used as the substrate in DMF for 1.5 days, no product formation was observed. On the other hand quantitative yield of product was observed when *p*-fluorobenzaldehyde was used as the substrate. 4-(Phenylthio)benzaldehyde (**6-2a**) was synthesized in a similar manner starting with benzenethiol. In the next step, Wittig reaction with (carboethoxymethylene)triphenylphosphorane was run in THF at ambient temperature and monitored by FIA. After 48 h and 72 h, the desired esters **6-1b** and **6-2b** respectively, were obtained as a mixture with triphenylphosphine oxide. For both the esters, the removal of triphenylphosphine oxide was difficult. In each case the crude mixture of product contaminated with triphenylphosphine oxide was subjected to hydrolysis with lithium hydroxide to give the products **6-1c** and **6-2c** in good yields.



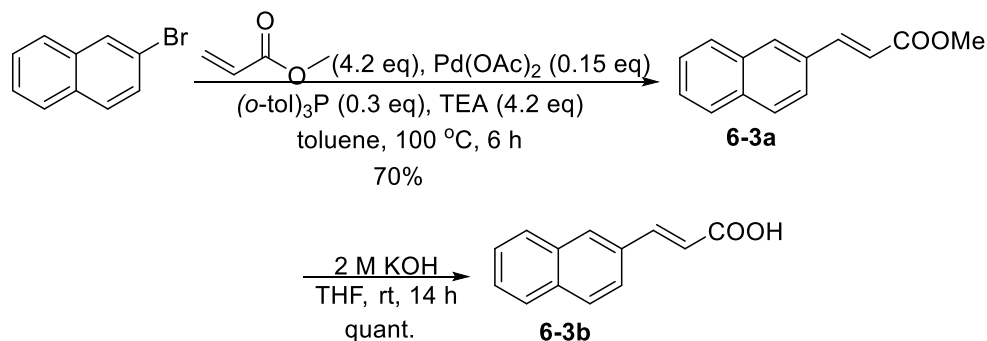
Scheme 6.1. Synthesis of C-13 side chain precursor

Additionally, to obtain the photoaffinity labeled analogues of **SB-RA-5011** and **SB-RA-5012**, the necessary side chains were synthesized starting from the aldehydes **6-1a** and **6-2a** (**Scheme 6.2**). The Friedel-Crafts reaction of benzoyl chloride with 4-(phenoxy)benzaldehyde (**6-1a**) in the presence of aluminum chloride and carbon disulfide afforded 4-(4-benzoyloxy)benzaldehyde (**6-1d**). Wittig reaction of **6-1d** with (carboethoxymethylene)triphenylphosphorane followed by hydrolysis of this ethyl ester gave the acid **6-1f** in good yield. (*E*)-3-(4-((4-Benzoylphenyl)thio)phenyl)acrylic acid (**6-2f**) was synthesized in a similar manner.



Scheme 6.2. Synthesis of photoaffinity labeled analogues of C-13 side chain precursors

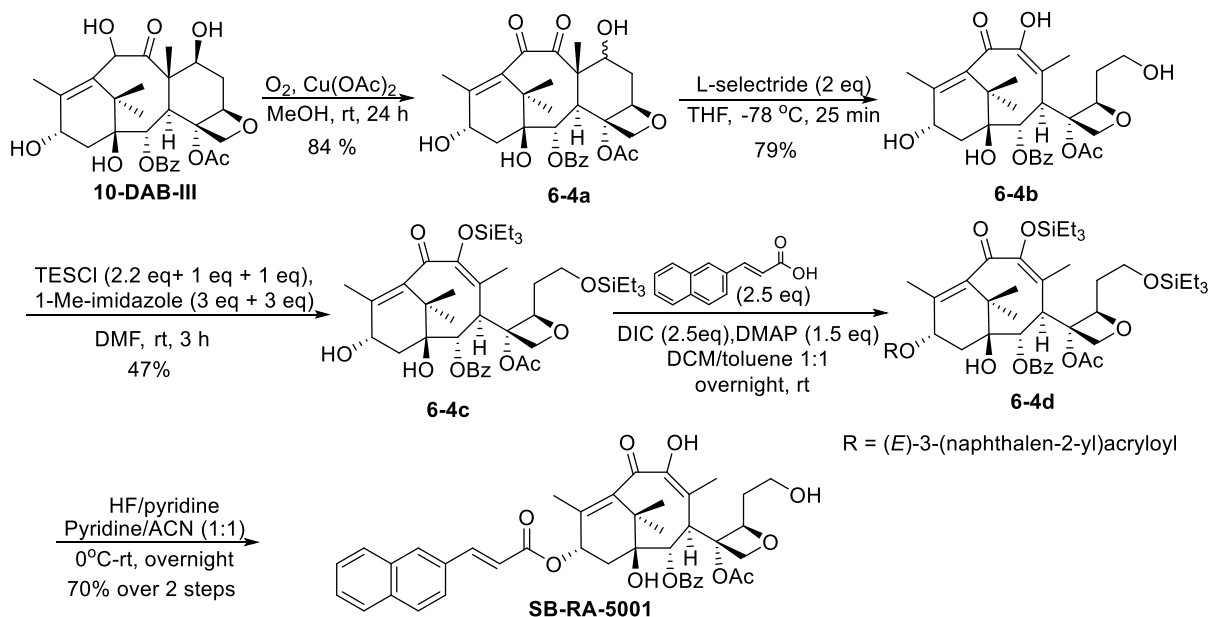
(*E*)-3-(Naphthalen-2-yl)acrylic acid (**6-3b**), the C-13 side chain precursor of **SB-RA-2001** and **SB-RA-5001**, was synthesized following **Scheme 6.3**. Heck reaction of 2-bromonaphthalene with methylacrylate gave methyl 3-(naphthalen-2-yl)acrylate, which was then hydrolyzed to the corresponding acid.



Scheme 6.3. Synthesis of (*E*)-3-(naphthalen-2-yl)acrylic acid

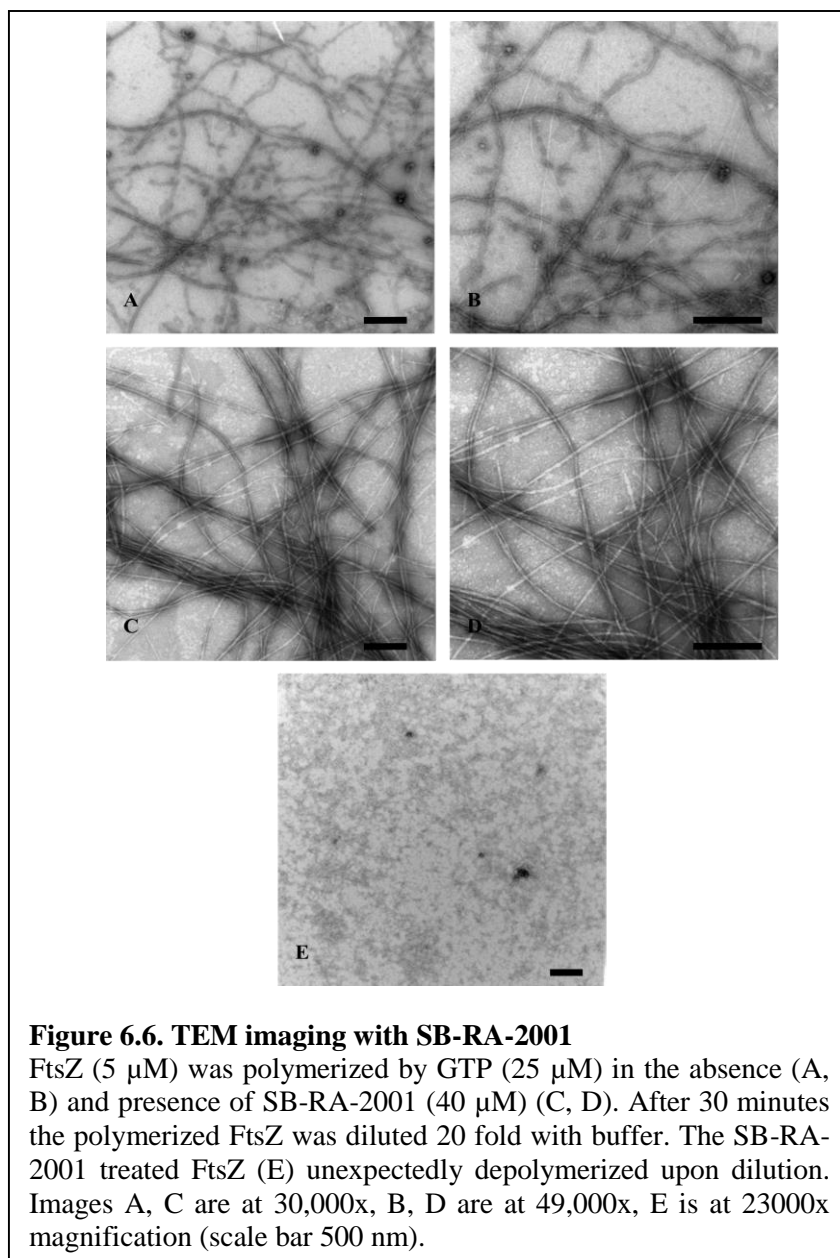
6.2.2. Synthesis of SB-RA-5001 and SB-RA-2001

The synthesis of **SB-RA-5001** is shown in **Scheme 6.4**.⁵ Air oxidation of 10-DAB III in the presence of copper (II) acetate afforded **6-4a**, which is a mixture of the C-7 epimerized hydroxyl group. The mixture of epimers was subjected to retro-aldol reductive fragmentation using L-selectride to afford **6-4b**. TES protection of the C-7 and C-9 hydroxyl groups afforded **6-4c**. This reaction requires optimization since a mixture of mono, di and tri TES protected compound was obtained. Coupling of 3-(2-naphthyl)acrylic acid to the C-13 position of **6-4d**, followed by HF/pyridine deprotection reaction afforded **SB-RA-5001**. The purification of this molecule is difficult since the product always co-elutes with DIU.



Scheme 6.4. Synthesis of SB-RA-5001⁵

For the synthesis of **SB-RA-2001**, 7,10-diTes DAB (III) prepared by previous group member was subjected to EDC/DMAP coupling condition using (*E*)-3-(naphthalen-2-yl)acrylic acid and even after 7 days at 40 °C the reaction showed no conversion. DIC/DMAP coupling conditions worked better, and the product was obtained in 88% yield over two steps (**Scheme 6.5**).



In addition to the preliminary target validation studies performed in our laboratory against *Mtb* FtsZ, Dr. Panda's research group carried out extensive studies against *B. subtilis* with **SB-RA-2001** provided by our laboratory.¹⁸ **SB-RA-2001** has been shown to interfere with the functioning of FtsZ isolated from *B. subtilis*. In the presence of 20, 40, and 60 μM **SB-RA-2001** the recovery of FtsZ polymer was found to increase by 13 ± 5 , 22 ± 7 and $46 \pm 4\%$ as compared to control confirming that the compound suppressed dilution induced disassembly of preformed FtsZ polymer. Additionally, the light scattering assay demonstrated that the compound increased

the initial rate of FtsZ assembly from 0.07 a.u./sec to 0.19 and 0.38 a.u./sec in presence of 20 and 40 μM compound, respectively. Also, the increase in sedimentable polymer mass of FtsZ in the presence of **SB-RA-2001** indicated that it enhances the assembly of FtsZ *in vitro*. The GTPase activity of the protein was inhibited by **SB-RA-2001** and by monitoring the increase of **SB-RA-2001** fluorescence upon binding to FtsZ, the dissociation constant for the compound was found to be $29 \pm 2 \mu\text{M}$. **SB-RA-2001** also caused cell elongation and filamentation of *B. subtilis* and *M. smegmatis* cells indicating that it inhibits cytokinesis in bacterial cells. The average length of the treated cells was 42 ± 18 and $35 \pm 25 \mu\text{m}$ for *B. subtilis* and *M. smegmatis*, respectively whereas the corresponding control cells were 3.4 ± 1 and $2.8 \pm 0.5 \mu\text{m}$ long (**Figure 6.7**).

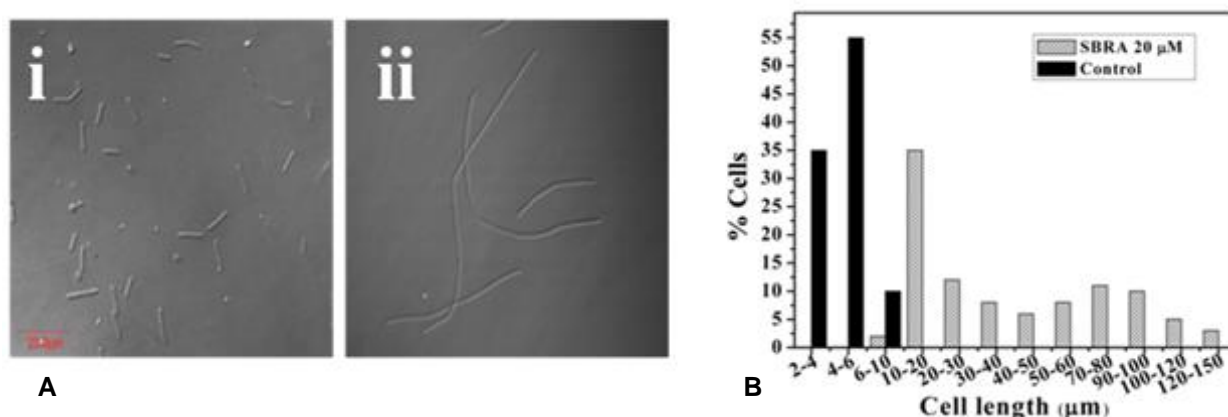


Figure 6.7. *Bacillus subtilis* 168 cells treated with SB-RA-2001

(A) *B. subtilis* 168 cells grown in the presence of either vehicle (i) or 20 μM **SB-RA-2001** (ii). The scale bar is 20 μm . (B) Distribution of *B. subtilis* 168 cell lengths in absence (vehicle treated) and presence of **SB-RA-2001** (20 μM). Adapted from Ref. 18

6.2.4. TEM Imaging with SB-RA-5001

Similar to **SB-RA-2001**, **SB-RA-5001** is expected to stabilize *Mtb* FtsZ polymers and this effect was visualized by transmission electron microscopy (**Figure 6.8**).¹⁹ *Mtb* FtsZ (5 μM) was polymerized in the presence of GTP (25 μM) at 37 $^{\circ}\text{C}$ for 30 minutes. The polymerized FtsZ was diluted 20 folds which resulted in de-polymerization of the polymers since the protein concentration dropped below the threshold value. On the other hand, *Mtb* FtsZ treated with **SB-RA-5001** wasn't susceptible to dilution induced de-polymerization as the compound stabilizes the polymers. These preliminary results give an insight into the mode of action of this series of compounds which is similar to the effect taxanes-based compounds have on tubulin.

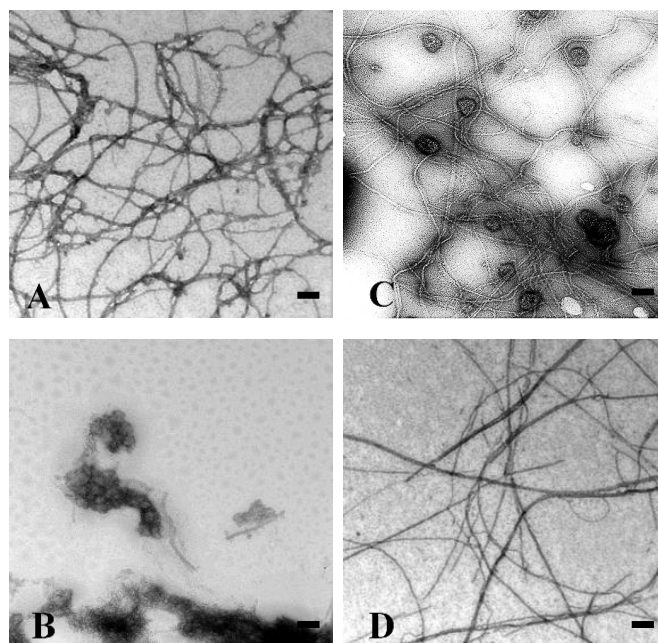


Figure 6.8. TEM Images of FtsZ with SB-RA-5001.

FtsZ (5 μM) was polymerized by GTP (25 μM) in the absence (A) and presence of SB-RA-5001 (160 μM) (C). After 30 minutes the polymerized FtsZ was diluted 20 folds with buffer. TEM images display the dilution induced de-polymerization of the untreated FtsZ protein (B) since the FtsZ concentration drops below the threshold value. The SB-RA-5001 treated FtsZ (D) doesn't depolymerize upon dilution because the compound stabilizes the FtsZ polymer. Images are at 68,000x magnification (scale bar 100 nm).

Adapted from Ref. 19

6.3. Conclusion

The taxanes based antibacterials have successfully been shown to stabilize *Mtb* FtsZ polymers and *B. subtilis* FtsZ polymers.^{18, 19} It is worth noting that the cytotoxicity of these taxanes-based compounds has been reversed to make them specific to prokaryotes versus eukaryotes. Further optimization studies are currently underway in our laboratory to develop these molecules as effective antibacterial agents.

6.4. Experimental Section

Methods. ^1H and ^{13}C NMR spectra were measured on a Bruker or Varian 300, 400 or 500 MHz NMR spectrometer. TLC was performed on silica coated aluminum sheets (thickness 200 μm) or alumina coated (thickness 200 μm) aluminum sheets supplied by Sorbent Technologies

and column chromatography was carried out on Siliaflash® P60 silica gel, 40-63 μm (230-400 mesh) supplied by Silicycle. Aluminum oxide, activated, neutral, Brockmann Grade I, 58 Å, was supplied by Alfa Aesar.

FEI Tecnai12 BioTwinG transmission electron microscope with an AMT XR-60 CCD digital camera system was used to acquire transmission electron microscopy images.

Synthesis of 4-Phenoxybenzaldehyde (6-1a): To a solution of phenol (417 mg, 4.4 mmol) and potassium carbonate anhydrous (1.8 g, 8.06 mmol) in *N,N*-dimethylformamide was added dropwise 4-fluorobenzaldehyde (500 mg, 4.03 mmol). The resulting solution was stirred overnight at reflux. The solution was cooled down and poured into ice-water mixture. The combined aqueous layers were extracted with methylene chloride and the combined organic layer was washed with water, brine, dried over MgSO_4 , filtered, and concentrated *in vacuo*. The crude product was purified on a silica gel column (hexane/EtOAc = 4/1) to afford the product as a brown oil (792 mg, 99% yield); ^1H NMR (300 MHz, CDCl_3) δ 7.03 - 7.12 (m, 4 H), 7.18 - 7.26 (m, 1 H), 7.35 - 7.47 (m, 2 H), 7.78 - 7.89 (m, 2 H), 9.90 (s, 1 H); MS (ESI) m/z 199.0 ($\text{M}+1$)⁺.

Same procedure was followed for the synthesis of **4-(phenylthio)benzaldehyde (6-2a)**: Pale yellow oil (75% yield); ^1H NMR (300 MHz, CDCl_3) δ 7.23 (d, $J = 8.52$ Hz, 2 H), 7.38 - 7.48 (m, 3 H), 7.48 - 7.58 (m, 2 H), 7.66 - 7.79 (m, 2 H), 9.90 (s, 1 H); MS (ESI) m/z 215.0 ($\text{M}+1$)⁺.

Synthesis of 4-[(4-benzoylphenyl)thio]benzaldehyde (6-2d): To a solution of benzoyl chloride (164 mg, 1.16 mmol) and AlCl_3 (920 mg, 6.9 mmol) in carbon disulfide (10 mL) was added dropwise 4-fluorobenzaldehyde (500 mg, 2.3 mmol) dissolved in carbon disulfide (5 mL). The reaction mixture was refluxed at 48 °C for 36 h. After completion the reaction was cooled on ice and quenched with 1 N HCl. The reaction mixture was transferred to a separatory funnel and extracted with ethyl acetate. The organic layer was dried over magnesium sulfate, filtered, and concentrated *in vacuo*. The crude product was purified on a silica gel column (hexane/EtOAc = 4/1) to afford the product as a white solid (339 mg, 91% yield); ^1H NMR (300 MHz, CDCl_3) δ 7.40 - 7.55 (m, 6 H), 7.56 - 7.67 (m, 1 H), 7.74 - 7.87 (m, 6 H), 9.97 (s, 1 H); MS (ESI) m/z 319.0 ($\text{M}+1$)⁺.

Same procedure was followed for the synthesis of **4-(4-benzoylphenoxy)benzaldehyde (6-1d)**: White solid (98% yield); ^1H NMR (300 MHz, CDCl_3) δ 7.16 (t, $J = 9.03$ Hz, 4 H), 7.50 (t,

$J = 7.45$ Hz, 2 H), 7.60 (t, $J = 7.26$ Hz, 1 H), 7.76 - 7.99 (m, 6 H), 9.97 (s, 1 H); MS (ESI) m/z 303.0 (M+1)⁺.

Synthesis of (*E*)-3-(4-(phenylthio)phenyl)acrylic acid (6-2c): To a solution of 4-(Phenylthio)benzaldehyde (863 mg, 4.0 mmol) in THF (15 mL) was added dropwise a solution of (carbethoxymethylene)triphenylphosphorane (1.53 g, 4.3 mmol) in THF (5 mL). The reaction was stirred for 72 h at room temperature after which it was quenched with saturated solution of aqueous ammonium chloride. The reaction was transferred to a separatory funnel and extracted with ethyl acetate. The organic layer was dried over magnesium sulfate, filtered and concentrated on a rotary evaporator. The crude contaminated with triphenylphosphine oxide was treated with lithium hydroxide dihydrate (335.7 mg, 13.8 mmol) in THF/MeOH/water (20/10/10) for 6 h. Following completion of reaction, the solution was concentrated on rotary evaporator. Small amount of triphenylphosphine oxide was removed by filtering the aqueous layer. The aqueous layer was then acidified, transferred to a separatory funnel and extracted with dichloromethane. The organic layer was dried over magnesium sulfate, filtered and concentrated on a rotary evaporator to obtain mixture of product and remaining triphenylphosphine oxide. The product was recrystallized from this mixture using cold dichloromethane (product has limited solubility in cold dichloromethane). Product was obtained as a white solid (715 mg, 70% yield over 2 steps); ¹H NMR (500 MHz, DMSO) δ 6.50 (d, $J = 16.17$ Hz, 1 H), 7.19 - 7.26 (m, $J = 8.54$ Hz, 2 H), 7.35 - 7.46 (m, 5 H), 7.55 (d, $J = 16.17$ Hz, 1 H), 7.61 - 7.67 (m, $J = 8.54$ Hz, 2 H); ¹³C NMR (126 MHz, DMSO) δ 119.3, 128.4, 129.1, 129.2, 129.9, 132.3, 132.7, 132.9, 138.6, 143.1, 167.6; MS (ESI) m/z 257.0 (M+1)⁺.

Same procedure was followed for the synthesis of **6-1c**, **6-1f**, **6-2f**

Ethyl (*E*)-3-(4-phenoxyphenyl)acrylate (6-1b) contaminated with Ph₃PO: ¹H NMR (300 MHz, CDCl₃) δ 1.31 (td, $J = 7.07, 1.24$ Hz, 3 H), 4.24 (qd, $J = 7.14, 1.10$ Hz, 2 H), 6.33 (dd, $J = 16.21, 0.82$ Hz, 1 H), 6.89 - 7.07 (m, 5 H), 7.08 - 7.19 (m, 1 H), 7.29 - 7.38 (m, 2 H), 7.38 - 7.58 (m, 13 H), 7.58 - 7.73 (m, 9 H); MS (ESI) m/z 269.0 (M+1)⁺.

(*E*)-3-(4-Phenoxyphenyl)acrylic acid (6-1c): Off white solid (99% yield); ¹H NMR (300 MHz, CDCl₃) δ 6.36 (d, $J = 15.83$ Hz, 1 H), 6.90 - 7.11 (m, 5 H), 7.17 (t, $J = 7.36$ Hz, 1 H), 7.38 (t, $J = 7.73$ Hz, 2 H), 7.51 (d, $J = 8.57$ Hz, 2 H), 7.75 (d, $J = 15.83$ Hz, 1 H), 8.59 (br. s, 1 H); ¹³C NMR

(75 MHz, CDCl₃) δ 116.2, 118.5, 120.0, 124.4, 128.9, 130.1, 130.3, 146.2, 156.1, 160.0, 172.4; MS (ESI) m/z 241.0 (M+1)⁺.

Ethyl (*E*)-3-[4-((4-benzoylphenyl)thio)phenyl]acrylate (6-2e): ester contaminated with Ph₃PO. ¹H NMR (300 MHz, CDCl₃) δ 1.32 (t, J = 7.14 Hz, 3 H), 4.25 (q, J = 7.05 Hz, 2 H), 6.44 (d, J = 15.93 Hz, 1 H), 7.33 (d, J = 8.52 Hz, 2 H), 7.39 - 7.58 (m, 19 H), 7.61 - 7.82 (m, 13 H); MS (ESI) 389.1(M+1)⁺.

(*E*)-3-[4-((4-benzoylphenyl)thio)phenyl]acrylic acid (6-2f): White solid (83% yield); ¹H NMR (300 MHz, DMSO) δ 6.59 (d, J = 16.21 Hz, 1 H), 7.41 (d, J = 8.79 Hz, 2 H), 7.46 - 7.60 (m, 5 H), 7.63 - 7.81 (m, 7 H); MS (ESI) 361.0 (M+1)⁺.

Ethyl (*E*)-3-(4-(4-benzoyloxy)phenyl)acrylate (6-1e): ester contaminated with Ph₃PO. ¹H NMR (300 MHz, CDCl₃) δ 1.31 (tt, J = 7.14, 0.69 Hz, 3 H), 4.19 - 4.31 (m, 2 H), 6.37 (dd, J = 15.93, 0.82 Hz, 1 H), 7.06 (d, J = 9.07 Hz, 4 H), 7.38 - 7.56 (m, 15 H), 7.59 - 7.71 (m, 8 H), 7.72 - 7.88 (m, 5 H); MS (ESI) m/z 373.1 (M+1)⁺.

(*E*)-3-(4-(4-benzoyloxy)phenyl)acrylic acid (6-1f): White solid (90% yield); ¹H NMR (300 MHz, Acetone) δ 6.51 (d, J = 15.93 Hz, 1 H), 7.13 - 7.25 (m, 4 H), 7.57 (d, J = 7.69 Hz, 2 H), 7.62 - 7.73 (m, 2 H), 7.79 (dd, J = 9.07, 2.20 Hz, 4 H), 7.83 - 7.92 (m, 2 H) MS (ESI) m/z 345.1 (M+1)⁺.

Synthesis of methyl (*E*)-3-(naphthalen-2-yl)acrylate (6-3a): Methyl acrylate (3.65 mL, 40.6 mmol) was added under N₂ to a suspension of 2-bromonaphthalene (2.0 g, 9.66 mmol), palladium (II) acetate (325 mg, 1.5 mmol), tri-*o*-tolylphosphine (882 mg, 2.9 mmol) and TEA (5.65 mL, 40.56 mmol) in toluene (6 mL). The mixture was stirred at 100°C for 6 h, cooled to room temperature, diluted with 100 ml of ethyl acetate and filtered over celite. After the solvent was evaporated, the crude material was purified by chromatography on silica gel with ethyl acetate/hexane (8:1) to give product **6-3a** as a white solid (1.426 g, 70% yield). ¹H NMR (300 MHz, CDCl₃) δ 3.84 (s, 3 H), 6.56 (d, J = 15.93 Hz, 1 H), 7.49 - 7.56 (m, 2 H), 7.67 (dd, J = 8.79, 1.65 Hz, 1 H), 7.79 - 7.91 (m, 4 H), 7.91 - 7.95 (m, 1 H).

Synthesis of (*E*)-3-(Naphthalen-2-yl)acrylic acid (6-3b): To a solution of **6-3a** (1.426 g, 6.72 mmol) in THF (13 mL) was added 17 mL of KOH (2 M). After stirring for 14 h, the solution was diluted with ethyl acetate, the aqueous phase was acidified to pH 1 with a 1 N solution of HCl,

and then extracted with ethyl acetate. The organic phase was dried over magnesium sulfate, filtered and evaporated under reduced pressure to give corresponding acid as white solid (1.339 g, 99% yield). ¹H NMR (500 MHz, DMSO) δ 6.69 (d, *J* = 15.87 Hz, 1 H), 7.51 - 7.58 (m, 2 H), 7.72 (d, *J* = 15.87 Hz, 1 H), 7.86 (dd, *J* = 8.54, 1.53 Hz, 1 H), 7.89 - 7.99 (m, 3 H), 8.15 (s, 1 H); ¹³C NMR (126 MHz, DMSO) δ 120.7, 123.9, 126.7, 127.1, 127.7, 128.4, 128.5, 129.4, 132.1, 132.9, 133.6, 143.1, 167.9; MS (ESI) *m/z* 199.1 (M+1)⁺.

Synthesis of 10-Dehydro-10-deacetylbaaccatin (6-4a): 10-DAB (1 g, 1.84 mmol) was suspended in methanol (30 mL), and Cu(OAc)₂ (1 g, 5.52 mmol) was added in small portions, with vigorous mechanical stirring, over ca. 10 min. The pale blue suspension darkened during the course of the reaction and stirring was continued with the flask neck unstoppered to allow contact with air. After 72 h, the reaction mixture was concentrated and the residue was purified by column chromatography on silica gel, with a 1% -5% methanol in dichloromethane to afforded **6-4a** (839 mg, 84% yield). ¹H NMR (300 MHz, CDCl₃) δ 1.04 - 1.30 (m, 18 H), 1.67 - 1.73 (m, 6 H), 1.77 - 2.13 (m, 18 H), 2.23 - 2.40 (m, 12 H), 2.49 - 2.64 (m, 2 H), 3.65 (d, *J* = 6.87 Hz, 1 H), 3.84 (d, *J* = 6.87 Hz, 1 H), 4.29 - 4.34 (m, 2 H), 4.40 - 4.44 (m, 0.5 H), 4.61 (d, *J* = 10.71 Hz, 0.5 H), 4.87 - 5.03 (m, 4 H), 5.72 - 5.84 (m, 2 H), 7.46 - 7.54 (m, 4 H), 7.59 - 7.67 (m, 2 H), 8.07 - 8.15 (m, 4 H)

Synthesis of 10-Dehydro-C-seco-10-deacetylbaaccatin (6-4b): In a two-necked 250 mL flask, **6-4a** (200 mg, 0.37 mmol) was suspended in dry THF (3 mL). With vigorous magnetic stirring, the reaction mixture was cooled to -78°C and L-selectride (1.0 M in THF, 1.1 mL) was added drop wise. At the end of the addition, the cooling bath was removed, and the reaction mixture was worked up by addition of ethyl acetate and 2 N H₂SO₄ (1.1 mL). The organic phase was washed sequentially with 2 N H₂SO₄ and brine. The crude material was purified by column chromatography on silica gel using 2%-5% methanol in dichloromethane to give **6-4b** (159 mg, 79% yield) as white powder. ¹H NMR (300 MHz, CDCl₃) δ 0.96 - 1.20 (m, 9 H), 1.80 (br. s., 6 H), 1.92 (s, 3 H), 2.00 - 2.17 (m, 2 H), 2.30 - 2.54 (m, 3 H), 2.61 - 2.94 (m, 3 H), 3.75 (d, *J* = 19.23 Hz, 2 H), 4.29 (br. s., 2 H), 4.83 - 4.96 (m, 1 H), 5.19 (br. s., 2 H), 5.56 (d, *J* = 9.07 Hz, 1 H), 6.50 (br. s., 1 H), 7.39 - 7.50 (m, 2 H), 7.53 - 7.62 (m, 1 H), 7.91 - 8.07 (m, 2 H).

Synthesis of 7,9-Bis(triethylsilyl)-10-dehydro-C-seco-10-deacetylbaaccatin (6-4c): 1-Methylimidazole (109.7 μL, 1.38 mmol) and TESCl (154 μL, 0.92 mmol) were added to a solution

of **6-4b** (250 mg, 0.46 mmol) in DMF at 0 °C. After stirring for 30 min, the reaction mixture was worked up by dilution with EtOAc and washing with water. The crude product was purified by column chromatography on silica gel using hexane/ethyl acetate 1/3 to get **6-4c** (169 mg, 47% yield). ¹H NMR (300 MHz, CDCl₃) δ 0.53 - 0.83 (m, 12 H), 0.97 (q, *J* = 7.51 Hz, 18 H), 1.13 (d, *J* = 6.87 Hz, 6 H), 1.63 - 2.16 (m, 10 H), 3.51 - 3.92 (m, 2 H), 4.07 - 4.60 (m, 2 H), 4.91 (q, *J* = 7.69 Hz, 1 H), 5.20 (br. s., 2 H), 5.57 (d, *J* = 9.07 Hz, 1 H), 7.43 - 7.52 (m, 2 H), 7.58 - 7.66 (m, 1 H), 8.01 (br. s., 2 H)

Synthesis of SB-RA-5001: To a solution of **6-4c** (32 mg, 0.04 mmol), DMAP (7.32 mg, 0.06 mmol) and the corresponding acid (20 mg, 0.1 mmol) in toluene/dichloromethane (1/2) was added DIC (12.6 mg, 0.1 mmol) at room temperature with stirring. After stirring for 72h, the solvent was evaporated *in vacuo*. Purification of the crude product by short silica gel chromatography using ethyl acetate/hexane (4:1) as eluent afforded TES protected C-13 coupling product contaminated by DIC-acid complex, which was directly used in the next step.

To a solution of TES protected C-13 coupling product in a (1:1) mixture of pyridine and acetonitrile (4 mL/100mg of starting material) at 0 °C was added a 70 % solution of HF in pyridine (1 mL/100 mg of starting material) with stirring. After stirring overnight at room temperature, the reaction was quenched with NaHCO₃ solution and extracted with ethyl acetate and then dried over magnesium sulfate. Purification of the crude product by silica gel chromatography (hexanes/EtOAc = 1/1) afforded **SB-RA-5001** contaminated with DIU (25 mg). The product was further purified by re-crystallization. ¹H NMR (300 MHz, CDCl₃) δ 1.02 - 1.32 (m, 9 H), 1.79 - 2.38 (m, 15 H), 3.90 (br. s., 2 H), 4.36 (br. s., 2 H), 5.18 - 5.52 (m, 2 H), 5.65 (d, *J* = 9.07 Hz, 1 H), 6.09 - 6.23 (m, 1 H), 6.53 (s, 1 H), 6.71 (d, *J* = 15.38 Hz, 1 H), 7.39 - 8.21 (m, 13 H)

SB-RA-2001 was synthesized following the same procedure. ¹H NMR (400 MHz, CDCl₃) δ 1.16 (s, 3 H), 1.26 (s, 3 H), 1.67 (s, 1 H), 1.79 (s, 3 H), 2.04 - 2.20 (m, 3 H), 2.21 - 2.37 (m, 4 H), 2.41 - 2.52 (m, 1 H), 2.57 - 2.73 (m, 1 H), 4.02 (d, *J* = 7.03 Hz, 1 H), 4.17 - 4.26 (m, 1 H), 4.32 (d, *J* = 8.03 Hz, 2 H), 5.01 (dd, *J* = 9.29, 1.51 Hz, 1 H), 5.29 (s, 1 H), 5.71 (d, *J* = 7.03 Hz, 1 H), 6.20 (t, *J* = 9.16 Hz, 1 H), 6.62 (d, *J* = 15.81 Hz, 1 H), 7.42 - 7.52 (m, 2 H), 7.53 - 7.63 (m, 3 H), 7.67 - 7.74 (m, *J* = 1.51 Hz, 1 H), 7.89 (d, *J* = 8.78 Hz, 3 H), 7.94 - 8.13 (m, 4 H)

Transmission Electron Microscopy (TEM) Analysis:²⁰ Stock solution of compounds was prepared in dimethylsulfoxide. *Mtb* FtsZ (5 μ M) was incubated with 40 μ M of SB-RA-2001 in polymerization buffer (50 mM MES, 5mM MgCl₂, 100 mM KCl, pH 6.5) for 15 min on ice. To each solution was added GTP to the final concentration of 25 μ M. The resulting solution was incubated at 37 °C for 30 min. The incubated solution was diluted 2 times with the polymerization buffer and immediately transferred to carbon coated 300 mesh formvar copper grid and negatively stained with 1% uranyl acetate. To visualize the effect of dilution, following 30 min incubation, the sample was diluted 20 fold in polymerization buffer. The resulting solution was transferred after 10 minutes to carbon coated 300 mesh formvar copper grid and negatively stained with 1% uranyl acetate. The samples were viewed at the Microscopy Imaging Center at Stony Brook University, with a FEI Tecnai12 BioTwinG transmission electron microscope at 80 kV. Digital images were acquired with an AMT XR-60 CCD digital camera system.

6.5. References

1. Nogales, E.; Downing, K. H.; Amos, L. A.; Lowe, J., Tubulin and FtsZ form a distinct family of GTPases. *Nat. Struct. Biol.* **1998**, *5*, 451-458
2. Rossmann, M. G.; Moras, D.; Olsen, K. W., Chemical and biological evolution of a nucleotide-binding protein. *Nature* **1974**, *250*, 194-9
3. Leung, A. K. W.; White, E. L.; Ross, L. J.; Reynolds, R. C.; DeVito, J. A.; Borhani, D. W., Structure of Mycobacterium tuberculosis FtsZ Reveals Unexpected, G Protein-like Conformational Switches. *J. Mol. Biol.* **2004**, *342*, 953-970
4. de Pereda, J. M.; Leynadier, D.; Evangelio, J. A.; Chacon, P.; Andreu, J. M., Tubulin secondary structure analysis, limited proteolysis sites, and homology to FtsZ. *Biochemistry* **1996**, *35*, 14203-14215
5. Huang, Q.; Kirikae, F.; Kirikae, T.; Pepe, A.; Amin, A.; Respicio, L.; Slayden, R. A.; Tonge, P. J.; Ojima, I., Targeting FtsZ for Antituberculosis Drug Discovery: Noncytotoxic Taxanes as Novel Antituberculosis Agents. *J. Med. Chem.* **2006**, *49*, 463-466
6. Georg, G. I.; Chen, T. T.; Ojima, I.; Wyas, D. M.; Editors, *Taxane Anticancer Agents: Basic Science and Current Status. ACS Symp. Ser.* 1995; Vol. 583, p 353.
7. Kingston, D. G. I.; Jagtap, P. G.; Yuan, H.; Samala, L., The chemistry of taxol and related taxoids. *Prog. Chem. Org. Nat. Prod.* **2002**, *84*, 53-225
8. Ojima, I.; Kuduk, S. D.; Chakravarty, S., Recent advances in the medicinal chemistry of taxoid anticancer agents. *Adv. Med. Chem.* **1999**, *4*, 69-124
9. Brooks, T. A.; Kennedy, D. R.; Gruol, D. J.; Ojima, I.; Baer, M. R.; Bernacki, R. J., Structure-activity analysis of taxane-based broad-spectrum multidrug resistance modulators. *Anticancer Res.* **2004**, *24*, 409-415
10. Brooks Tracy, A.; Minderman, H.; O'Loughlin Kieran, L.; Pera, P.; Ojima, I.; Baer Maria, R.; Bernacki Ralph, J.; Brooks, T., Taxane-based reversal agents modulate drug resistance mediated by P-glycoprotein, multidrug resistance protein, and breast cancer resistance protein. *Mol. Cancer Ther.* **2003**, *2*, 1195-205
11. Minderman, H.; Brooks, T. A.; O'Loughlin, K. L.; Ojima, I.; Bernacki, R. J.; Baer, M. R., Broad-spectrum modulation of ATP-binding cassette transport proteins by the taxane

- derivatives ortataxel (IDN-5109, BAY 59-8862) and tRA96023. *Cancer Chemother. Pharmacol.* **2004**, *53*, 363-369
12. Ojima, I.; Borella, C. P.; Wu, X.; Bounaud, P.-Y.; Oderda, C. F.; Sturm, M.; Miller, M. L.; Chakravarty, S.; Chen, J.; Huang, Q.; Pera, P.; Brooks, T. A.; Baer, M. R.; Bernacki, R. J., Design, Synthesis and Structure-Activity Relationships of Novel Taxane-Based Multidrug Resistance Reversal Agents. *J. Med. Chem.* **2005**, *48*, 2218-2228
 13. Ojima, I.; Bounaud, P.-Y.; Bernacki, R. J., New weapons in the fight against cancer. *Chemtech* **1998**, *28*, 31-36
 14. Ojima, I.; Bounaud, P.-Y.; Bernacki, R. J., Designing taxanes to treat multidrug-resistant tumors. *Mod. Drug Discovery* **1999**, *2*, 45,47-48,51-52
 15. Ojima, I.; Bounaud, P.-Y.; Oderda, C. F., Recent strategies for the treatment of multi-drug resistance in cancer cells. *Expert Opin. Ther. Pat.* **1998**, *8*, 1587-1598
 16. Appendino, G.; Danieli, B.; Jakupovic, J.; Belloro, E.; Scambia, G.; Bombardelli, E., The chemistry and occurrence of taxane derivatives. XXX. Synthesis and evaluation of C-seco paclitaxel analogs. *Tetrahedron Lett.* **1997**, *38*, 4273-4276
 17. Taraboletti, G.; Micheletti, G.; Rieppi, M.; Poli, M.; Turatto, M.; Rossi, C.; Borsotti, P.; Roccabianca, P.; Scanziani, E.; Nicoletti, M. I.; Bombardelli, E.; Morazzoni, P.; Riva, A.; Giavazzi, R., Antiangiogenic and antitumor activity of IDN 5390, a new taxane derivative. *Clin. Cancer Res.* **2002**, *8*, 1182-1188
 18. Singh, D.; Bhattacharya, A.; Rai, A.; Dhaked, H. P. S.; Awasthi, D.; Ojima, I.; Panda, D., SB-RA-2001 inhibits bacterial proliferation by targeting FtsZ assembly. *Biochemistry* **2014**, *53*, 2979-2992
 19. Ojima, I.; Kumar, K.; Awasthi, D.; Vineberg, J. G., Drug discovery targeting cell division proteins, microtubules and FtsZ. *Bioorg. Med. Chem.*,
 20. Kumar, K.; Awasthi, D.; Lee, S.-Y.; Zanardi, I.; Ruzsicska, B.; Knudson, S.; Tonge, P. J.; Slayden, R. A.; Ojima, I., Novel Trisubstituted Benzimidazoles, Targeting Mtb FtsZ, as a New Class of Antitubercular Agents. *J. Med. Chem.* **2011**, *54*, 374-381

Bibliography

Chapter 1

1. World Health Organization, Tuberculosis: data and country profiles. <http://www.who.int/tb/country/en/>.
2. Gandhi, N. R.; Moll, A.; Sturm, A. W.; Pawinski, R.; Govender, T.; Lalloo, U.; Zeller, K.; Andrews, J.; Friedland, G., Extensively drug-resistant tuberculosis as a cause of death in patients co-infected with tuberculosis and HIV in a rural area of South Africa. *Lancet* **2006**, *368*, 1575-80
3. Bloom, B. R.; Murray, C. J., Tuberculosis: commentary on a reemerging killer. *Science* **1992**, *257*, 1055-64
4. Errington, J.; Daniel, R. A.; Scheffers, D.-J., Cytokinesis in bacteria. *Microbiol. Mol. Biol. Rev.* **2003**, *67*, 52-65
5. Raviglione, M. C., Issues facing TB control (7). Multiple drug-resistant tuberculosis. *Scott Med J* **2000**, *45*, 52-5; discussion 56
6. World Health Organization, Tuberculosis: Data and Country Profiles. Available at http://www.who.int/tb/publications/global_report/gtbr13_executive_summary.pdf?ua=1.
7. Miller, J. R.; Waldrop, G. L., Discovery of novel antibacterials. *Expert Opin. Drug Discovery* **2010**, *5*, 145-154
8. Diacon, A. H.; Pym, A.; Grobusch, M.; Patientia, R.; Rustomjee, R.; Page-Shipp, L.; Pistorius, C.; Krause, R.; Bogoshi, M.; Churchyard, G.; Venter, A.; Allen, J.; Palomino, J. C.; De Marez, T.; van Heeswijk, R. P.; Lounis, N.; Meyvisch, P.; Verbeeck, J.; Parys, W.; de Beule, K.; Andries, K.; Mc Neeley, D. F., The diarylquinoline TMC207 for multidrug-resistant tuberculosis. *N Engl J Med* **2009**, *360*, 2397-405
9. Slayden, R. A.; Knudson, D. L.; Belisle, J. T., Identification of cell cycle regulators in *Mycobacterium tuberculosis* by inhibition of septum formation and global transcriptional analysis. *Microbiology* **2006**, *152*, 1789-1797
10. Vollmer, W., The prokaryotic cytoskeleton: A putative target for inhibitors and antibiotics? *Appl. Microbiol. Biotechnol.* **2006**, *73*, 37-47
11. Margalit, D. N.; Romberg, L.; Mets, R. B.; Hebert, A. M.; Mitchison, T. J.; Kirschner, M. W.; RayChaudhuri, D., Targeting cell division: Small-molecule inhibitors of FtsZ GTPase perturb

- cytokinetic ring assembly and induce bacterial lethality. *Proc. Natl. Acad. Sci. U. S. A.* **2004**, *101*, 11821-11826
12. Ben-Yehuda, S.; Losick, R., Asymmetric cell division in *B. subtilis* involves a spiral-like intermediate of the cytokinetic protein FtsZ. *Cell* **2002**, *109*, 257-266
 13. Goehring, N. W.; Beckwith, J., Diverse paths to midcell: assembly of the bacterial cell division machinery. *Curr. Biol.* **2005**, *15*, R514-R526
 14. Leung, A. K. W.; White, E. L.; Ross, L. J.; Reynolds, R. C.; DeVito, J. A.; Borhani, D. W., Structure of *Mycobacterium tuberculosis* FtsZ Reveals Unexpected, G Protein-like Conformational Switches. *J. Mol. Biol.* **2004**, *342*, 953-970
 15. Moller-Jensen, J.; Loewe, J., Increasing complexity of the bacterial cytoskeleton. *Curr. Opin. Cell Biol.* **2005**, *17*, 75-81
 16. Thanedar, S.; Margolin, W., FtsZ Exhibits Rapid Movement and Oscillation Waves in Helix-like Patterns in *Escherichia coli*. *Curr. Biol.* **2004**, *14*, 1167-1173
 17. de Boer, P.; Crossley, R.; Rothfield, L., The essential bacterial cell-division protein FtsZ is a GTPase. *Nature* **1992**, *359*, 254-6
 18. RayChaudhuri, D.; Park, J. T., *Escherichia coli* cell-division gene *ftsZ* encodes a novel GTP-binding protein. *Nature* **1992**, *359*, 251-4
 19. Adams, D. W.; Errington, J., Bacterial cell division: assembly, maintenance and disassembly of the Z ring. *Nat. Rev. Microbiol.* **2009**, *7*, 642-653
 20. Erickson Harold, P.; Anderson David, E.; Osawa, M., FtsZ in bacterial cytokinesis: cytoskeleton and force generator all in one. *Microbiol. Mol. Biol. Rev.* **2010**, *74*, 504-28
 21. Mukherjee, A.; Dai, K.; Lutkenhaus, J., *Escherichia coli* cell division protein FtsZ is a guanine nucleotide binding protein. *Proc. Natl. Acad. Sci. U. S. A.* **1993**, *90*, 1053-1057
 22. Erickson, H. P.; O'Brien, E. T., Microtubule Dynamic Instability and GTP Hydrolysis. *Annu. Rev. Biophys. Biomol. Struct.* **1992**, *21*, 145-166
 23. Mukherjee, A.; Lutkenhaus, J., Guanine nucleotide-dependent assembly of FtsZ into filaments. *J. Bacteriol.* **1994**, *176*, 2754-8
 24. Li, Z.; Trimble, M. J.; Brun, Y. V.; Jensen, G. J., The structure of FtsZ filaments in vivo suggests a force-generating role in cell division. *Embo J.* **2007**, *26*, 4694-4708

25. Caplan, M. R.; Erickson, H. P., Apparent Cooperative Assembly of the Bacterial Cell Division Protein FtsZ Demonstrated by Isothermal Titration Calorimetry. *J. Biol. Chem.* **2003**, *278*, 13784-13788
26. Chen, Y.; Bjornson, K.; Redick, S. D.; Erickson, H. P., A rapid fluorescence assay for FtsZ assembly indicates cooperative assembly with a dimer nucleus. *Biophys. J.* **2005**, *88*, 505-514
27. Romberg, L.; Simon, M.; Erickson, H. P., Polymerization of FtsZ, a bacterial homolog of tubulin. Is assembly cooperative? *J. Biol. Chem.* **2001**, *276*, 11743-11753
28. Huecas, S.; Andreu, J. M., Polymerization of nucleotide-free, GDP- and GTP-bound cell division protein FtsZ: GDP makes the difference. *FEBS Lett.* **2004**, *569*, 43-48
29. Romberg, L.; Mitchison, T. J., Rate-Limiting Guanosine 5'-Triphosphate Hydrolysis during Nucleotide Turnover by FtsZ, a Prokaryotic Tubulin Homologue Involved in Bacterial Cell Division. *Biochemistry* **2004**, *43*, 282-288
30. Lu, C.; Reedy, M.; Erickson, H. P., Straight and curved conformations of FtsZ are regulated by GTP hydrolysis. *J. Bacteriol.* **2000**, *182*, 164-170
31. Mukherjee, A.; Saez, C.; Lutkenhaus, J., Assembly of an FtsZ mutant deficient in GTPase activity has implications for FtsZ assembly and the role of the Z ring in cell division. *J. Bacteriol.* **2001**, *183*, 7190-7197
32. Oliva, M. A.; Trambaiolo, D.; Loewe, J., Structural Insights into the Conformational Variability of FtsZ. *J. Mol. Biol.* **2007**, *373*, 1229-1242
33. Osawa, M.; Anderson, D. E.; Erickson, H. P., Reconstitution of Contractile FtsZ Rings in Liposomes. *Science* **2008**, *320*, 792-794
34. Erickson Harold, P.; Anderson David, E.; Osawa, M., FtsZ in bacterial cytokinesis: cytoskeleton and force generator all in one. *Microbiol Molecul. Biol. Rev.* **2010**, *74*, 504-28
35. Yanagisawa, M.; Imai, M.; Taniguchi, T., Shape Deformation of Ternary Vesicles Coupled with Phase Separation. *Phys. Rev. Lett.* **2008**, *100*, 148102/1-148102/4
36. Zhu, T. F.; Szostak, J. W., Coupled Growth and Division of Model protocell membranes. *J. Am. Chem. Soc.* **2009**, *131*, 5705-5713
37. de Boer, P. A. J.; Crossley, R. E.; Rothfield, L. I., A division inhibitor and a topological specificity factor coded for by the minicell locus determine proper placement of the division septum in *E. coli*. *Cell* **1989**, *56*, 641-649

38. De Boer, P. A. J.; Crossley, R. E.; Rothfield, L. I., Roles of MinC and MinD in the site-specific septation block mediated by the MinCDE system of Escherichia coli. *J. Bacteriol.* **1992**, *174*, 63-70
39. Edwards, D. H.; Errington, J., The Bacillus subtilis DivIVA protein targets to the division septum and controls the site specificity of cell division. *Mol Microbiol.* **1997**, *24*, 905-15
40. Marston, A. L.; Thomaides, H. B.; Edwards, D. H.; Sharpe, M. E.; Errington, J., Polar localization of the MinD protein of Bacillus subtilis and its role in selection of the mid-cell division site. *Genes Dev.* **1998**, *12*, 3419-30
41. Marston, A. L.; Errington, J., Selection of the midcell division site in Bacillus subtilis through MinD-dependent polar localization and activation of MinC. *Mol Microbiol.* **1999**, *33*, 84-96
42. Bernhardt, T. G.; de Boer, P. A. J., SlmA, a Nucleoid-Associated, FtsZ Binding Protein Required for Blocking Septal Ring Assembly over Chromosomes in E. coli. *Molecular Cell* **2005**, *18*, 555-564
43. Tonthat, N. K.; Milam, S. L.; Chinnam, N.; Whitfill, T.; Margolin, W.; Schumacher, M. A., SlmA forms a higher-order structure on DNA that inhibits cytokinetic Z-ring formation over the nucleoid. *Proc. Natl. Acad. Sci. U. S. A.* **2013**, *110*, 10586-10591
44. Tonthat, N. K.; Arold, S. T.; Pickering, B. F.; Van Dyke, M. W.; Liang, S.; Lu, Y.; Beuria, T. K.; Margolin, W.; Schumacher, M. A., Molecular mechanism by which the nucleoid occlusion factor, SlmA, keeps cytokinesis in check. *The EMBO Journal* **2011**, *30*, 154-164
45. Cho, H.; McManus, H. R.; Dove, S. L.; Bernhardt, T. G., Nucleoid occlusion factor SlmA is a DNA-activated FtsZ polymerization antagonist. *Proc. Natl. Acad. Sci. U. S. A.* **2011**, *108*, 3773-3778
46. Wu, L. J.; Errington, J., Coordination of cell division and chromosome segregation by a nucleoid occlusion protein in Bacillus subtilis. *Cell.* **2004**, *117*, 917-25
47. Wu, L. J.; Errington, J., Nucleoid occlusion and bacterial cell division. *Nat. Rev. Microbiol.* **2011**, *10*, 8-12
48. Monahan, L. G.; Liew, A. T. F.; Bottomley, A. L.; Harry, E. J., Division site positioning in bacteria: one size does not fit all. *Front. Microbiol.* **2014**, *5*,
49. Rodrigues, C. D. A.; Harry, E. J., The Min System and Nucleoid Occlusion Are Not Required for Identifying the Division Site in Bacillus subtilis but Ensure Its Efficient Utilization. *PLoS Genet* **2012**, *8*, e1002561

50. Moriya, S.; Rashid, R. A.; Rodrigues, C. D. A.; Harry, E. J., Influence of the nucleoid and the early stages of DNA replication on positioning the division site in *Bacillus subtilis*. *Mol. Microbiol.* **2010**, *76*, 634-647
51. Awasthi, D.; Kumar, K.; Ojima, I., Therapeutic potential of FtsZ inhibition: a patent perspective. *Expert Opin. Ther. Pat.* **2011**, *21*, 657-679
52. Kumar, K.; Awasthi, D.; Berger, W. T.; Tonge, P. J.; Slayden, R. A.; Ojima, I., Discovery of anti-TB agents that target the cell-division protein FtsZ. *Future Med. Chem.* **2010**, *2*, 1305-1323
53. Beuria, T. K.; Singh, P.; Surolia, A.; Panda, D., Promoting assembly and bundling of FtsZ as a strategy to inhibit bacterial cell division: A new approach for developing novel antibacterial drugs. *Biochem. J.* **2009**, *423*, 61-69
54. White, E. L.; Suling, W. J.; Ross, L. J.; Seitz, L. E.; Reynolds, R. C., 2-Alkoxy-carbonylaminopyridines: inhibitors of *Mycobacterium tuberculosis* FtsZ. *J. Antimicrob. Chemother.* **2002**, *50*, 111-114
55. Reynolds, R. C.; Srivastava, S.; Ross, L. J.; Suling, W. J.; White, E. L., A new 2-carbamoyl pteridine that inhibits mycobacterial FtsZ. *Bioorg. Med. Chem. Lett.* **2004**, *14*, 3161-3164
56. Huang, Q.; Kirikae, F.; Kirikae, T.; Pepe, A.; Amin, A.; Respicio, L.; Slayden, R. A.; Tonge, P. J.; Ojima, I., Targeting FtsZ for Antituberculosis Drug Discovery: Noncytotoxic Taxanes as Novel Antituberculosis Agents. *J. Med. Chem.* **2006**, *49*, 463-466
57. Kumar, K.; Awasthi, D.; Lee, S.-Y.; Zanardi, I.; Ruzsicska, B.; Knudson, S.; Tonge, P. J.; Slayden, R. A.; Ojima, I., Novel Trisubstituted Benzimidazoles, Targeting *Mtb* FtsZ, as a New Class of Antitubercular Agents. *J. Med. Chem.* **2011**, *54*, 374-381
58. Laeppchen, T.; Hartog, A. F.; Pinas, V. A.; Koomen, G.-J.; Den Blaauwen, T., GTP Analogue Inhibits Polymerization and GTPase Activity of the Bacterial Protein FtsZ without Affecting Its Eukaryotic Homologue Tubulin. *Biochemistry* **2005**, *44*, 7879-7884
59. Paradis-Bleau, C.; Beaumont, M.; Sanschagrín, F.; Voyer, N.; Levesque, R. C., Parallel solid synthesis of inhibitors of the essential cell division FtsZ enzyme as a new potential class of antibacterials. *Bioorg. Med. Chem.* **2007**, *15*, 1330-1340
60. Parhi, A.; Kelley, C.; Kaul, M.; Pilch, D. S.; LaVoie, E. J., Antibacterial activity of substituted 5-methylbenzo[c]phenanthridinium derivatives. *Bioorg. Med. Chem. Lett.* **2012**, *22*, 7080-7083

61. Beuria, T. K.; Santra, M. K.; Panda, D., Sanguinarine Blocks Cytokinesis in Bacteria by Inhibiting FtsZ Assembly and Bundling. *Biochemistry* **2005**, *44*, 16584-16593
62. Mathew, B.; Ross, L.; Reynolds, R. C., A novel quinoline derivative that inhibits mycobacterial FtsZ. *Tuberculosis* **2013**, *93*, 398-400
63. Kelley, C.; Zhang, Y.; Parhi, A.; Kaul, M.; Pilch, D. S.; LaVoie, E. J., 3-Phenyl substituted 6,7-dimethoxyisoquinoline derivatives as FtsZ-targeting antibacterial agents. *Bioorg. Med. Chem.* **2012**, *20*, 7012-7029
64. Parhi, A.; Lu, S.; Kelley, C.; Kaul, M.; Pilch, D. S.; LaVoie, E. J., Antibacterial activity of substituted dibenzo[a,g]quinolizin-7-ium derivatives. *Bioorg. Med. Chem. Lett.* **2012**, *22*, 6962-6966
65. Haydon, D. J.; Stokes, N. R.; Ure, R.; Galbraith, G.; Bennett, J. M.; Brown, D. R.; Baker, P. J.; Barynin, V. V.; Rice, D. W.; Sedelnikova, S. E.; Heal, J. R.; Sheridan, J. M.; Aiwale, S. T.; Chauhan, P. K.; Srivastava, A.; Taneja, A.; Collins, I.; Errington, J.; Czaplowski, L. G., An Inhibitor of FtsZ with Potent and Selective Anti-Staphylococcal Activity. *Science* **2008**, *321*, 1673-1675
66. Haydon, D. J.; Bennett, J. M.; Brown, D.; Collins, I.; Galbraith, G.; Lancett, P.; Macdonald, R.; Stokes, N. R.; Chauhan, P. K.; Sutariya, J. K.; Nayal, N.; Srivastava, A.; Beanland, J.; Hall, R.; Henstock, V.; Noula, C.; Rockley, C.; Czaplowski, L., Creating an antibacterial with in vivo efficacy: synthesis and characterization of potent inhibitors of the bacterial cell division protein FtsZ with improved pharmaceutical properties. *J. Med. Chem.* **2010**, *53*, 3927-3936
67. Margalit, D. N.; Romberg, L.; Mets, R. B.; Hebert, A. M.; Mitchison, T. J.; Kirschner, M. W.; RayChaudhuri, D., Targeting cell division: Small-molecule inhibitors of FtsZ GTPase perturb cytokinetic ring assembly and induce bacterial lethality. [Erratum to document cited in CA141:271048]. *Proc. Natl. Acad. Sci. U. S. A.* **2004**, *101*, 13969
68. Plaza, A.; Keffer, J. L.; Bifulco, G.; Lloyd, J. R.; Bewley, C. A., Chrysopaentins A-H, antibacterial bisdiarylbutene macrocycles that inhibit the bacterial cell division protein FtsZ. *J. Am. Chem. Soc.* **2010**, *132*, 9069-9077
69. Mathew, B.; Srivastava, S.; Ross, L. J.; Suling, W. J.; White, E. L.; Woolhiser, L. K.; Lenaerts, A. J.; Reynolds, R. C., Novel pyridopyrazine and pyrimidothiazine derivatives as FtsZ inhibitors. *Bioorg. Med. Chem.* **2011**, *19*, 7120-7128

70. Erickson, H. P.; Taylor, D. W.; Taylor, K. A.; Bramhill, D., Bacterial cell division protein FtsZ assembles into protofilament sheets and minirings, structural homologs of tubulin polymers. *Proc. Natl. Acad. Sci. USA* **1996**, *93*, 519-23
71. Lowe, J.; Amos, L. A., Crystal structure of the bacterial cell-division protein FtsZ. *Nature* **1998**, *391*, 203-6
72. Lowe, J.; Amos, L. A., Tubulin-like protofilaments in Ca²⁺-induced FtsZ sheets. *Embo J.* **1999**, *18*, 2364-71
73. Lappchen, T.; Hartog Aloysius, F.; Pinas Victorine, A.; Koomen, G.-J.; den Blaauwen, T., GTP analogue inhibits polymerization and GTPase activity of the bacterial protein FtsZ without affecting its eukaryotic homologue tubulin. *Biochemistry* **2005**, *44*, 7879-84
74. Huang, Q.; Tonge Peter, J.; Slayden Richard, A.; Kirikae, T.; Ojima, I., FtsZ: a novel target for tuberculosis drug discovery. *Curr. Top. Med. Chem.* **2007**, *7*, 527-43
75. Georg, G. I.; Chen, T. T.; Ojima, I.; Wyas, D. M.; Editors, *Taxane Anticancer Agents: Basic Science and Current Status. ACS Symp. Ser.* 1995; Vol. 583, p 353.
76. Kingston, D. G. I.; Jagtap, P. G.; Yuan, H.; Samala, L., The chemistry of taxol and related taxoids. *Prog. Chem. Org. Nat. Prod.* **2002**, *84*, 53-225
77. Ojima, I.; Kuduk, S. D.; Chakravarty, S., Recent advances in the medicinal chemistry of taxoid anticancer agents. *Adv. Med. Chem.* **1999**, *4*, 69-124
78. Brooks, T. A.; Kennedy, D. R.; Gruol, D. J.; Ojima, I.; Baer, M. R.; Bernacki, R. J., Structure-activity analysis of taxane-based broad-spectrum multidrug resistance modulators. *Anticancer Res.* **2004**, *24*, 409-415
79. Brooks Tracy, A.; Minderman, H.; O'Loughlin Kieran, L.; Pera, P.; Ojima, I.; Baer Maria, R.; Bernacki Ralph, J.; Brooks, T., Taxane-based reversal agents modulate drug resistance mediated by P-glycoprotein, multidrug resistance protein, and breast cancer resistance protein. *Mol. Cancer Ther.* **2003**, *2*, 1195-205
80. Minderman, H.; Brooks, T. A.; O'Loughlin, K. L.; Ojima, I.; Bernacki, R. J.; Baer, M. R., Broad-spectrum modulation of ATP-binding cassette transport proteins by the taxane derivatives ortataxel (IDN-5109, BAY 59-8862) and tRA96023. *Cancer Chemother. Pharmacol.* **2004**, *53*, 363-369
81. Ojima, I.; Borella, C. P.; Wu, X.; Bounaud, P.-Y.; Oderda, C. F.; Sturm, M.; Miller, M. L.; Chakravarty, S.; Chen, J.; Huang, Q.; Pera, P.; Brooks, T. A.; Baer, M. R.; Bernacki, R. J.,

- Design, Synthesis and Structure-Activity Relationships of Novel Taxane-Based Multidrug Resistance Reversal Agents. *J. Med. Chem.* **2005**, *48*, 2218-2228
82. Ojima, I.; Bounaud, P.-Y.; Bernacki, R. J., New weapons in the fight against cancer. *Chemtech* **1998**, *28*, 31-36
83. Ojima, I.; Bounaud, P.-Y.; Bernacki, R. J., Designing taxanes to treat multidrug-resistant tumors. *Mod. Drug Discovery* **1999**, *2*, 45,47-48,51-52
84. Ojima, I.; Bounaud, P.-Y.; Oderda, C. F., Recent strategies for the treatment of multi-drug resistance in cancer cells. *Expert Opin. Ther. Pat.* **1998**, *8*, 1587-1598
85. Appendino, G.; Danieli, B.; Jakupovic, J.; Belloro, E.; Scambia, G.; Bombardelli, E., The chemistry and occurrence of taxane derivatives. XXX. Synthesis and evaluation of C-seco paclitaxel analogs. *Tetrahedron Lett.* **1997**, *38*, 4273-4276
86. Taraboletti, G.; Micheletti, G.; Rieppi, M.; Poli, M.; Turatto, M.; Rossi, C.; Borsotti, P.; Roccabianca, P.; Scanziani, E.; Nicoletti, M. I.; Bombardelli, E.; Morazzoni, P.; Riva, A.; Giavazzi, R., Antiangiogenic and antitumor activity of IDN 5390, a new taxane derivative. *Clin. Cancer Res.* **2002**, *8*, 1182-1188

Chapter 2

1. Vollmer, W., The prokaryotic cytoskeleton: A putative target for inhibitors and antibiotics? *Appl. Microbiol. Biotechnol.* **2006**, *73*, 37-47
2. Margalit, D. N.; Romberg, L.; Mets, R. B.; Hebert, A. M.; Mitchison, T. J.; Kirschner, M. W.; RayChaudhuri, D., Targeting cell division: Small-molecule inhibitors of FtsZ GTPase perturb cytokinetic ring assembly and induce bacterial lethality. *Proc. Natl. Acad. Sci. U. S. A.* **2004**, *101*, 11821-11826
3. Ben-Yehuda, S.; Losick, R., Asymmetric cell division in *B. subtilis* involves a spiral-like intermediate of the cytokinetic protein FtsZ. *Cell* **2002**, *109*, 257-266
4. Goehring, N. W.; Beckwith, J., Diverse paths to midcell: assembly of the bacterial cell division machinery. *Curr. Biol.* **2005**, *15*, R514-R526
5. Leung, A. K. W.; White, E. L.; Ross, L. J.; Reynolds, R. C.; DeVito, J. A.; Borhani, D. W., Structure of *Mycobacterium tuberculosis* FtsZ Reveals Unexpected, G Protein-like Conformational Switches. *J. Mol. Biol.* **2004**, *342*, 953-970

6. Moller-Jensen, J.; Loewe, J., Increasing complexity of the bacterial cytoskeleton. *Curr. Opin. Cell Biol.* **2005**, *17*, 75-81
7. Thanedar, S.; Margolin, W., FtsZ Exhibits Rapid Movement and Oscillation Waves in Helix-like Patterns in Escherichia coli. *Curr. Biol.* **2004**, *14*, 1167-1173
8. de Boer, P.; Crossley, R.; Rothfield, L., The essential bacterial cell-division protein FtsZ is a GTPase. *Nature* **1992**, *359*, 254-6
9. RayChaudhuri, D.; Park, J. T., Escherichia coli cell-division gene ftsZ encodes a novel GTP-binding protein. *Nature* **1992**, *359*, 251-4
10. Adams, D. W.; Errington, J., Bacterial cell division: assembly, maintenance and disassembly of the Z ring. *Nat. Rev. Microbiol.* **2009**, *7*, 642-653
11. Erickson Harold, P.; Anderson David, E.; Osawa, M., FtsZ in bacterial cytokinesis: cytoskeleton and force generator all in one. *Microbiol. Mol. Biol. Rev.* **2010**, *74*, 504-28
12. Errington, J.; Daniel, R. A.; Scheffers, D.-J., Cytokinesis in bacteria. *Microbiol. Mol. Biol. Rev.* **2003**, *67*, 52-65
13. Huang, Q.; Kirikae, F.; Kirikae, T.; Pepe, A.; Amin, A.; Respicio, L.; Slayden, R. A.; Tonge, P. J.; Ojima, I., Targeting FtsZ for Antituberculosis Drug Discovery: Noncytotoxic Taxanes as Novel Antituberculosis Agents. *J. Med. Chem.* **2006**, *49*, 463-466
14. Kumar, K.; Awasthi, D.; Berger, W. T.; Tonge, P. J.; Slayden, R. A.; Ojima, I., Discovery of anti-TB agents that target the cell-division protein FtsZ. *Future Med. Chem.* **2010**, *2*, 1305-1323
15. Respicio, L.; Nair, P. A.; Huang, Q.; Burcu, A. B.; Tracz, S.; Truglio, J. J.; Kisker, C.; Raleigh, D. P.; Ojima, I.; Knudson, D. L.; Tonge, P. J.; Slayden, R. A., Characterizing Septum Inhibition in Mycobacterium tuberculosis for Novel Drug Discovery. *Tuberculosis* **2008**, *88*, 420-429
16. Slayden, R. A.; Knudson, D. L.; Belisle, J. T., Identification of cell cycle regulators in Mycobacterium tuberculosis by inhibition of septum formation and global transcriptional analysis. *Microbiology* **2006**, *152*, 1789-1797
17. Huang, Q.; Tonge Peter, J.; Slayden Richard, A.; Kirikae, T.; Ojima, I., FtsZ: a novel target for tuberculosis drug discovery. *Curr. Top. Med. Chem.* **2007**, *7*, 527-43
18. Lock, R. L.; Harry, E. J., Cell-division inhibitors: new insights for future antibiotics. *Nat. Rev. Drug Discovery* **2008**, *7*, 324-338

19. Margolin, W., Themes and variations in prokaryotic cell division. *FEMS Microbiol. Rev.* **2000**, *24*, 531-548
20. Rothfield, L.; Justice, S.; Garcia-Lara, J., Bacterial cell division. *Annu. Rev. Genet.* **1999**, *33*, 423-448
21. Haydon, D. J.; Stokes, N. R.; Ure, R.; Galbraith, G.; Bennett, J. M.; Brown, D. R.; Baker, P. J.; Barynin, V. V.; Rice, D. W.; Sedelnikova, S. E.; Heal, J. R.; Sheridan, J. M.; Aiwale, S. T.; Chauhan, P. K.; Srivastava, A.; Taneja, A.; Collins, I.; Errington, J.; Czaplewski, L. G., An Inhibitor of FtsZ with Potent and Selective Anti-Staphylococcal Activity. *Science* **2008**, *321*, 1673-1675
22. Awasthi, D.; Kumar, K.; Ojima, I., Therapeutic potential of FtsZ inhibition: a patent perspective. *Expert Opin. Ther. Pat.* **2011**, *21*, 657-679
23. Beuria, T. K.; Singh, P.; Surolia, A.; Panda, D., Promoting assembly and bundling of FtsZ as a strategy to inhibit bacterial cell division: A new approach for developing novel antibacterial drugs. *Biochem. J.* **2009**, *423*, 61-69
24. White, E. L.; Suling, W. J.; Ross, L. J.; Seitz, L. E.; Reynolds, R. C., 2-Alkoxy-carbonylaminopyridines: inhibitors of Mycobacterium tuberculosis FtsZ. *J. Antimicrob. Chemother.* **2002**, *50*, 111-114
25. Reynolds, R. C.; Srivastava, S.; Ross, L. J.; Suling, W. J.; White, E. L., A new 2-carbamoyl pteridine that inhibits mycobacterial FtsZ. *Bioorg. Med. Chem. Lett.* **2004**, *14*, 3161-3164
26. Kumar, K.; Awasthi, D.; Lee, S.-Y.; Zanardi, I.; Ruzsicska, B.; Knudson, S.; Tonge, P. J.; Slayden, R. A.; Ojima, I., Novel Trisubstituted Benzimidazoles, Targeting Mtb FtsZ, as a New Class of Antitubercular Agents. *J. Med. Chem.* **2011**, *54*, 374-381
27. Laeppchen, T.; Hartog, A. F.; Pinas, V. A.; Koomen, G.-J.; Den Blaauwen, T., GTP Analogue Inhibits Polymerization and GTPase Activity of the Bacterial Protein FtsZ without Affecting Its Eukaryotic Homologue Tubulin. *Biochemistry* **2005**, *44*, 7879-7884
28. Paradis-Bleau, C.; Beaumont, M.; Sanschagrín, F.; Voyer, N.; Levesque, R. C., Parallel solid synthesis of inhibitors of the essential cell division FtsZ enzyme as a new potential class of antibacterials. *Bioorg. Med. Chem.* **2007**, *15*, 1330-1340
29. Parhi, A.; Kelley, C.; Kaul, M.; Pilch, D. S.; LaVoie, E. J., Antibacterial activity of substituted 5-methylbenzo[c]phenanthridinium derivatives. *Bioorg. Med. Chem. Lett.* **2012**, *22*, 7080-7083

30. Beuria, T. K.; Santra, M. K.; Panda, D., Sanguinarine Blocks Cytokinesis in Bacteria by Inhibiting FtsZ Assembly and Bundling. *Biochemistry* **2005**, *44*, 16584-16593
31. Mathew, B.; Ross, L.; Reynolds, R. C., A novel quinoline derivative that inhibits mycobacterial FtsZ. *Tuberculosis* **2013**, *93*, 398-400
32. Kelley, C.; Zhang, Y.; Parhi, A.; Kaul, M.; Pilch, D. S.; LaVoie, E. J., 3-Phenyl substituted 6,7-dimethoxyisoquinoline derivatives as FtsZ-targeting antibacterial agents. *Bioorg. Med. Chem.* **2012**, *20*, 7012-7029
33. Parhi, A.; Lu, S.; Kelley, C.; Kaul, M.; Pilch, D. S.; LaVoie, E. J., Antibacterial activity of substituted dibenzo[a,g]quinolizin-7-ium derivatives. *Bioorg. Med. Chem. Lett.* **2012**, *22*, 6962-6966
34. Haydon, D. J.; Bennett, J. M.; Brown, D.; Collins, I.; Galbraith, G.; Lancett, P.; Macdonald, R.; Stokes, N. R.; Chauhan, P. K.; Sutariya, J. K.; Nayal, N.; Srivastava, A.; Beanland, J.; Hall, R.; Henstock, V.; Noula, C.; Rockley, C.; Czaplowski, L., Creating an antibacterial with in vivo efficacy: synthesis and characterization of potent inhibitors of the bacterial cell division protein FtsZ with improved pharmaceutical properties. *J. Med. Chem.* **2010**, *53*, 3927-3936
35. Margalit, D. N.; Romberg, L.; Mets, R. B.; Hebert, A. M.; Mitchison, T. J.; Kirschner, M. W.; RayChaudhuri, D., Targeting cell division: Small-molecule inhibitors of FtsZ GTPase perturb cytokinetic ring assembly and induce bacterial lethality. [Erratum to document cited in CA141:271048]. *Proc. Natl. Acad. Sci. U. S. A.* **2004**, *101*, 13969
36. Plaza, A.; Keffer, J. L.; Bifulco, G.; Lloyd, J. R.; Bewley, C. A., Chrysopaentins A-H, antibacterial bisdiarylbutene macrocycles that inhibit the bacterial cell division protein FtsZ. *J. Am. Chem. Soc.* **2010**, *132*, 9069-9077
37. Mathew, B.; Srivastava, S.; Ross, L. J.; Suling, W. J.; White, E. L.; Woolhiser, L. K.; Lenaerts, A. J.; Reynolds, R. C., Novel pyridopyrazine and pyrimidothiazine derivatives as FtsZ inhibitors. *Bioorg. Med. Chem.* **2011**, *19*, 7120-7128
38. Sarcina, M.; Mullineaux, C. W., Effects of tubulin assembly inhibitors on cell division in prokaryotes in vivo. *FEMS Microbiol. Lett.* **2000**, *191*, 25-29
39. Slayden, R. A.; Knudson, D. L.; Belisle, J. T., Identification of cell cycle regulators in *Mycobacterium tuberculosis* by inhibition of septum formation and global transcriptional analysis. *Microbiology* **2006**, *152*, 1789-1797

40. Awasthi, D.; Kumar, K.; Knudson, S. E.; Slayden, R. A.; Ojima, I., SAR Studies on Trisubstituted Benzimidazoles as Inhibitors of Mtb FtsZ for the Development of Novel Antitubercular Agents. *J. Med. Chem.* **2013**, *56*, 9756-9770
41. Knudson, S. E.; Kumar, K.; Awasthi, D.; Ojima, I.; Slayden, R. A., Potency of benzimidazoles and in vitro activity–efficacy relationship against Mycobacteria tuberculosis. *Tuberculosis* **2014**, *94*, 271-276
42. Knudson, S. E.; Awasthi, D.; Kumar, K.; Ojima, I.; Slayden, R. A., A Trisubstituted benzimidazole cell division inhibitor with efficacy against Mycobacteria tuberculosis. *PLoS ONE* **2014**, *9*, e93953 (2014)
43. Yoakim, C.; Ogilvie, W. W.; Cameron, D. R.; Chabot, C.; Guse, I.; Hache, B.; Naud, J.; O'Meara, J. A.; Plante, R.; Deziel, R., Î²-Lactam Derivatives as Inhibitors of Human Cytomegalovirus Protease. *J. Med. Chem.* **1998**, *41*, 2882-2891
44. Iranpoor, N.; Firouzabadi, H.; Nowrouzi, N.; Khalili, D., Selective mono- and di-N-alkylation of aromatic amines with alcohols and acylation of aromatic amines using Ph₃P/DDQ. *Tetrahedron* **2009**, *65*, 3893-3899

Chapter 3

1. Ben-Yehuda, S.; Losick, R., Asymmetric cell division in *B. subtilis* involves a spiral-like intermediate of the cytokinetic protein FtsZ. *Cell (Cambridge, MA, U. S.)* **2002**, *109*, 257-266
2. Goehring, N. W.; Beckwith, J., Diverse paths to midcell: assembly of the bacterial cell division machinery. *Curr. Biol.* **2005**, *15*, R514-R526
3. Leung, A. K. W.; White, E. L.; Ross, L. J.; Reynolds, R. C.; DeVito, J. A.; Borhani, D. W., Structure of Mycobacterium tuberculosis FtsZ Reveals Unexpected, G Protein-like Conformational Switches. *J. Mol. Biol.* **2004**, *342*, 953-970
4. Moller-Jensen, J.; Loewe, J., Increasing complexity of the bacterial cytoskeleton. *Curr. Opin. Cell Biol.* **2005**, *17*, 75-81
5. Thanedar, S.; Margolin, W., FtsZ Exhibits Rapid Movement and Oscillation Waves in Helix-like Patterns in *Escherichia coli*. *Curr. Biol.* **2004**, *14*, 1167-1173
6. Pelham, R. J.; Chang, F., Actin dynamics in the contractile ring during cytokinesis in fission yeast. *Nature* **2002**, *419*, 82-86

7. Li, Y.; Hsin, J.; Zhao, L.; Cheng, Y.; Shang, W.; Huang, K. C.; Wang, H.-W.; Ye, S., FtsZ Protofilaments Use a Hinge-Opening Mechanism for Constrictive Force Generation. *Science* **2013**, *341*, 392-395
8. Erickson, H. P.; Taylor, D. W.; Taylor, K. A.; Bramhill, D., Bacterial cell division protein FtsZ assembles into protofilament sheets and minirings, structural homologs of tubulin polymers. *Proc. Natl. Acad. Sci. U. S. A.* **1996**, *93*, 519-23
9. Awasthi, D.; Kumar, K.; Ojima, I., Therapeutic potential of FtsZ inhibition: a patent perspective. *Expert Opin. Ther. Pat.* **2011**, *21*, 657-679
10. Kumar, K.; Awasthi, D.; Berger, W. T.; Tonge, P. J.; Slayden, R. A.; Ojima, I., Discovery of anti-TB agents that target the cell-division protein FtsZ. *Future Med. Chem.* **2010**, *2*, 1305-1323
11. Beuria, T. K.; Singh, P.; Surolia, A.; Panda, D., Promoting assembly and bundling of FtsZ as a strategy to inhibit bacterial cell division: A new approach for developing novel antibacterial drugs. *Biochem. J.* **2009**, *423*, 61-69
12. White, E. L.; Suling, W. J.; Ross, L. J.; Seitz, L. E.; Reynolds, R. C., 2-Alkoxy-carbonylaminopyridines: inhibitors of Mycobacterium tuberculosis FtsZ. *J. Antimicrob. Chemother.* **2002**, *50*, 111-114
13. Reynolds, R. C.; Srivastava, S.; Ross, L. J.; Suling, W. J.; White, E. L., A new 2-carbamoyl pteridine that inhibits mycobacterial FtsZ. *Bioorg. Med. Chem. Lett.* **2004**, *14*, 3161-3164
14. Huang, Q.; Kirikae, F.; Kirikae, T.; Pepe, A.; Amin, A.; Respicio, L.; Slayden, R. A.; Tonge, P. J.; Ojima, I., Targeting FtsZ for Antituberculosis Drug Discovery: Noncytotoxic Taxanes as Novel Antituberculosis Agents. *J. Med. Chem.* **2006**, *49*, 463-466
15. Kumar, K.; Awasthi, D.; Lee, S.-Y.; Zanardi, I.; Ruzsicska, B.; Knudson, S.; Tonge, P. J.; Slayden, R. A.; Ojima, I., Novel Trisubstituted Benzimidazoles, Targeting Mtb FtsZ, as a New Class of Antitubercular Agents. *J. Med. Chem.* **2011**, *54*, 374-381
16. Awasthi, D.; Kumar, K.; Knudson, S. E.; Slayden, R. A.; Ojima, I., SAR Studies on Trisubstituted Benzimidazoles as Inhibitors of Mtb FtsZ for the Development of Novel Antitubercular Agents. *J. Med. Chem.* **2013**, *56*, 9756-9770
17. Park, B.; Awasthi, D.; Chowdhury, S. R.; Melief, E. H.; Kumar, K.; Knudson, S. E.; Slayden, R. A.; Ojima, I., Design, synthesis and evaluation of novel 2,5,6-trisubstituted benzimidazoles targeting FtsZ as antitubercular agents. *Bioorg. Med. Chem.* **2014**, *22*, 2602-2612

18. Laeppchen, T.; Hartog, A. F.; Pinas, V. A.; Koomen, G.-J.; Den Blaauwen, T., GTP Analogue Inhibits Polymerization and GTPase Activity of the Bacterial Protein FtsZ without Affecting Its Eukaryotic Homologue Tubulin. *Biochemistry* **2005**, *44*, 7879-7884
19. Paradis-Bleau, C.; Beaumont, M.; Sanschagrín, F.; Voyer, N.; Levesque, R. C., Parallel solid synthesis of inhibitors of the essential cell division FtsZ enzyme as a new potential class of antibacterials. *Bioorg. Med. Chem.* **2007**, *15*, 1330-1340
20. Parhi, A.; Kelley, C.; Kaul, M.; Pilch, D. S.; LaVoie, E. J., Antibacterial activity of substituted 5-methylbenzo[c]phenanthridinium derivatives. *Bioorg. Med. Chem. Lett.* **2012**, *22*, 7080-7083
21. Beuria, T. K.; Santra, M. K.; Panda, D., Sanguinarine Blocks Cytokinesis in Bacteria by Inhibiting FtsZ Assembly and Bundling. *Biochemistry* **2005**, *44*, 16584-16593
22. Mathew, B.; Ross, L.; Reynolds, R. C., A novel quinoline derivative that inhibits mycobacterial FtsZ. *Tuberculosis* **2013**, *93*, 398-400
23. Kelley, C.; Zhang, Y.; Parhi, A.; Kaul, M.; Pilch, D. S.; LaVoie, E. J., 3-Phenyl substituted 6,7-dimethoxyisoquinoline derivatives as FtsZ-targeting antibacterial agents. *Bioorg. Med. Chem.* **2012**, *20*, 7012-7029
24. Parhi, A.; Lu, S.; Kelley, C.; Kaul, M.; Pilch, D. S.; LaVoie, E. J., Antibacterial activity of substituted dibenzo[a,g]quinolizin-7-ium derivatives. *Bioorg. Med. Chem. Lett.* **2012**, *22*, 6962-6966
25. Haydon, D. J.; Stokes, N. R.; Ure, R.; Galbraith, G.; Bennett, J. M.; Brown, D. R.; Baker, P. J.; Barynin, V. V.; Rice, D. W.; Sedelnikova, S. E.; Heal, J. R.; Sheridan, J. M.; Aiwale, S. T.; Chauhan, P. K.; Srivastava, A.; Taneja, A.; Collins, I.; Errington, J.; Czaplewski, L. G., An Inhibitor of FtsZ with Potent and Selective Anti-Staphylococcal Activity. *Science* **2008**, *321*, 1673-1675
26. Haydon, D. J.; Bennett, J. M.; Brown, D.; Collins, I.; Galbraith, G.; Lancett, P.; Macdonald, R.; Stokes, N. R.; Chauhan, P. K.; Sutariya, J. K.; Nayal, N.; Srivastava, A.; Beanland, J.; Hall, R.; Henstock, V.; Noula, C.; Rockley, C.; Czaplewski, L., Creating an antibacterial with in vivo efficacy: synthesis and characterization of potent inhibitors of the bacterial cell division protein FtsZ with improved pharmaceutical properties. *J. Med. Chem.* **2010**, *53*, 3927-3936

27. Margalit, D. N.; Romberg, L.; Mets, R. B.; Hebert, A. M.; Mitchison, T. J.; Kirschner, M. W.; RayChaudhuri, D., Targeting cell division: Small-molecule inhibitors of FtsZ GTPase perturb cytokinetic ring assembly and induce bacterial lethality. [Erratum to document cited in CA141:271048]. *Proc. Natl. Acad. Sci. U. S. A.* **2004**, *101*, 13969
28. Plaza, A.; Keffer, J. L.; Bifulco, G.; Lloyd, J. R.; Bewley, C. A., Chrysopaentins A-H, antibacterial bisdiarylbutene macrocycles that inhibit the bacterial cell division protein FtsZ. *J. Am. Chem. Soc.* **2010**, *132*, 9069-9077
29. Mathew, B.; Srivastava, S.; Ross, L. J.; Suling, W. J.; White, E. L.; Woolhiser, L. K.; Lenaerts, A. J.; Reynolds, R. C., Novel pyridopyrazine and pyrimidothiazine derivatives as FtsZ inhibitors. *Bioorg. Med. Chem.* **2011**, *19*, 7120-7128
30. White, E. L.; Ross, L. J.; Reynolds, R. C.; Seitz, L. E.; Moore, G. D.; Borhani, D. W., Slow Polymerization of *Mycobacterium tuberculosis* FtsZ. *J. Bacteriol.* **2000**, *182*, 4028 -4034
31. Geladopoulos, T. P.; Sotiroudis, T. G.; Evangelopoulos, A. E., A malachite green colorimetric assay for protein phosphatase activity. *Anal. Biochem.* **1991**, *192*, 112–116
32. Knudson, S. E.; Awasthi, D.; Kumar, K.; Ojima, I.; Slayden, R. A., A Trisubstituted benzimidazole cell division inhibitor with efficacy against *Mycobacteria tuberculosis*. *PLoS ONE* **2014**, *9*, e93953 (2014)
33. Knudson, S. E.; Kumar, K.; Awasthi, D.; Ojima, I.; Slayden, R. A., Potency of benzimidazoles and in vitro activity–efficacy relationship against *Mycobacteria tuberculosis*. *Tuberculosis* **2014**, *94*, 271-276

Chapter 4

1. Gould, I. M.; David, M. Z.; Esposito, S.; Garau, J.; Lina, G.; Mazzei, T.; Peters, G., New insights into meticillin-resistant *Staphylococcus aureus* (MRSA) pathogenesis, treatment and resistance. *Int. J. Antimicrob. Agents* **2012**, *39*, 96-104
2. Wang, J.-L.; Hsueh, P.-R., Therapeutic options for infections due to vancomycin-resistant enterococci. *Expert Opin. Pharmacother.* **2009**, *10*, 785-796
3. McLendon, M. K.; Apicella, M. A.; Allen, L.-A. H., *Francisella tularensis*: taxonomy, genetics, and immunopathogenesis of a potential agent of biowarfare. *Annu. Rev. Microbiol.* **2006**, *60*, 167-185

4. Feodorova, V. A.; Corbel, M. J., Prospects for new plague vaccines. *Expert Rev. Vaccines* **2009**, *8*, 1721-1738
5. Oyston, P. C. F.; Sjoestedt, A.; Titball, R. W., Tularaemia: bioterrorism defence renews interest in *Francisella tularensis*. *Nature Reviews Microbiology* **2004**, *2*, 967-978
6. Ryan, K. J.; Ray, C. G., *Sherris Medical Microbiology: An Introduction to Infectious Diseases*. McGraw Hill: 2004; p 488-490.
7. Evans, M. E.; Gregory, D. W.; Schaffner, W.; McGee, Z. A. *Tularemia: a 30-year experience with 88 cases*; United States FIELD Citation:, 1985; pp 251-69.
8. Dennis, D. T.; Inglesby, T. V.; Henderson, D. A.; Bartlett, J. G.; Ascher, M. S.; Eitzen, E.; Fine, A. D.; Friedlander, A. M.; Hauer, J.; Layton, M.; Lillibridge, S. R.; McDade, J. E.; Osterholm, M. T.; O'Toole, T.; Parker, G.; Perl, T. M.; Russell, P. K.; Tonat, K., Tularemia as a biological weapon: medical and public health management. *Jama* **2001**, *285*, 2763-73
9. Larsson, P.; Oyston, P. C. F.; Chain, P.; Chu, M. C.; Duffield, M.; Fuxelius, H.-H.; Garcia, E.; Haelltorp, G.; Johansson, D.; Isherwood, K. E.; Karp, P. D.; Larsson, E.; Liu, Y.; Michell, S.; Prior, J.; Prior, R.; Malfatti, S.; Sjoestedt, A.; Svensson, K.; Thompson, N.; Vergez, L.; Wagg, J. K.; Wren, B. W.; Lindler, L. E.; Andersson, S. G. E.; Forsman, M.; Titball, R. W., The complete genome sequence of *Francisella tularensis*, the causative agent of tularemia. *Nat. Genet.* **2004**, *37*, 153-159
10. Saslaw, S.; Eigelsbach, H. T.; Wilson, H. E.; Prior, J. A.; Carhart, S., Tularemia vaccine study. I. Intracutaneous challenge. *Arch Intern Med* **1961**, *107*, 689-701
11. Saslaw, S.; Eigelsbach, H. T.; Prior, J. A.; Wilson, H. E.; Carhart, S., Tularemia vaccine study. II. Respiratory challenge. *Arch Intern Med* **1961**, *107*, 702-14
12. Health Aspects of Chemical and Biological Weapons. *World Health Organization* **1970**,
13. Miller, J. R.; Waldrop, G. L., Discovery of novel antibacterials. *Expert Opin. Drug Discovery* **2010** *5*, 145-154
14. World Health Organization, Tuberculosis: Data and Country Profiles. Available at http://www.who.int/tb/publications/global_report/gtbr13_executive_summary.pdf?ua=1.
15. Enderlin, G.; Morales, L.; Jacobs, R. F.; Cross, J. T., Streptomycin and alternative agents for the treatment of tularemia: review of the literature. *Clinical infectious diseases an official publication of the Infectious Diseases Society of America* **1994**, *19*, 42-7

16. Ikaheimo, I.; Syrjala, H.; Karhukorpi, J.; Schildt, R.; Koskela, M., In vitro antibiotic susceptibility of *Francisella tularensis* isolated from humans and animals. *J. Antimicrob. Chemother.* **2000**, *46*, 287-290
17. Awasthi, D.; Kumar, K.; Knudson, S. E.; Slayden, R. A.; Ojima, I., SAR Studies on Trisubstituted Benzimidazoles as Inhibitors of Mtb FtsZ for the Development of Novel Antitubercular Agents. *J. Med. Chem.* **2013**, *56*, 9756-9770
18. Kumar, K.; Awasthi, D.; Lee, S.-Y.; Zanardi, I.; Ruzsicska, B.; Knudson, S.; Tonge, P. J.; Slayden, R. A.; Ojima, I., Novel Trisubstituted Benzimidazoles, Targeting Mtb FtsZ, as a New Class of Antitubercular Agents. *J. Med. Chem.* **2011**, *54*, 374-381
19. Kumar, K.; Awasthi, D.; Lee, S.-Y.; Cummings, J. E.; Knudson, S. E.; Slayden, R. A.; Ojima, I., Benzimidazole-based antibacterial agents against *Francisella tularensis*. *Bioorg. Med. Chem.* **2013**, *21*, 3318-26

Chapter 5

1. Awasthi, D.; Kumar, K.; Knudson, S. E.; Slayden, R. A.; Ojima, I., SAR Studies on Trisubstituted Benzimidazoles as Inhibitors of Mtb FtsZ for the Development of Novel Antitubercular Agents. *J. Med. Chem.* **2013**, *56*, 9756-9770
2. Kumar, K.; Awasthi, D.; Lee, S.-Y.; Zanardi, I.; Ruzsicska, B.; Knudson, S.; Tonge, P. J.; Slayden, R. A.; Ojima, I., Novel Trisubstituted Benzimidazoles, Targeting Mtb FtsZ, as a New Class of Antitubercular Agents. *J. Med. Chem.* **2011**, *54*, 374-381
3. Peng, J.; Zong, C.; Ye, M.; Chen, T.; Gao, D.; Wang, Y.; Chen, C., Direct transition-metal-free intramolecular C-O bond formation: synthesis of benzoxazole derivatives. *Org. Biomol. Chem.* **2011**, *9*, 1225-1230
4. Muller, C.; Bauer, A.; Bach, T., Light-driven enantioselective organocatalysis. *Angew Chem Int Ed Engl* **2009**, *48*, 6640-2
5. Wang, B.; Zhang, Y.; Li, P.; Wang, L., An efficient and practical synthesis of benzoxazoles from acyl chlorides and 2-aminophenols catalyzed by Lewis acid In(OTf)₃ under solvent-free reaction conditions. *Chin. J. Chem.* **2010**, *28*, 1697-1703
6. Kuroyanagi, J.-i.; Kanai, K.; Sugimoto, Y.; Horiuchi, T.; Achiwa, I.; Takeshita, H.; Kawakami, K., 1,3-Benzoxazole-4-carbonitrile as a novel antifungal scaffold of β -1,6-glucan synthesis inhibitors. *Bioorg. Med. Chem.* **2010**, *18*, 7593-7606

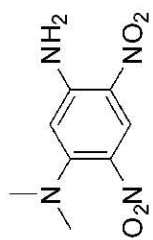
Chapter 6

1. Nogales, E.; Downing, K. H.; Amos, L. A.; Lowe, J., Tubulin and FtsZ form a distinct family of GTPases. *Nat. Struct. Biol.* **1998**, *5*, 451-458
2. Rossmann, M. G.; Moras, D.; Olsen, K. W., Chemical and biological evolution of a nucleotide-binding protein. *Nature* **1974**, *250*, 194-9
3. Leung, A. K. W.; White, E. L.; Ross, L. J.; Reynolds, R. C.; DeVito, J. A.; Borhani, D. W., Structure of Mycobacterium tuberculosis FtsZ Reveals Unexpected, G Protein-like Conformational Switches. *J. Mol. Biol.* **2004**, *342*, 953-970
4. de Pereda, J. M.; Leynadier, D.; Evangelio, J. A.; Chacon, P.; Andreu, J. M., Tubulin secondary structure analysis, limited proteolysis sites, and homology to FtsZ. *Biochemistry* **1996**, *35*, 14203-14215
5. Huang, Q.; Kirikae, F.; Kirikae, T.; Pepe, A.; Amin, A.; Respicio, L.; Slayden, R. A.; Tonge, P. J.; Ojima, I., Targeting FtsZ for Antituberculosis Drug Discovery: Noncytotoxic Taxanes as Novel Antituberculosis Agents. *J. Med. Chem.* **2006**, *49*, 463-466
6. Georg, G. I.; Chen, T. T.; Ojima, I.; Wyas, D. M.; Editors, *Taxane Anticancer Agents: Basic Science and Current Status. ACS Symp. Ser.* 1995; Vol. 583, p 353.
7. Kingston, D. G. I.; Jagtap, P. G.; Yuan, H.; Samala, L., The chemistry of taxol and related taxoids. *Prog. Chem. Org. Nat. Prod.* **2002**, *84*, 53-225
8. Ojima, I.; Kuduk, S. D.; Chakravarty, S., Recent advances in the medicinal chemistry of taxoid anticancer agents. *Adv. Med. Chem.* **1999**, *4*, 69-124
9. Brooks, T. A.; Kennedy, D. R.; Gruol, D. J.; Ojima, I.; Baer, M. R.; Bernacki, R. J., Structure-activity analysis of taxane-based broad-spectrum multidrug resistance modulators. *Anticancer Res.* **2004**, *24*, 409-415
10. Brooks Tracy, A.; Minderman, H.; O'Loughlin Kieran, L.; Pera, P.; Ojima, I.; Baer Maria, R.; Bernacki Ralph, J.; Brooks, T., Taxane-based reversal agents modulate drug resistance mediated by P-glycoprotein, multidrug resistance protein, and breast cancer resistance protein. *Mol. Cancer Ther.* **2003**, *2*, 1195-205
11. Minderman, H.; Brooks, T. A.; O'Loughlin, K. L.; Ojima, I.; Bernacki, R. J.; Baer, M. R., Broad-spectrum modulation of ATP-binding cassette transport proteins by the taxane derivatives ortataxel (IDN-5109, BAY 59-8862) and tRA96023. *Cancer Chemother. Pharmacol.* **2004**, *53*, 363-369

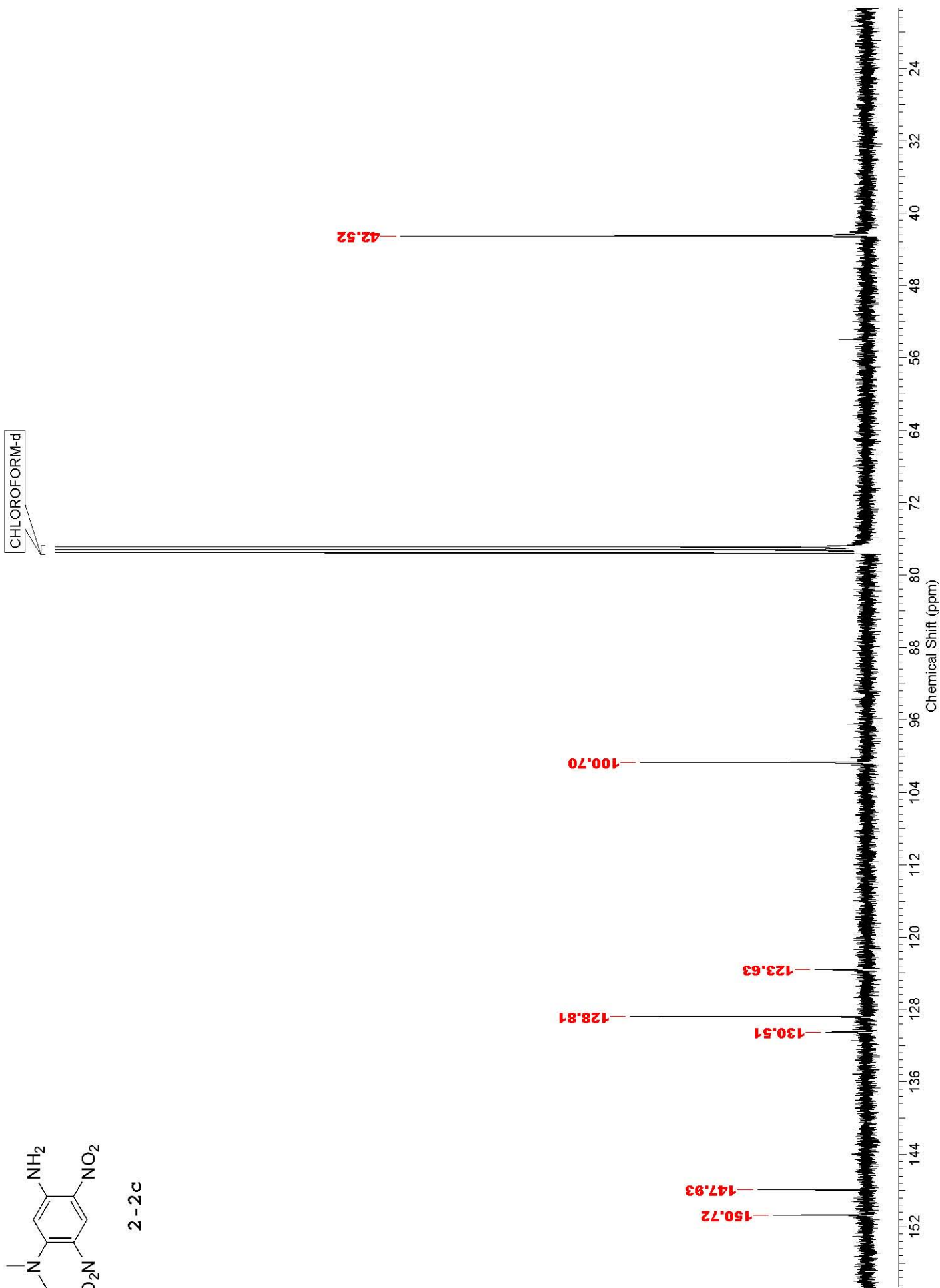
12. Ojima, I.; Borella, C. P.; Wu, X.; Bounaud, P.-Y.; Oderda, C. F.; Sturm, M.; Miller, M. L.; Chakravarty, S.; Chen, J.; Huang, Q.; Pera, P.; Brooks, T. A.; Baer, M. R.; Bernacki, R. J., Design, Synthesis and Structure-Activity Relationships of Novel Taxane-Based Multidrug Resistance Reversal Agents. *J. Med. Chem.* **2005**, *48*, 2218-2228
13. Ojima, I.; Bounaud, P.-Y.; Bernacki, R. J., New weapons in the fight against cancer. *Chemtech* **1998**, *28*, 31-36
14. Ojima, I.; Bounaud, P.-Y.; Bernacki, R. J., Designing taxanes to treat multidrug-resistant tumors. *Mod. Drug Discovery* **1999**, *2*, 45,47-48,51-52
15. Ojima, I.; Bounaud, P.-Y.; Oderda, C. F., Recent strategies for the treatment of multi-drug resistance in cancer cells. *Expert Opin. Ther. Pat.* **1998**, *8*, 1587-1598
16. Appendino, G.; Danieli, B.; Jakupovic, J.; Belloro, E.; Scambia, G.; Bombardelli, E., The chemistry and occurrence of taxane derivatives. XXX. Synthesis and evaluation of C-seco paclitaxel analogs. *Tetrahedron Lett.* **1997**, *38*, 4273-4276
17. Taraboletti, G.; Micheletti, G.; Rieppi, M.; Poli, M.; Turatto, M.; Rossi, C.; Borsotti, P.; Roccabianca, P.; Scanziani, E.; Nicoletti, M. I.; Bombardelli, E.; Morazzoni, P.; Riva, A.; Giavazzi, R., Antiangiogenic and antitumor activity of IDN 5390, a new taxane derivative. *Clin. Cancer Res.* **2002**, *8*, 1182-1188
18. Singh, D.; Bhattacharya, A.; Rai, A.; Dhaked, H. P. S.; Awasthi, D.; Ojima, I.; Panda, D., SB-RA-2001 inhibits bacterial proliferation by targeting FtsZ assembly. *Biochemistry* **2014**, *53*, 2979-2992
19. Ojima, I.; Kumar, K.; Awasthi, D.; Vineberg, J. G., Drug discovery targeting cell division proteins, microtubules and FtsZ. *Bioorg. Med. Chem.*,
20. Kumar, K.; Awasthi, D.; Lee, S.-Y.; Zanardi, I.; Ruzsicska, B.; Knudson, S.; Tonge, P. J.; Slayden, R. A.; Ojima, I., Novel Trisubstituted Benzimidazoles, Targeting Mtb FtsZ, as a New Class of Antitubercular Agents. *J. Med. Chem.* **2011**, *54*, 374-381

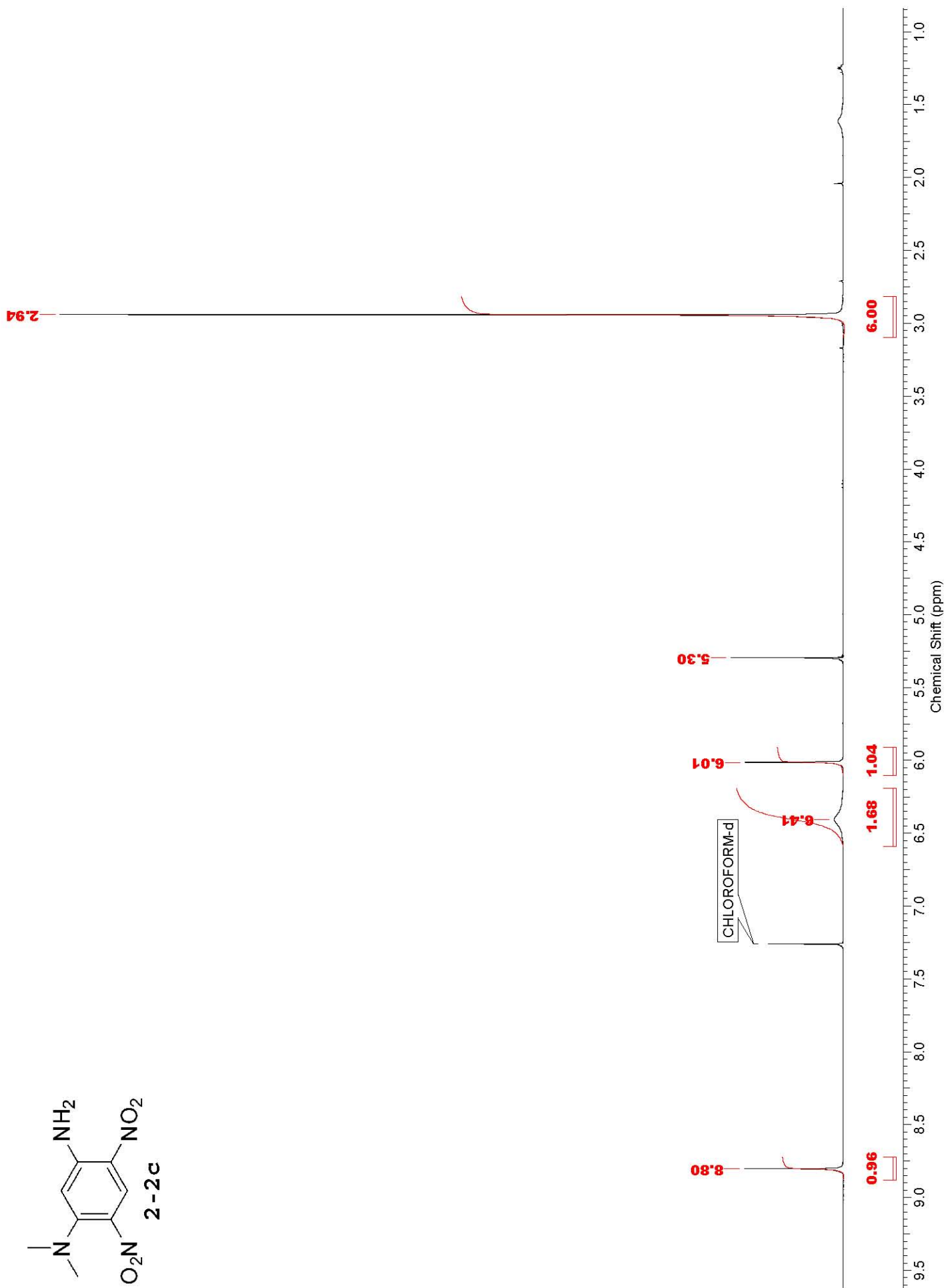
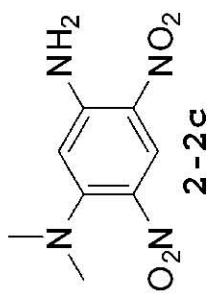
Appendices

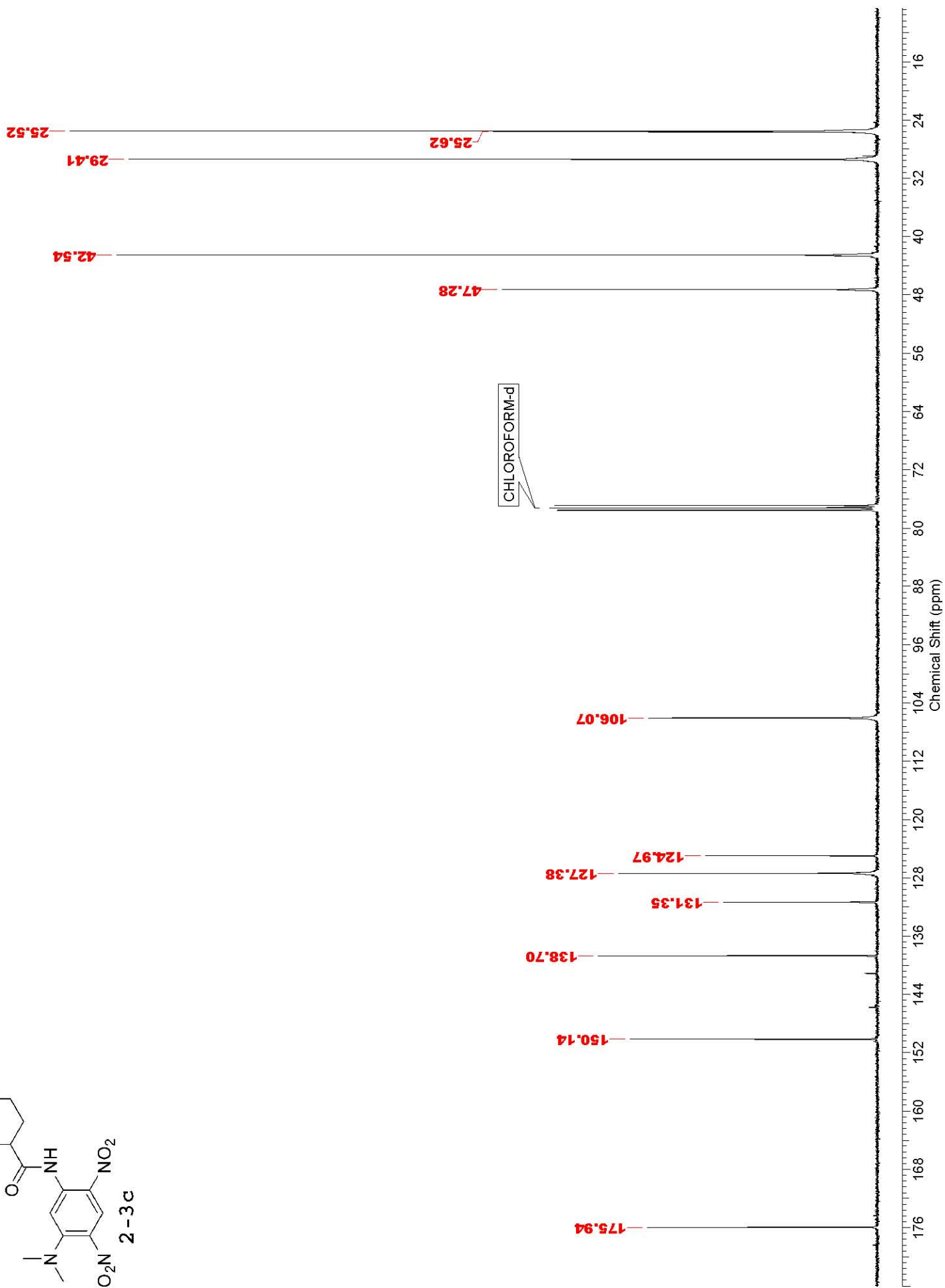
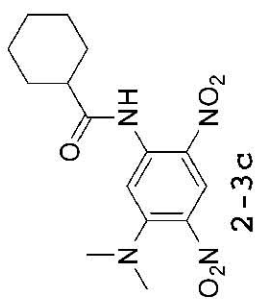
| | |
|-----------------------------|-----|
| A1. Appendix Chapter 2..... | 190 |
| A2. Appendix Chapter 3..... | 336 |
| A3. Appendix Chapter 4..... | 346 |
| A4. Appendix Chapter 5..... | 356 |
| A5. Appendix Chapter 6..... | 415 |

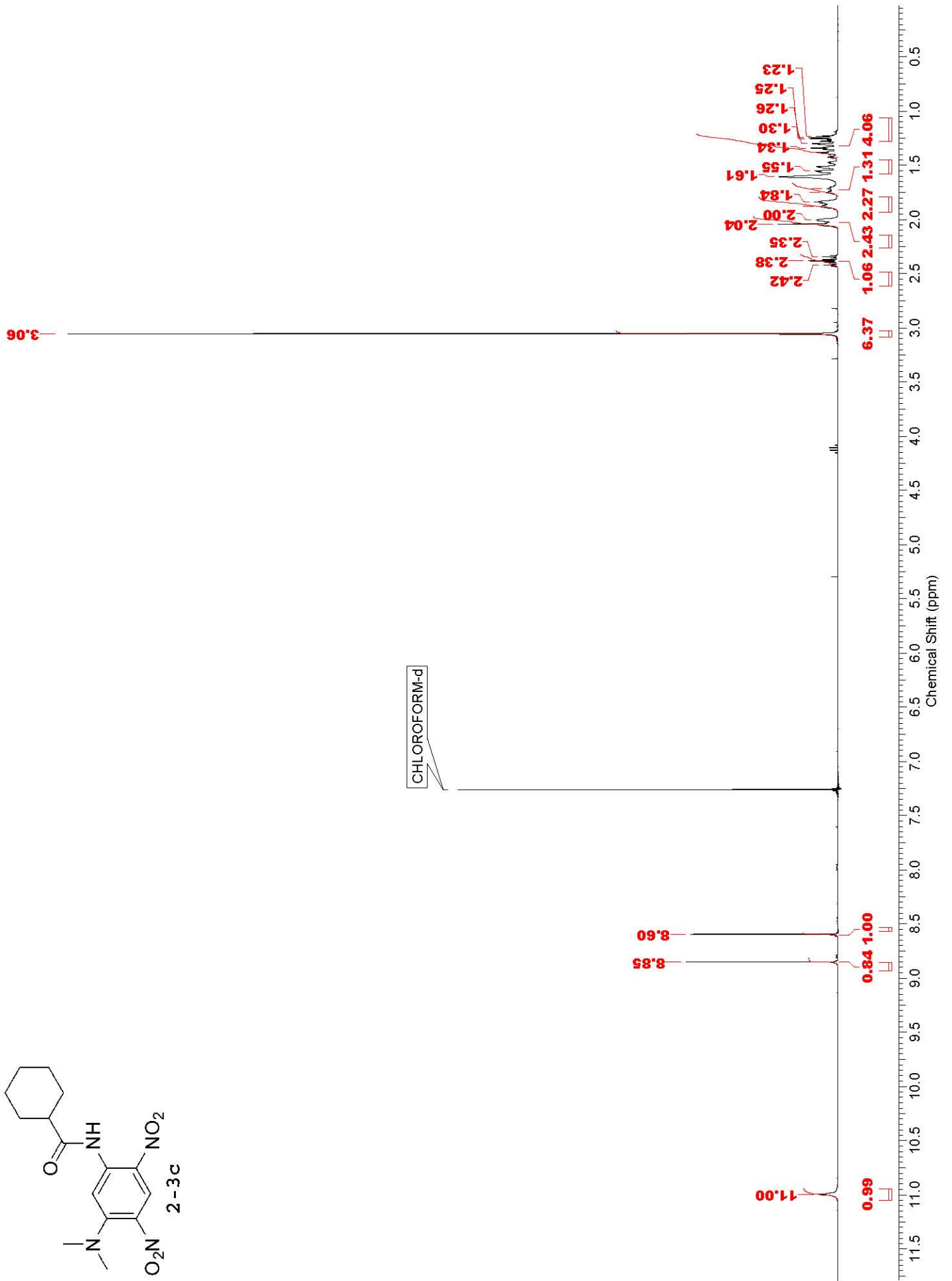
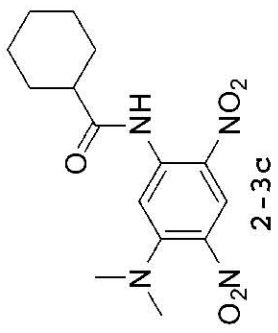


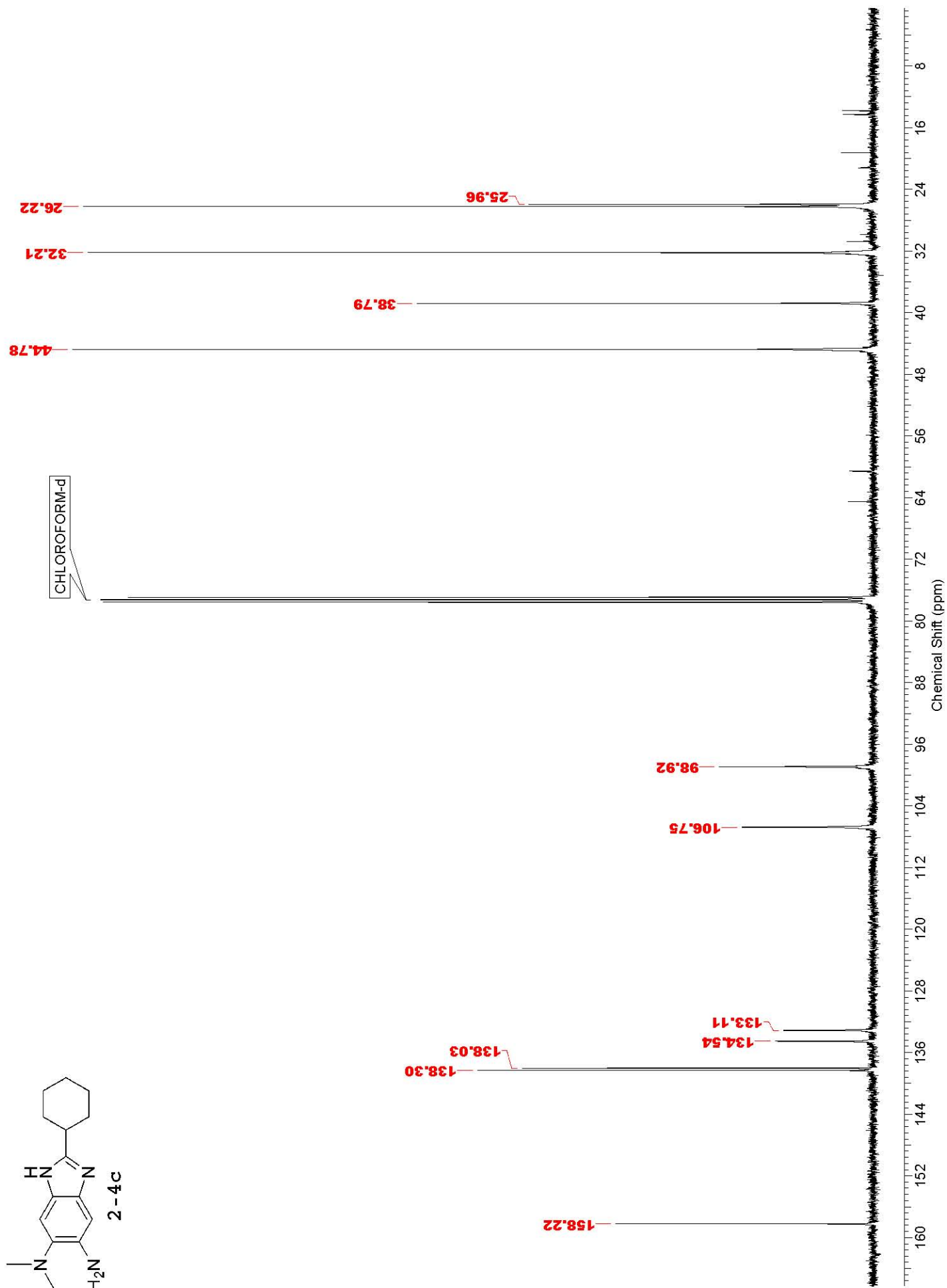
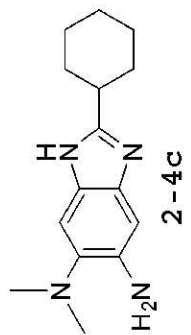
2-2c

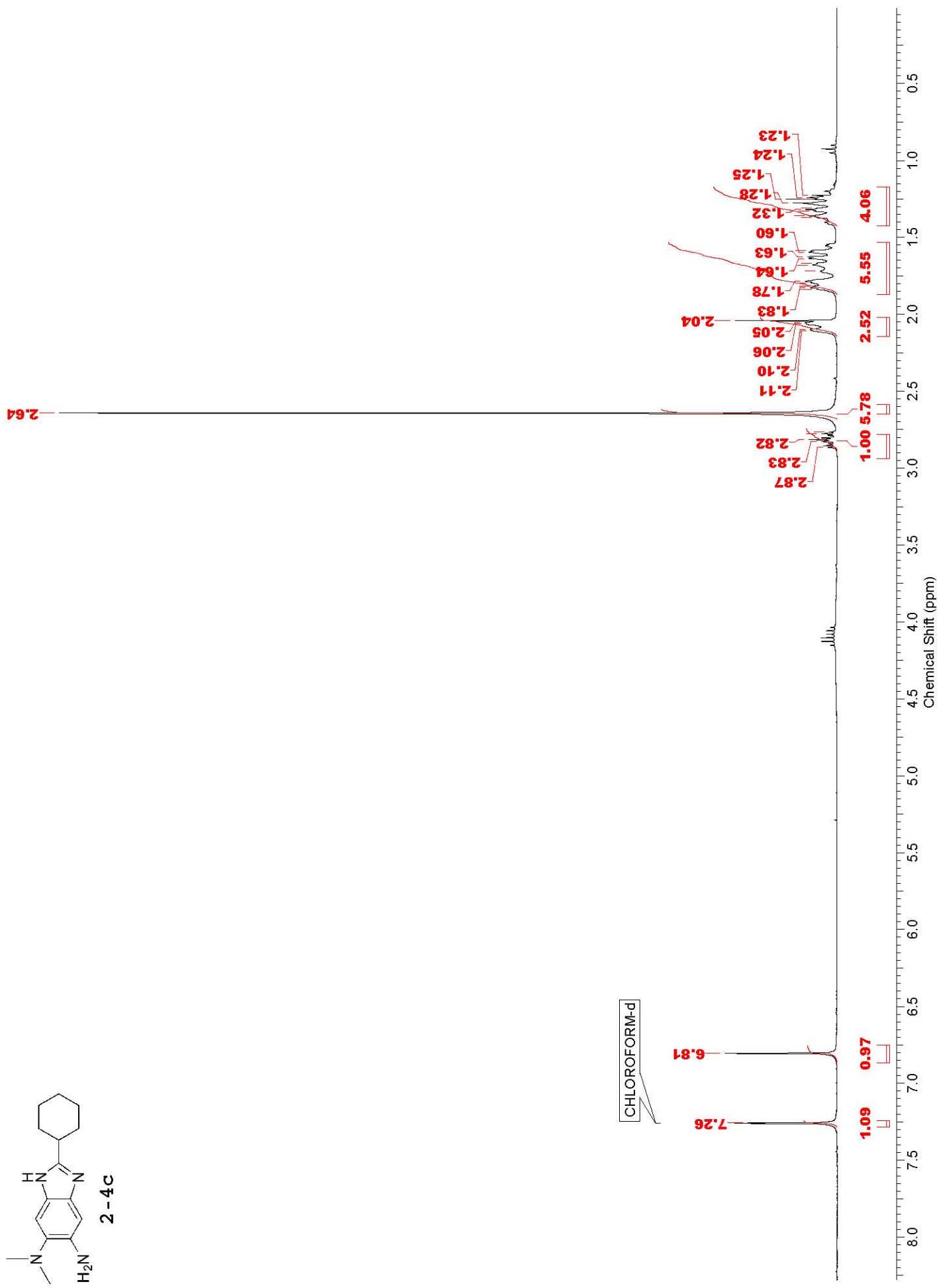
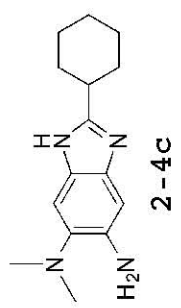


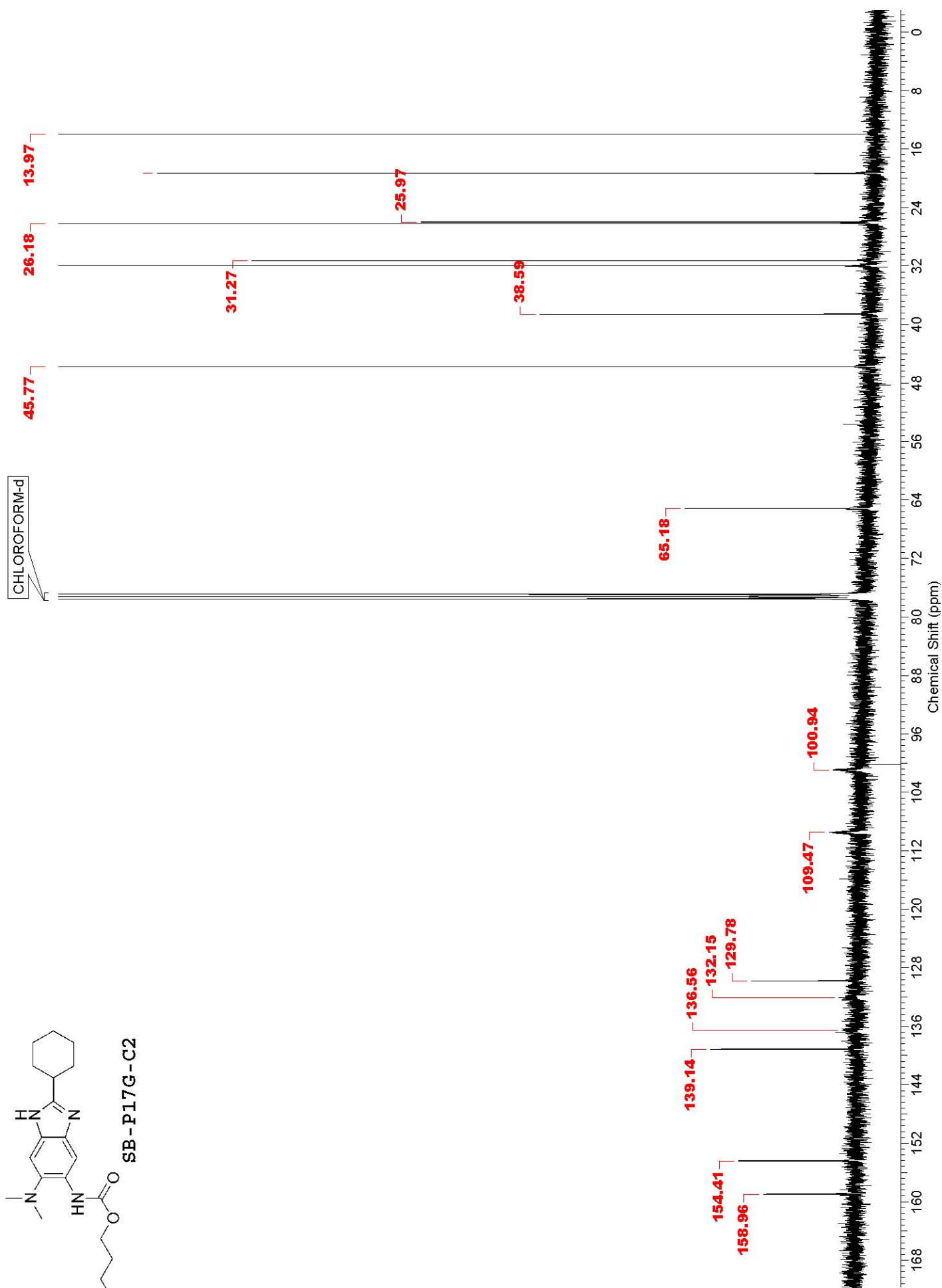
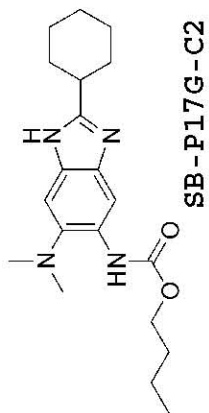


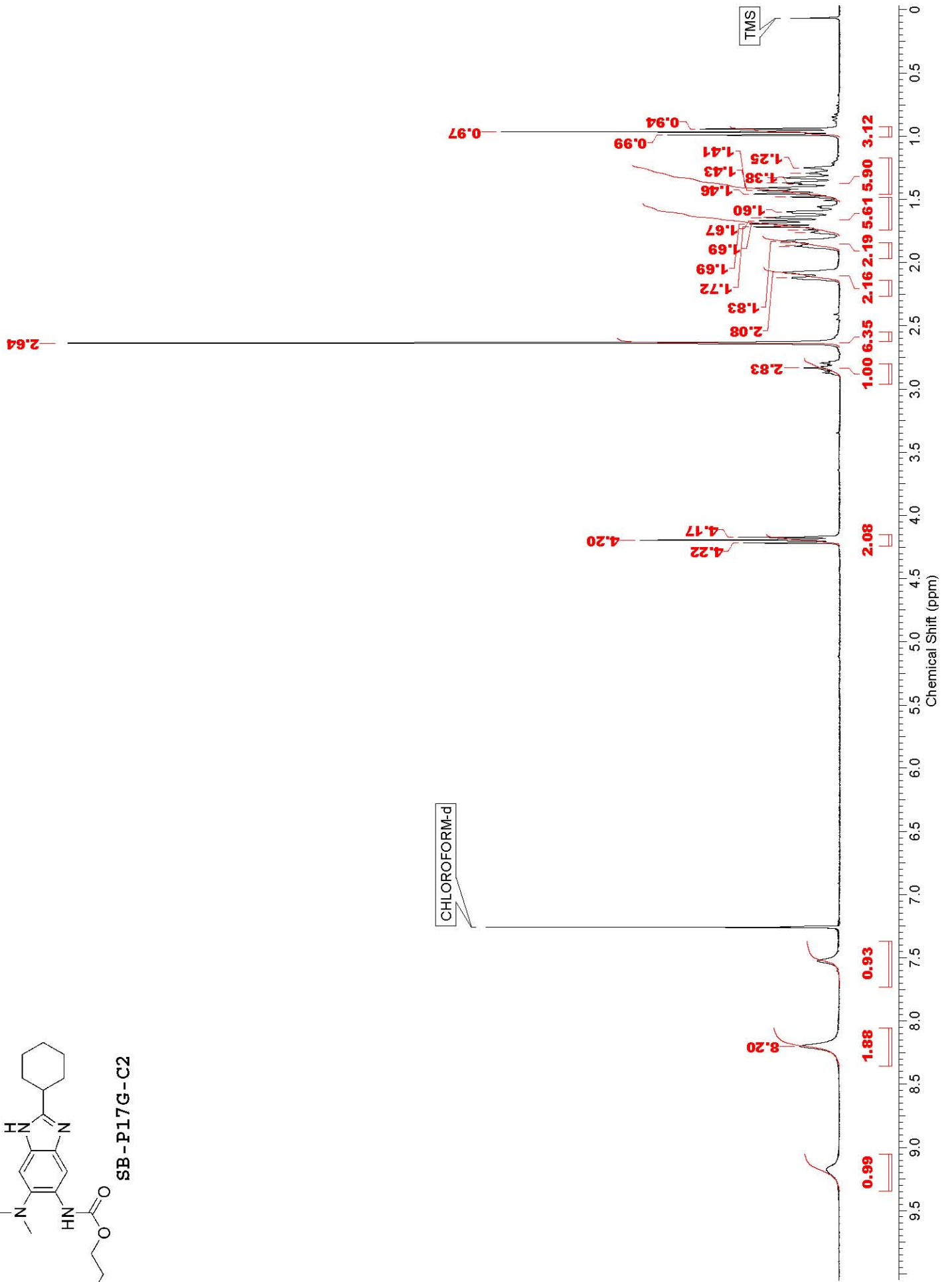
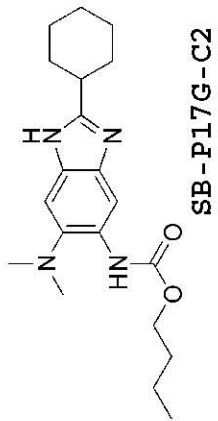


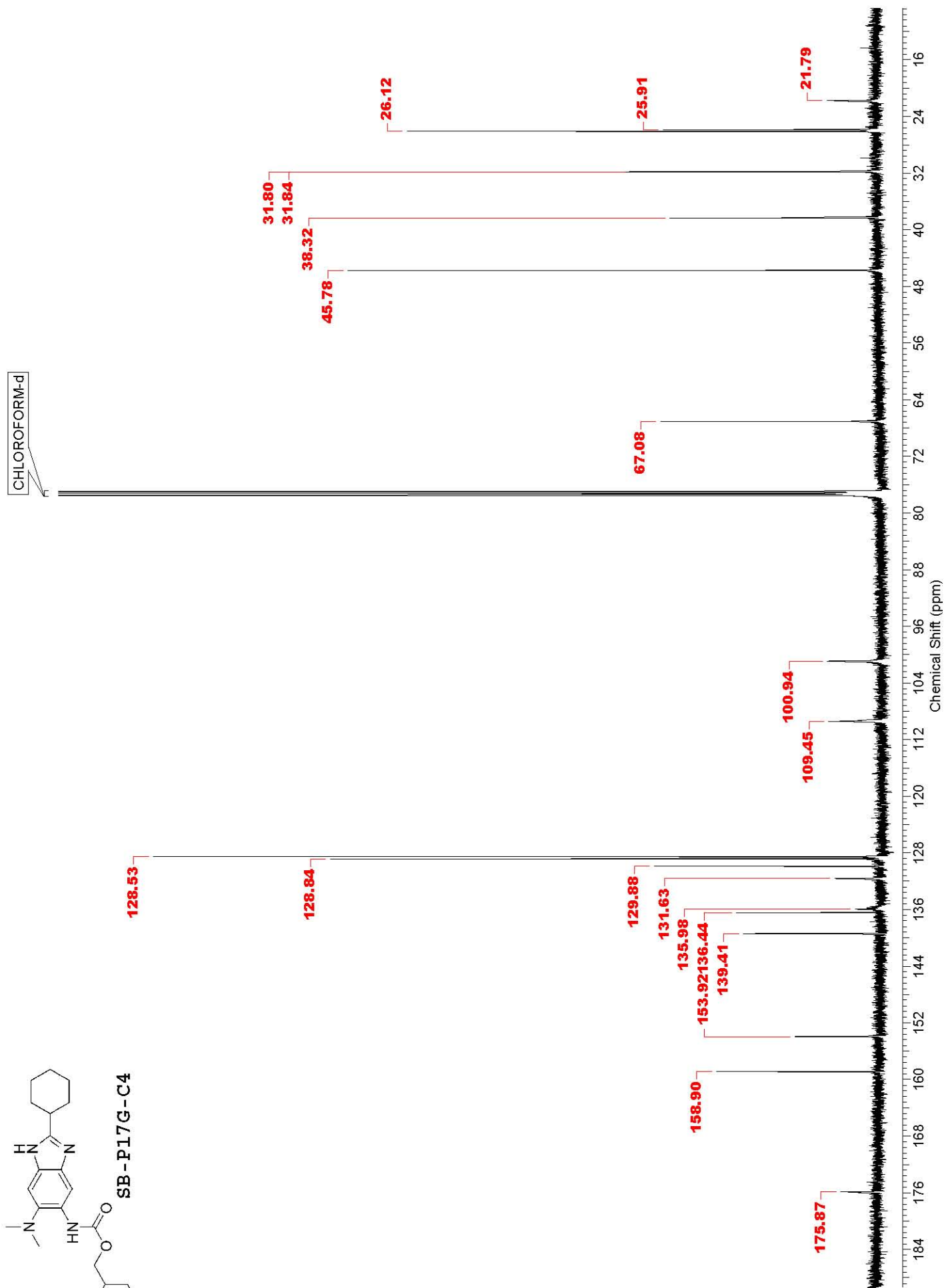
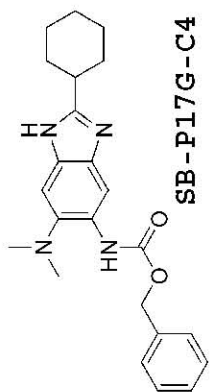


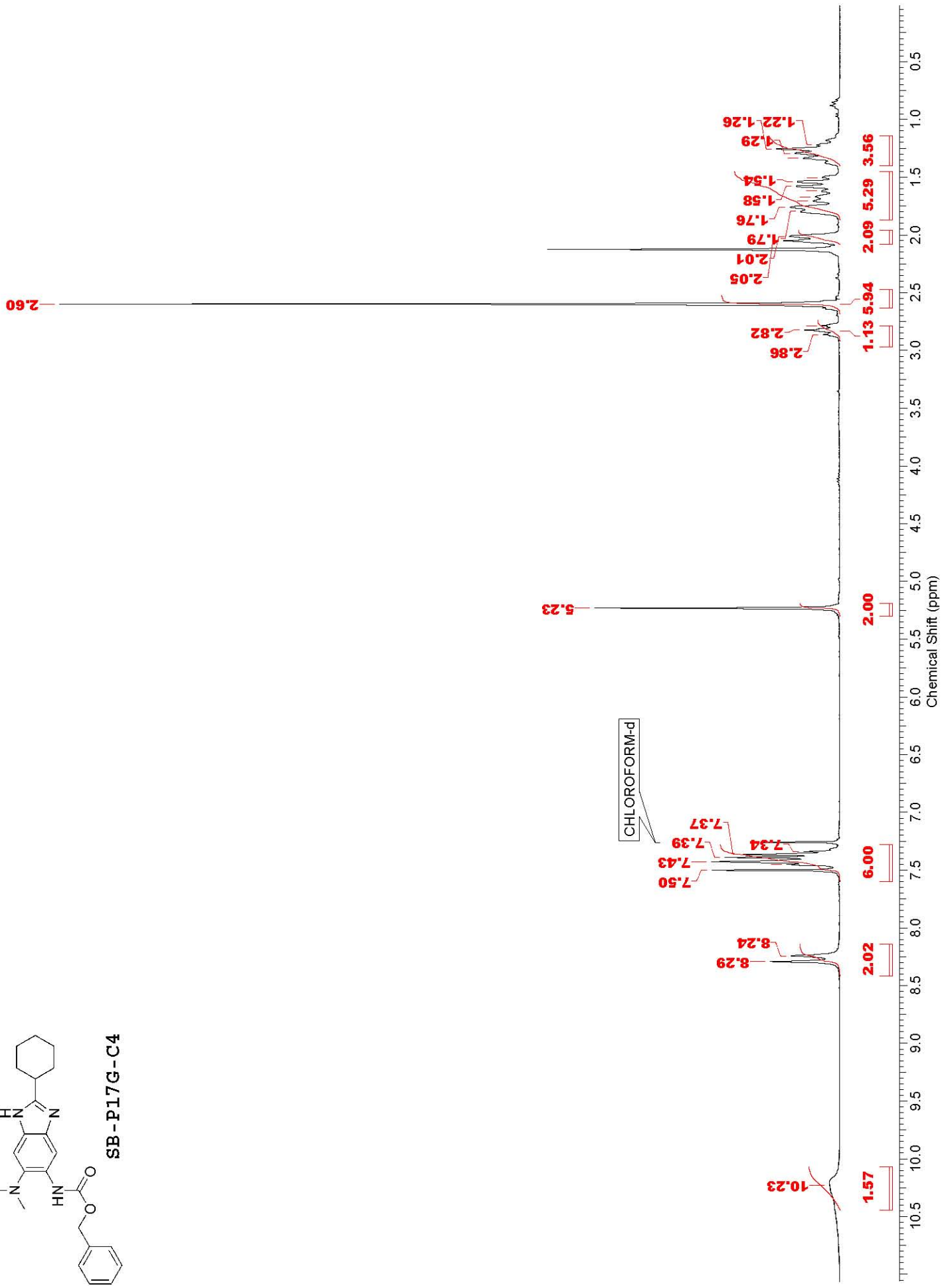
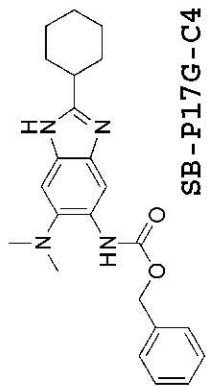


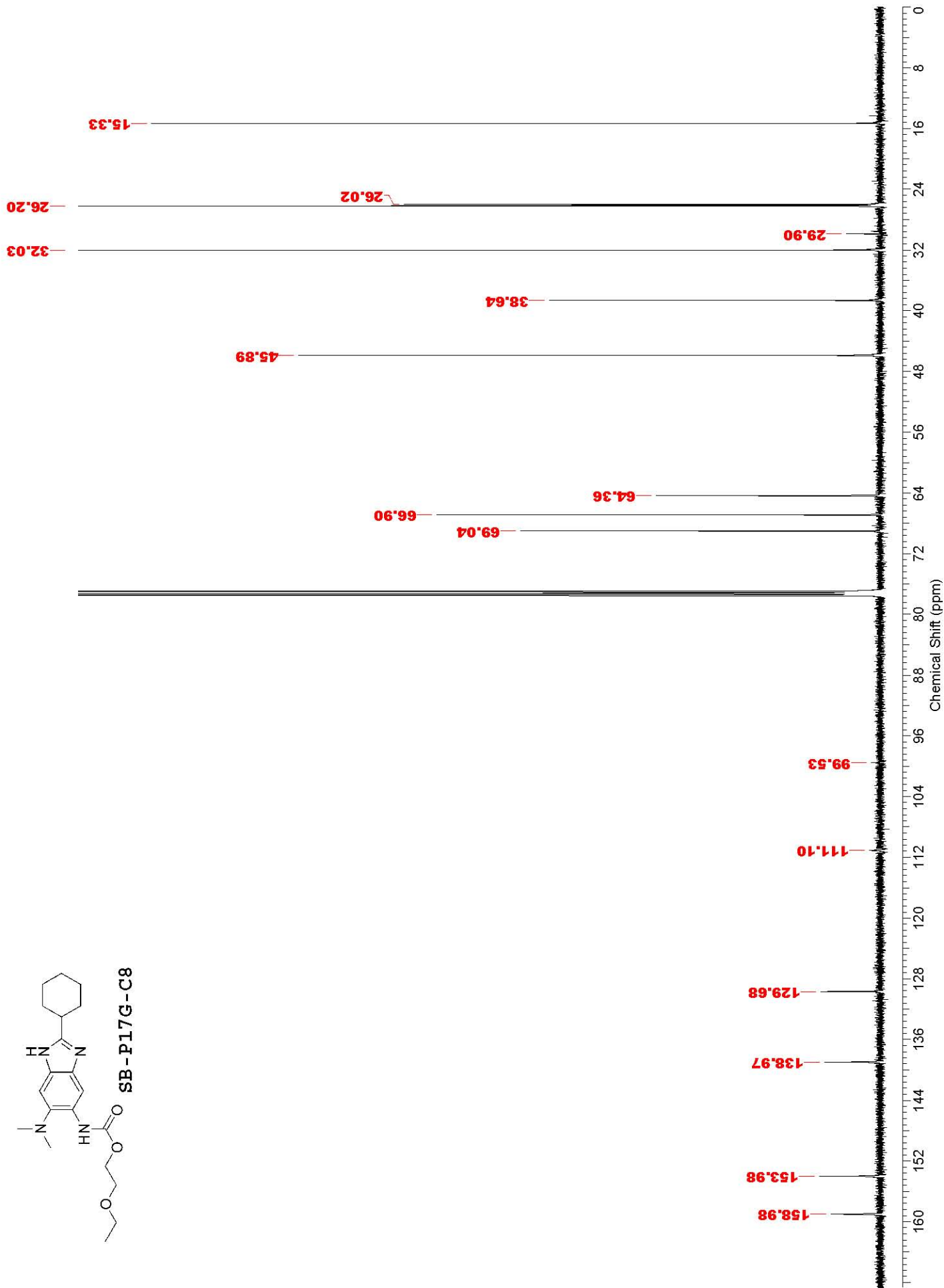
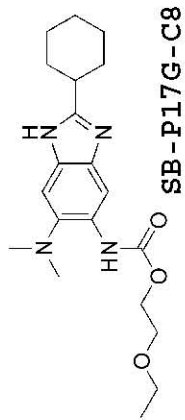


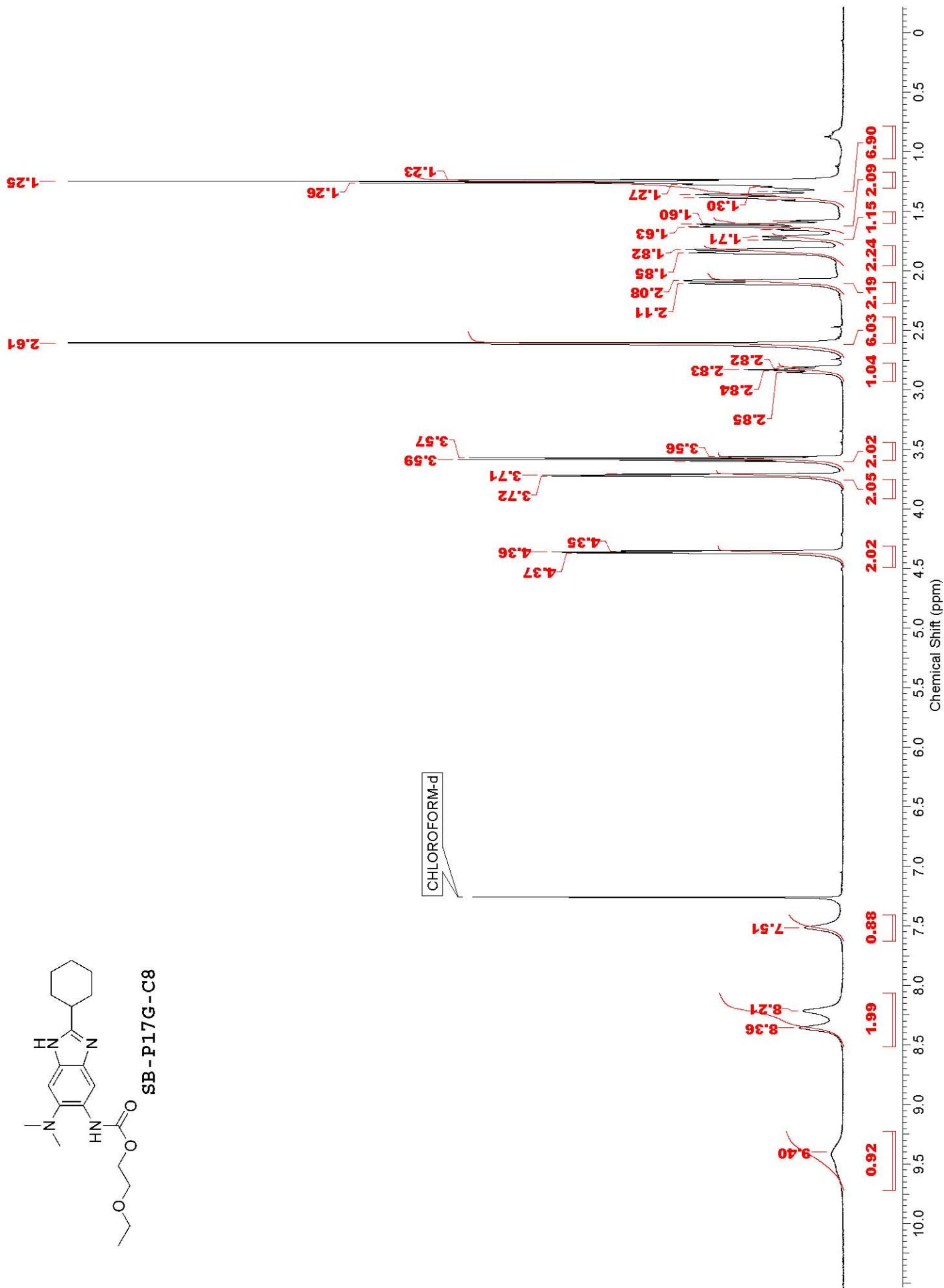
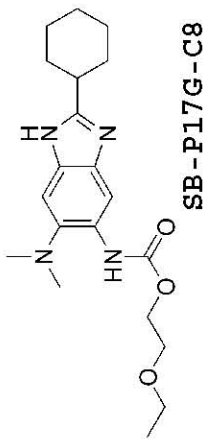


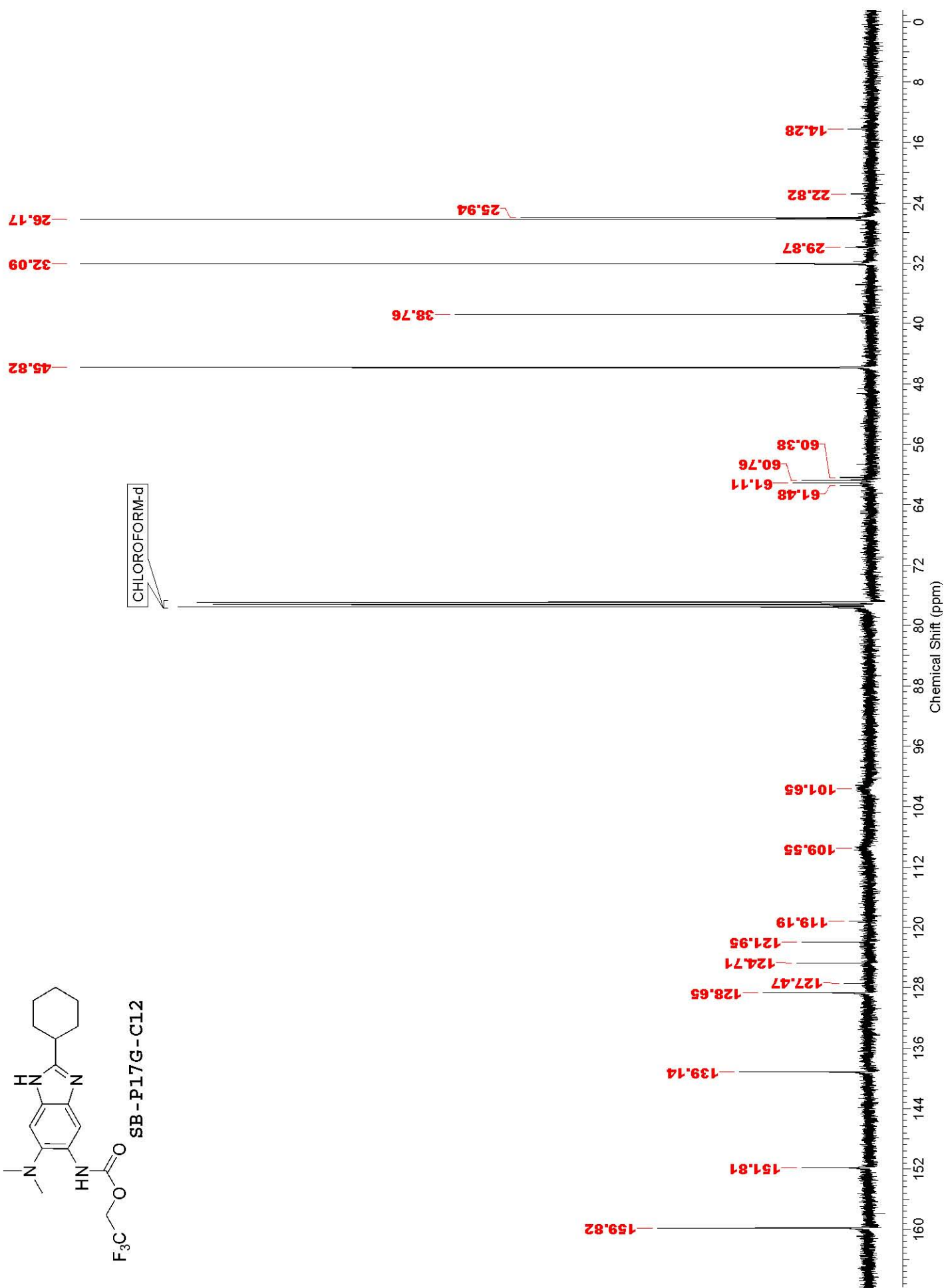
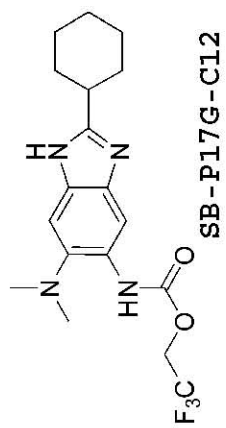


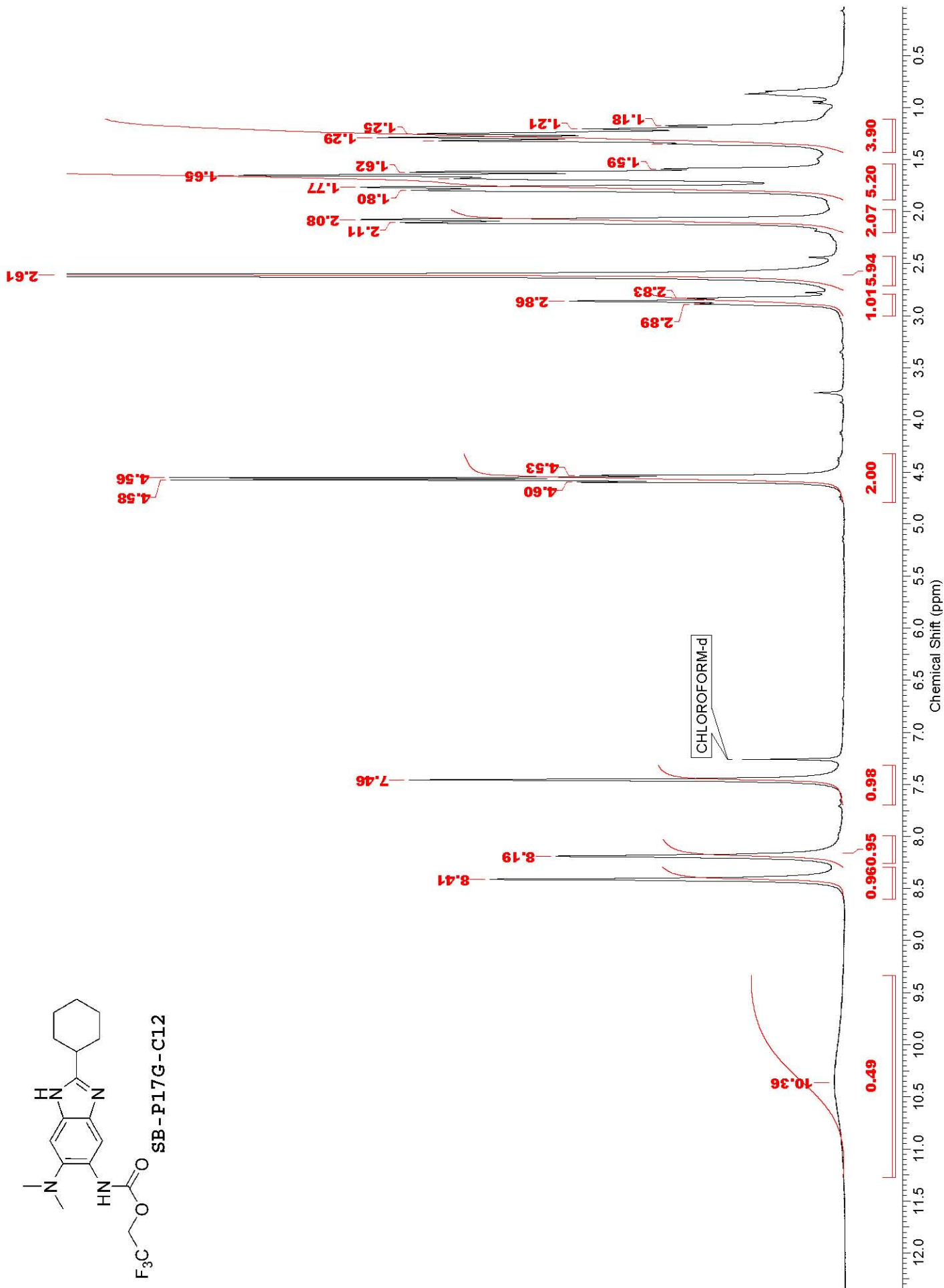
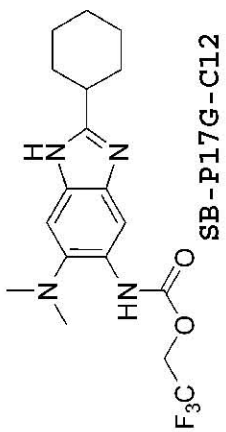


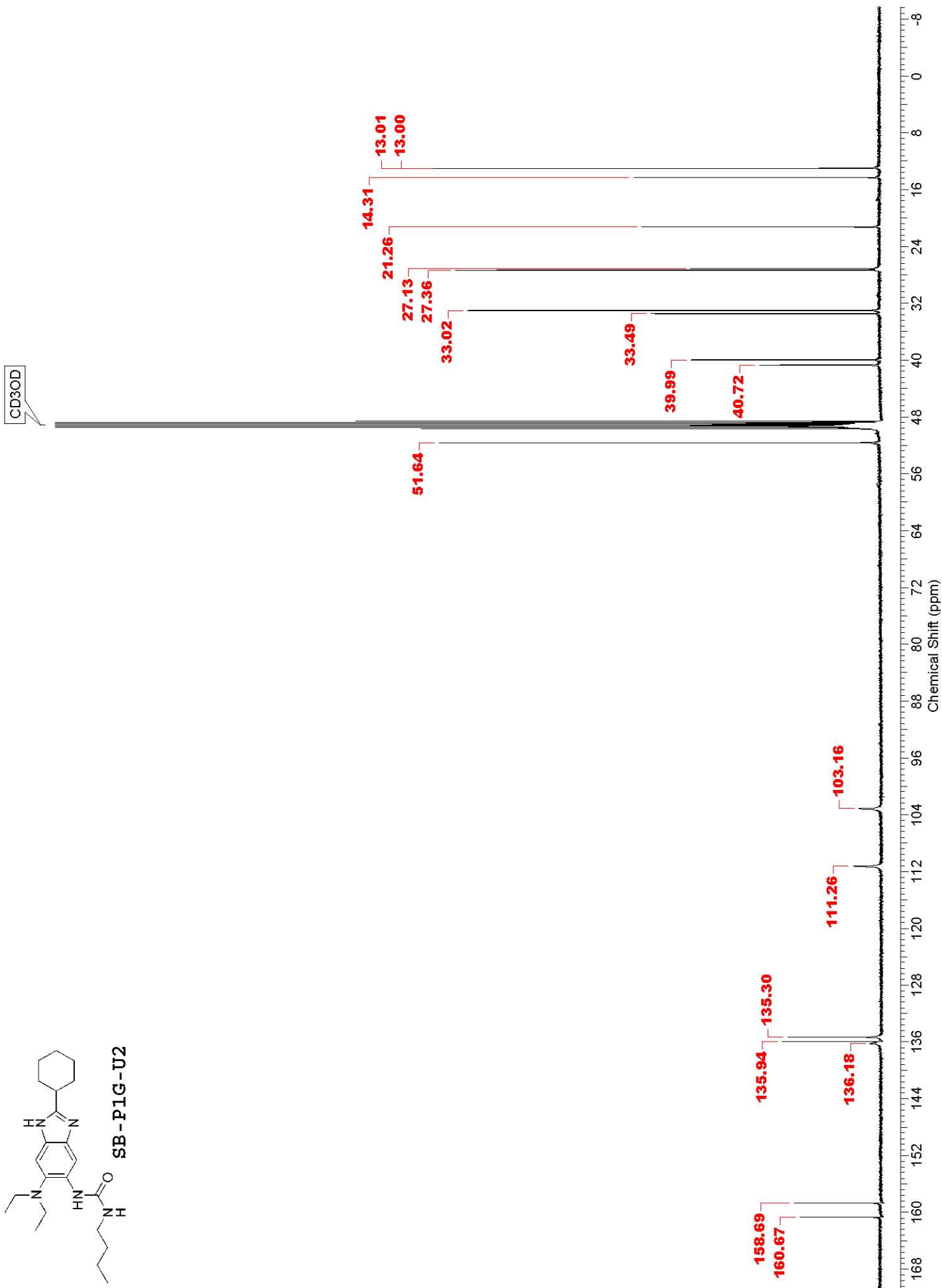
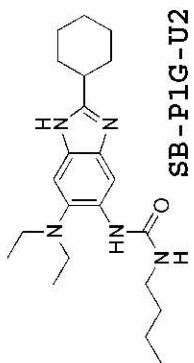


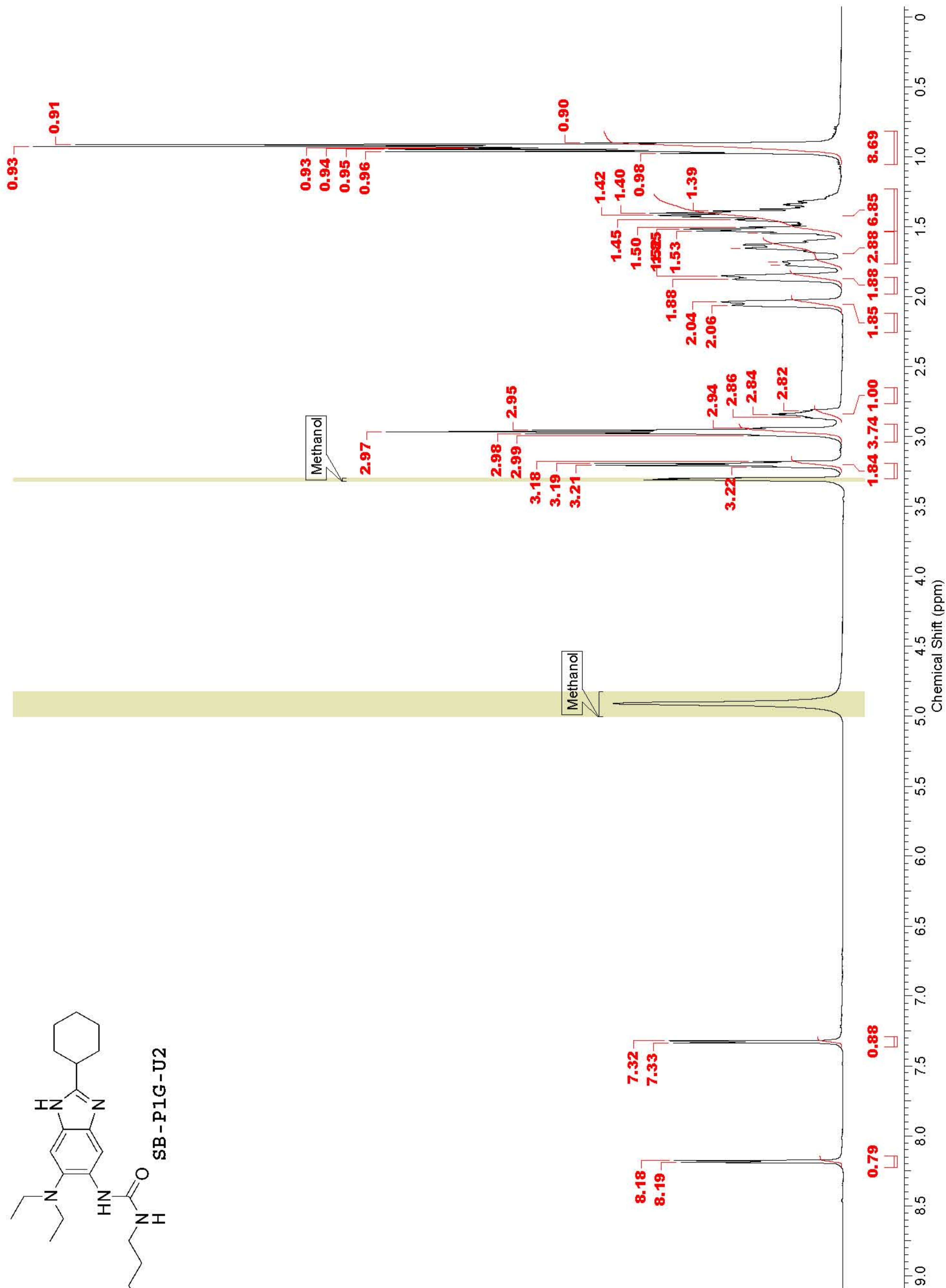
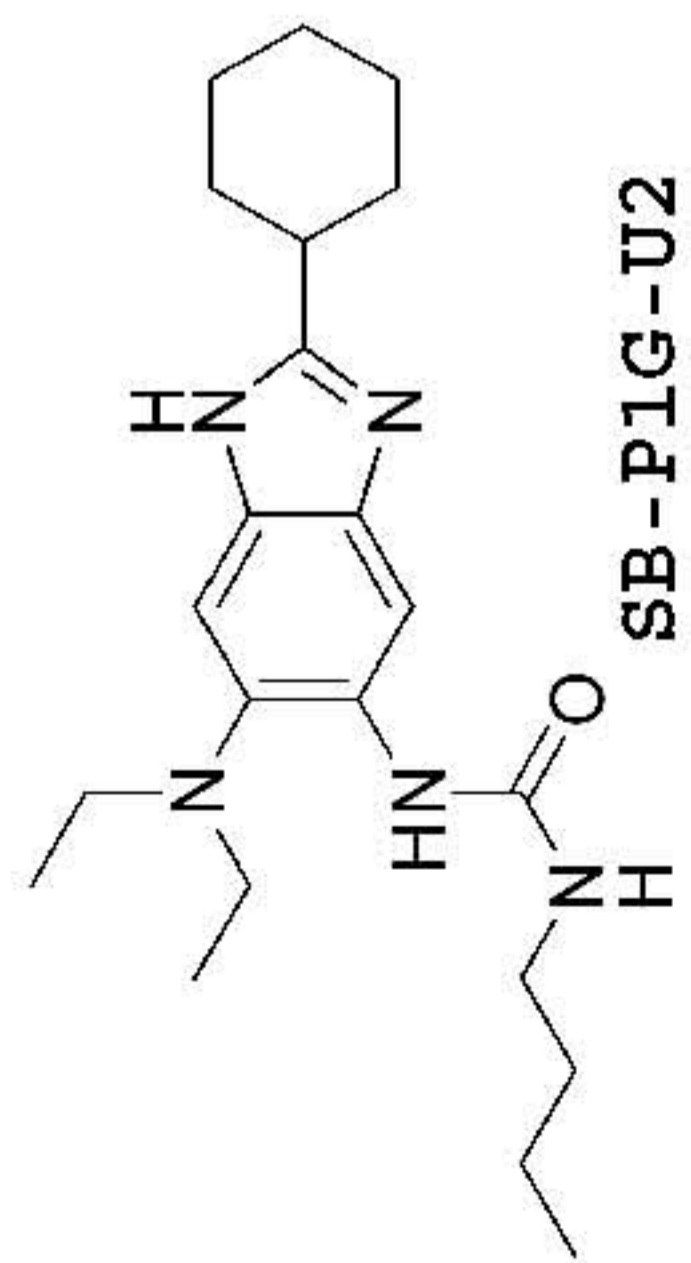


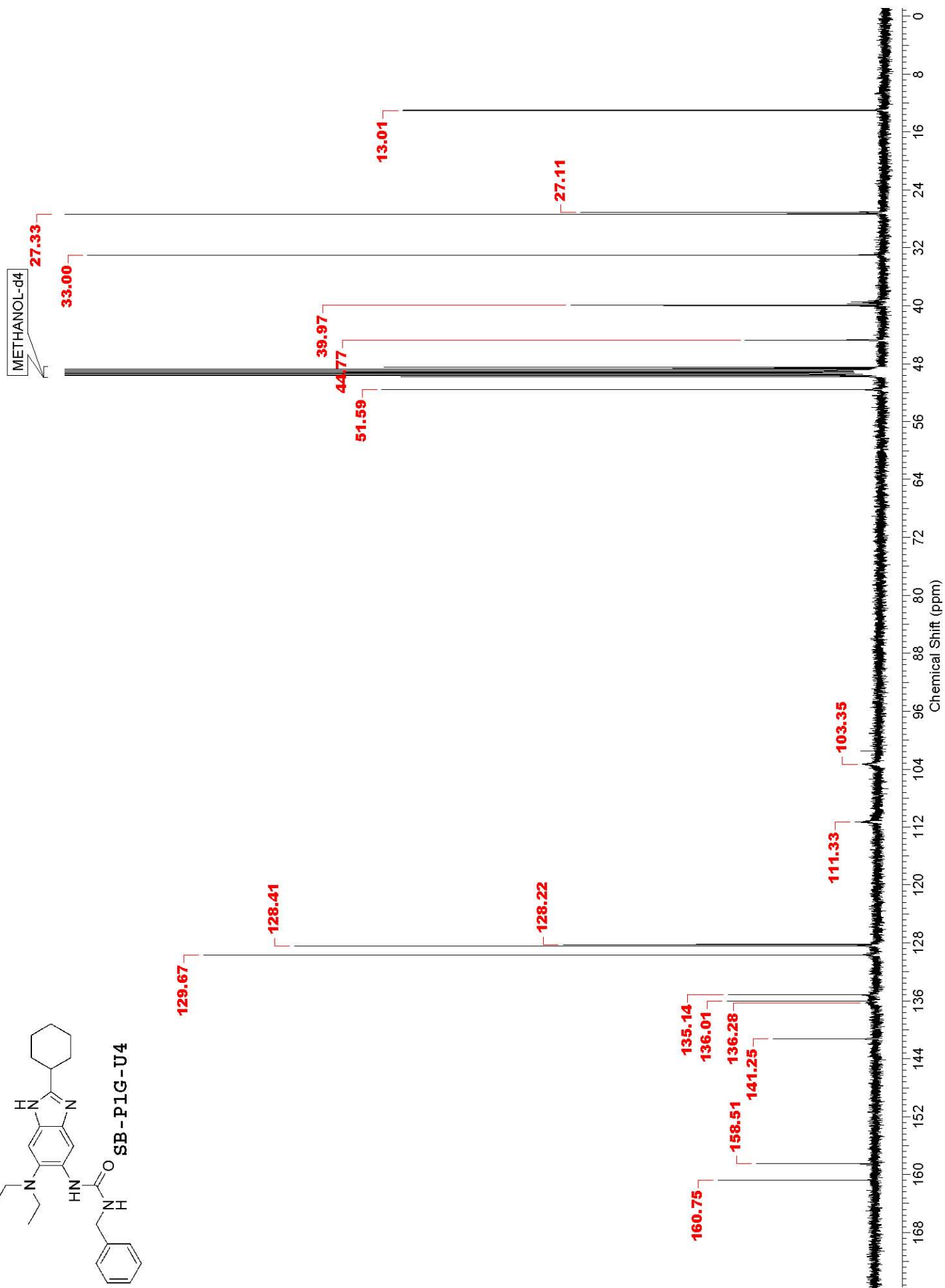
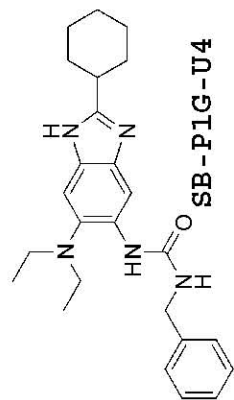


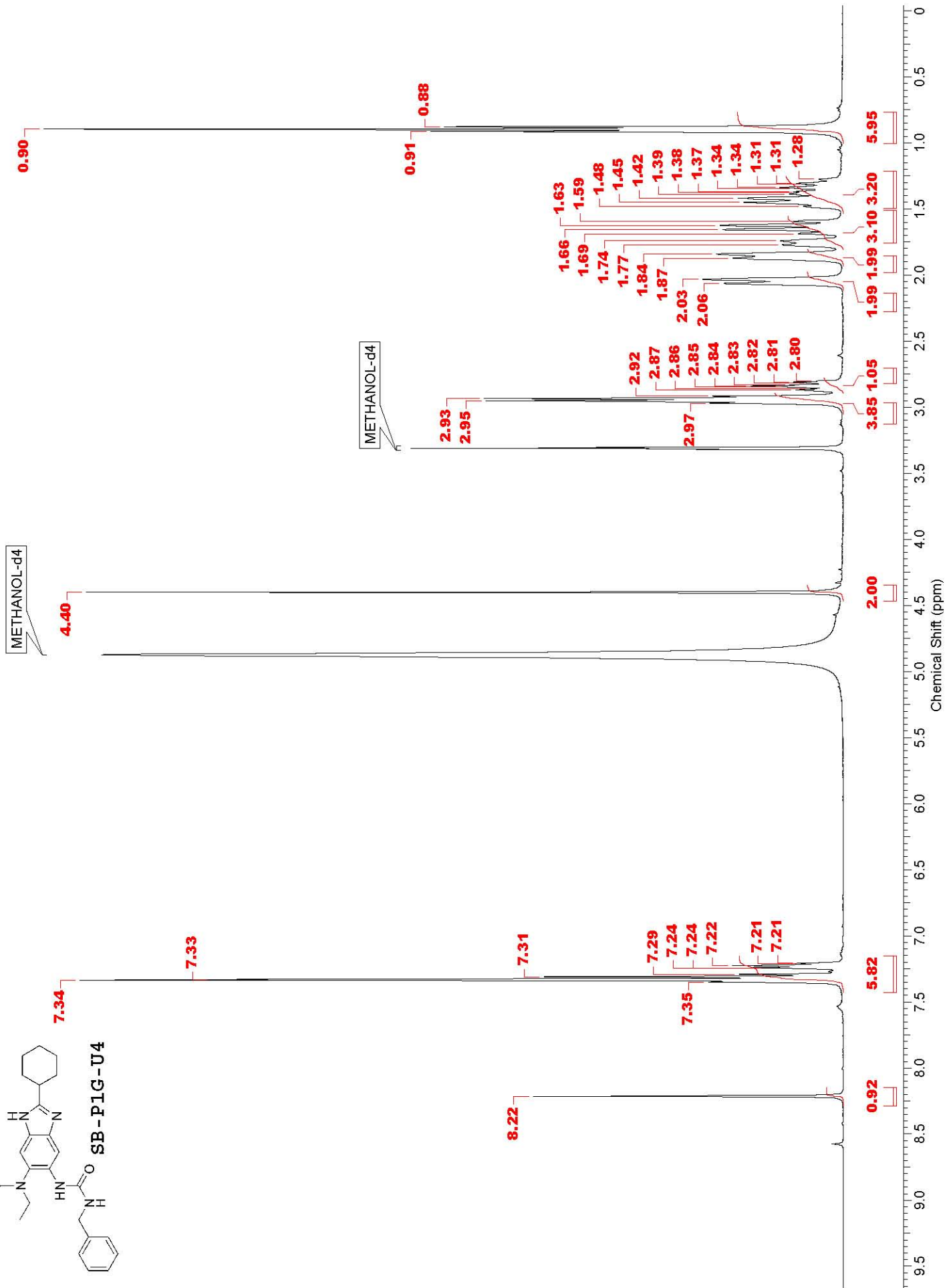
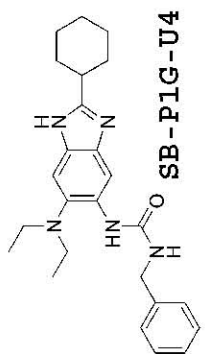


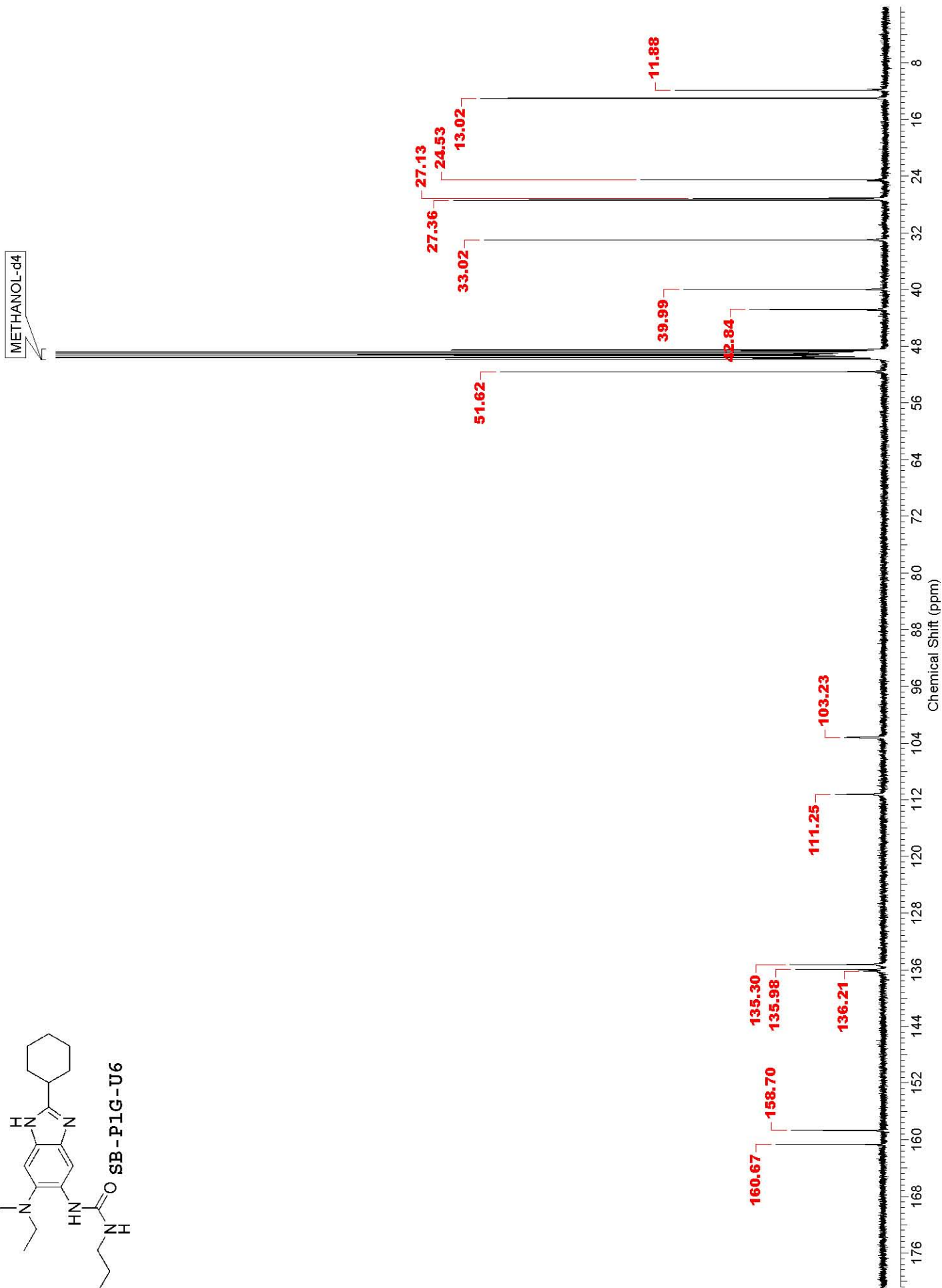
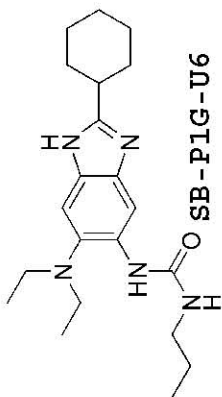


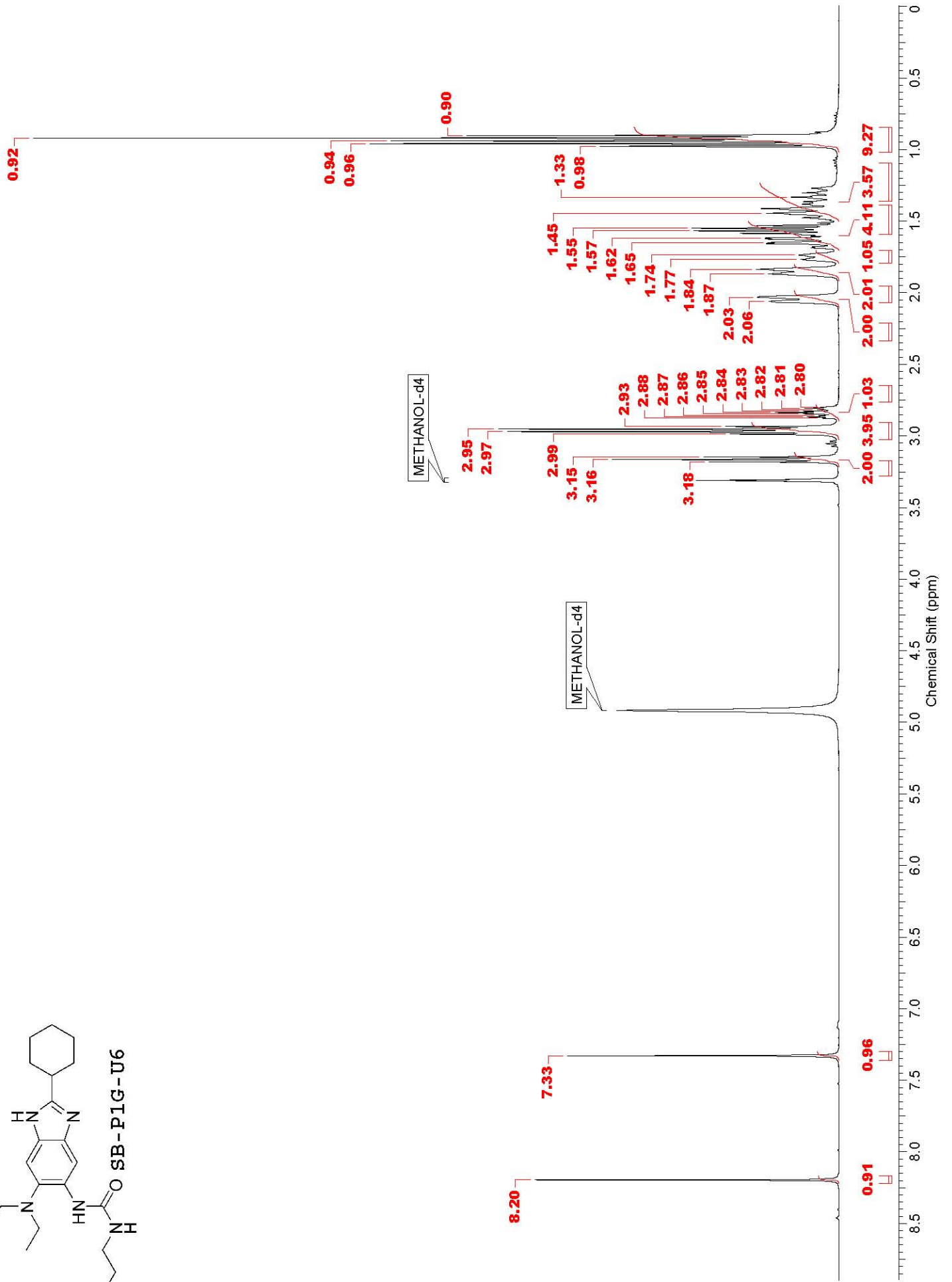
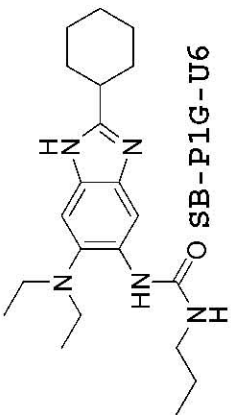


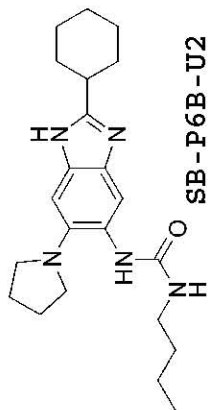




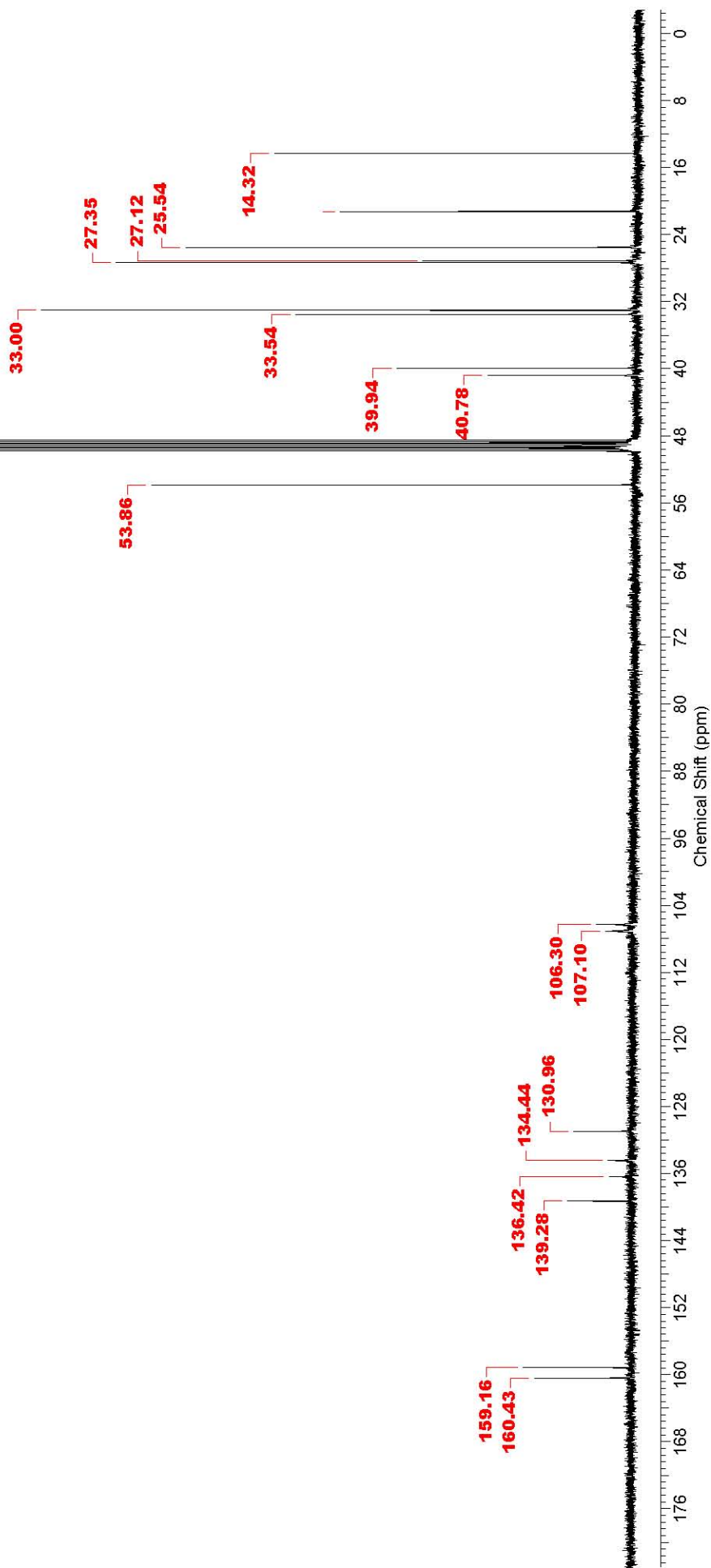


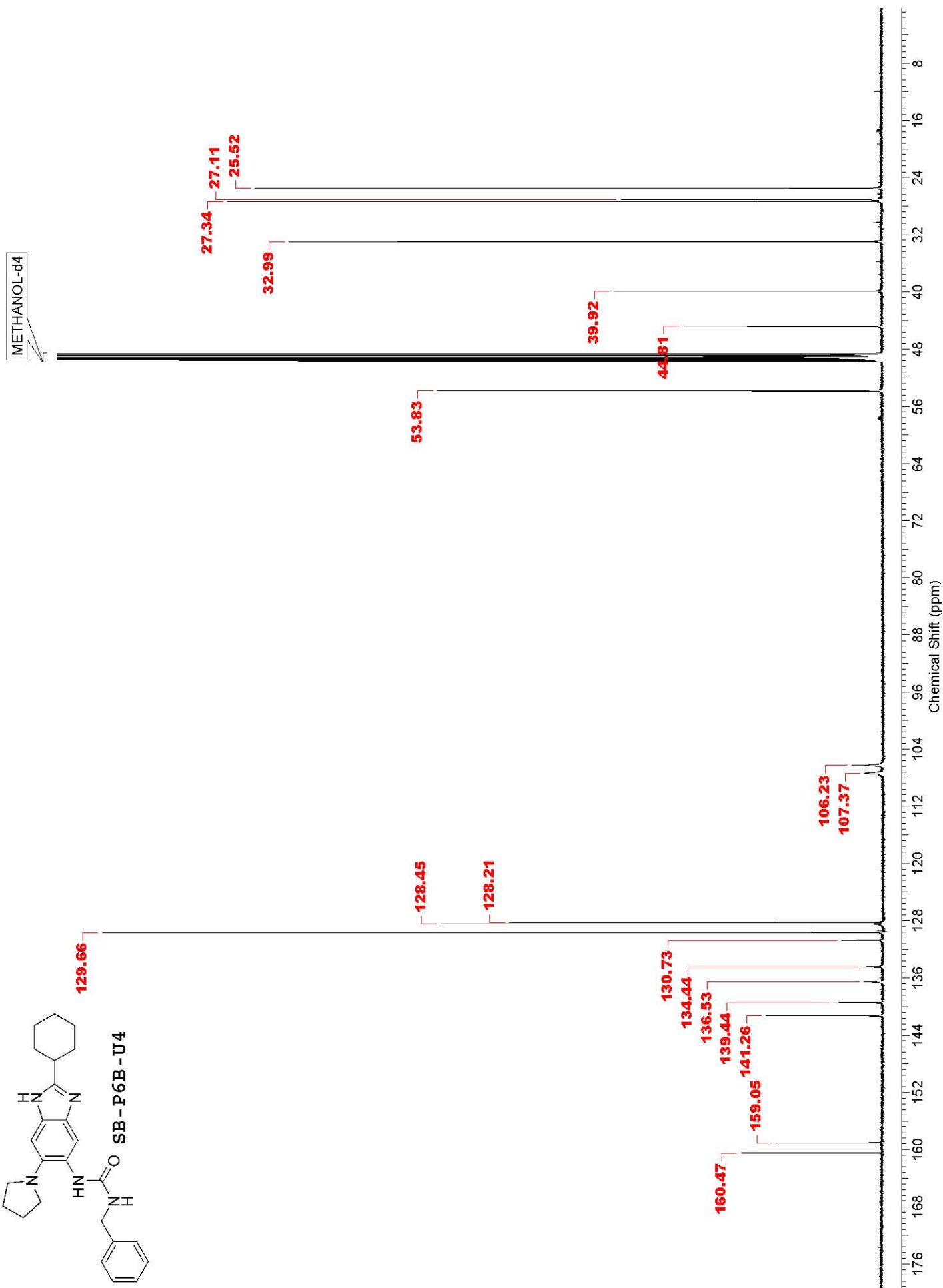
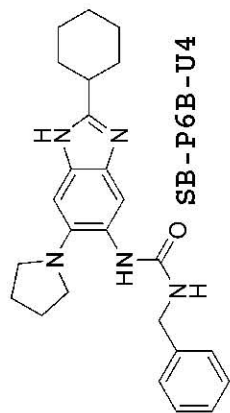


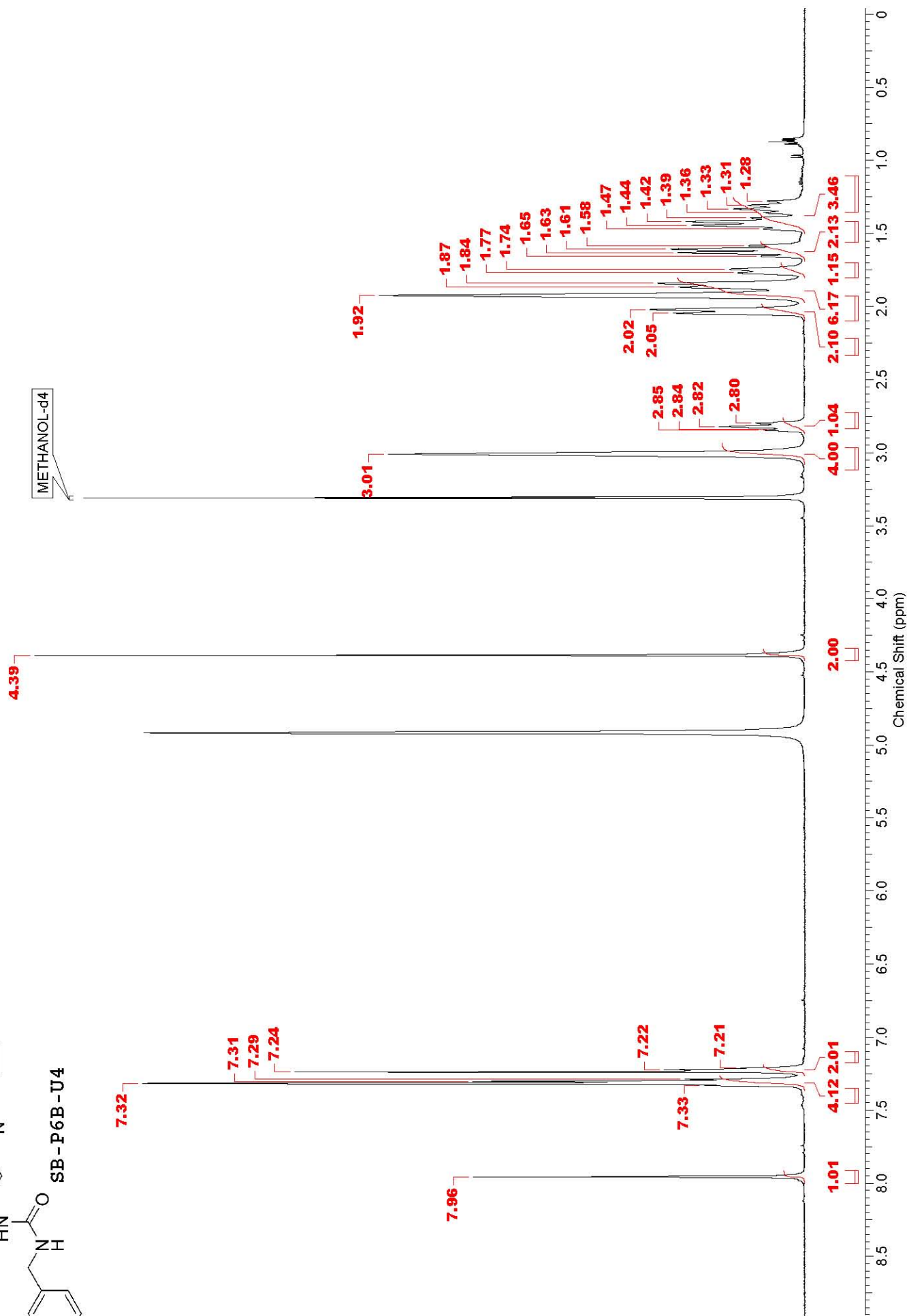
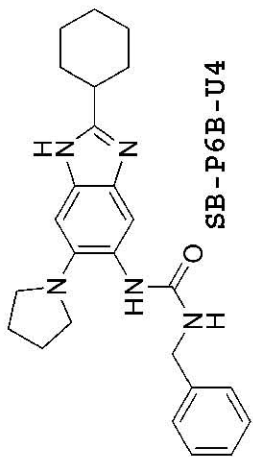


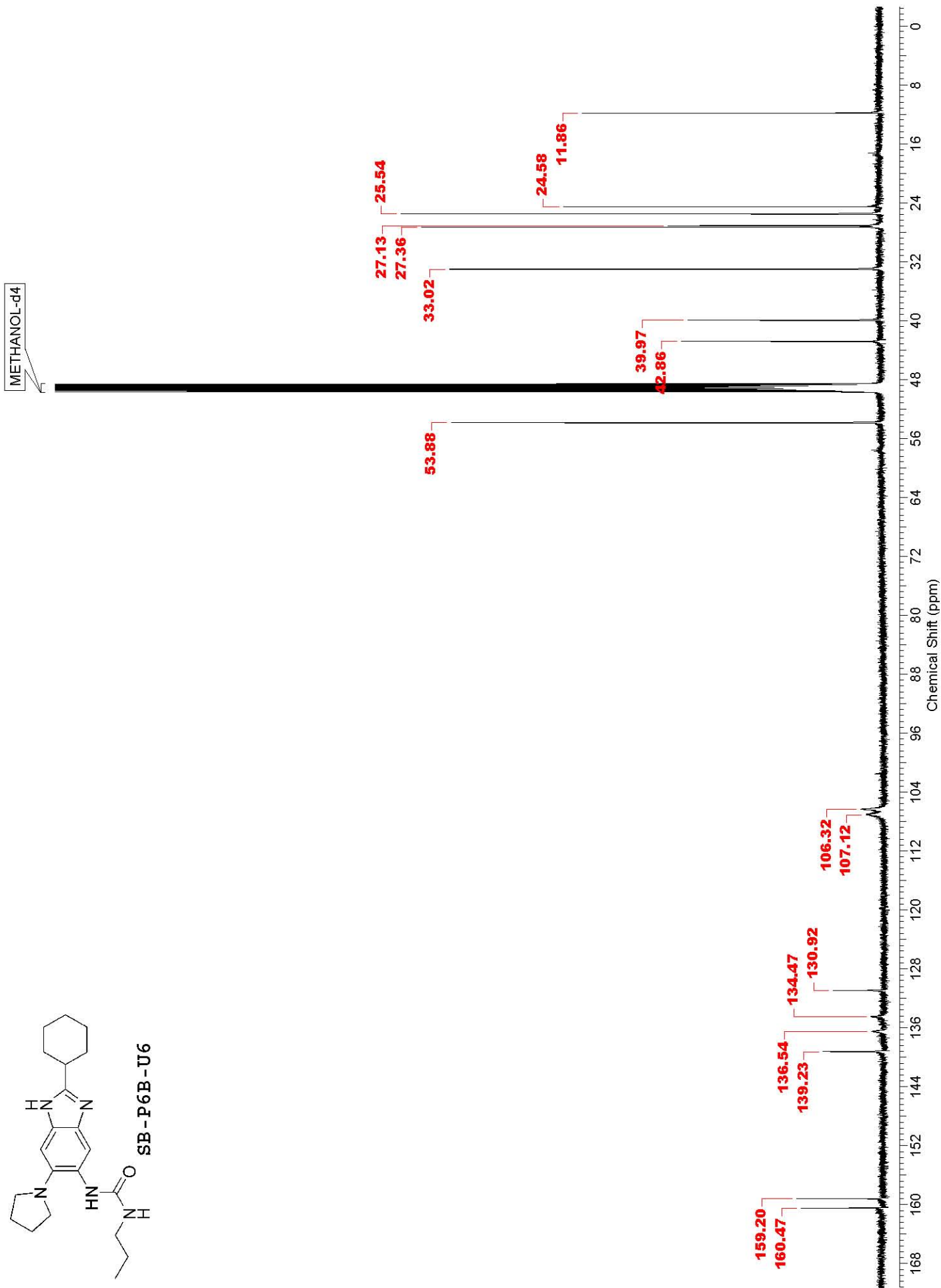
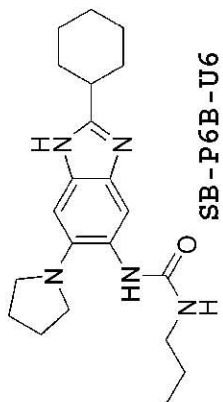


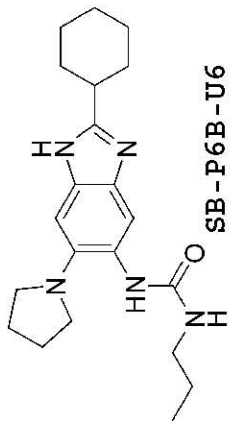
METHANOL-d4





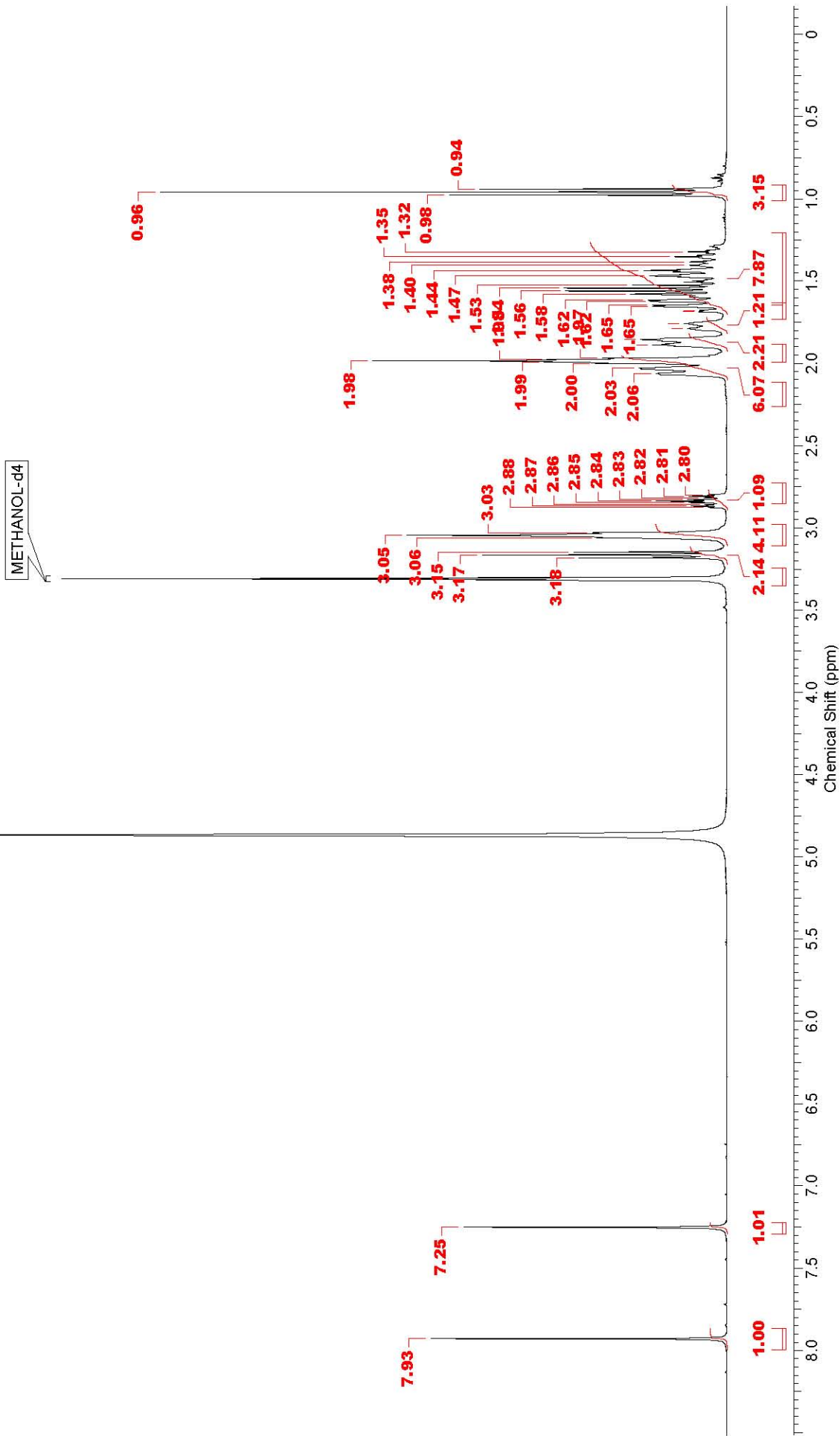


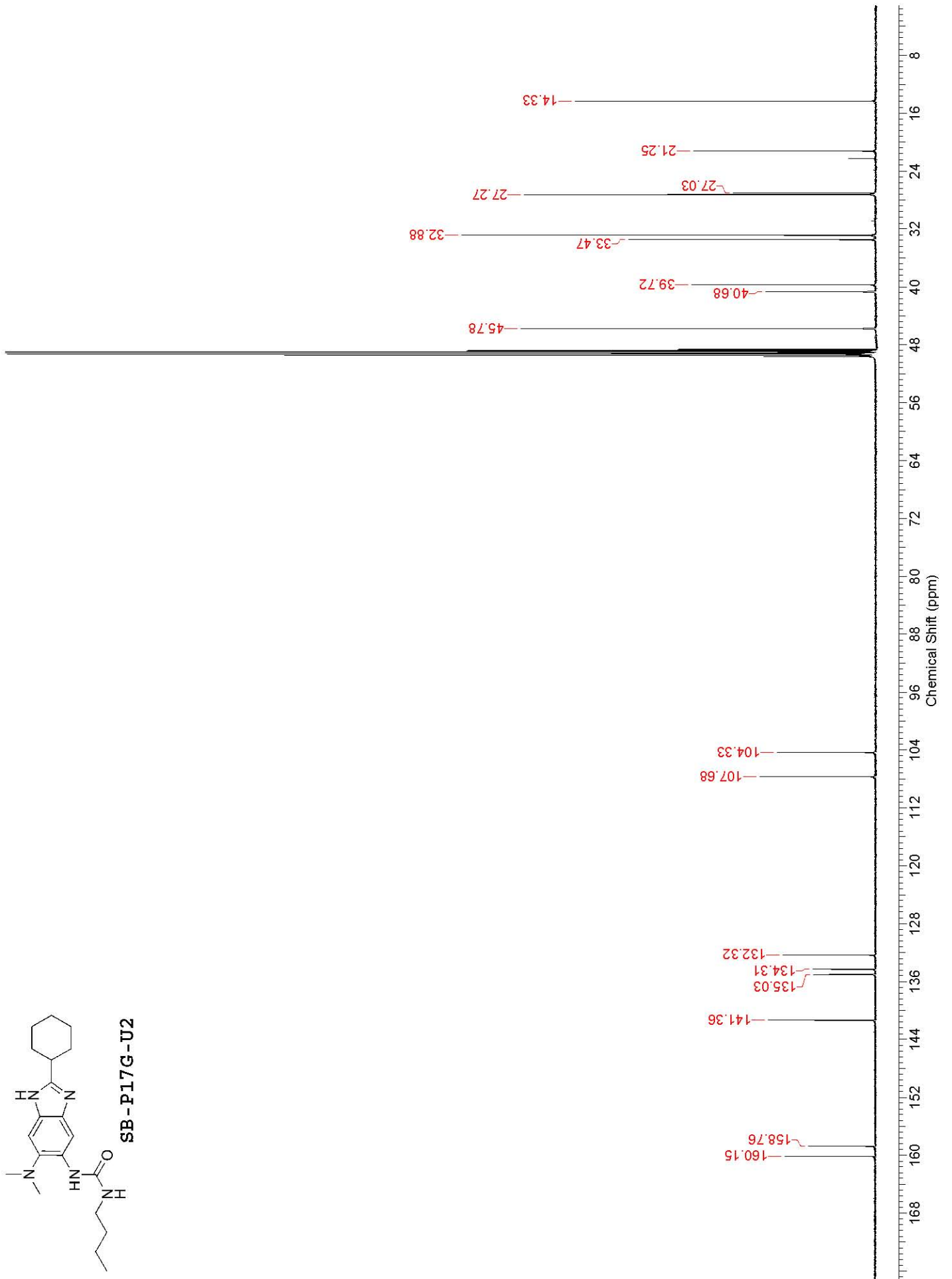
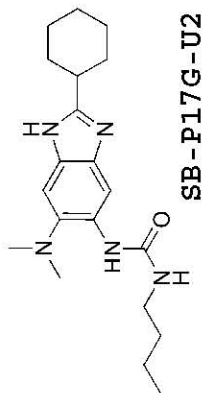


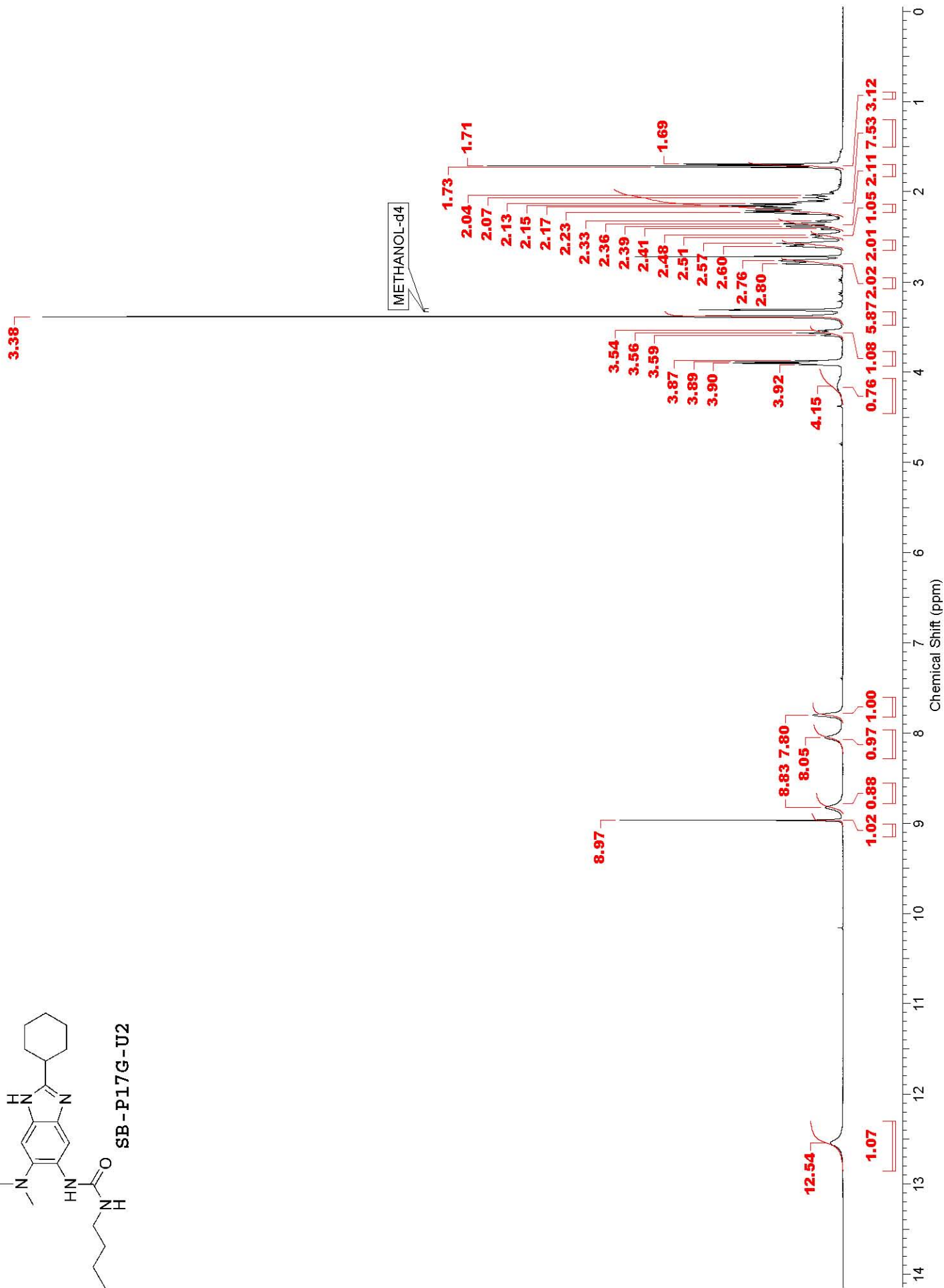
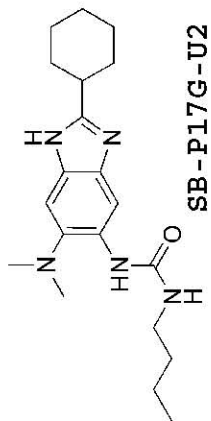


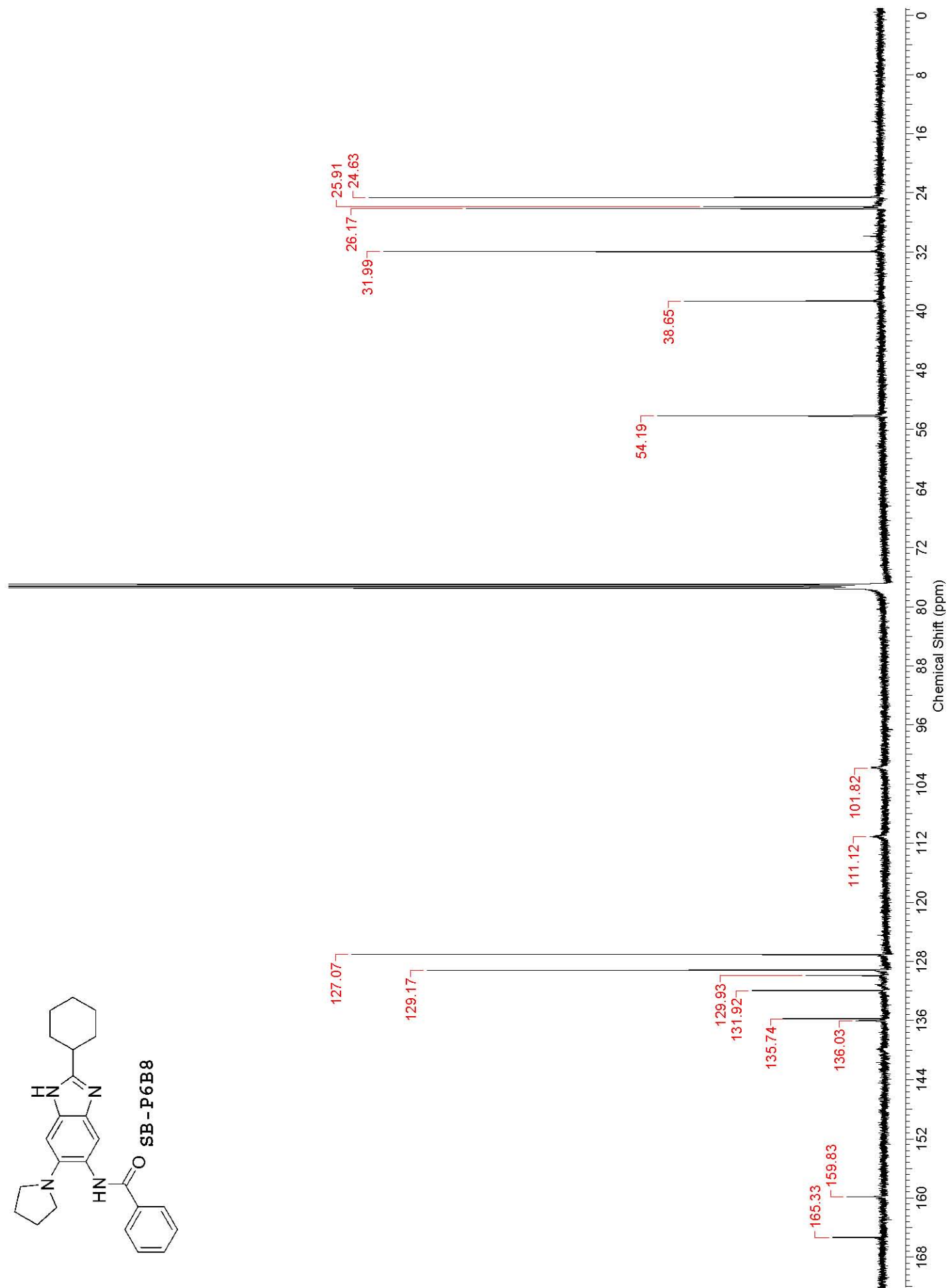
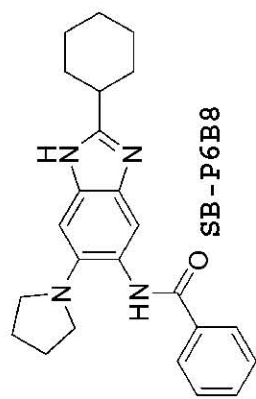
METHANOL-d4

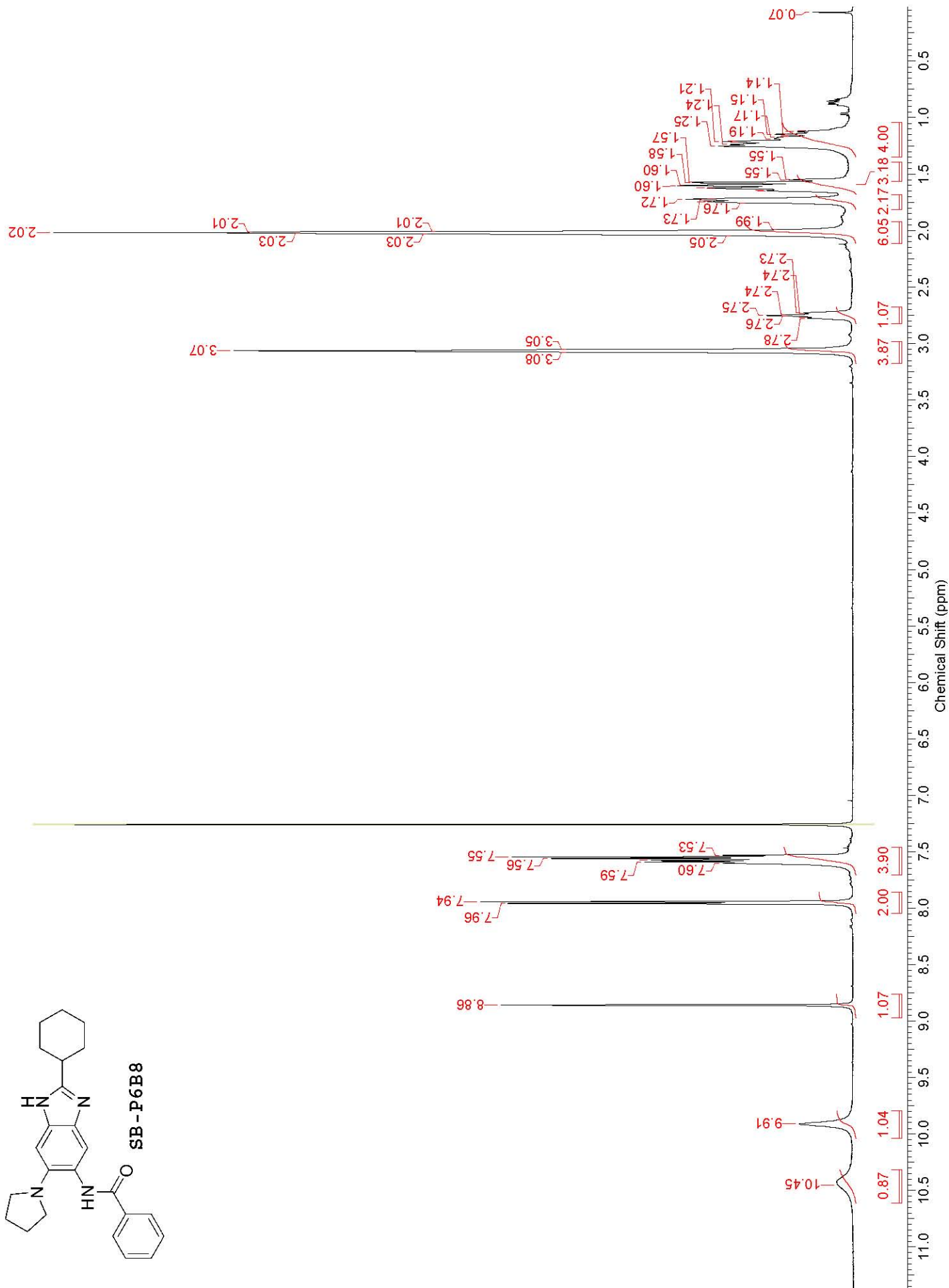
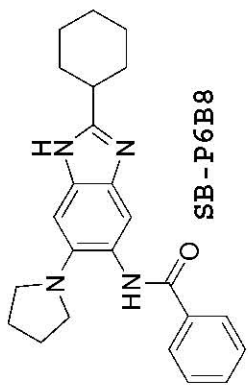
METHANOL-d4

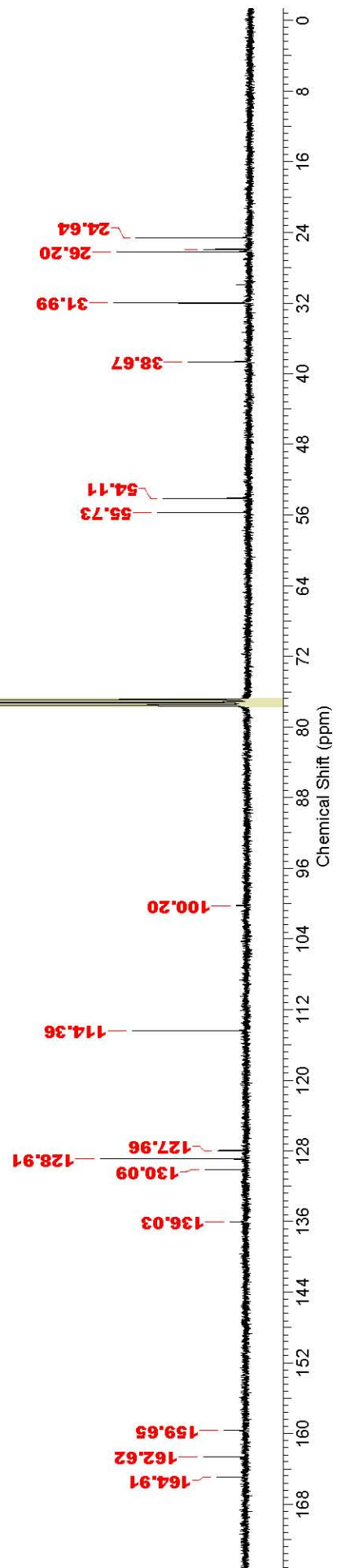
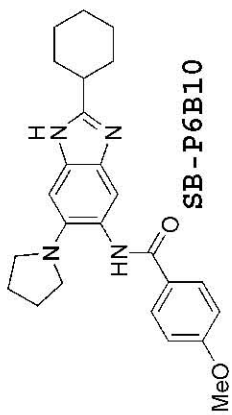


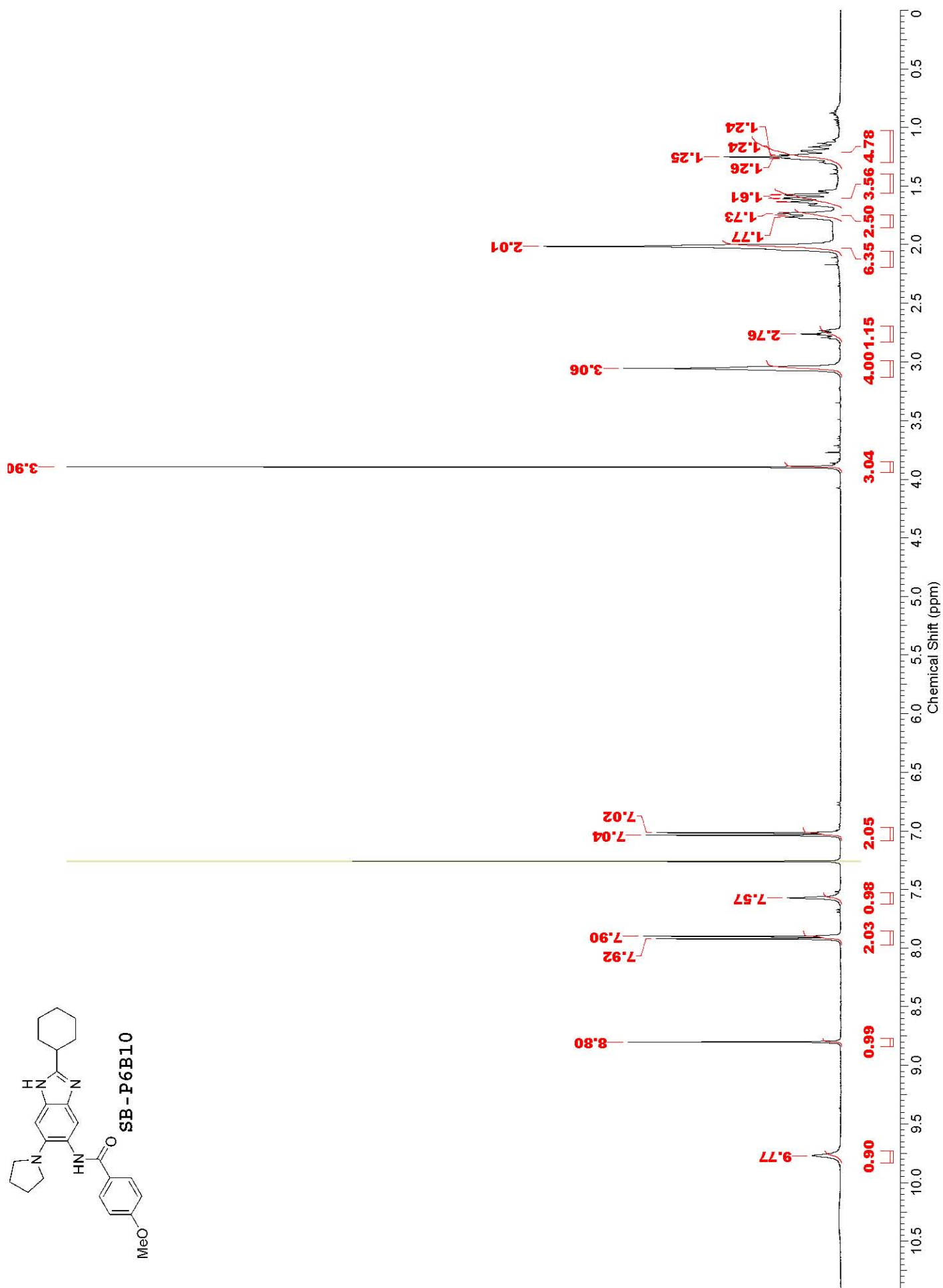
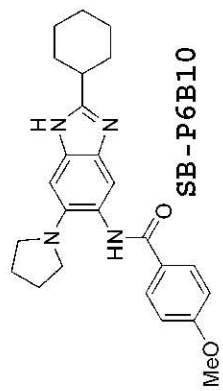


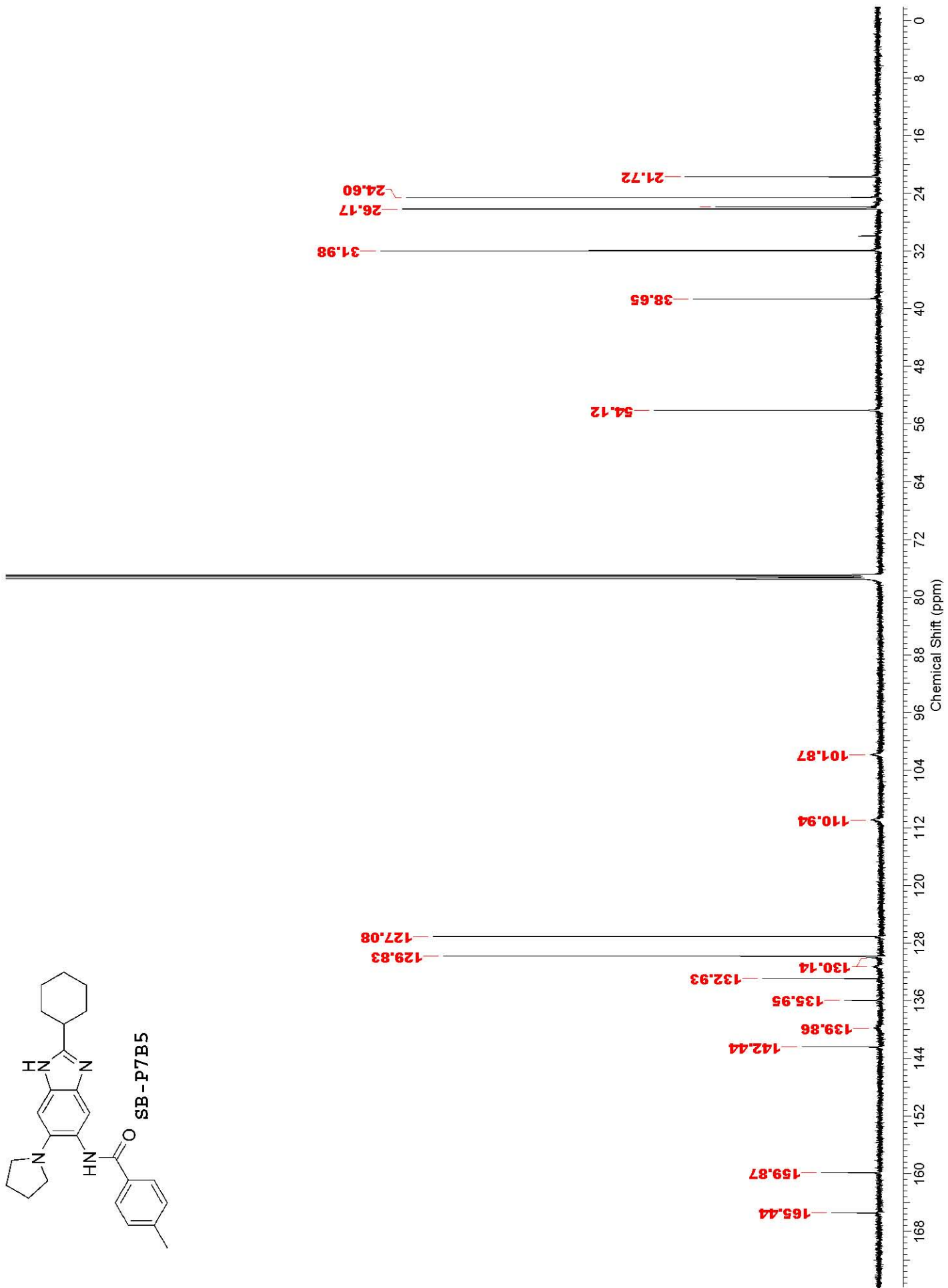
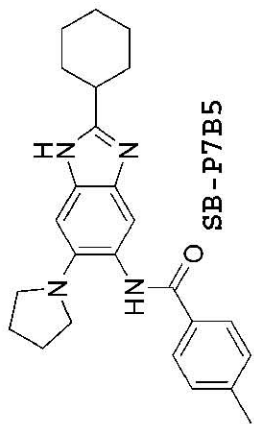


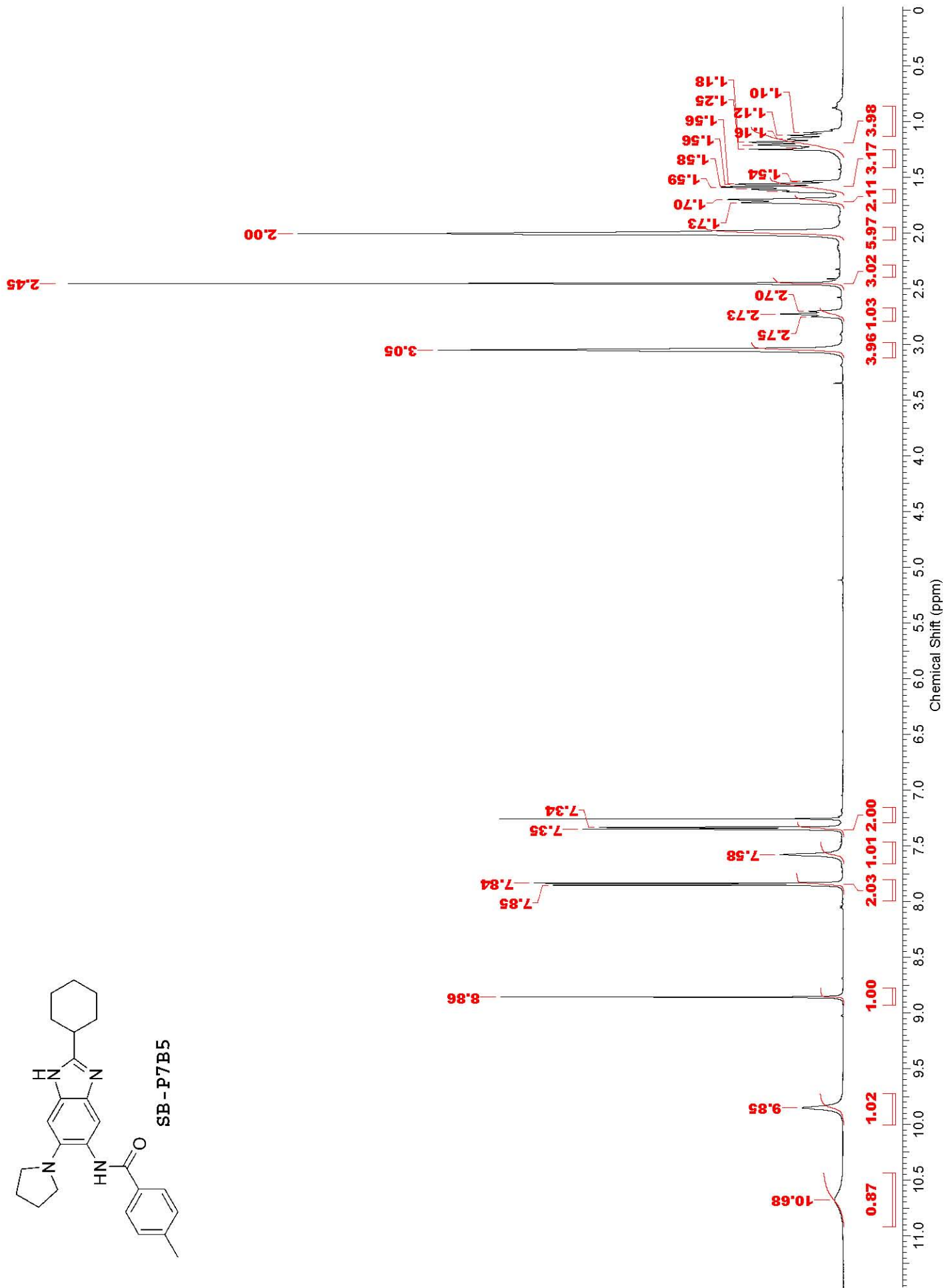
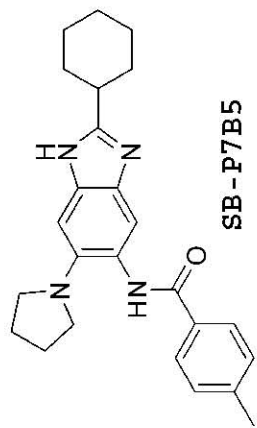


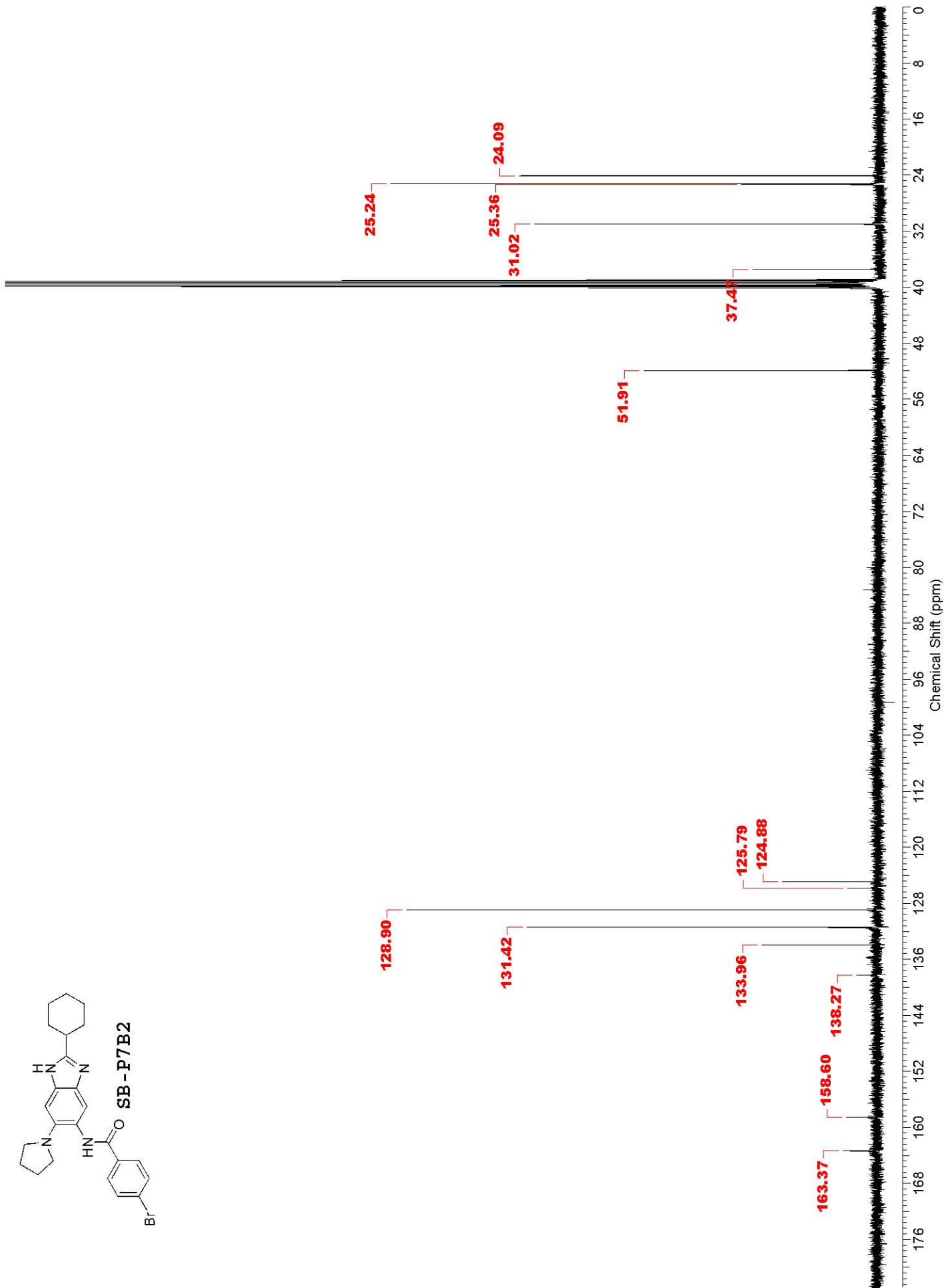
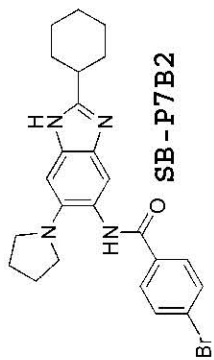


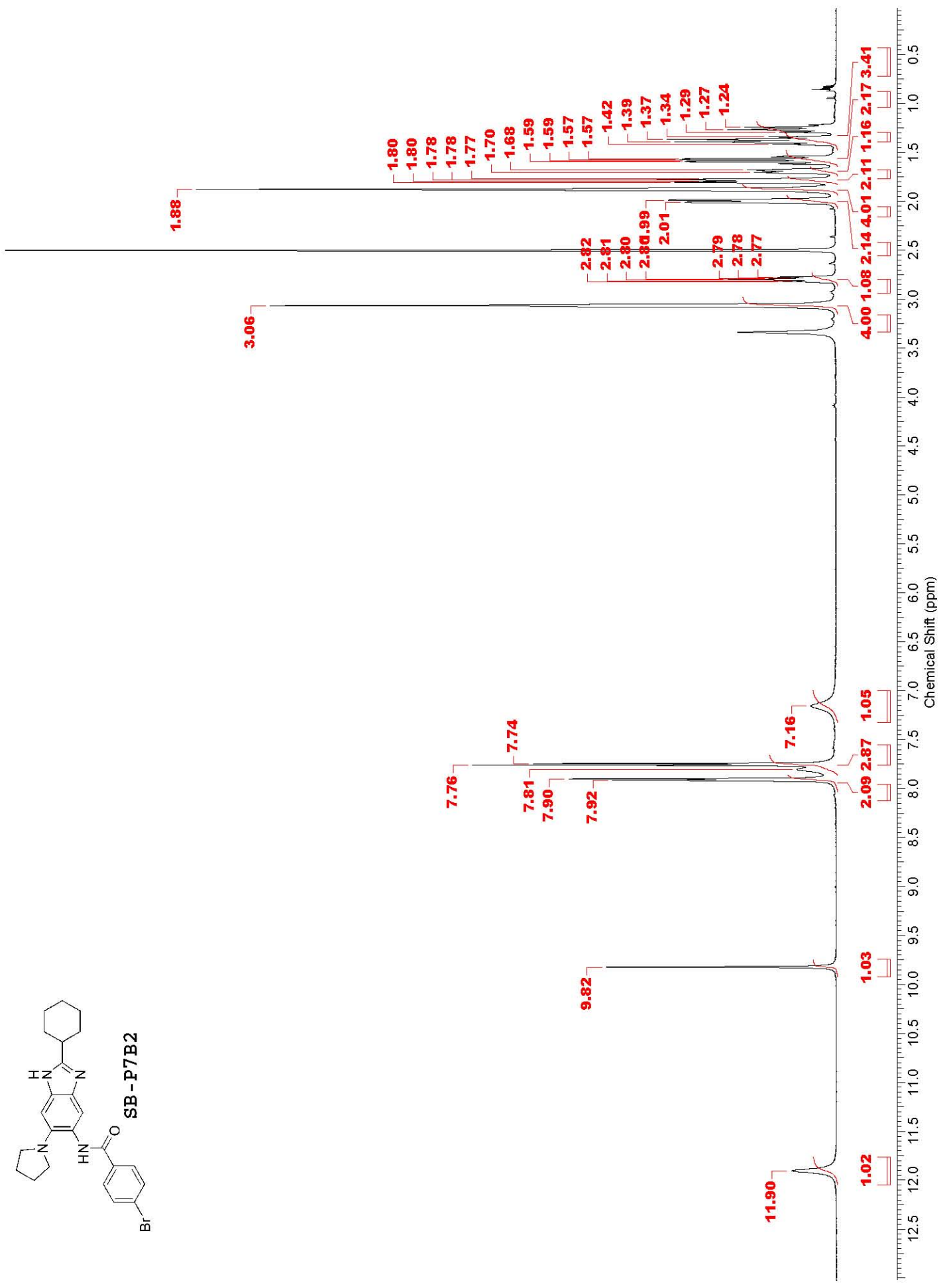
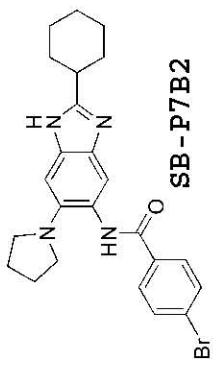


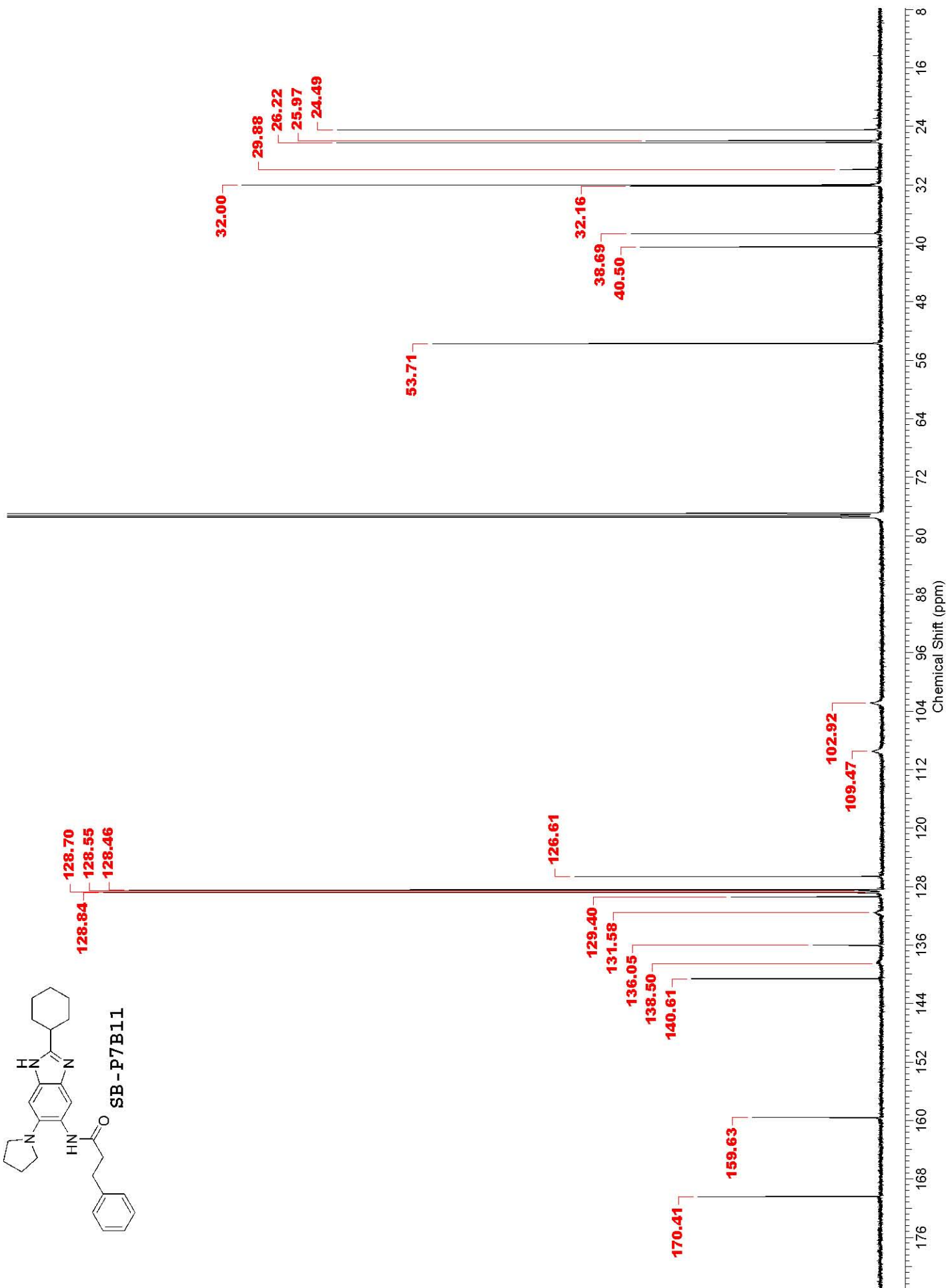
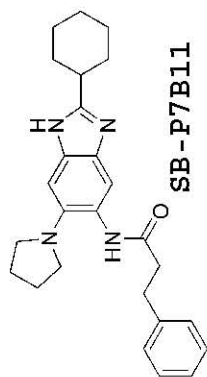


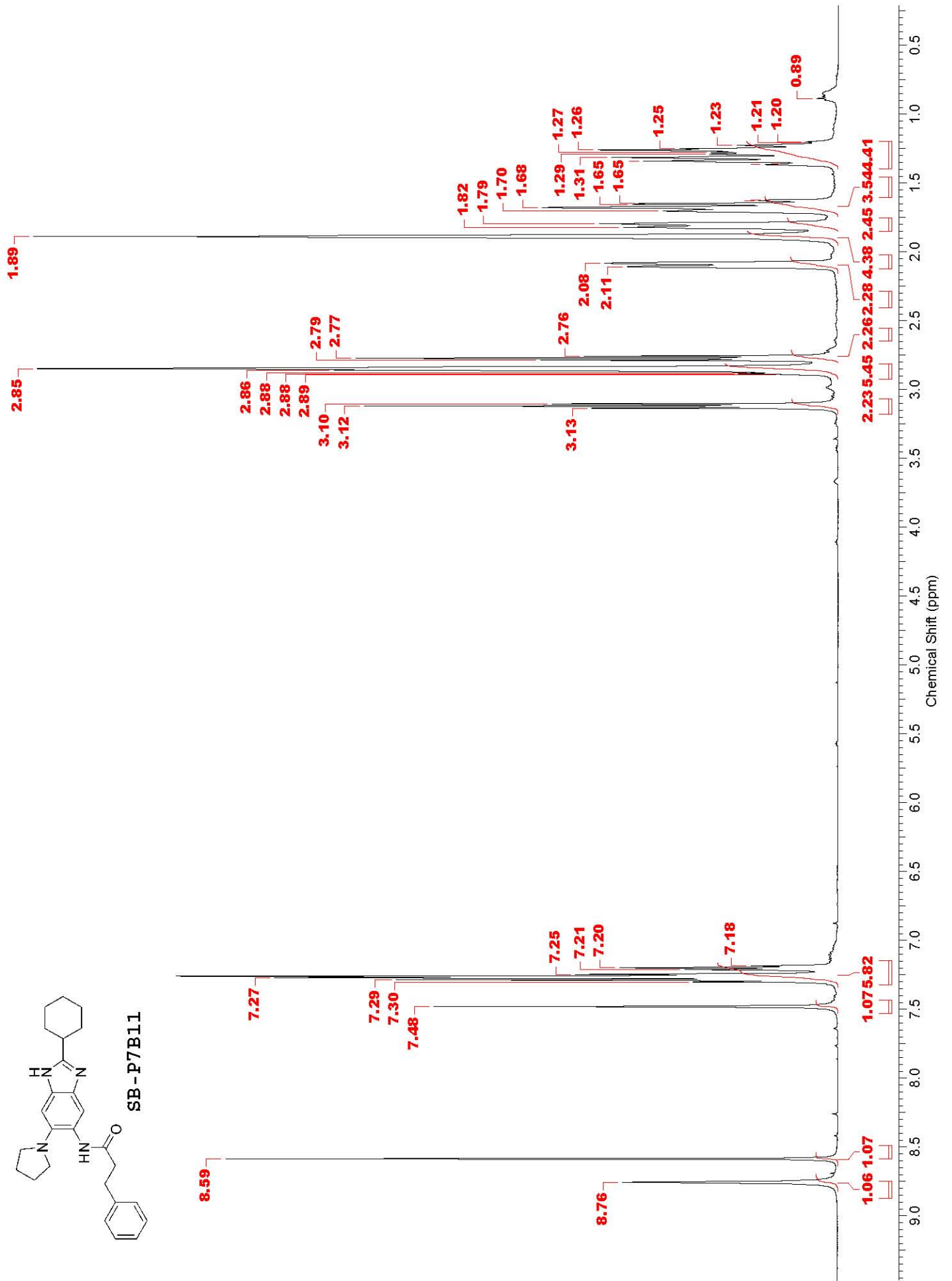
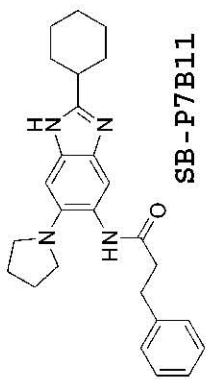


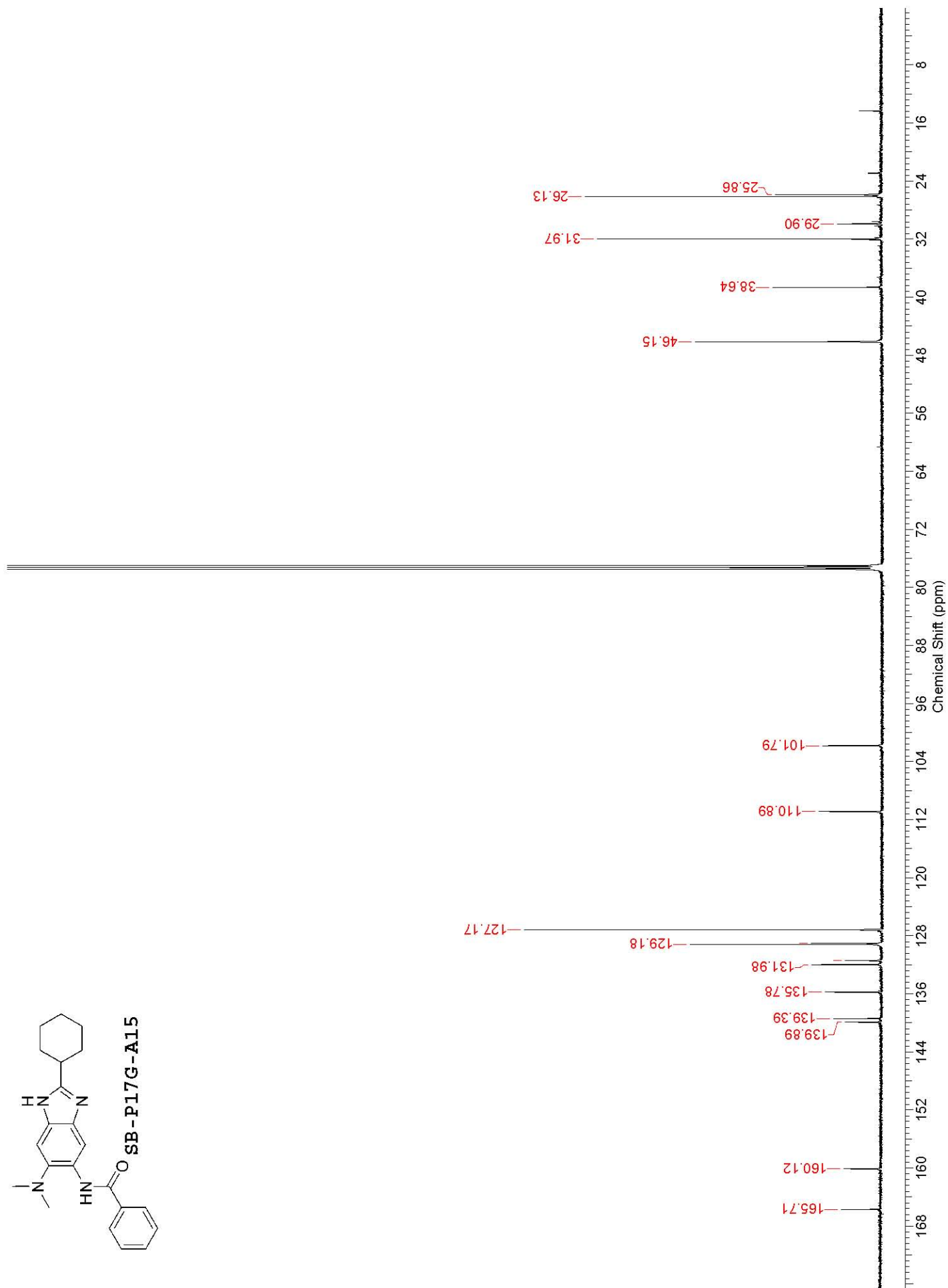
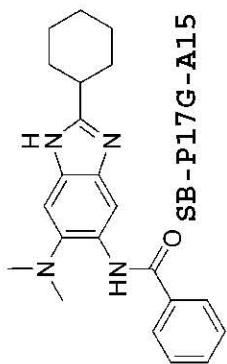


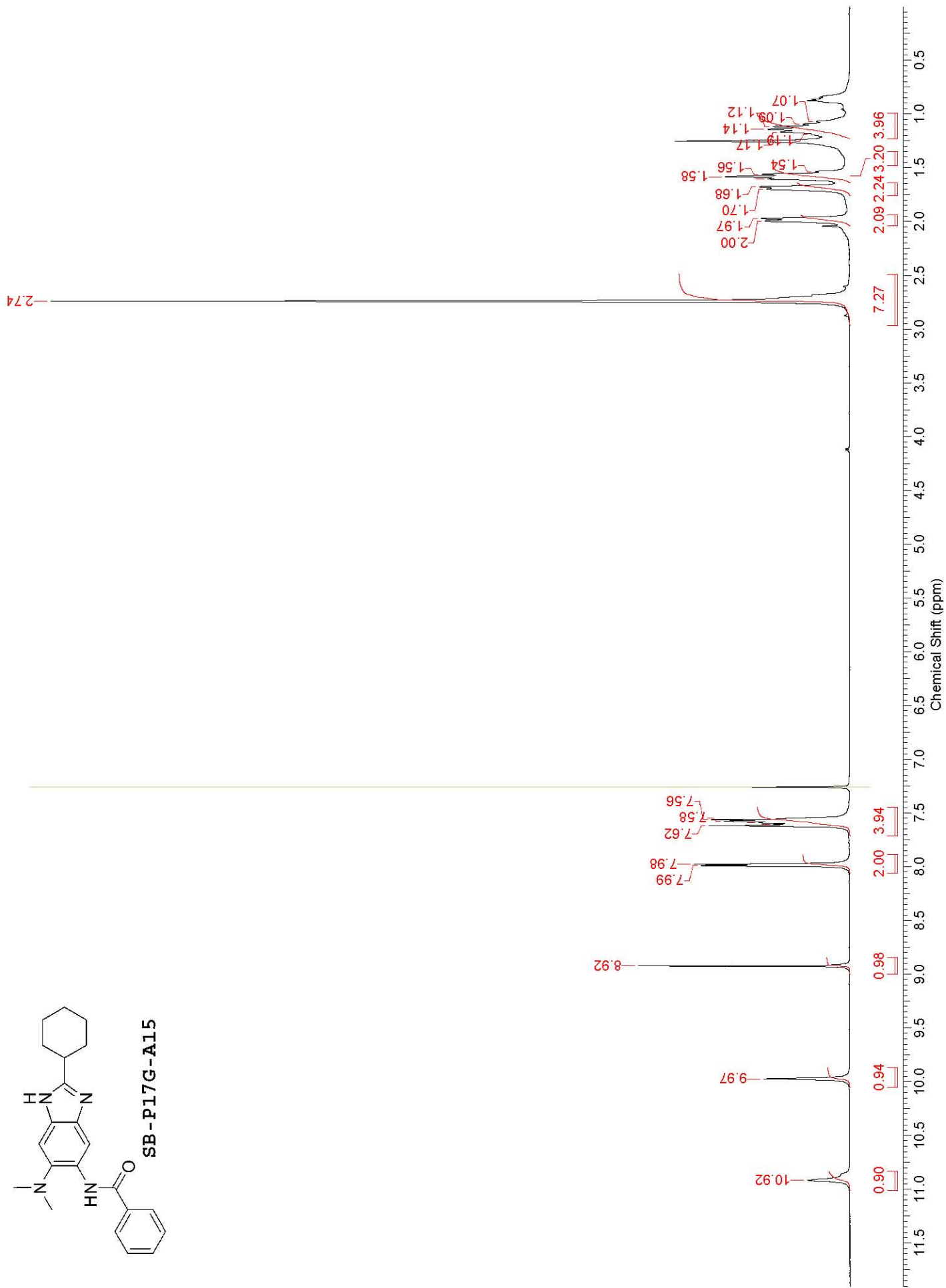
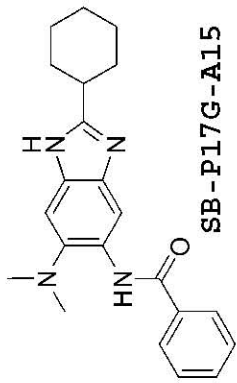


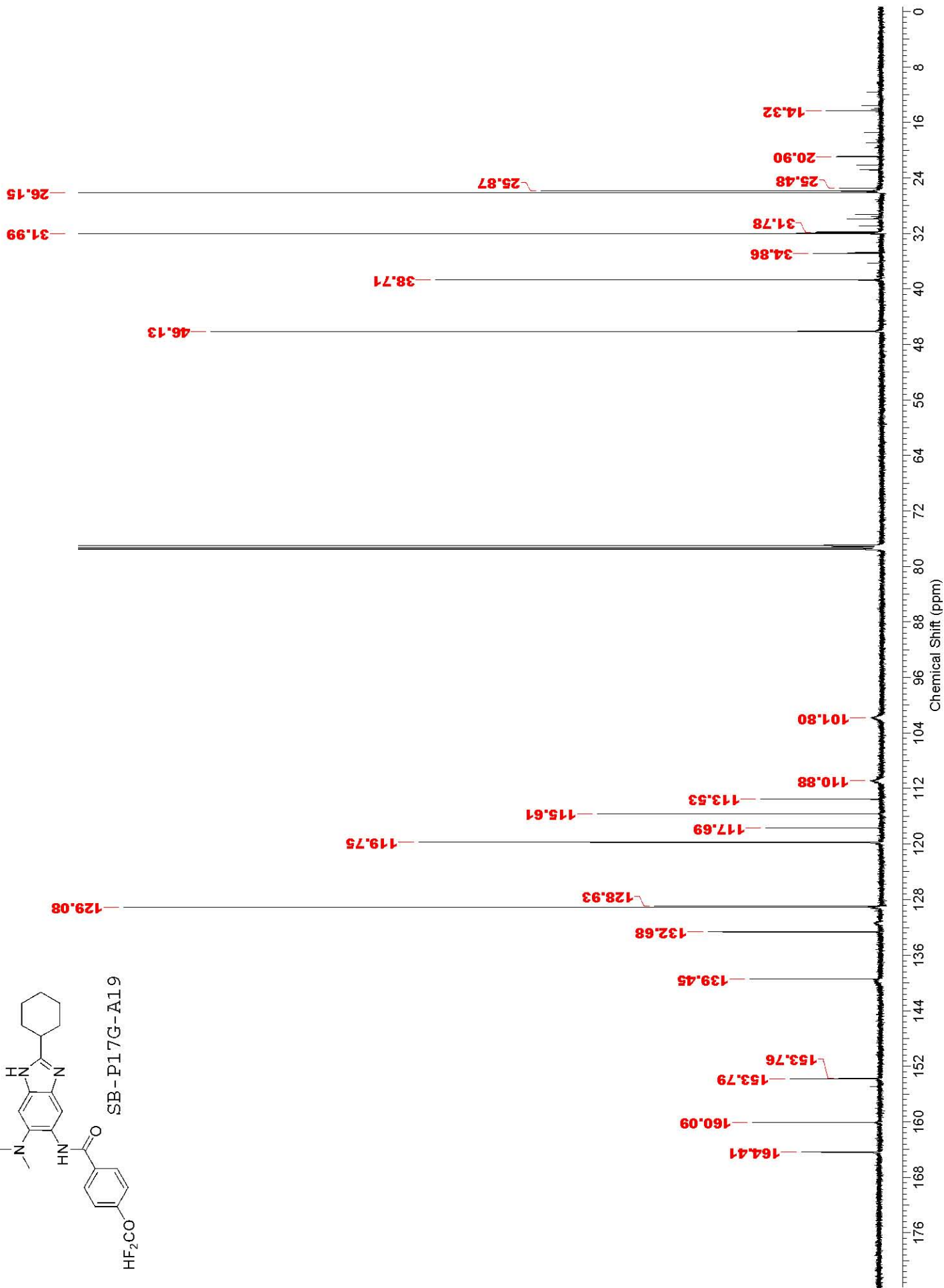
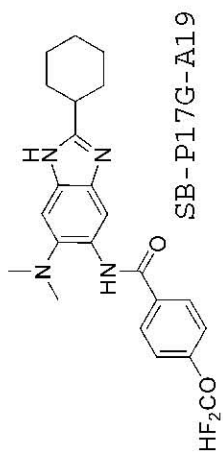


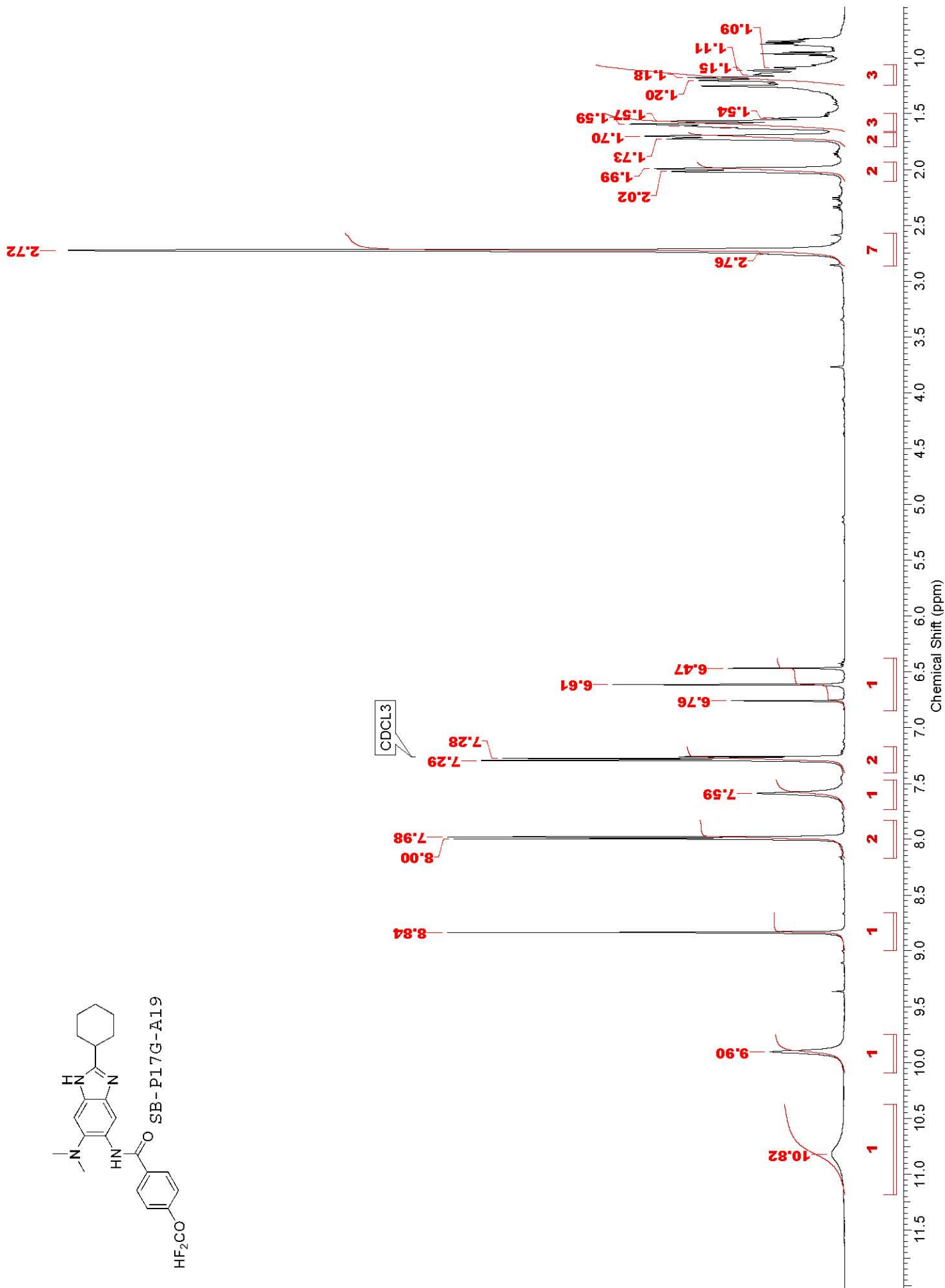
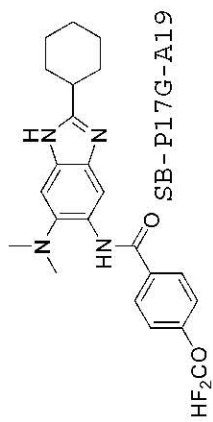


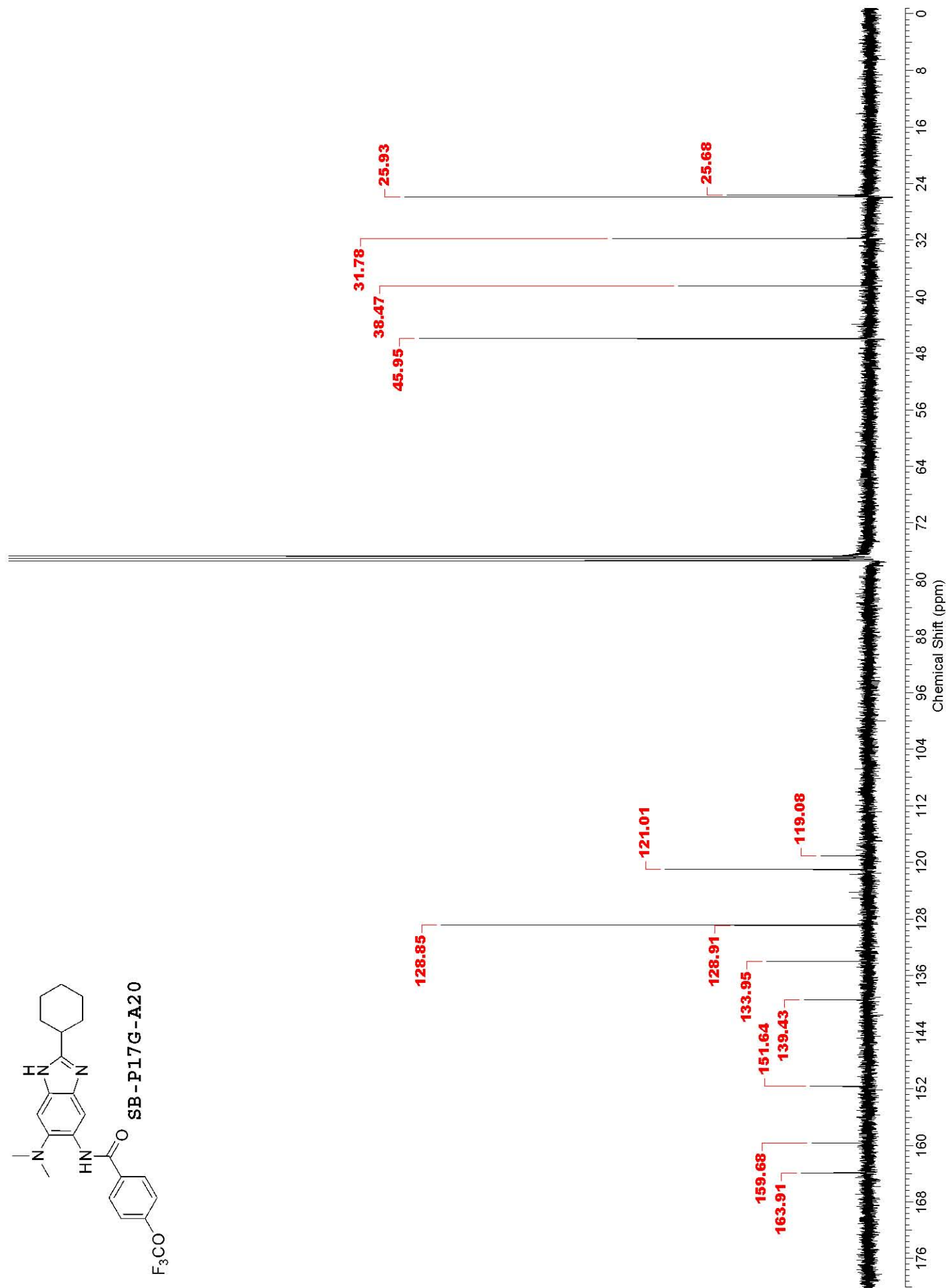
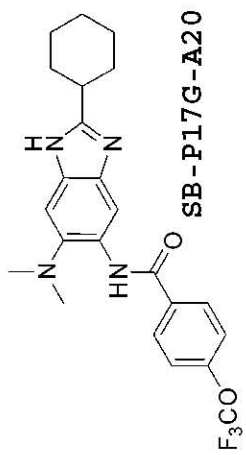


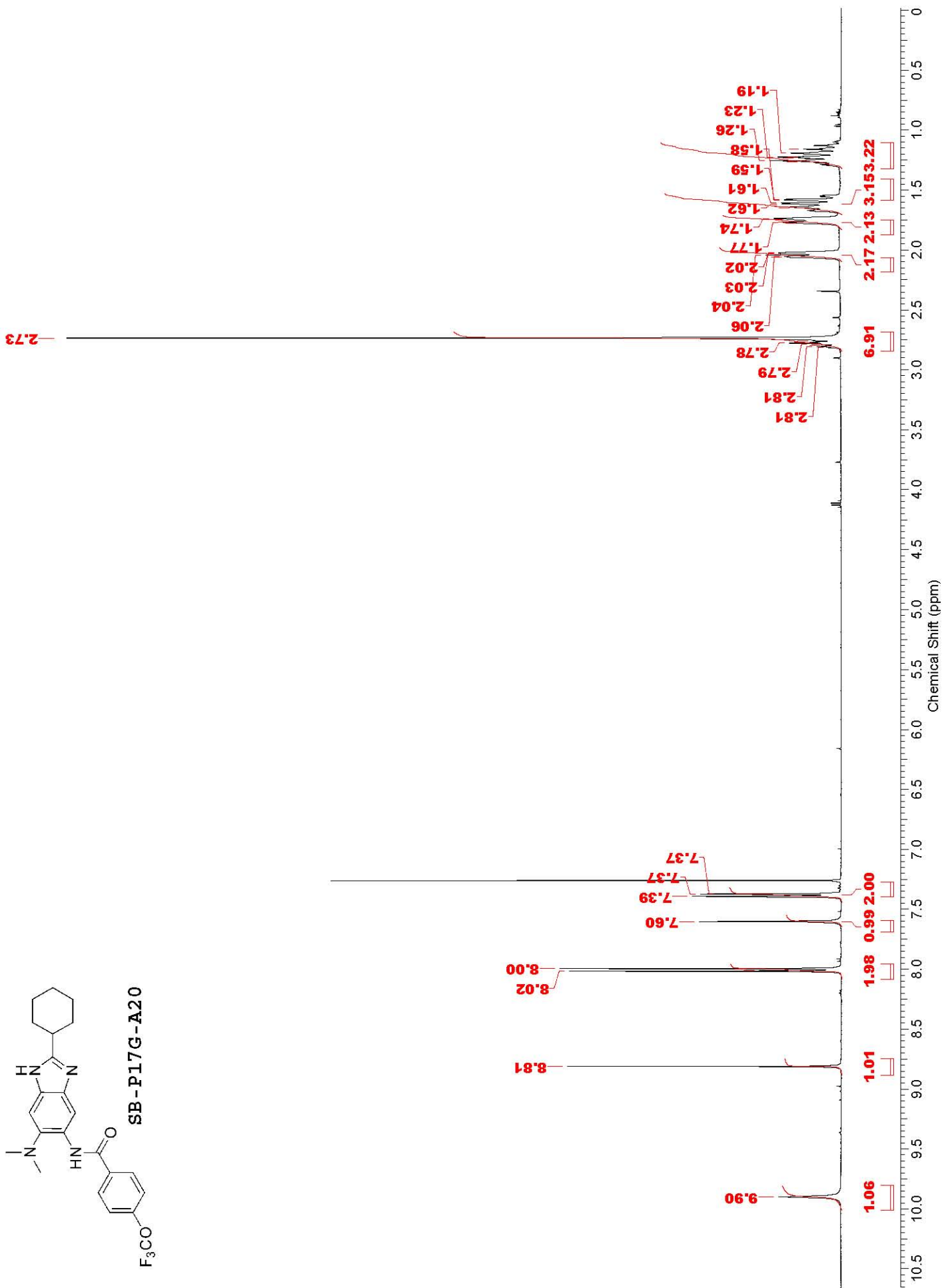
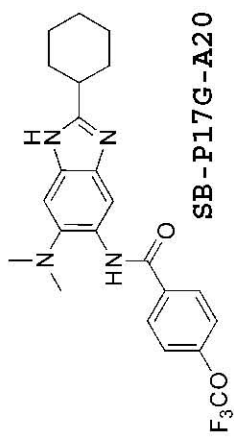


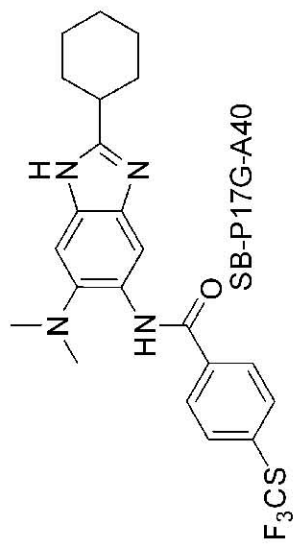




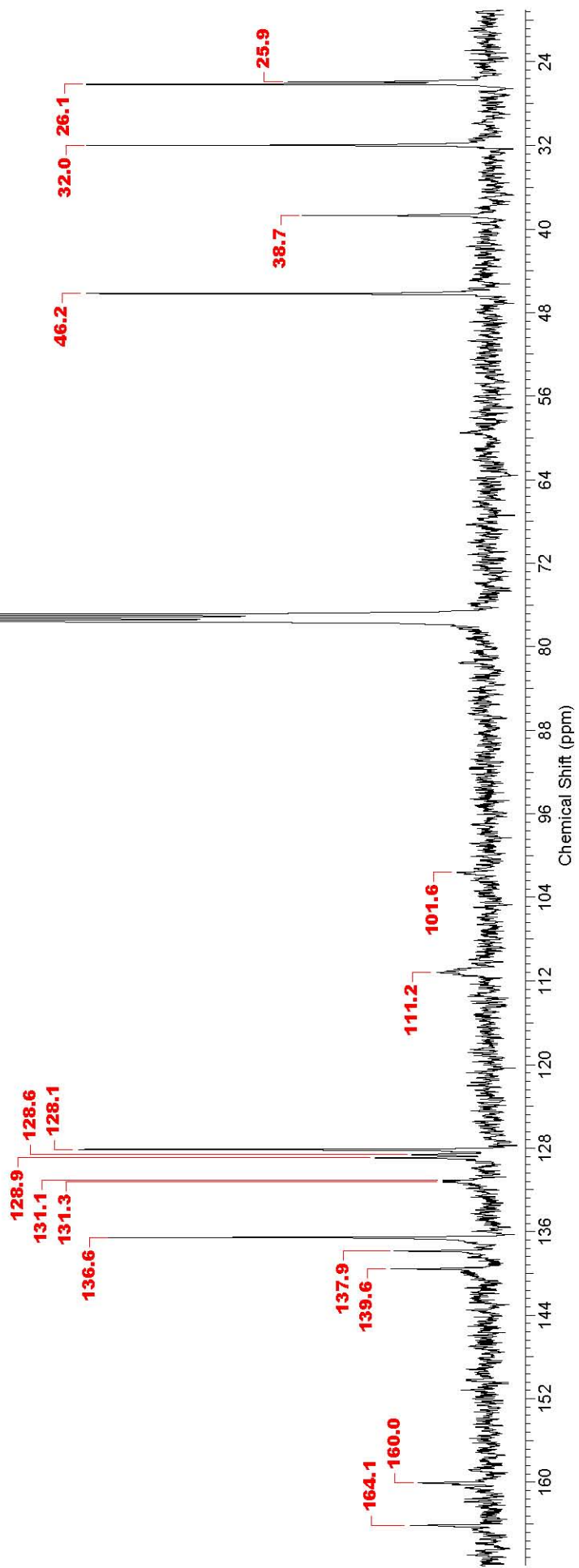


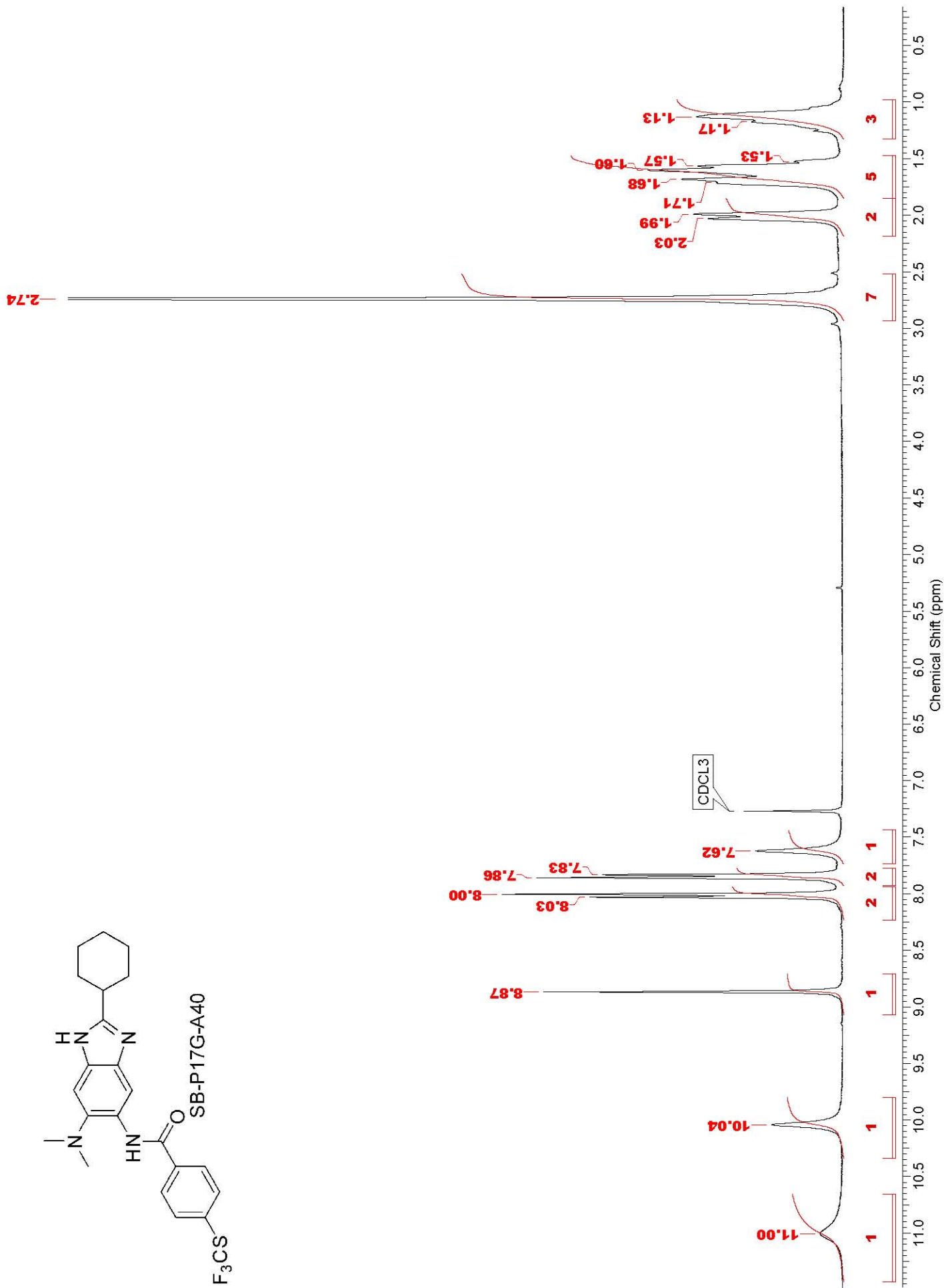
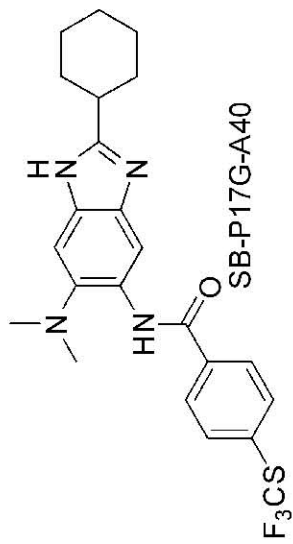


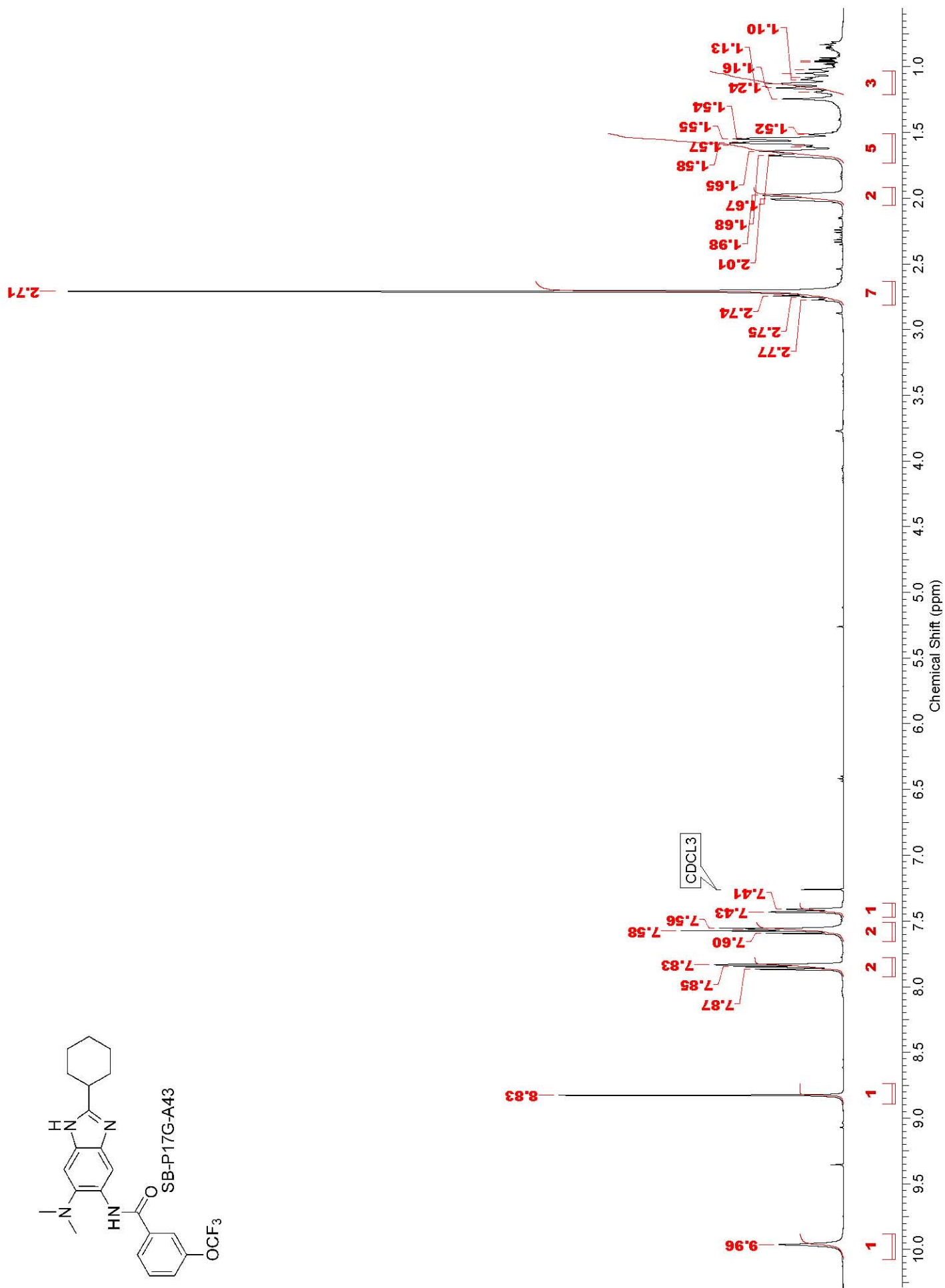
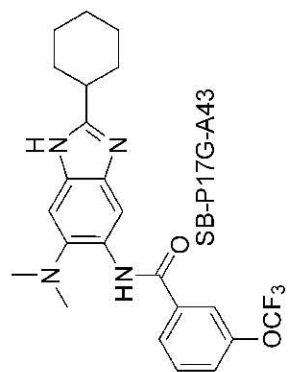


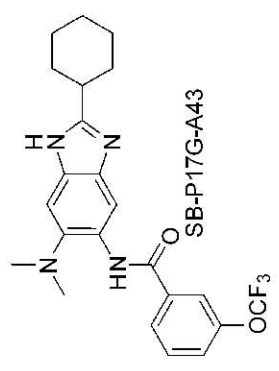
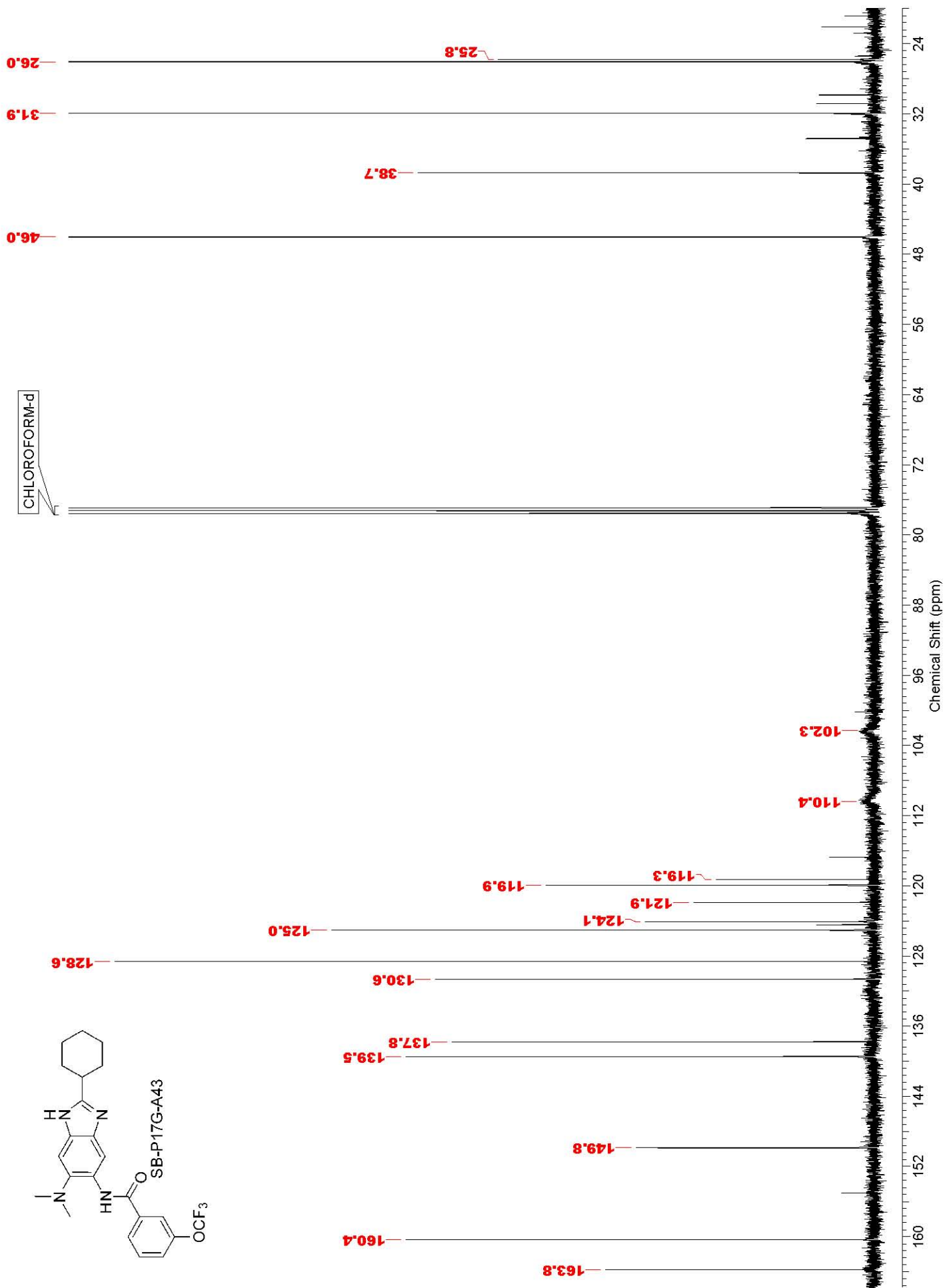


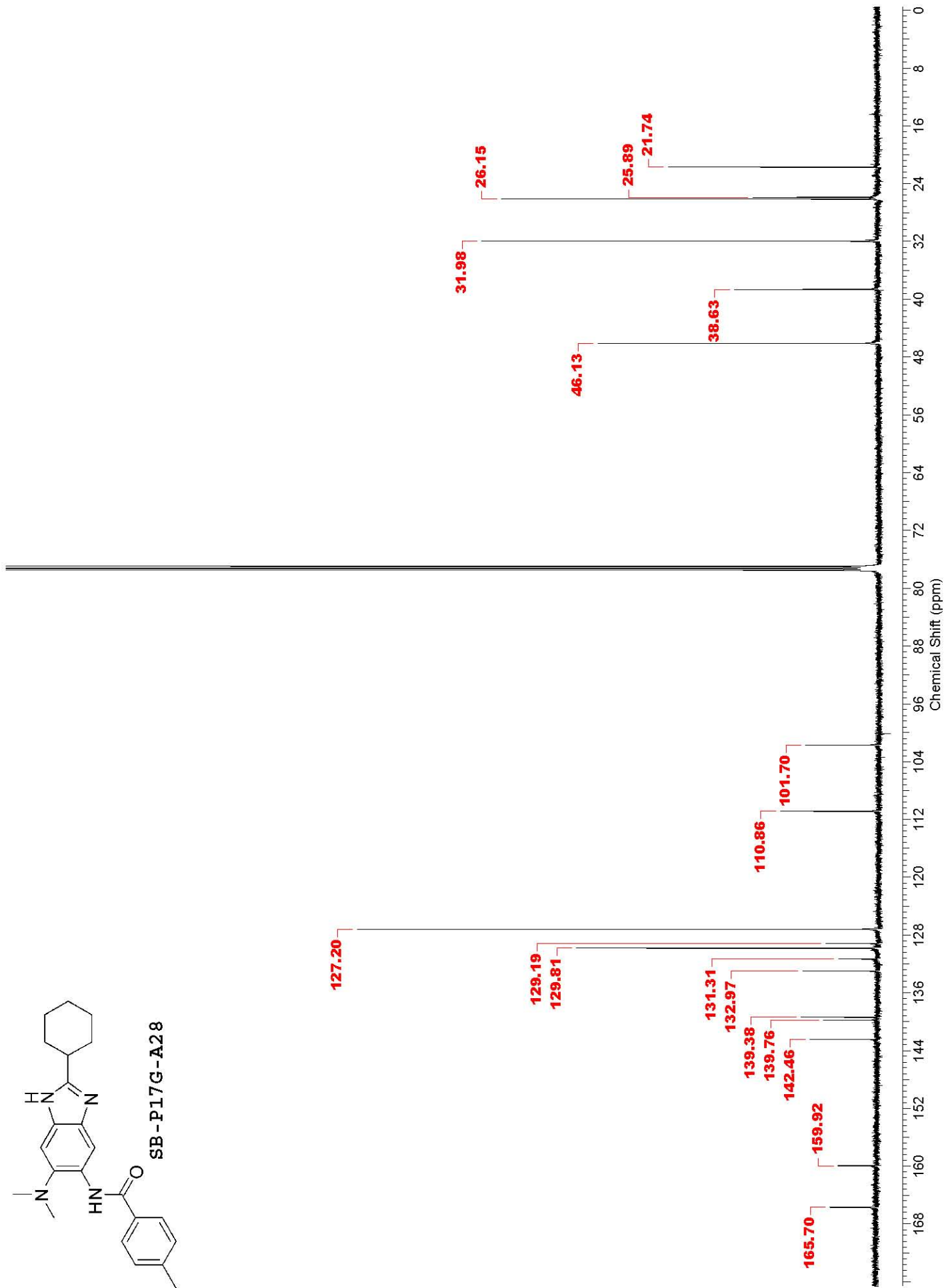
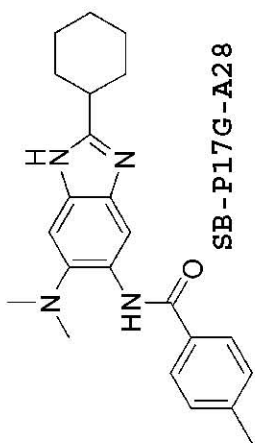
CHLOROFORM-d

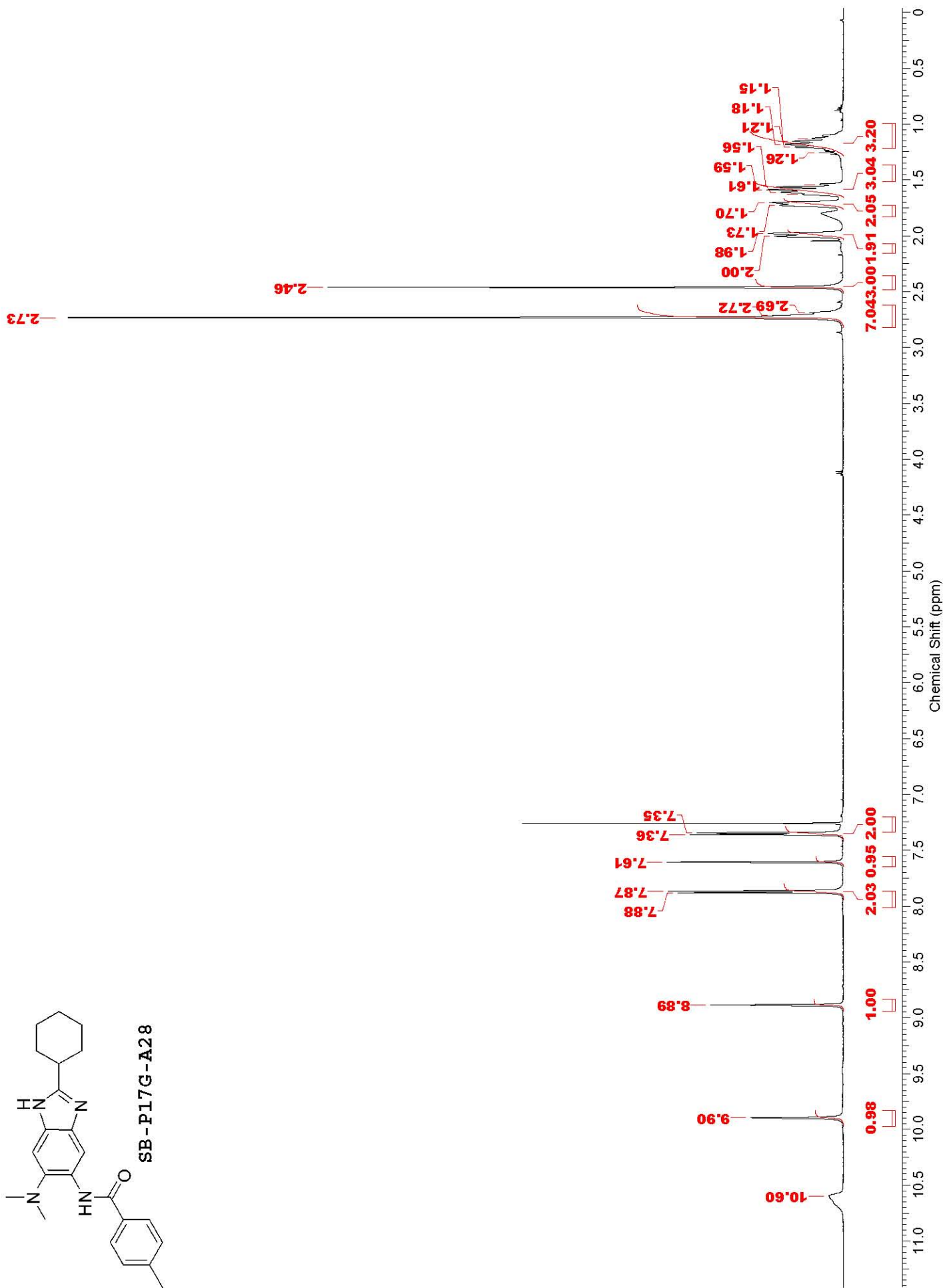
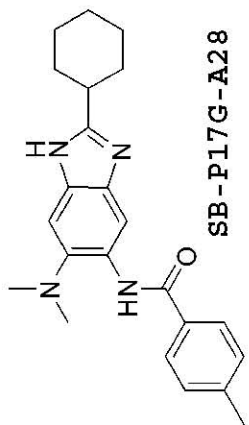


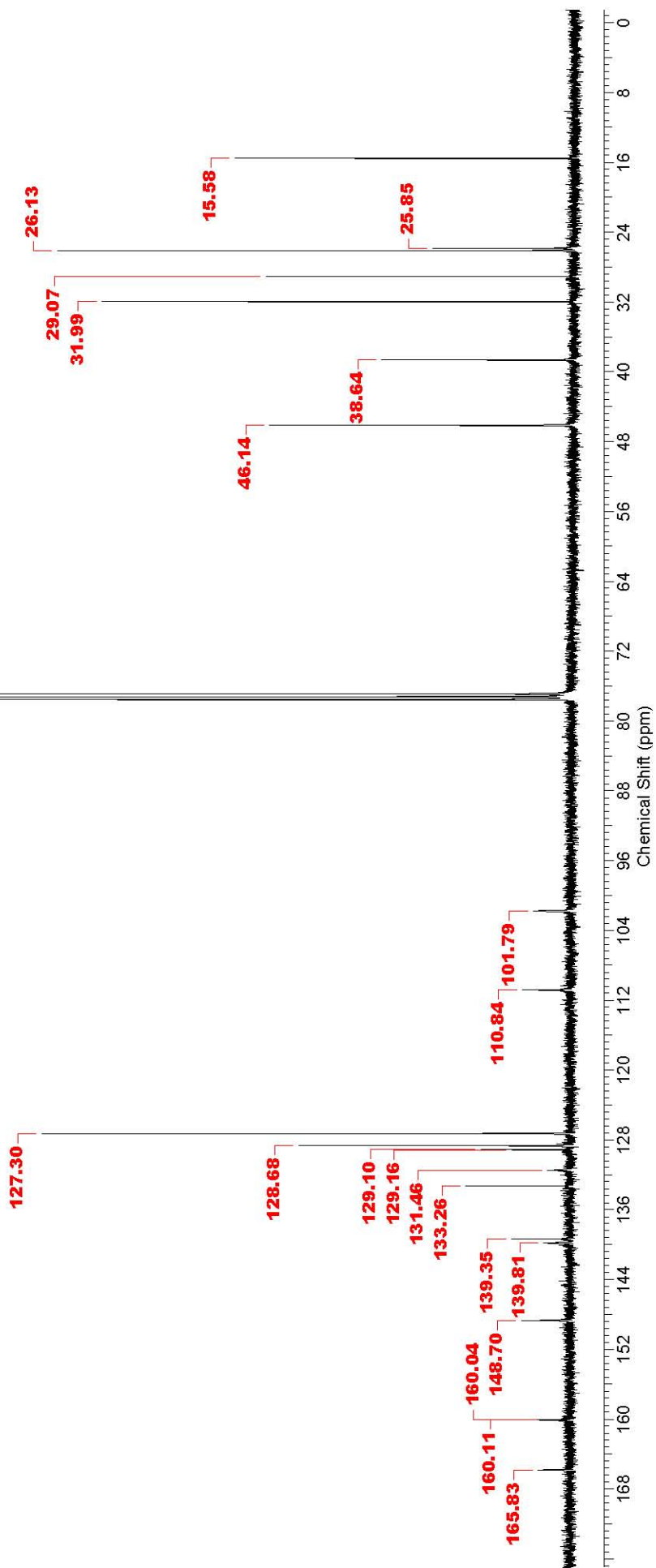
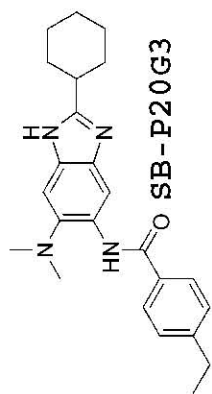


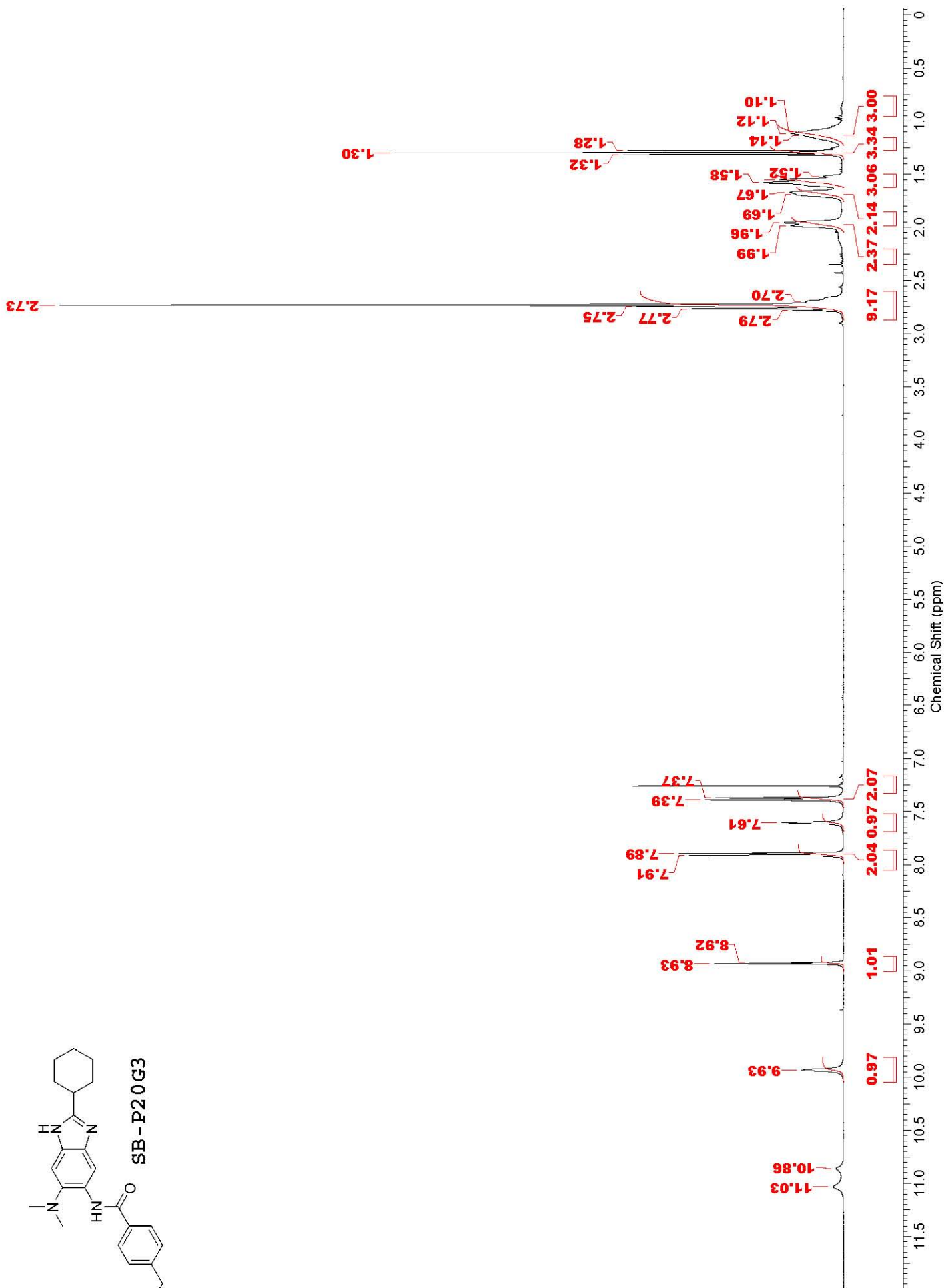
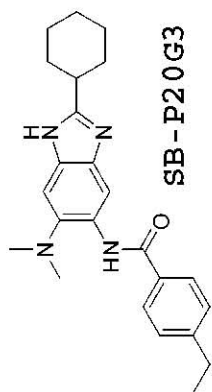


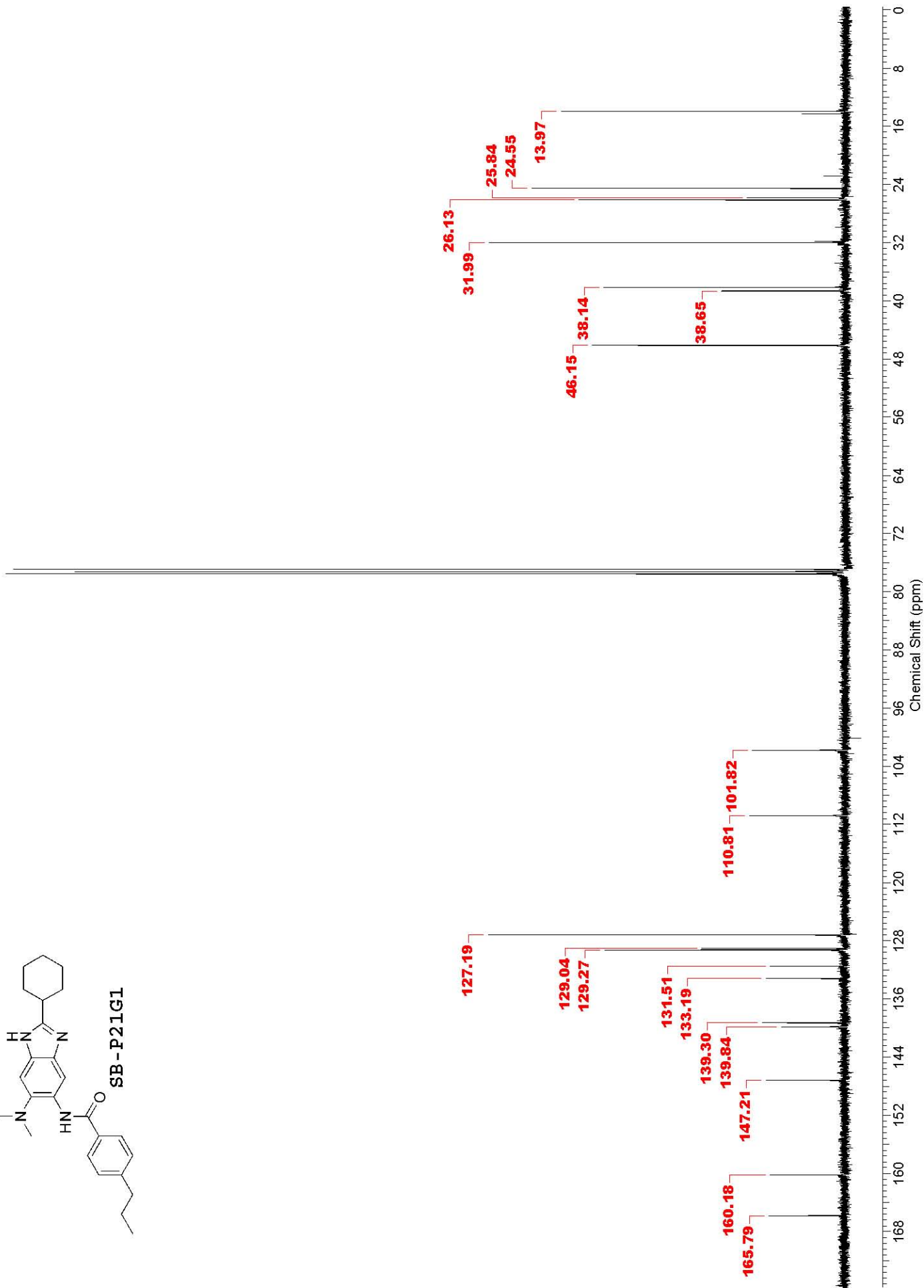
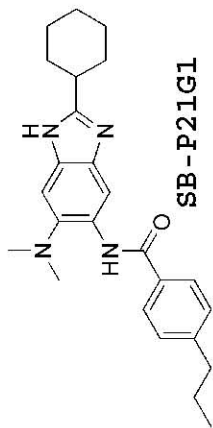


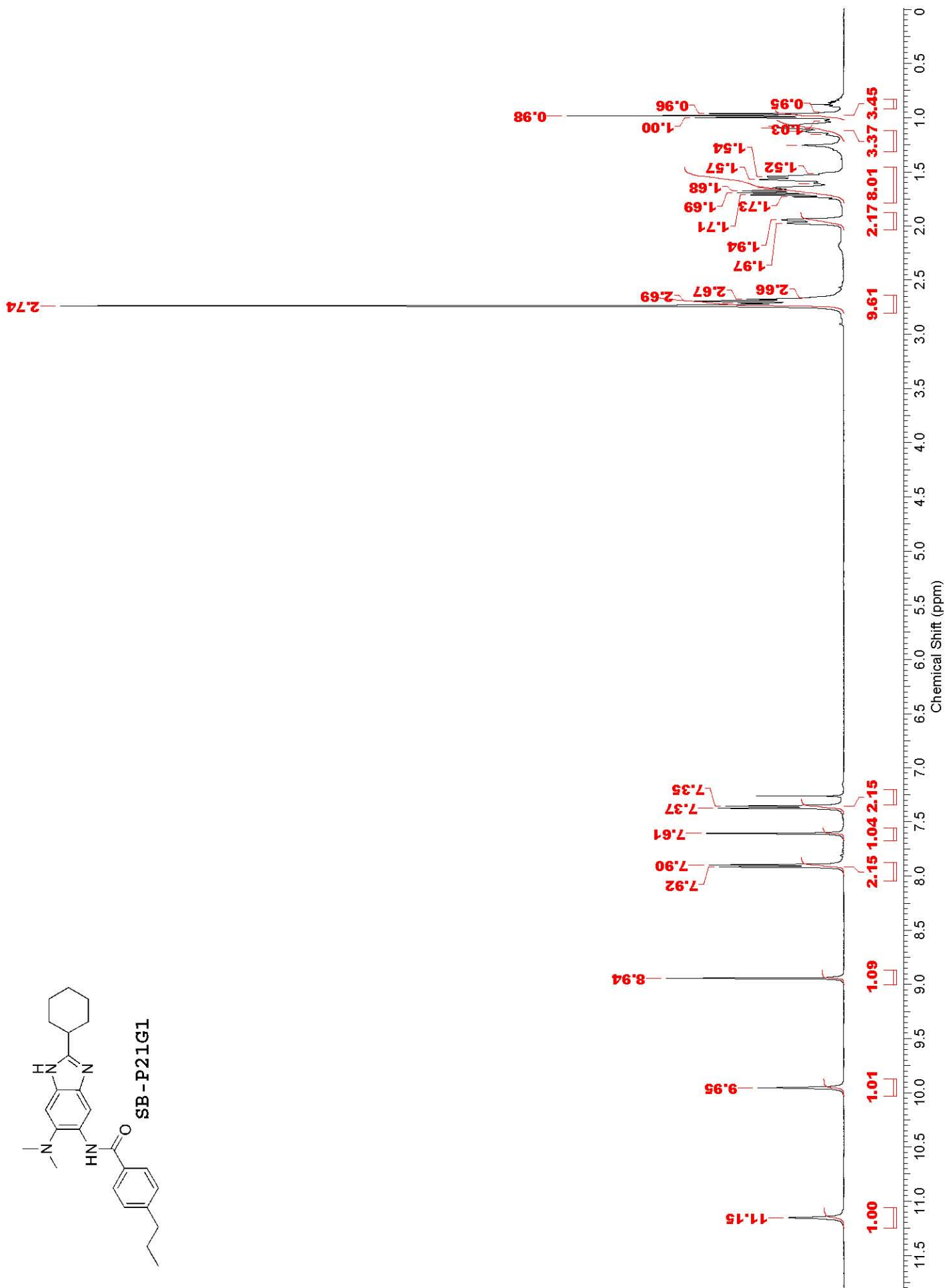
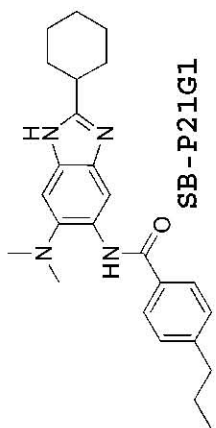


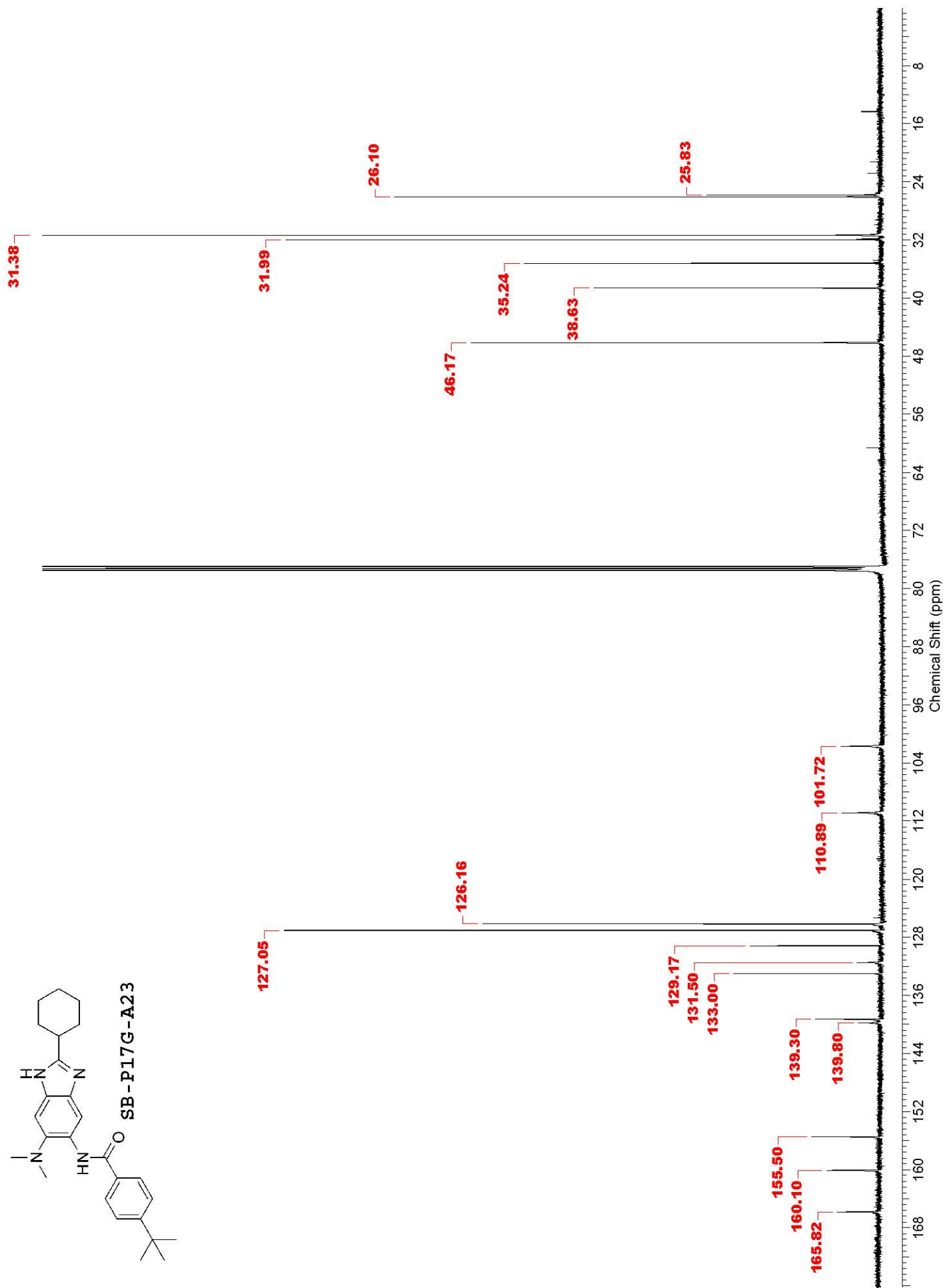
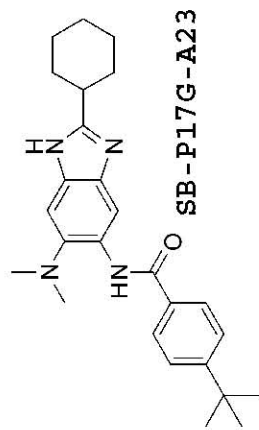


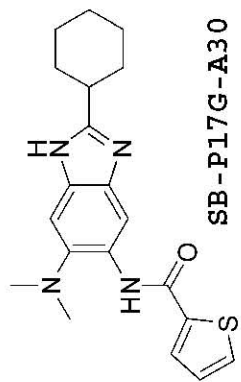




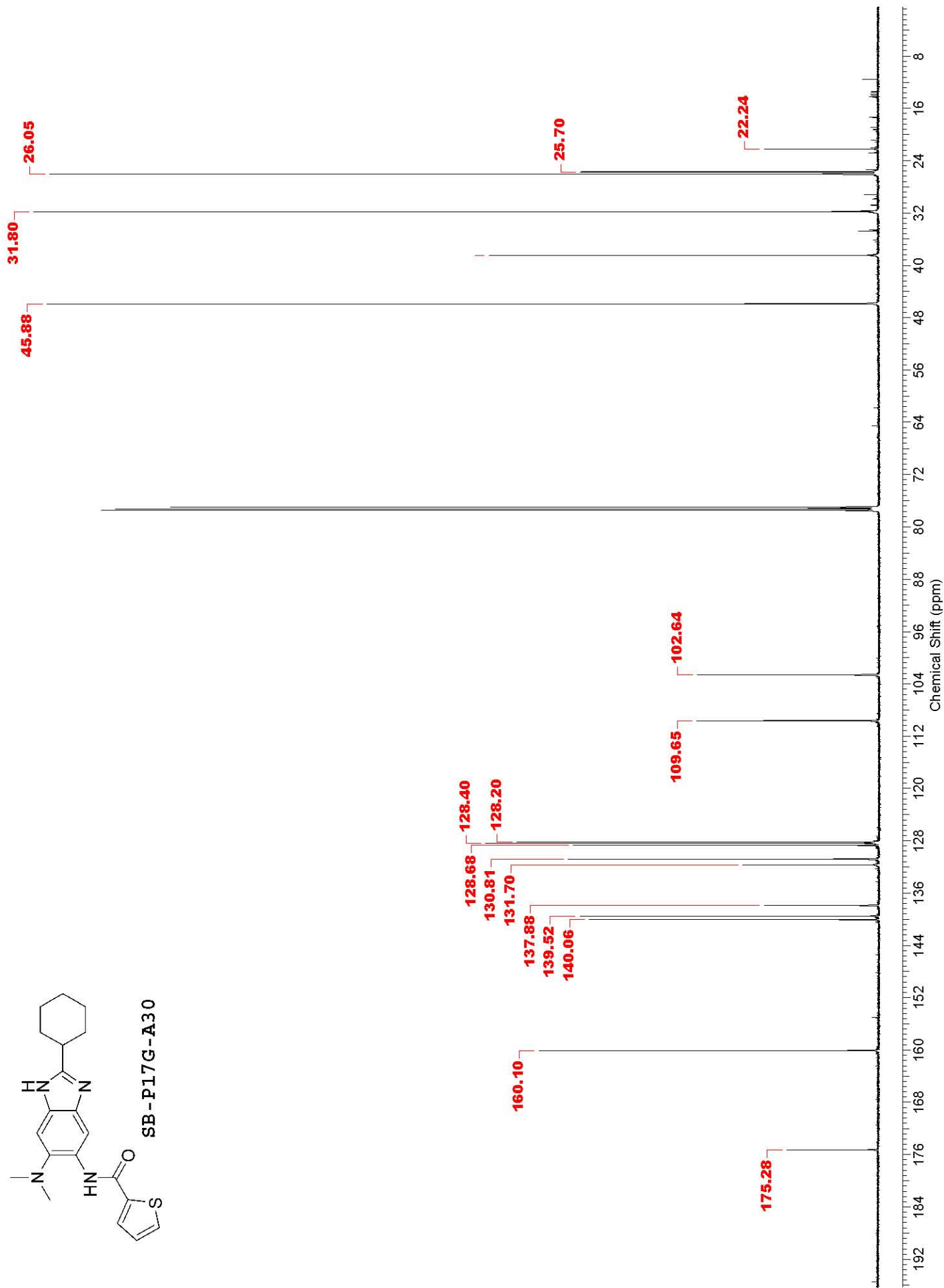


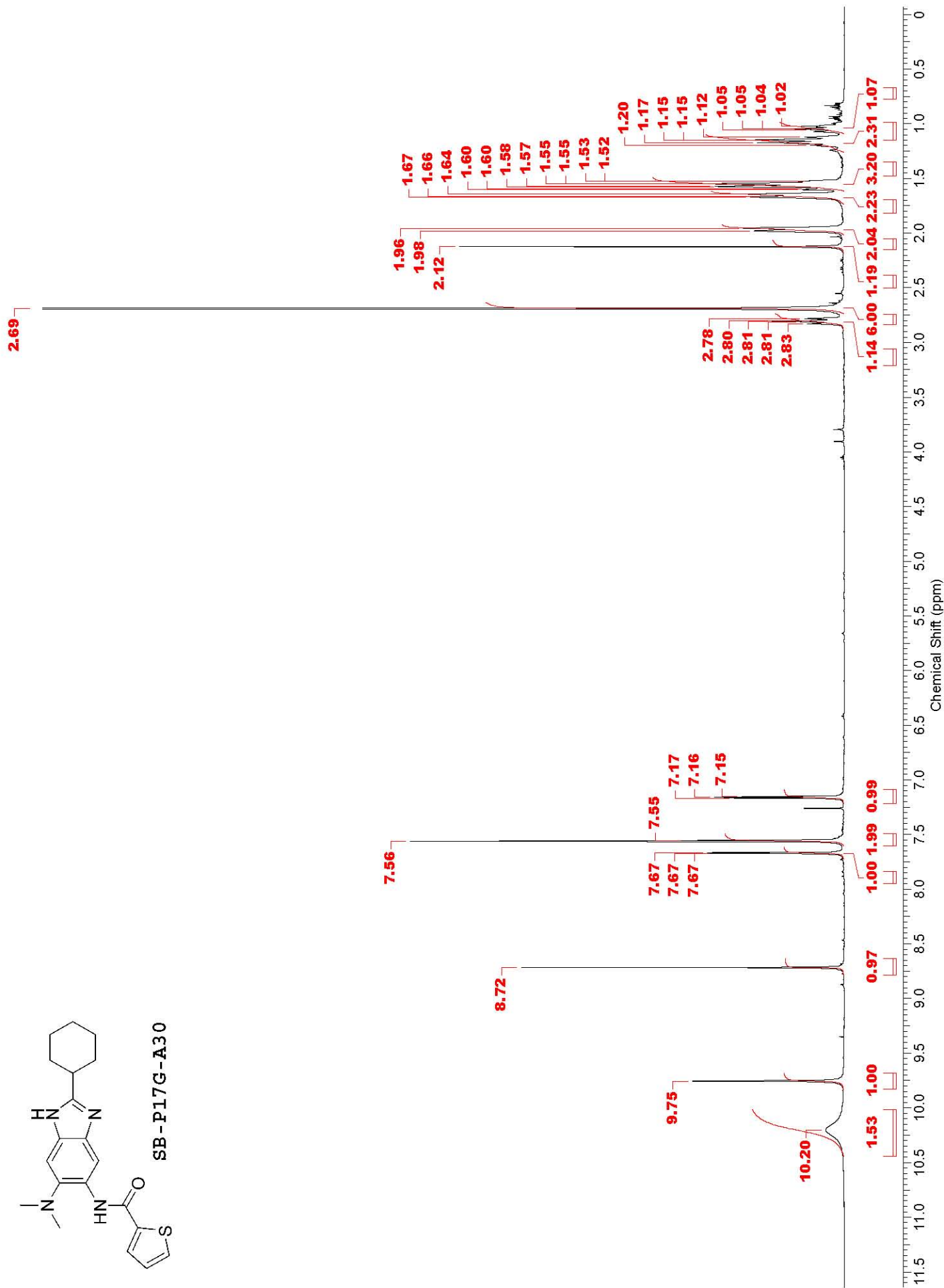
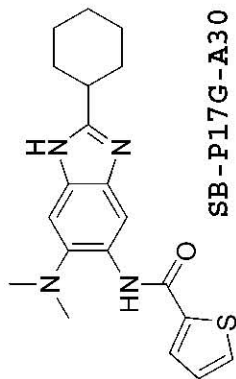


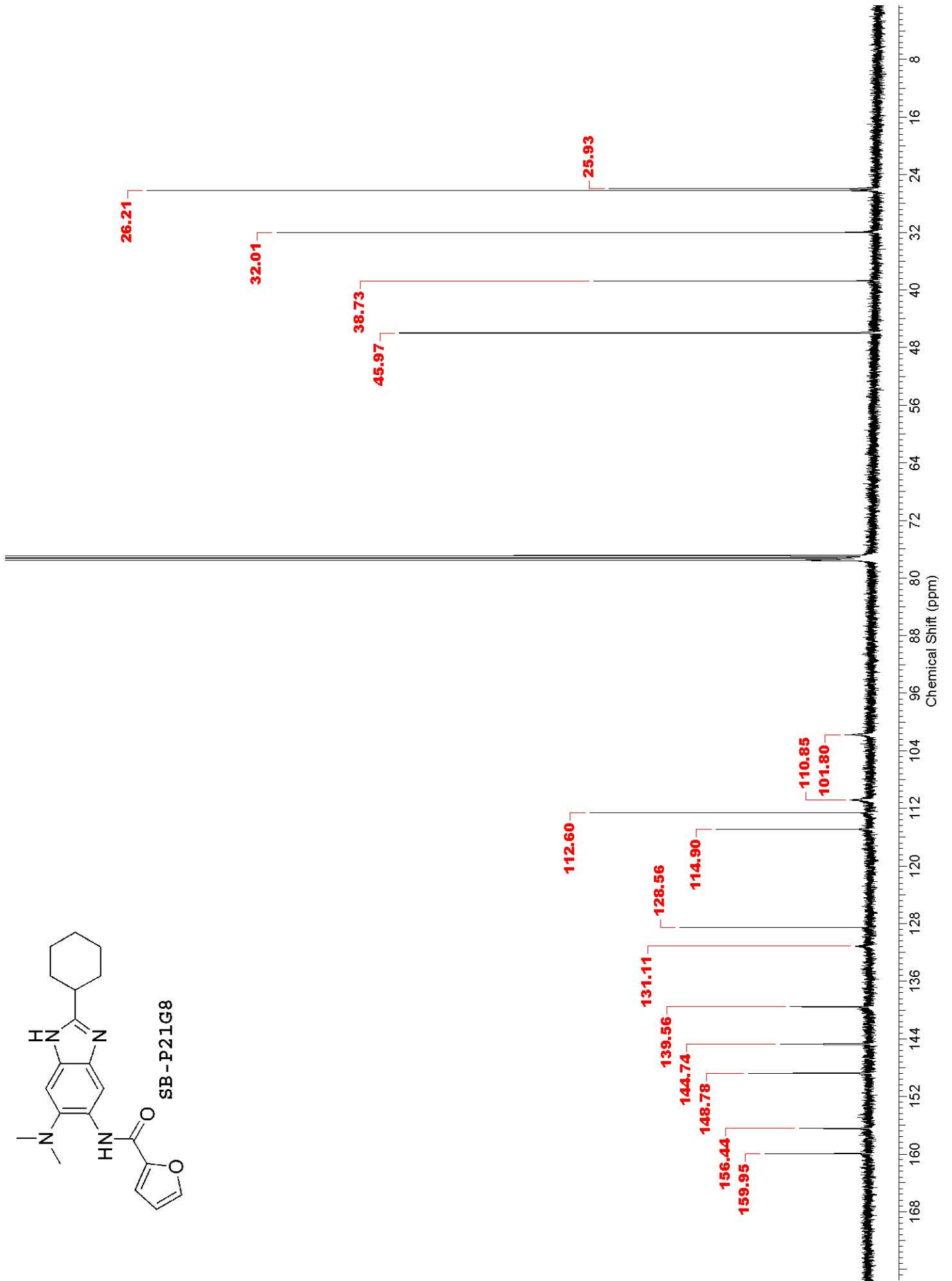
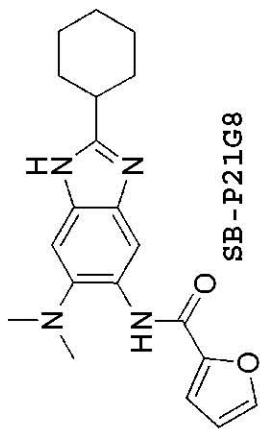


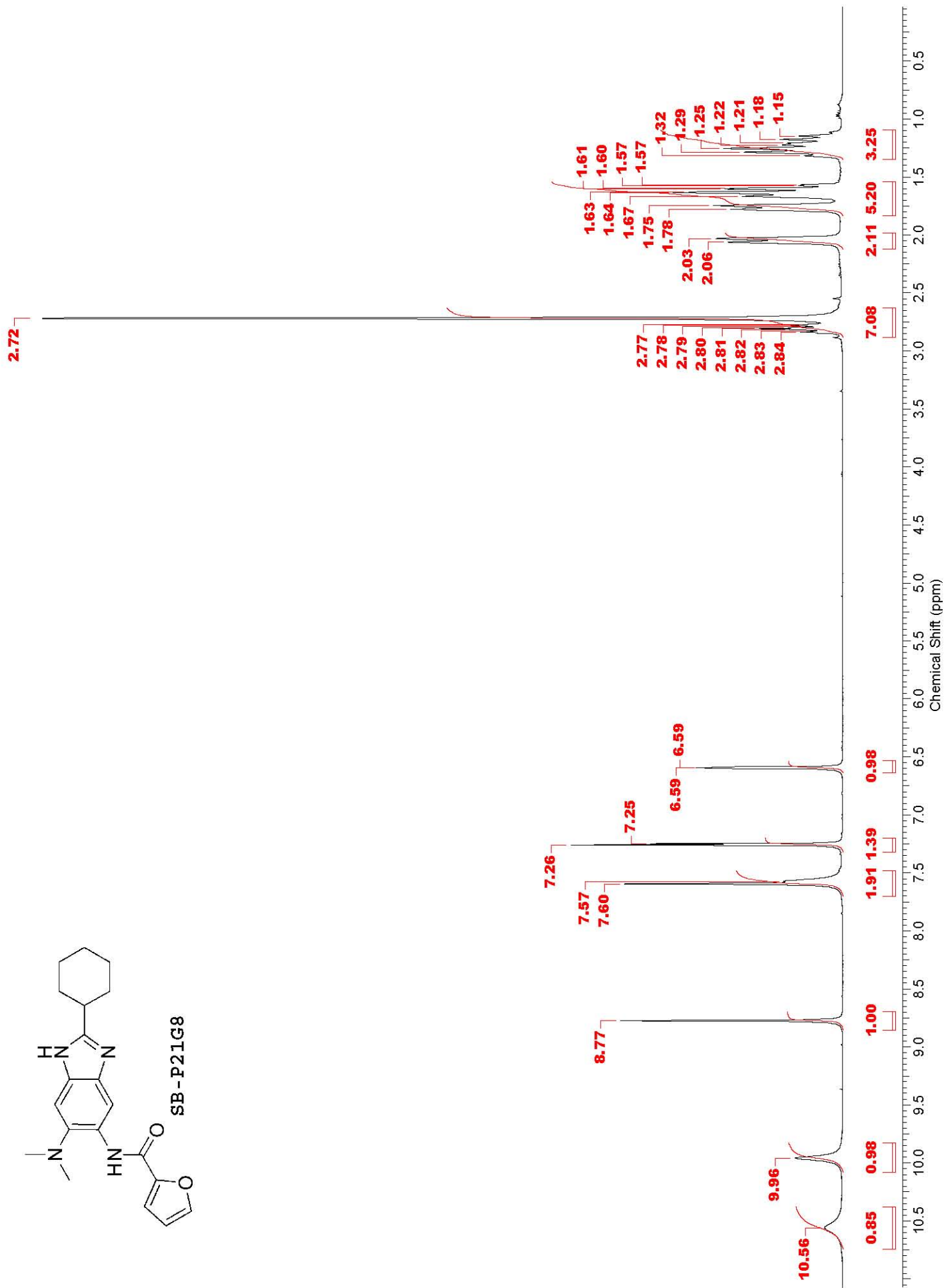
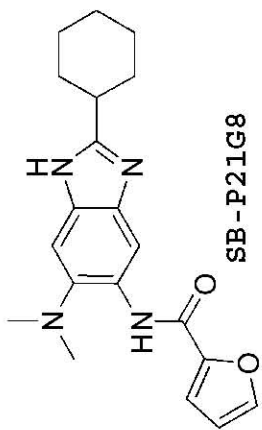


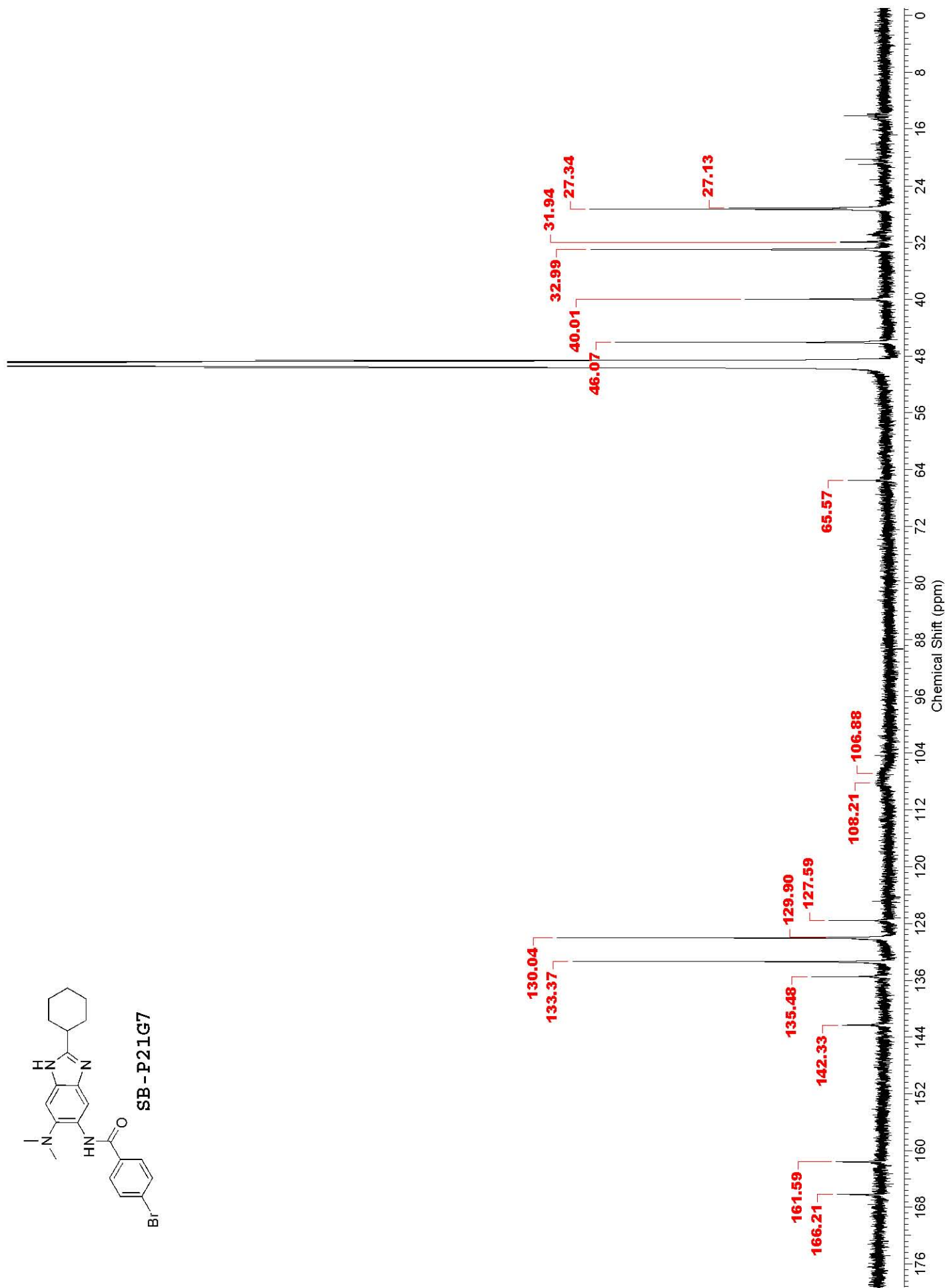
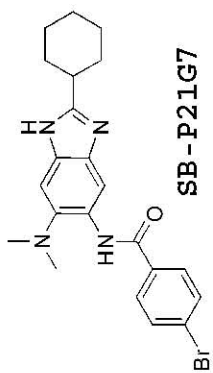
SB-P17G-A30

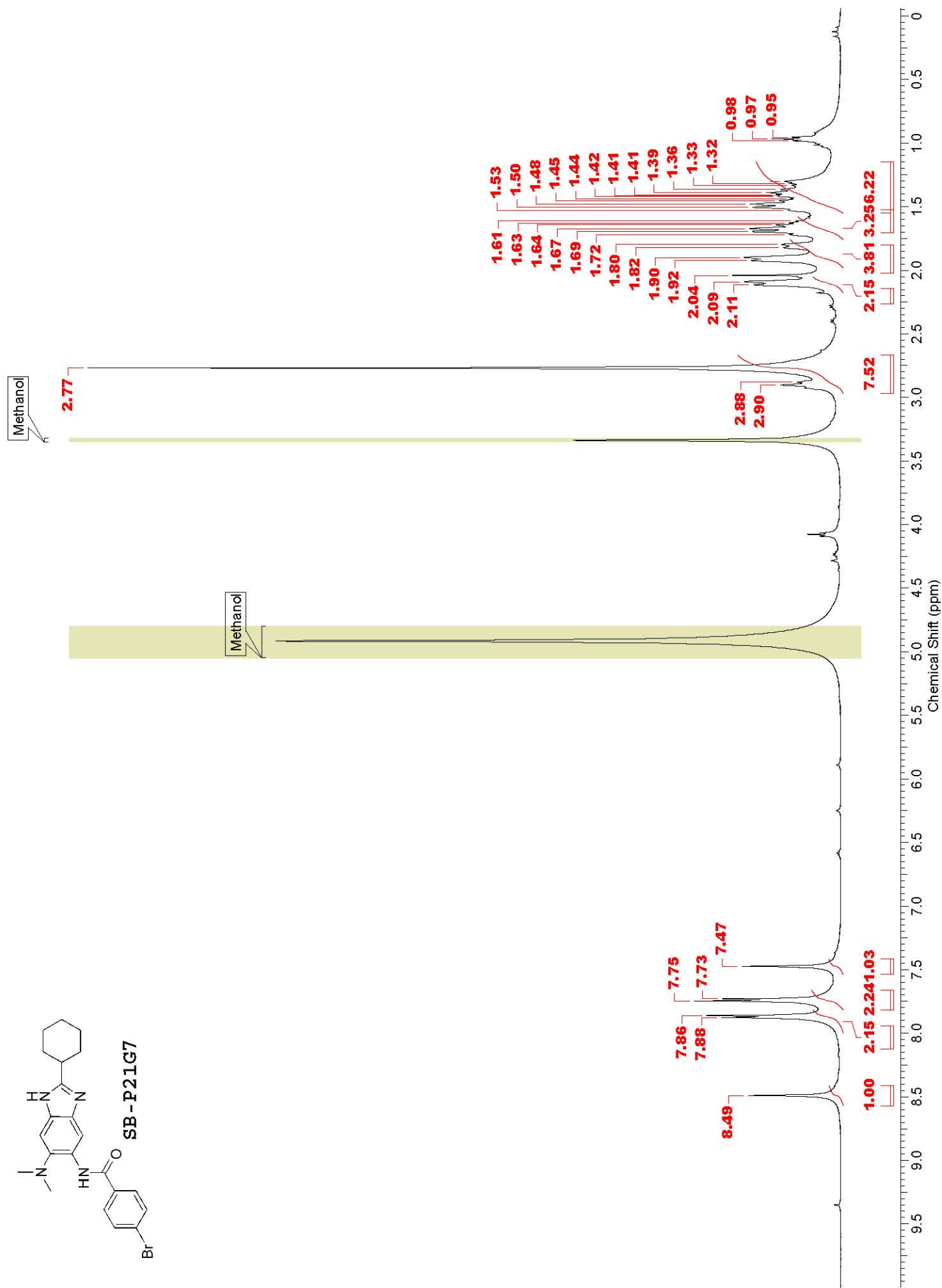
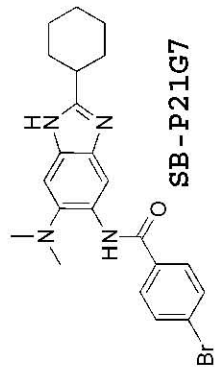


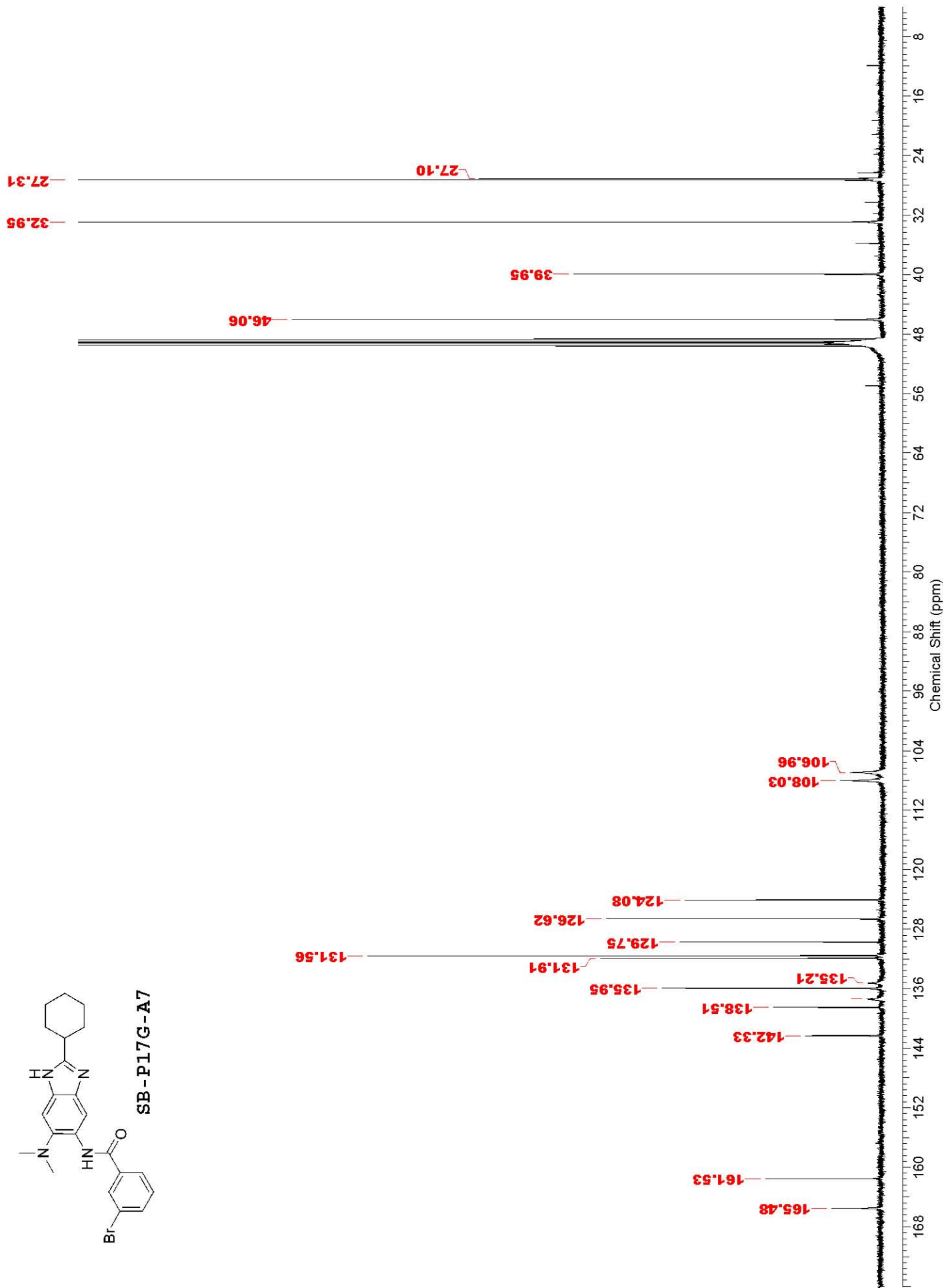
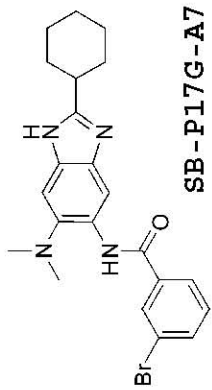


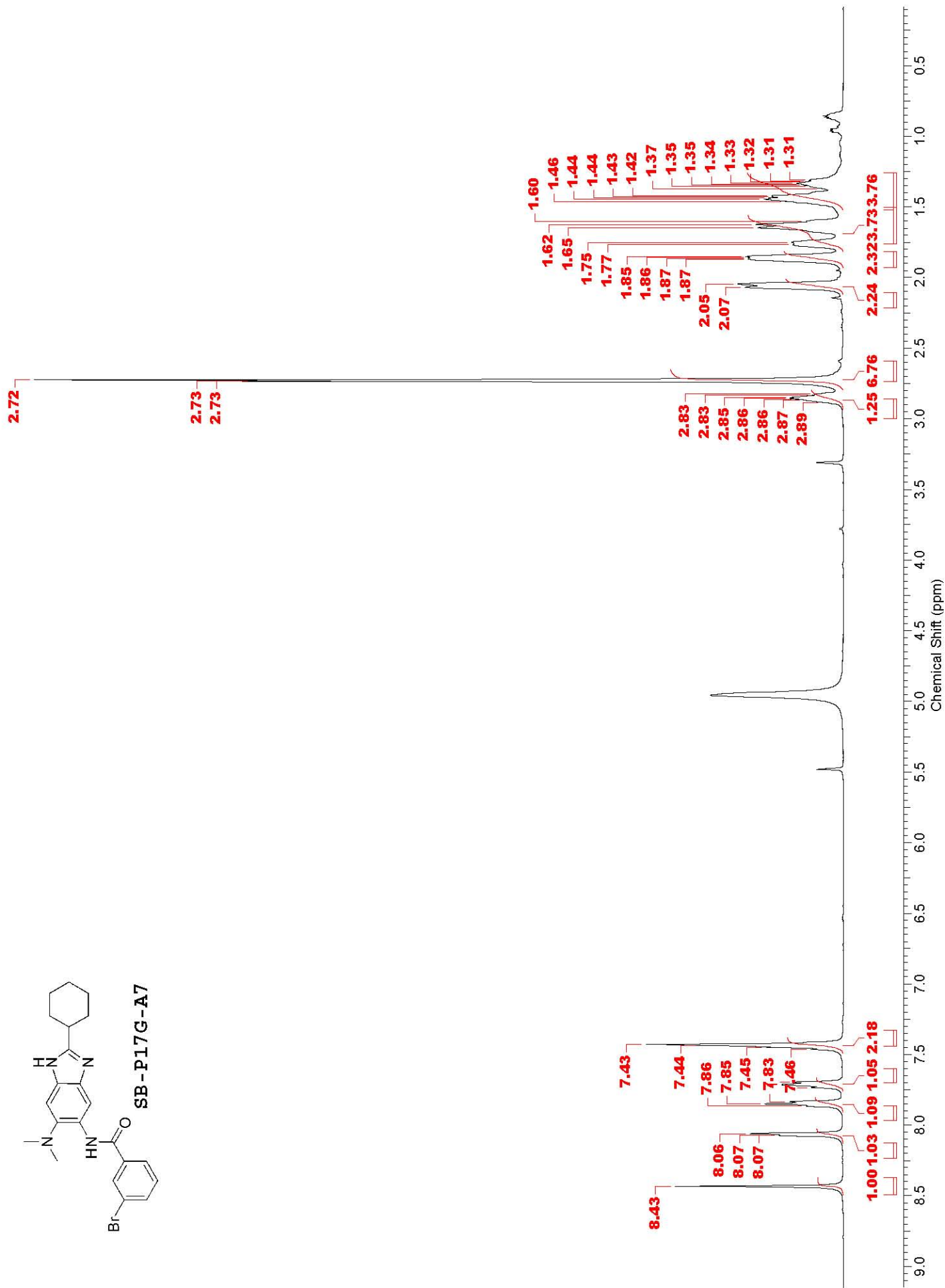
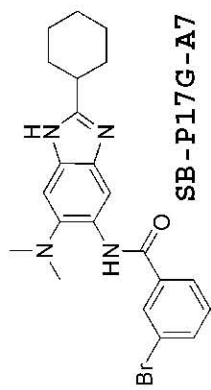


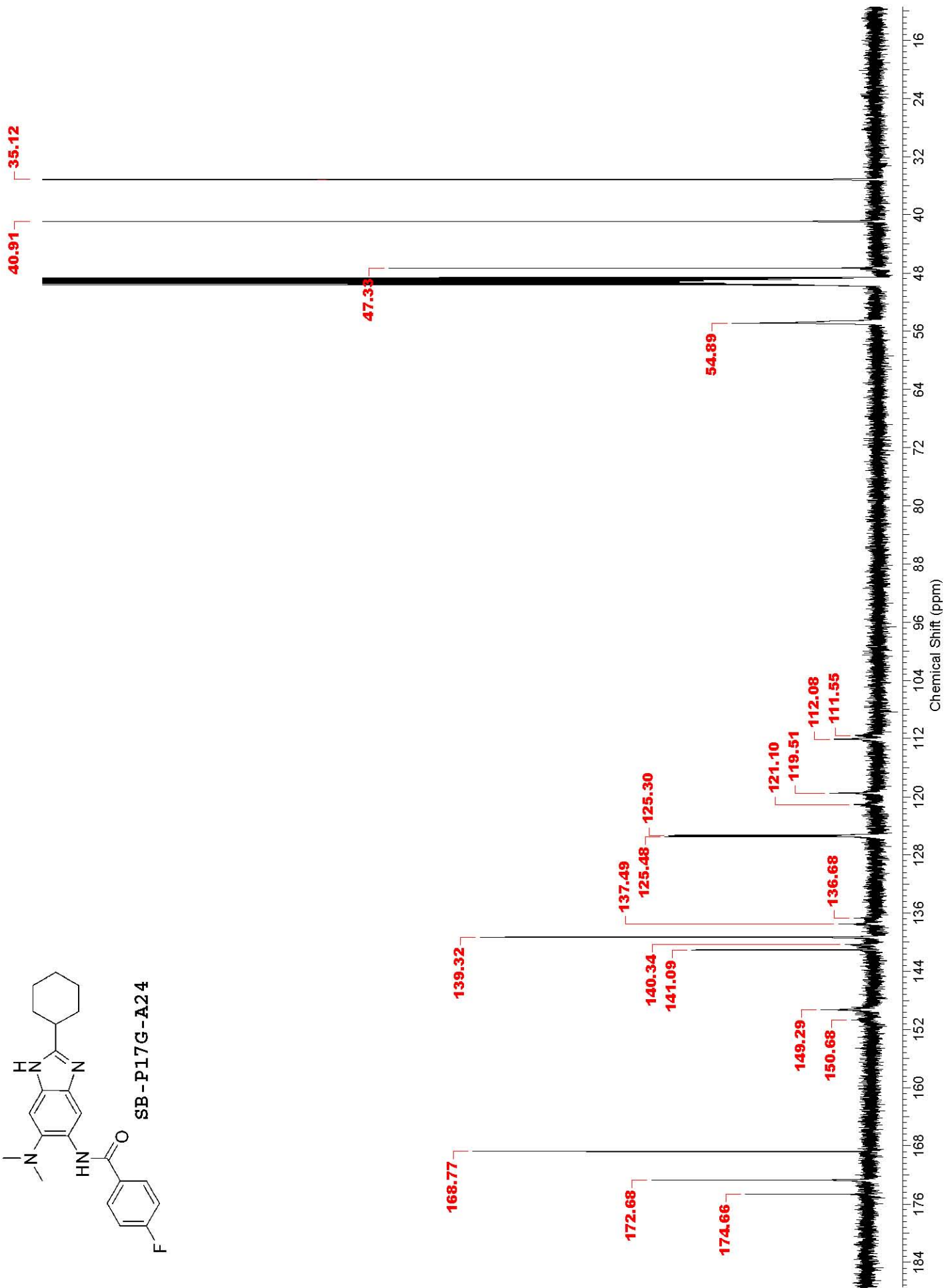
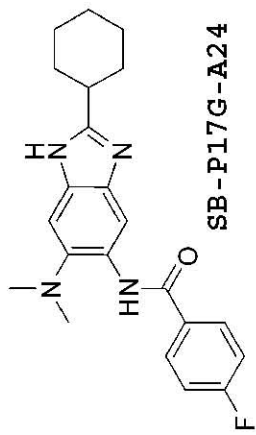


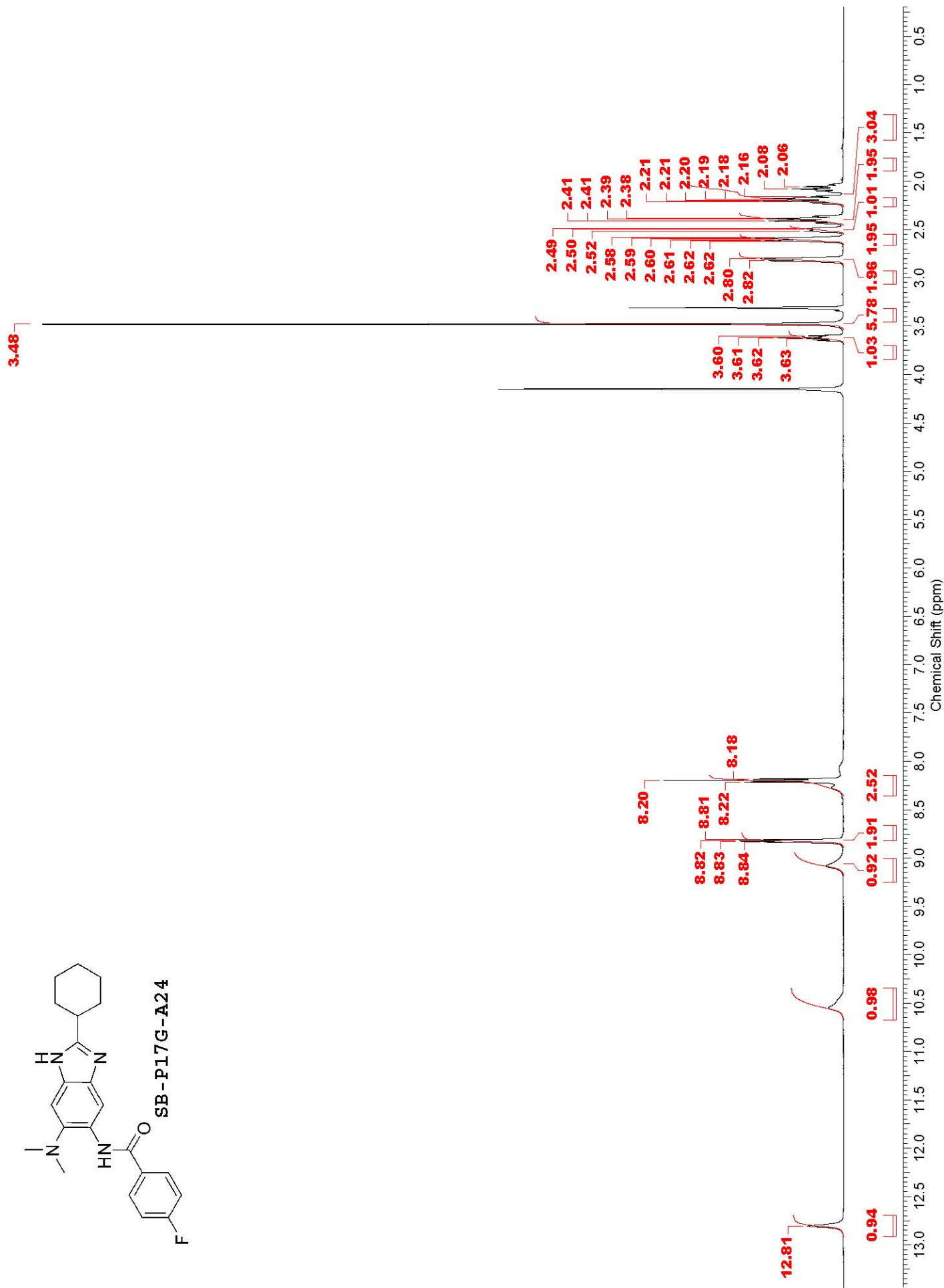
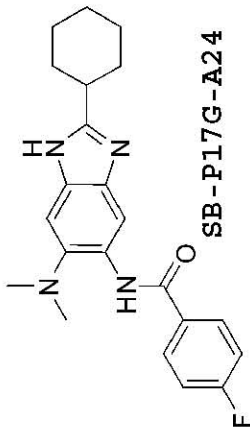


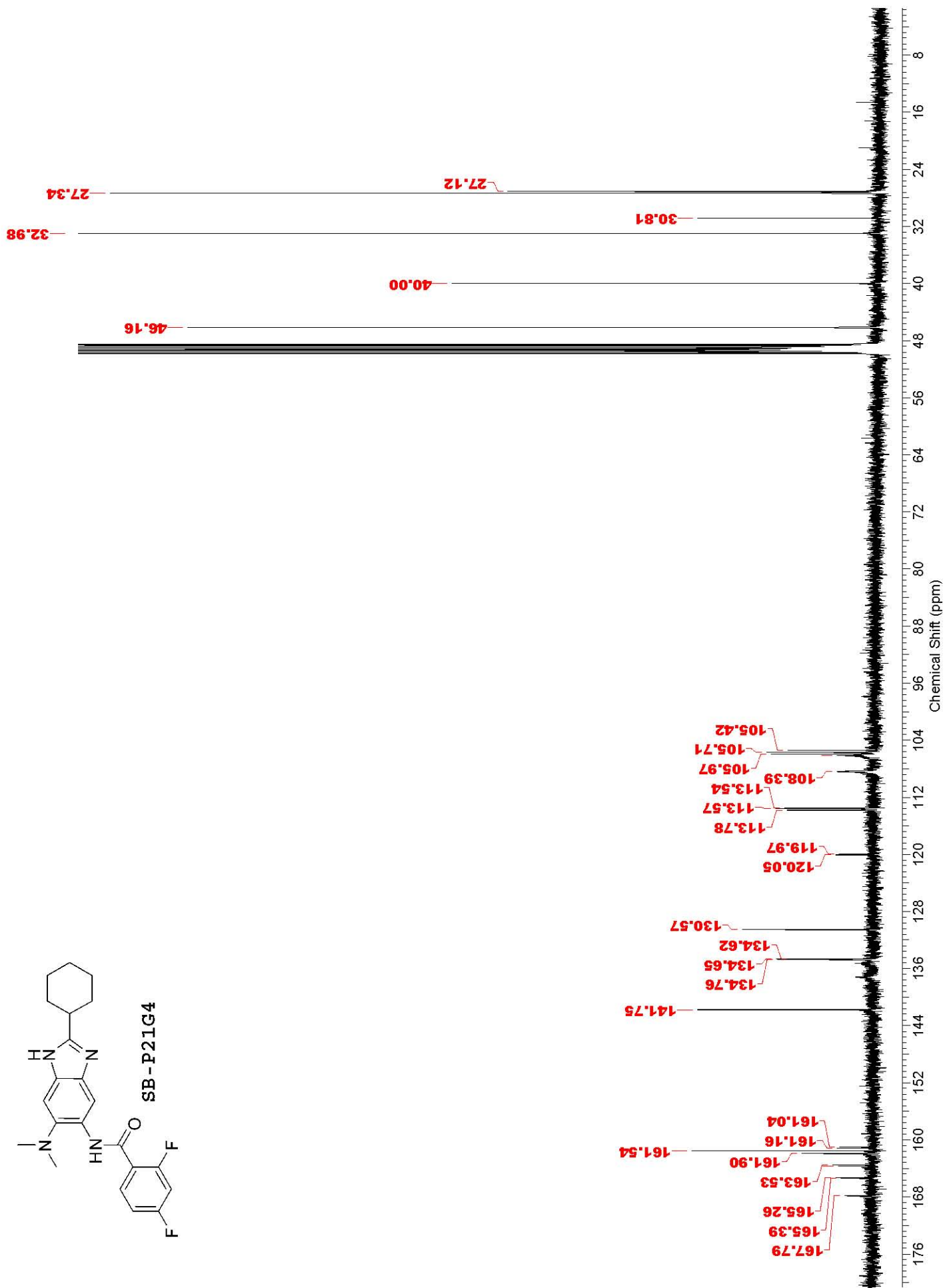
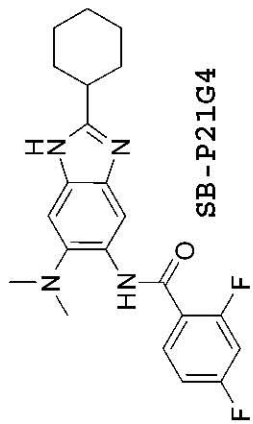


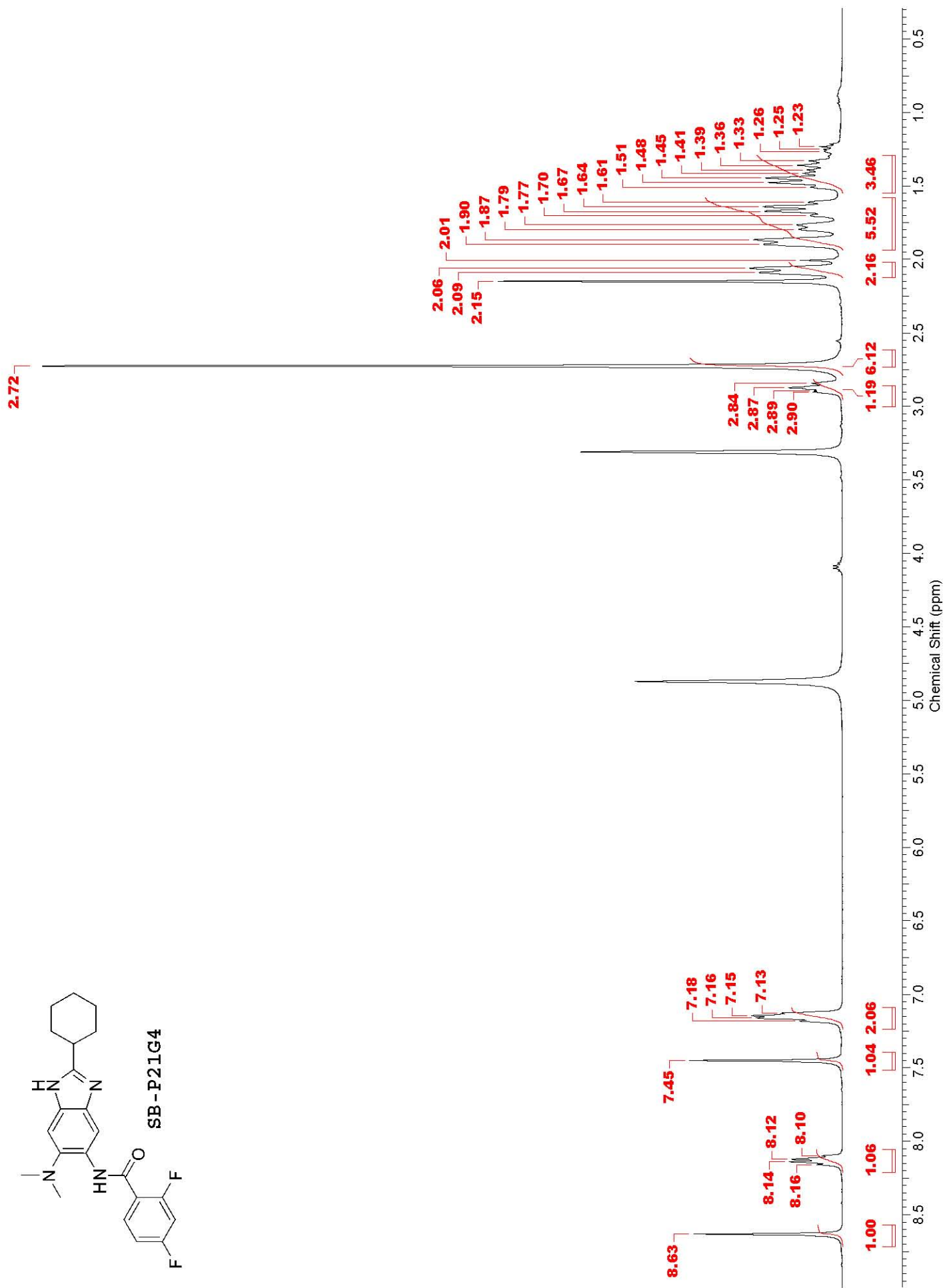
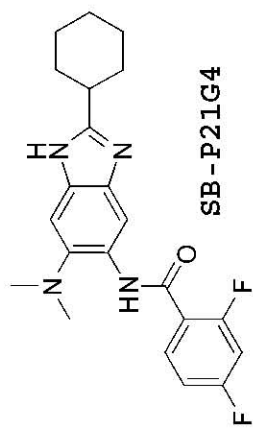


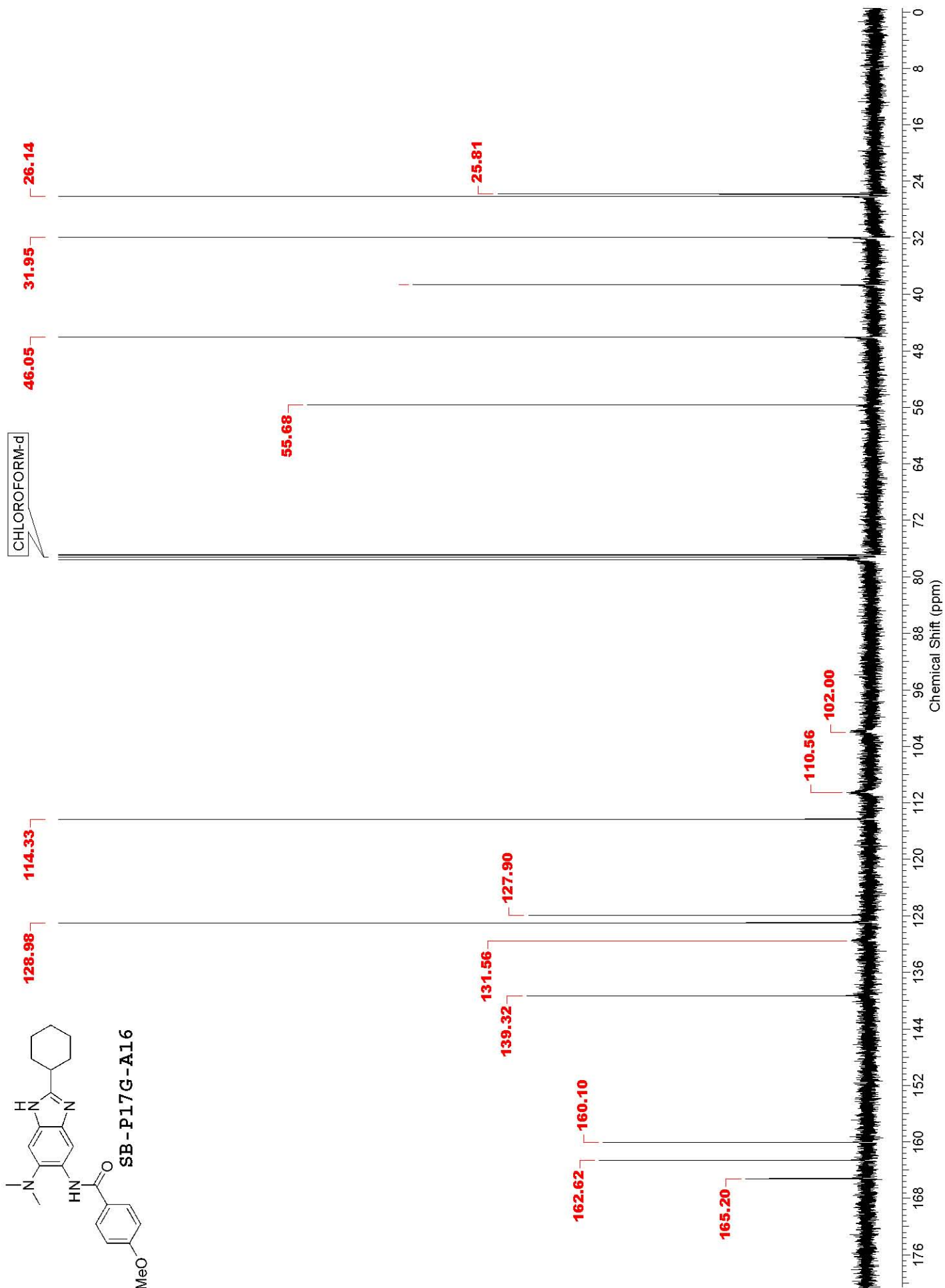
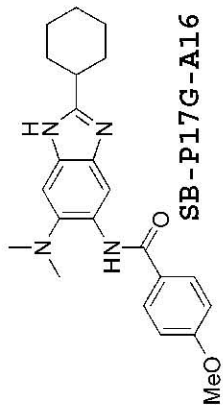


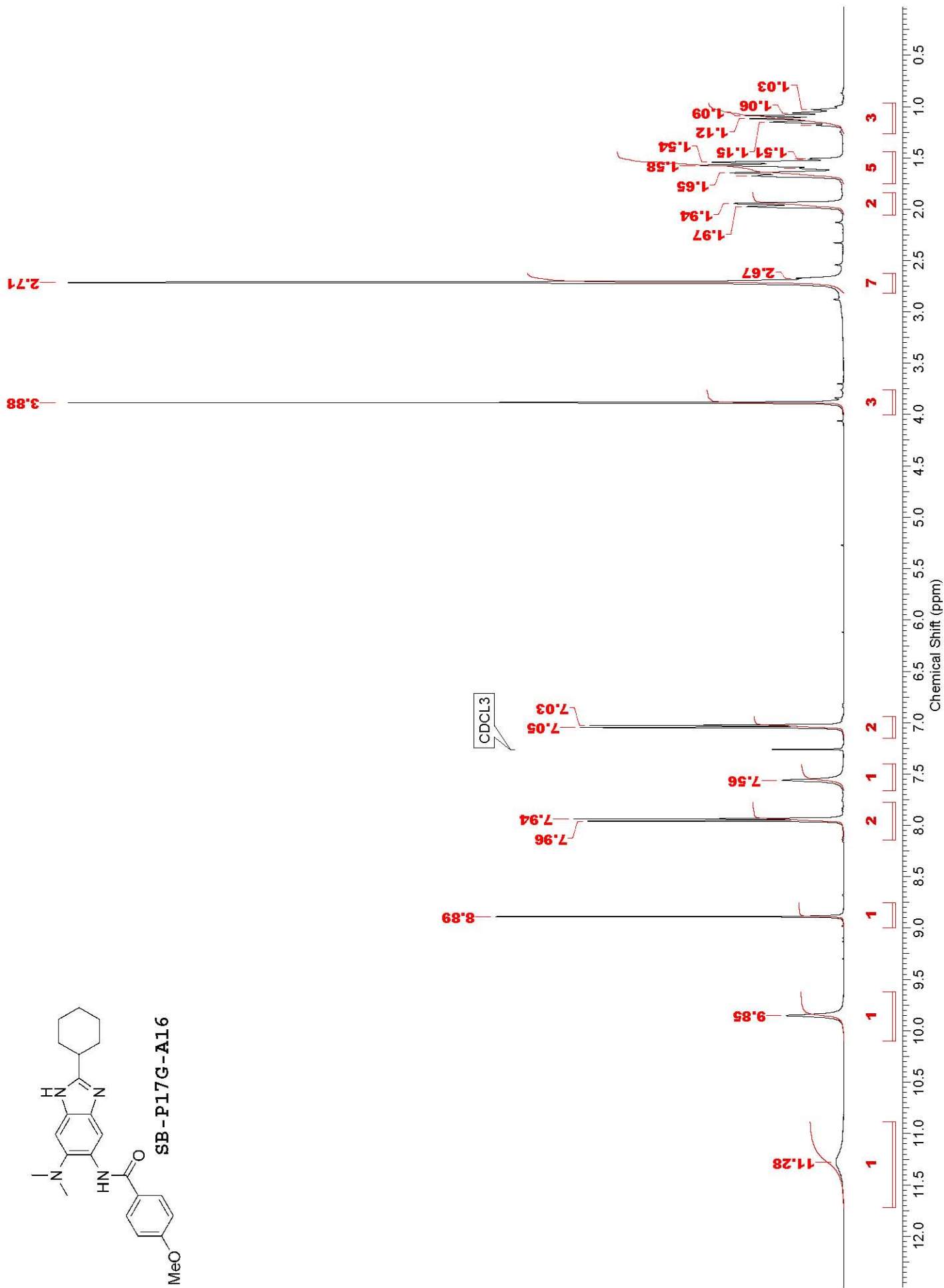
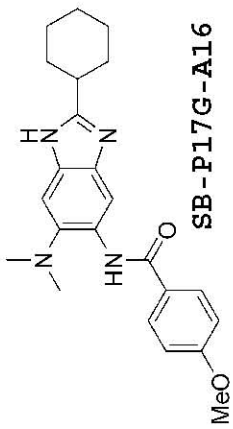


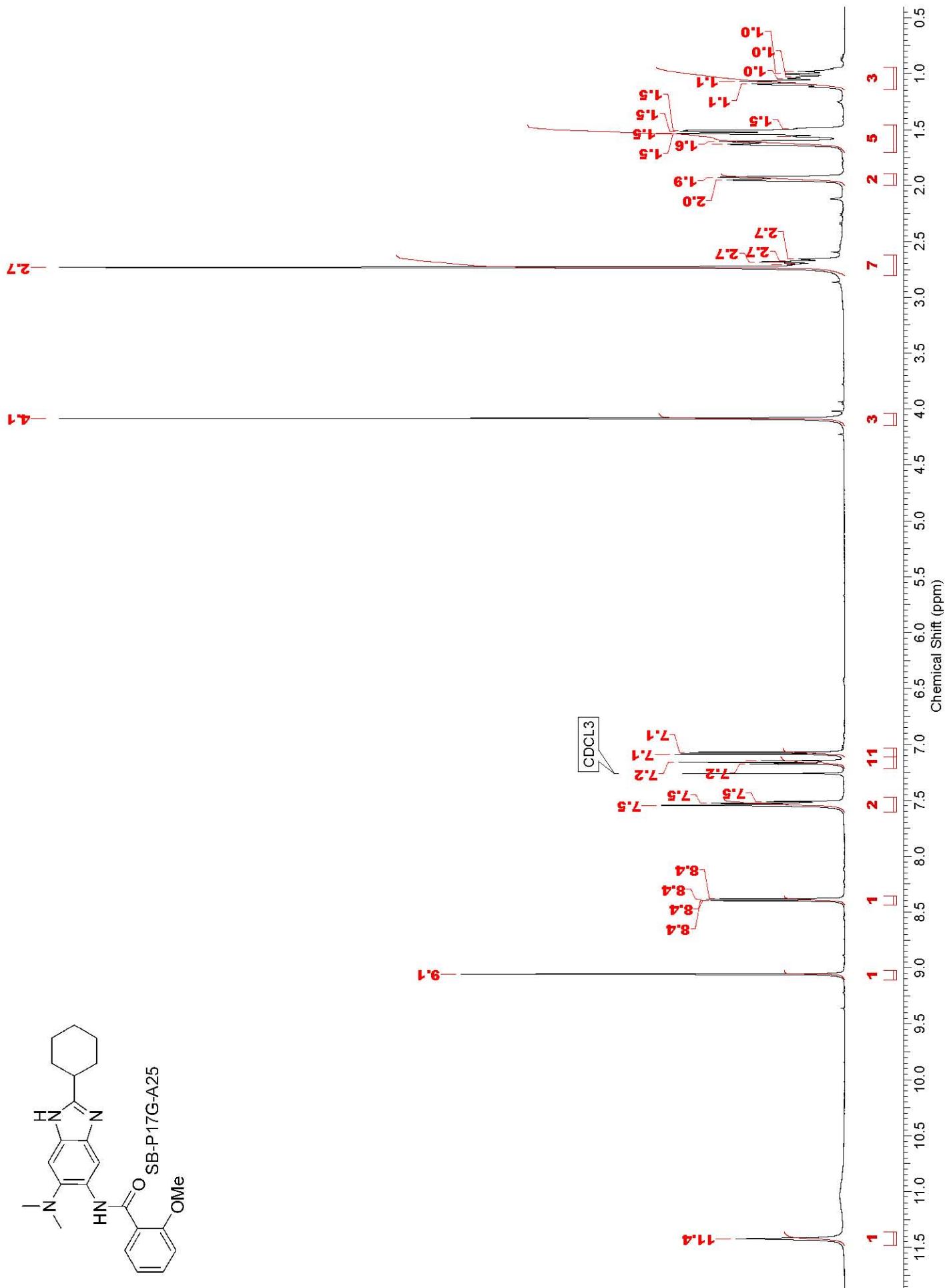
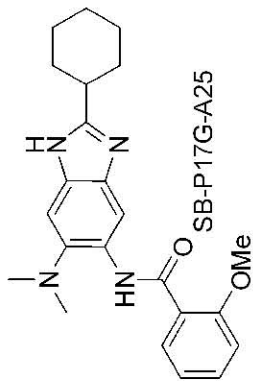


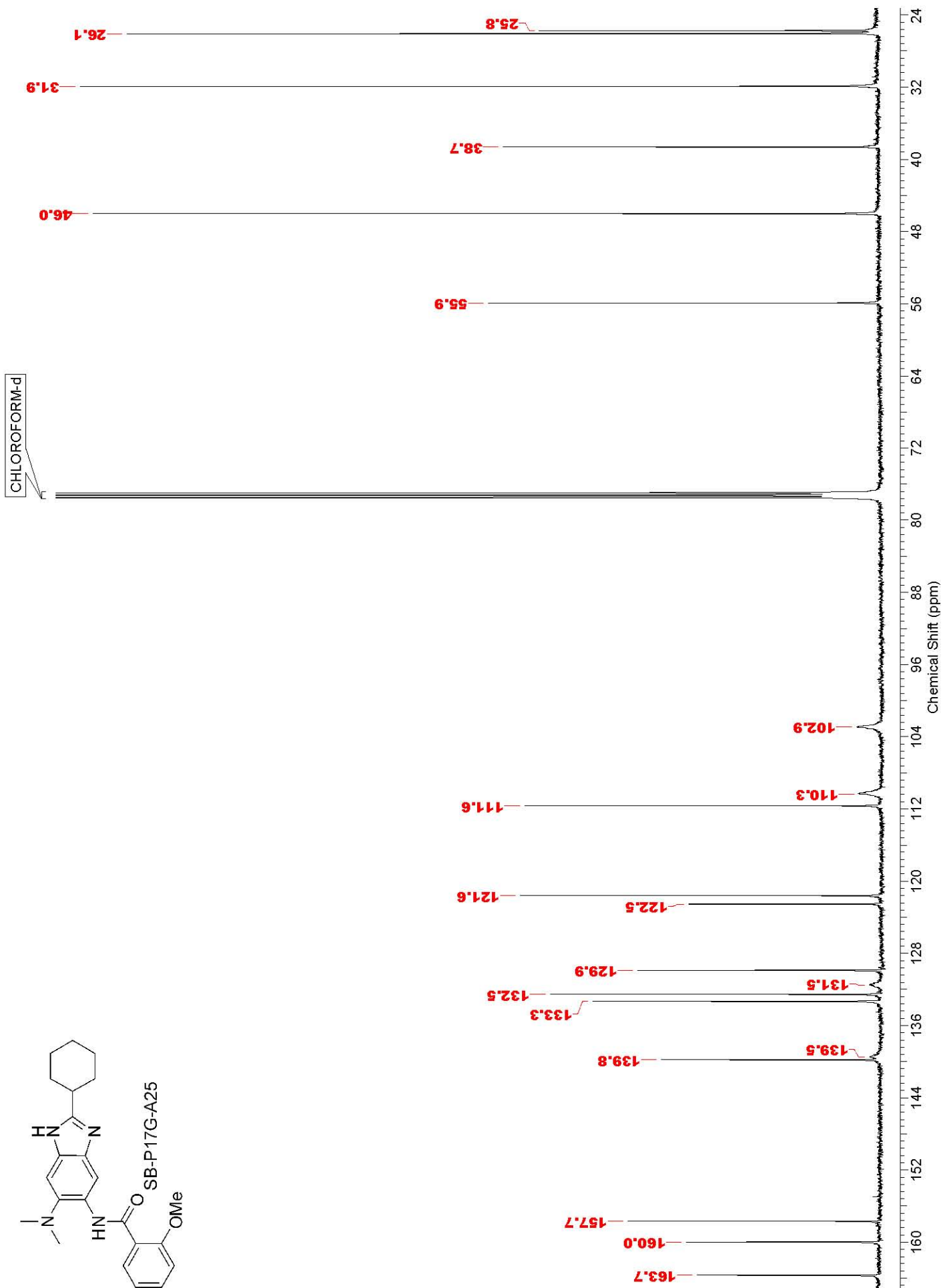
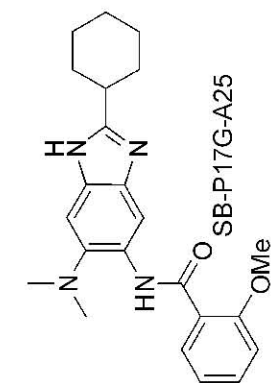


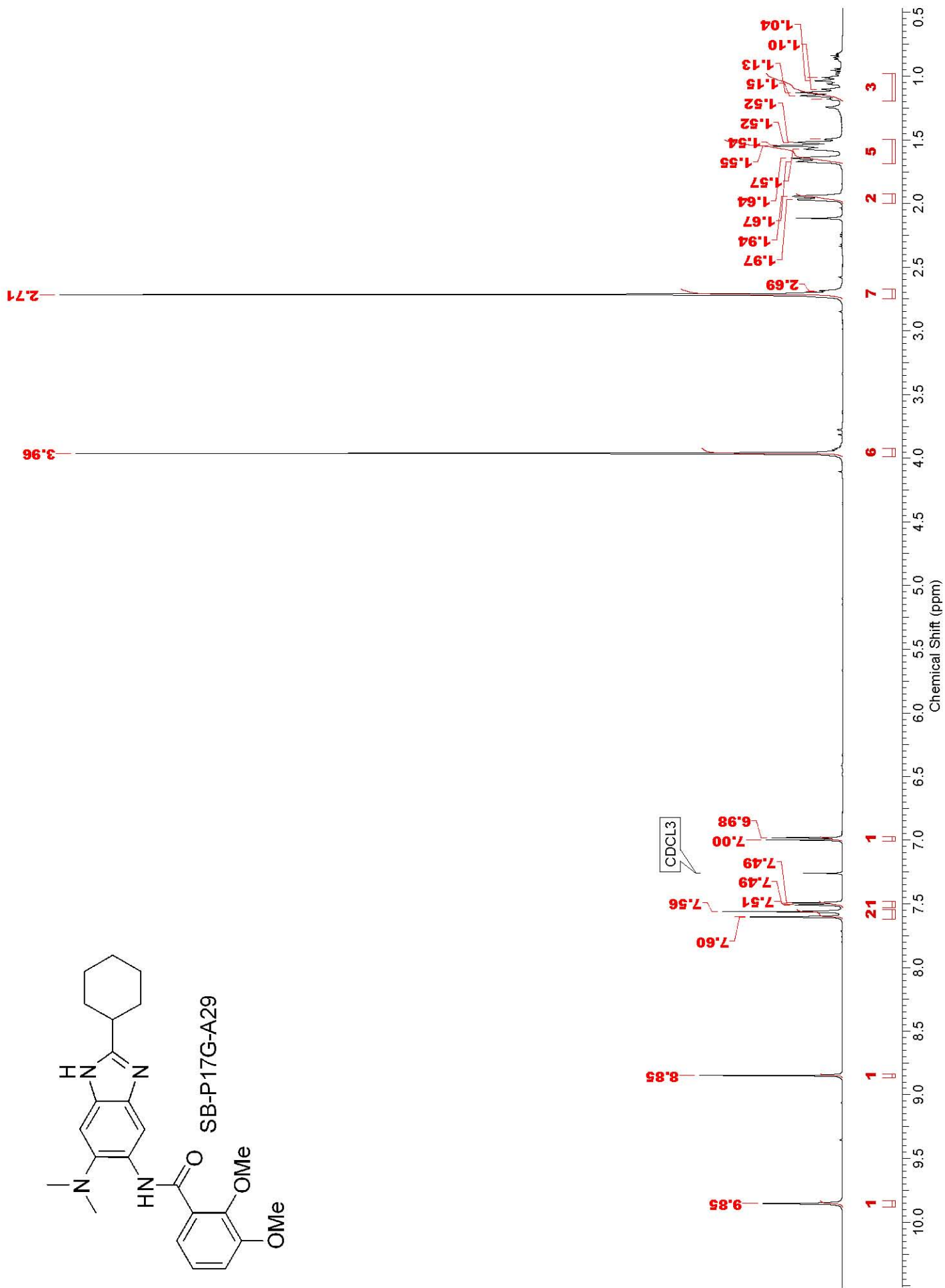
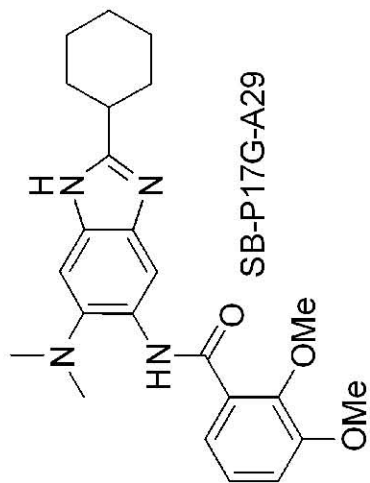




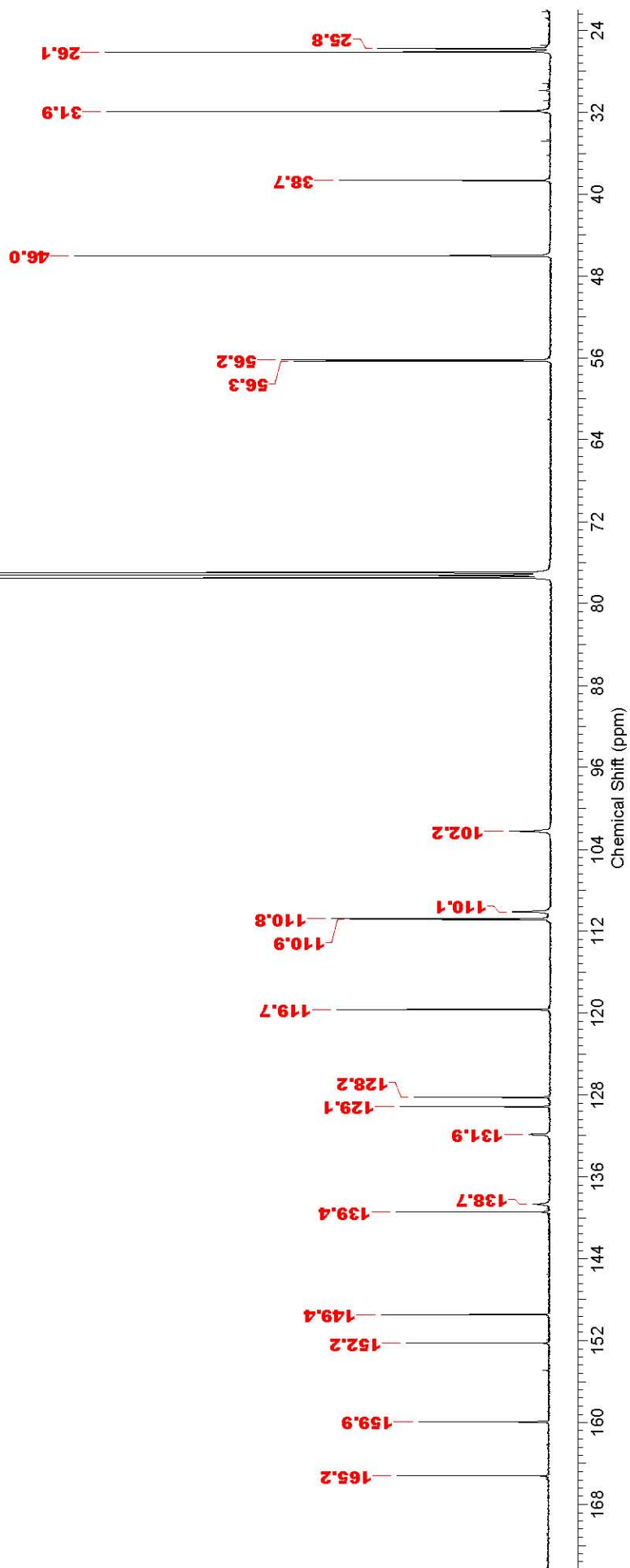
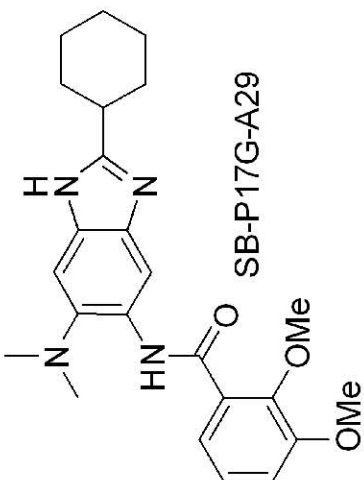


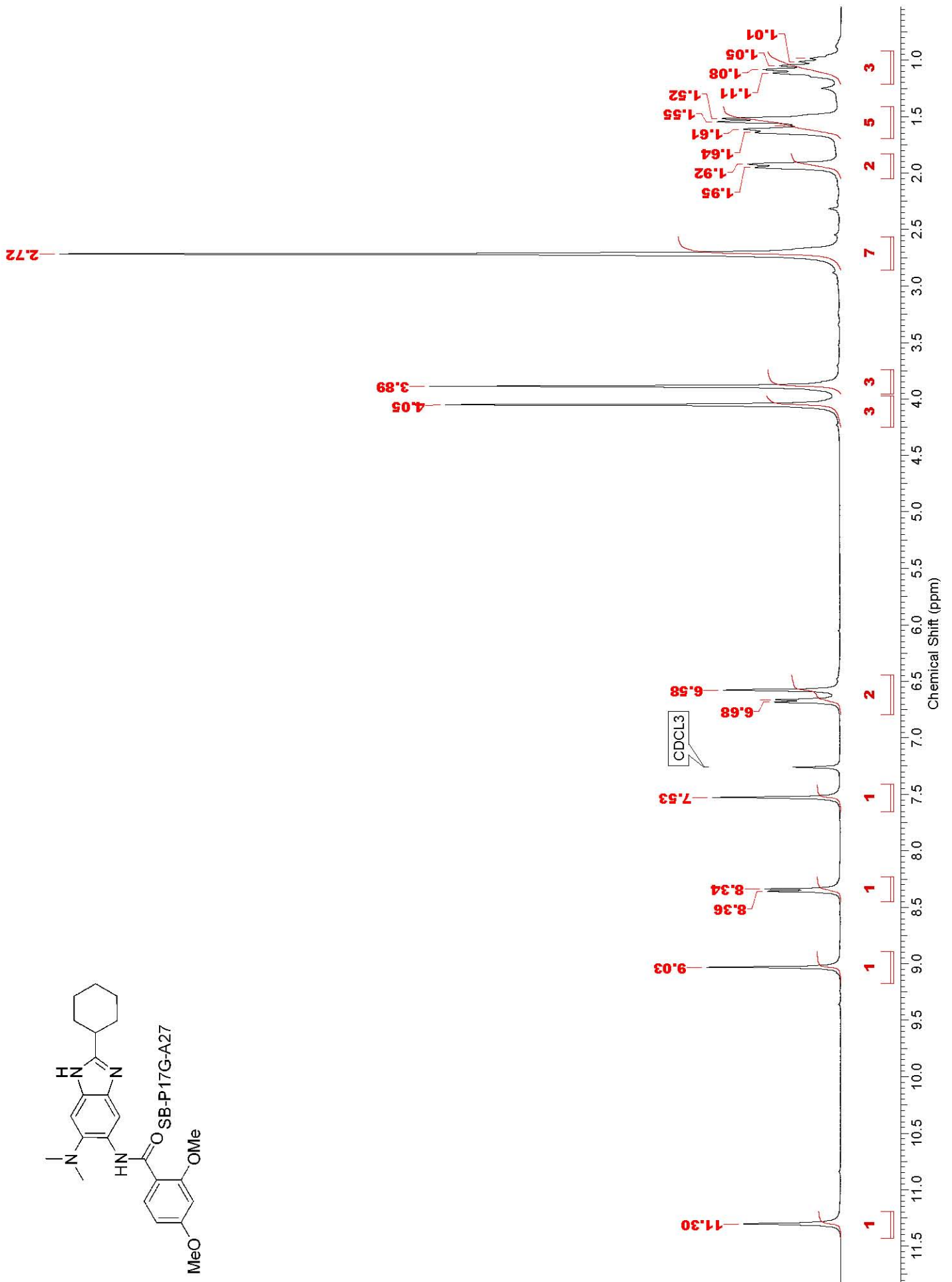
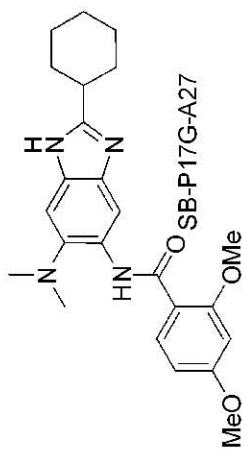


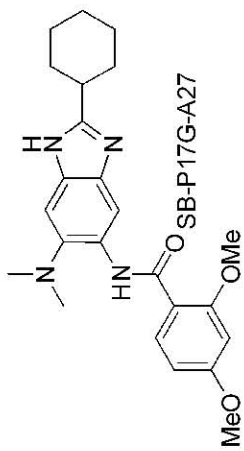




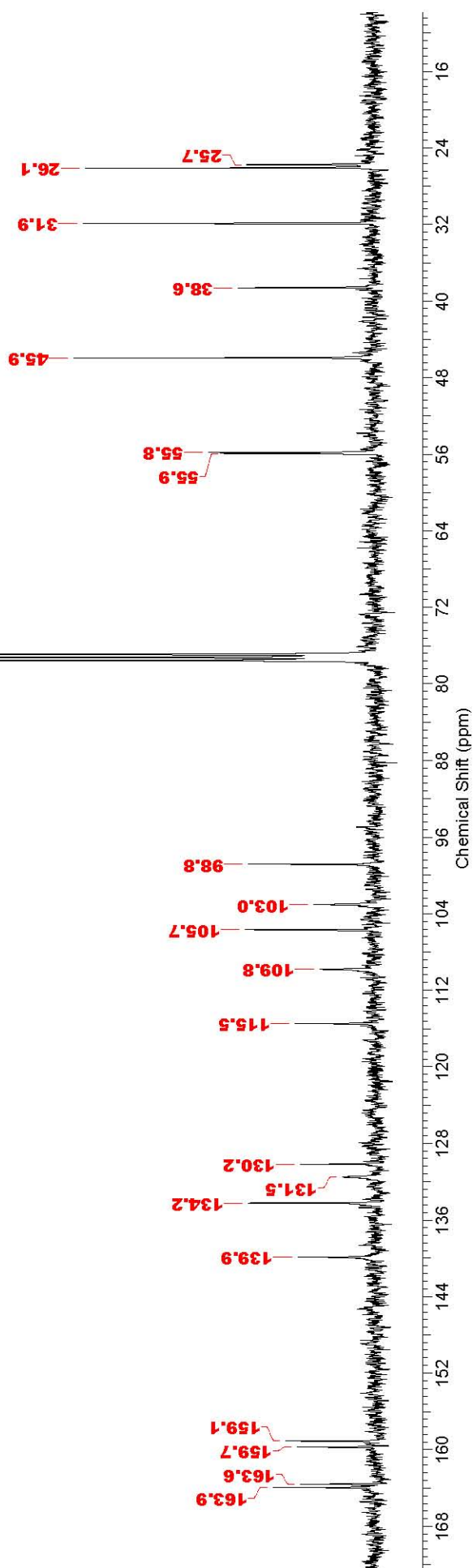
CHLOROFORM-d

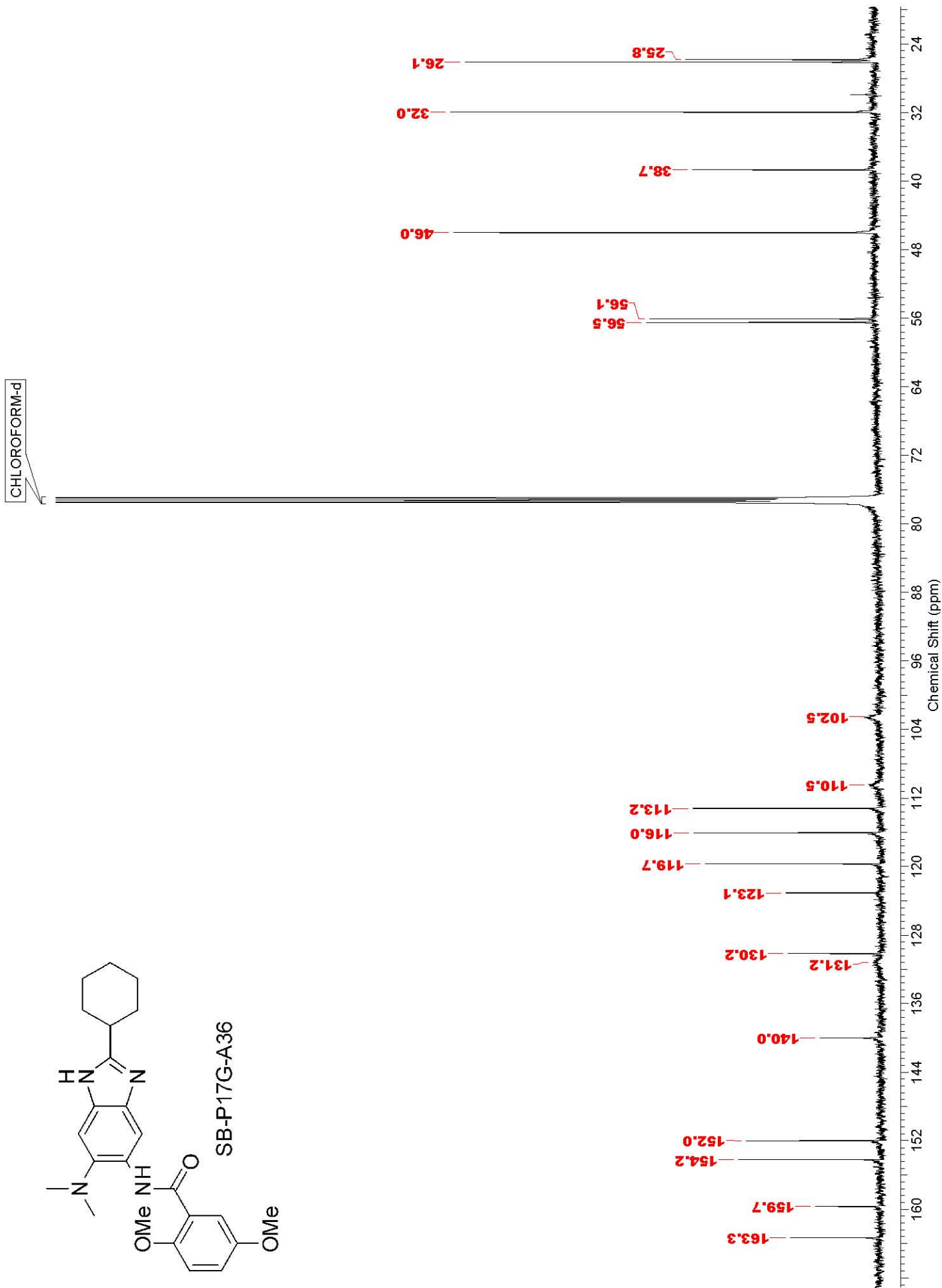
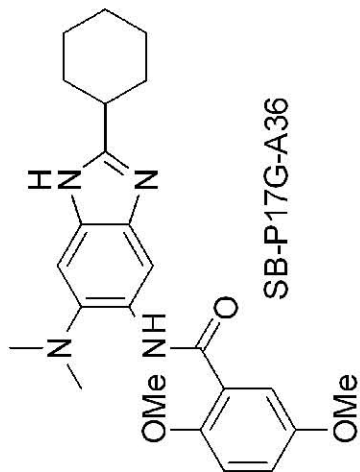


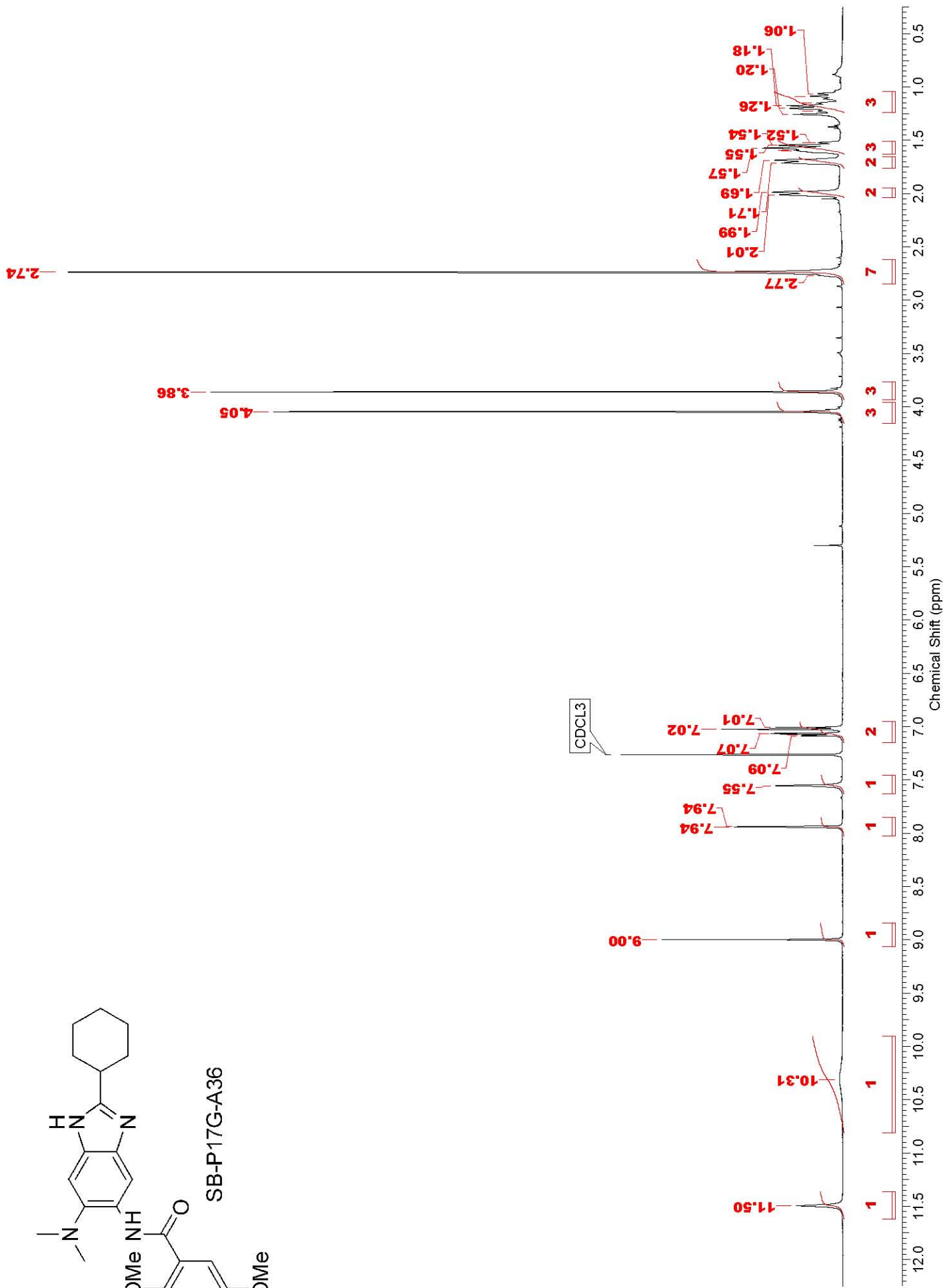
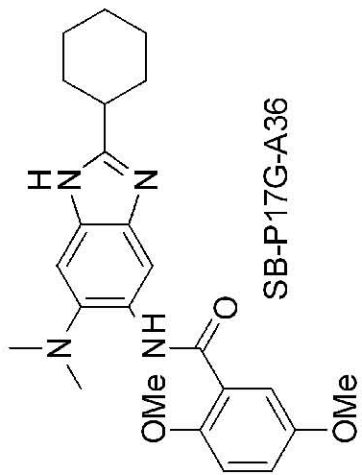




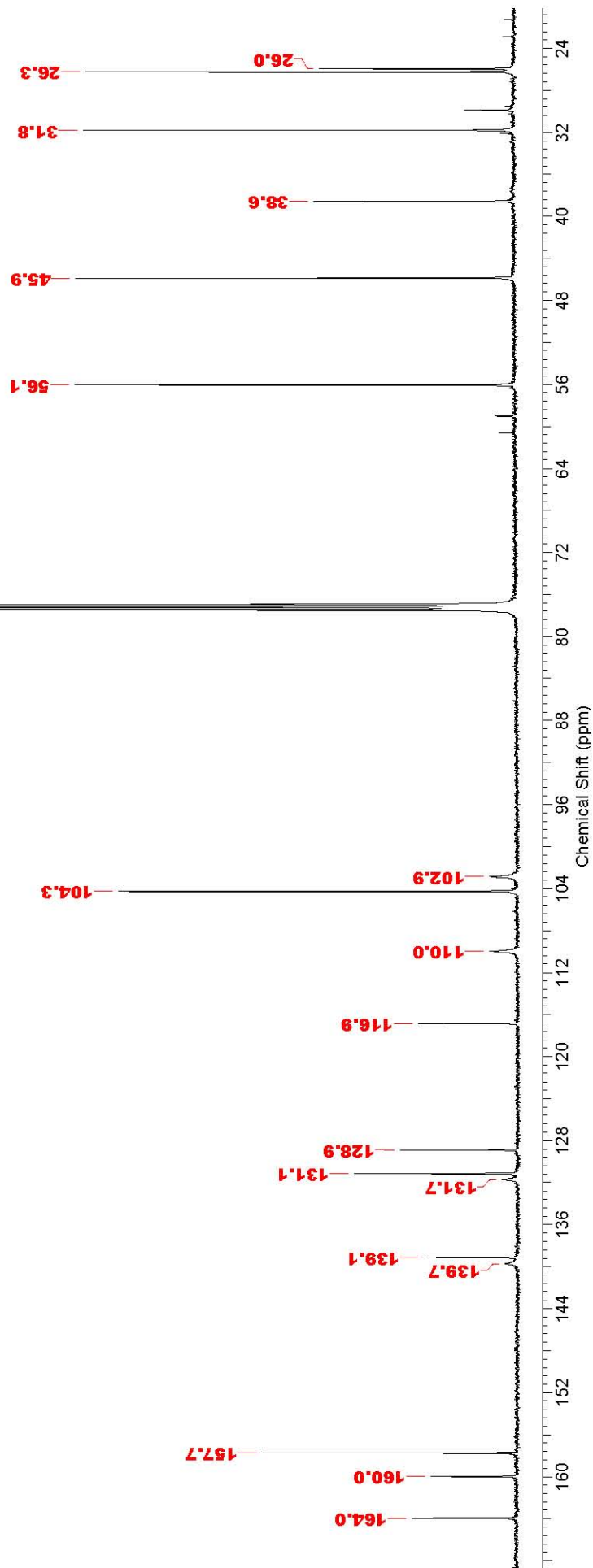
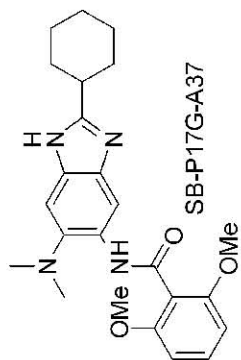
CHLOROFORM-d

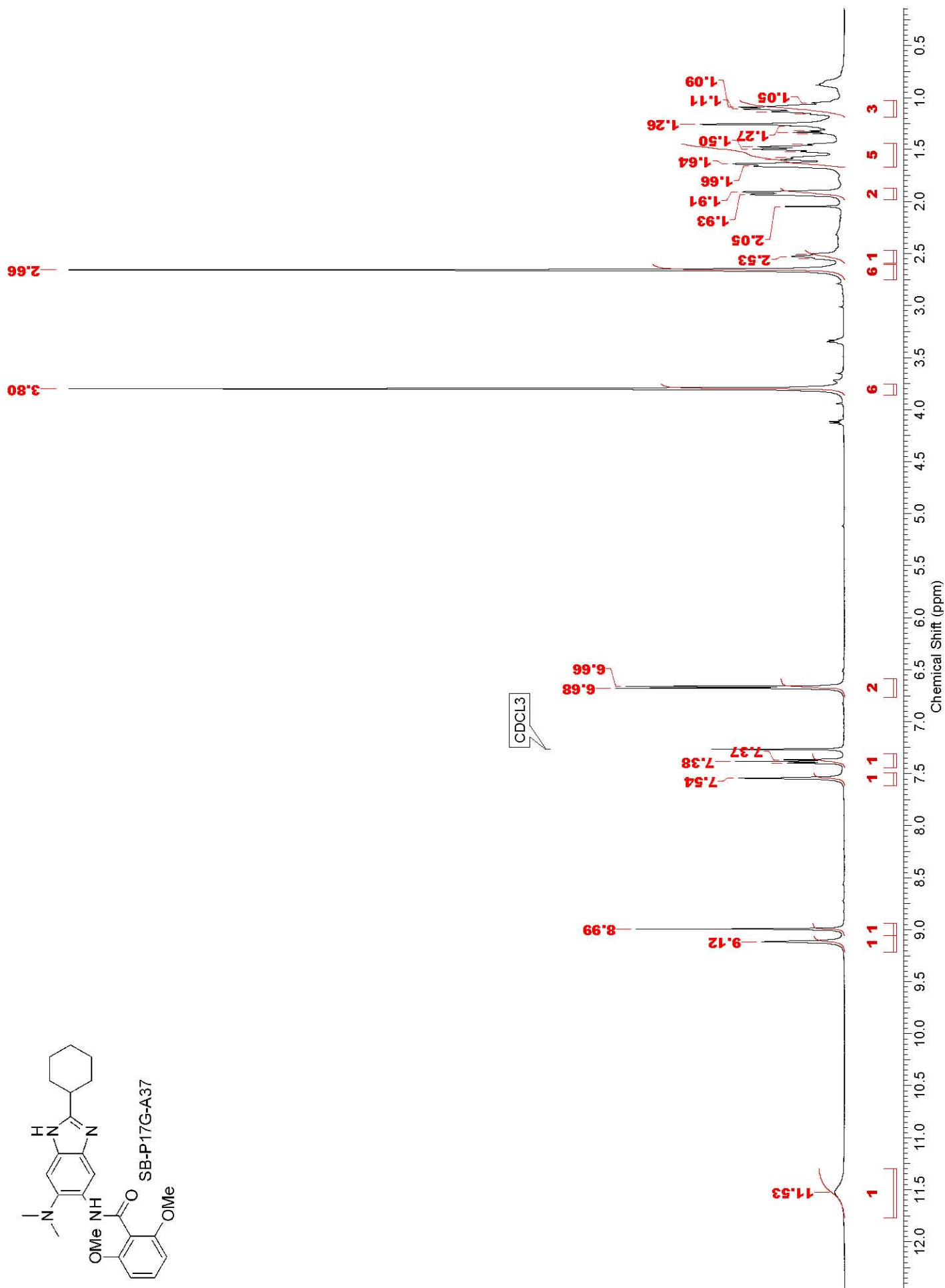
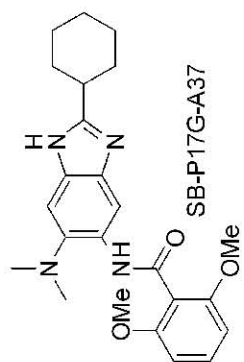


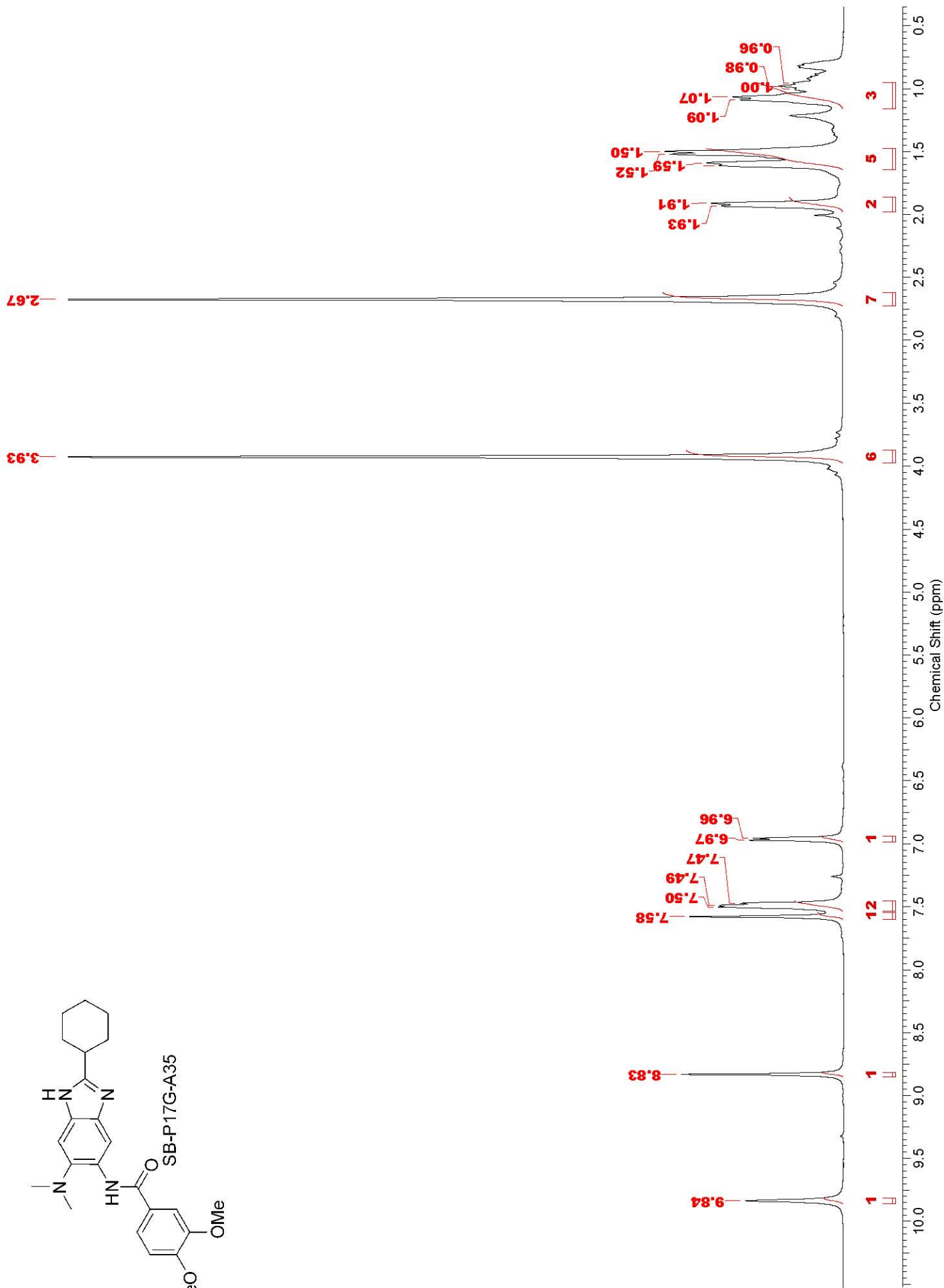
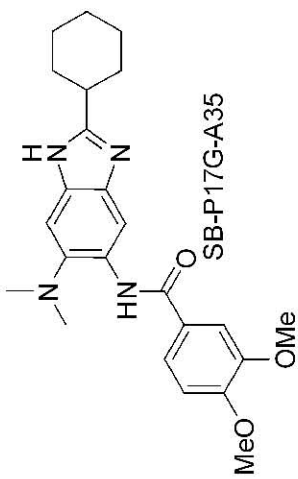


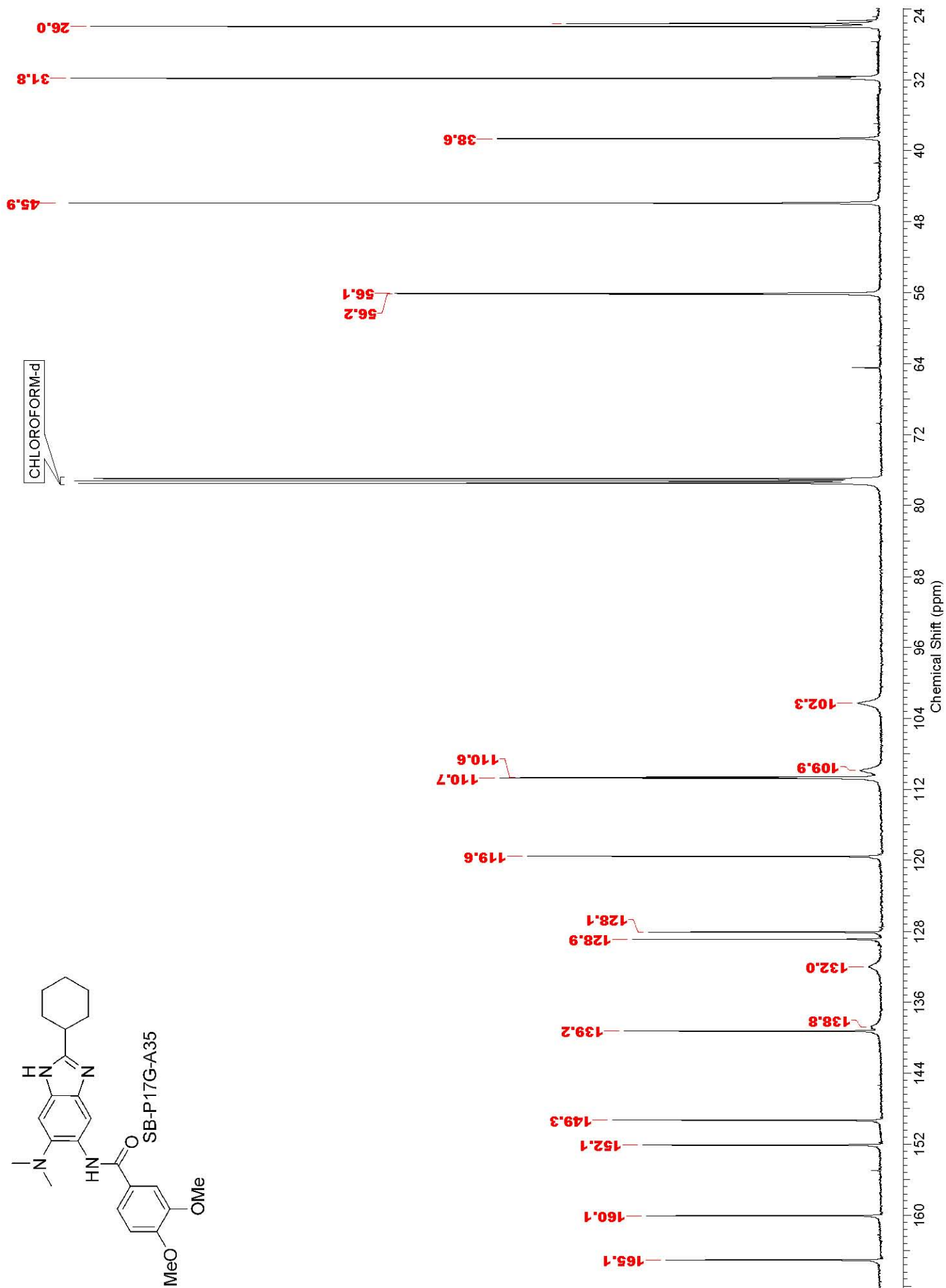
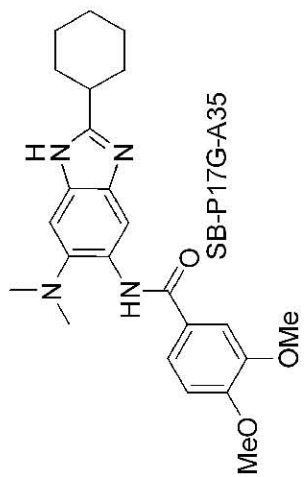


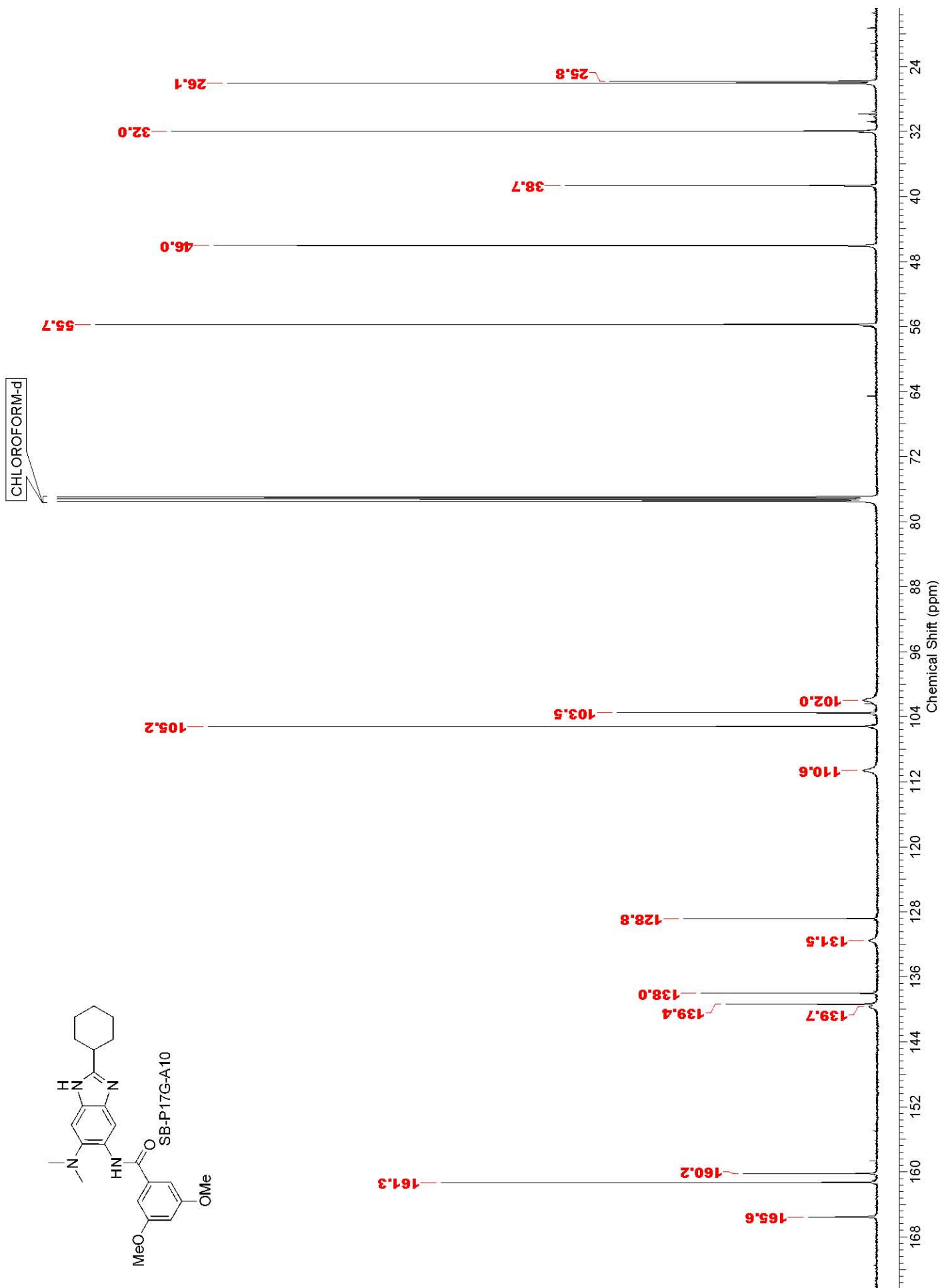
CHLOROFORM-d

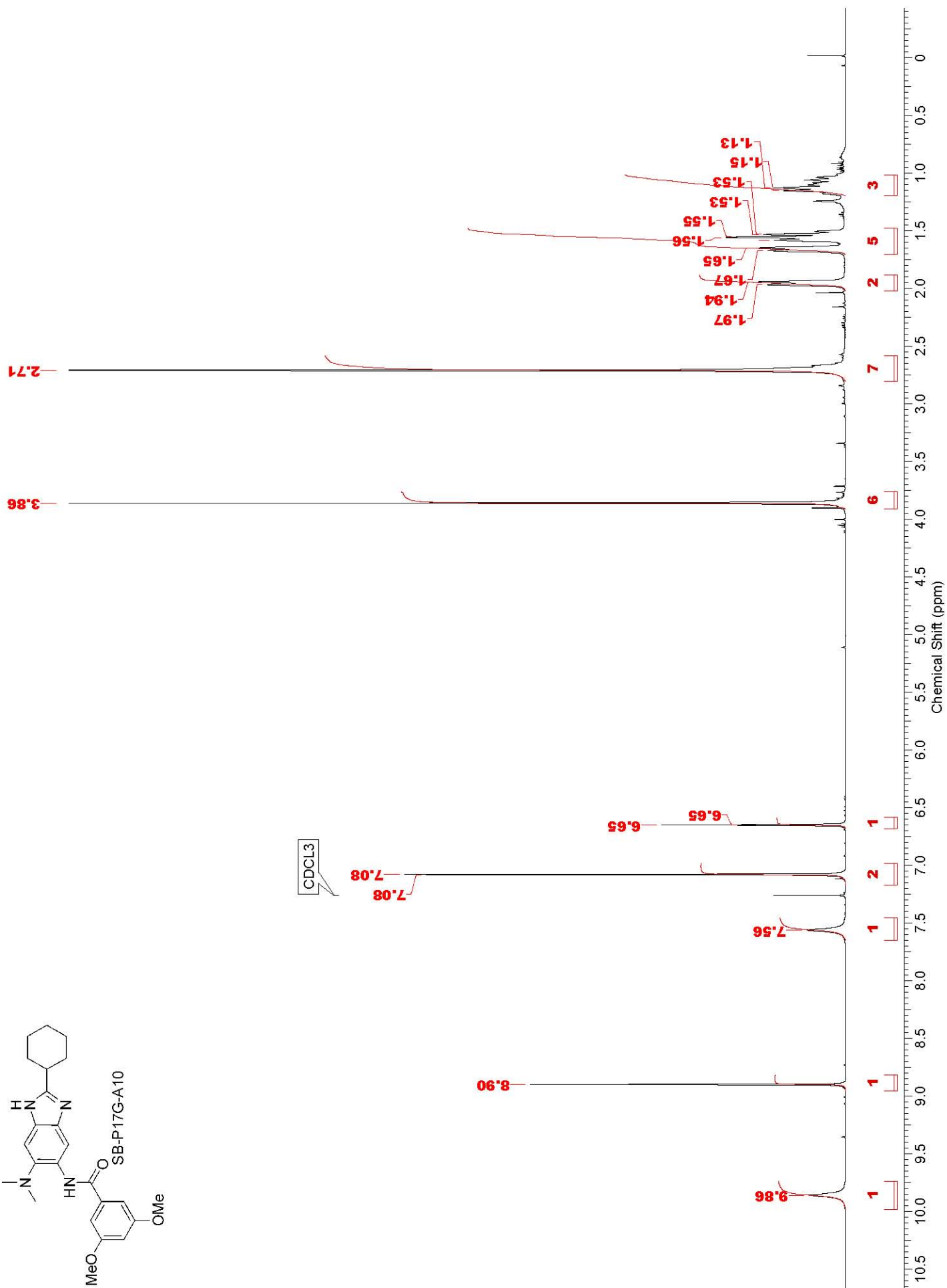
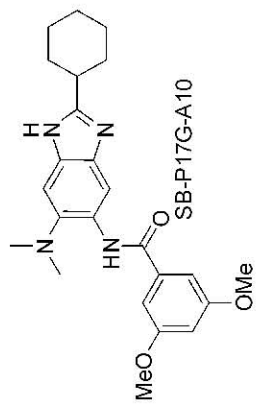


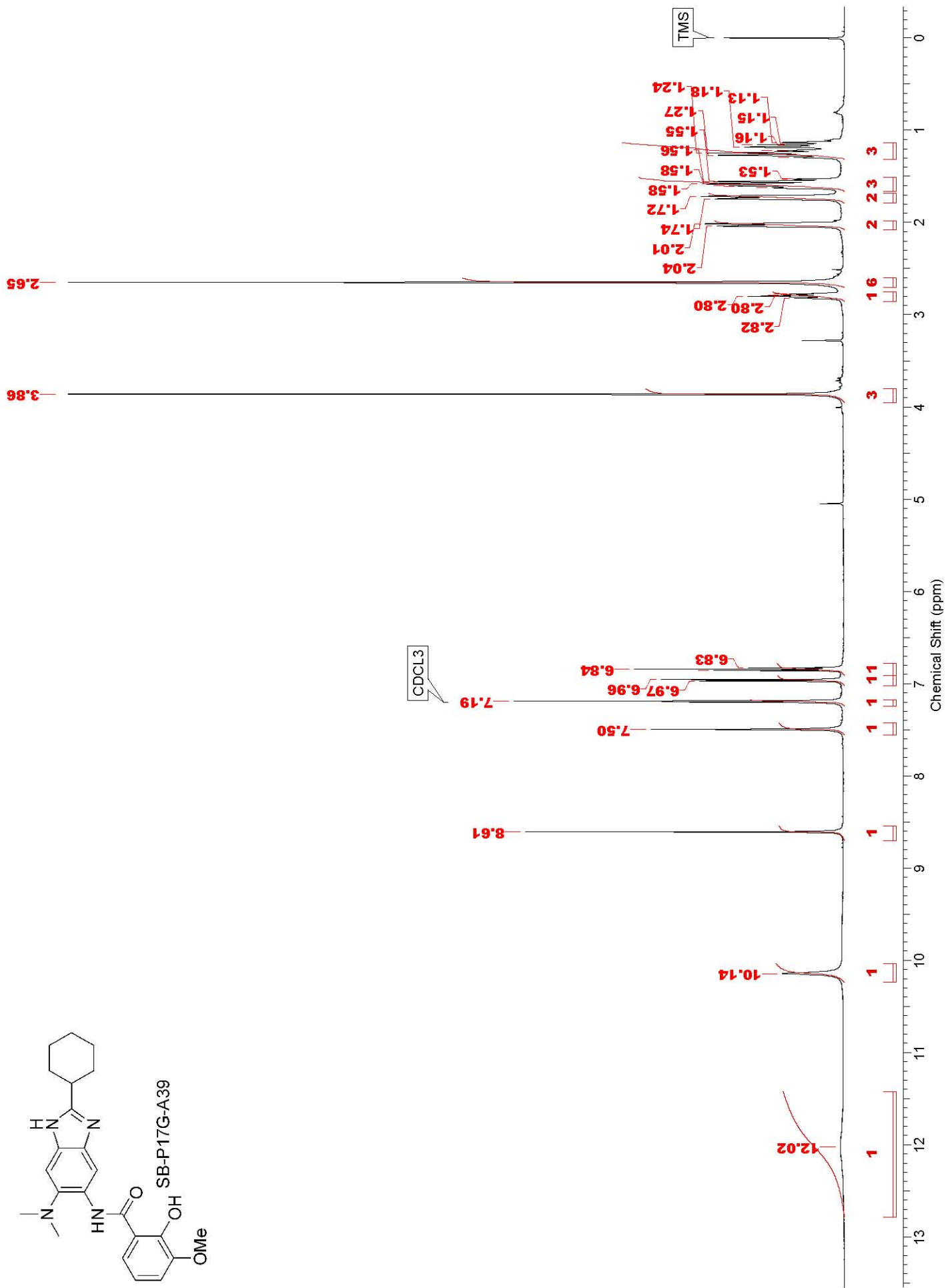
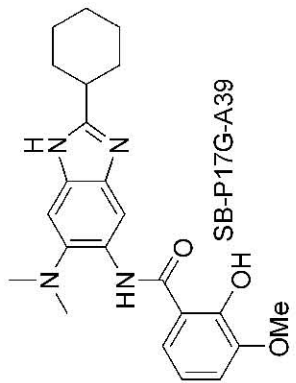




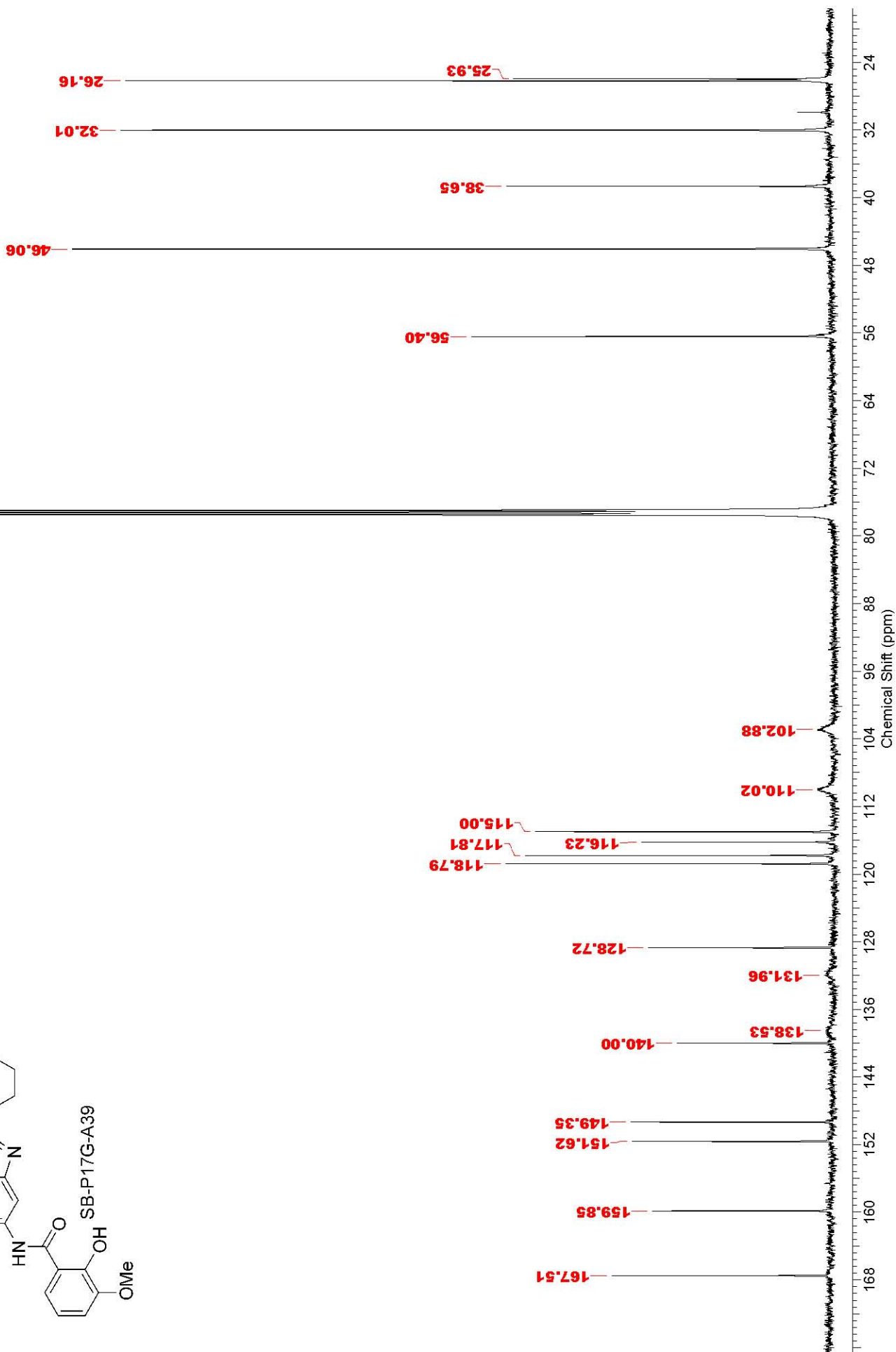
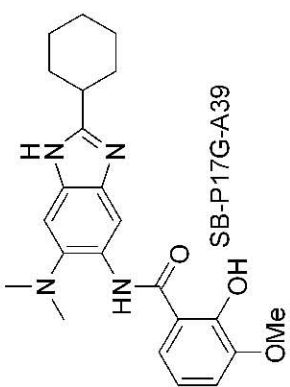




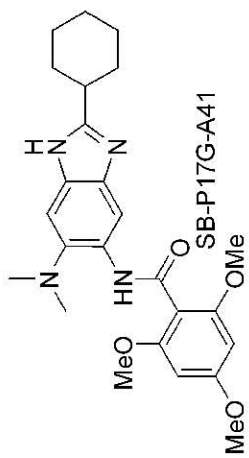
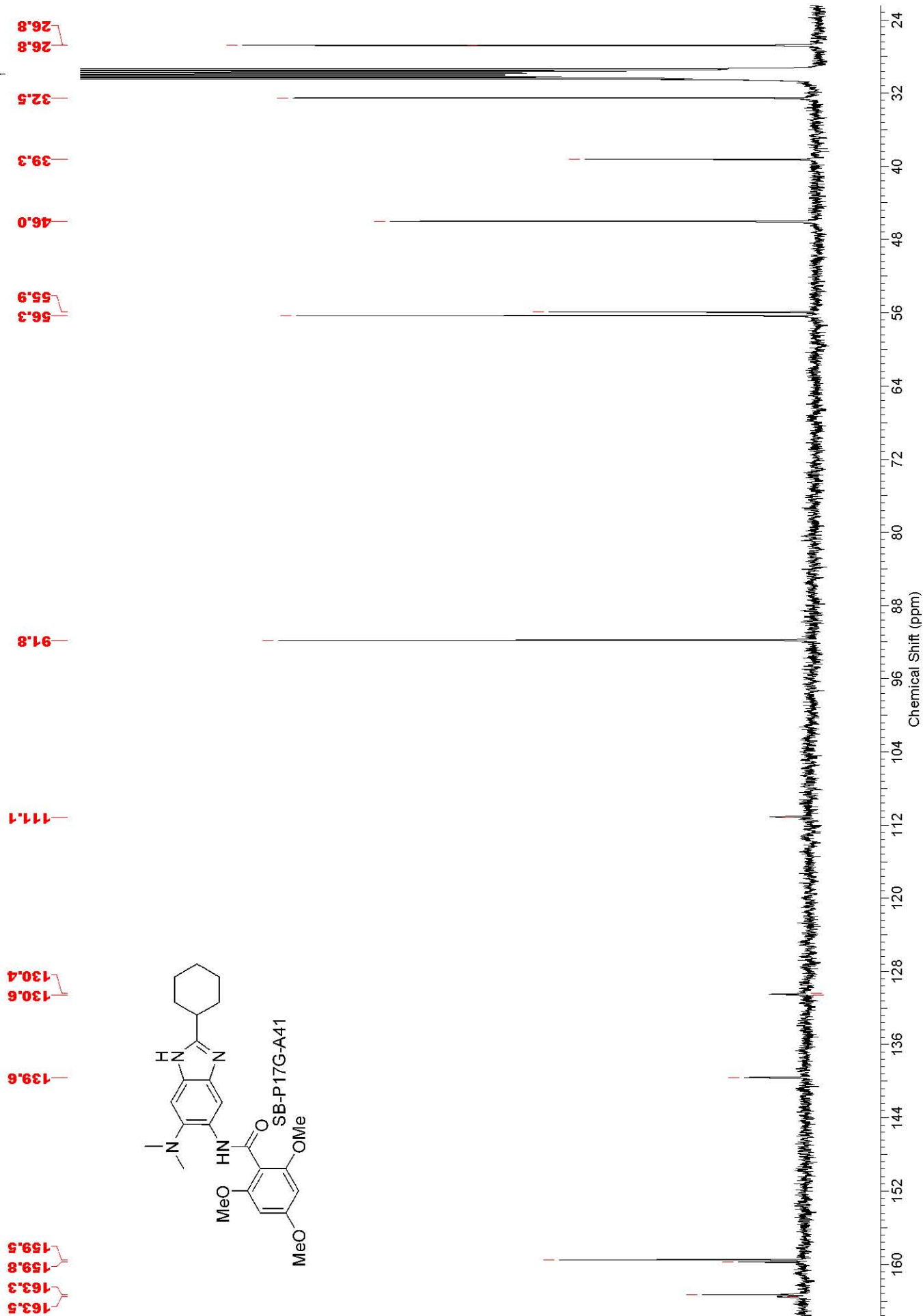


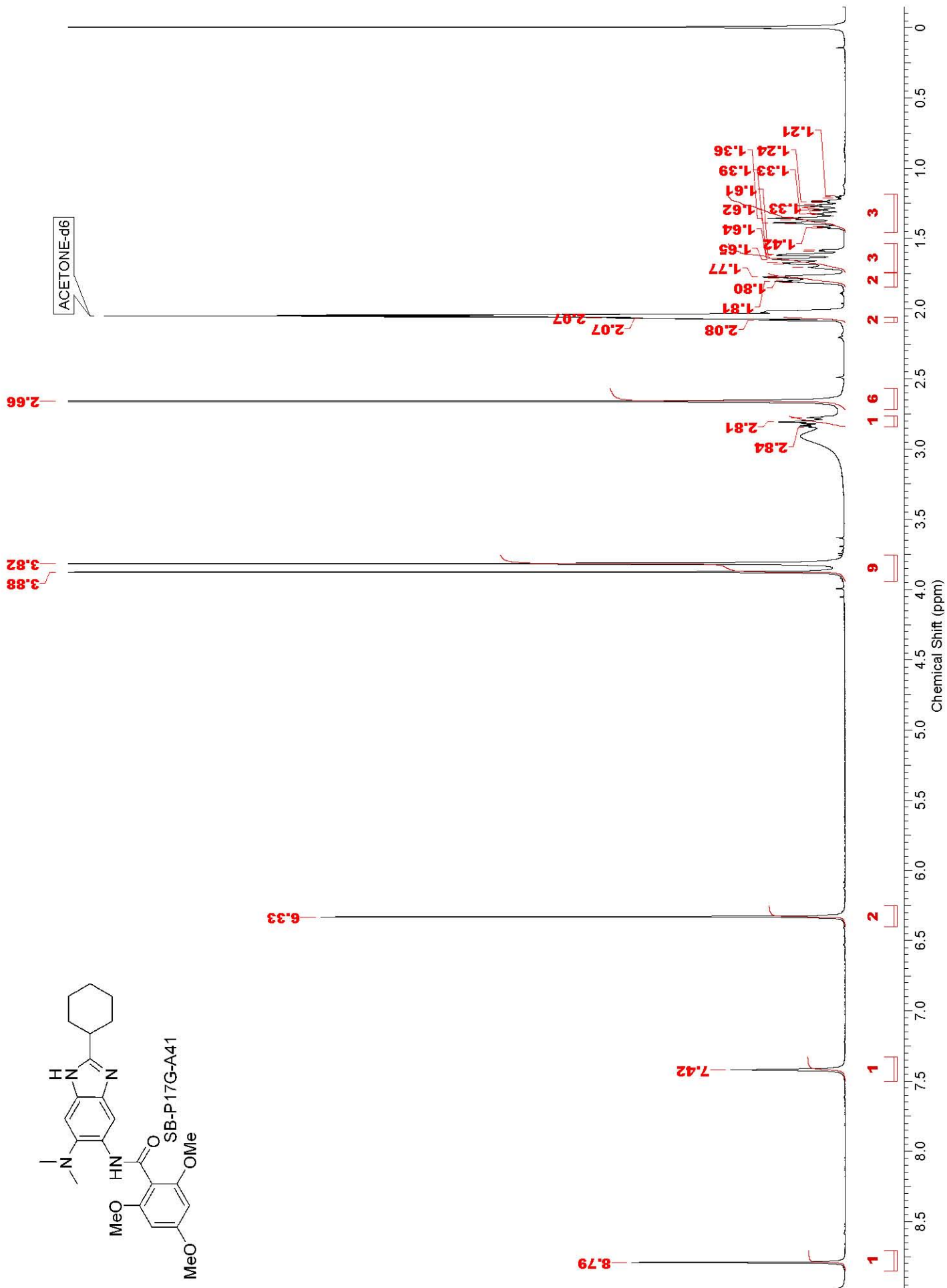
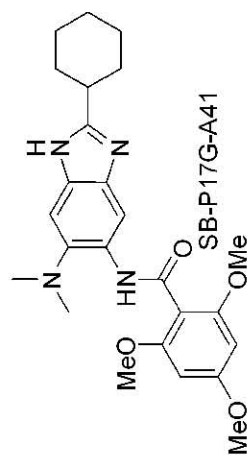


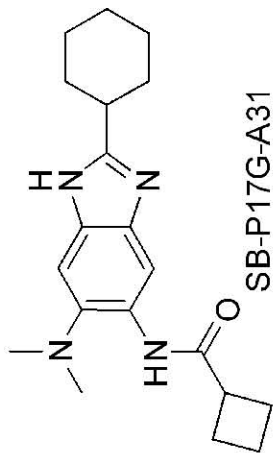
CHLOROFORM-d



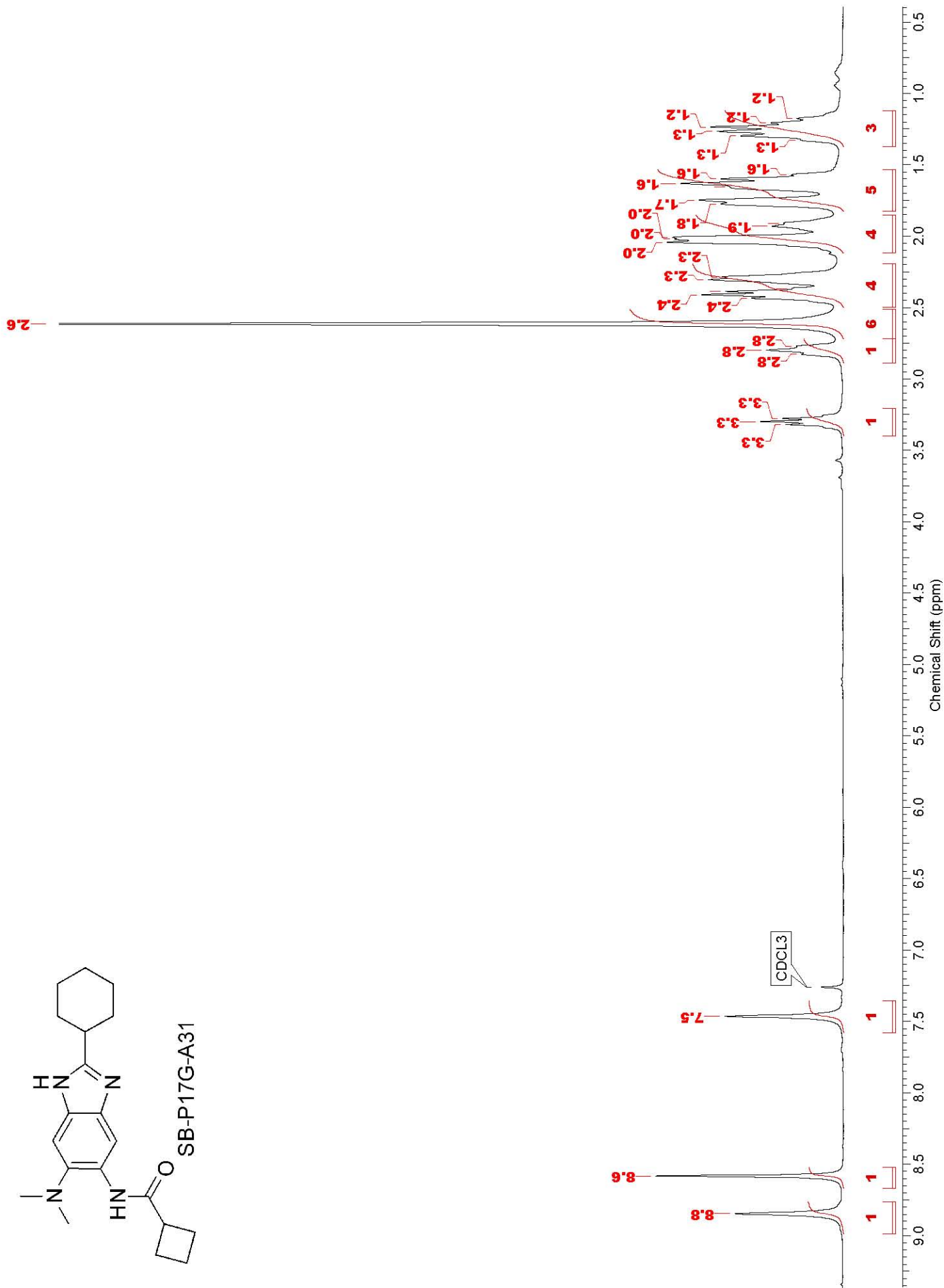
ACETONE-d6

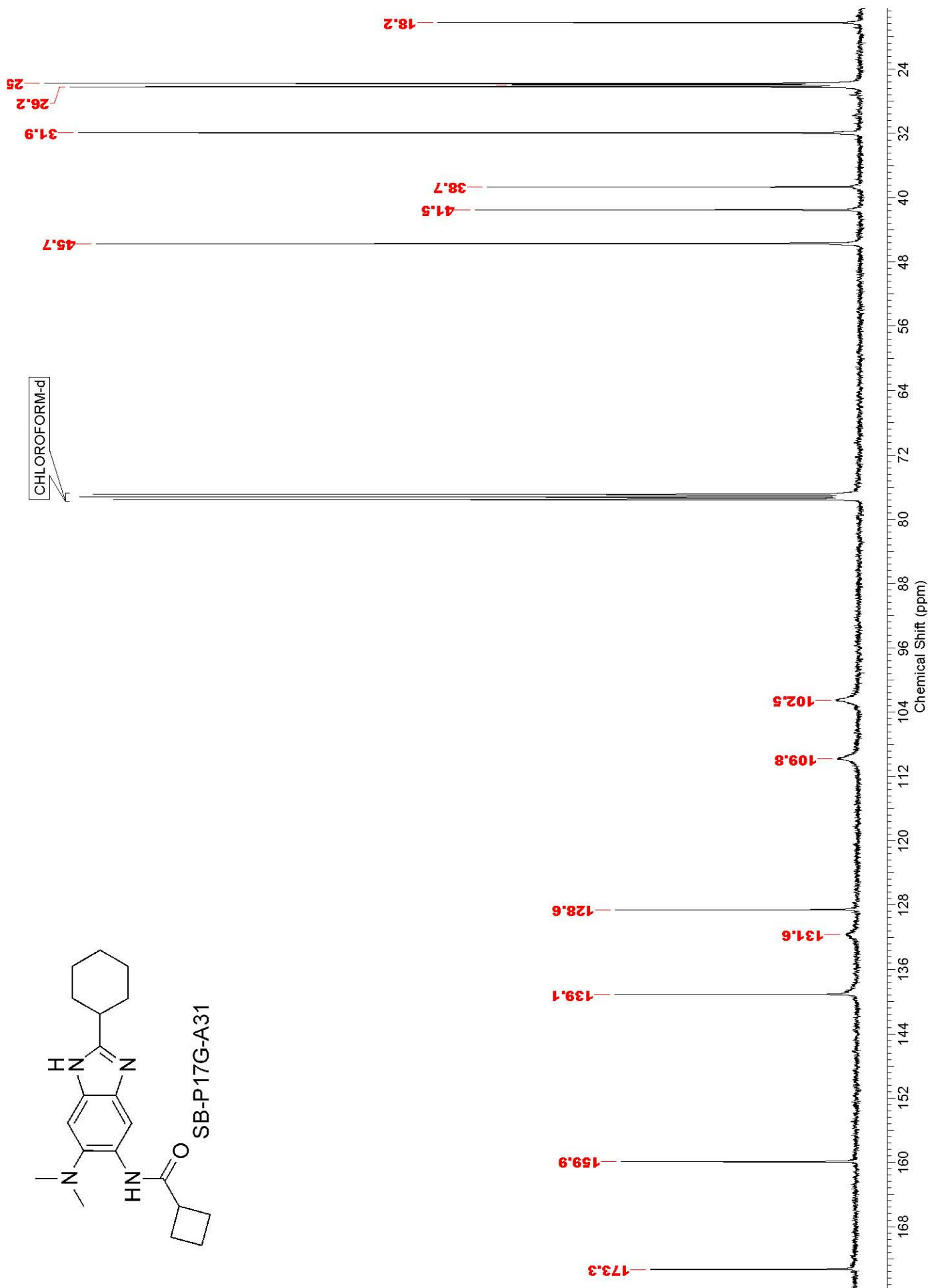
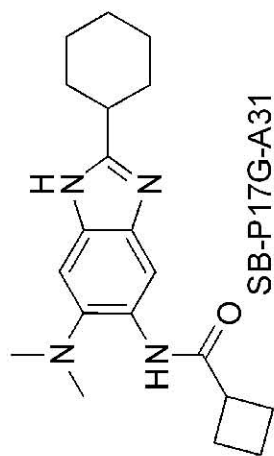


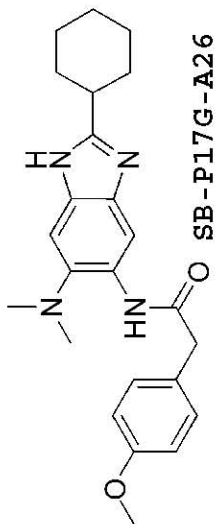




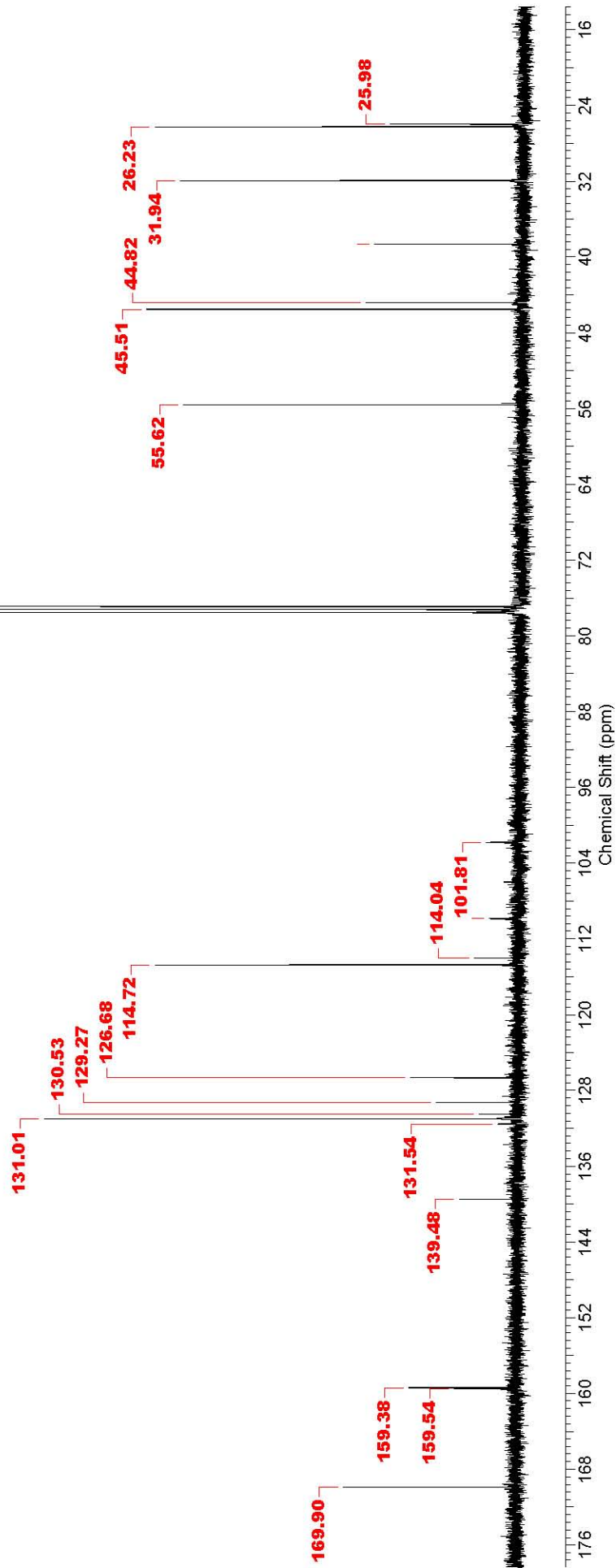
SB-P17G-A31

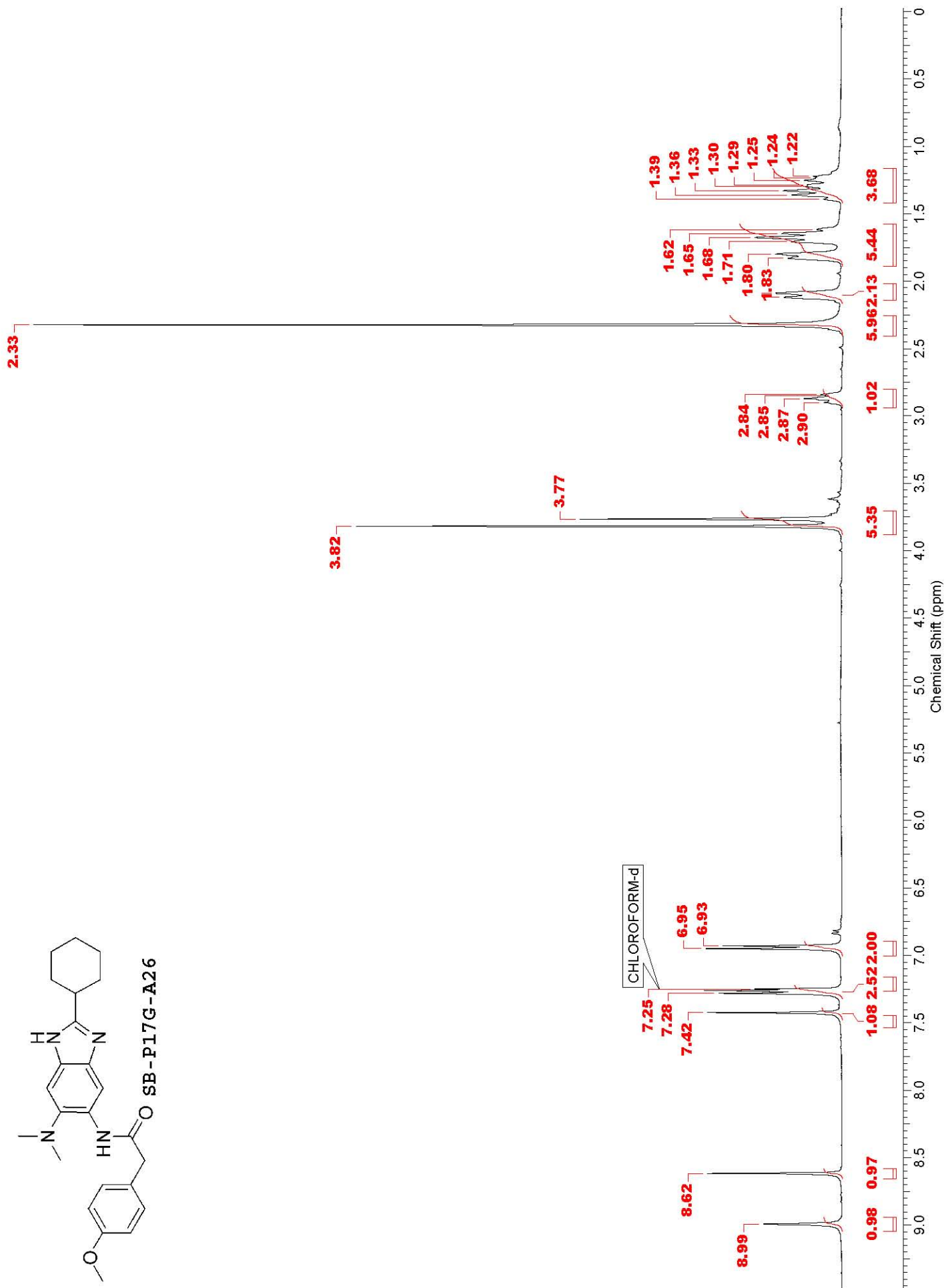
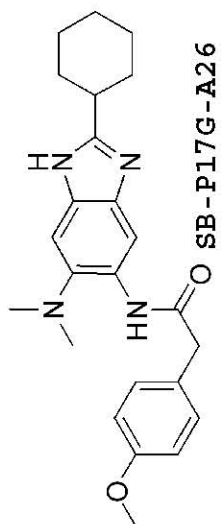


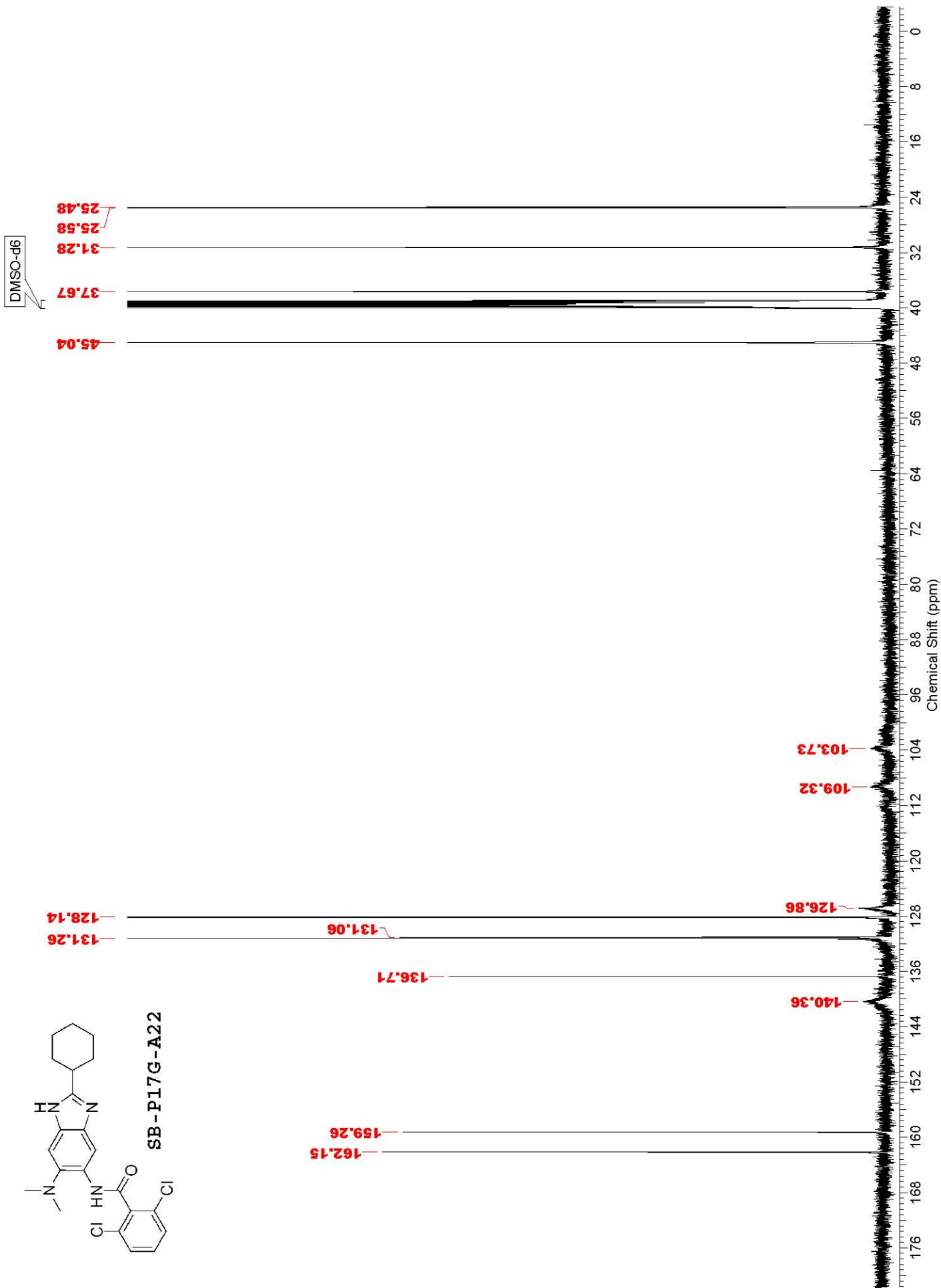


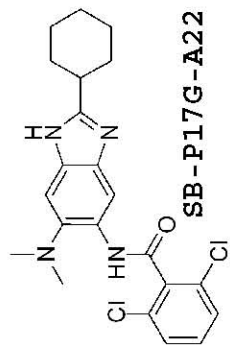


CHLOROFORM-d

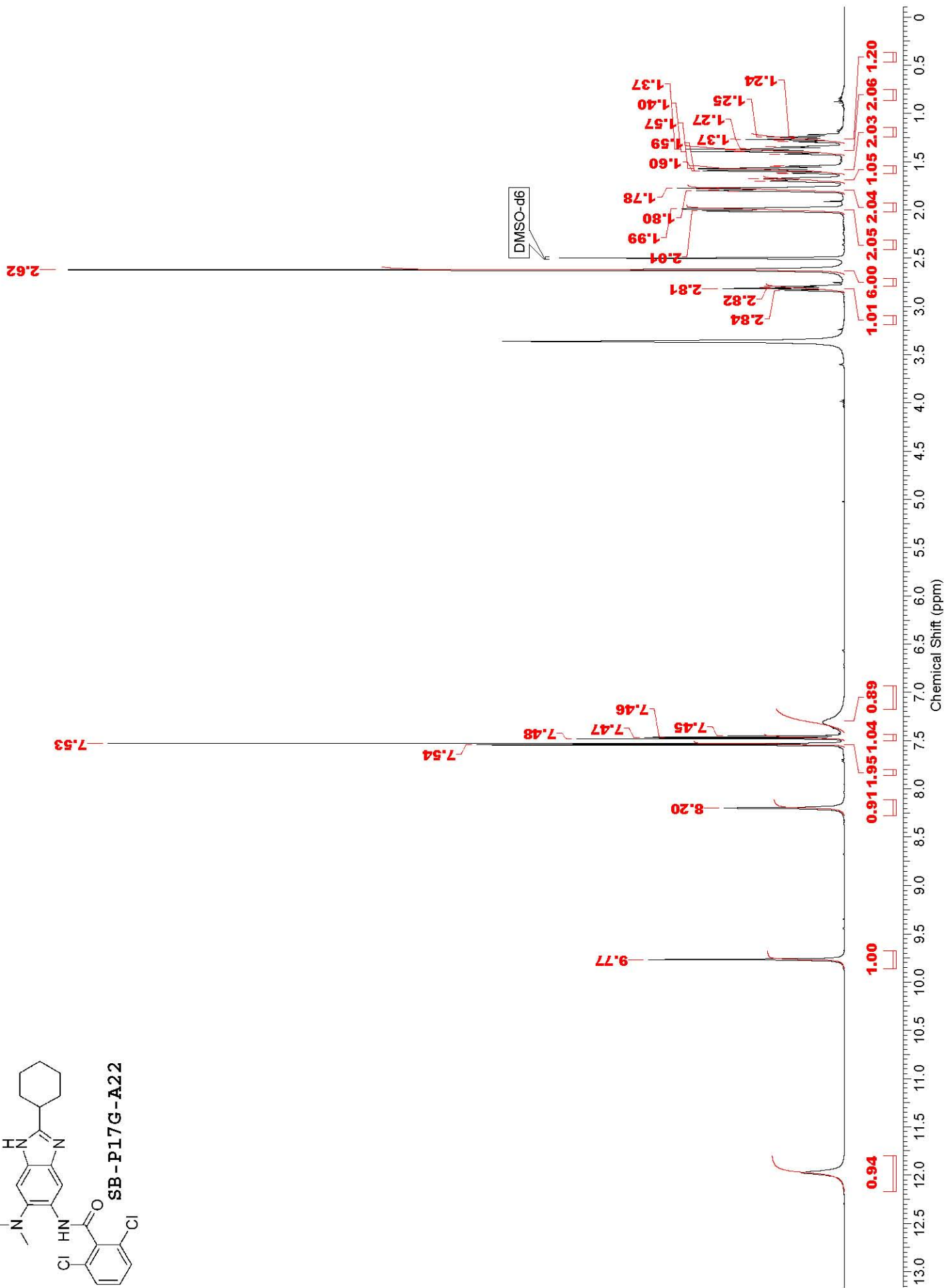




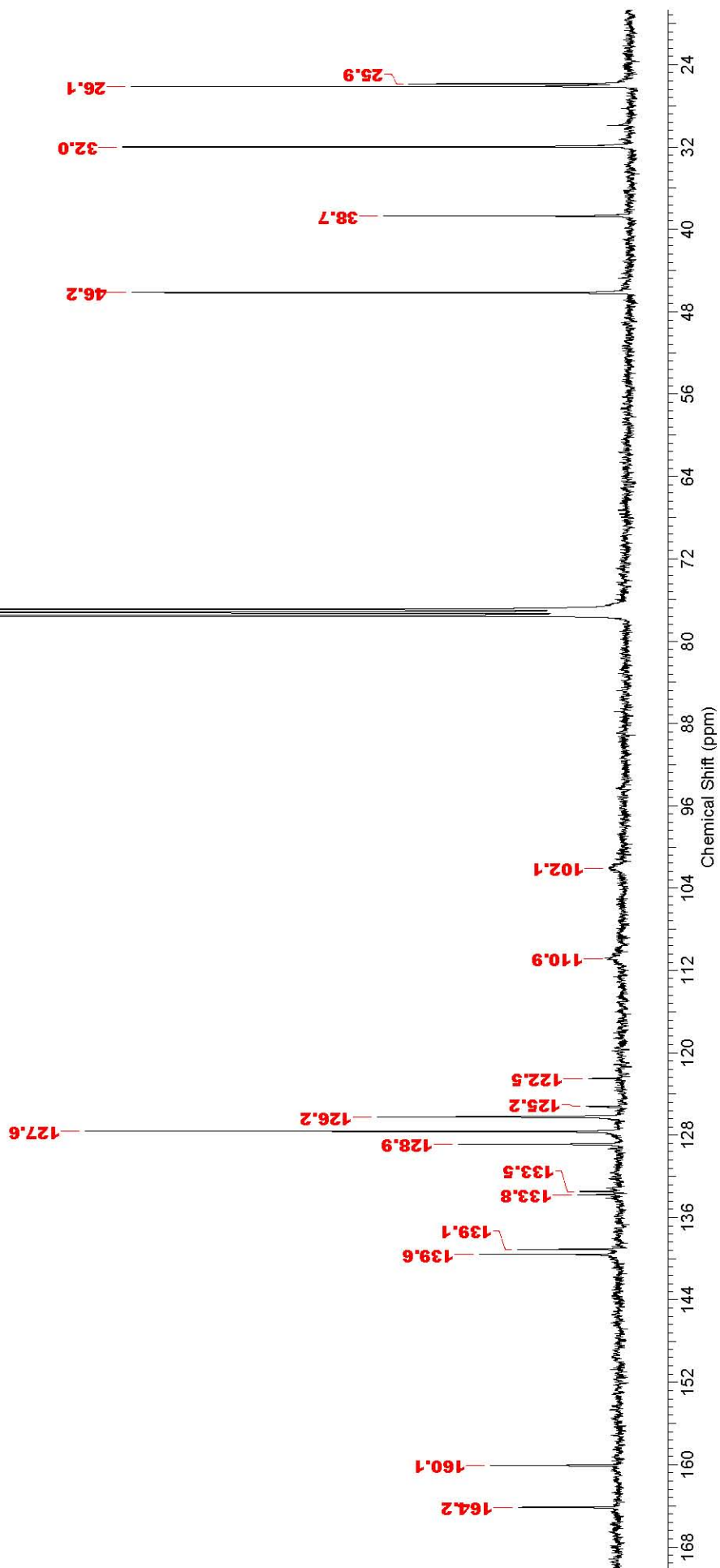
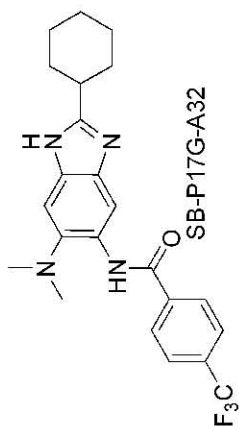


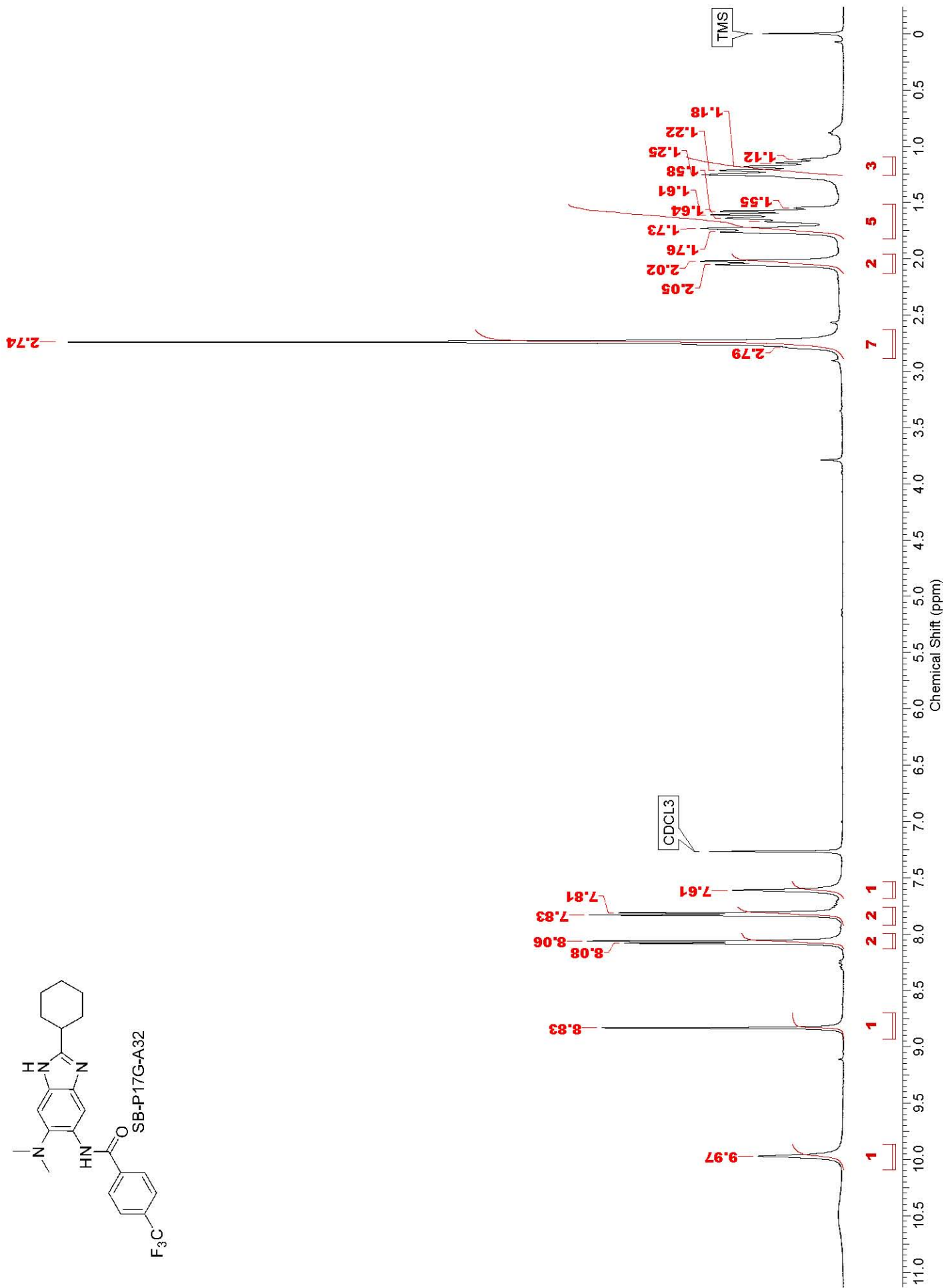
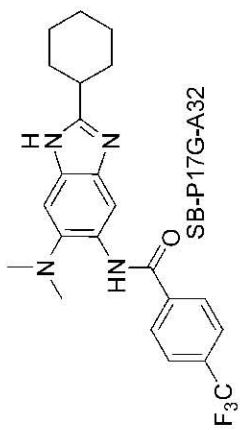


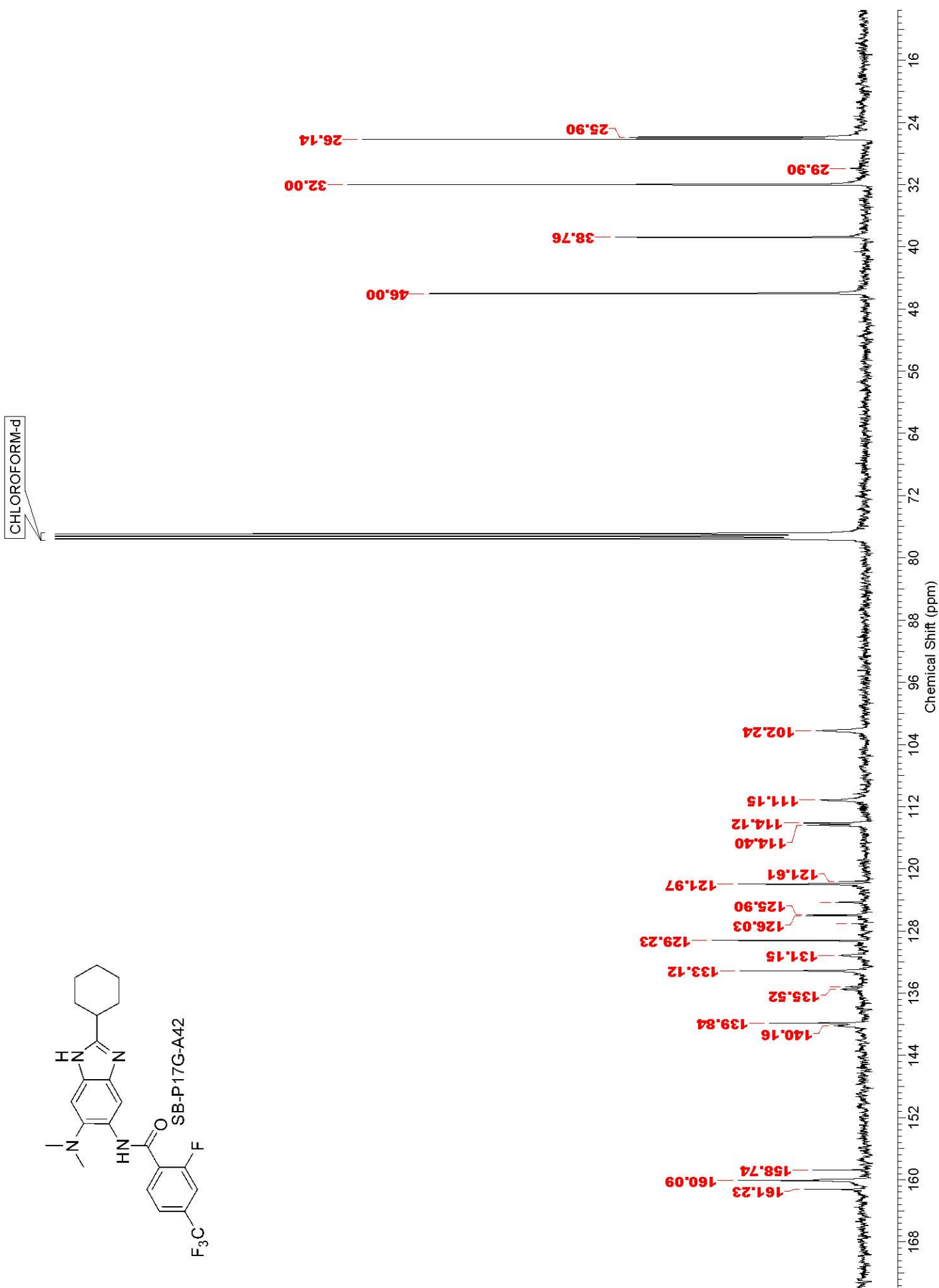
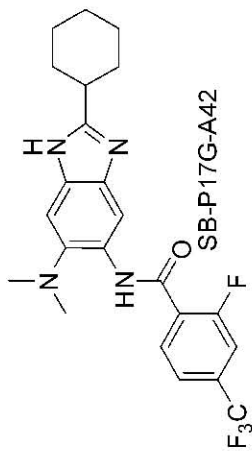
SB-P17G-A22

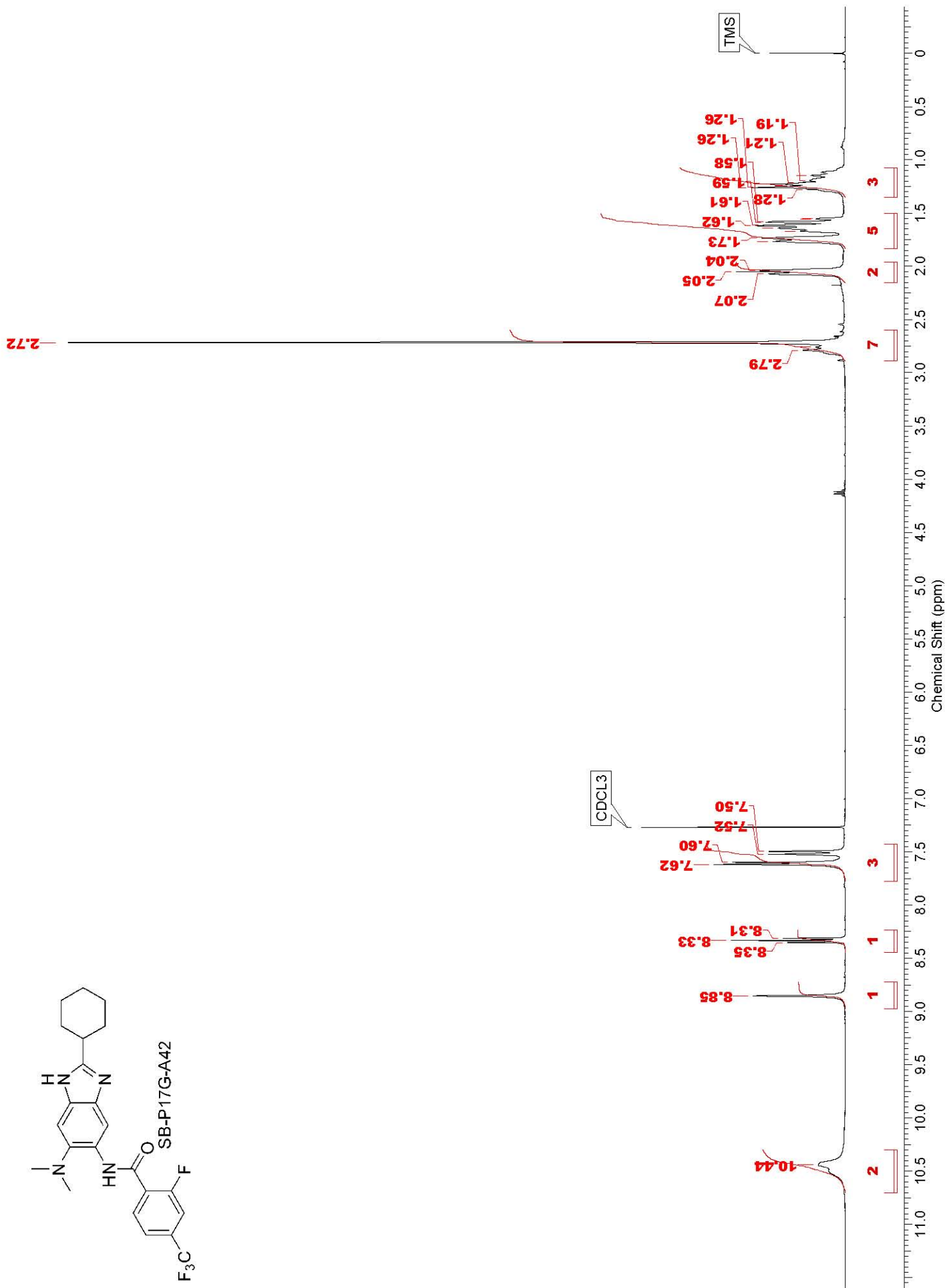
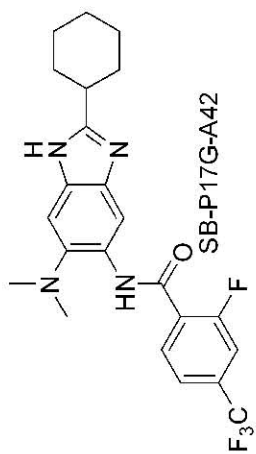


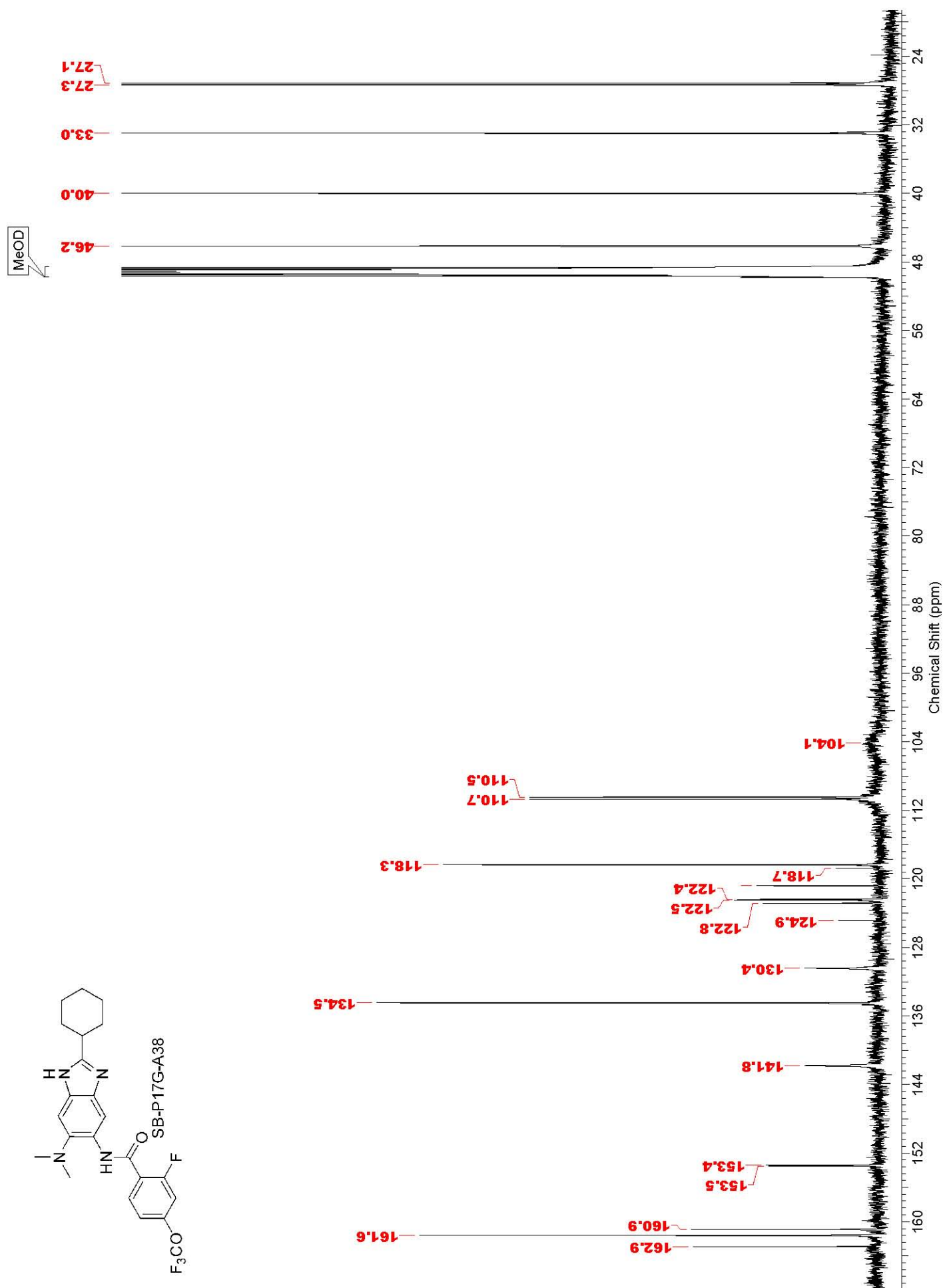
CHLOROFORM-d

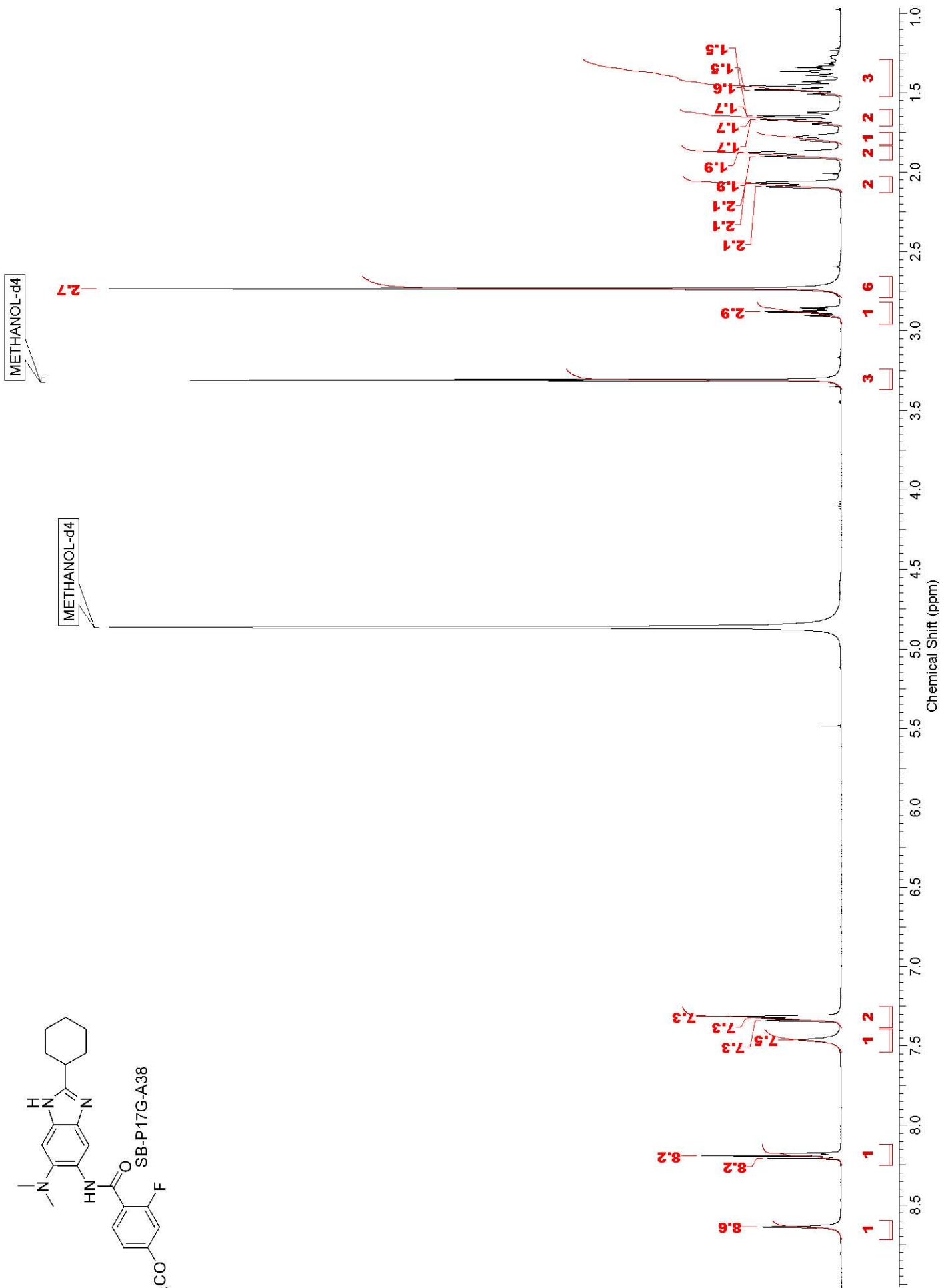
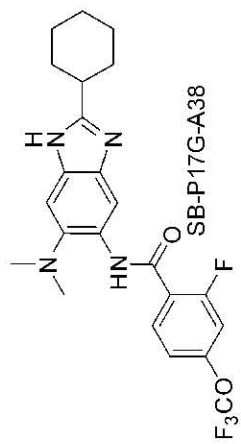


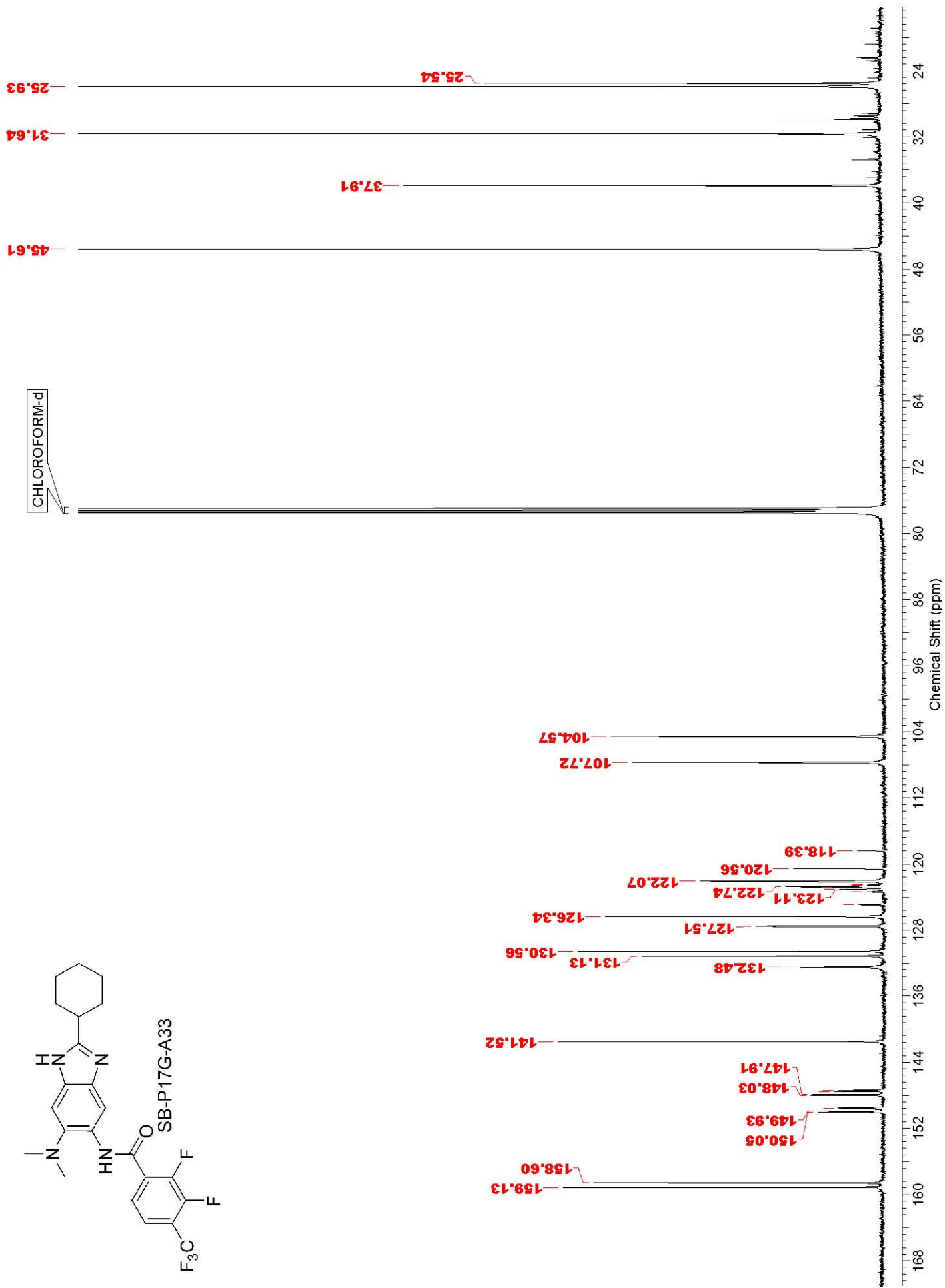
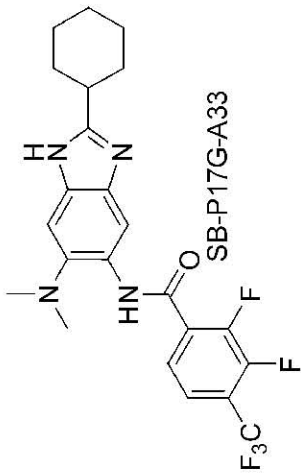


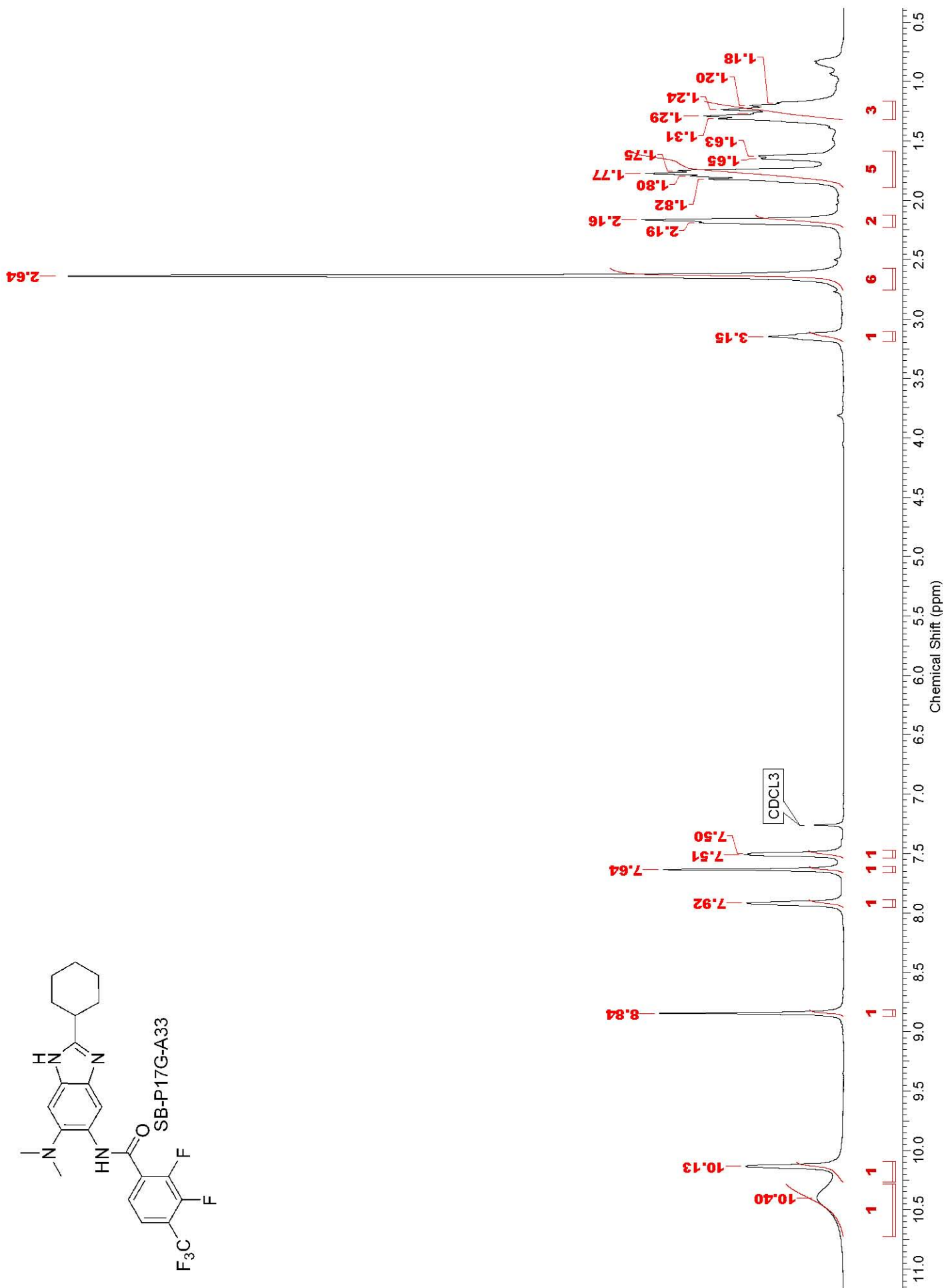
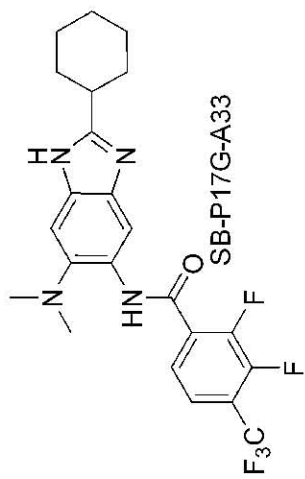


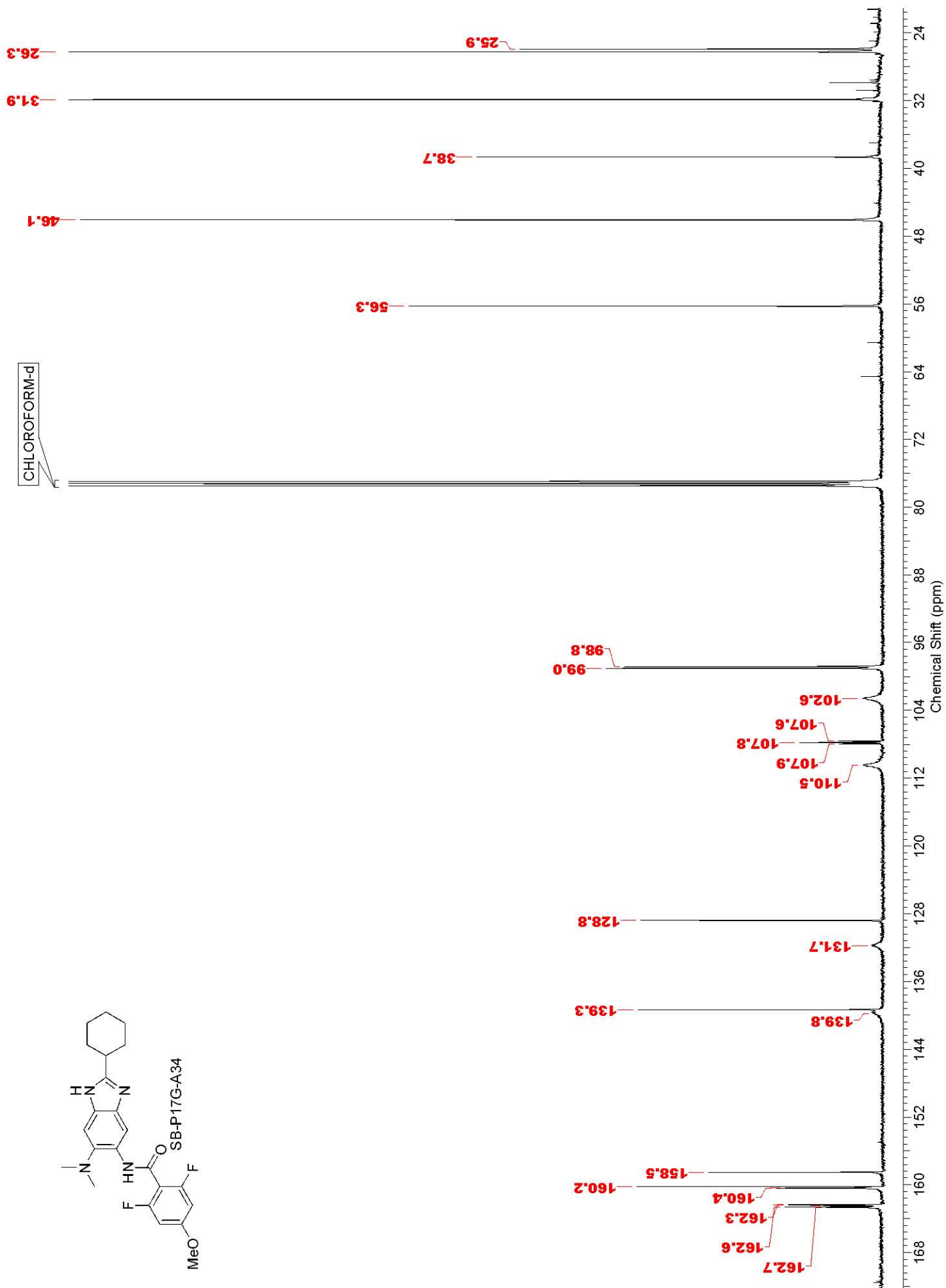
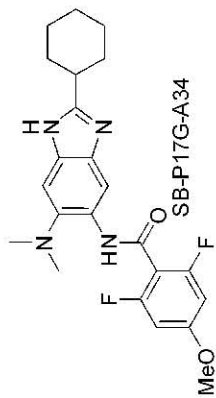


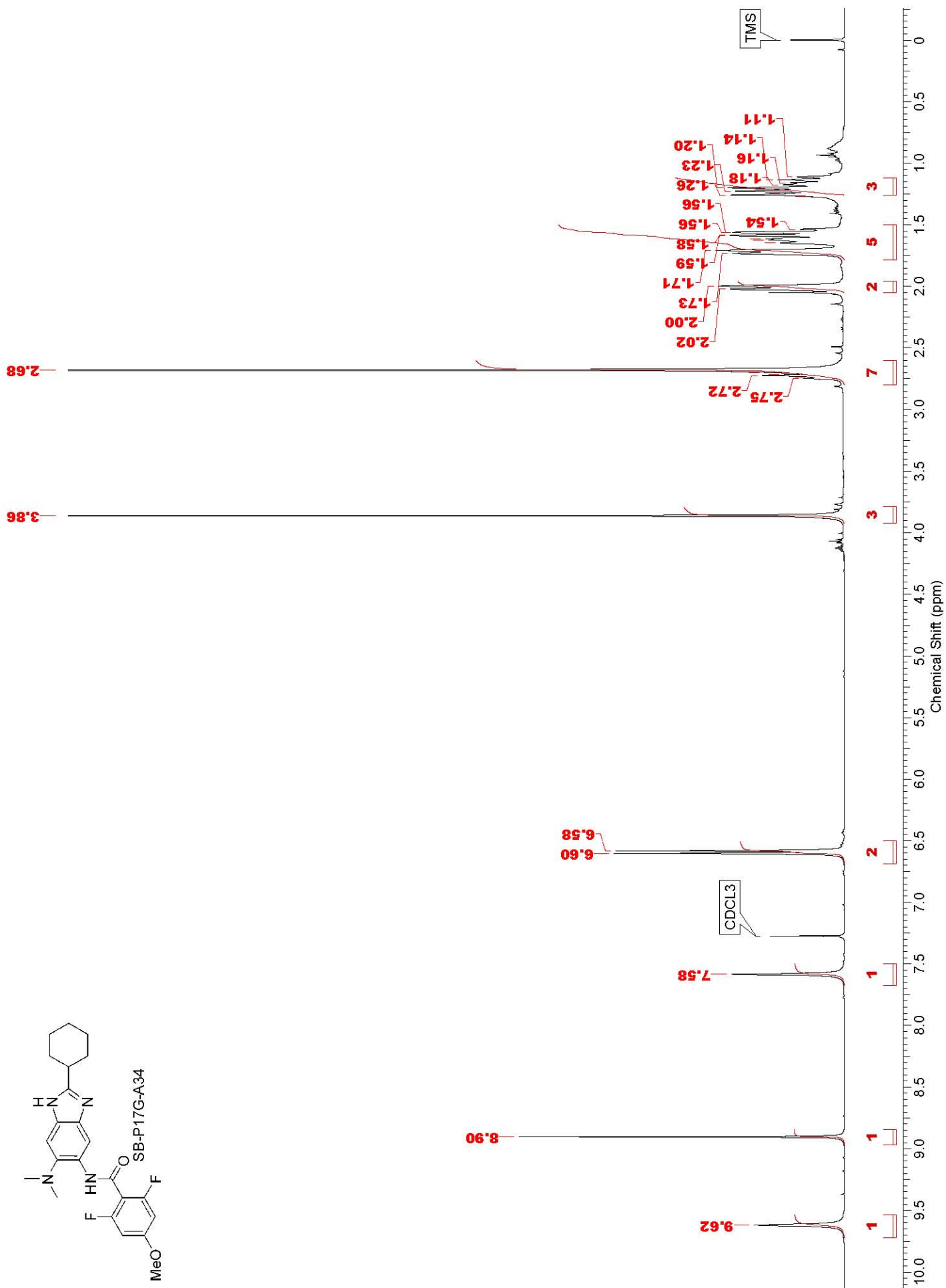
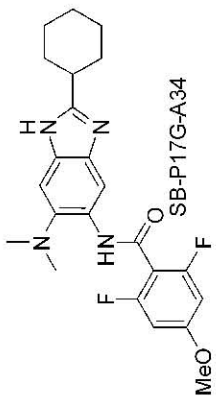




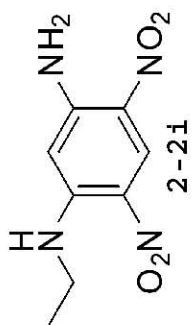




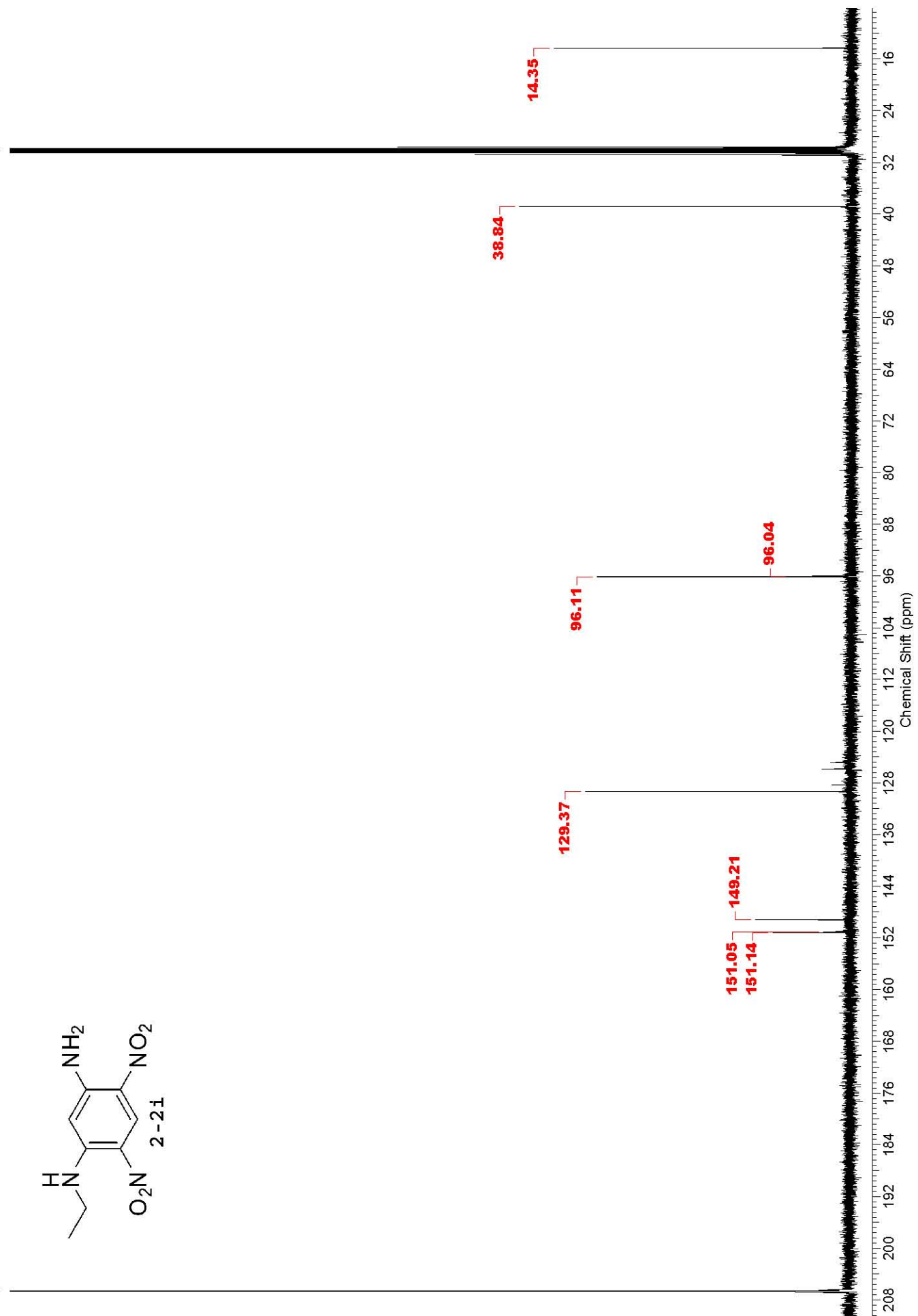


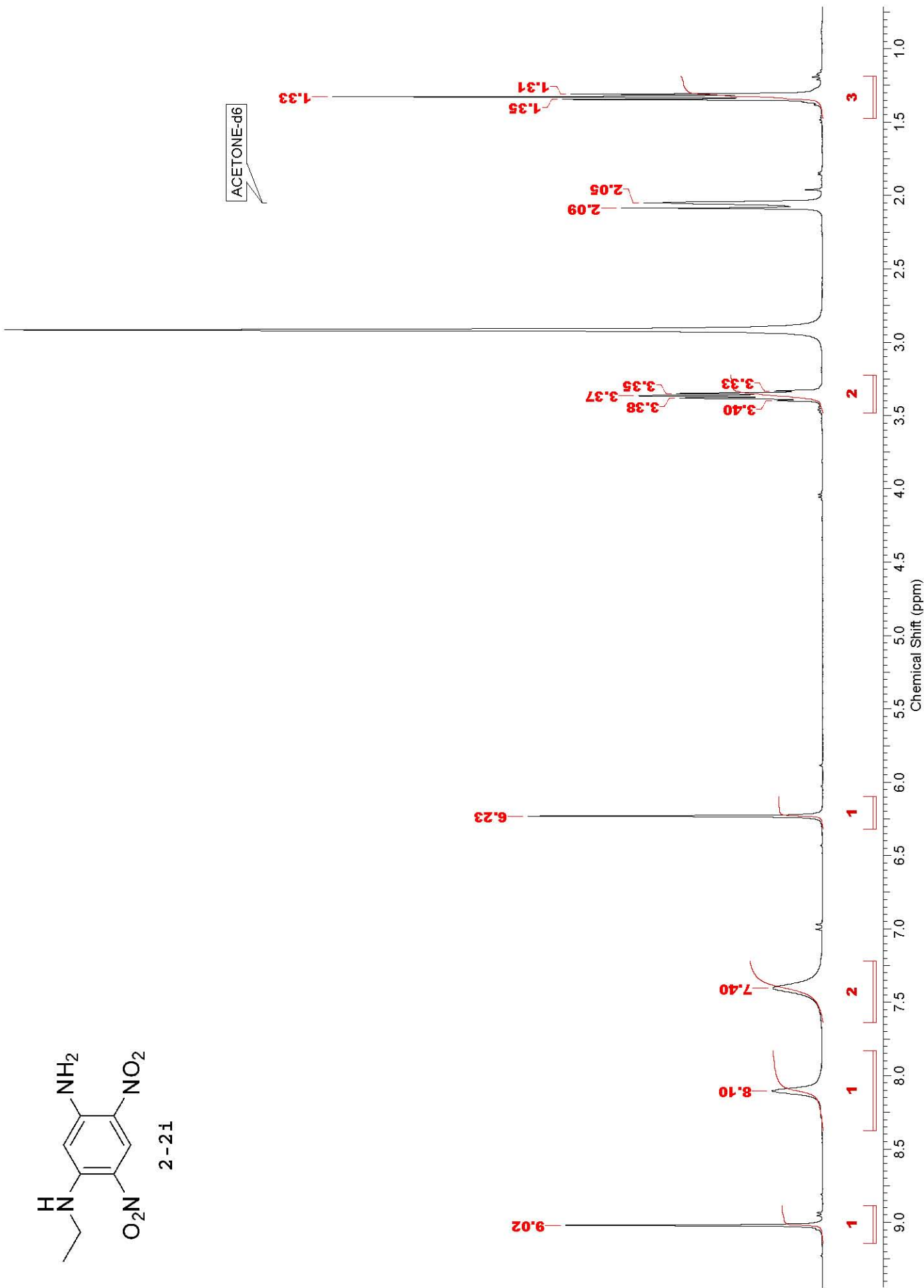
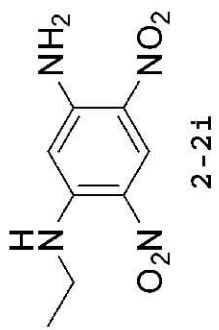


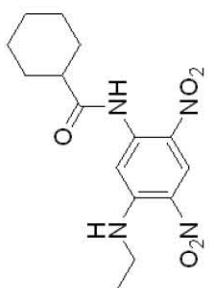
ACETONE-d6



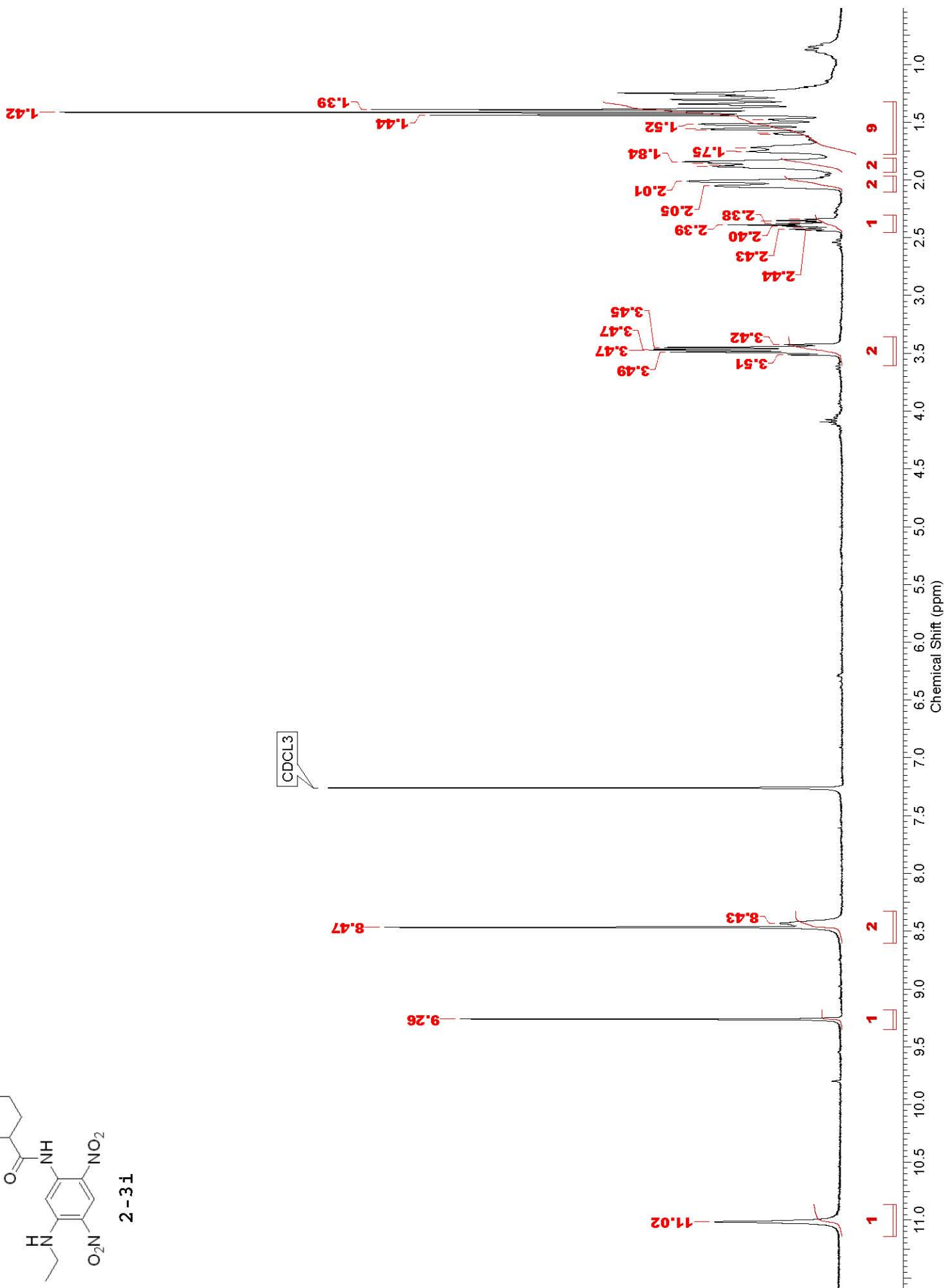
ACETONE-d6

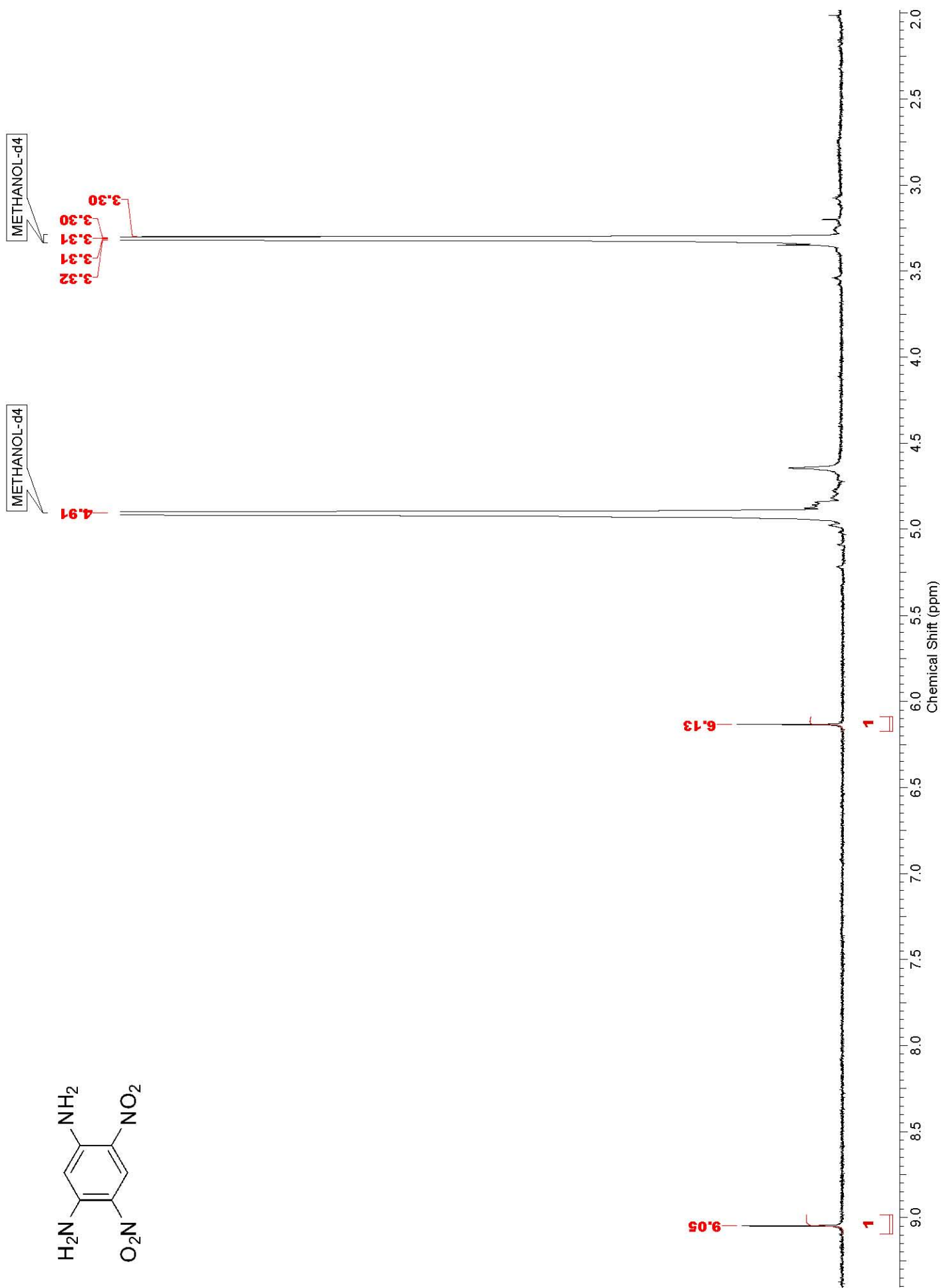
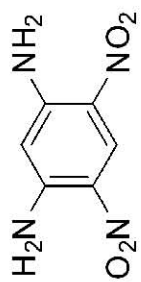


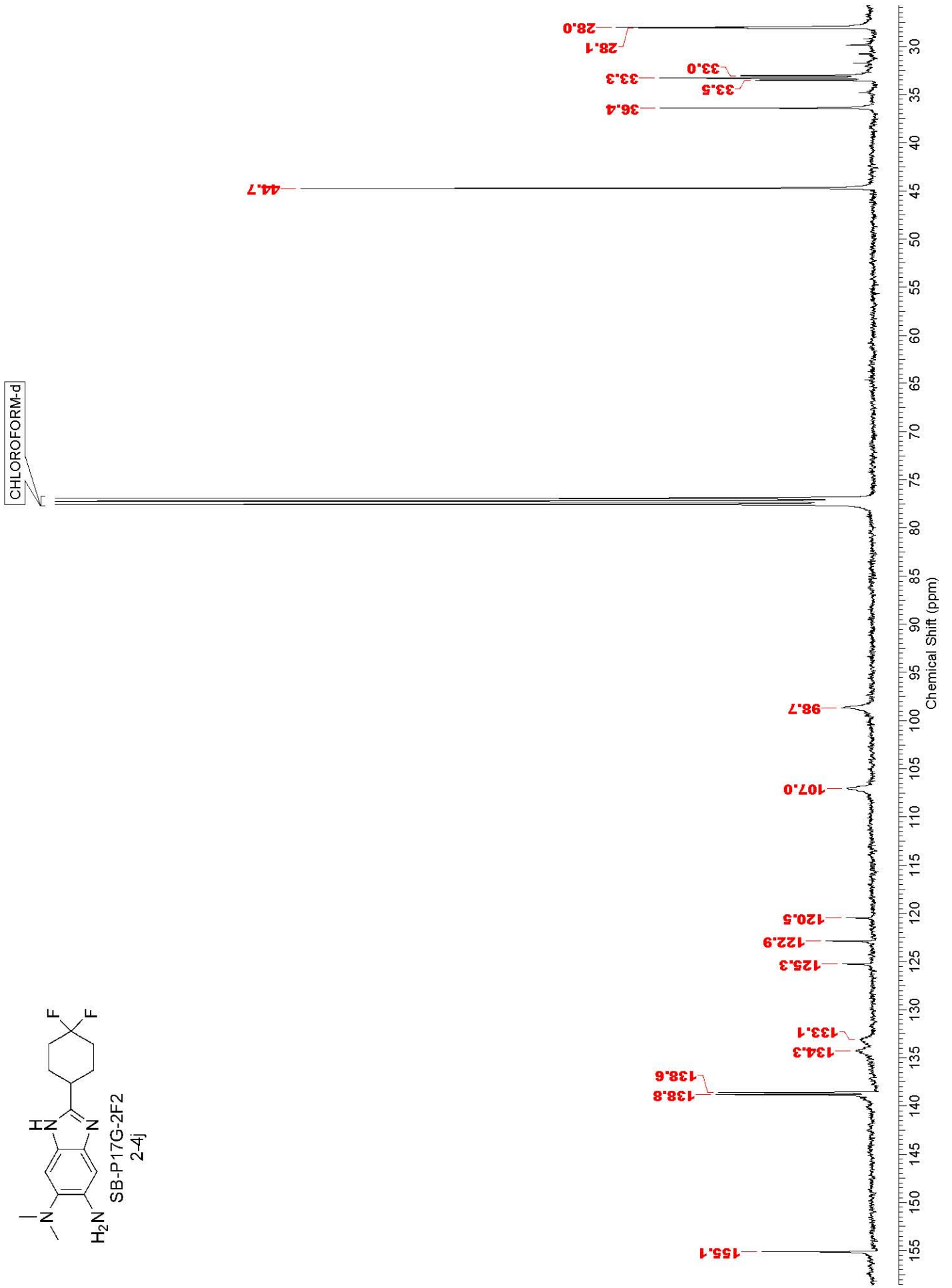
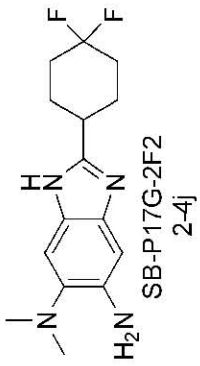


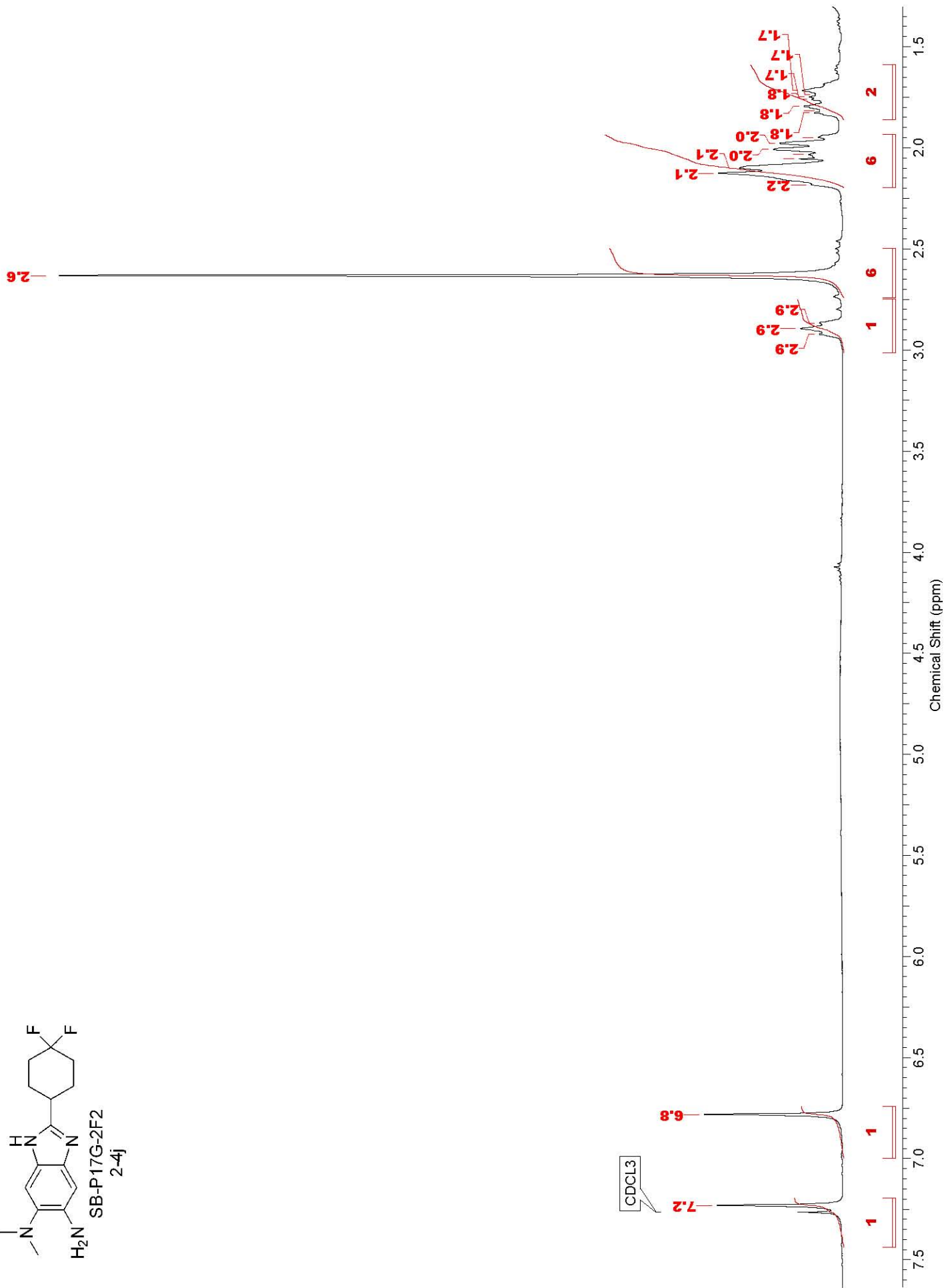
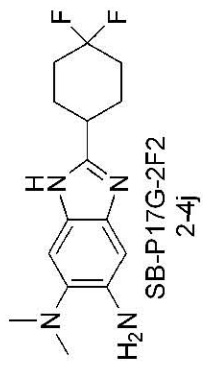


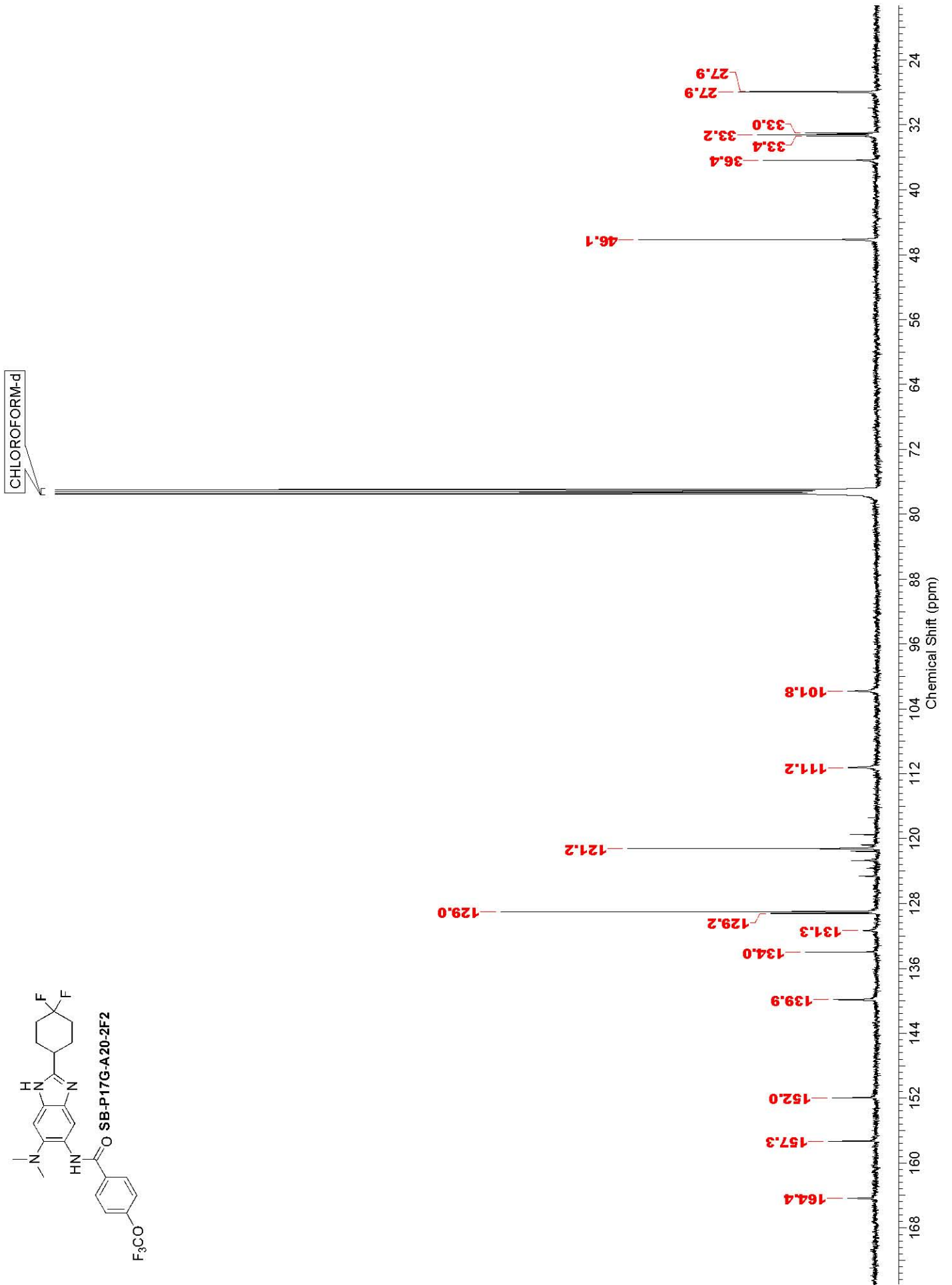
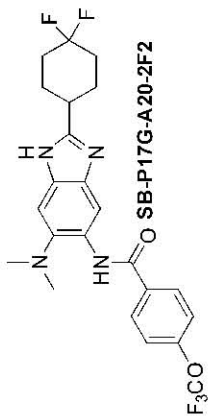
2-31

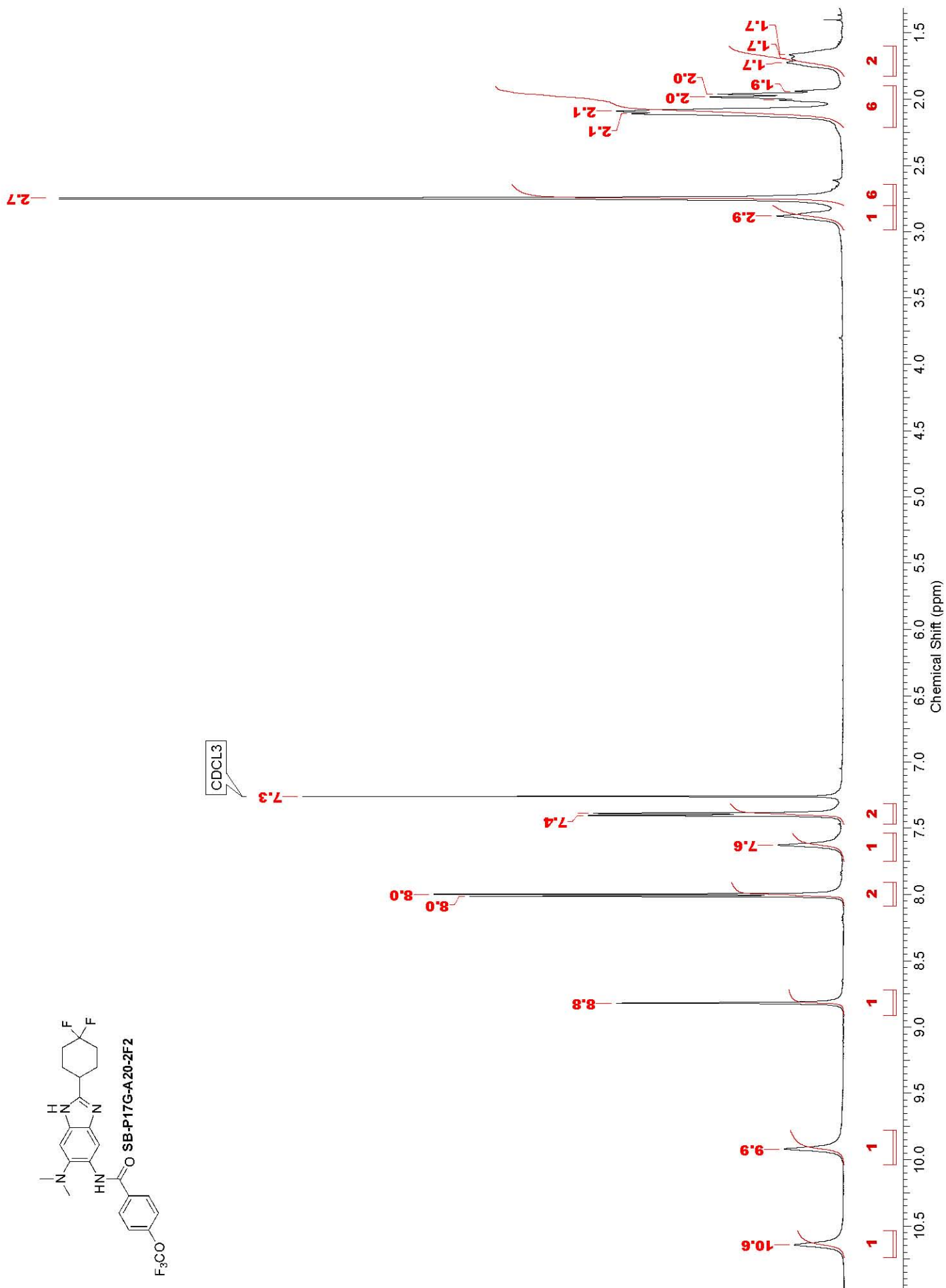
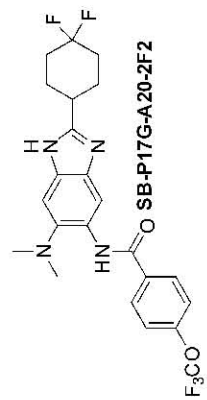


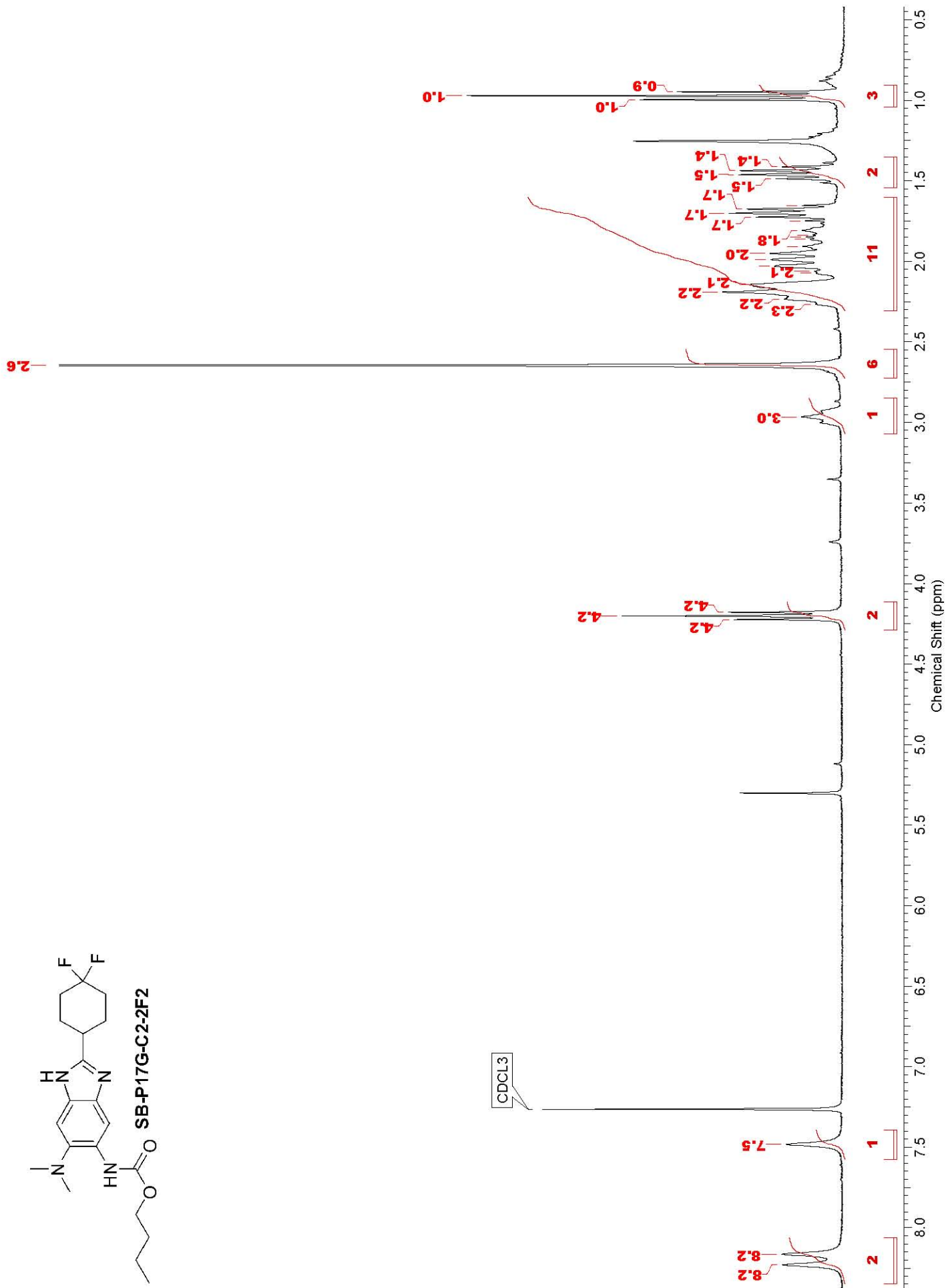
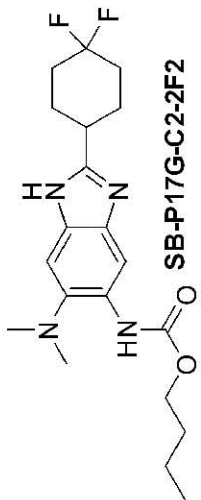


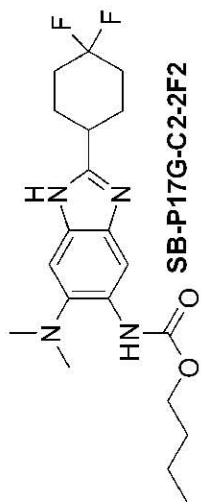




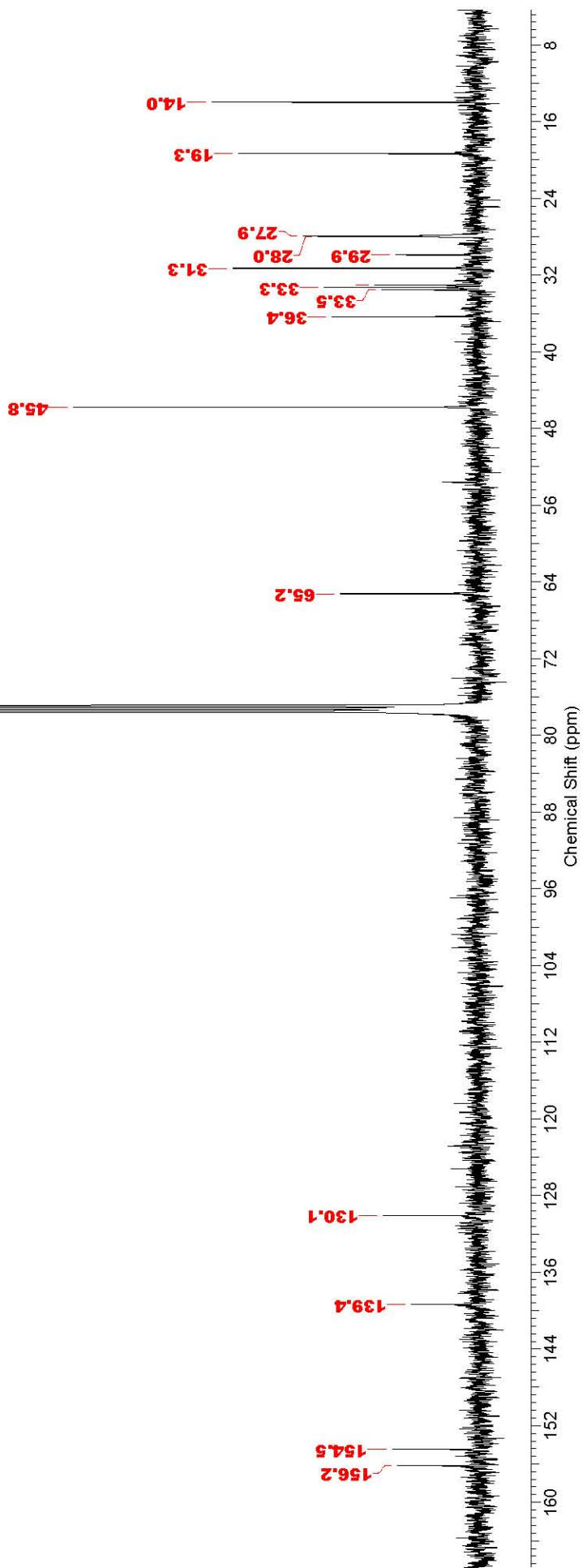


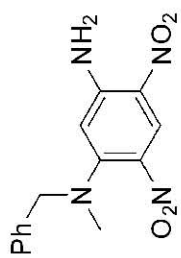




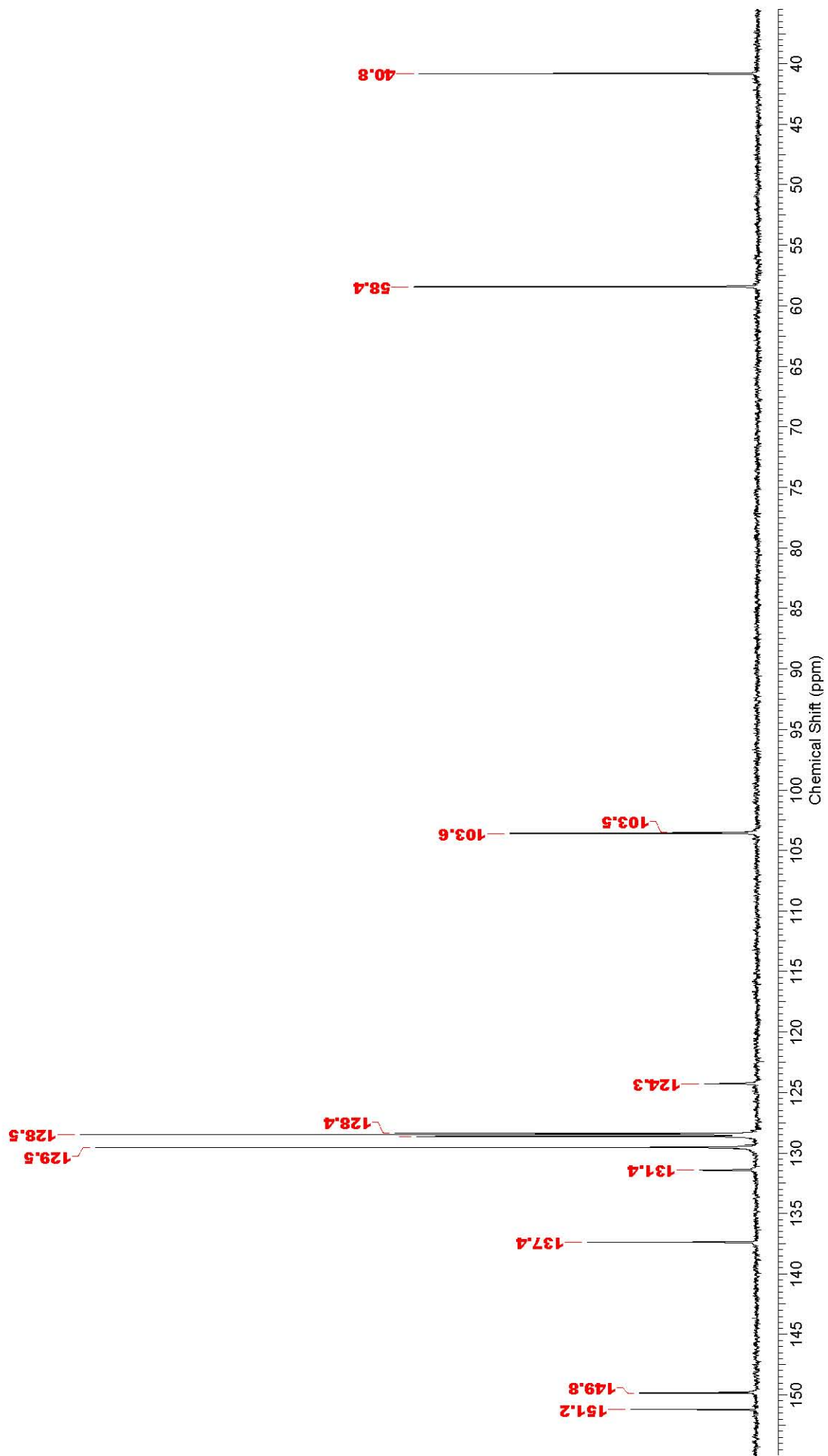


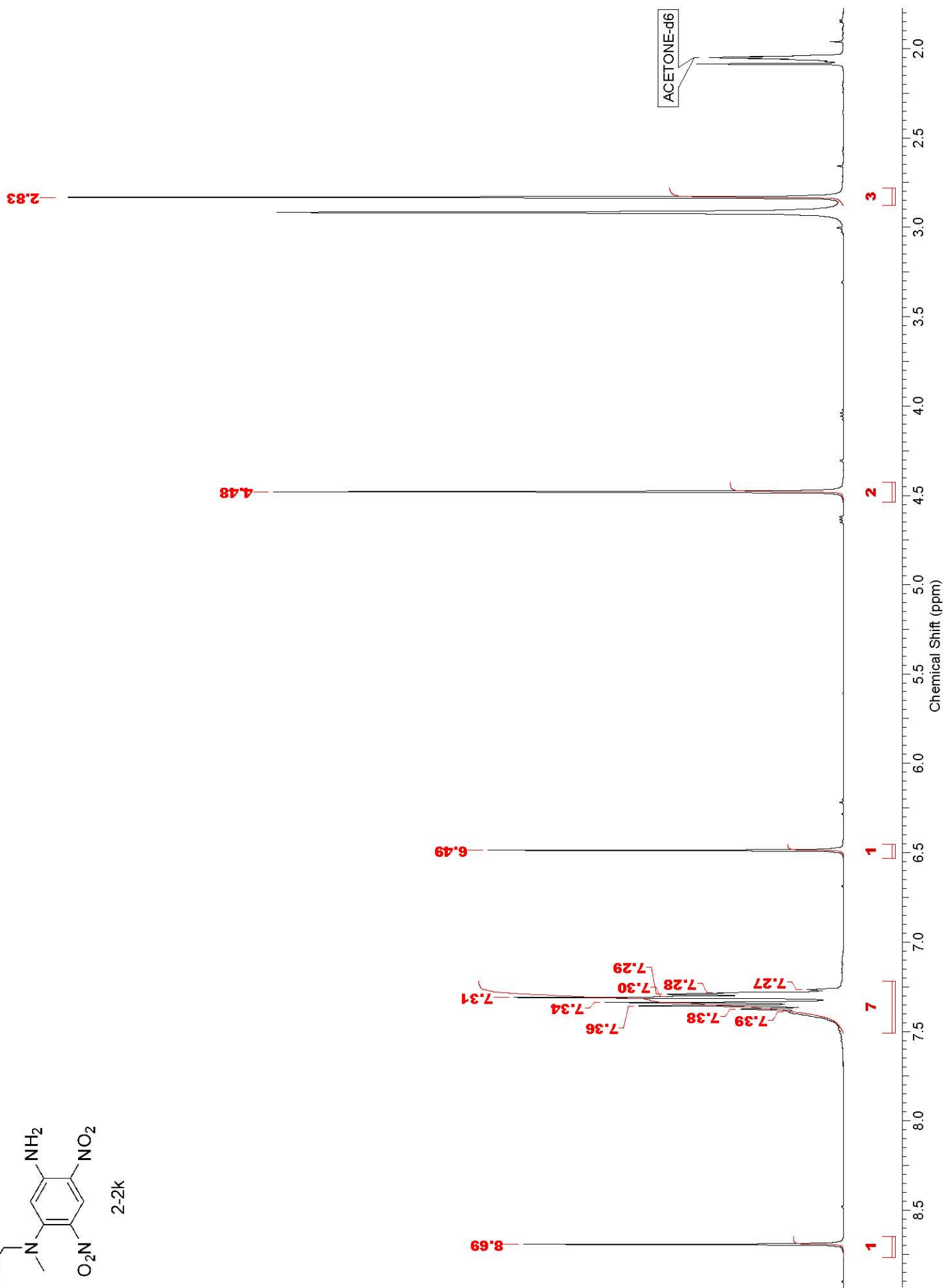
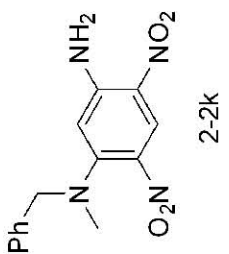
CHLOROFORM-d

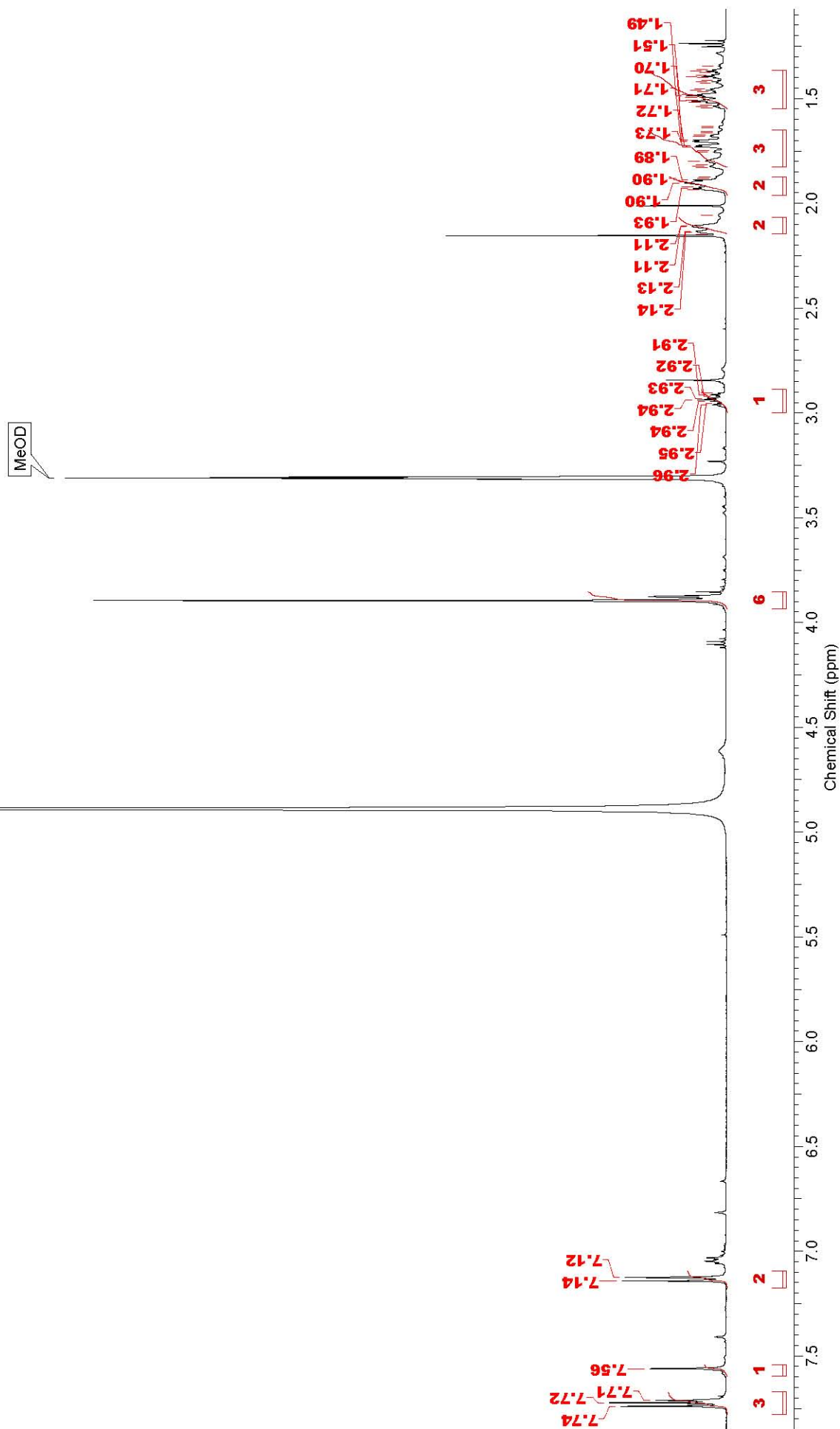
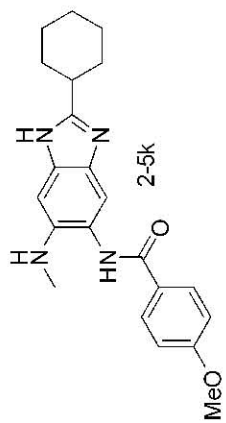


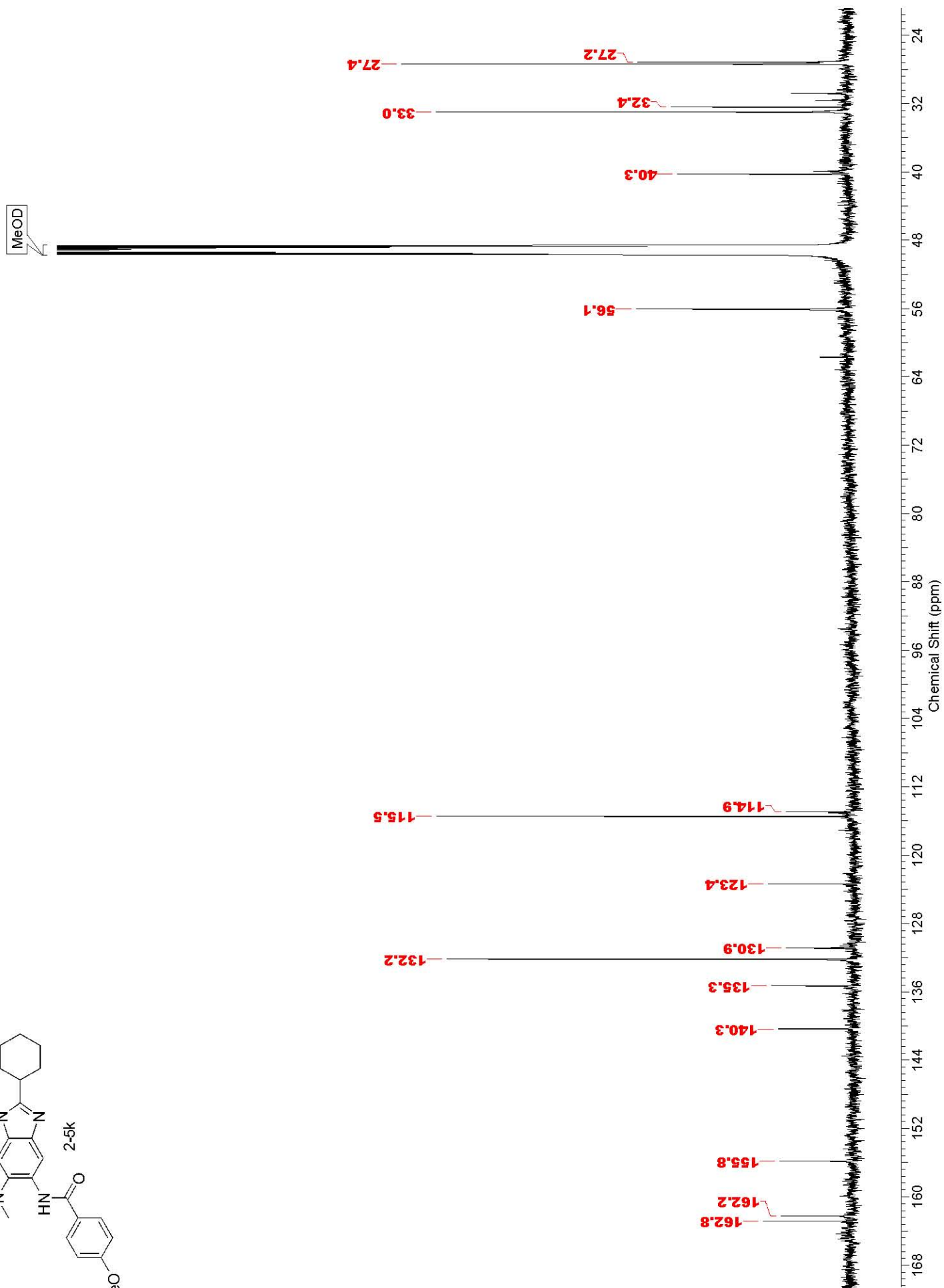
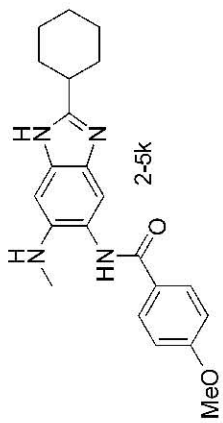


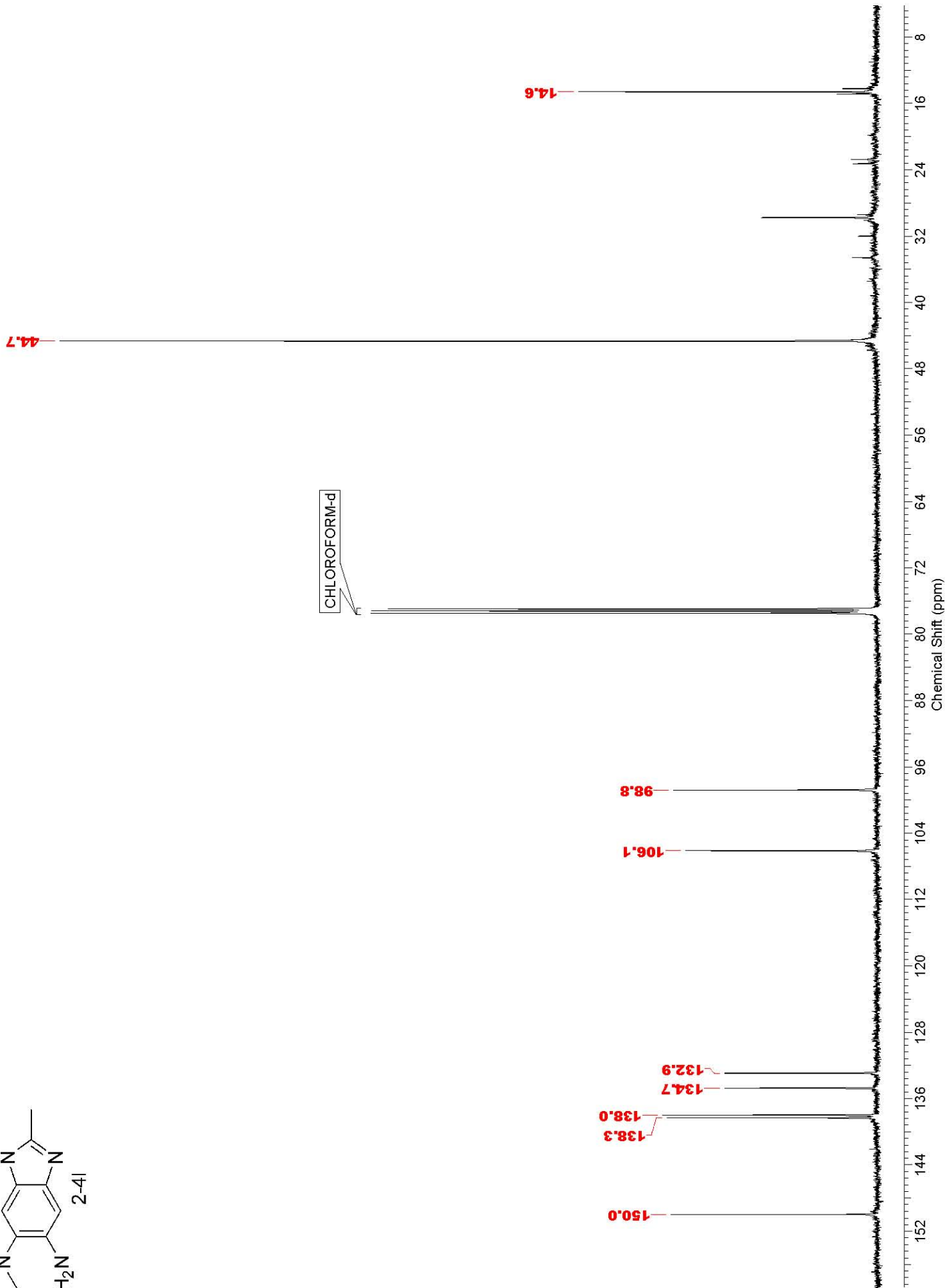
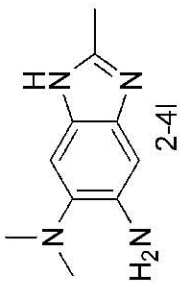
2-2k

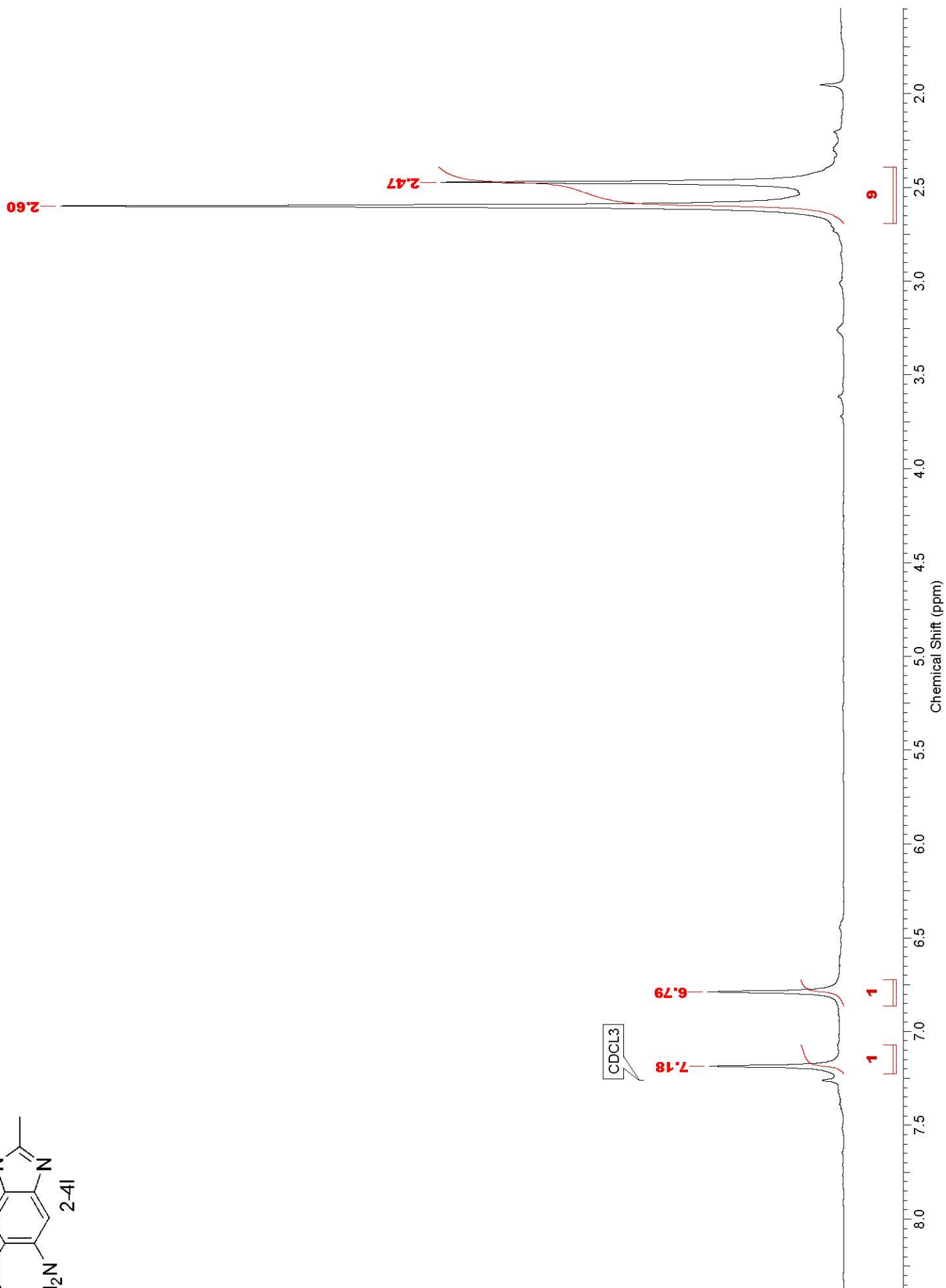
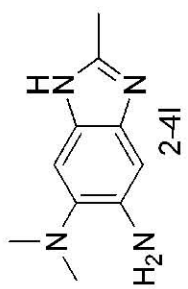


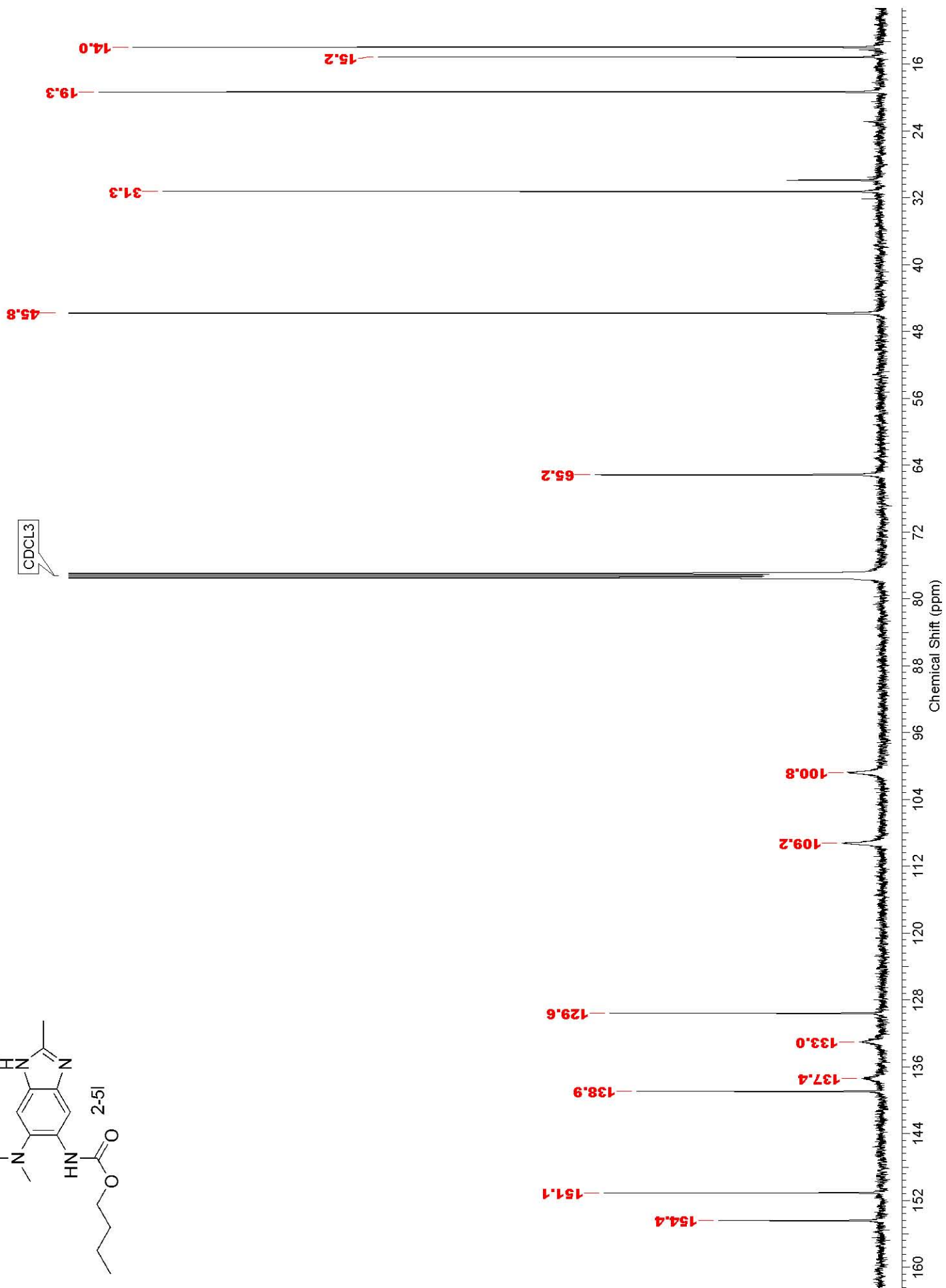
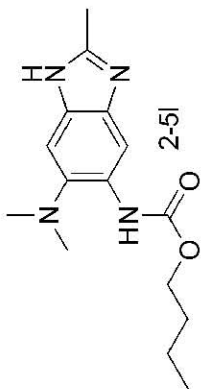


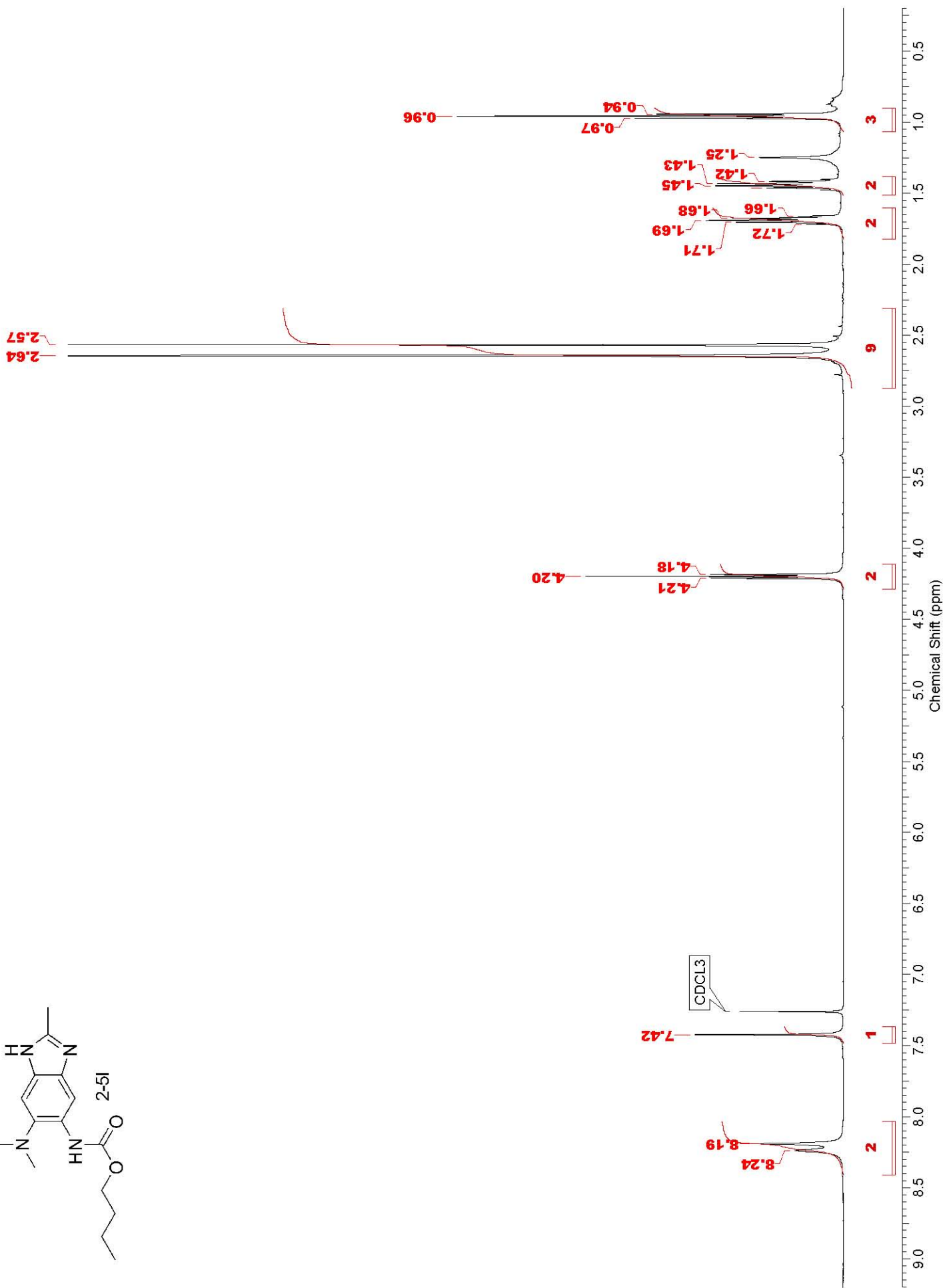
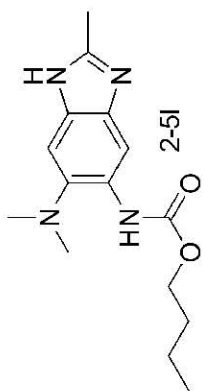


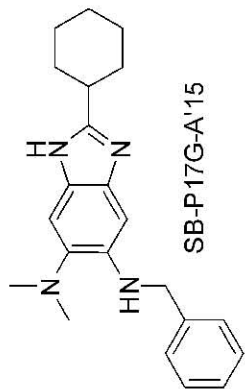




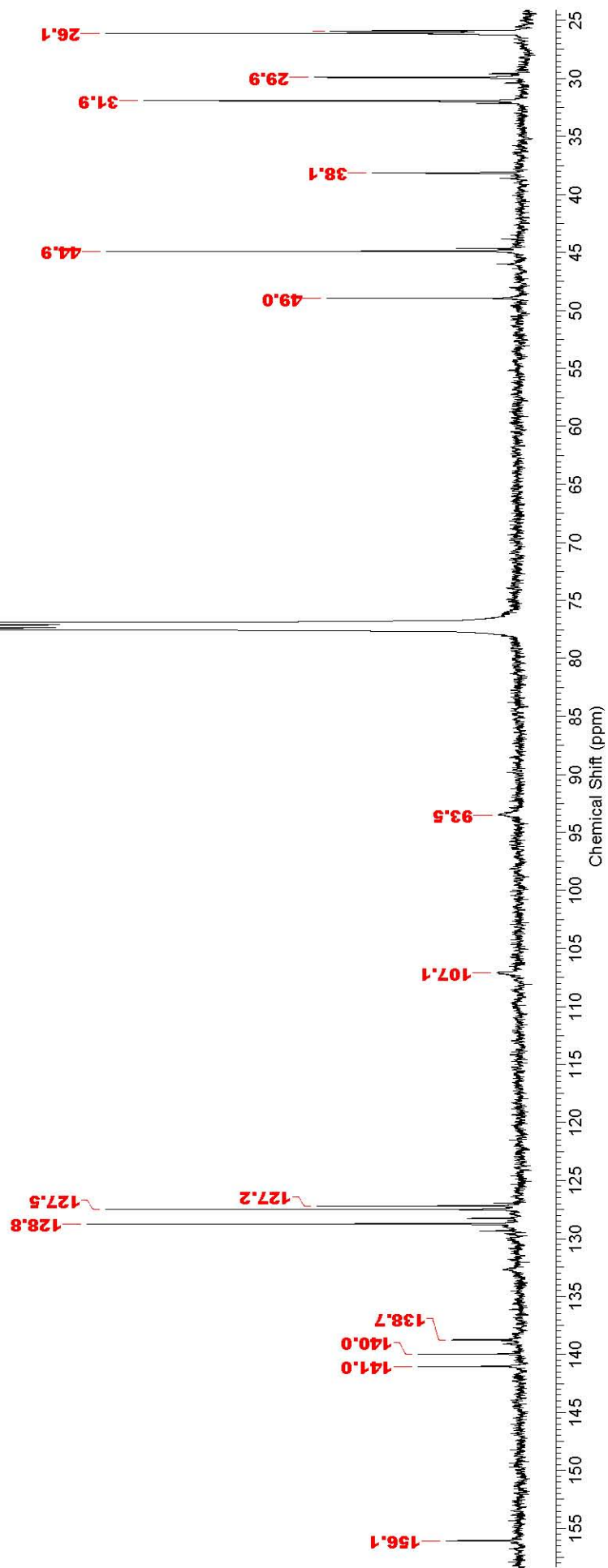


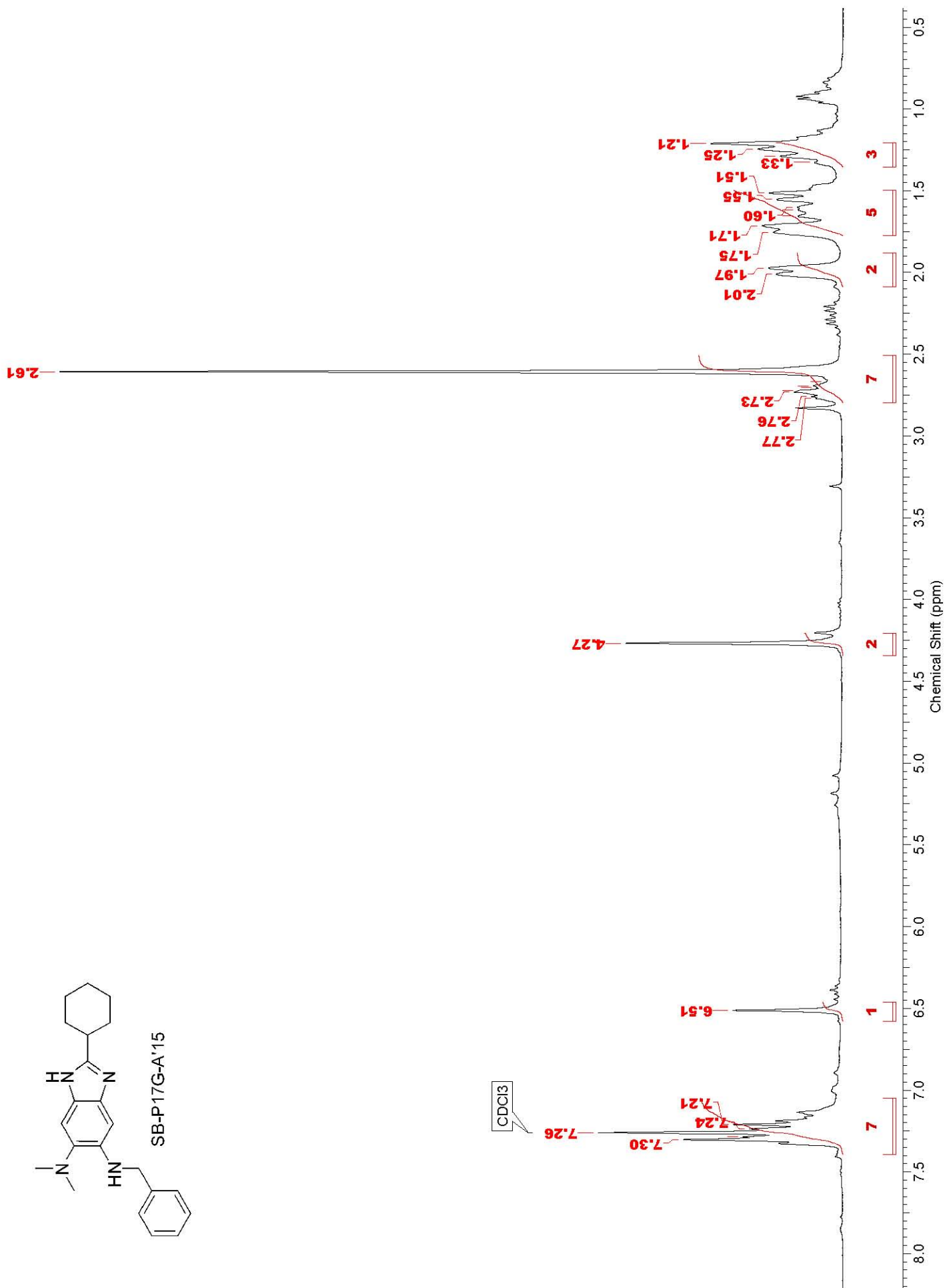
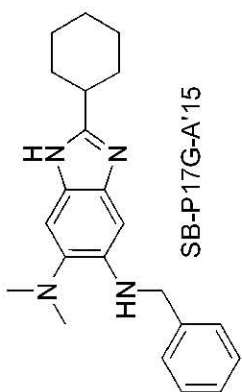


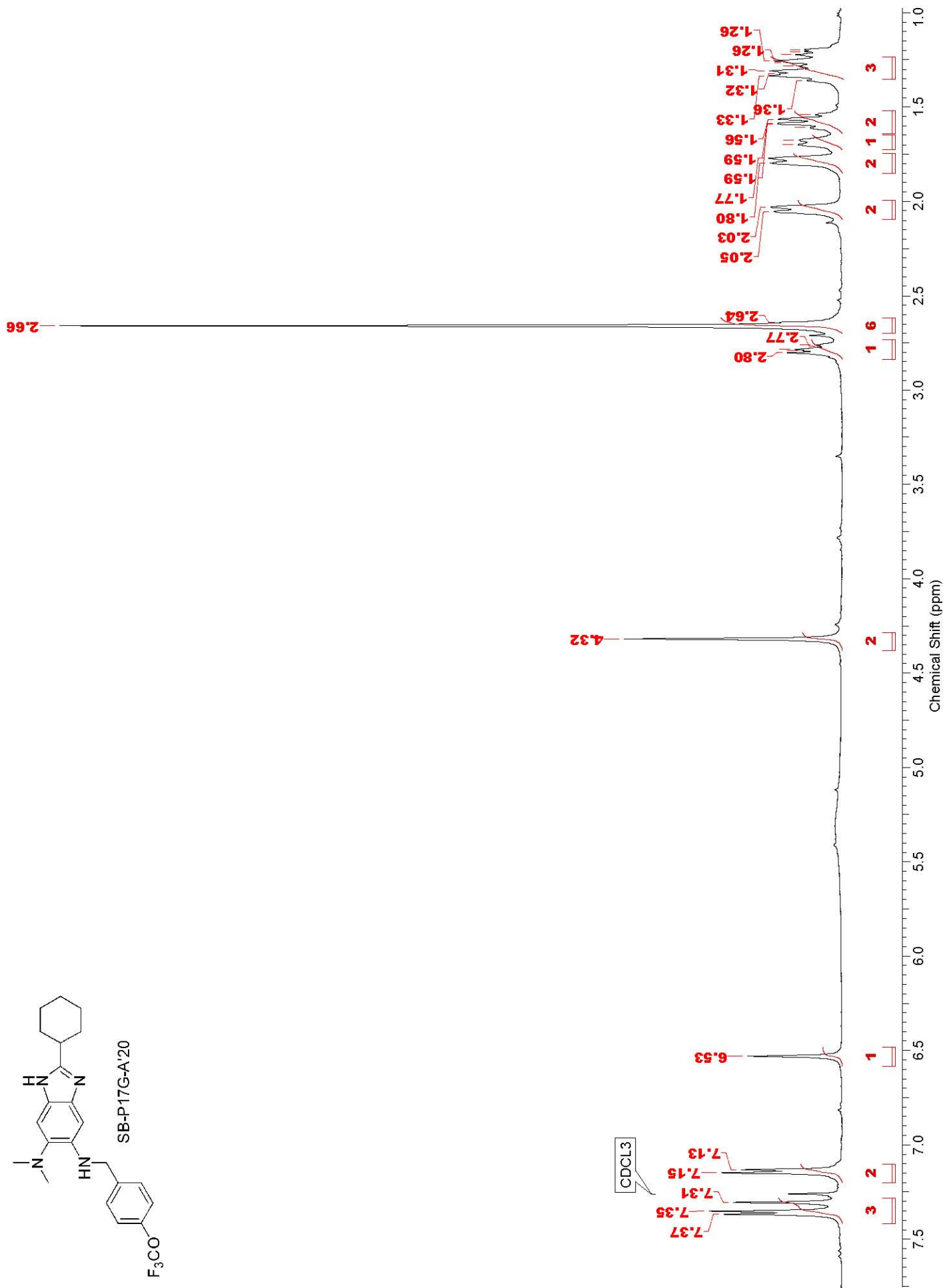
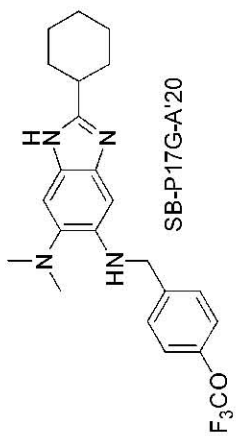


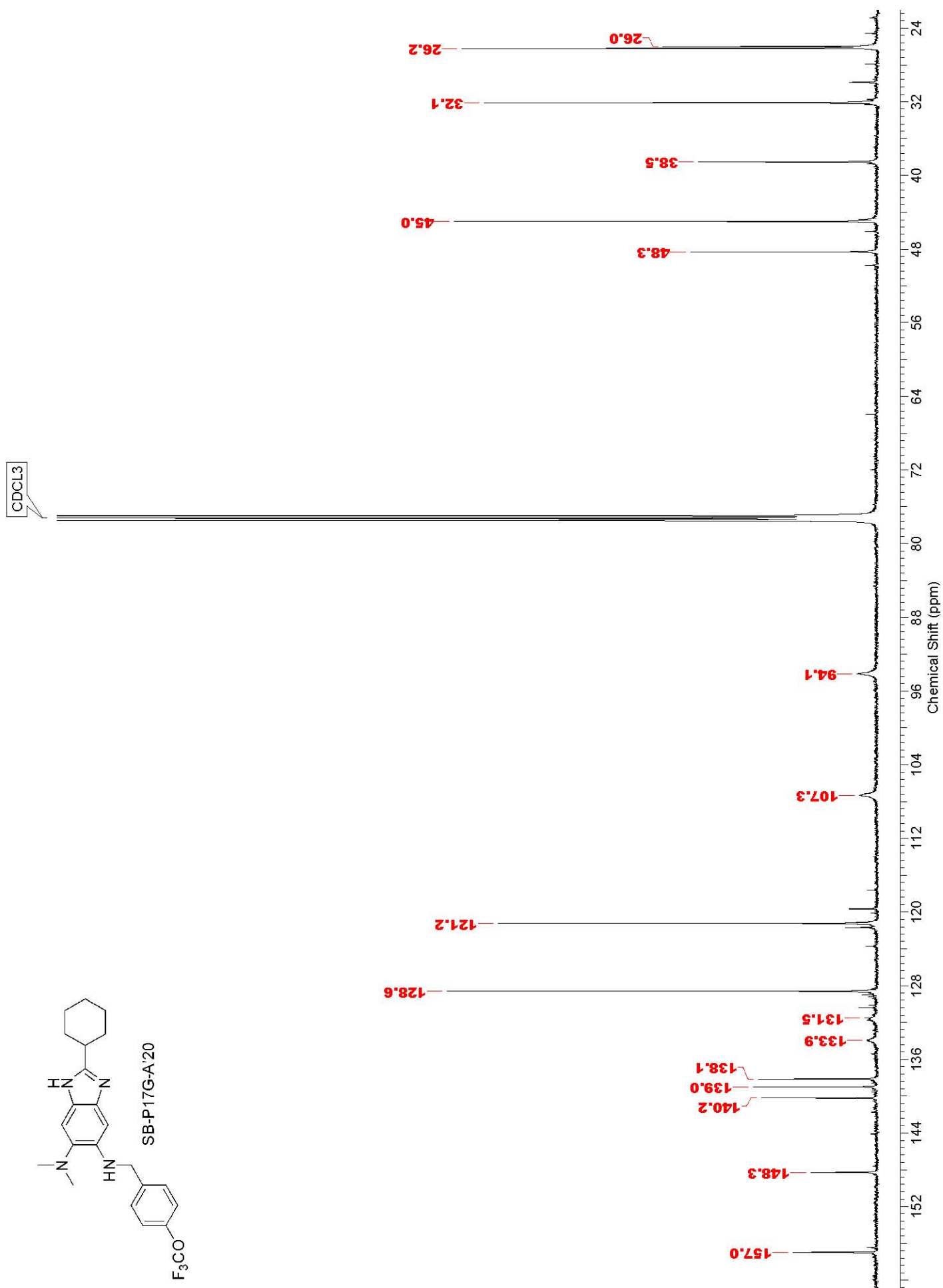
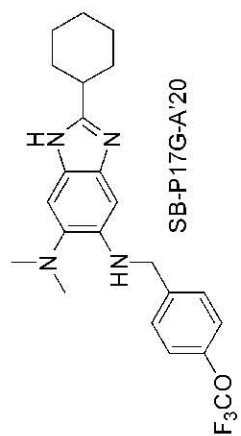


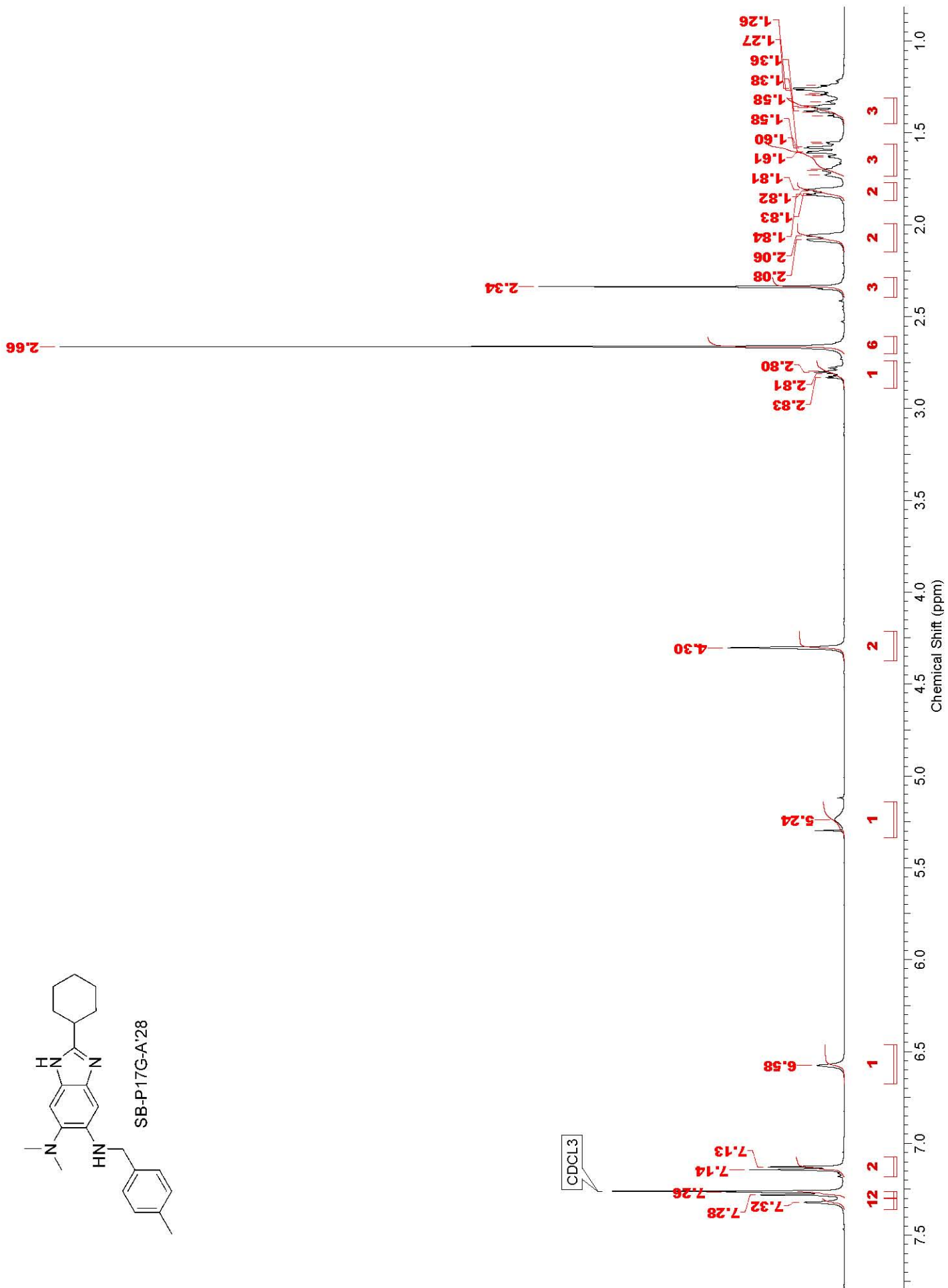
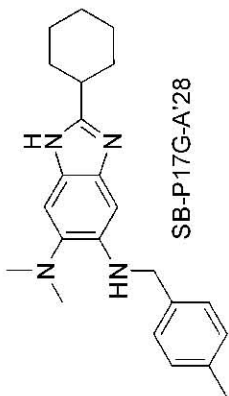
CHLOROFORM-d

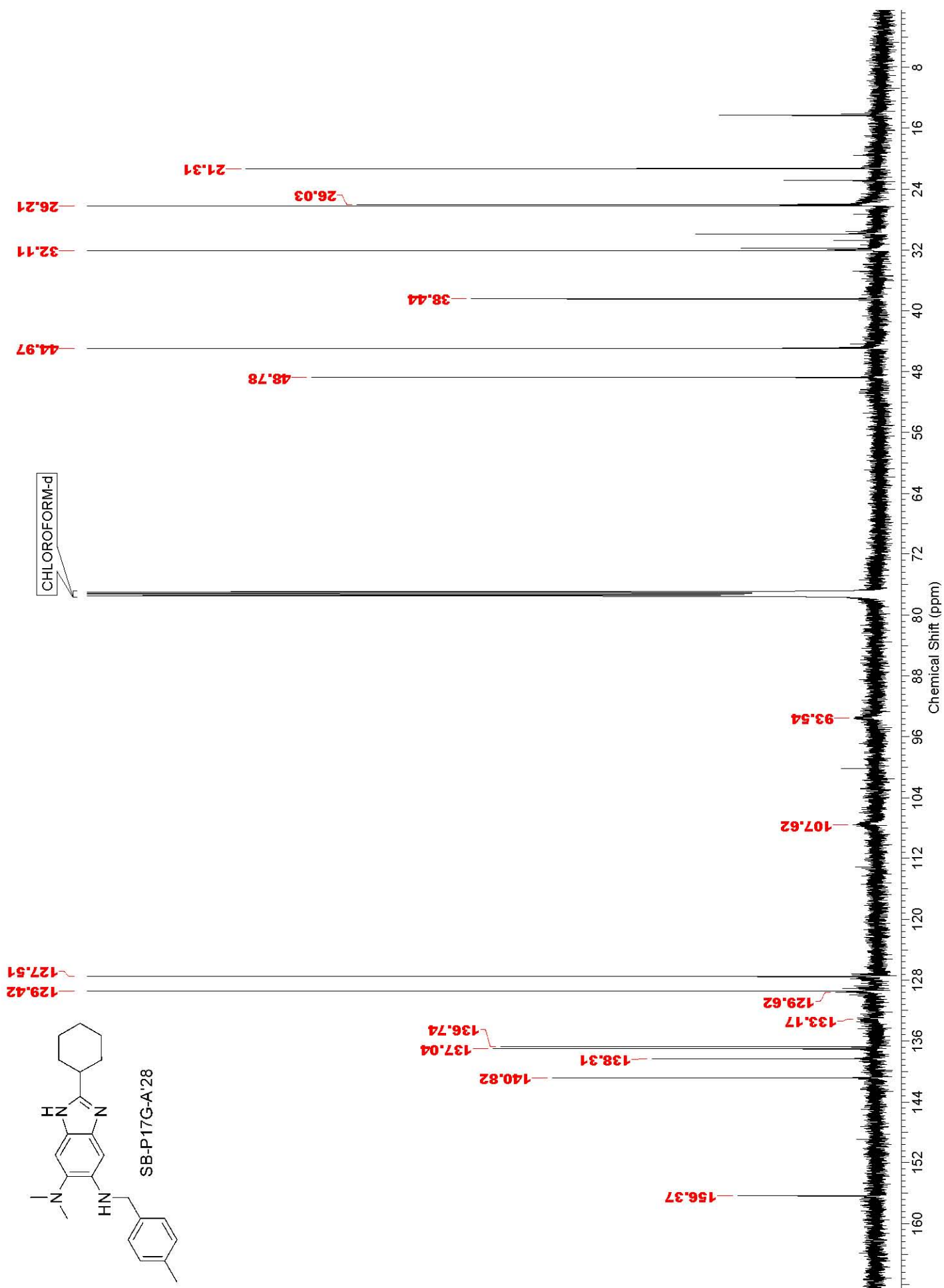


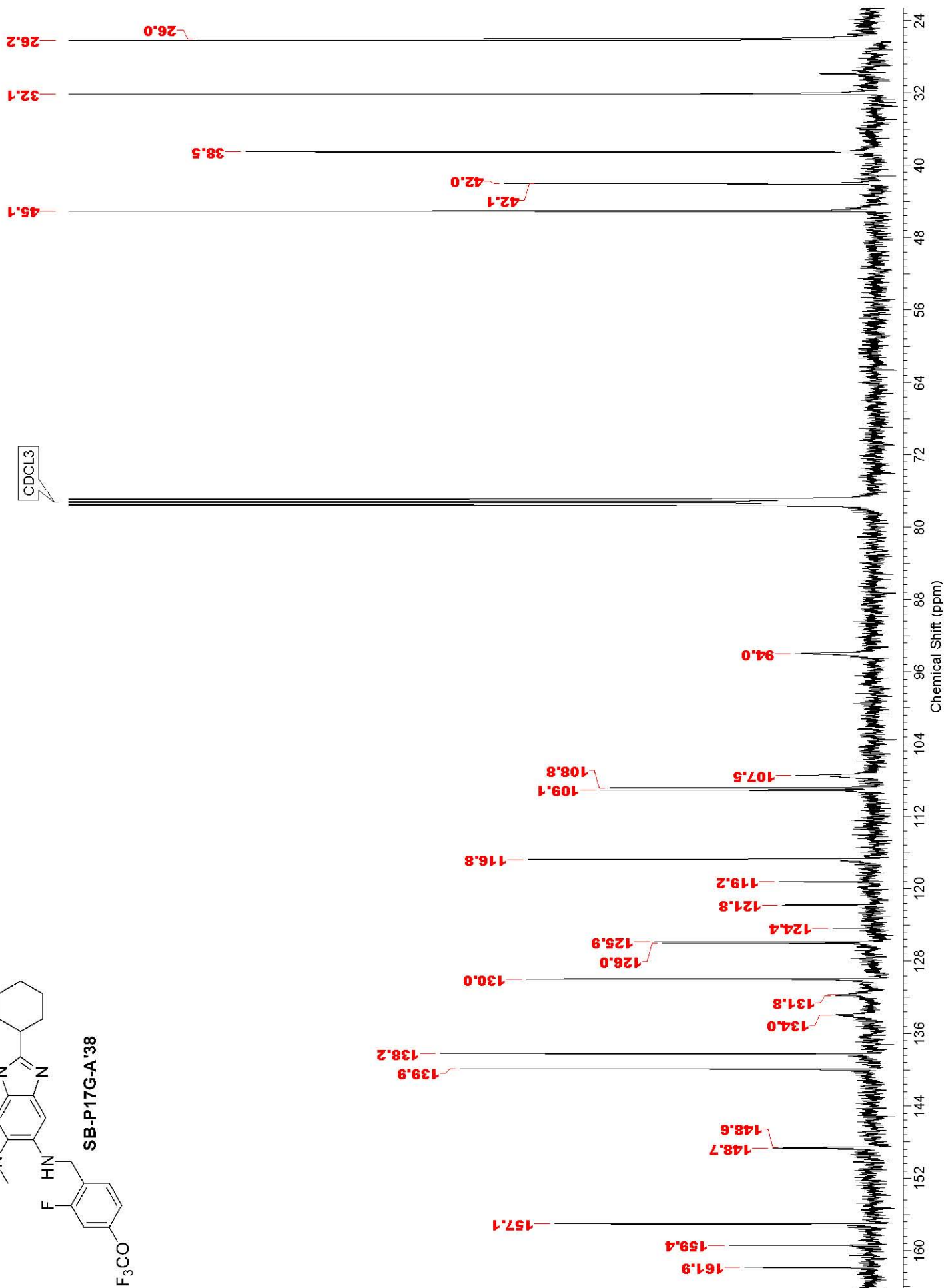
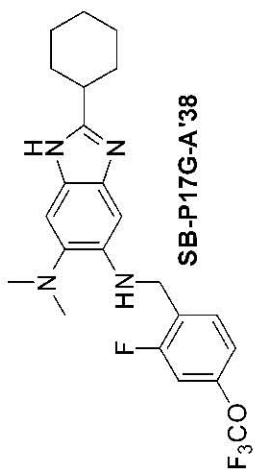


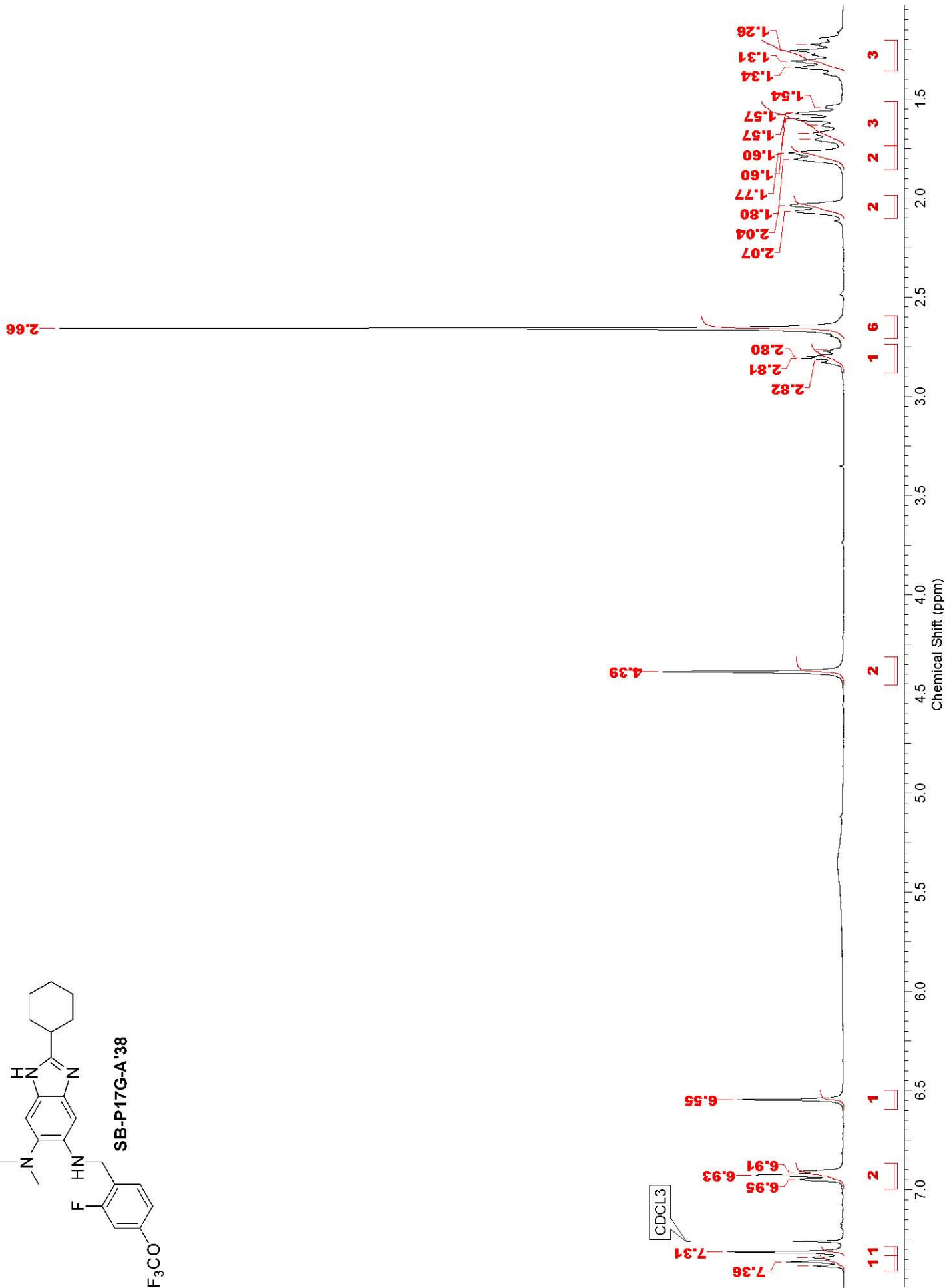
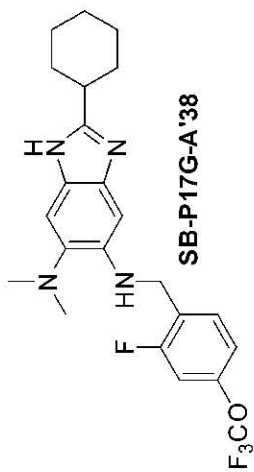




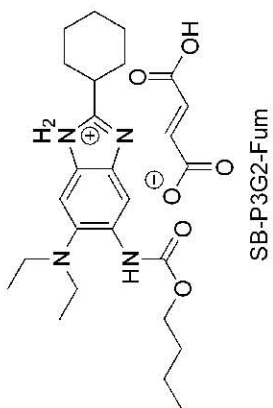
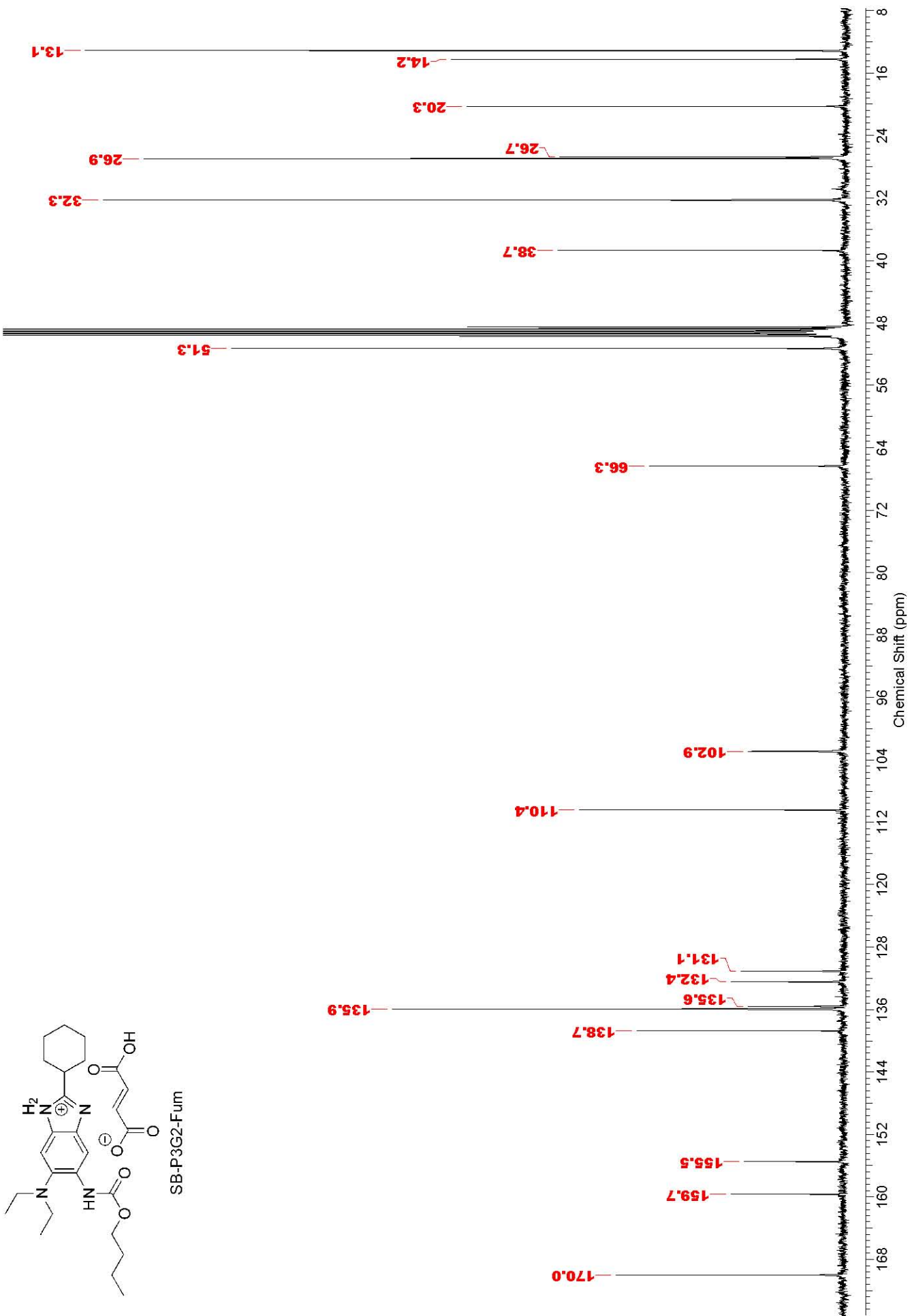


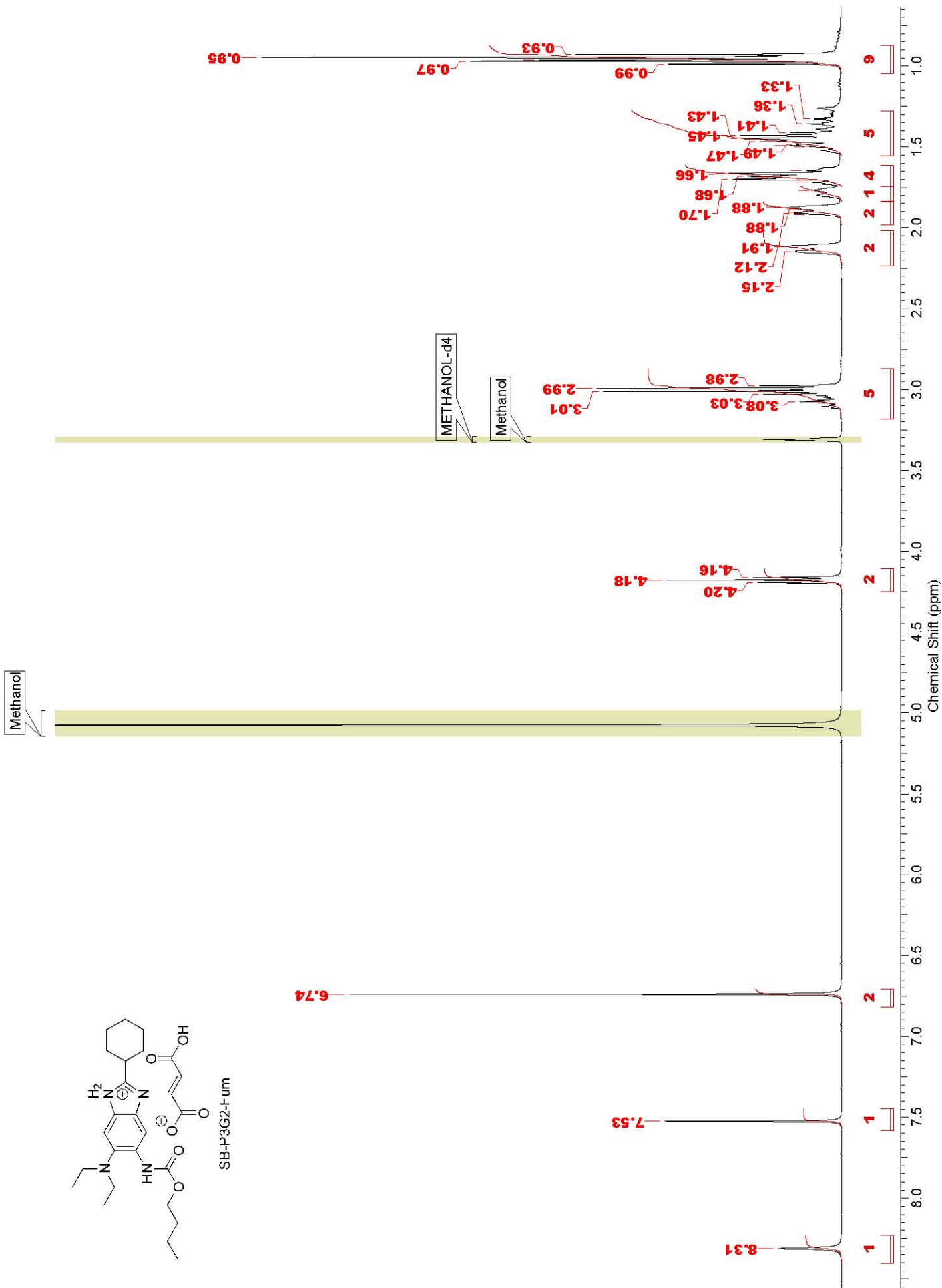


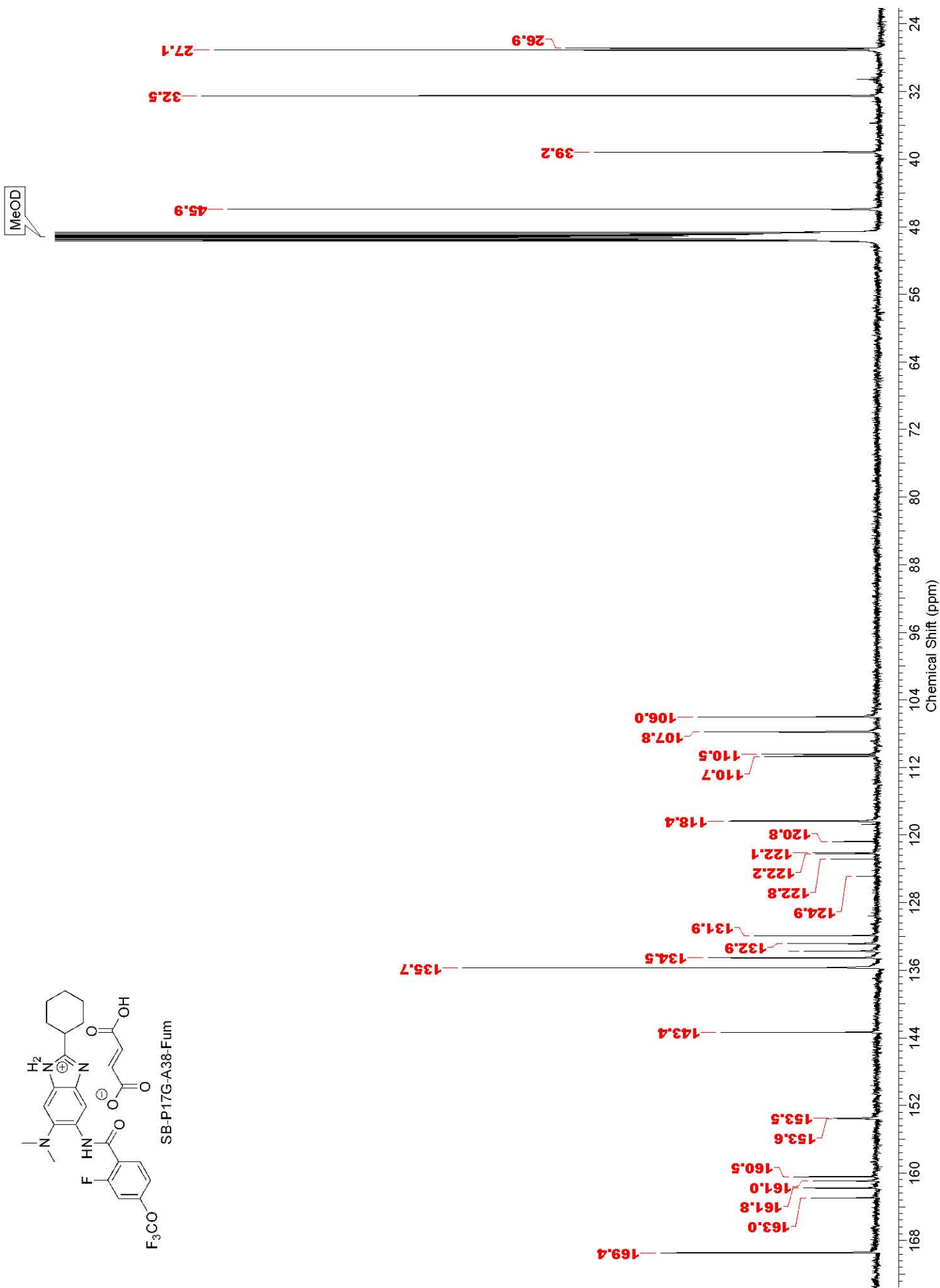
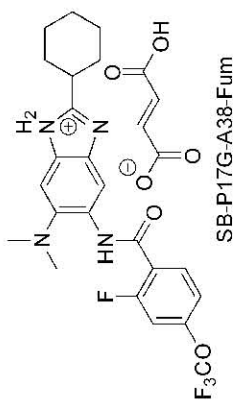


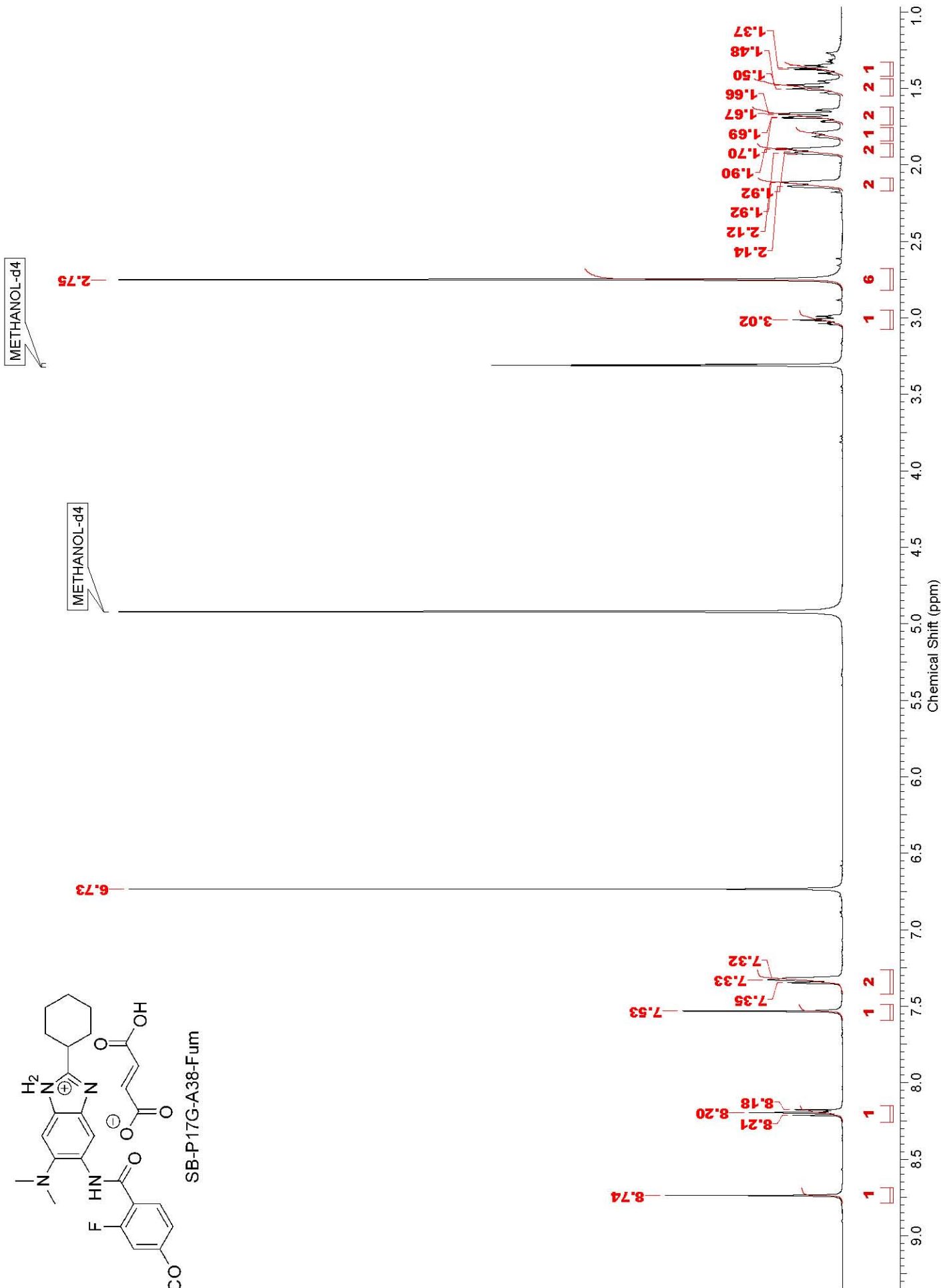
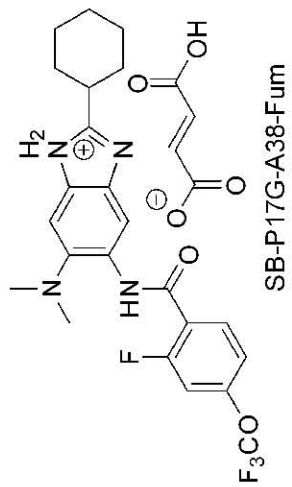


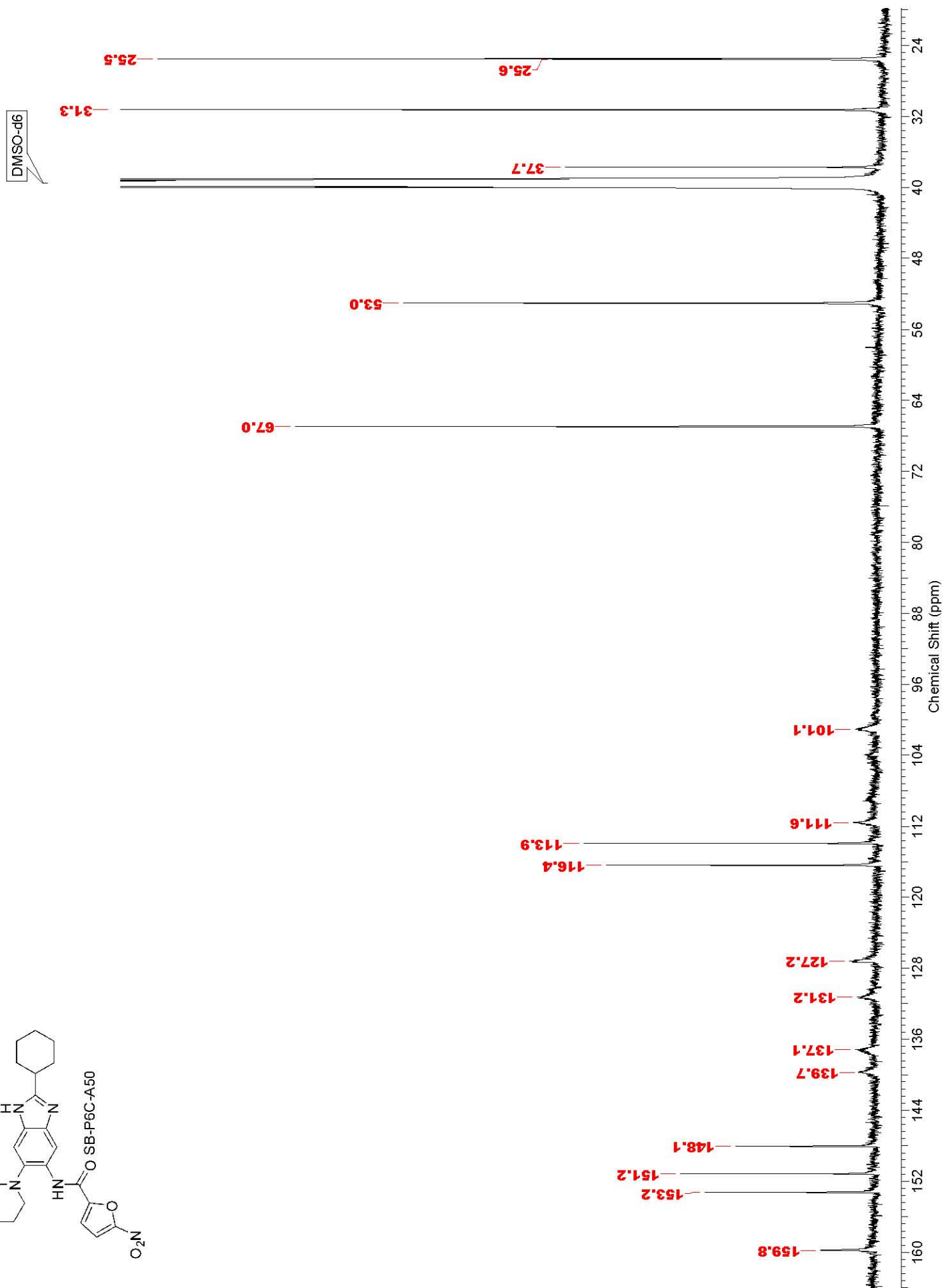
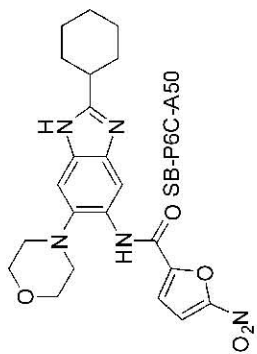
METHANOL-d4

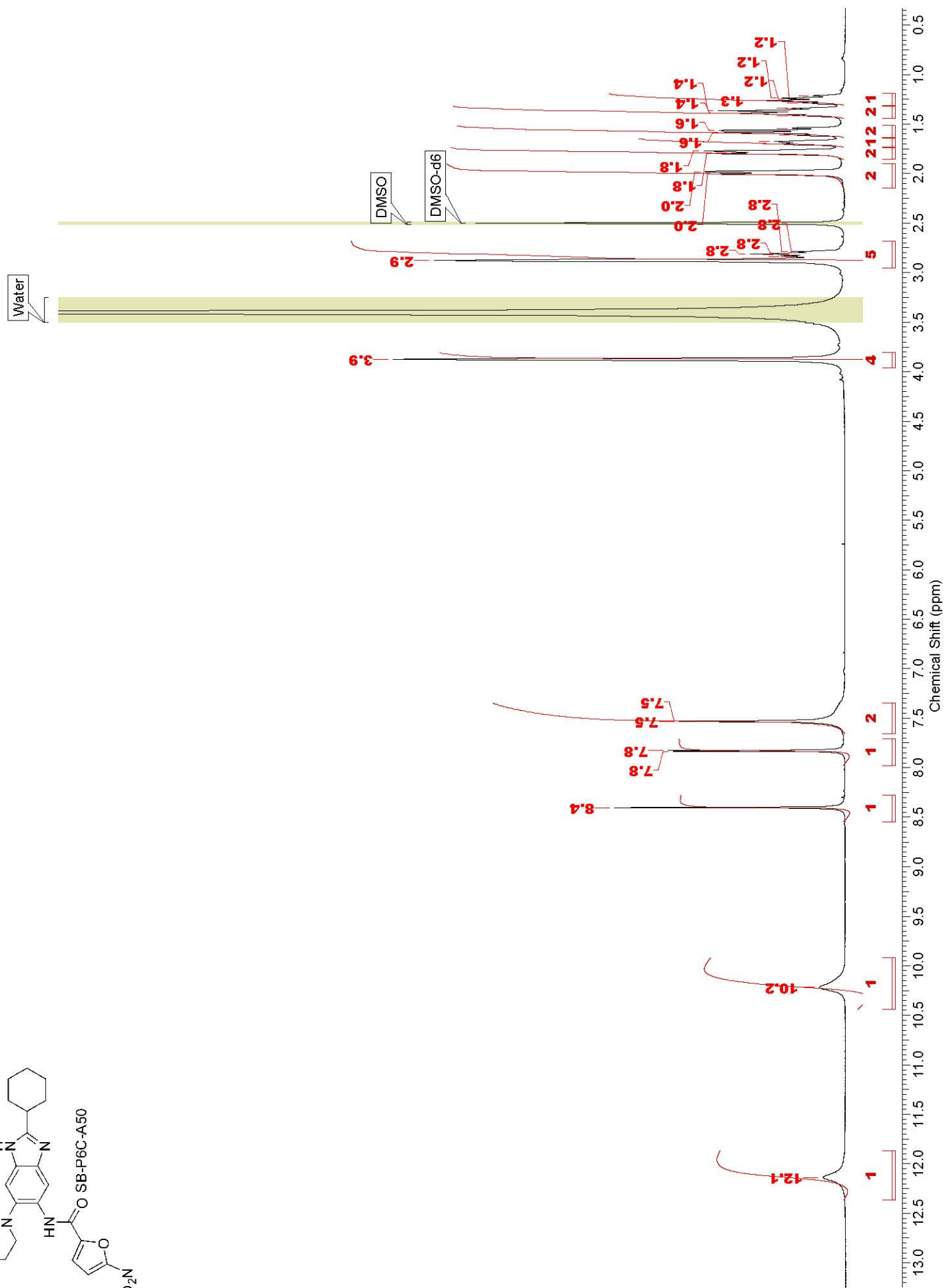
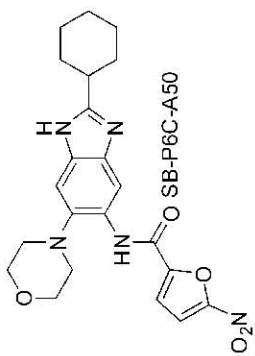


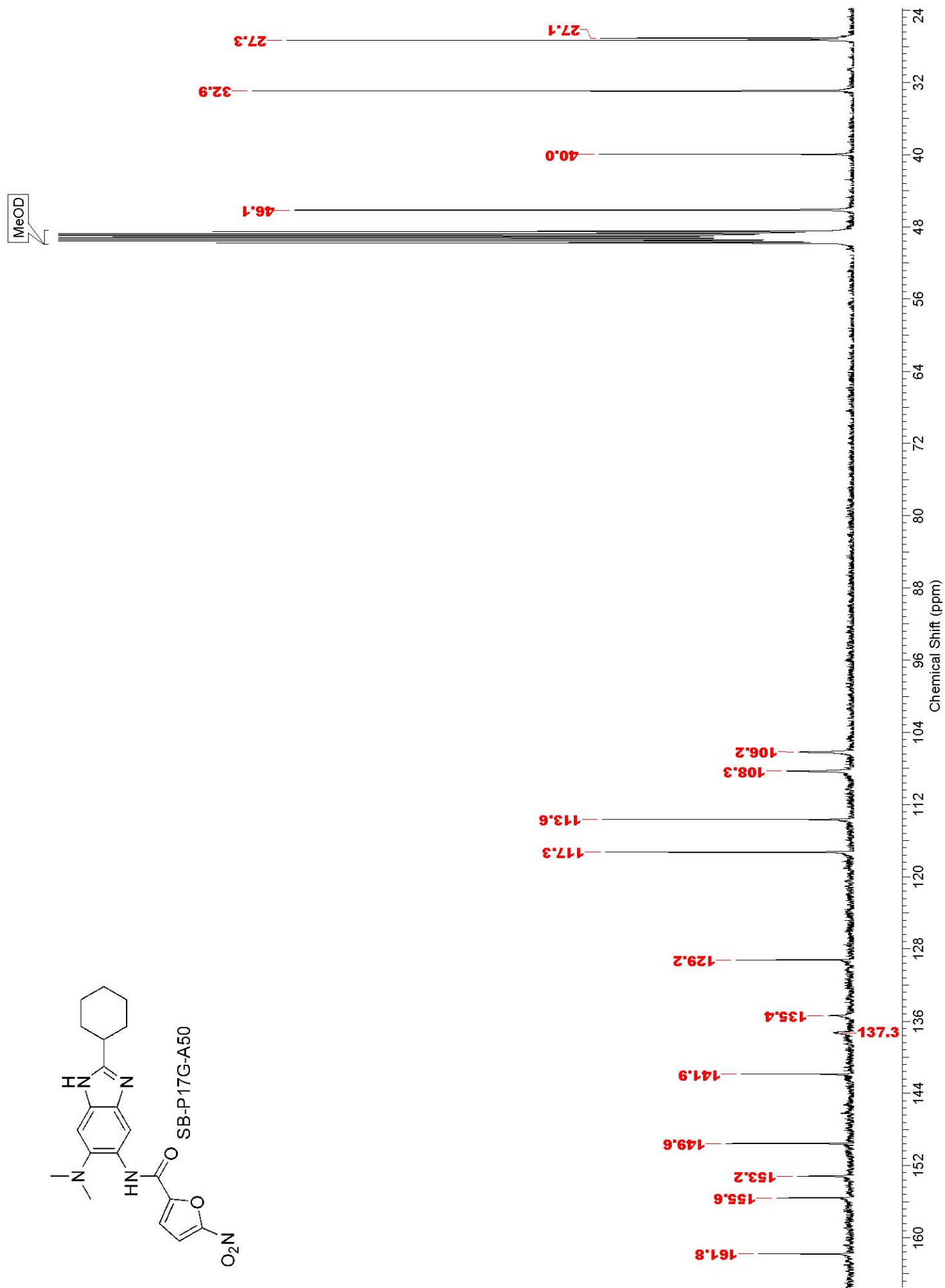
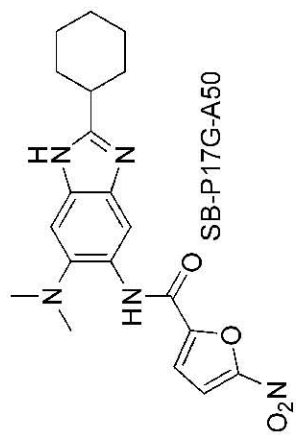


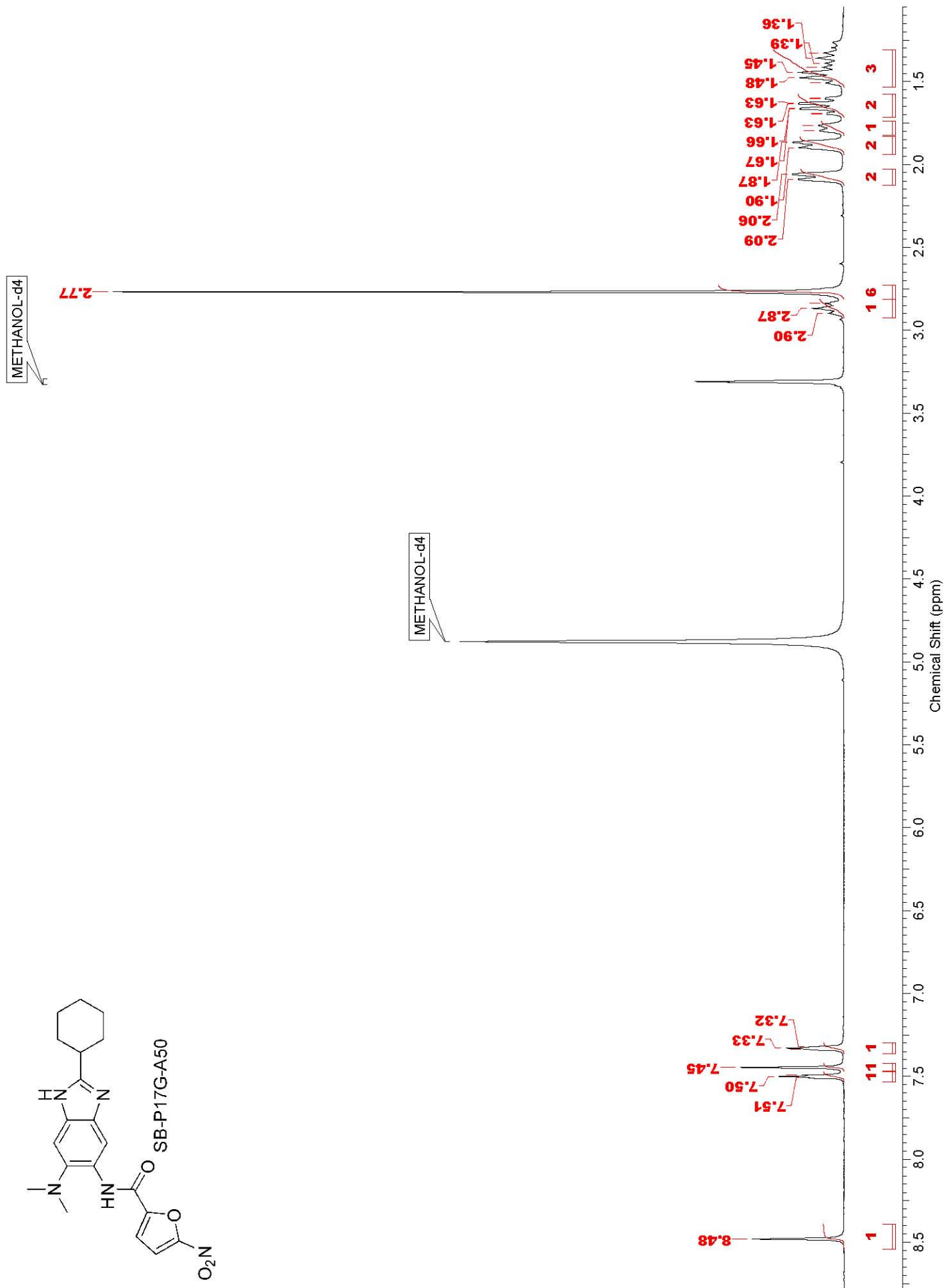
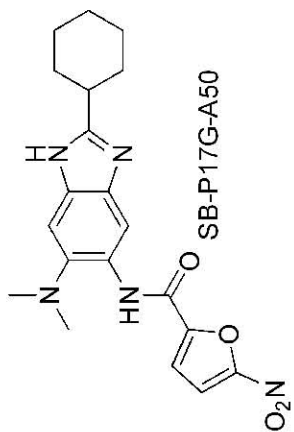


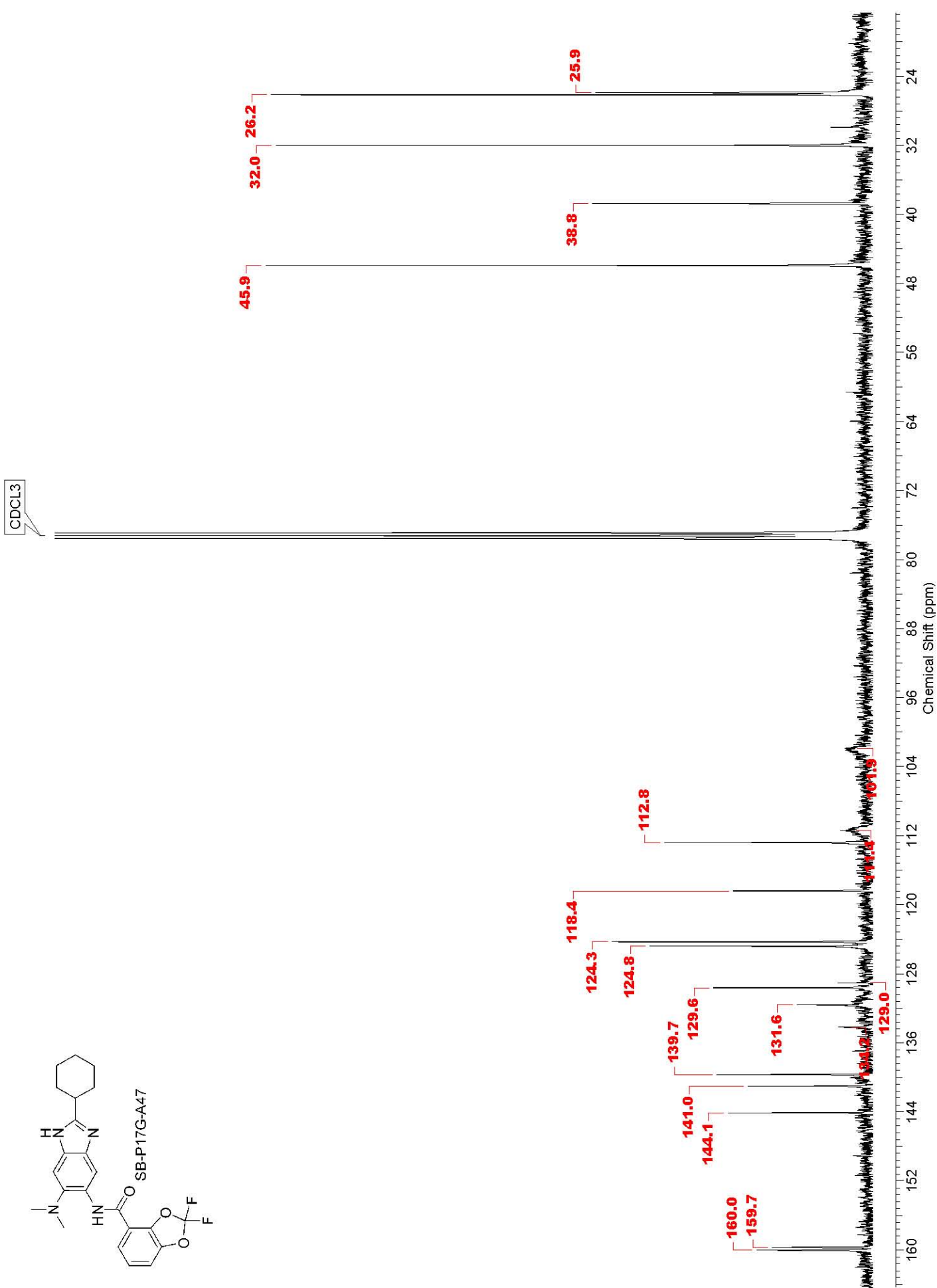
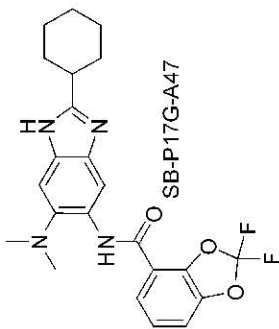


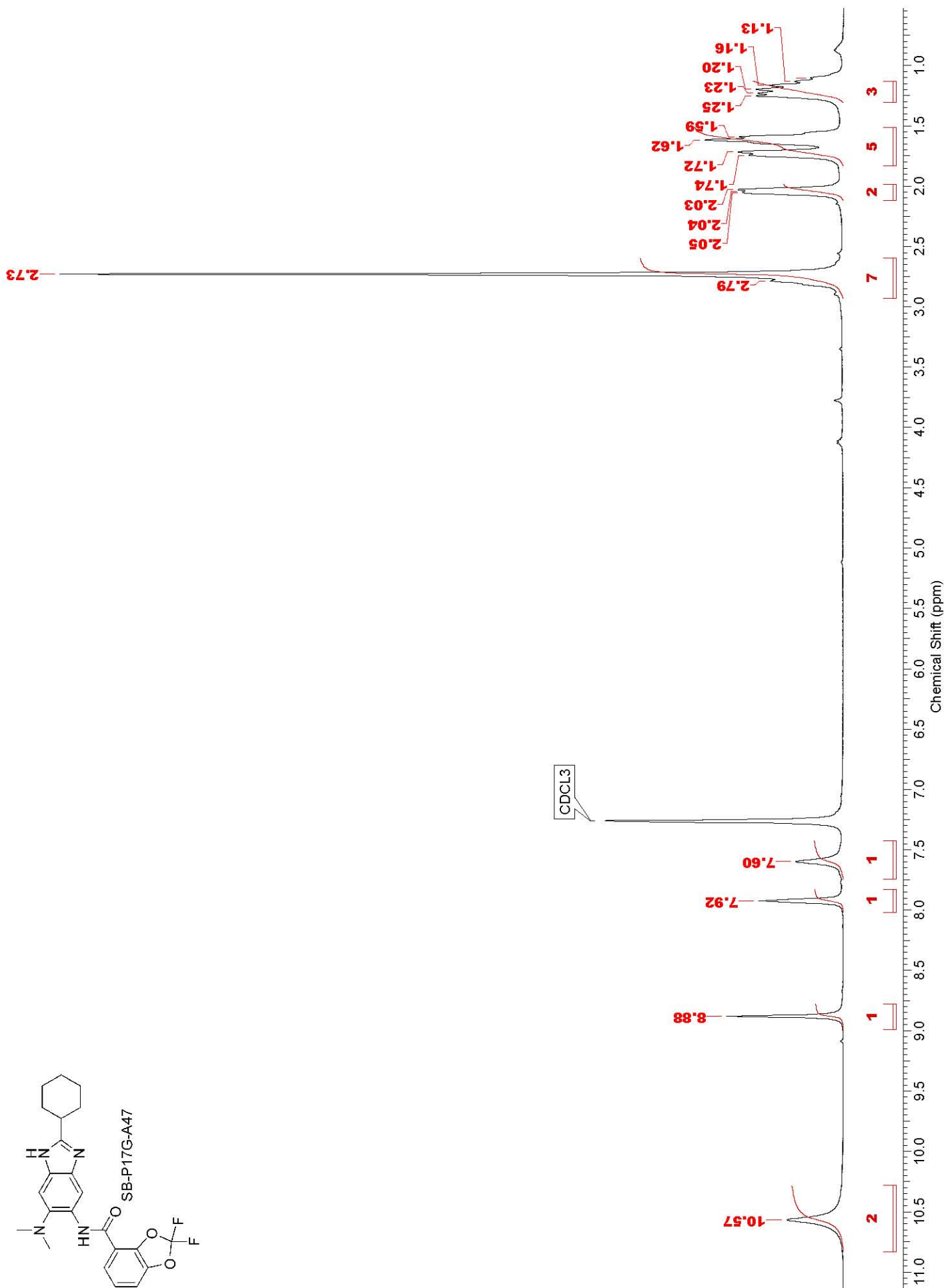
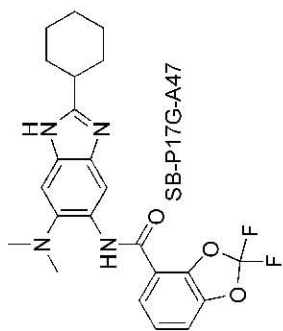


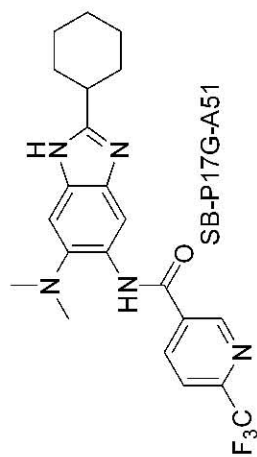




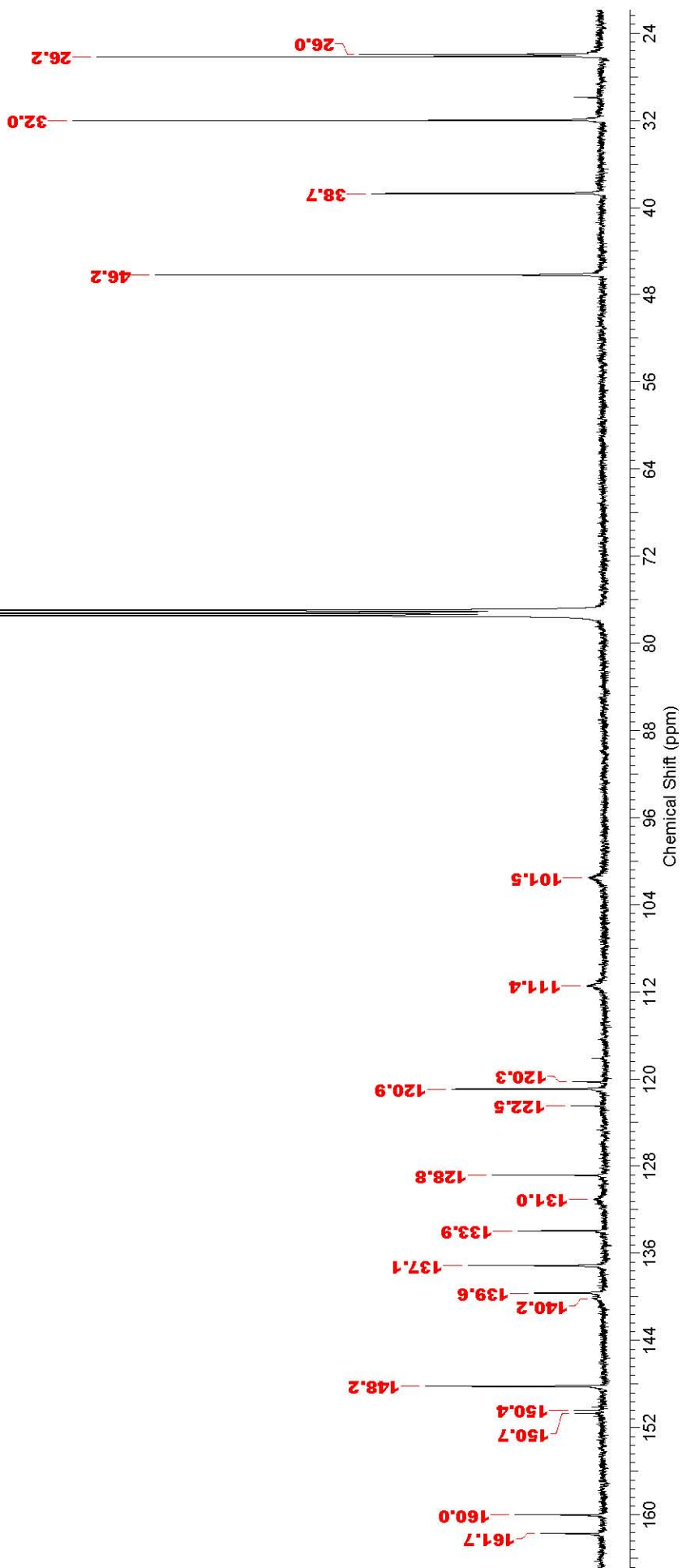


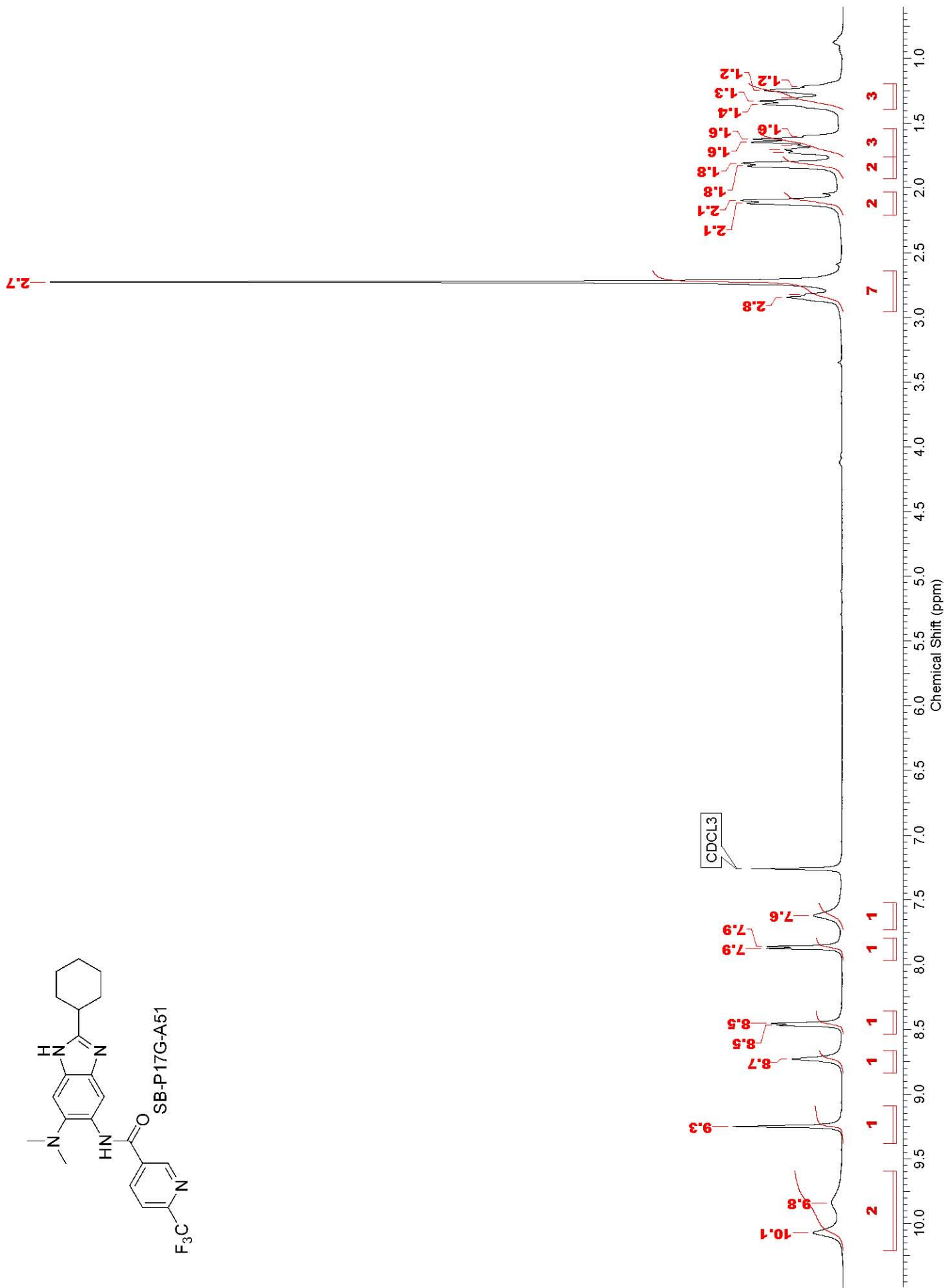
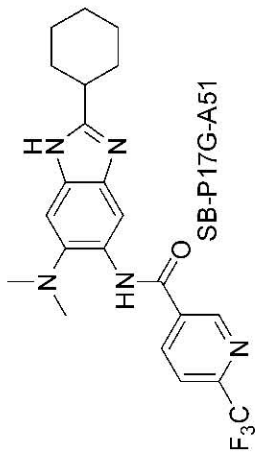


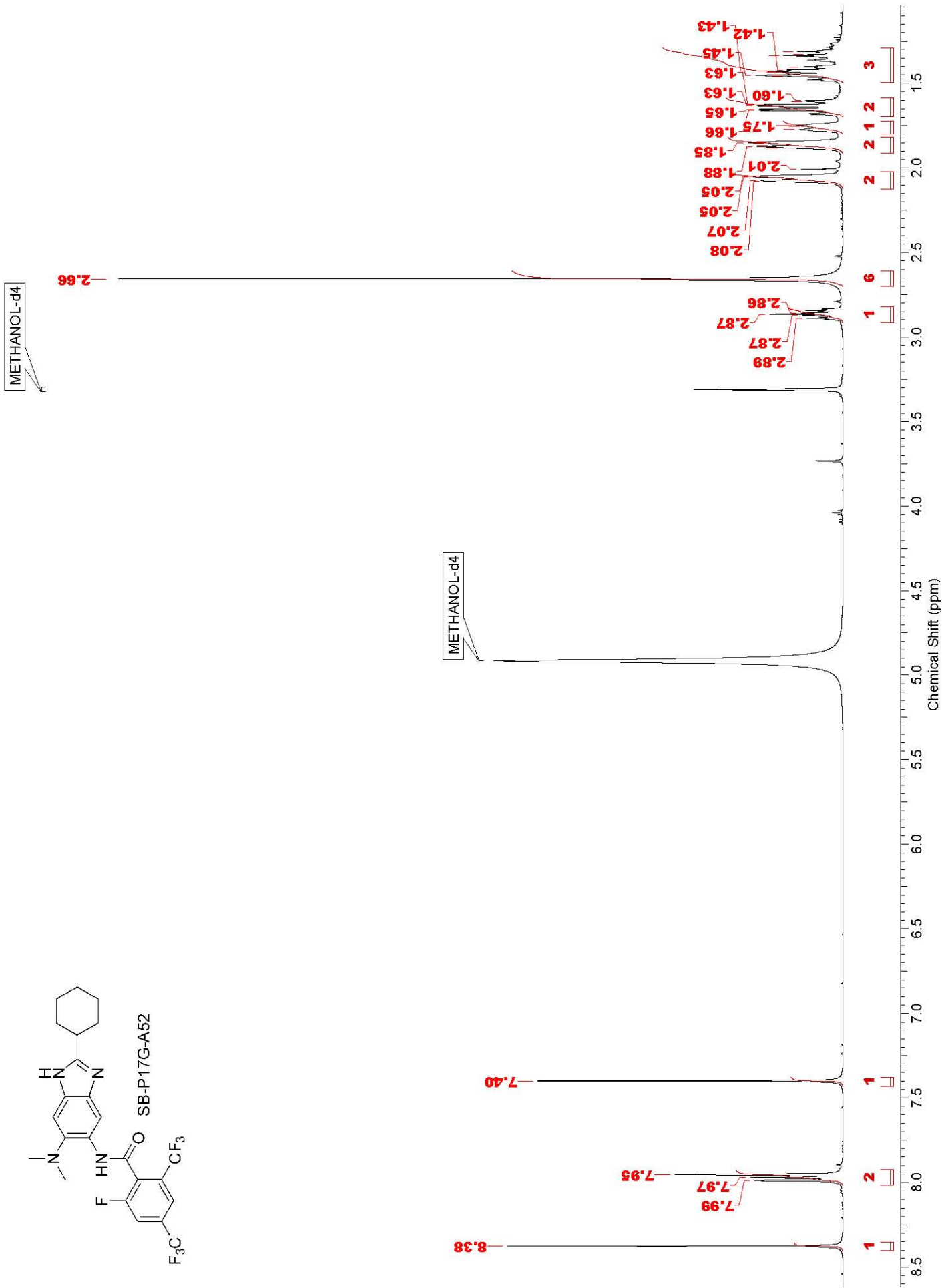
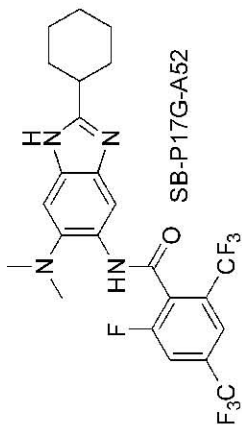


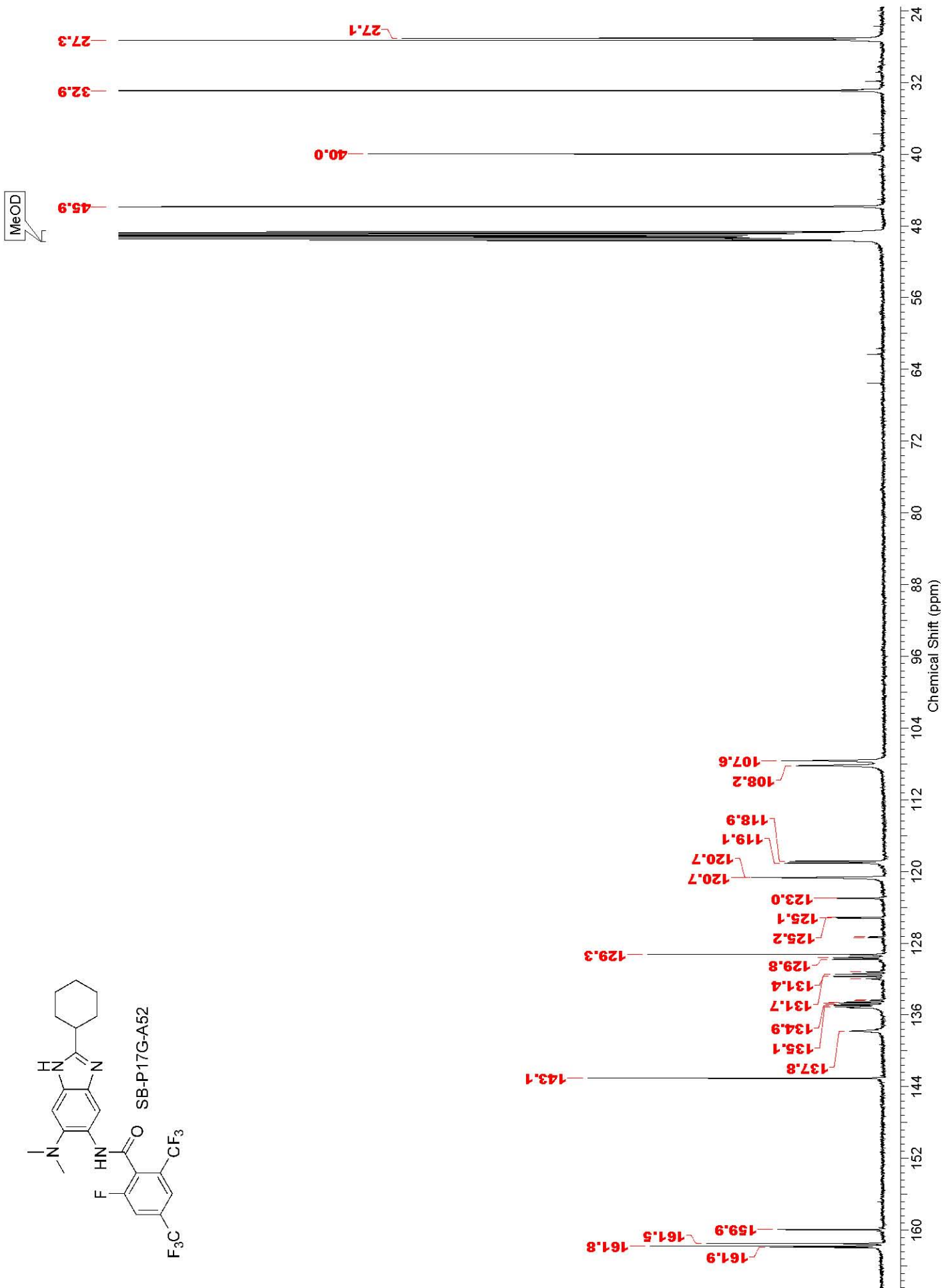


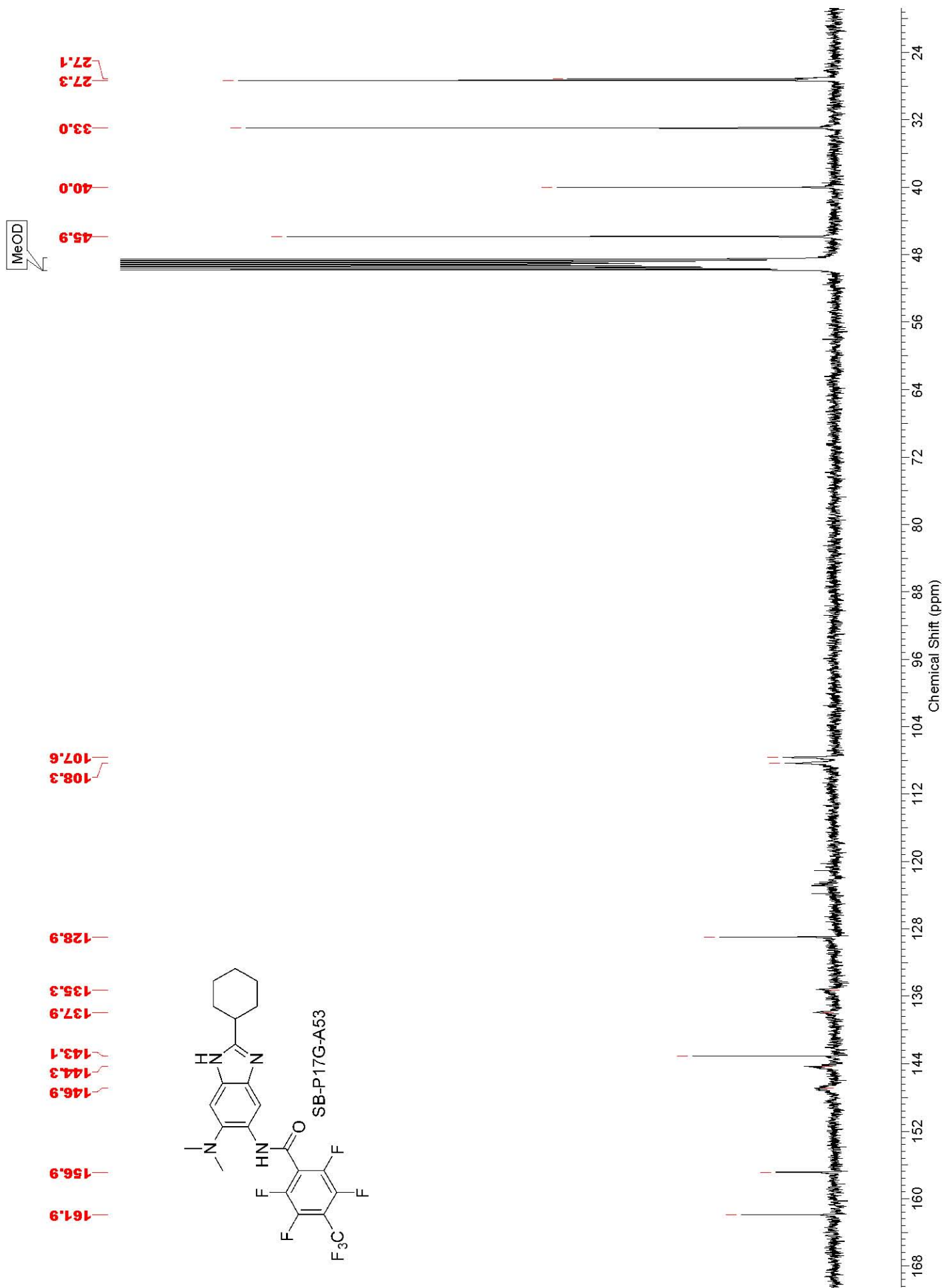
CHLOROFORM-d

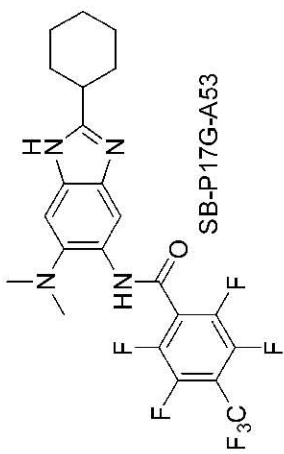










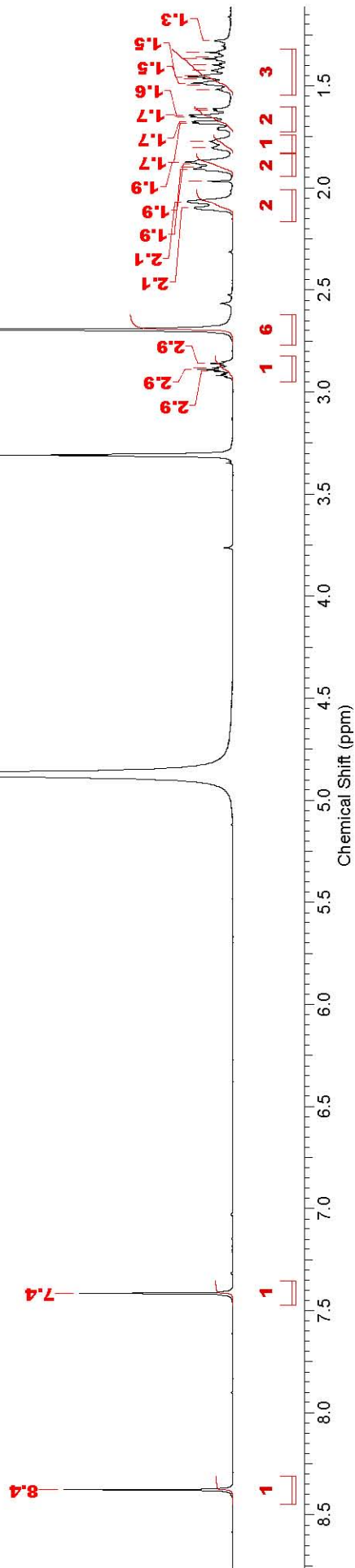


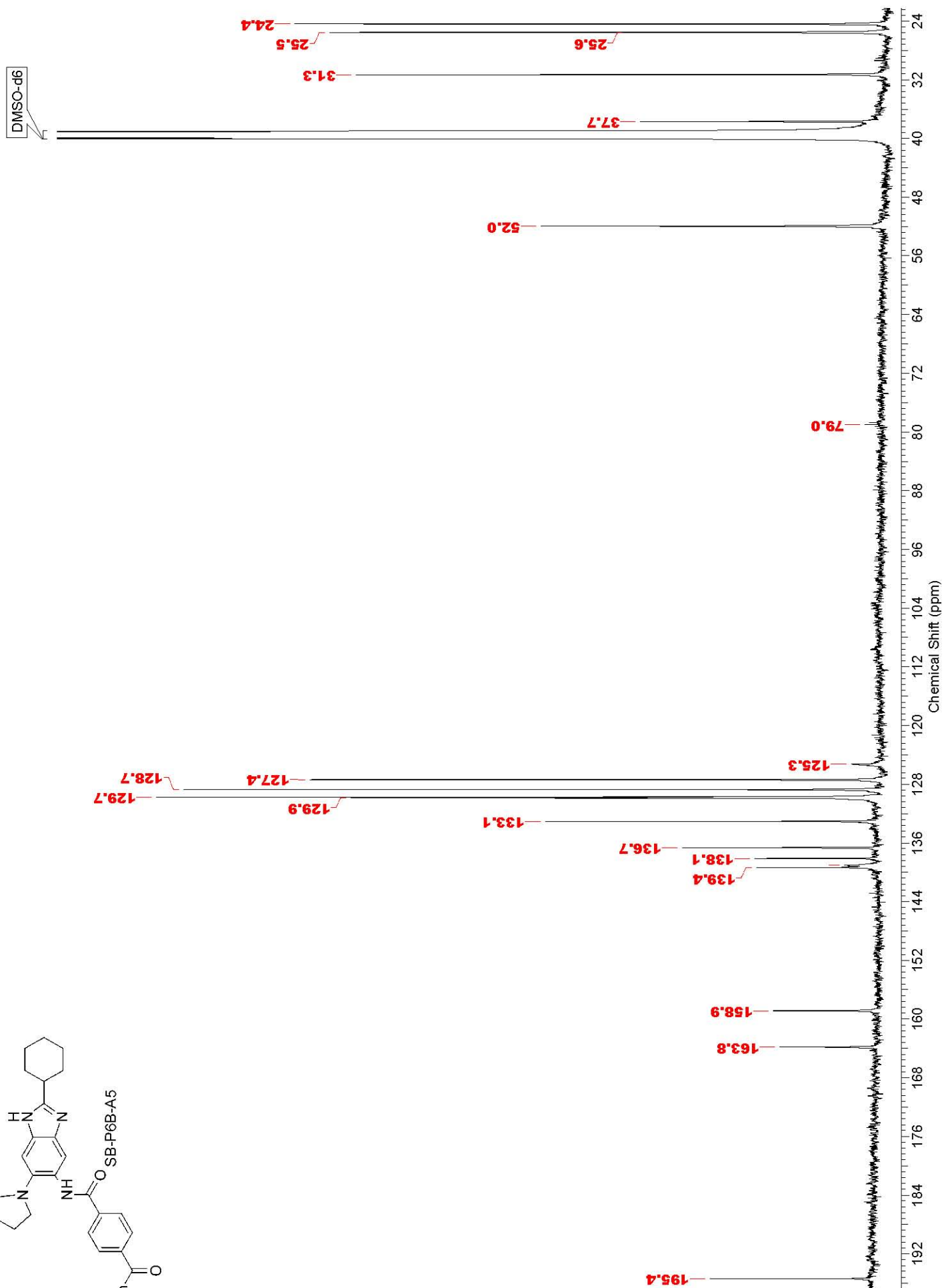
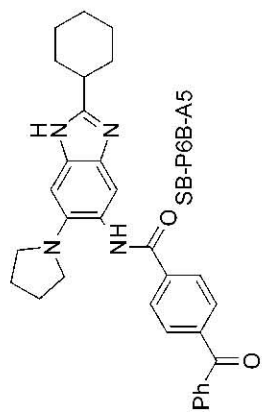
SB-P17G-A53

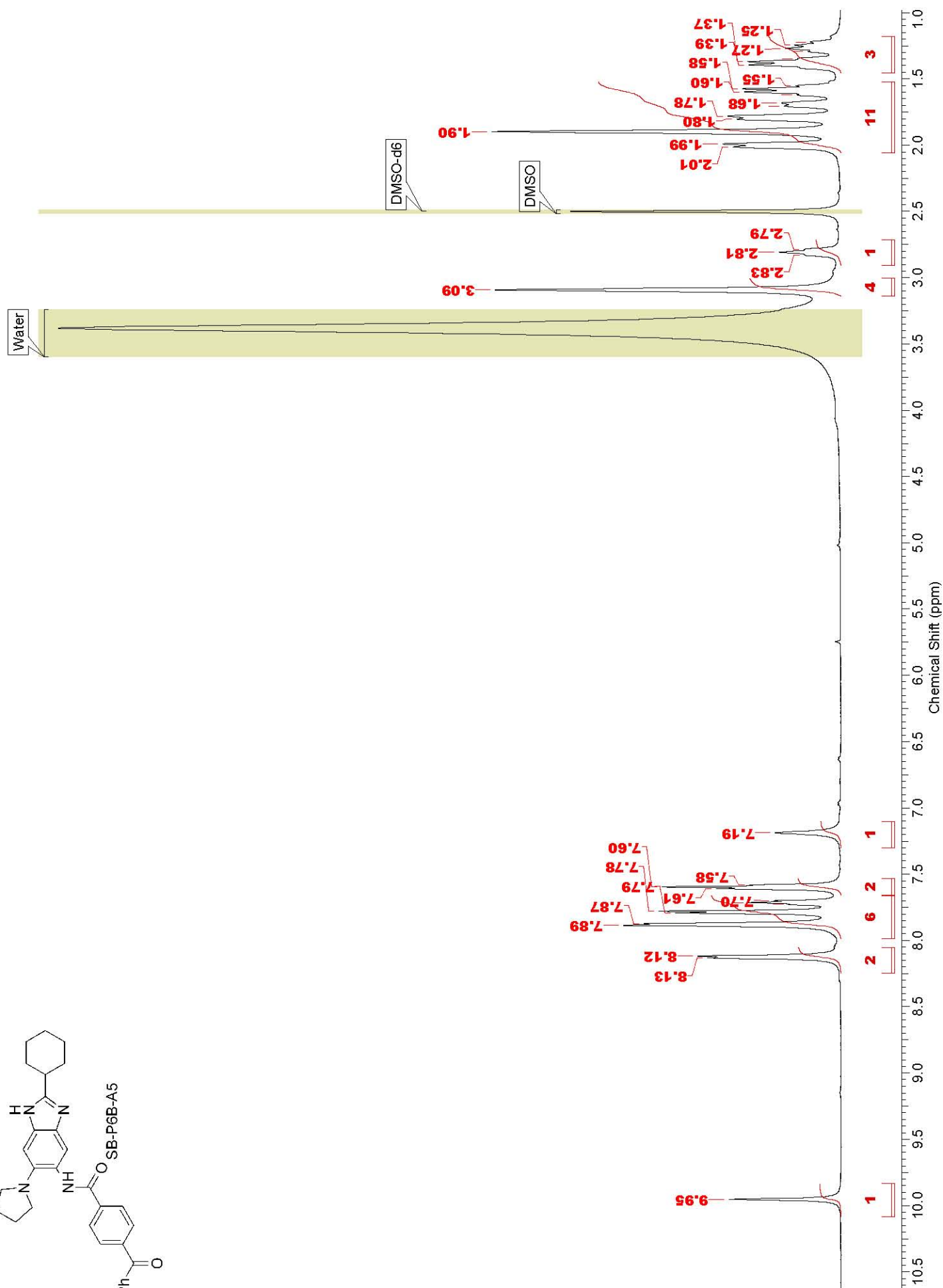
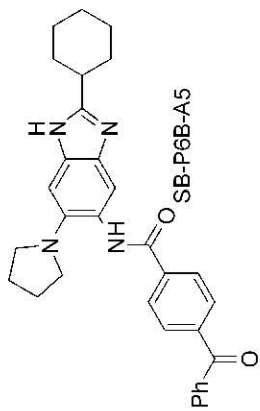
METHANOL-d4

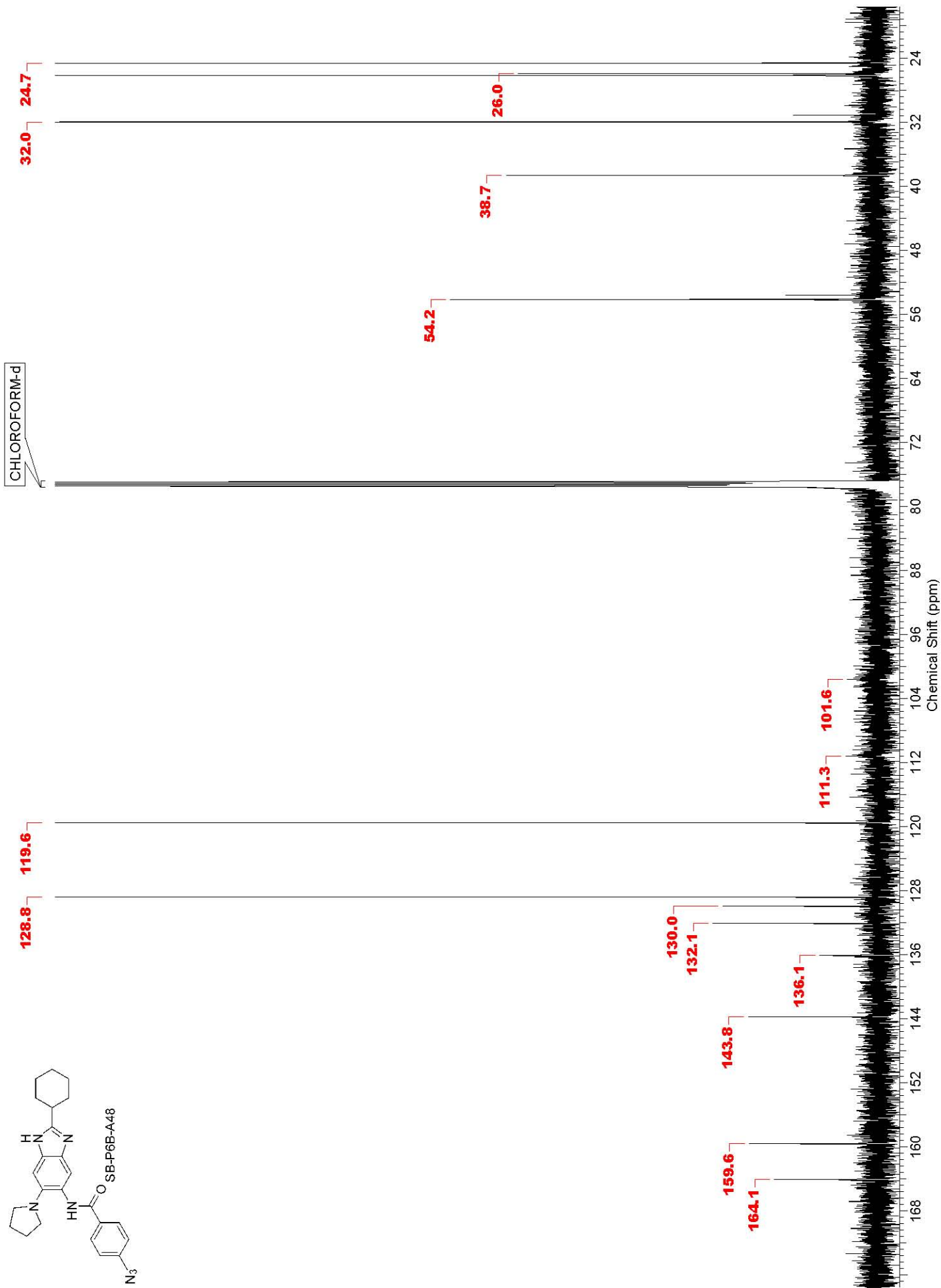
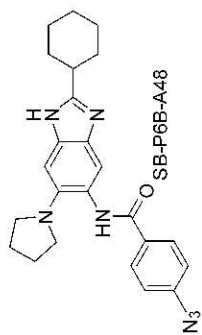
2.7

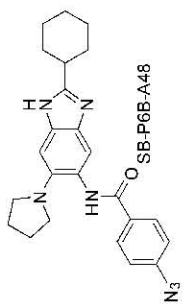
METHANOL-d4



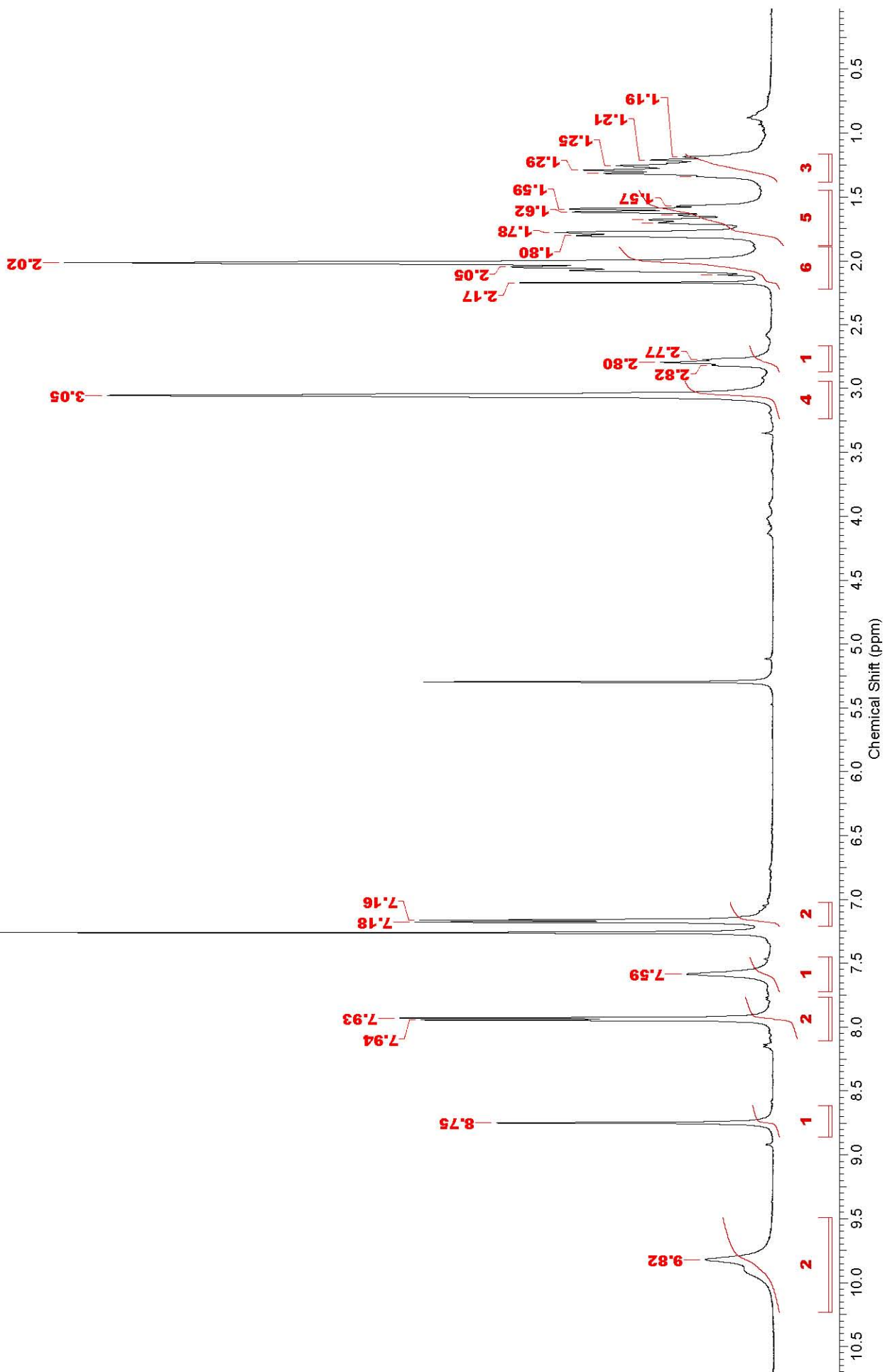


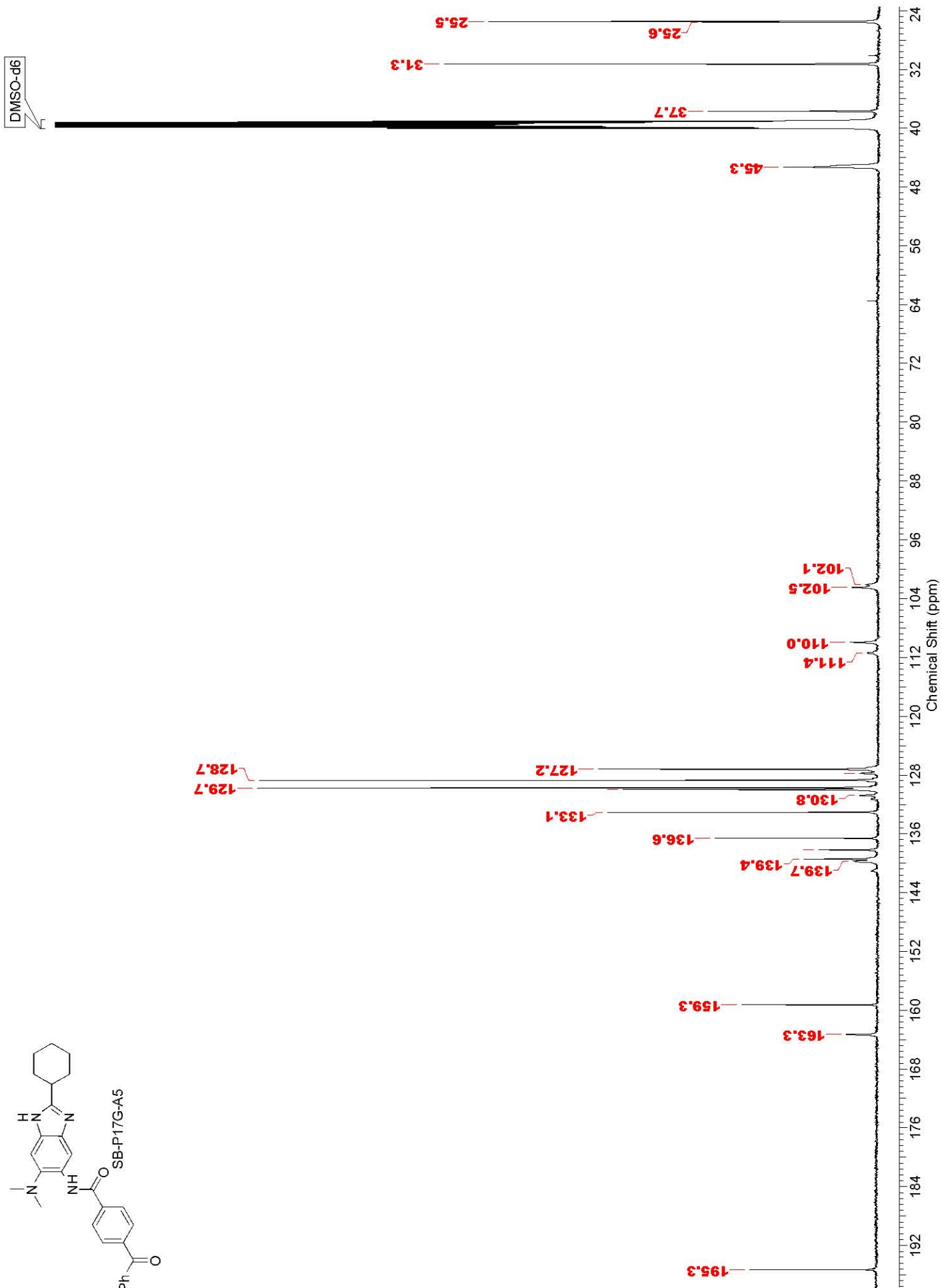
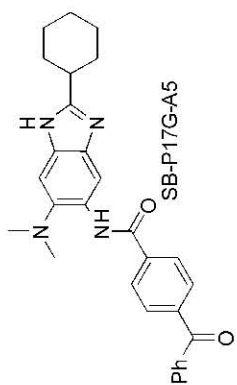


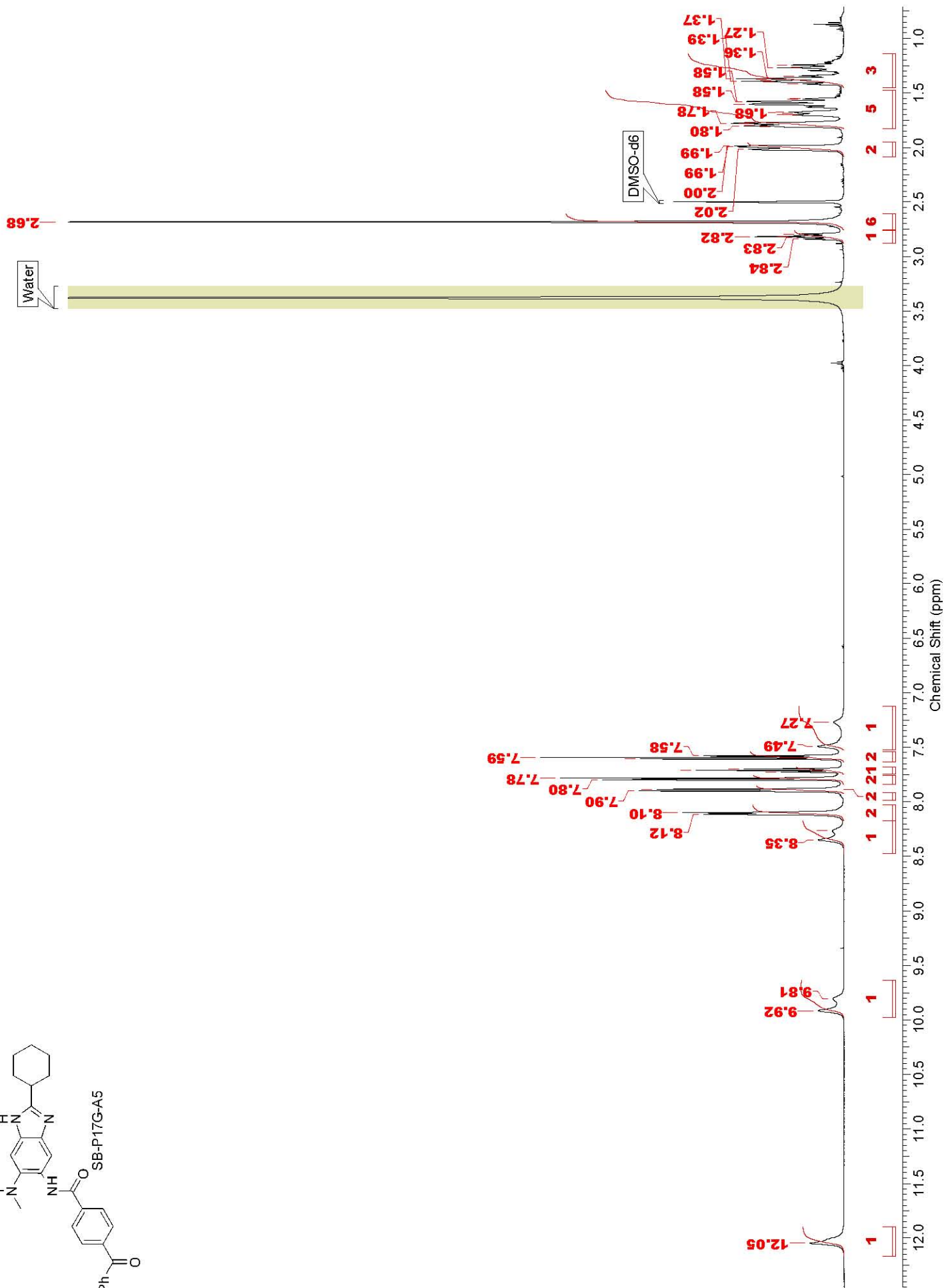
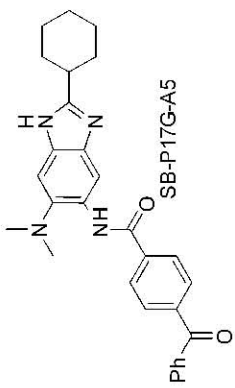


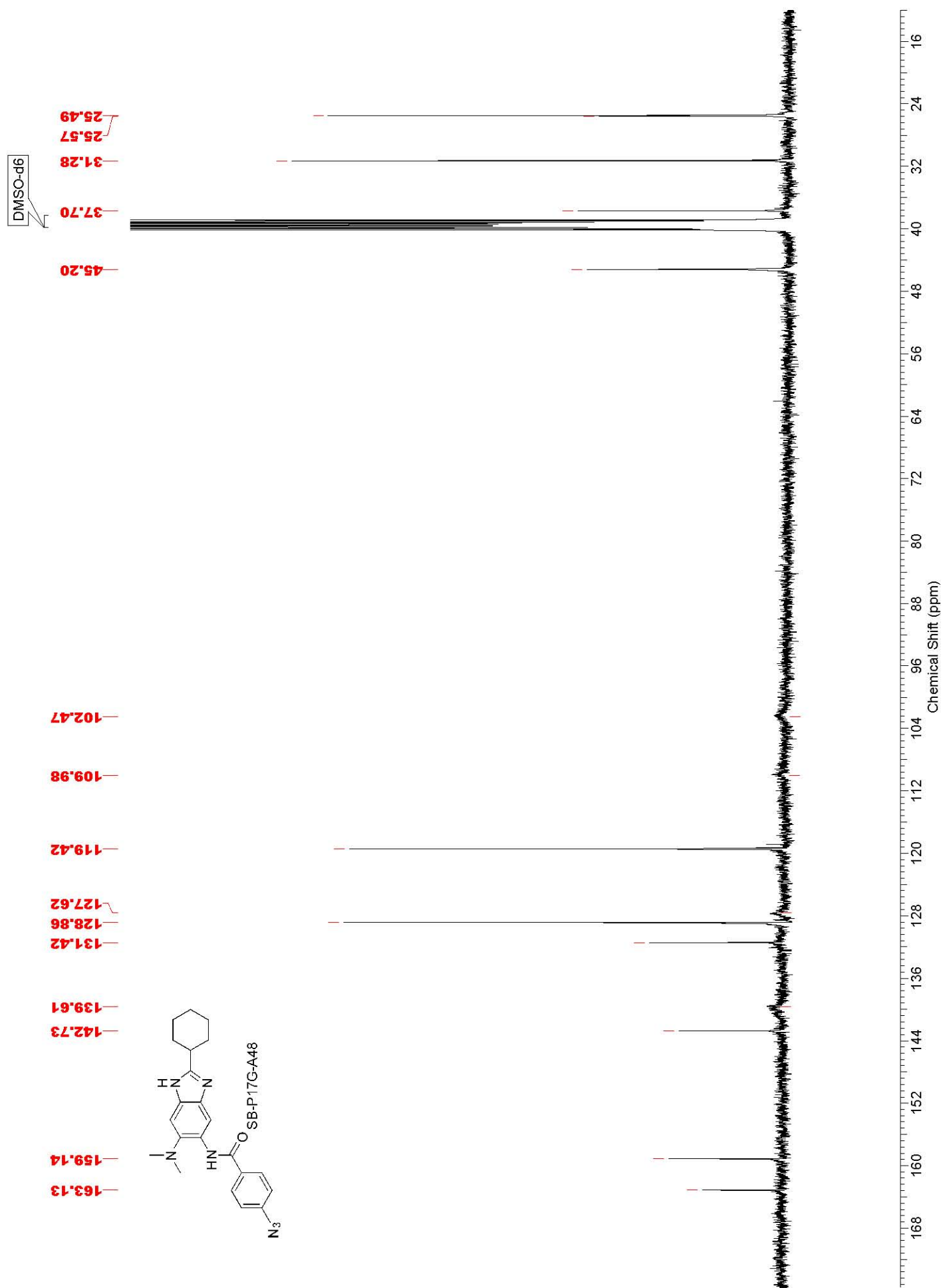


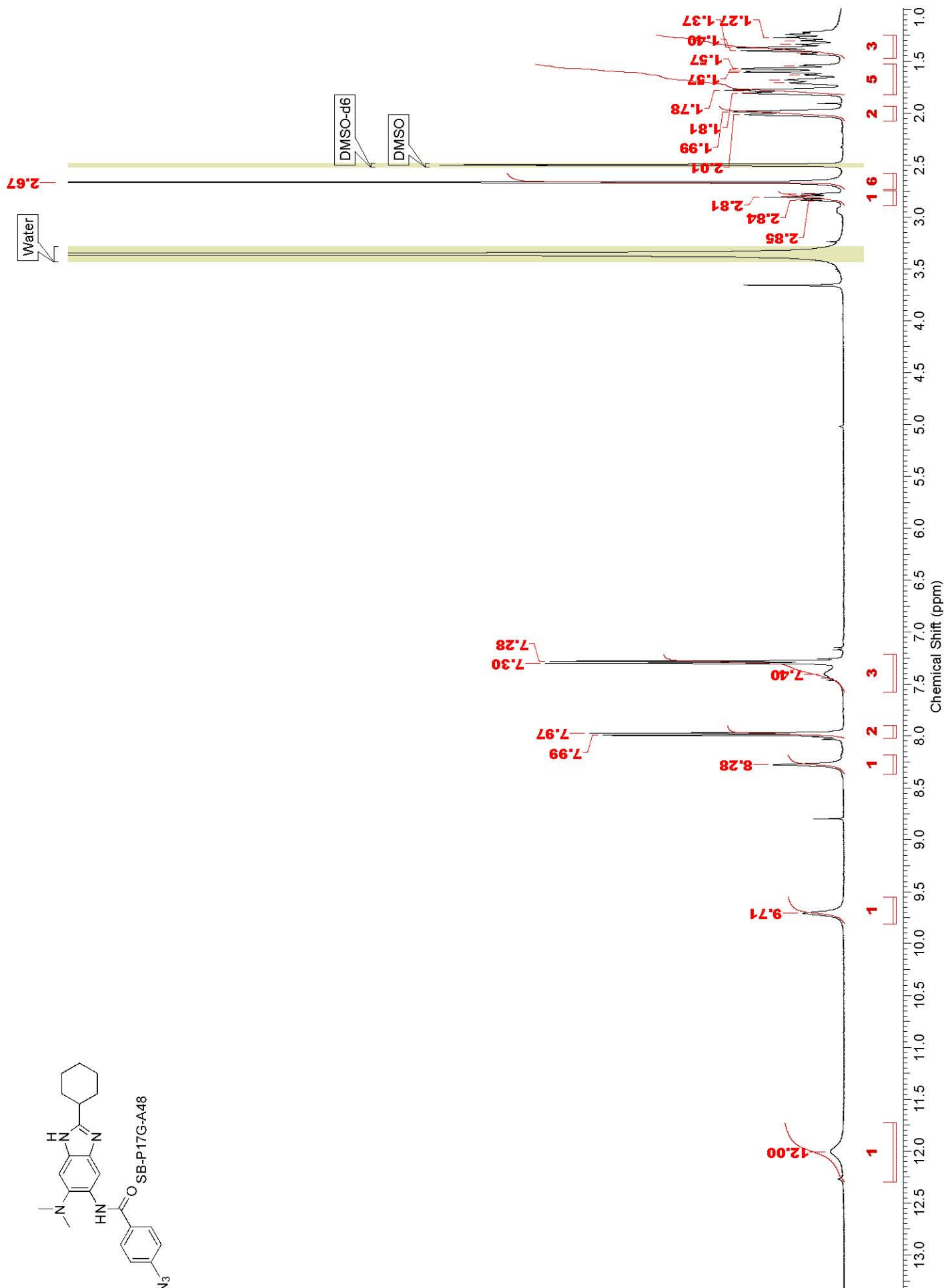
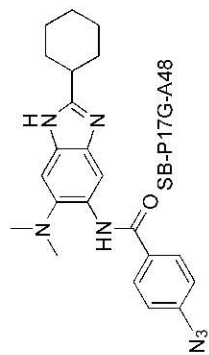
CDCl₃

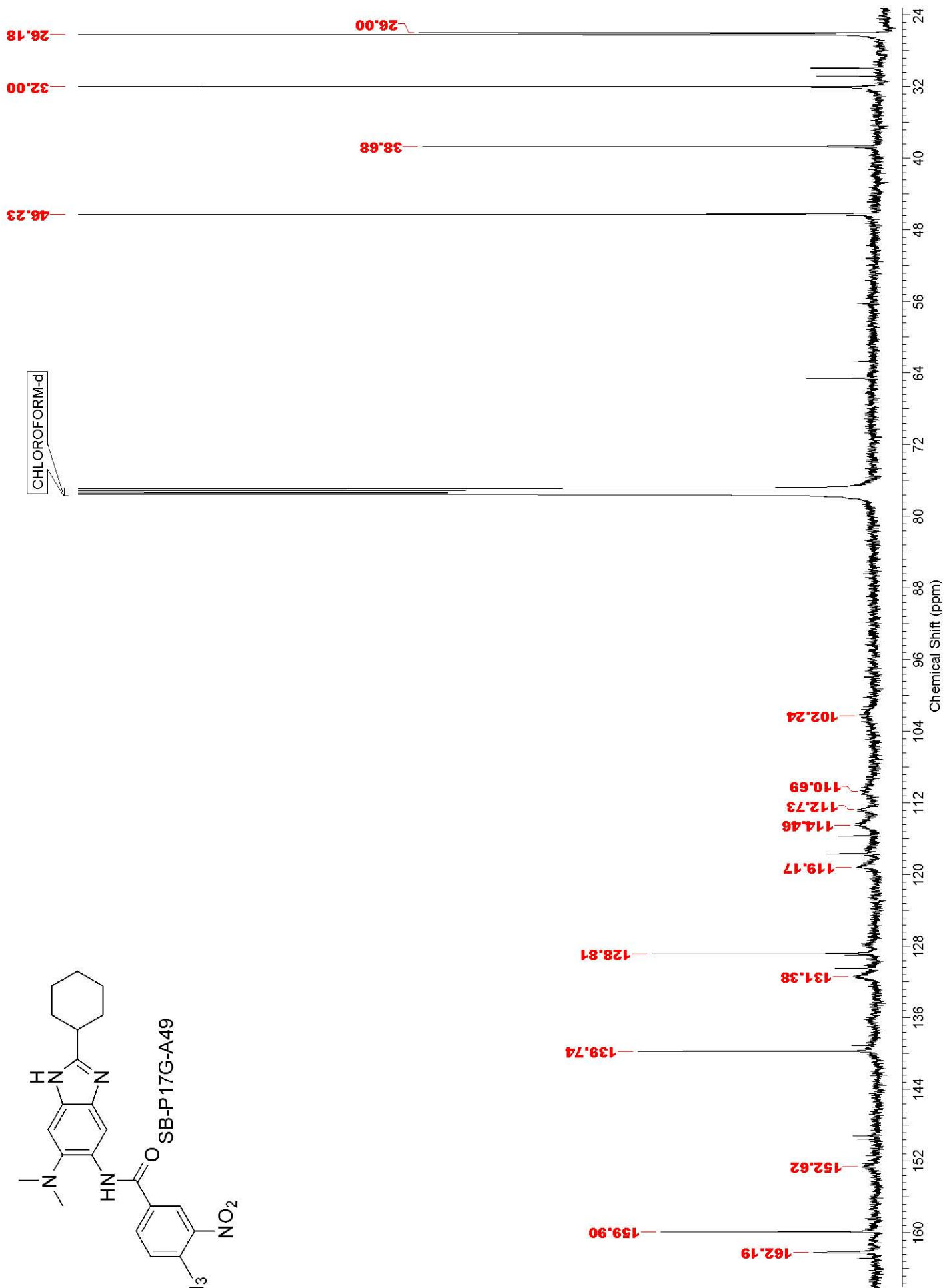
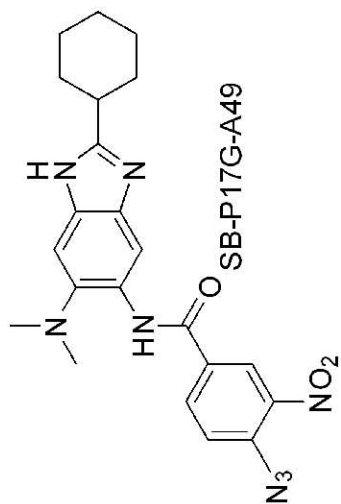


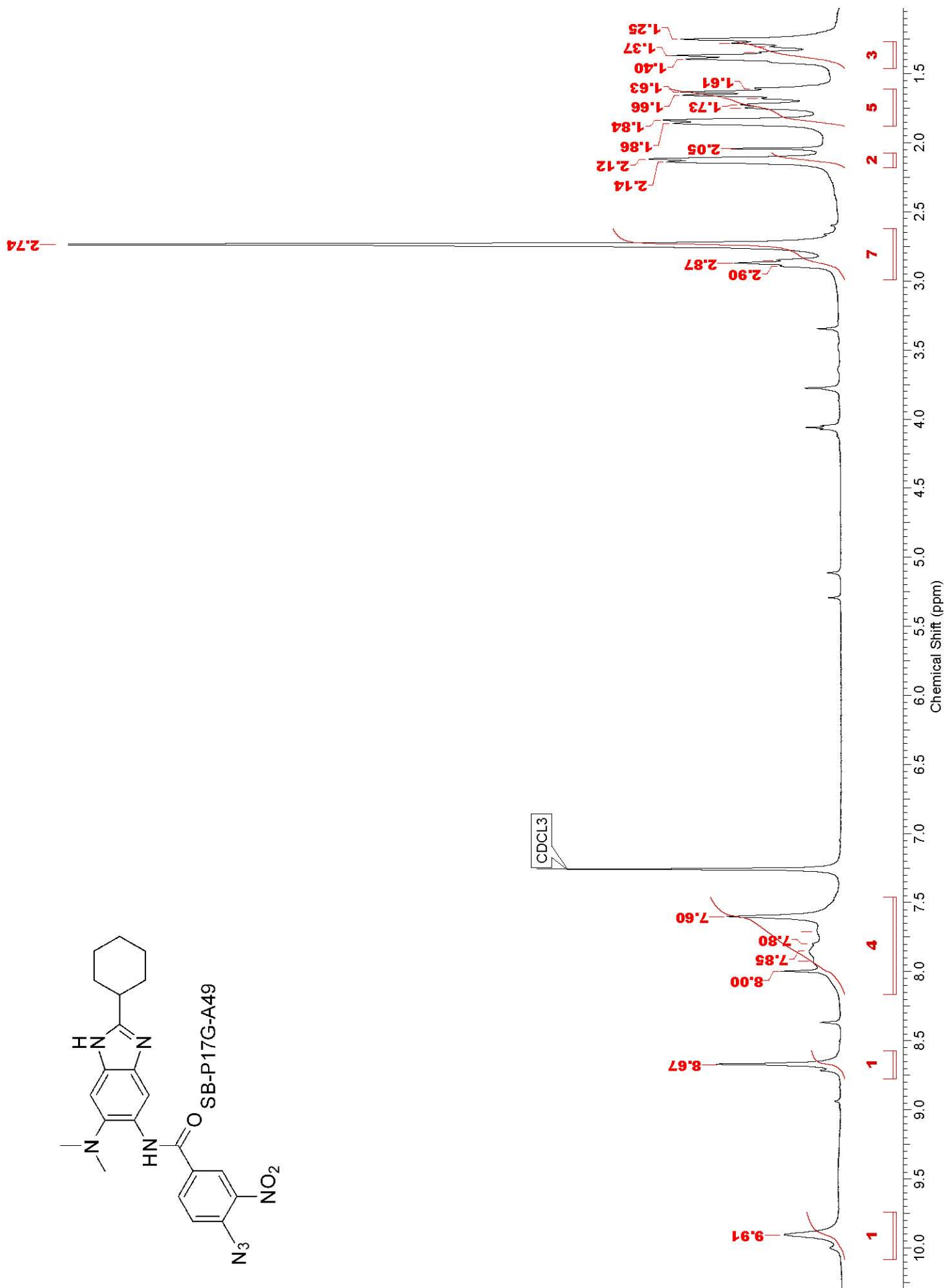
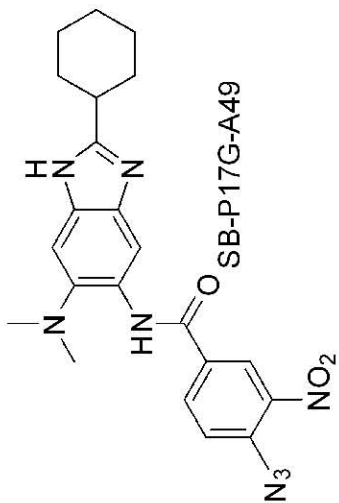


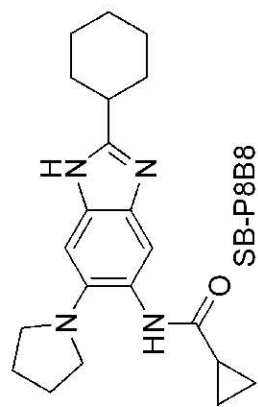






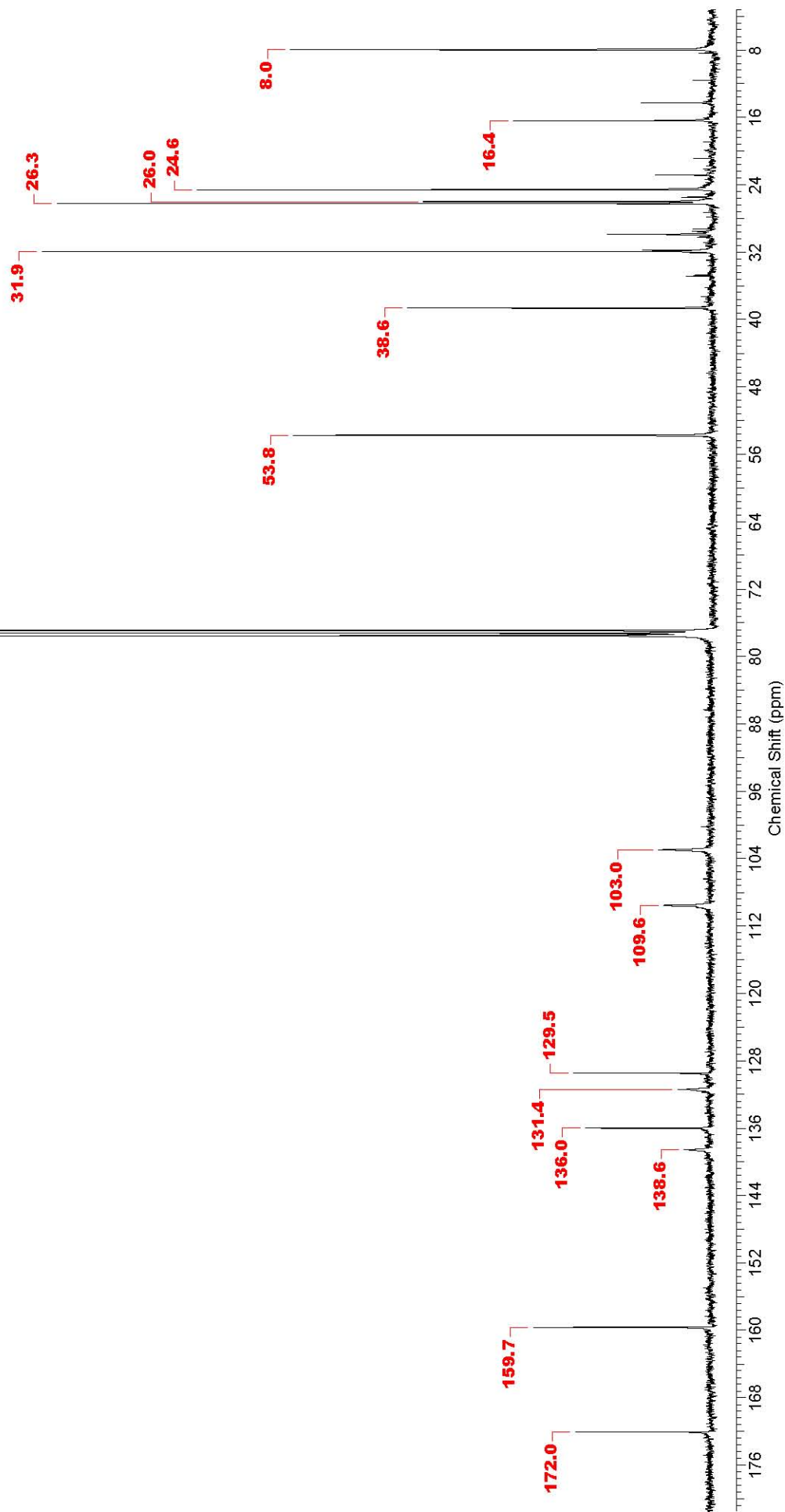


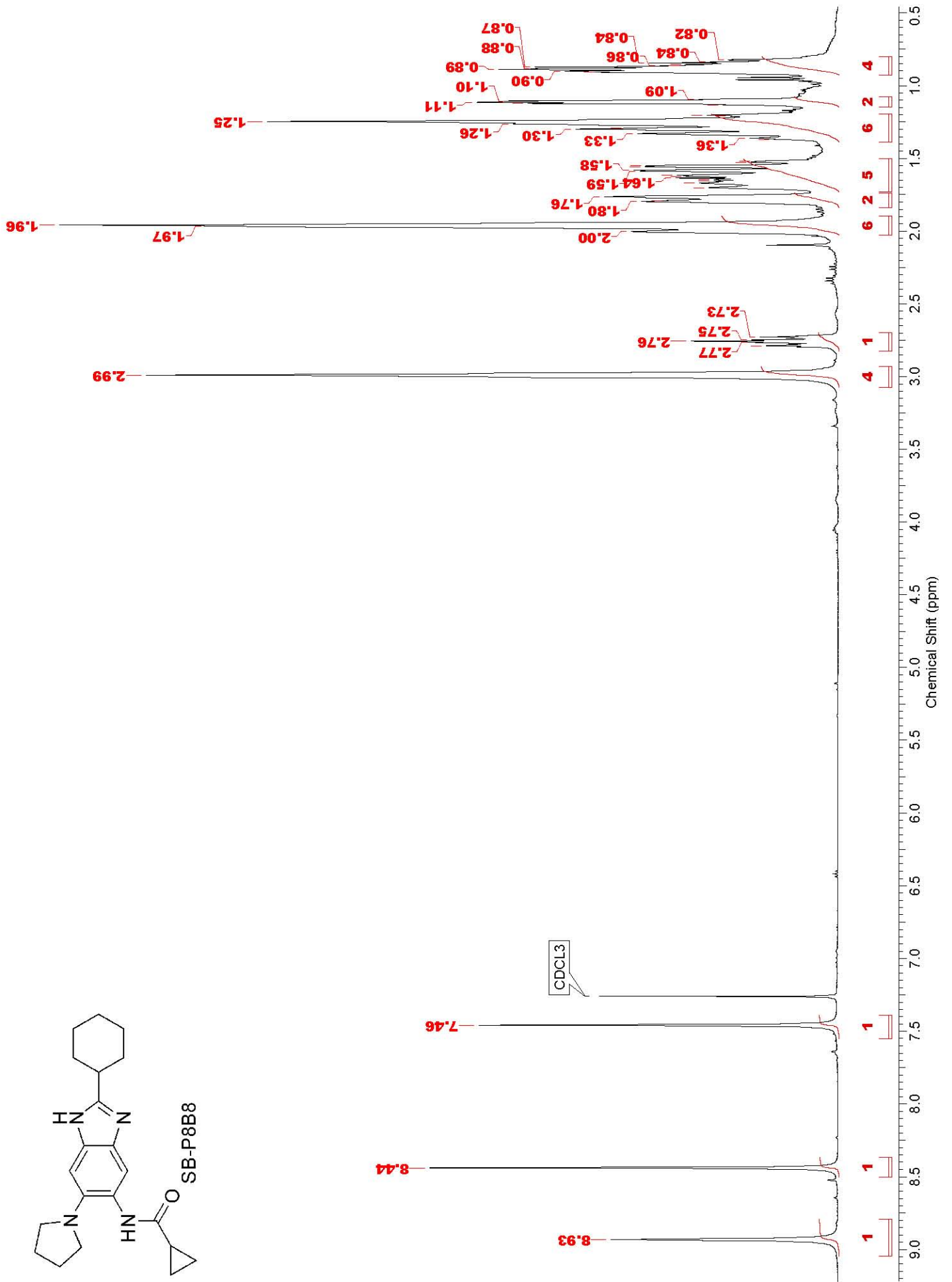
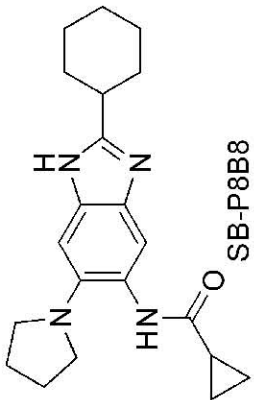




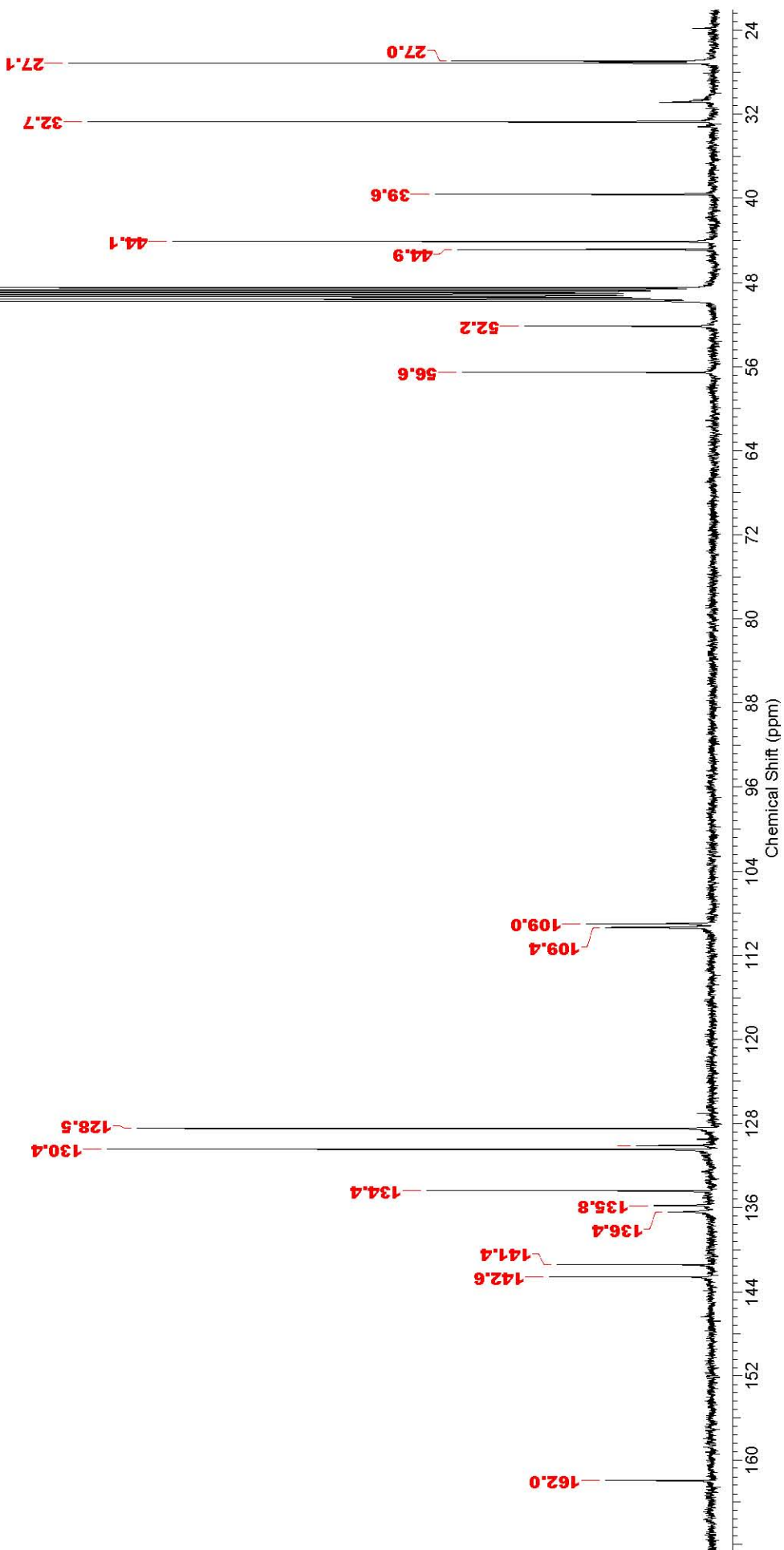
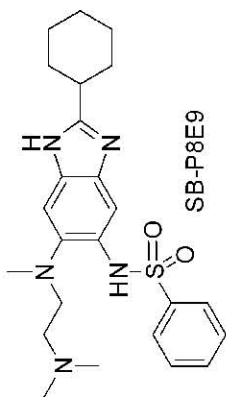
SB-P8B8

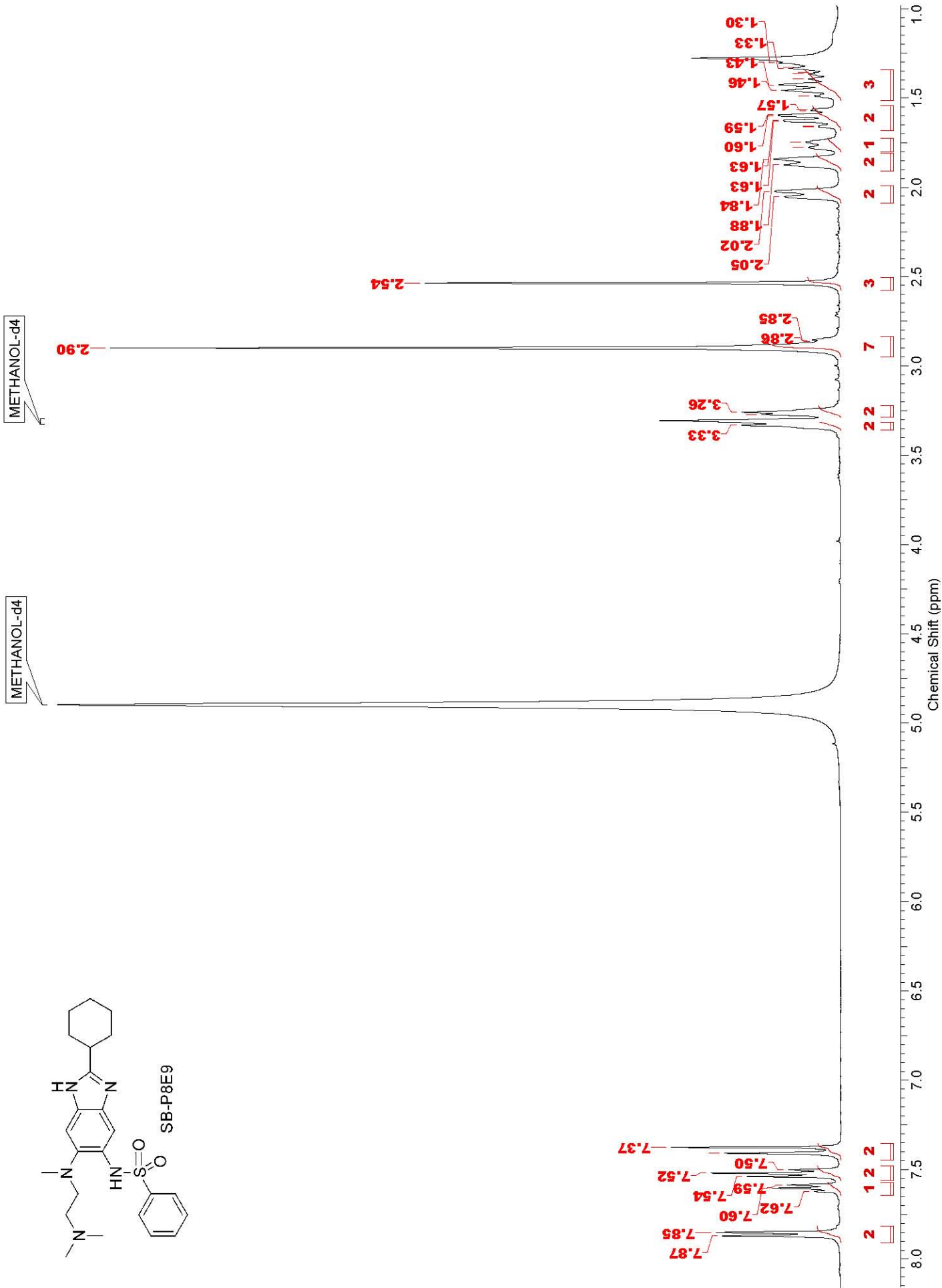
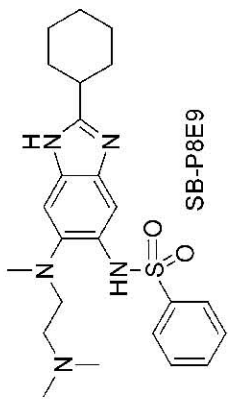
CDCl₃

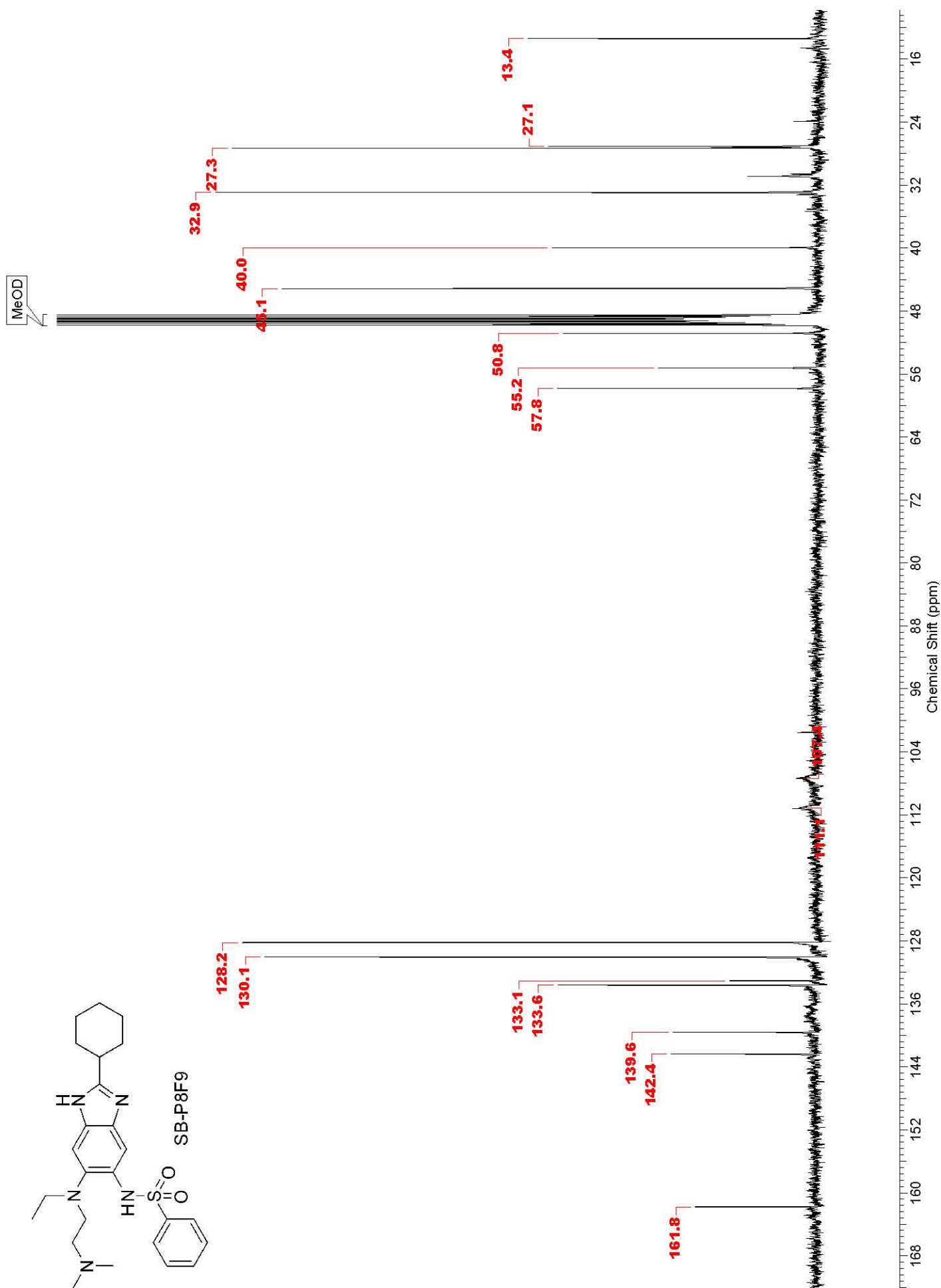
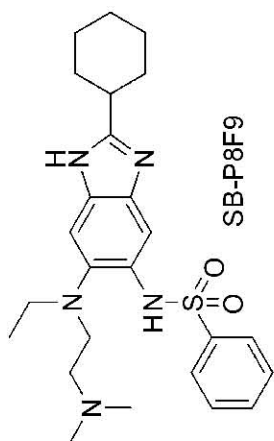


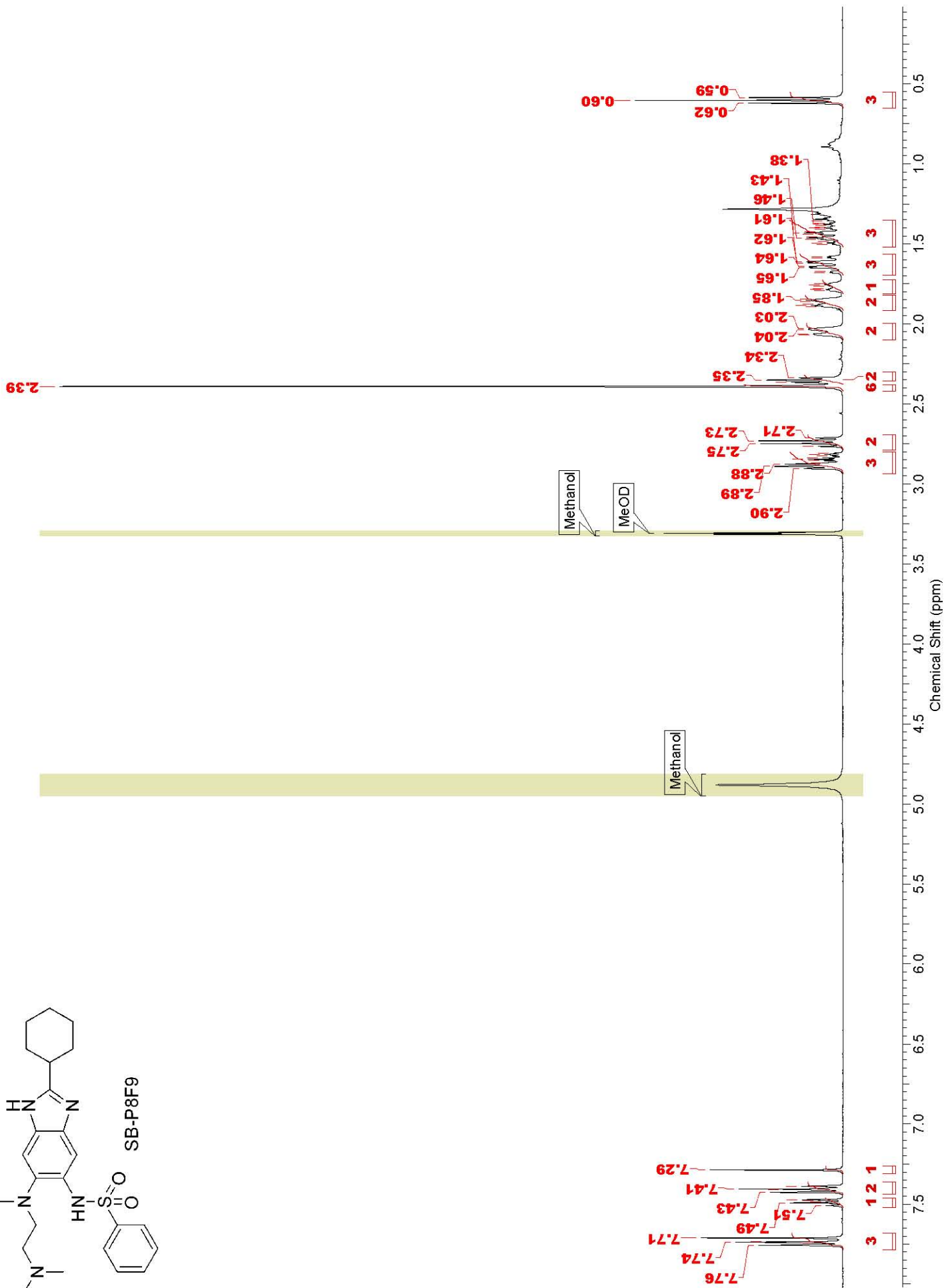
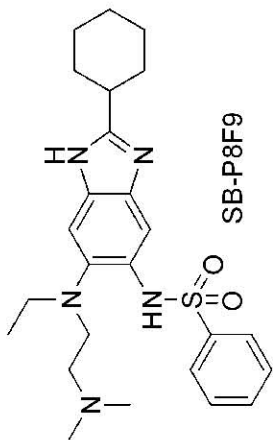


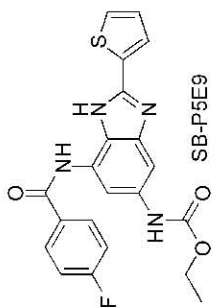
METHANOL-d4



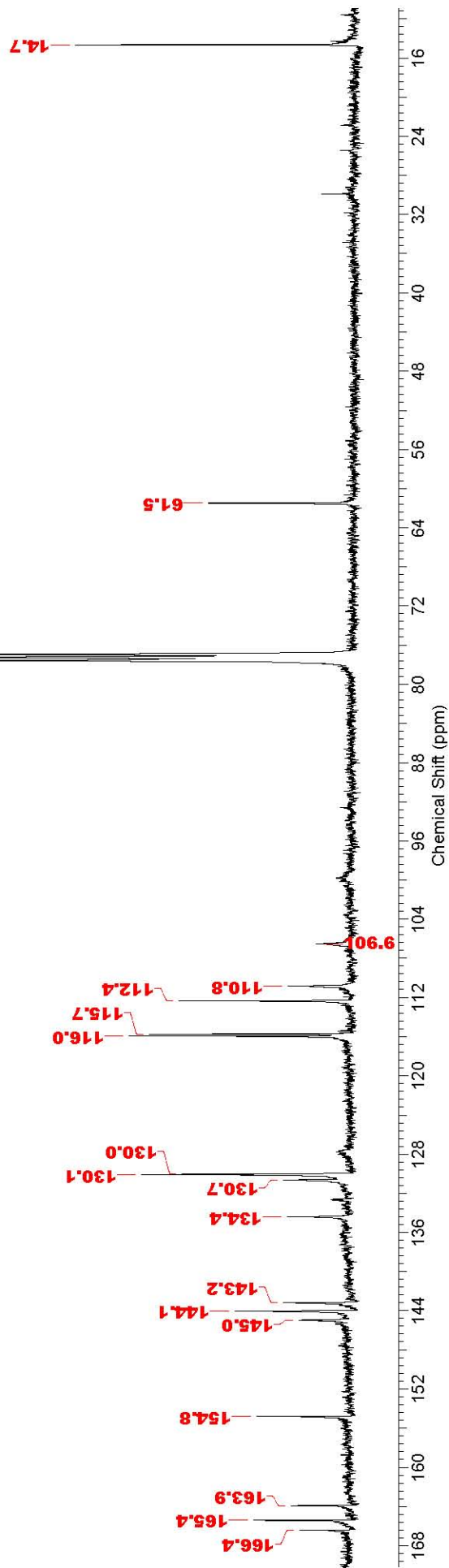


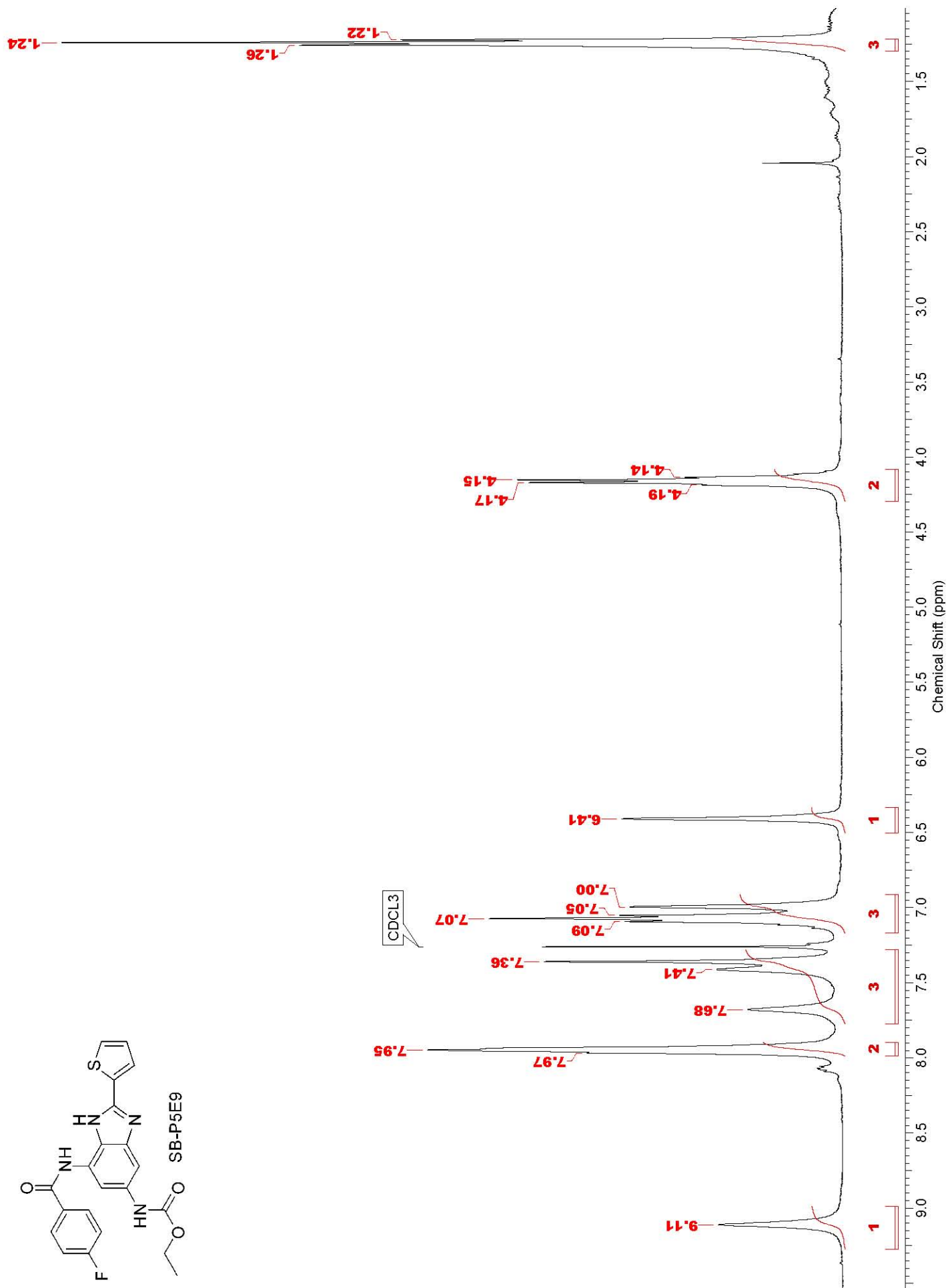
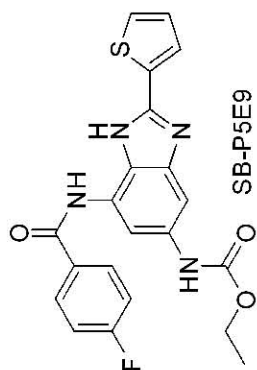


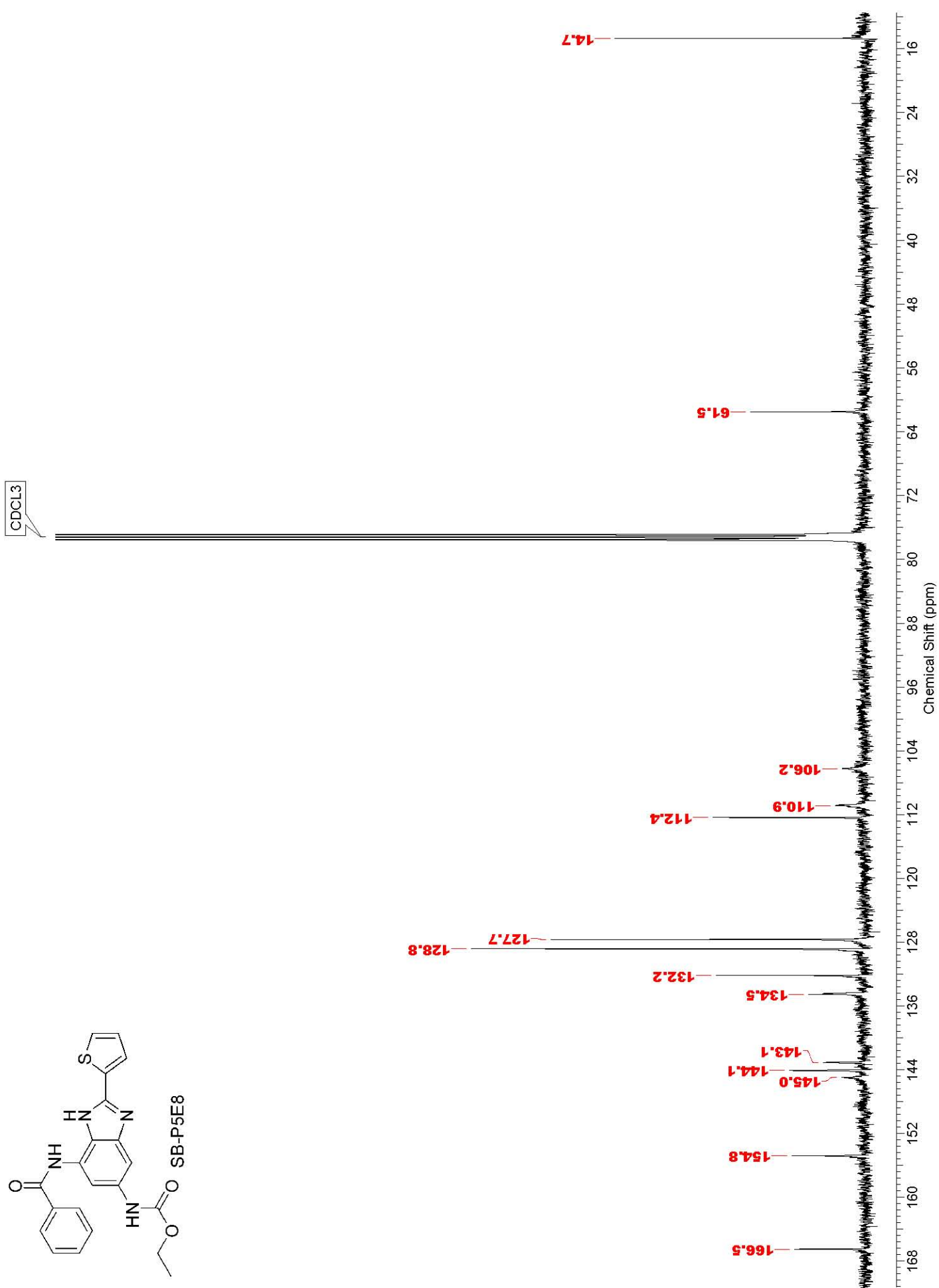
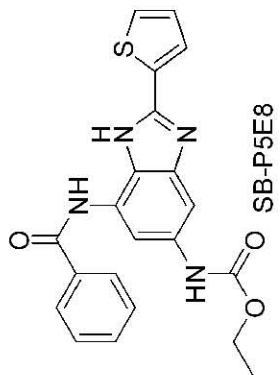


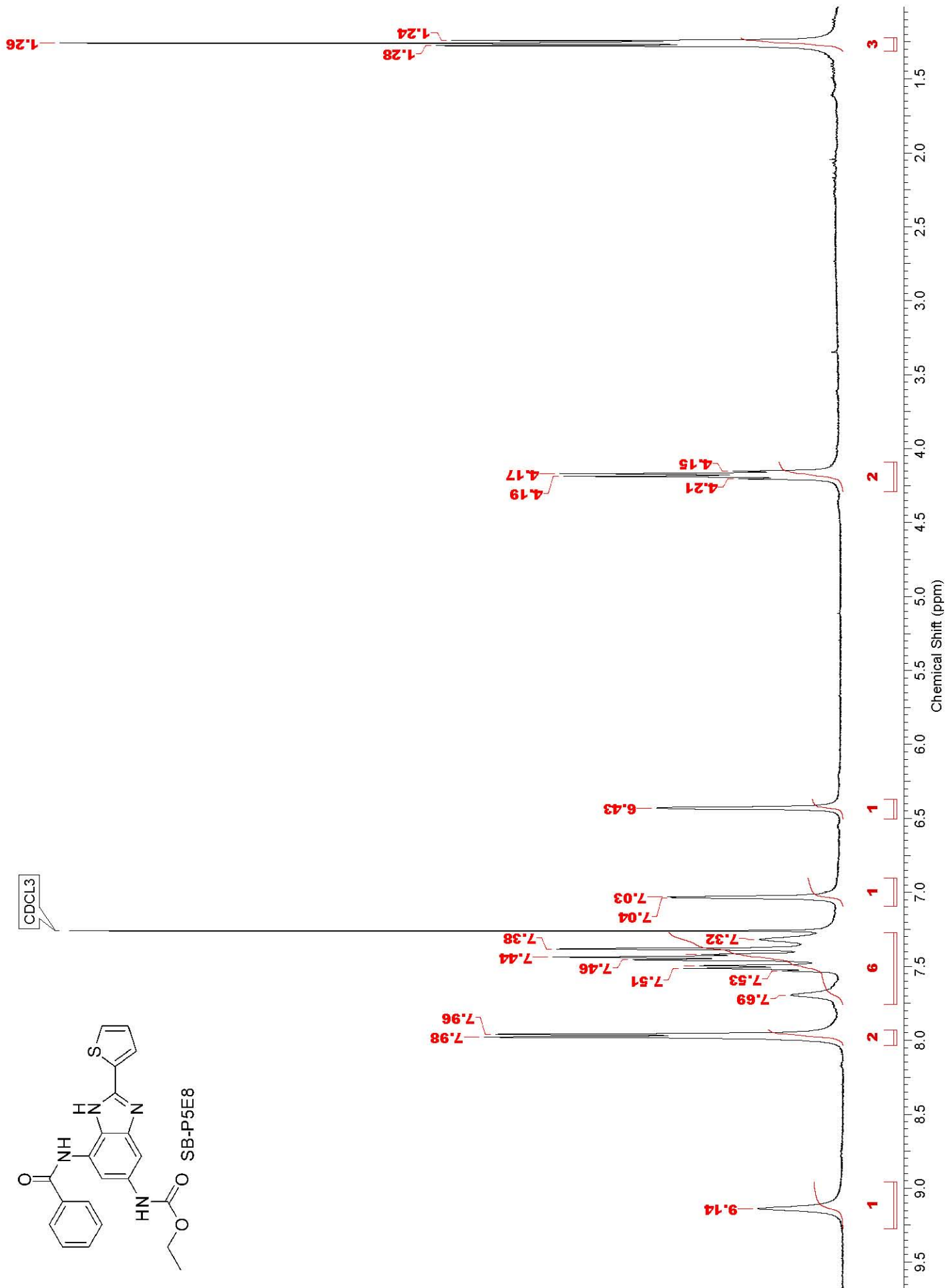
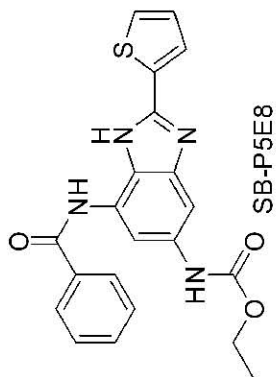


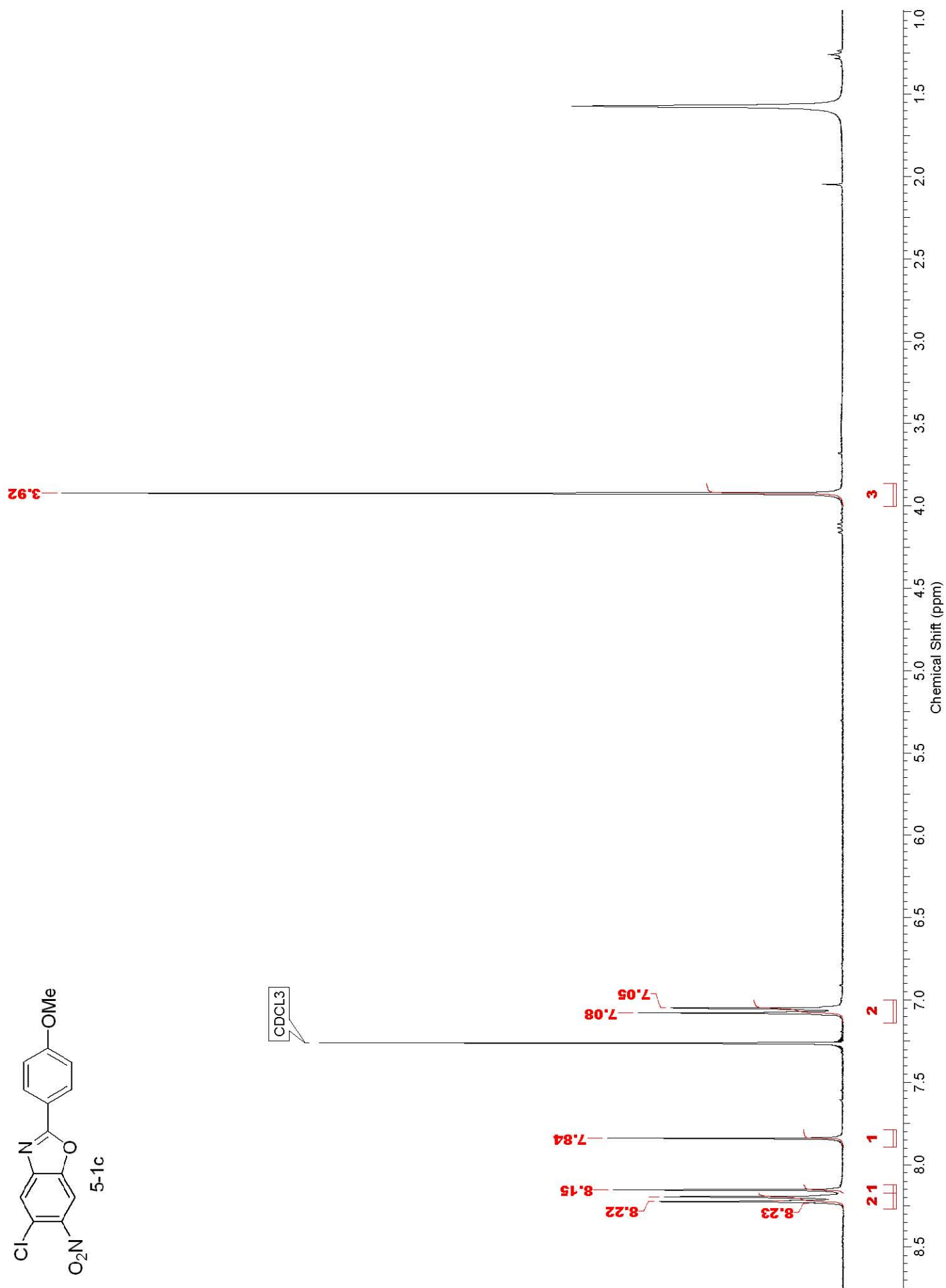
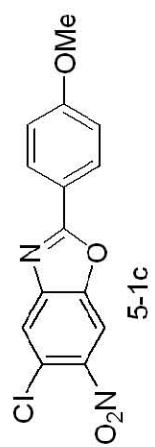
CHLOROFORM-d





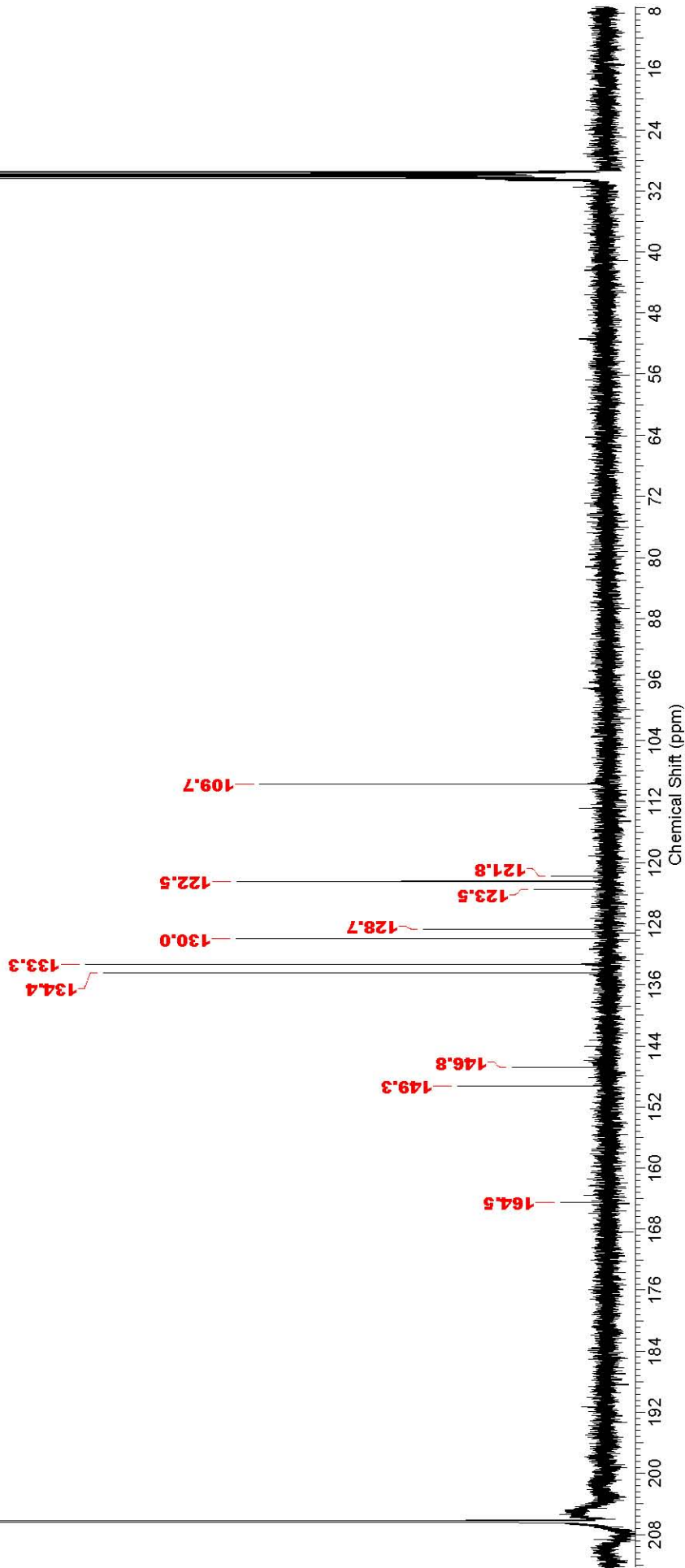
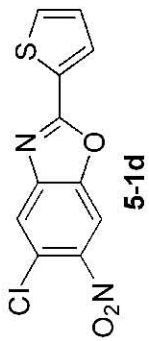


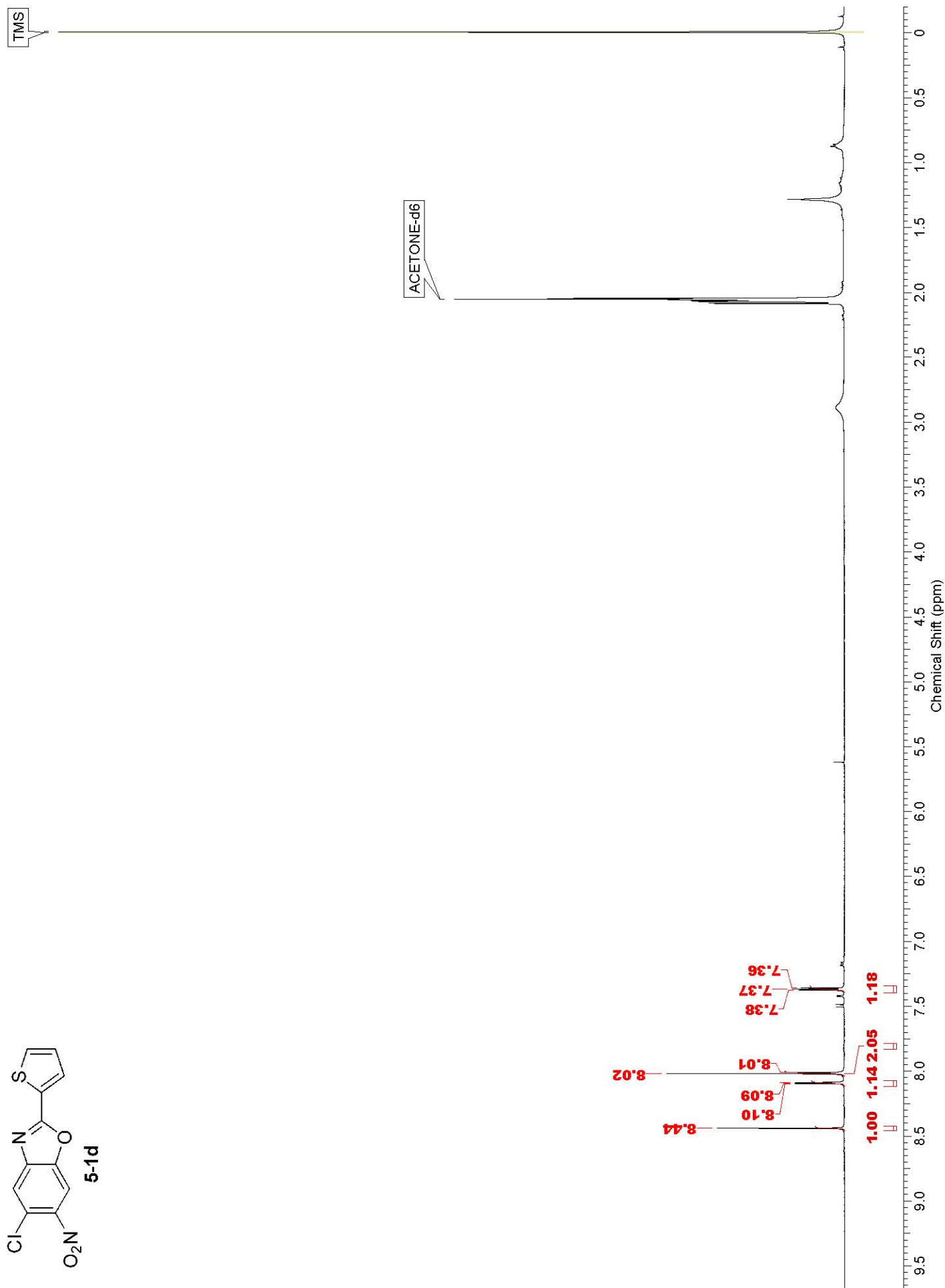
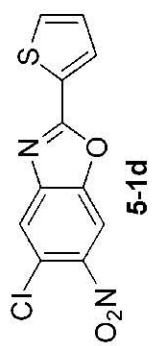


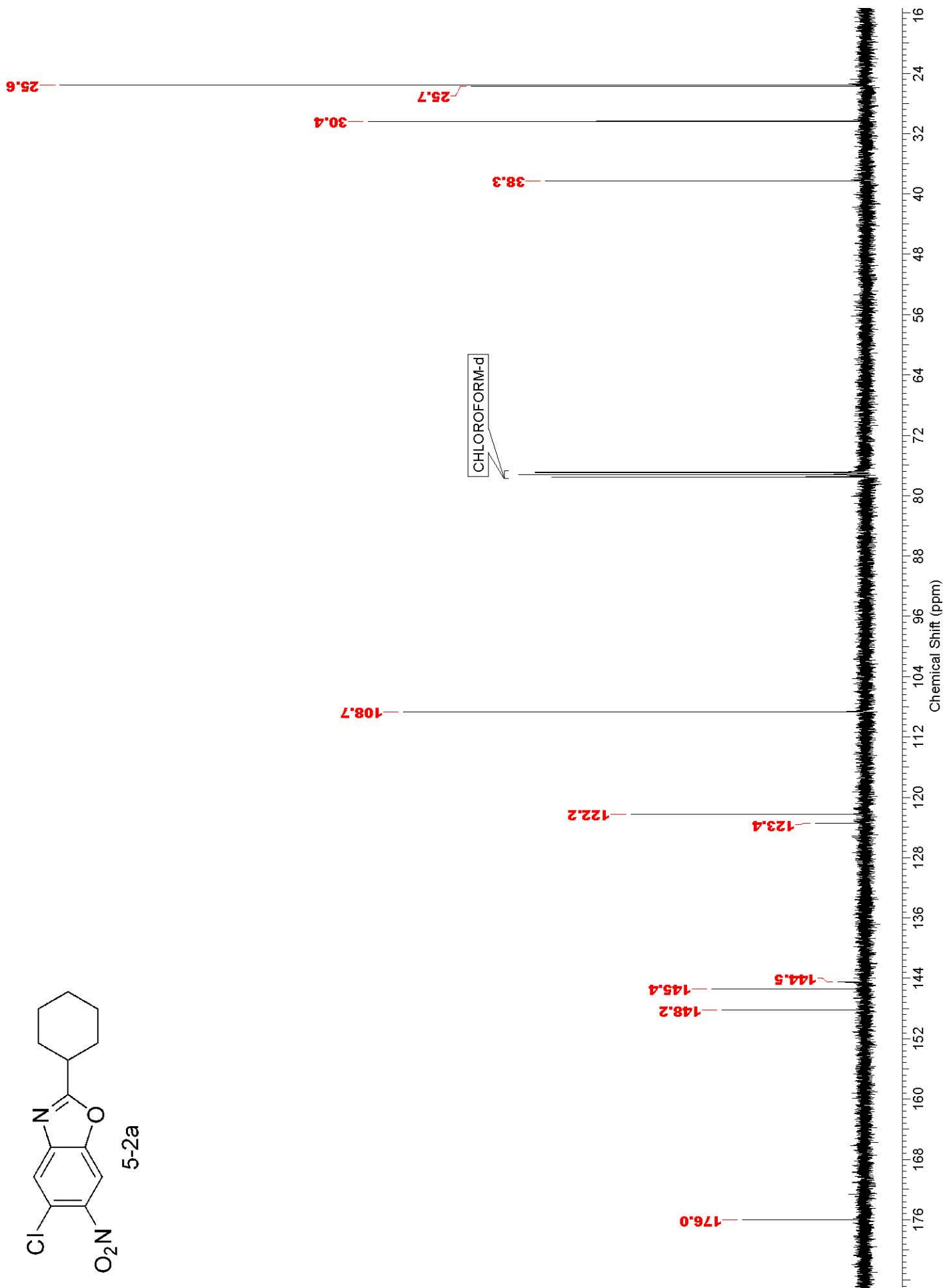
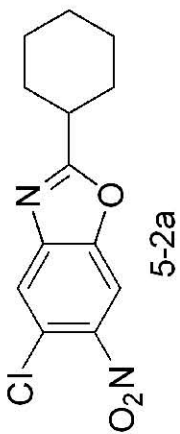


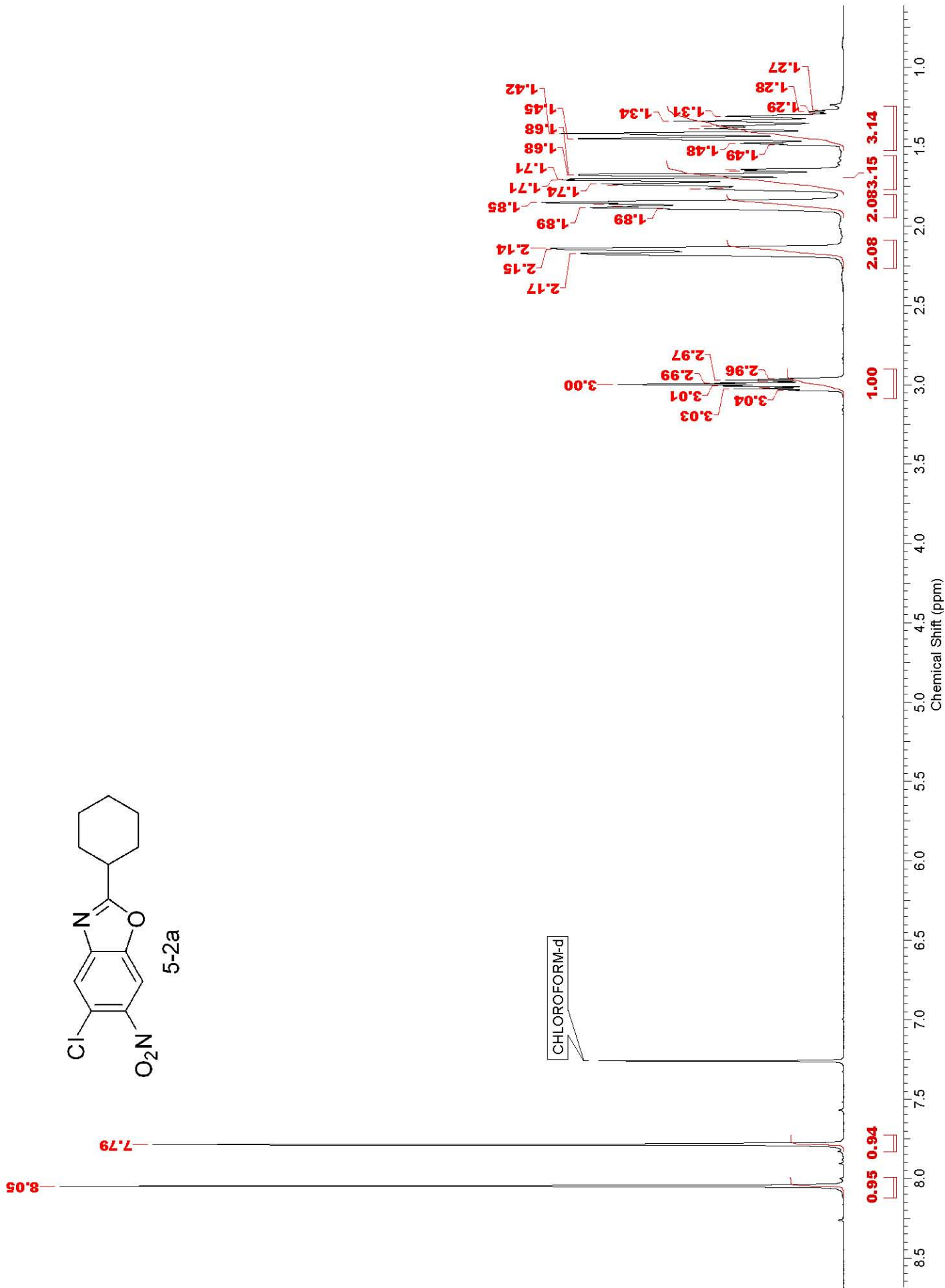
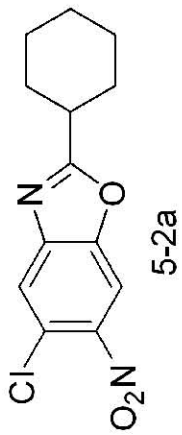
ACETONE-d6

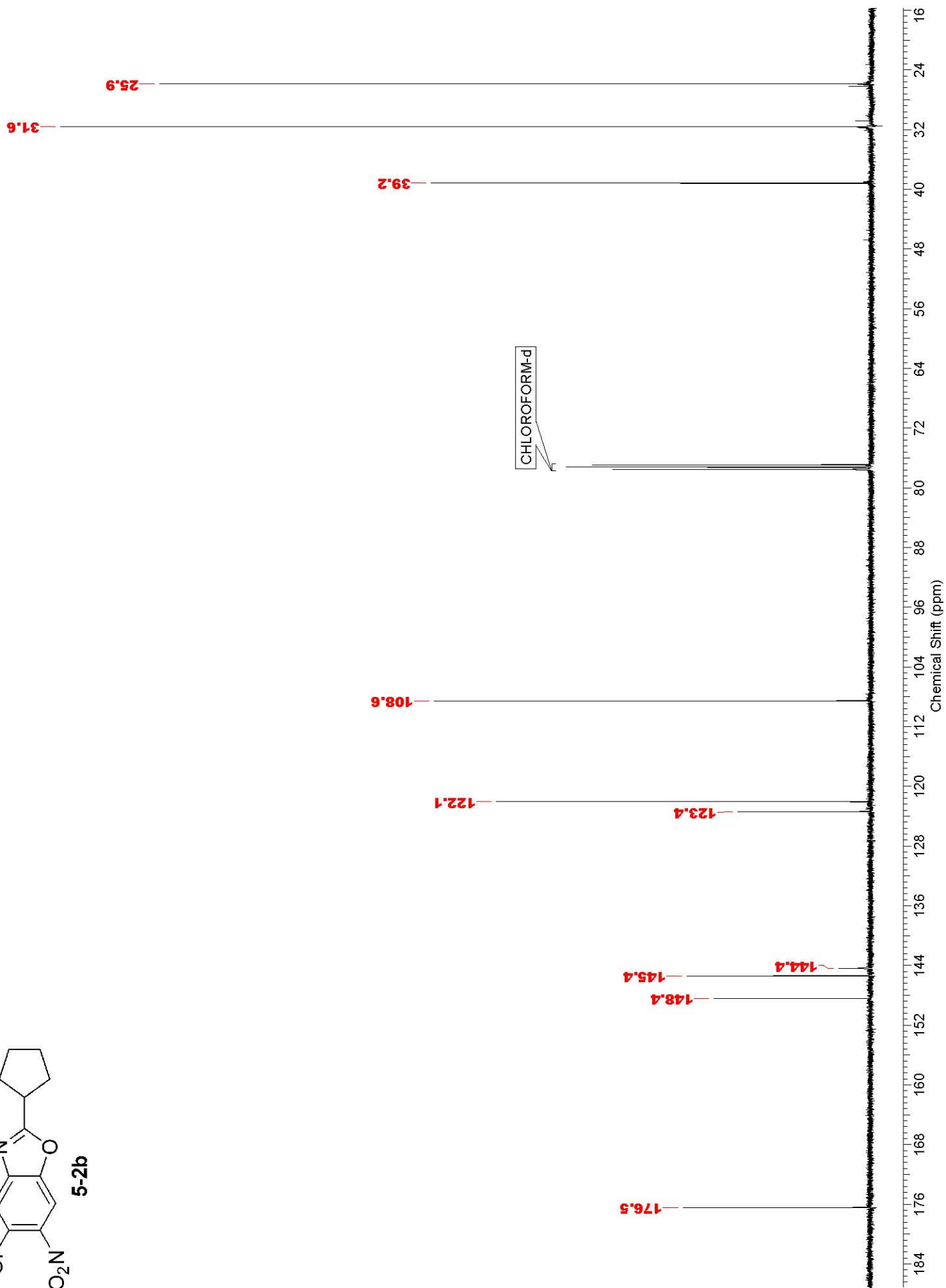
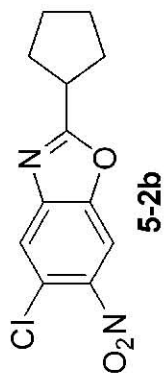
ACETONE-d6

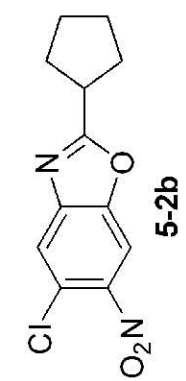




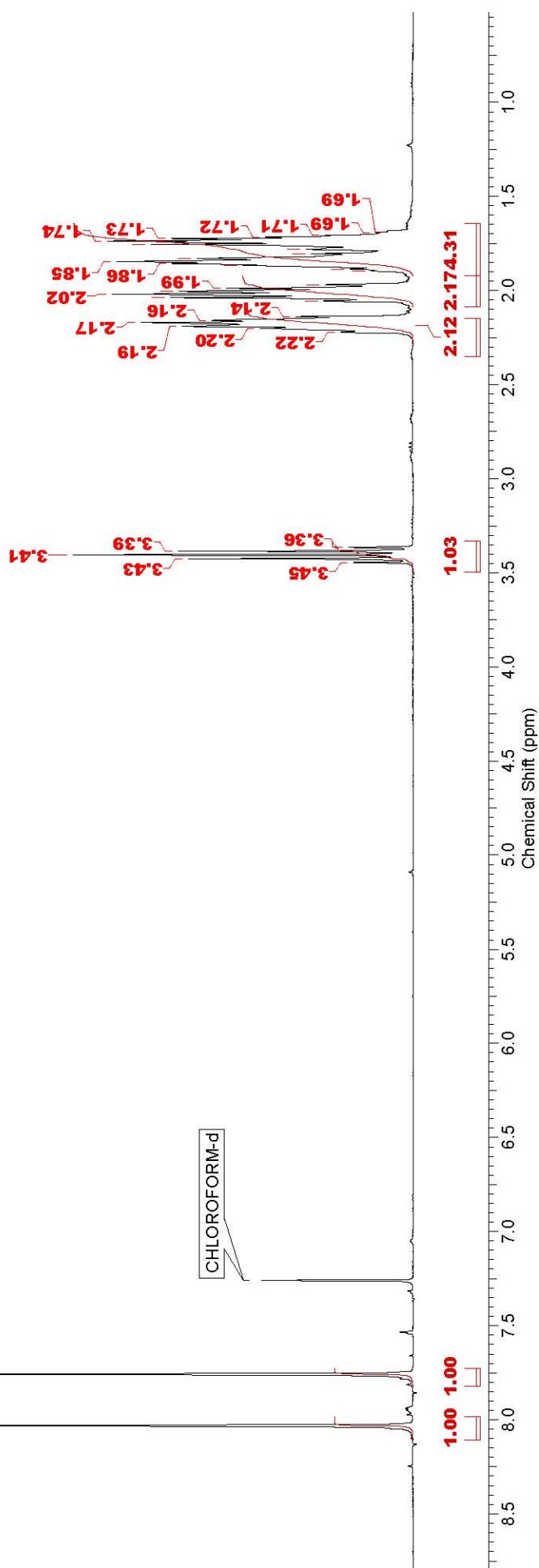


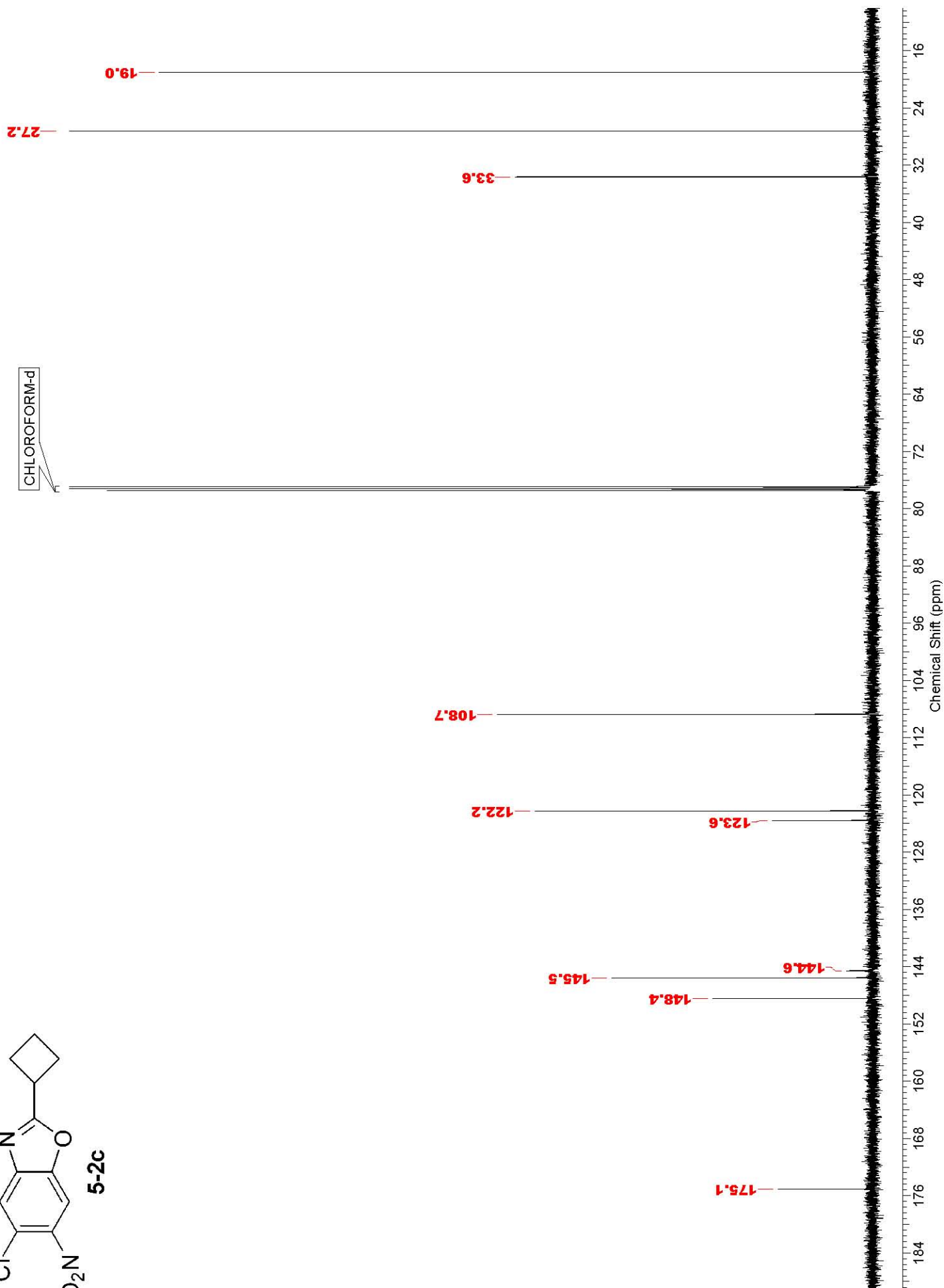
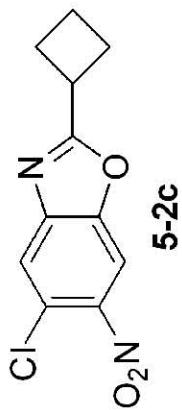


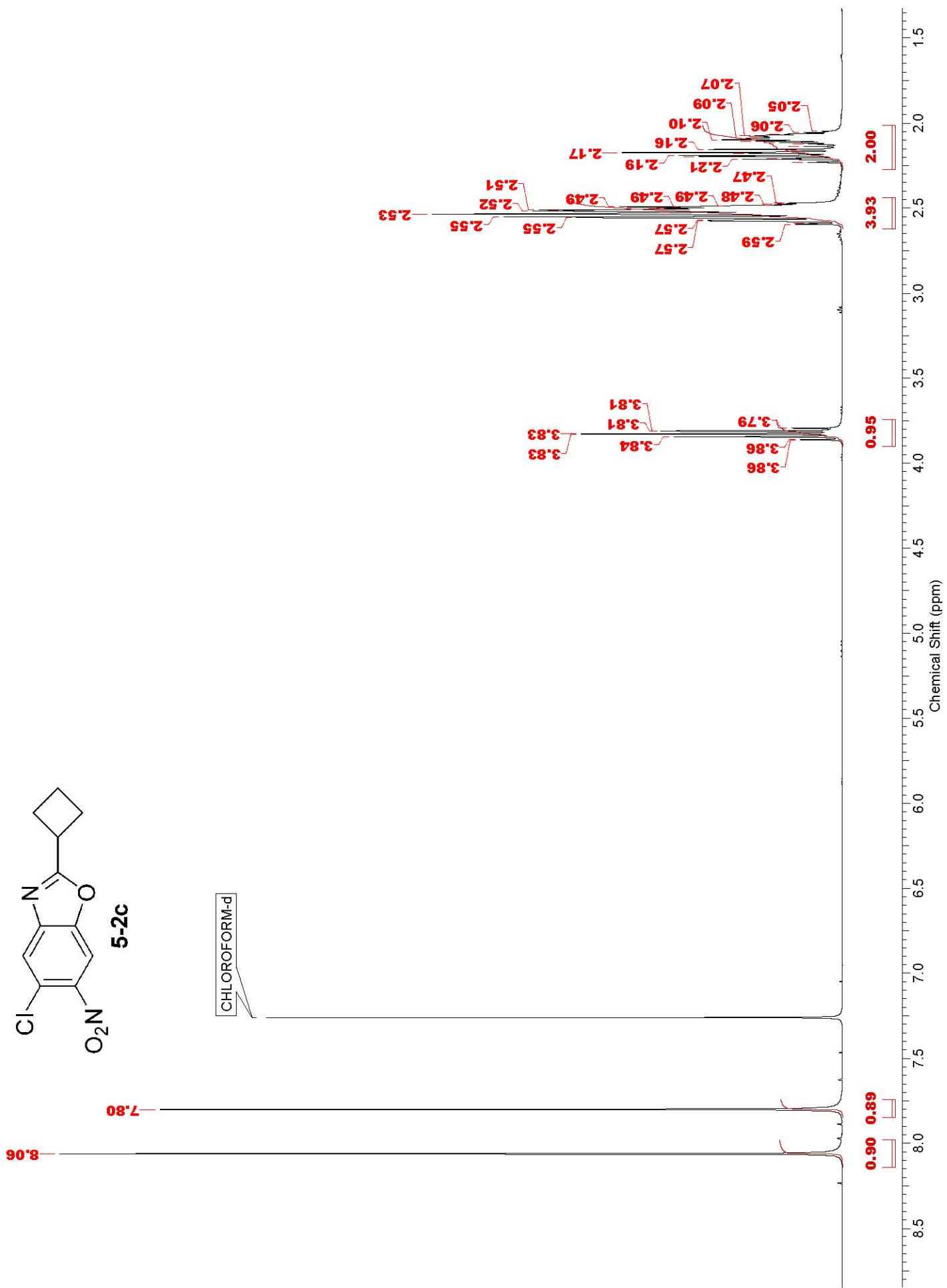
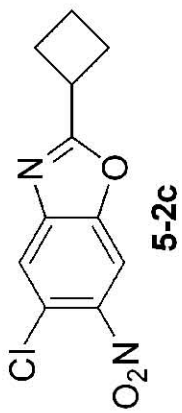


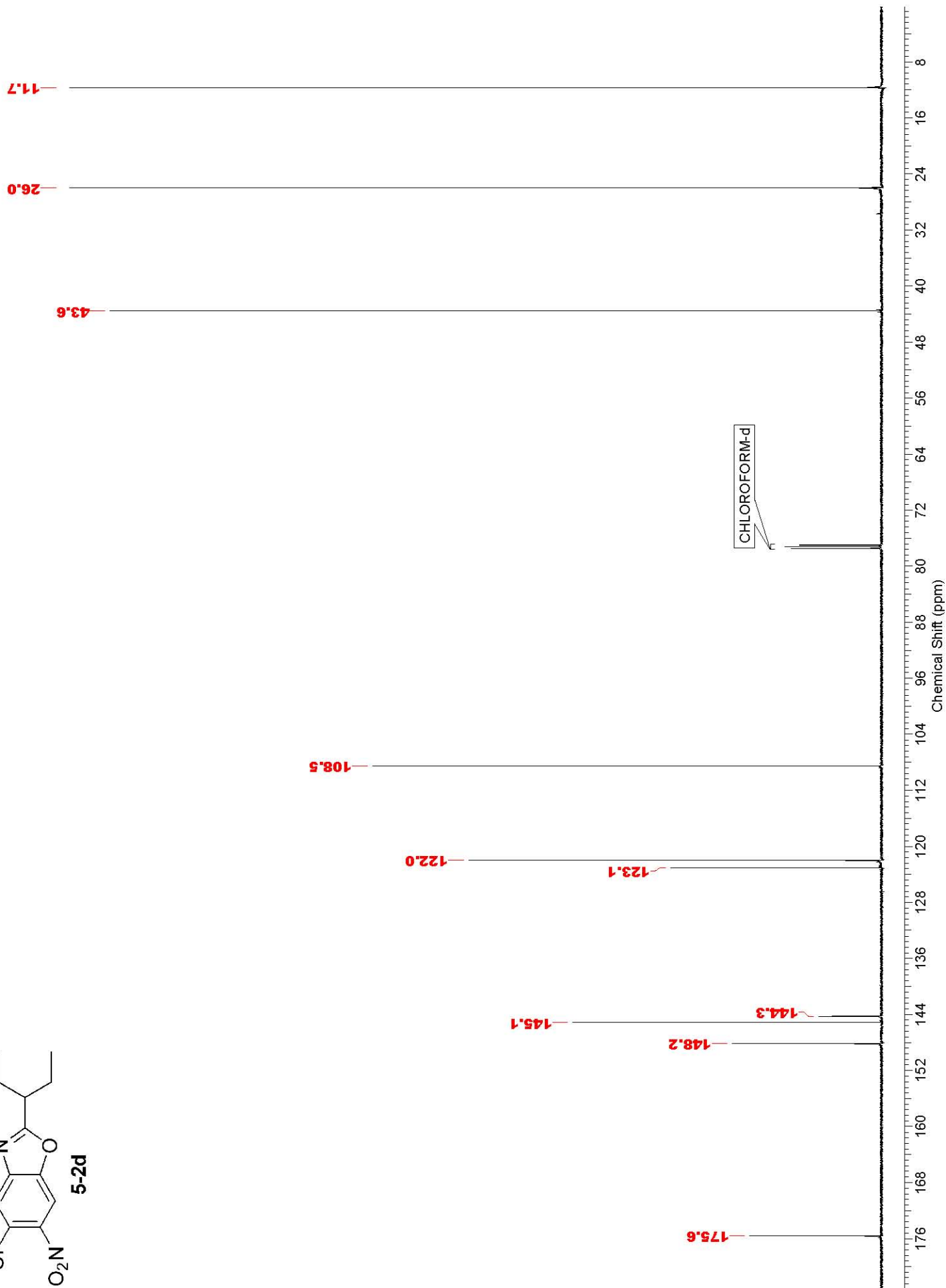
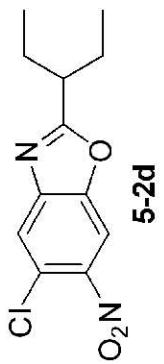


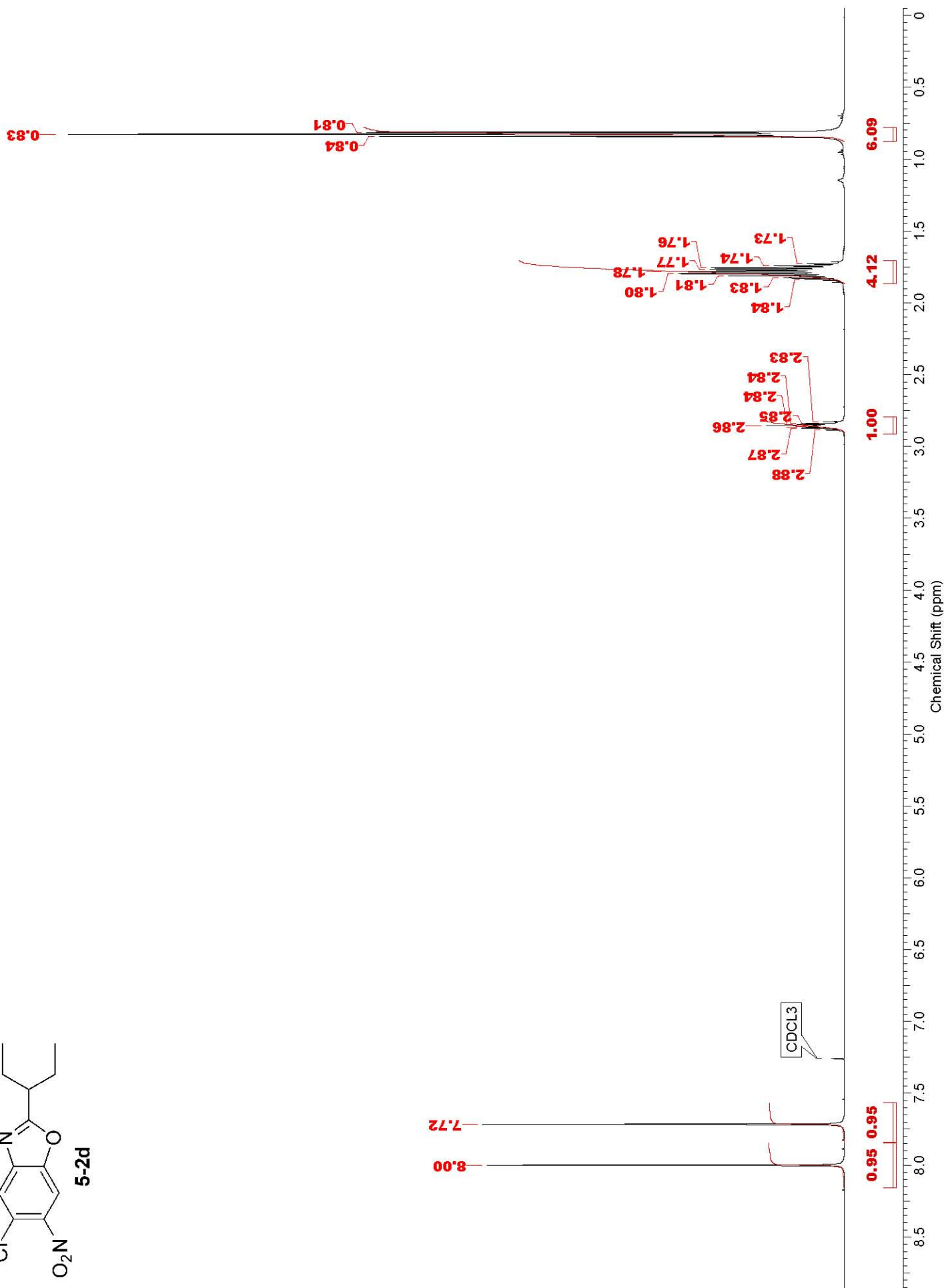
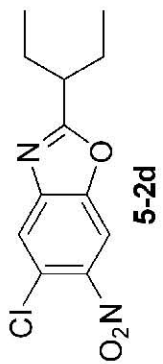
8.03
7.76

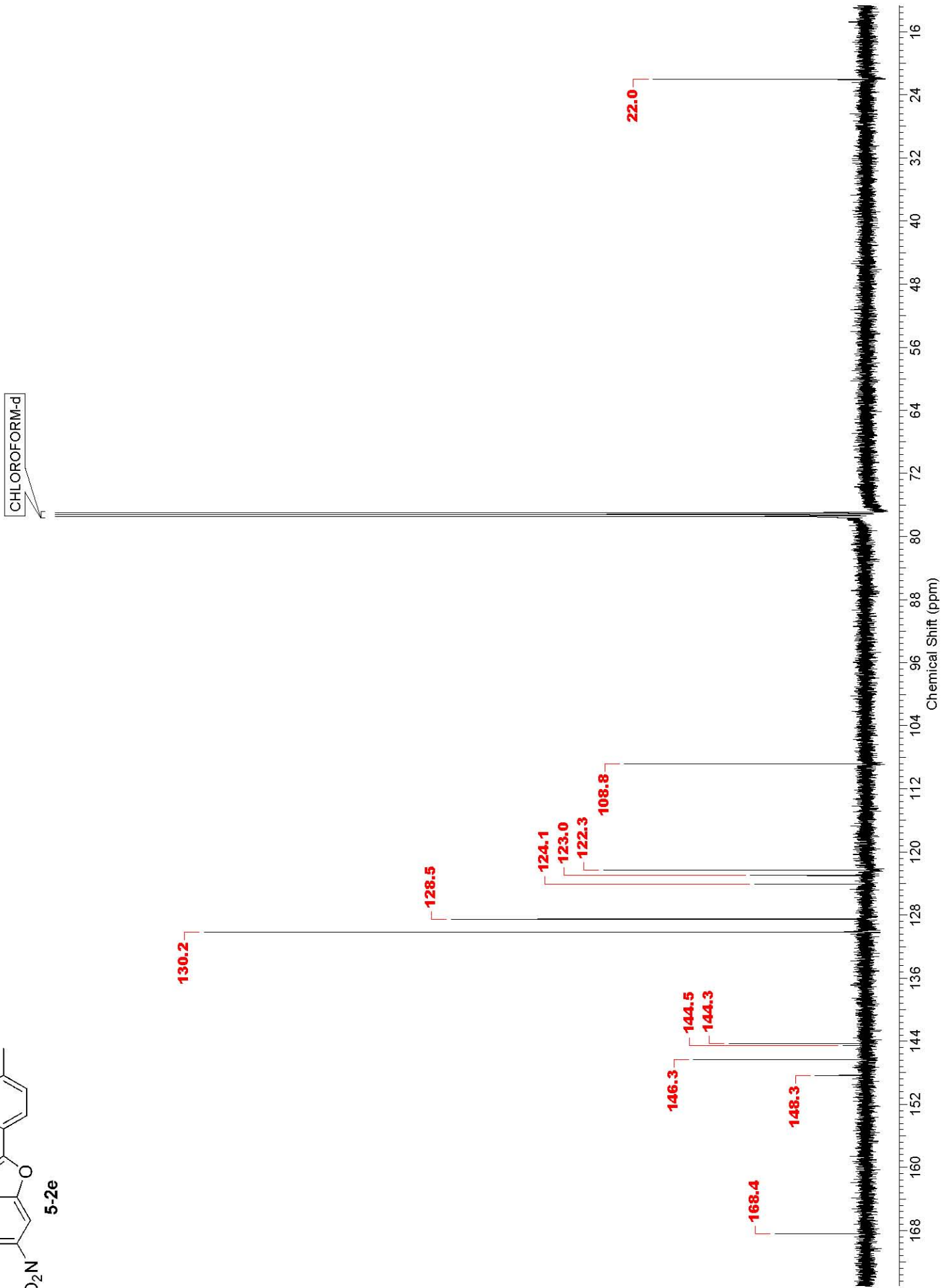
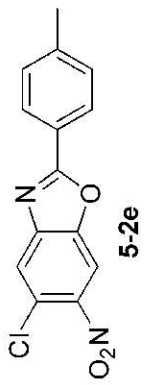


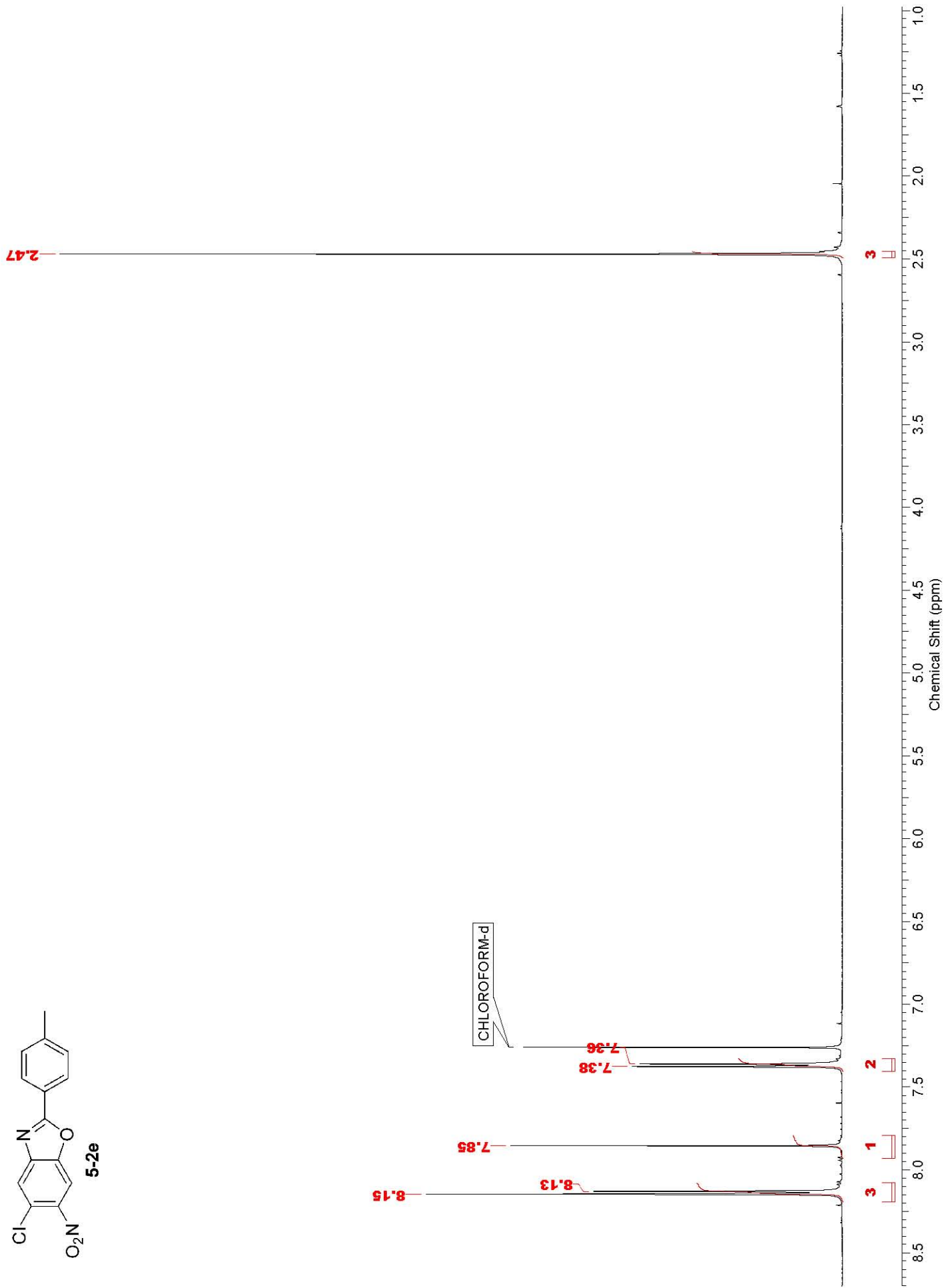
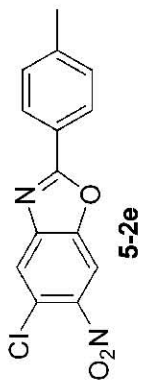


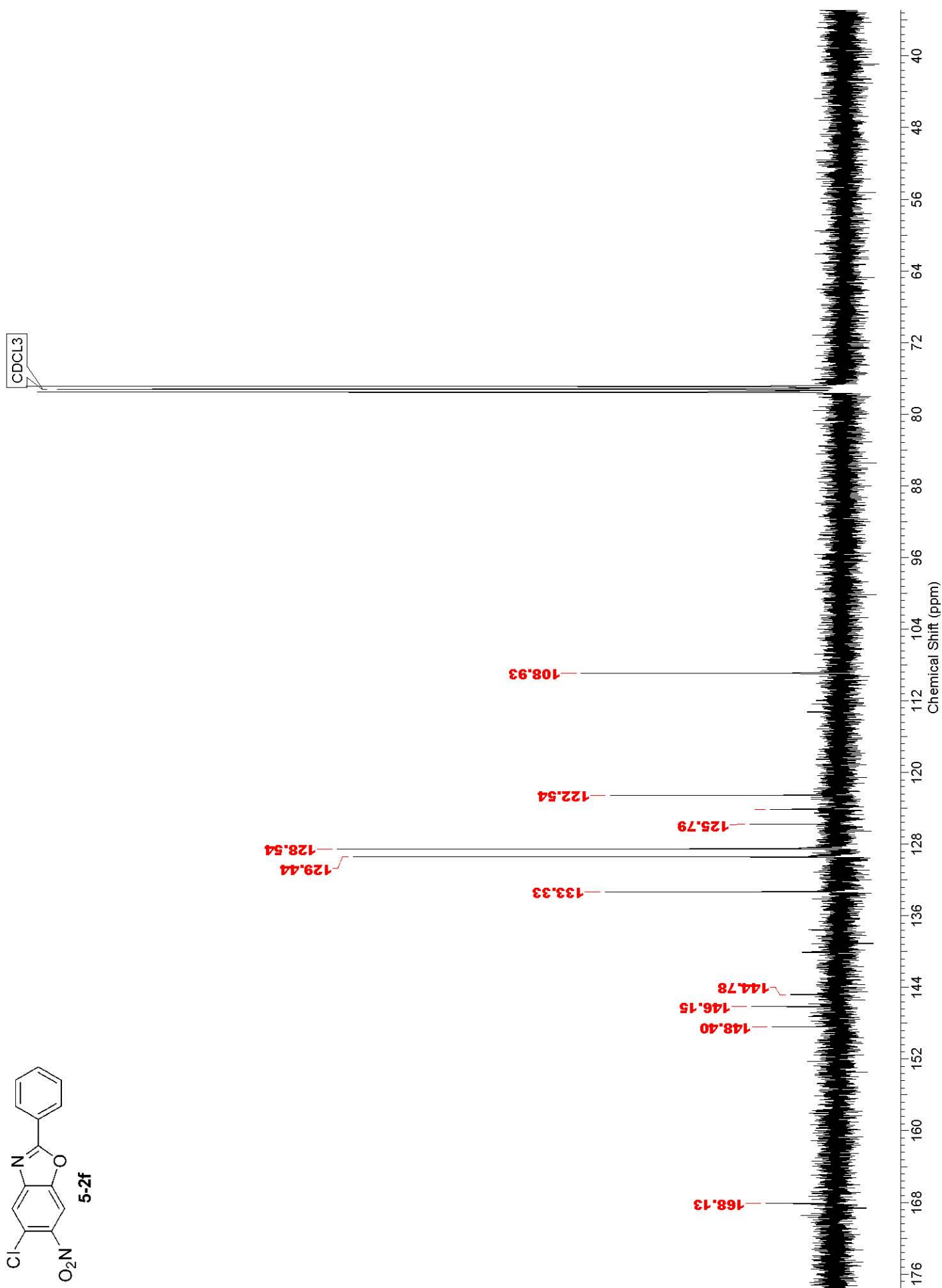
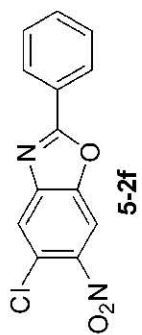


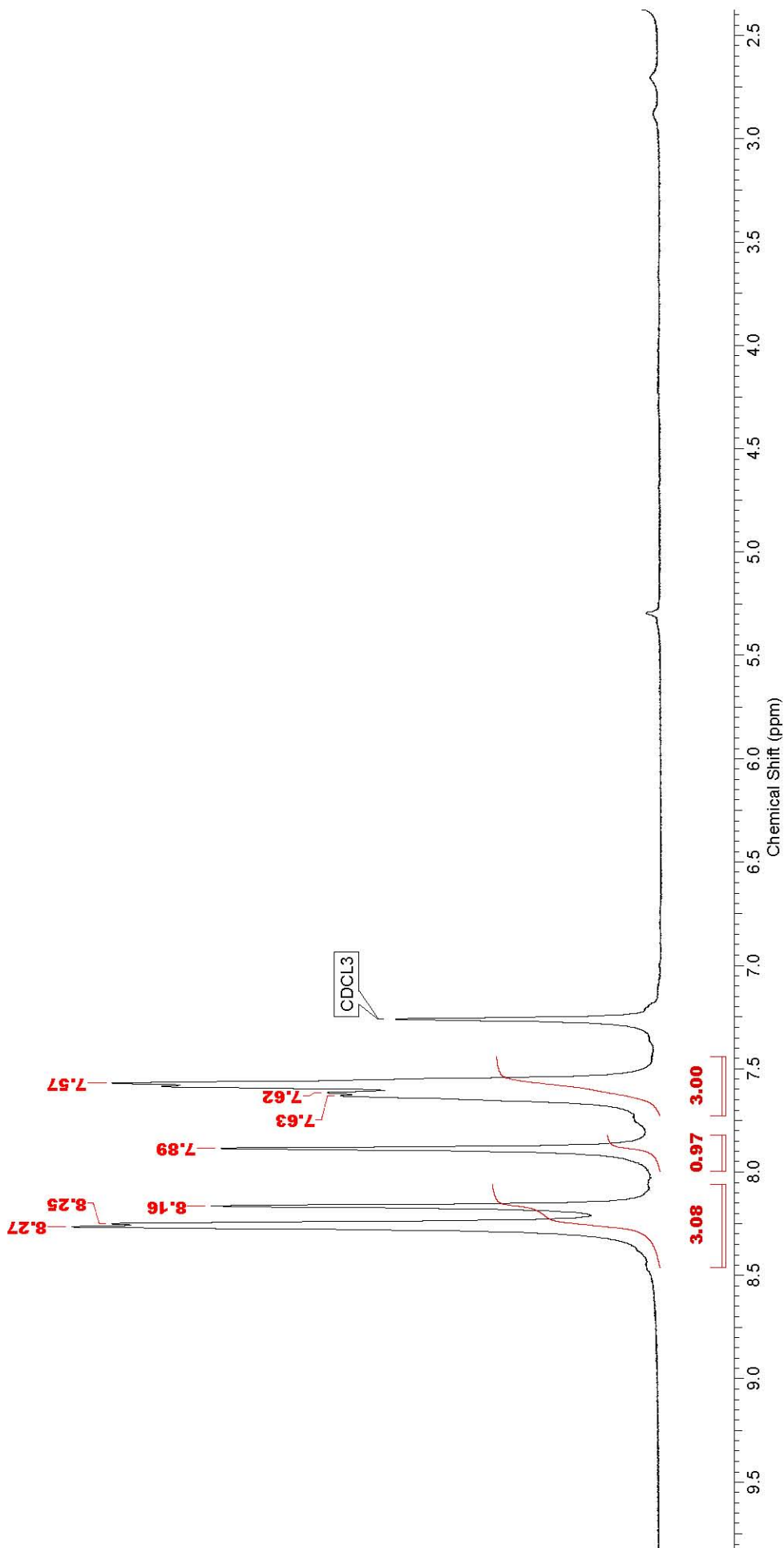
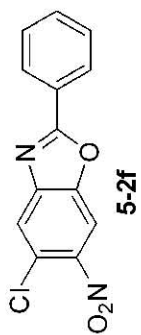


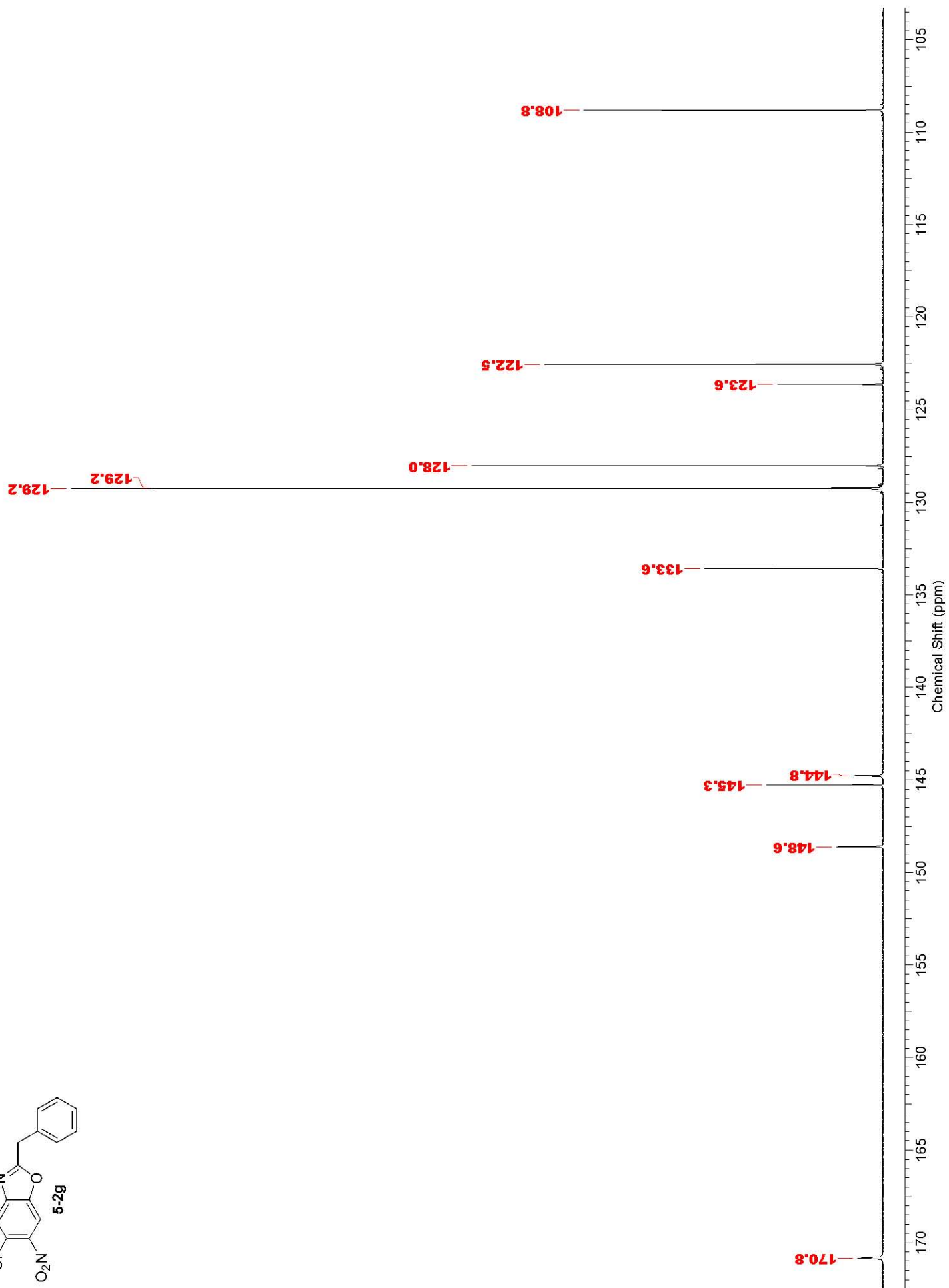
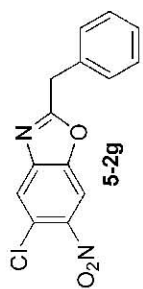


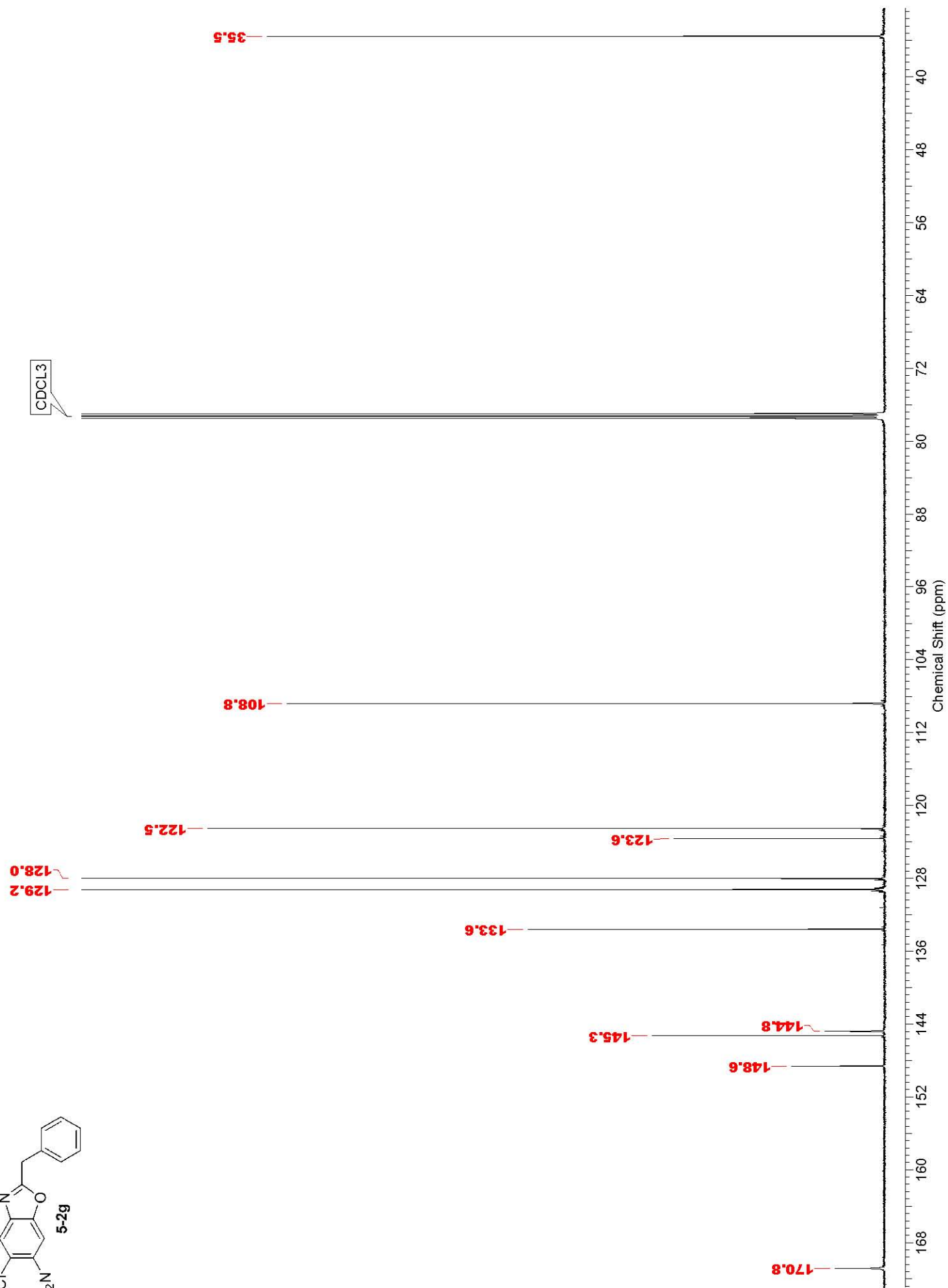
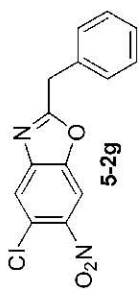


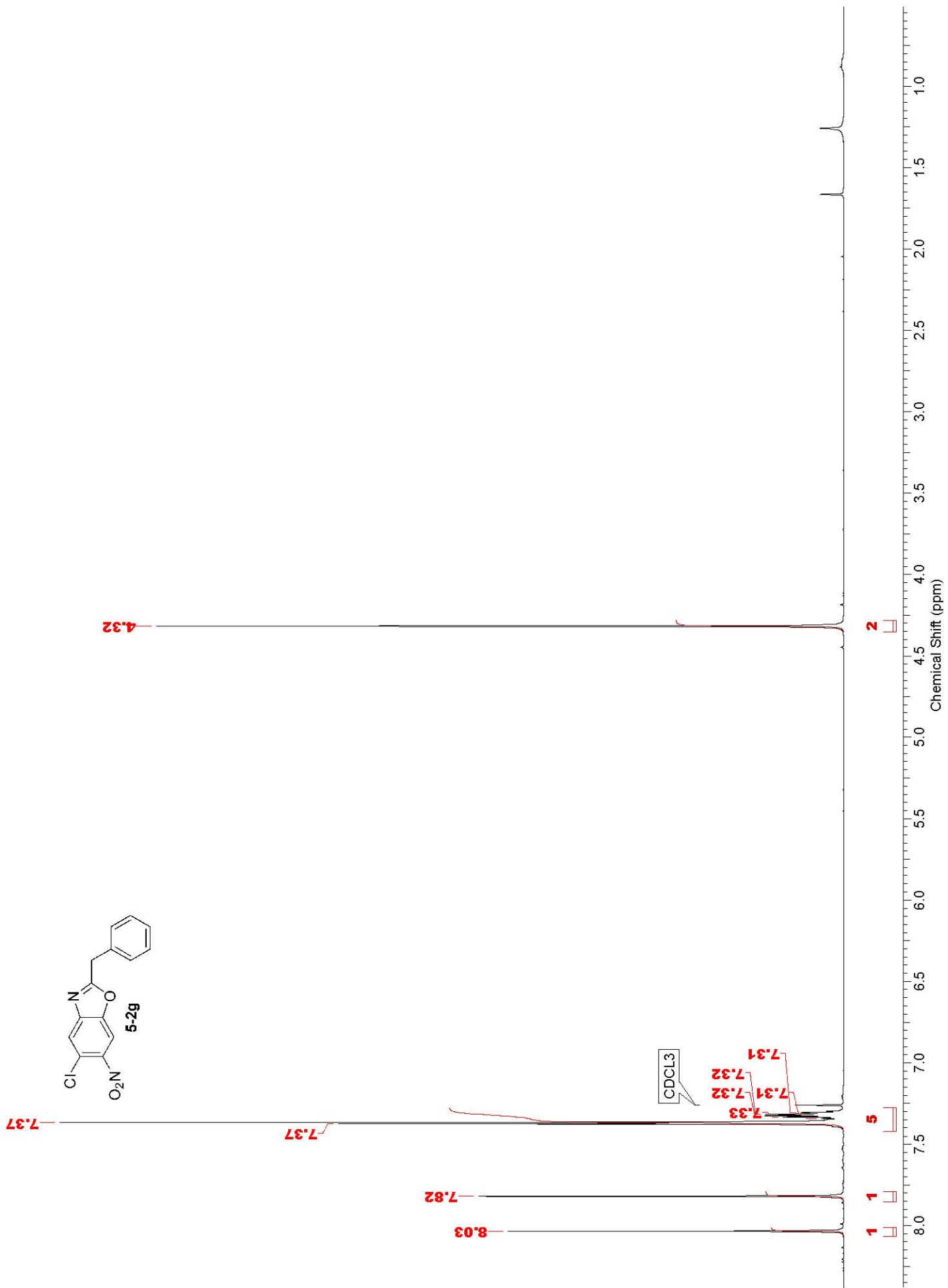


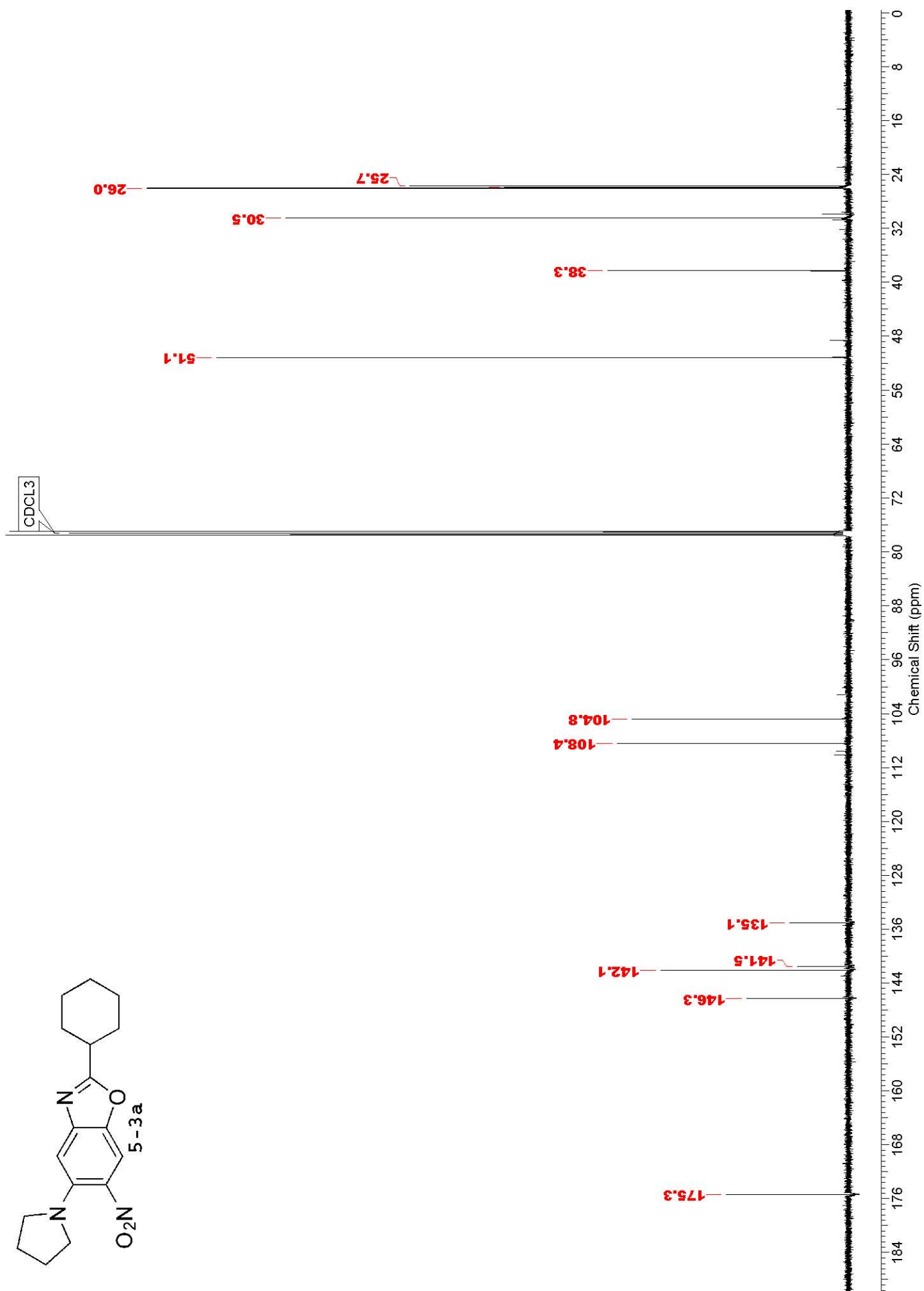
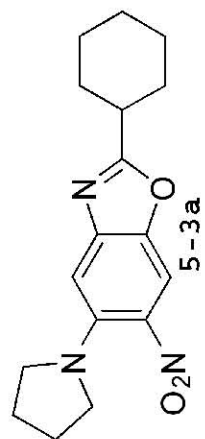


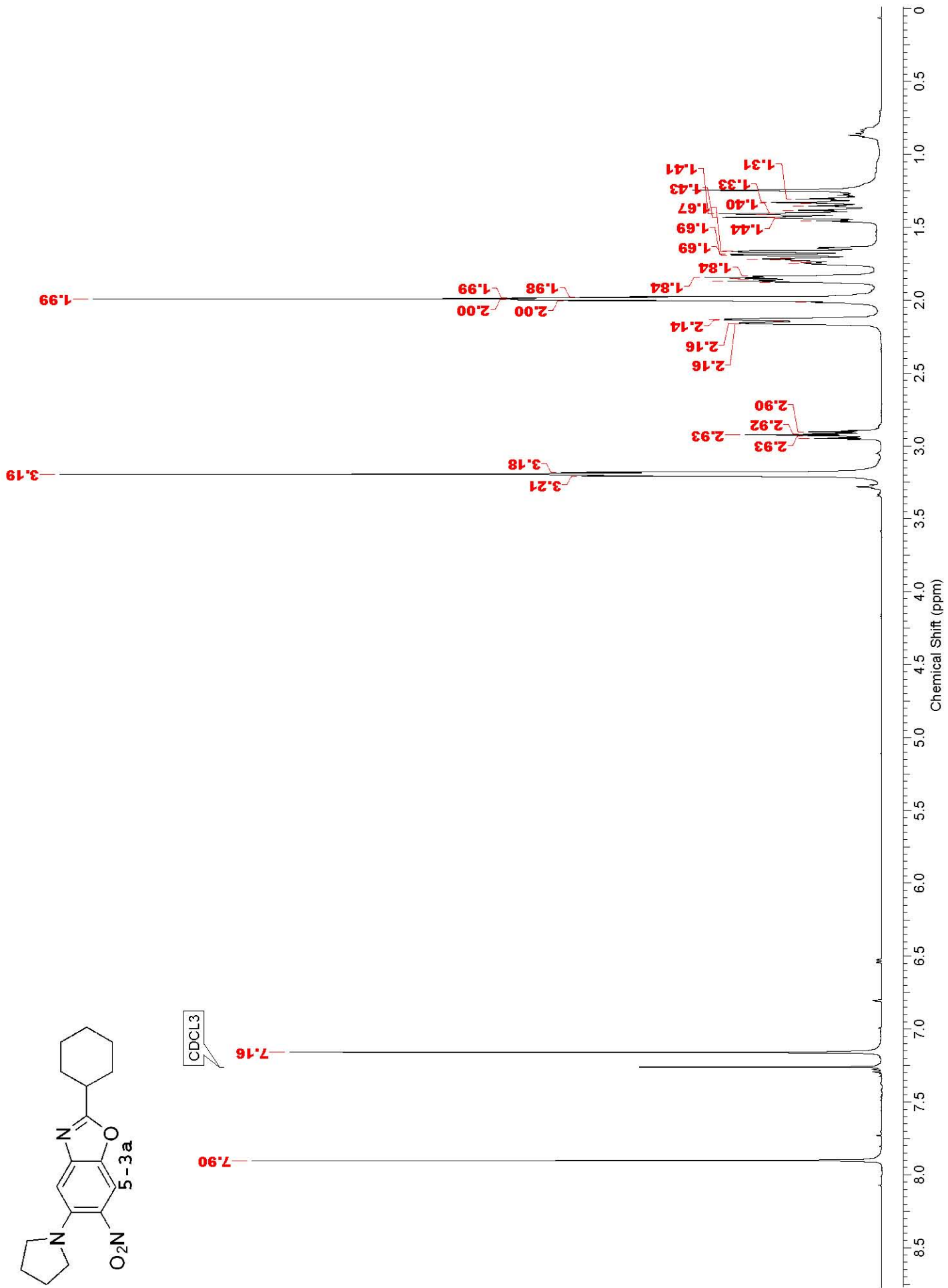
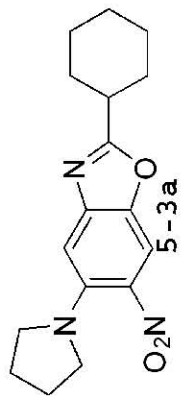


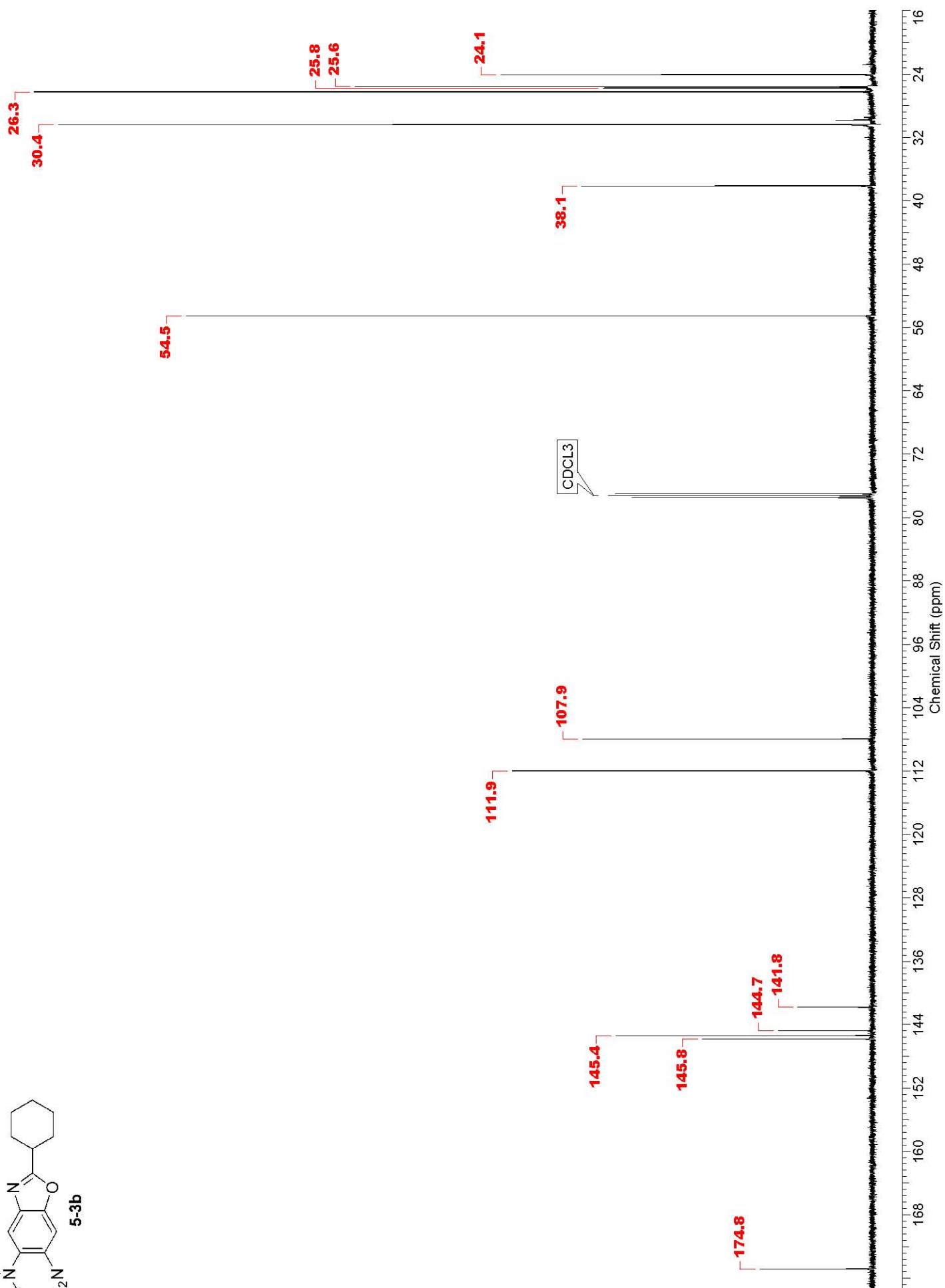
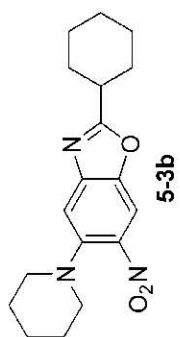


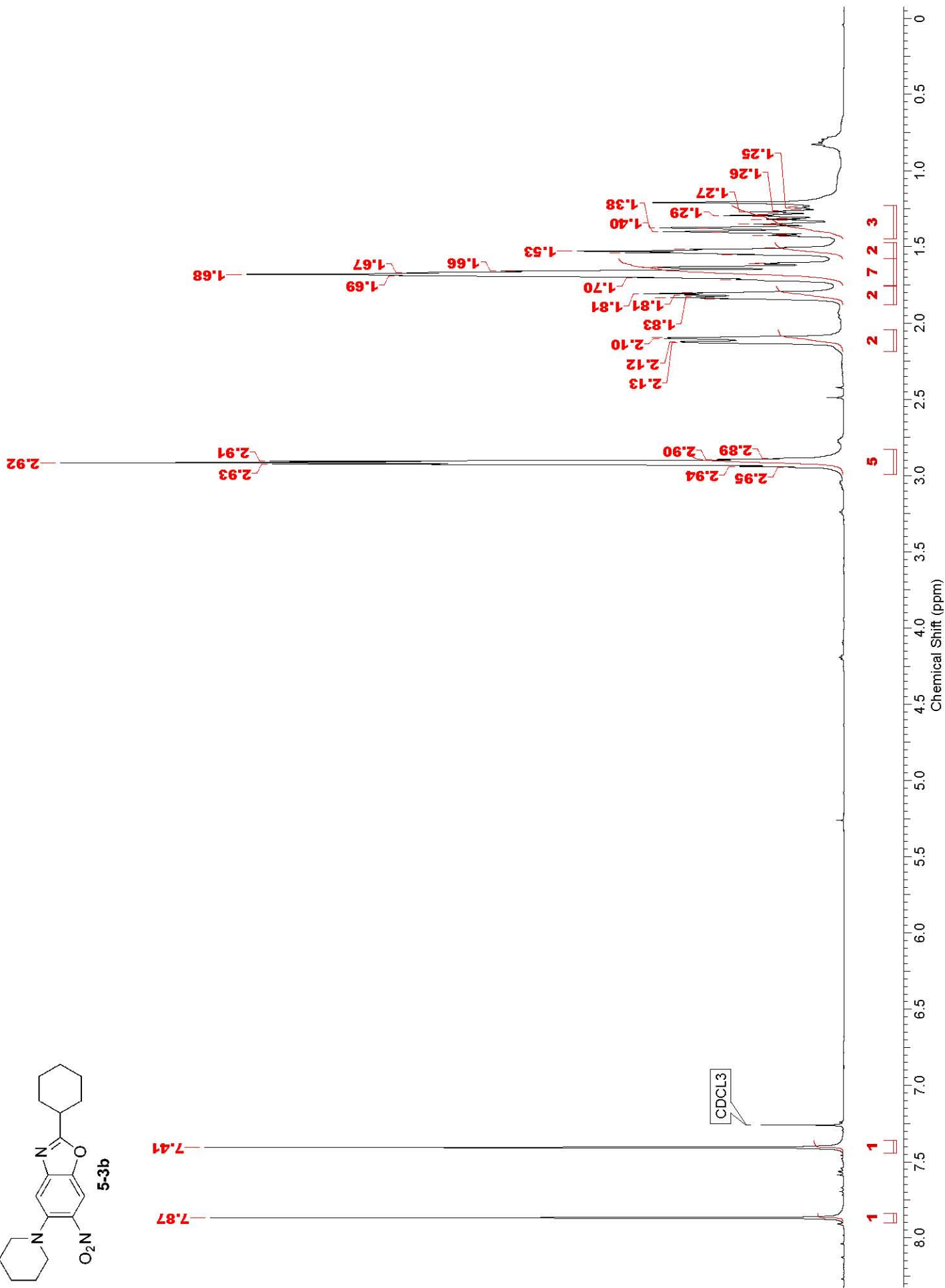
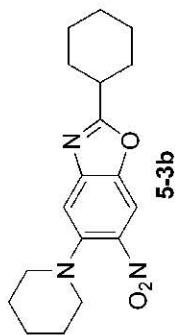


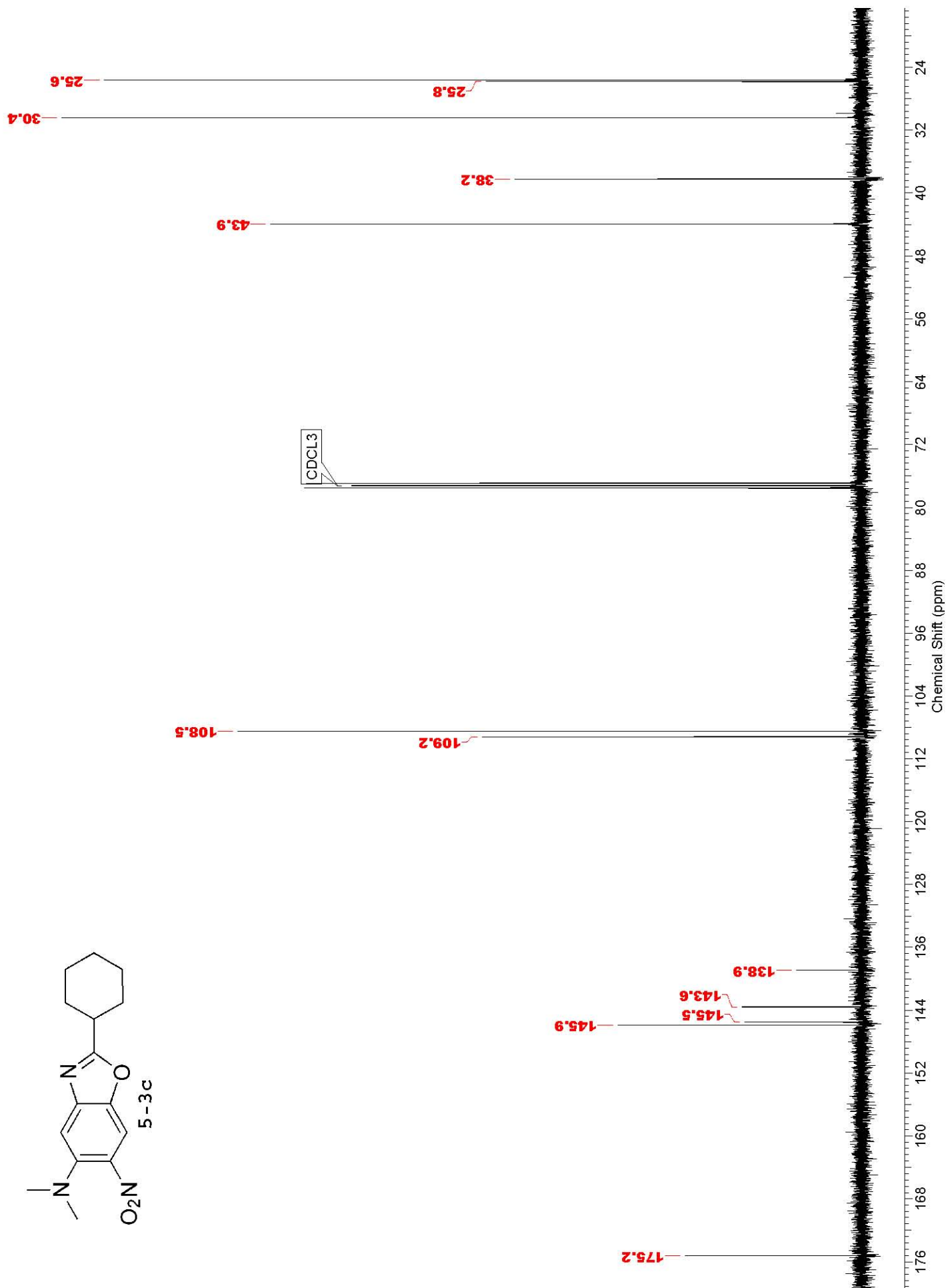
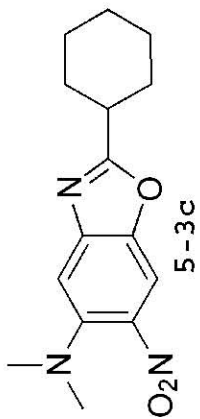


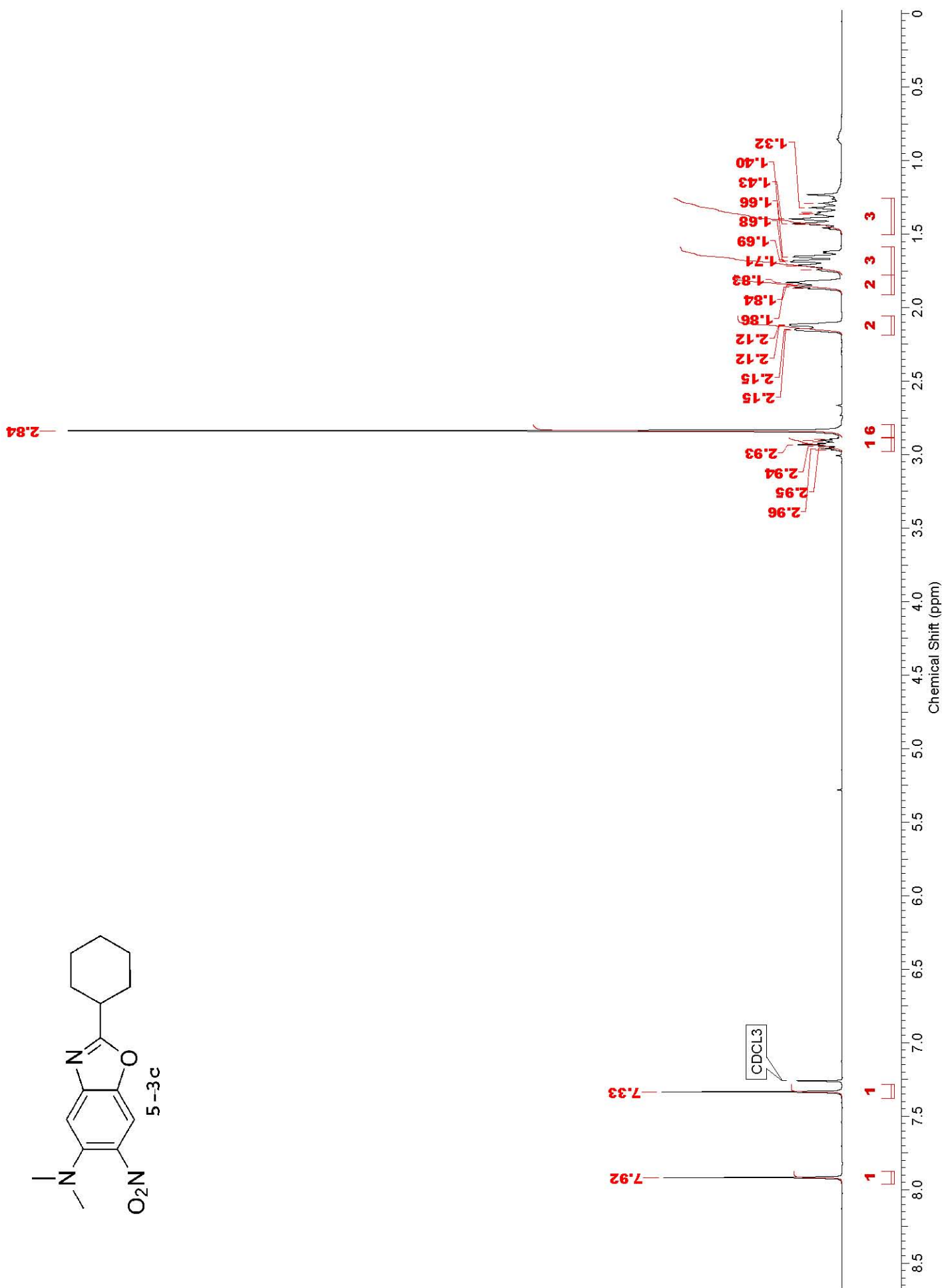
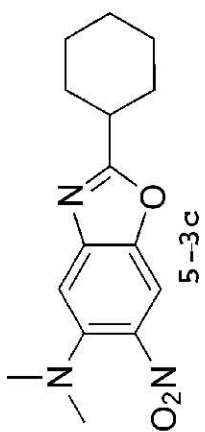


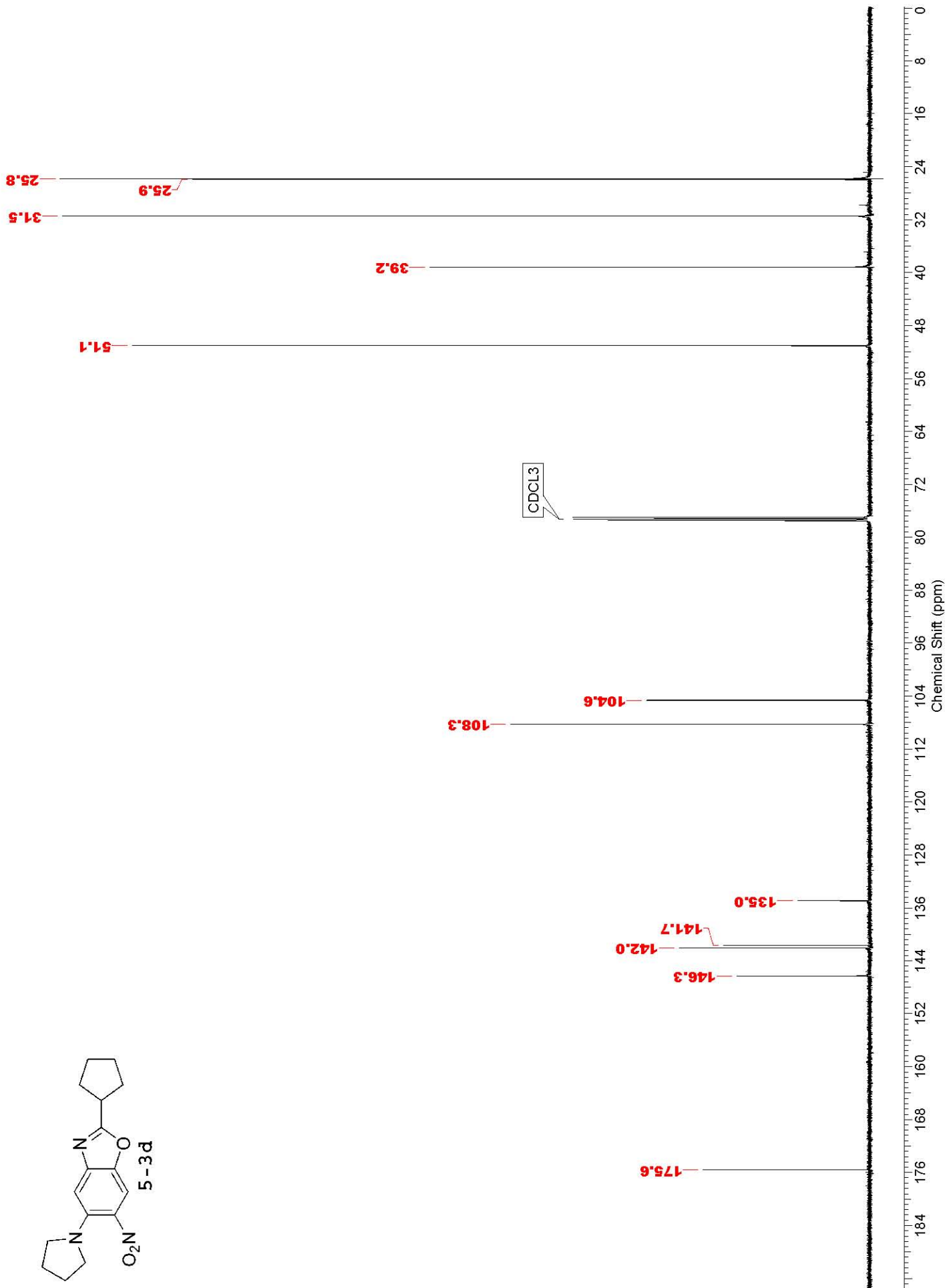
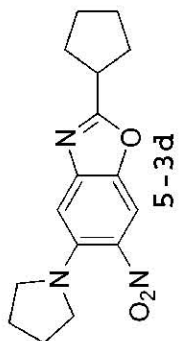


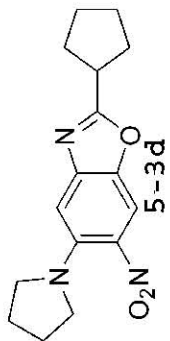




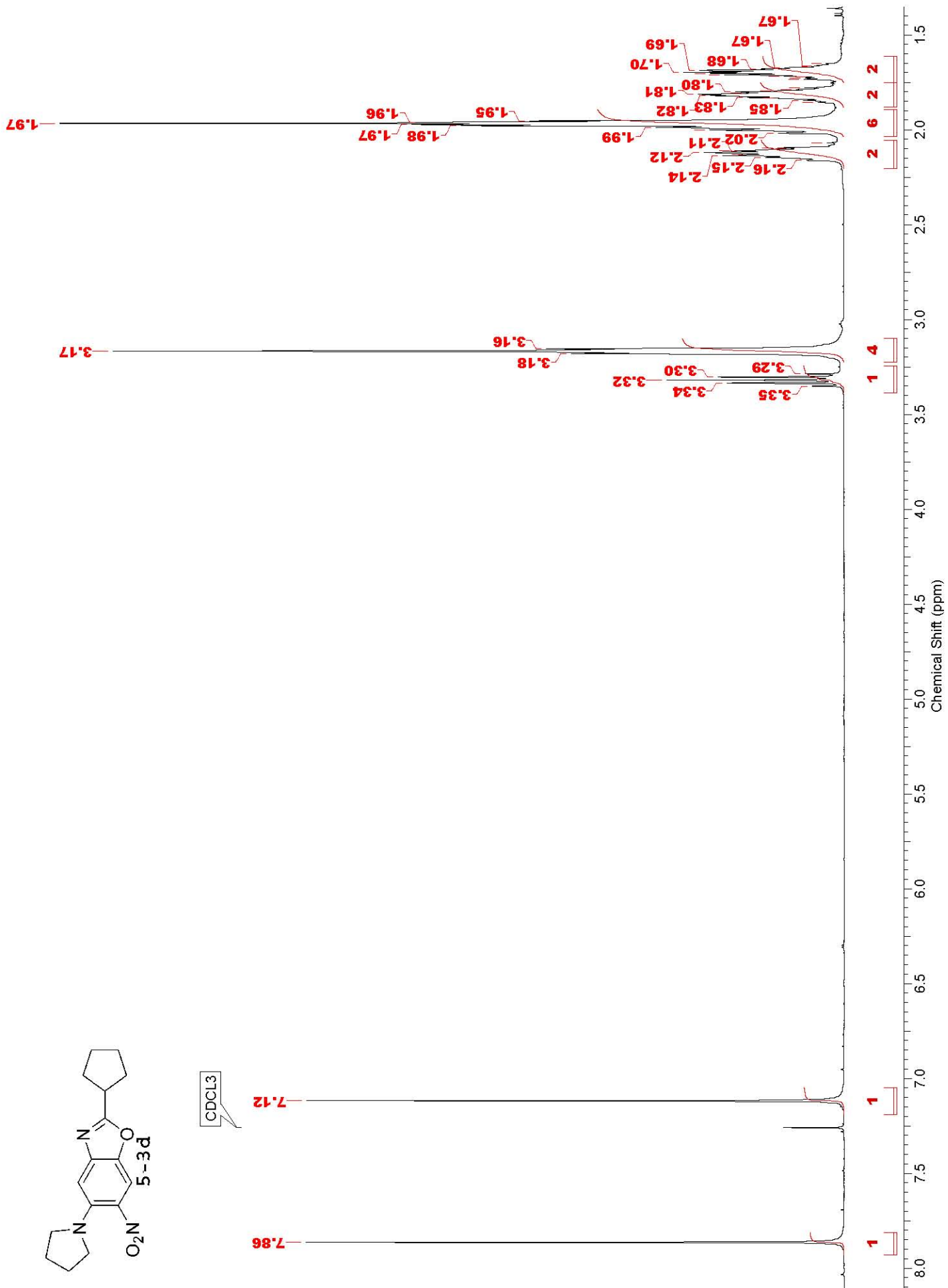


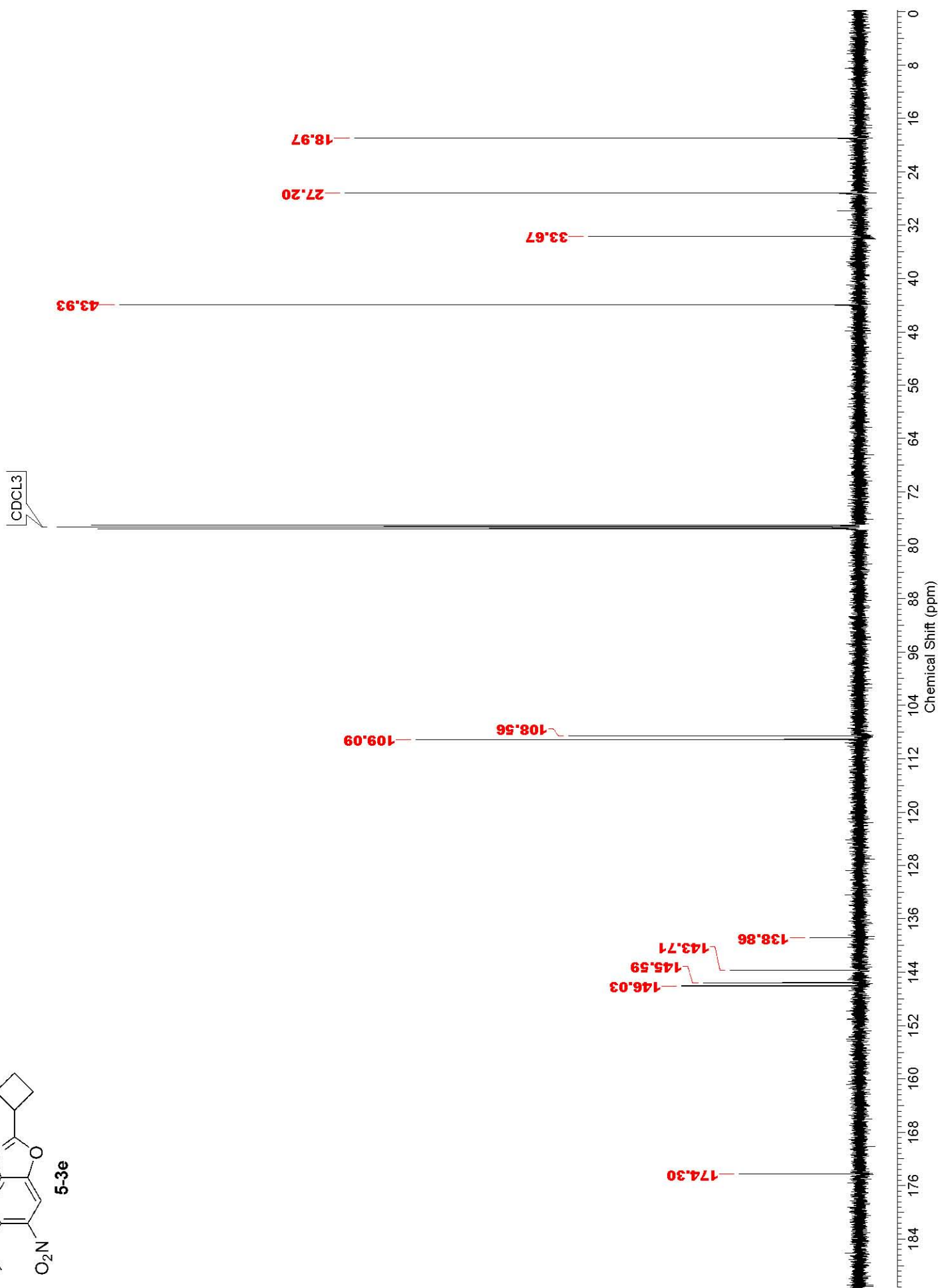
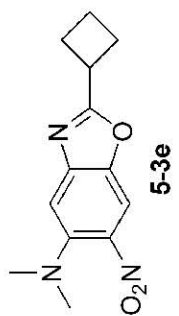


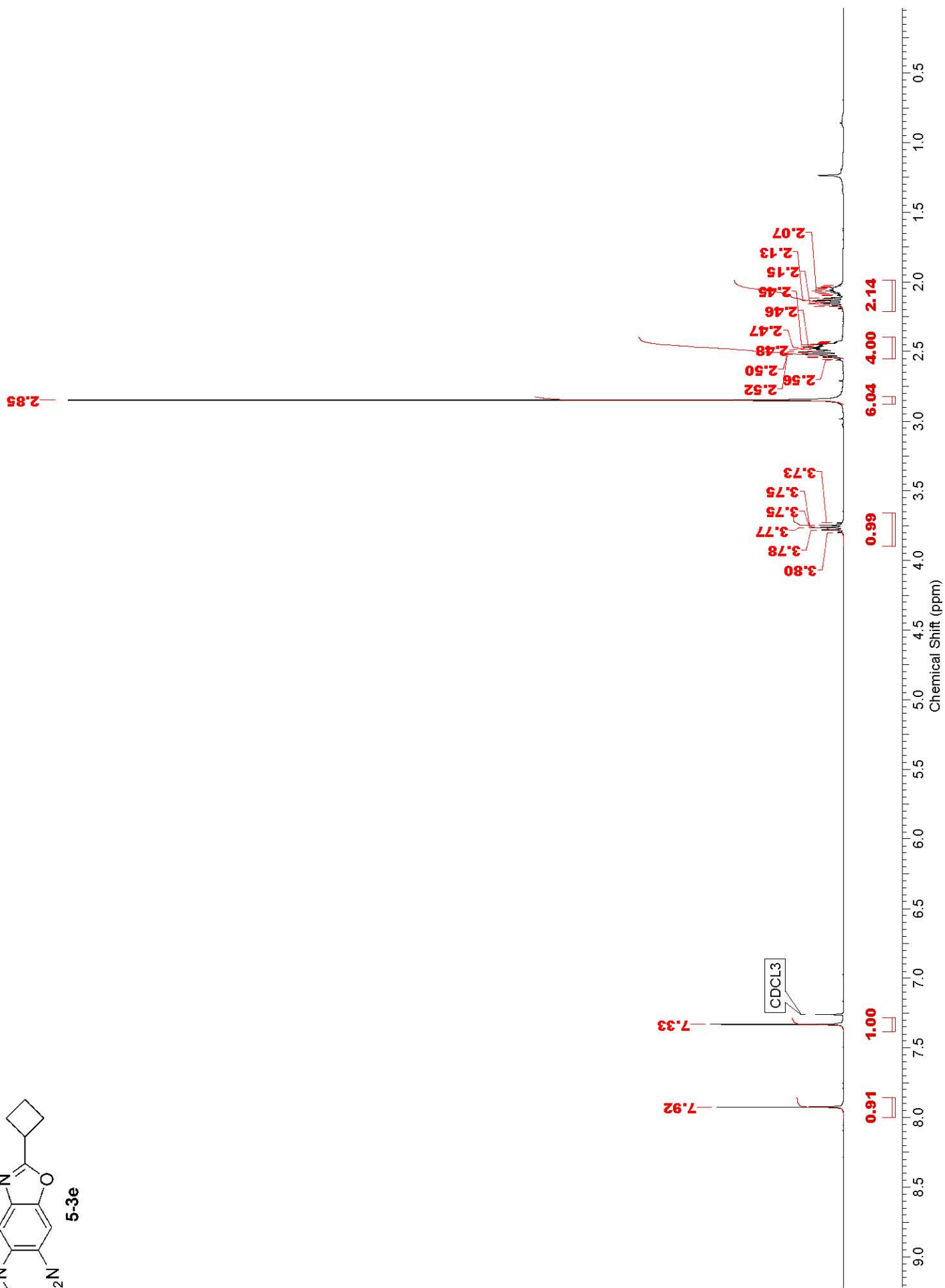
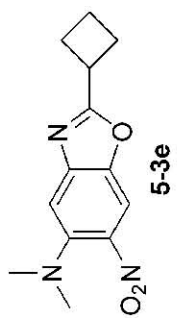


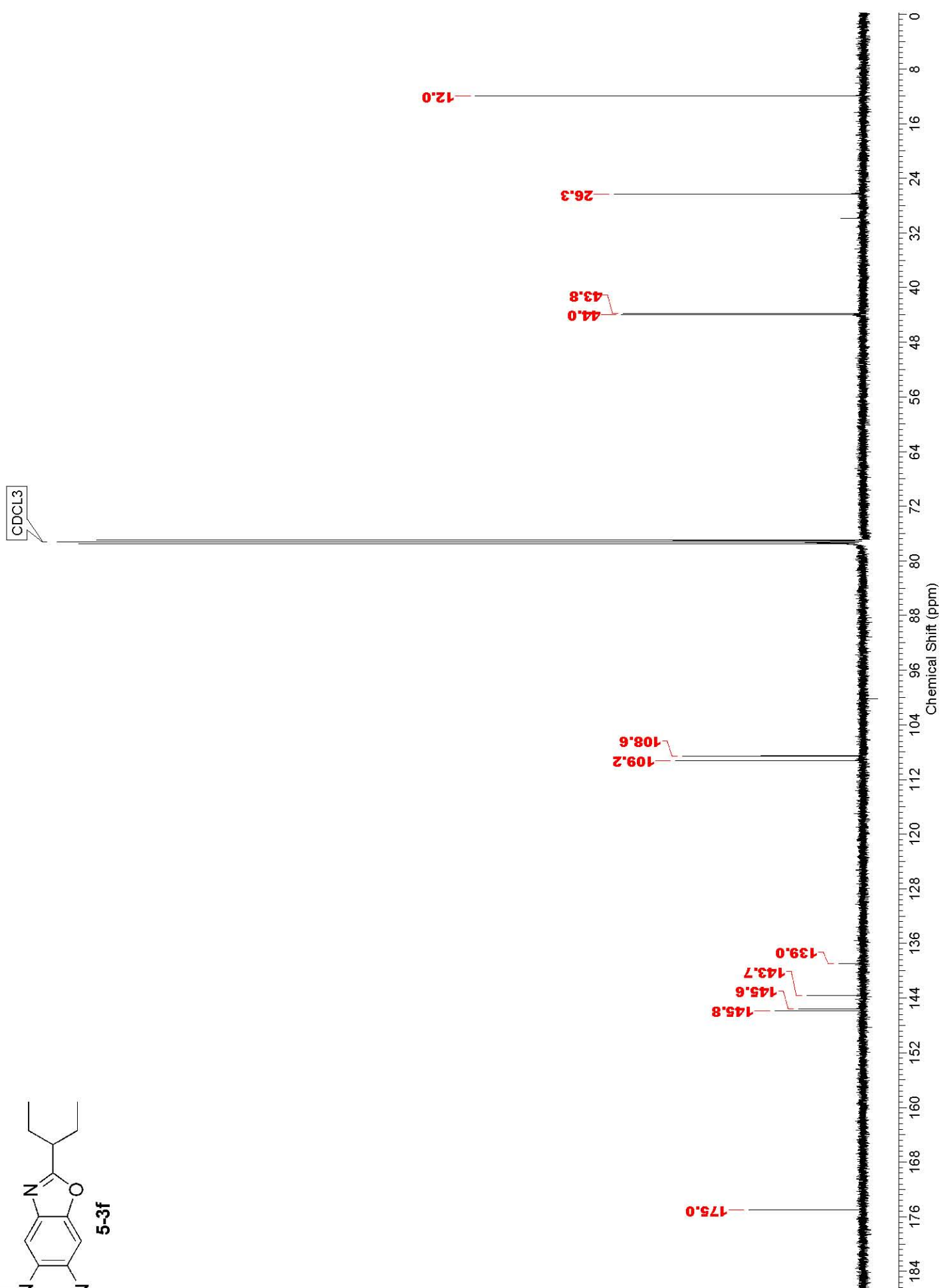
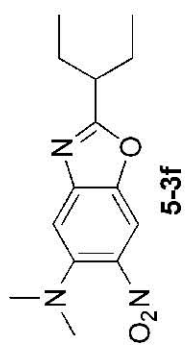


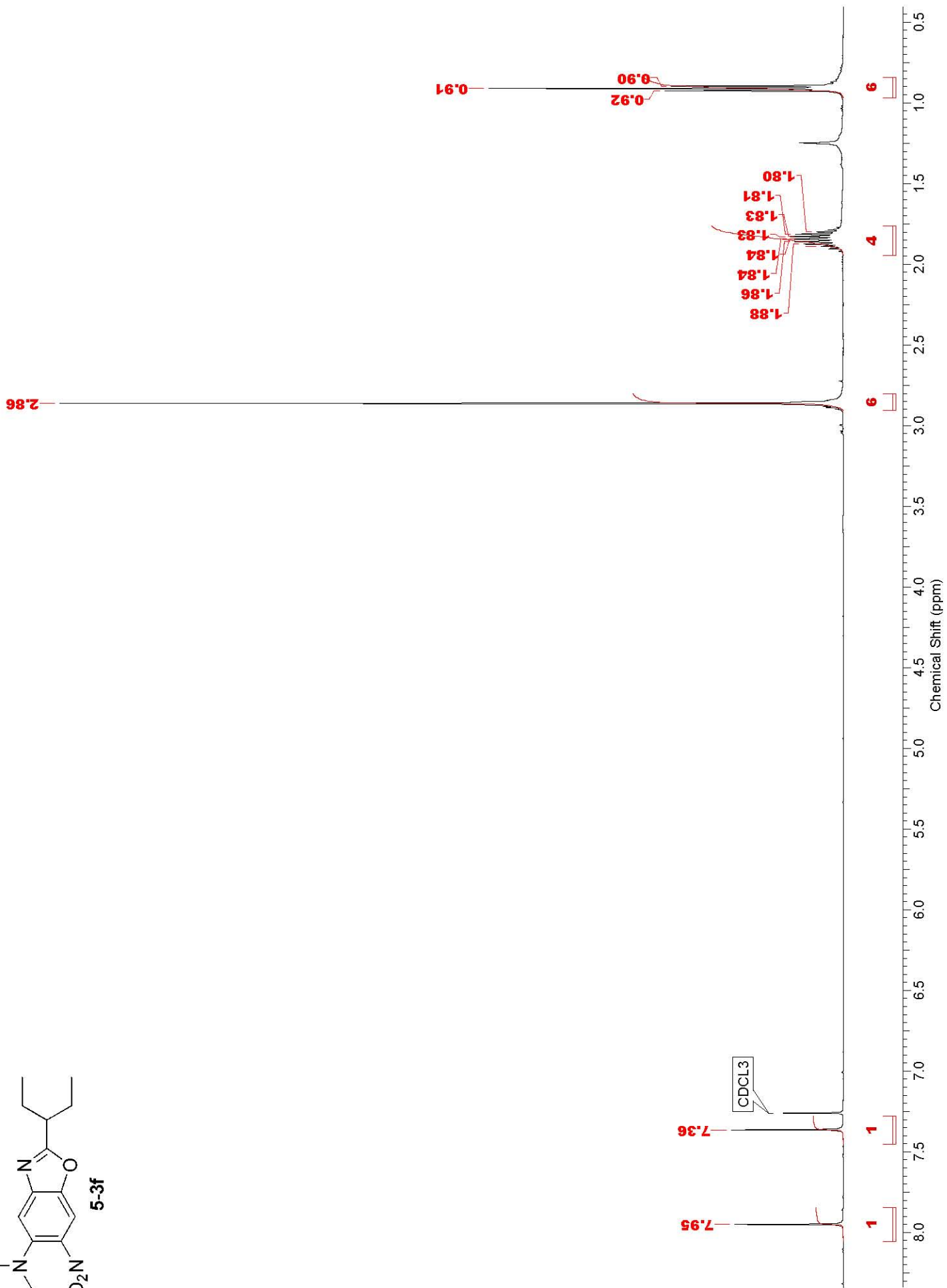
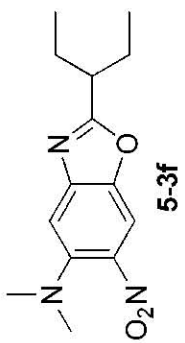
CDCl₃

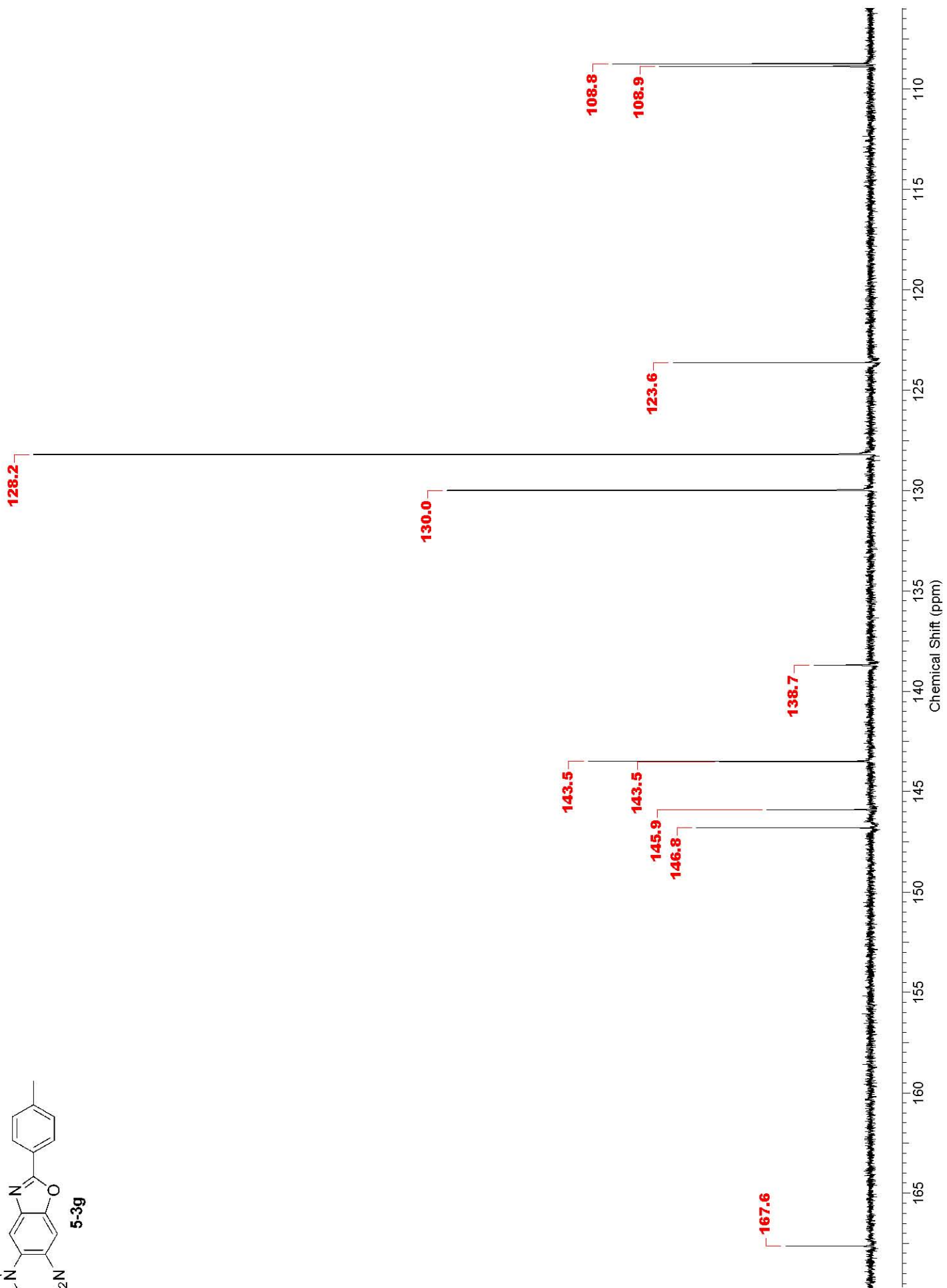
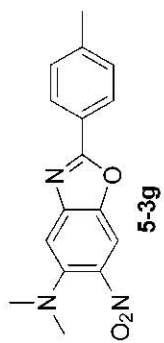


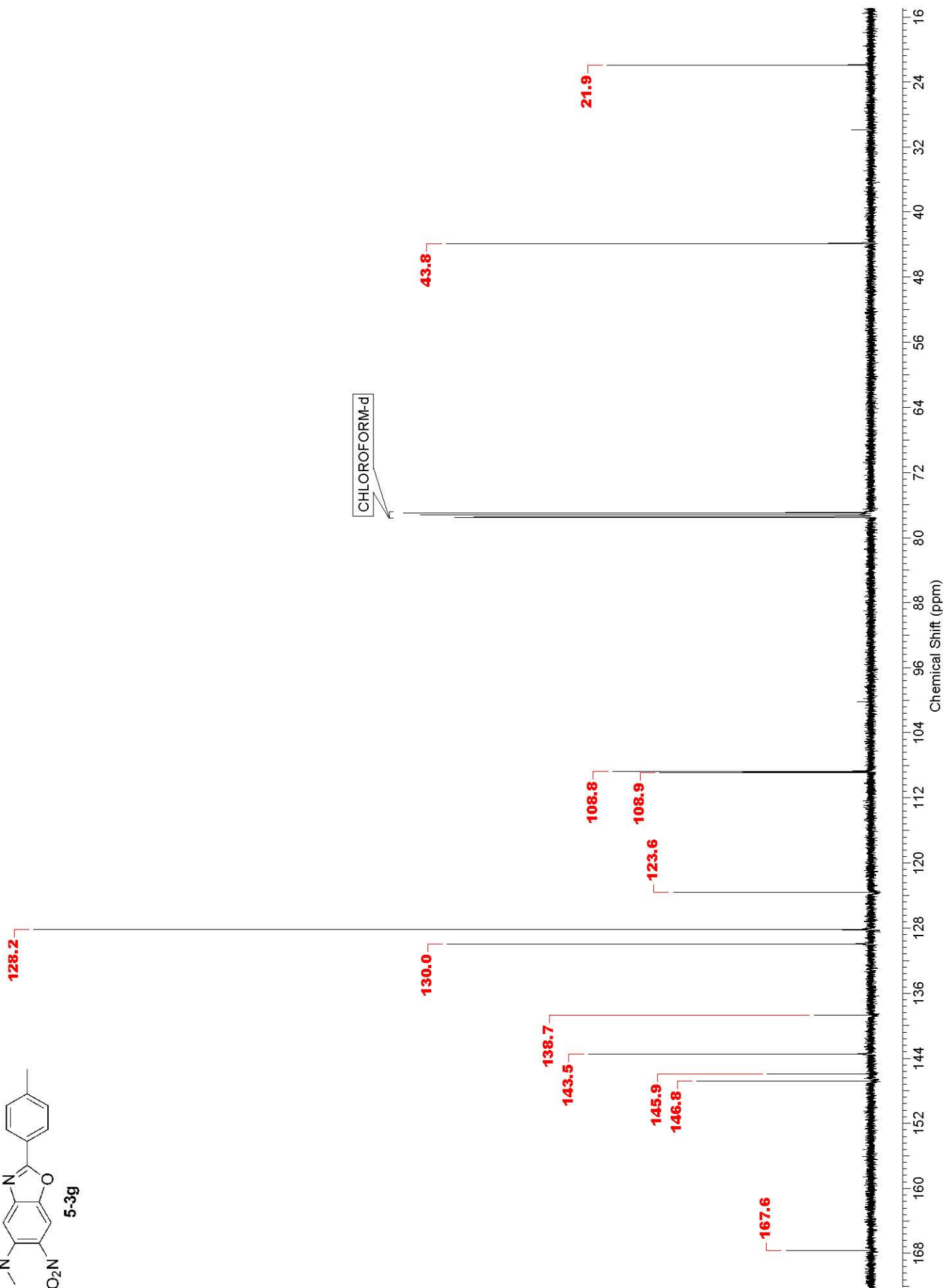
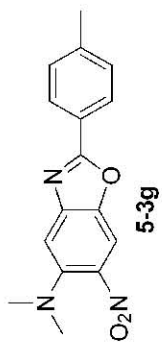


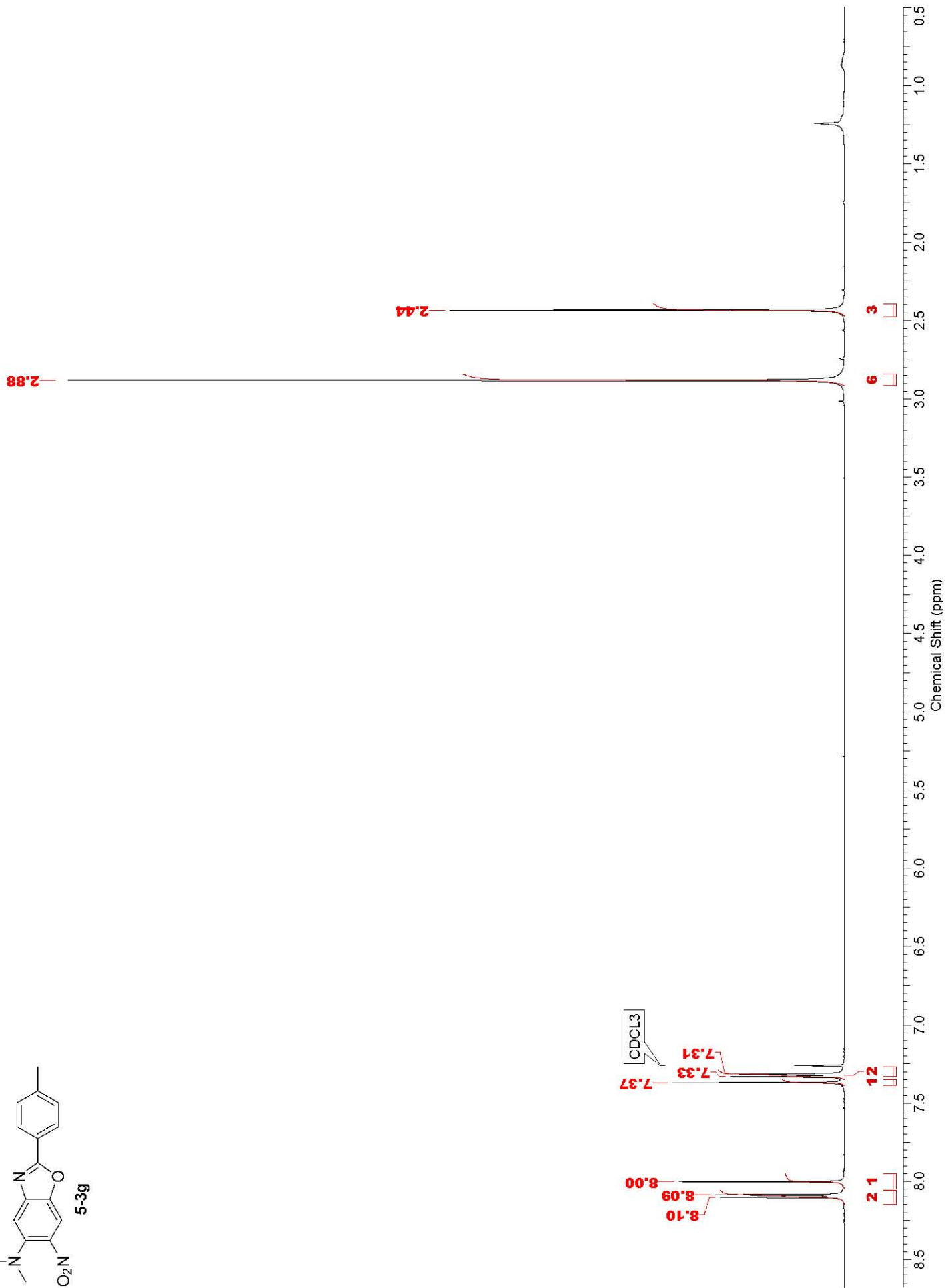
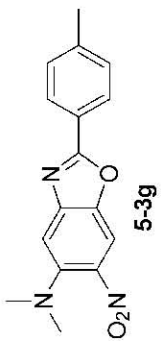


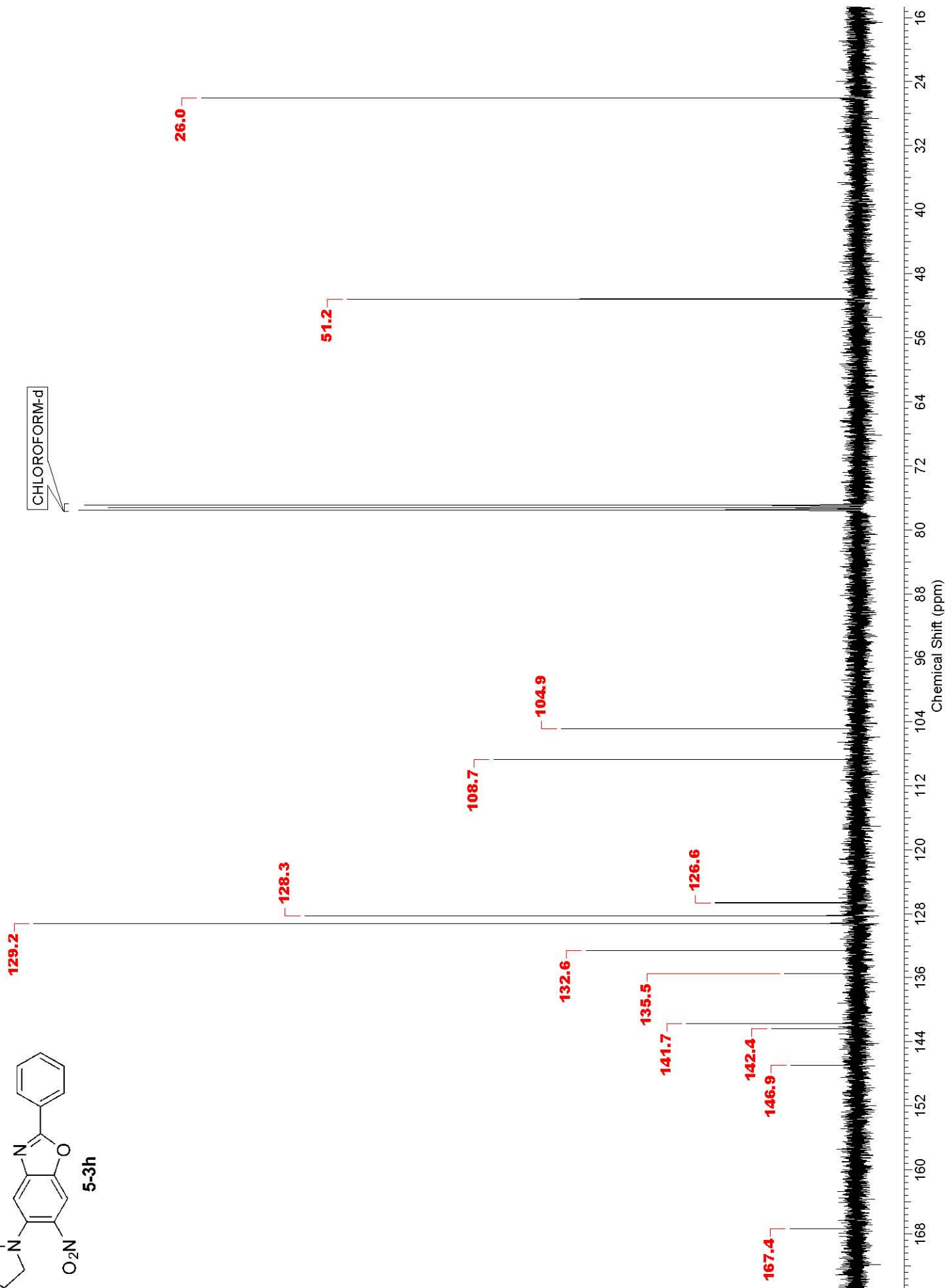
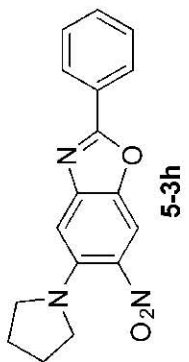


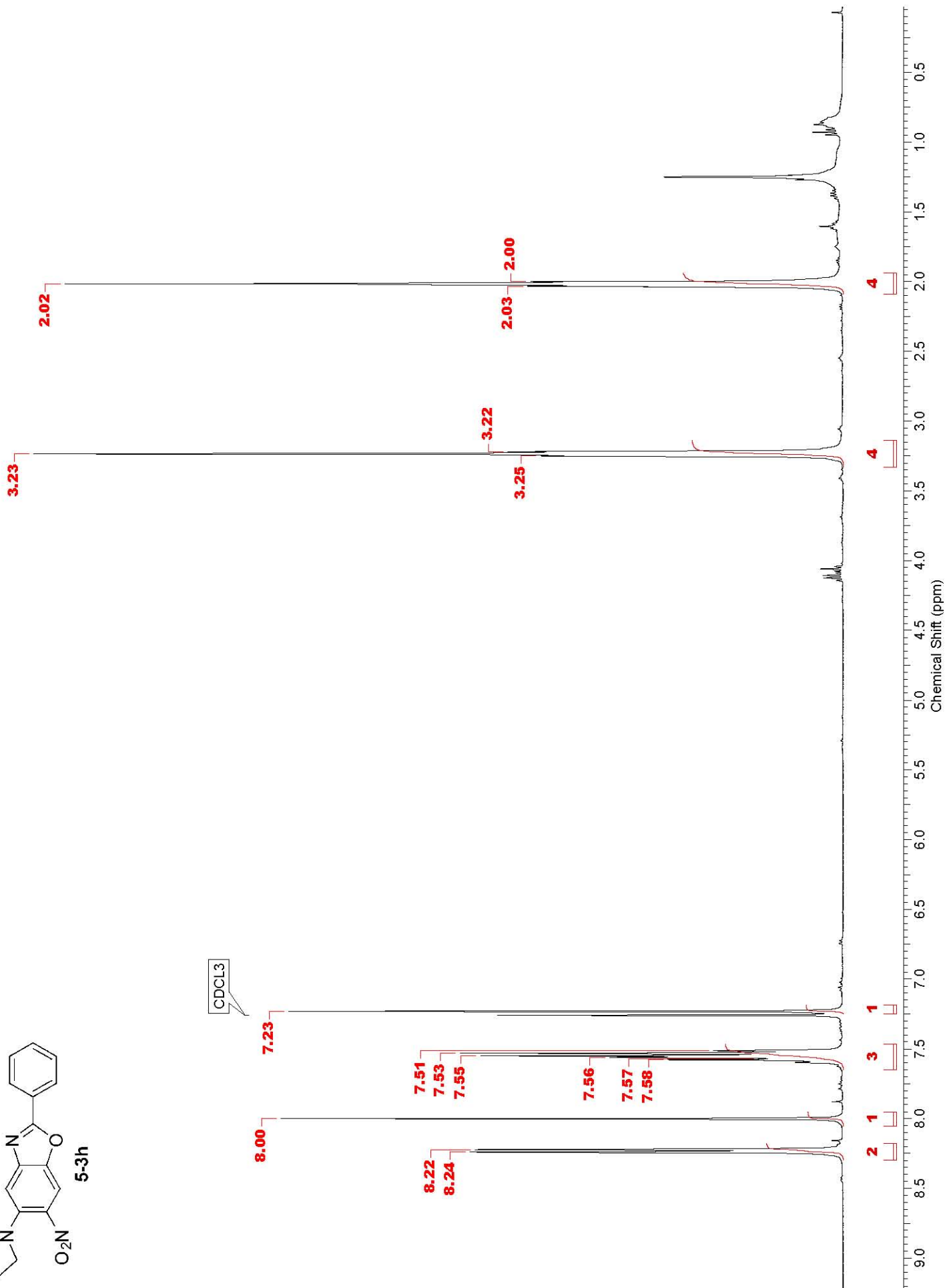
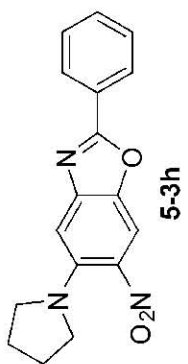


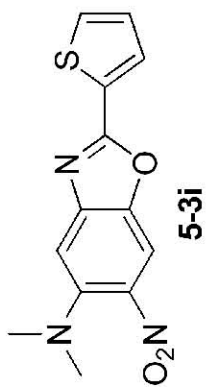












CDCl₃

43.8

108.8

128.8

131.6

132.1

138.6

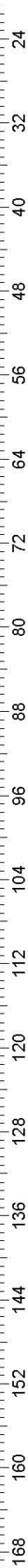
143.3

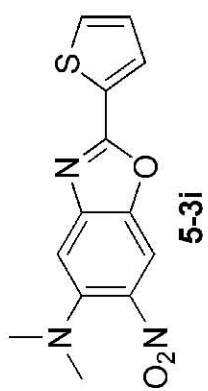
146.1

146.7

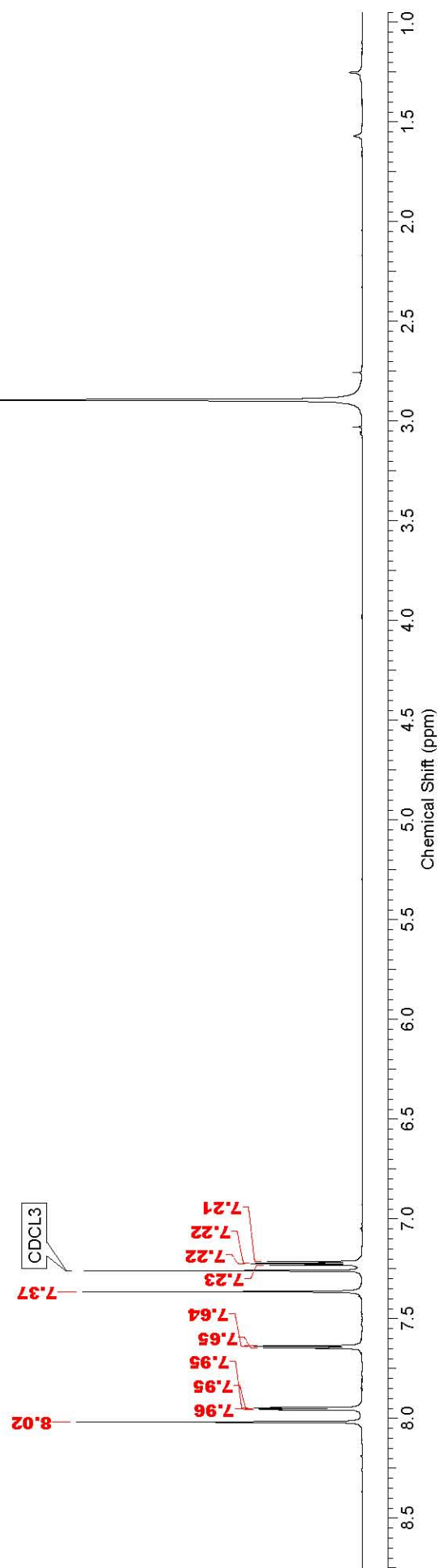
163.3

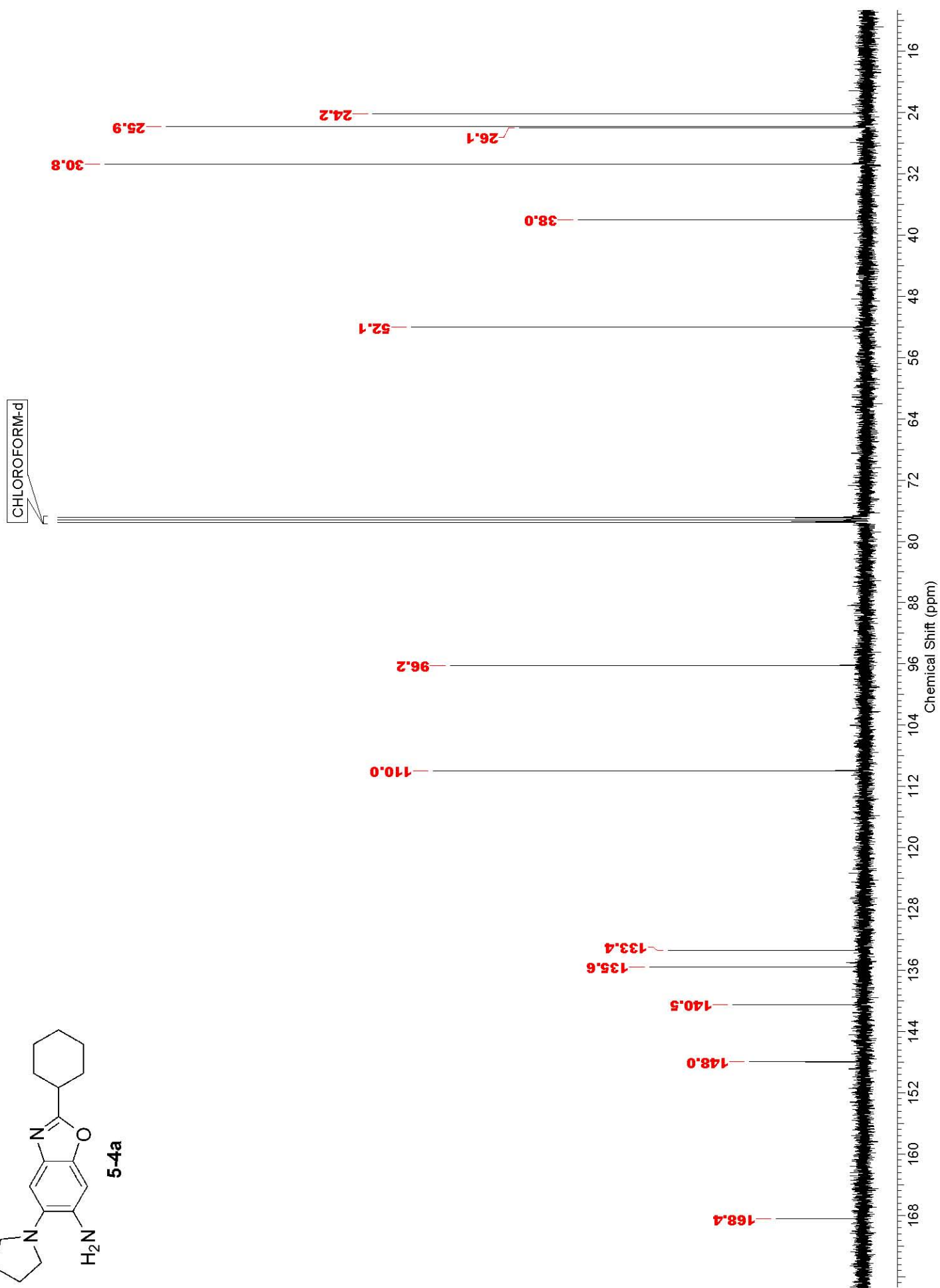
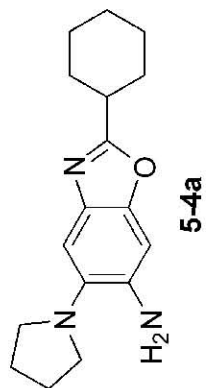
Chemical Shift (ppm)

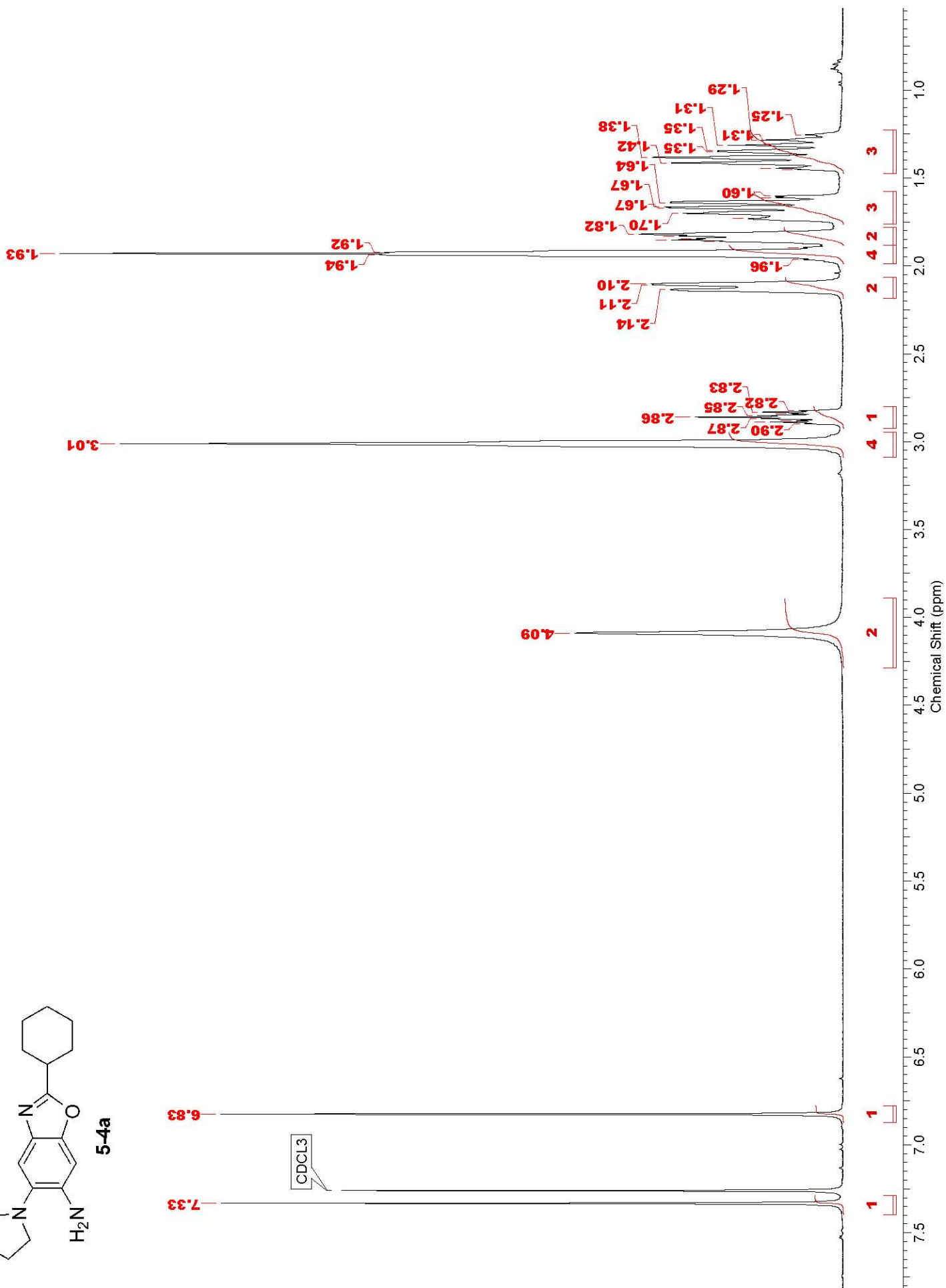
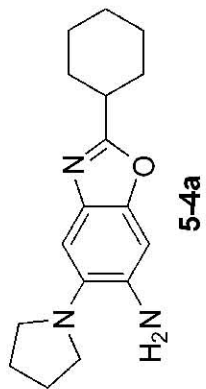


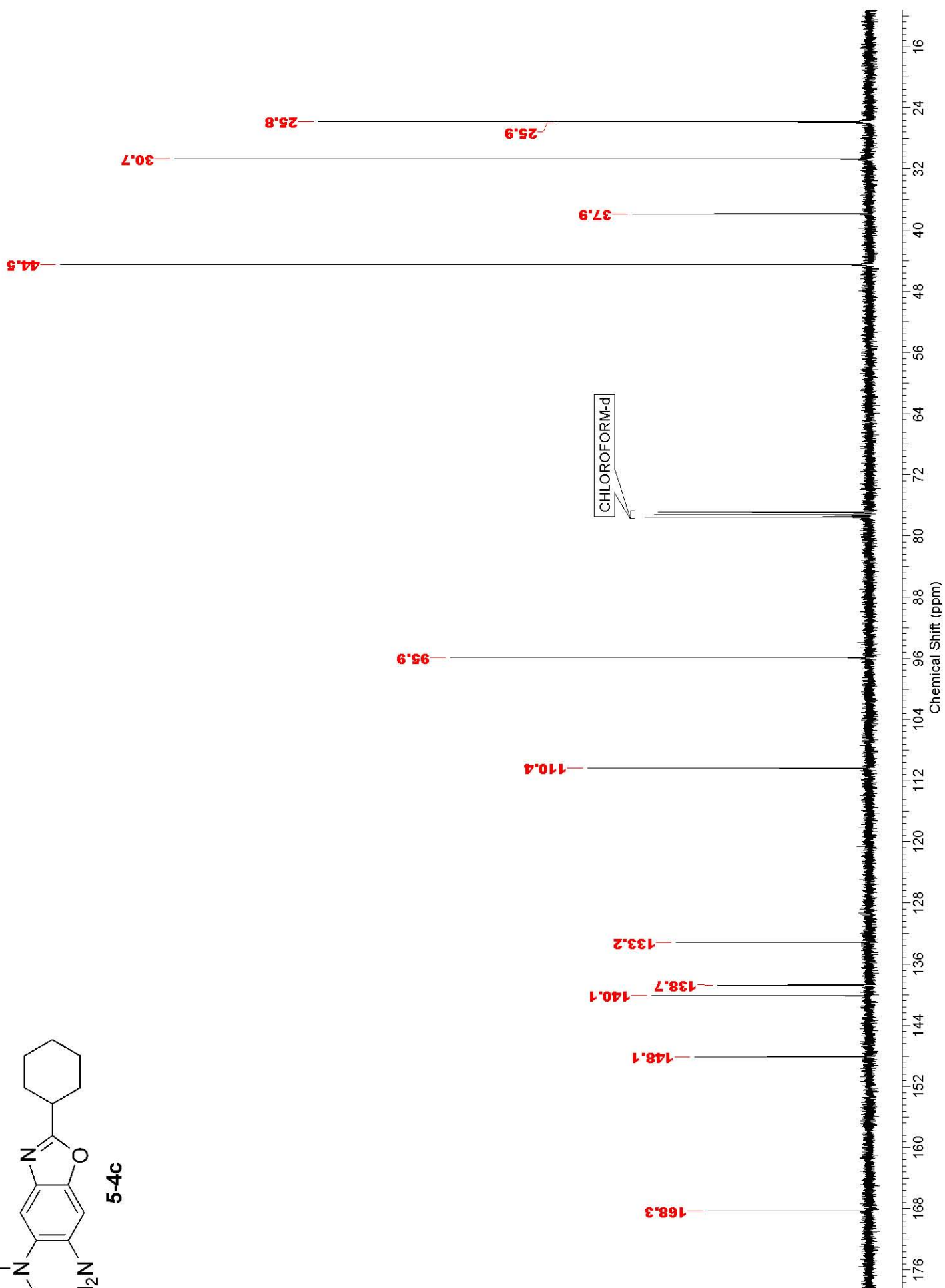
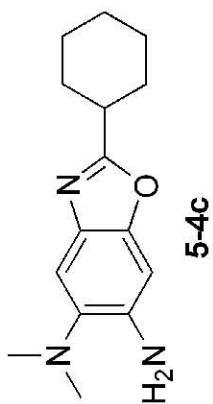


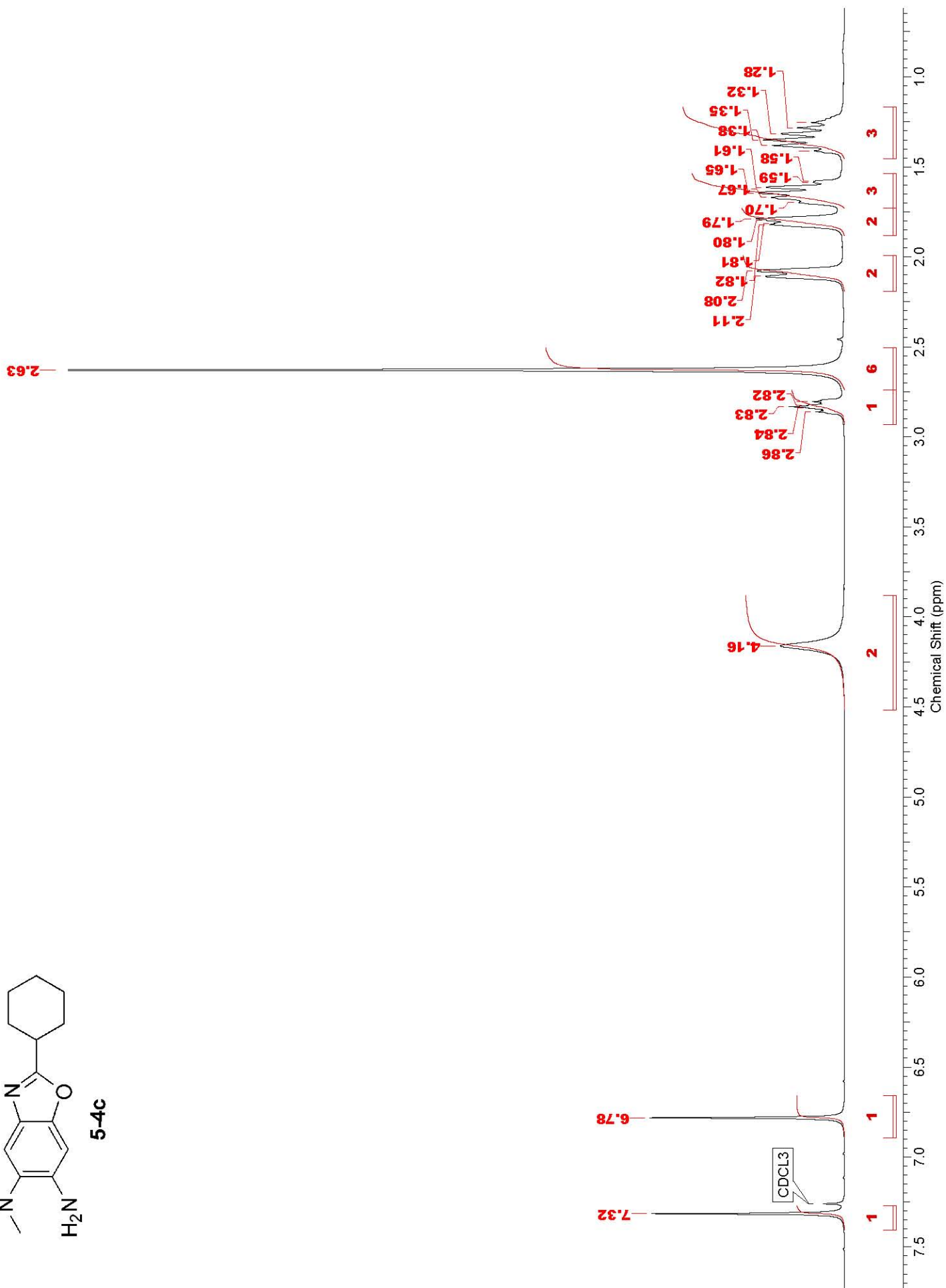
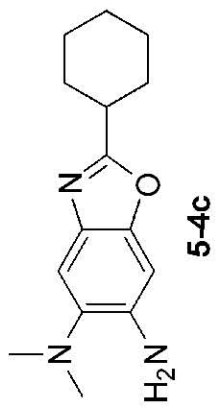
2.89

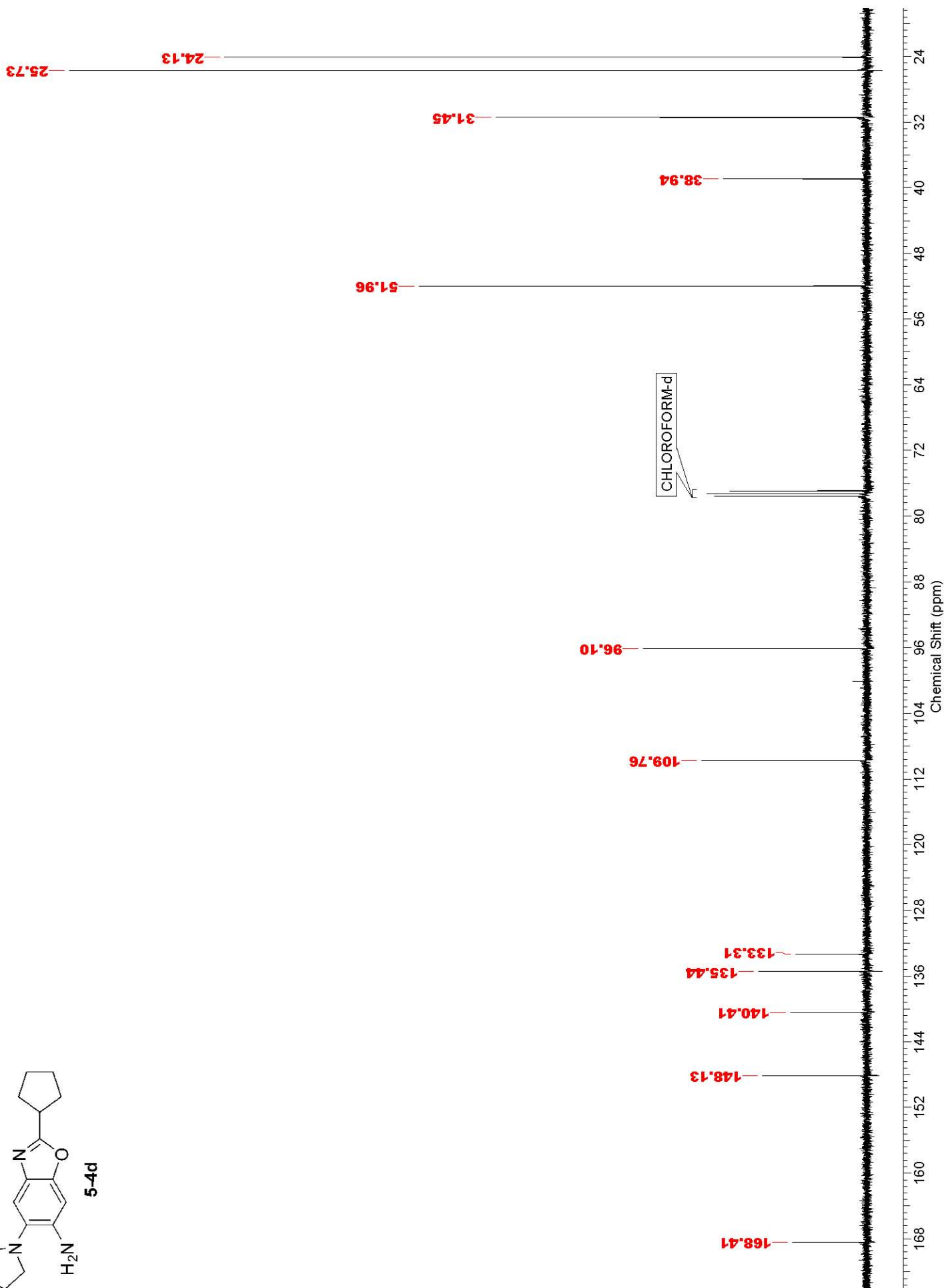
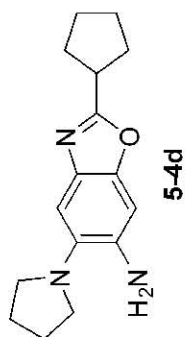


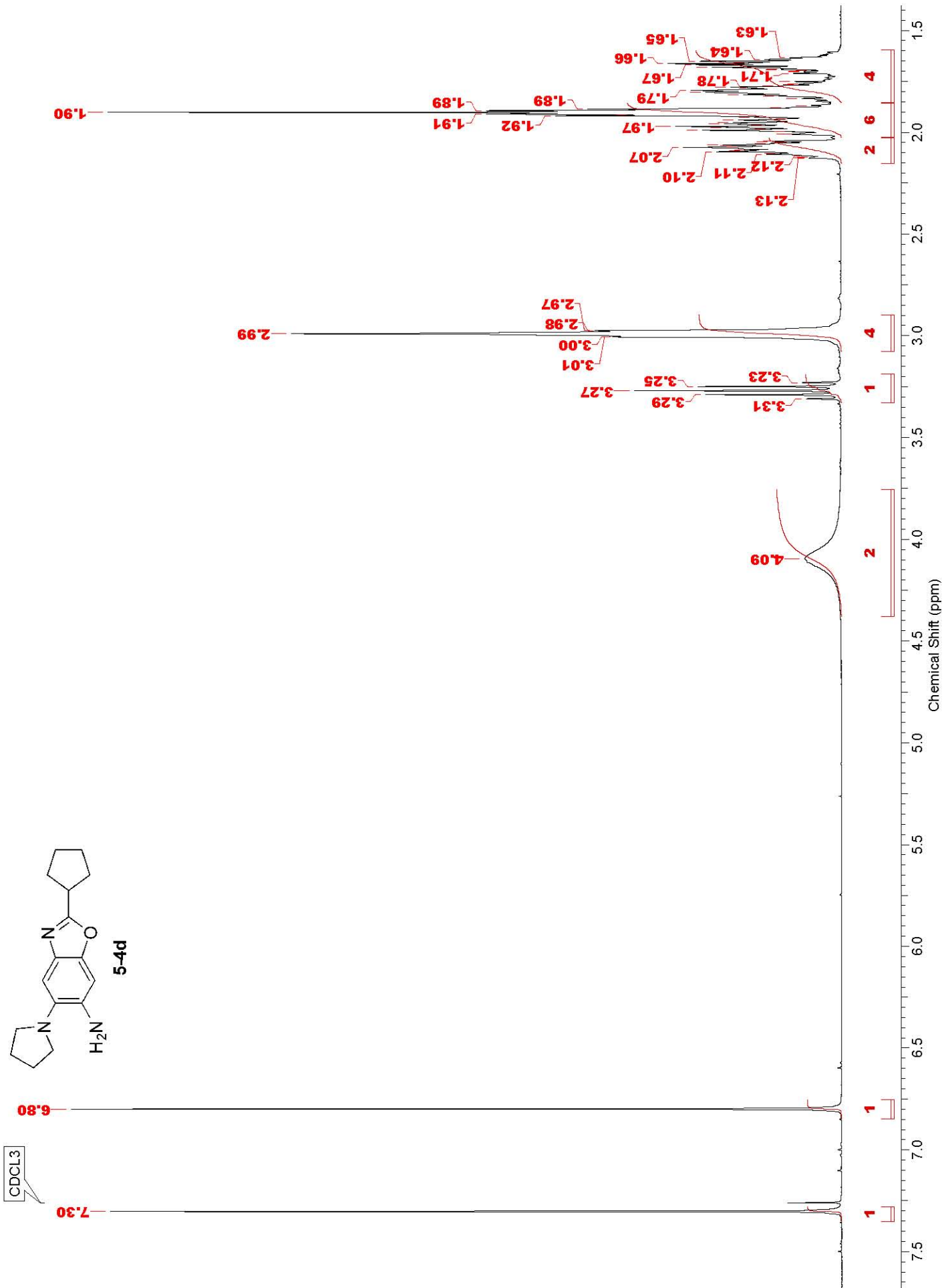
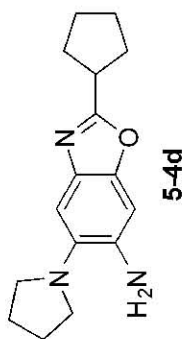


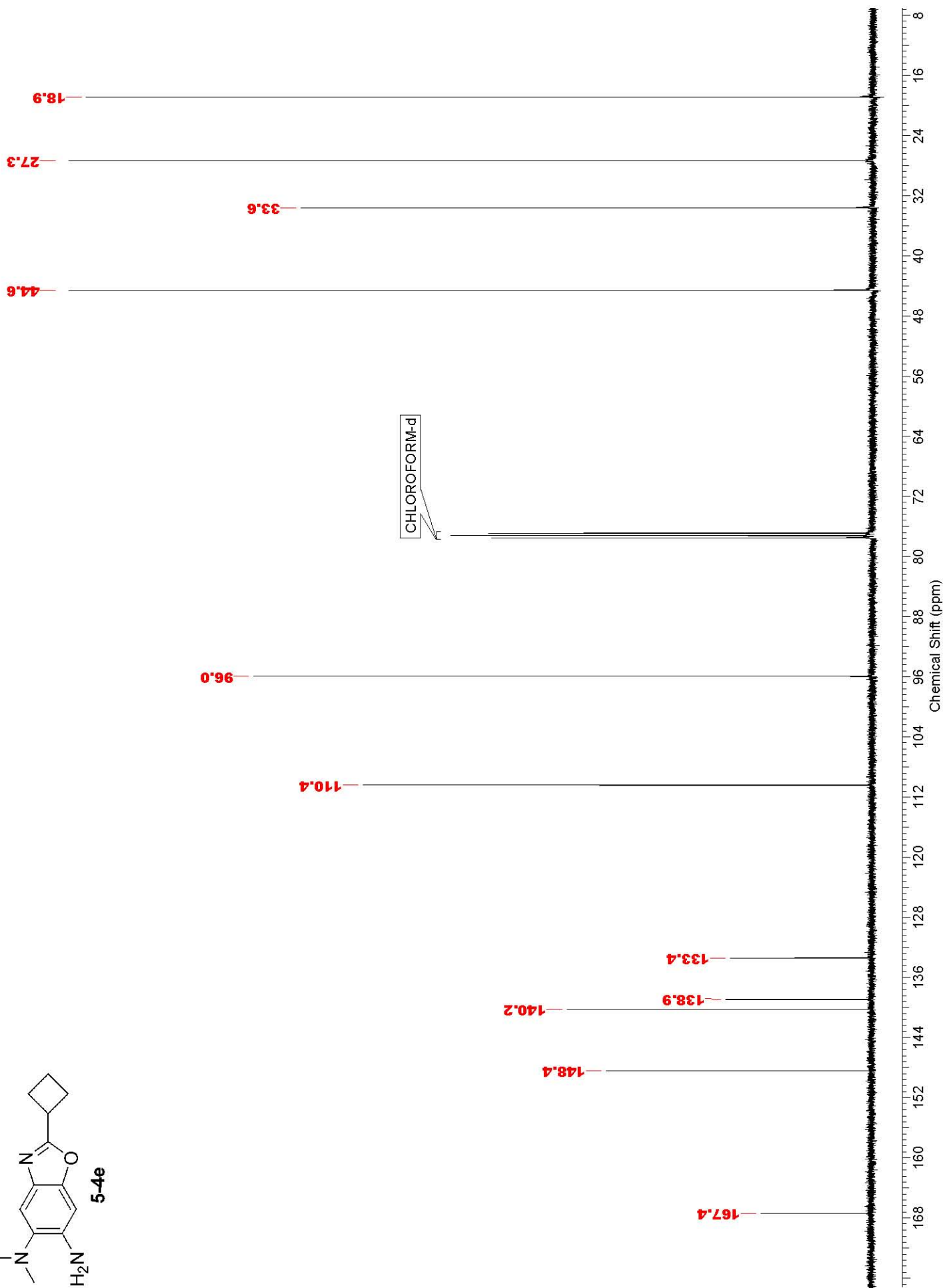
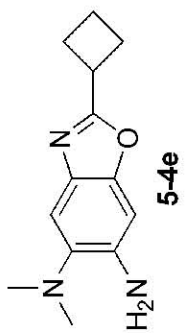


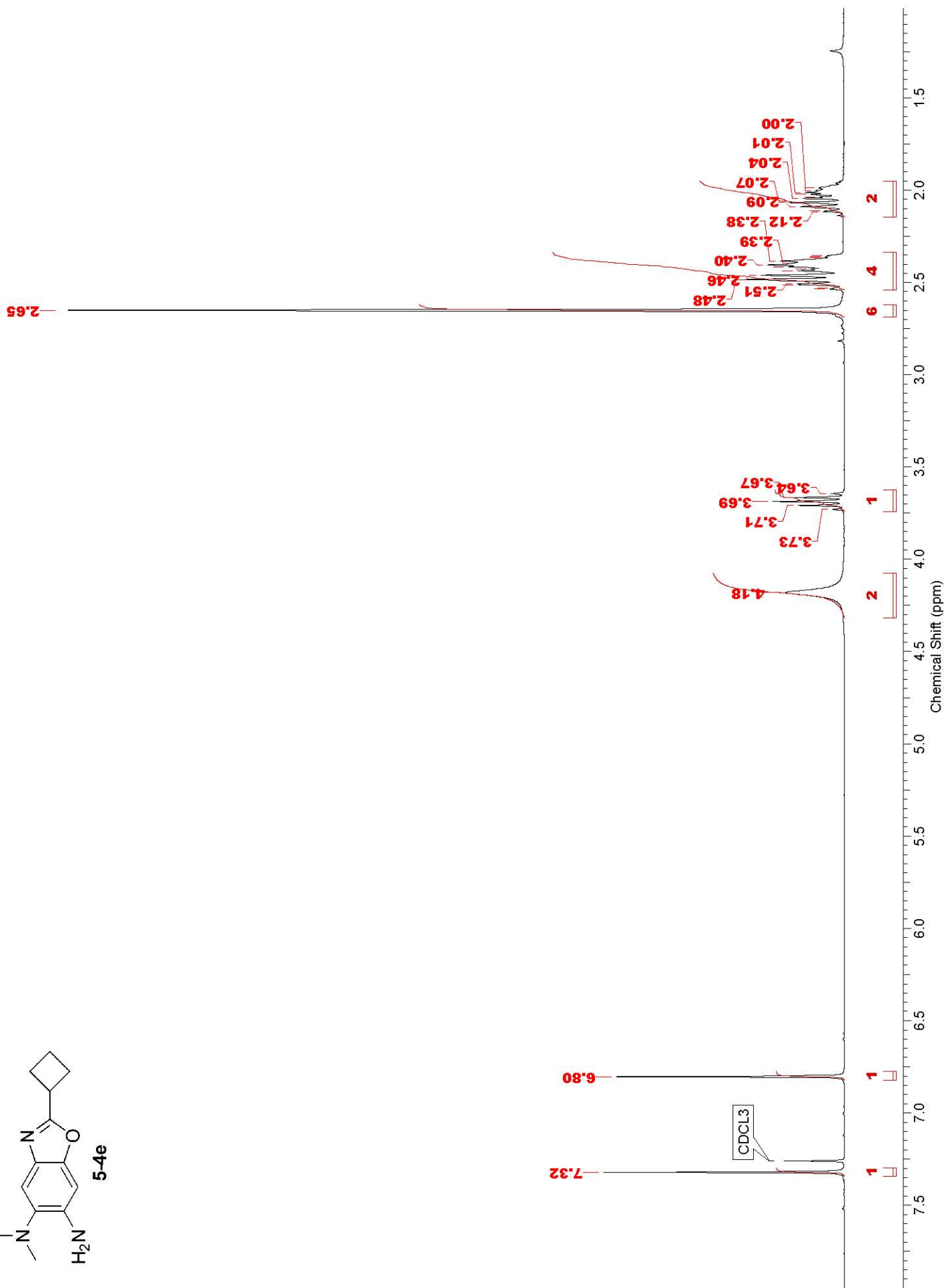
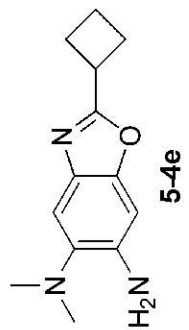


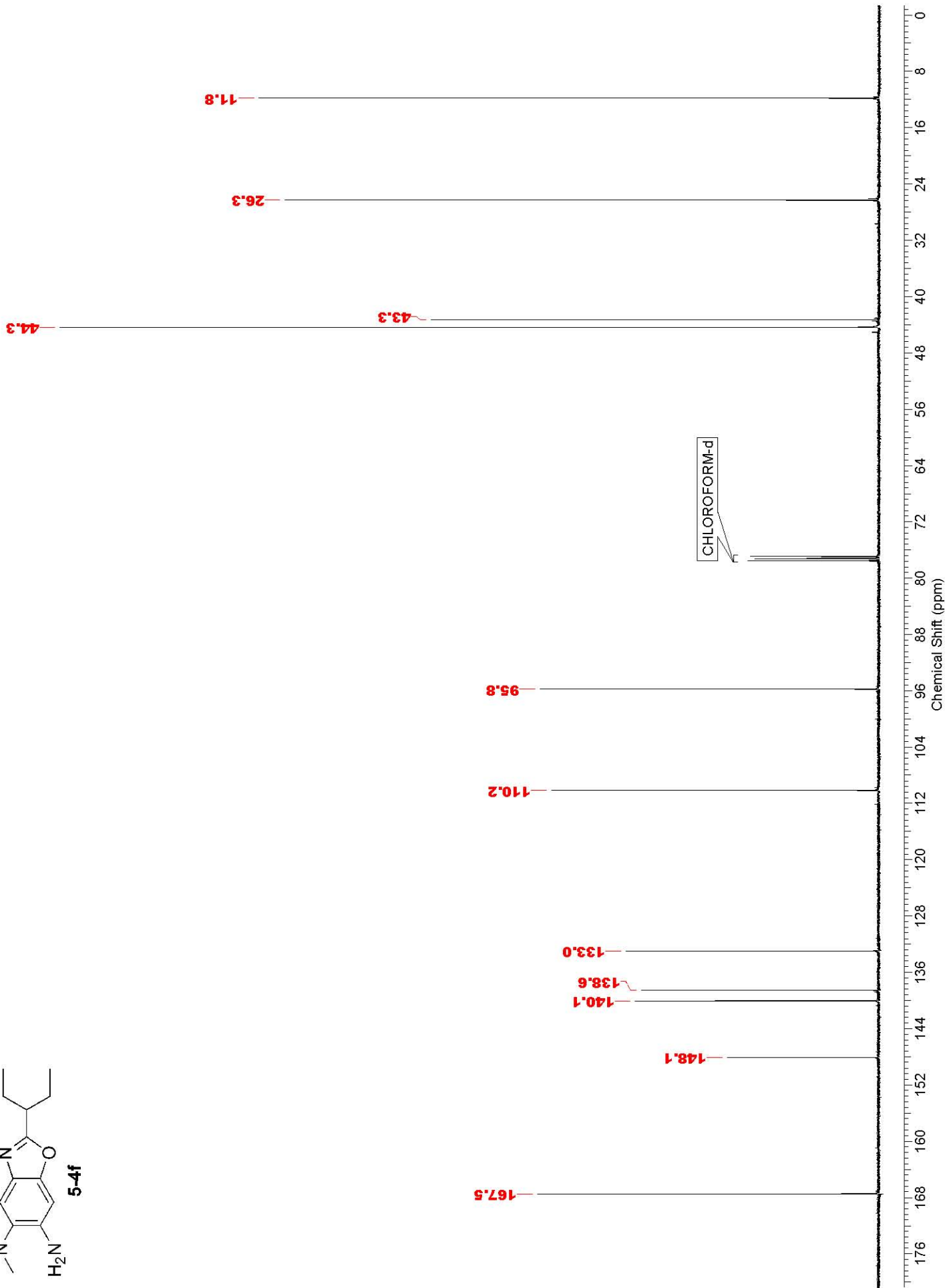
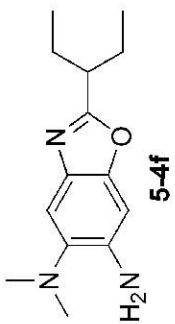


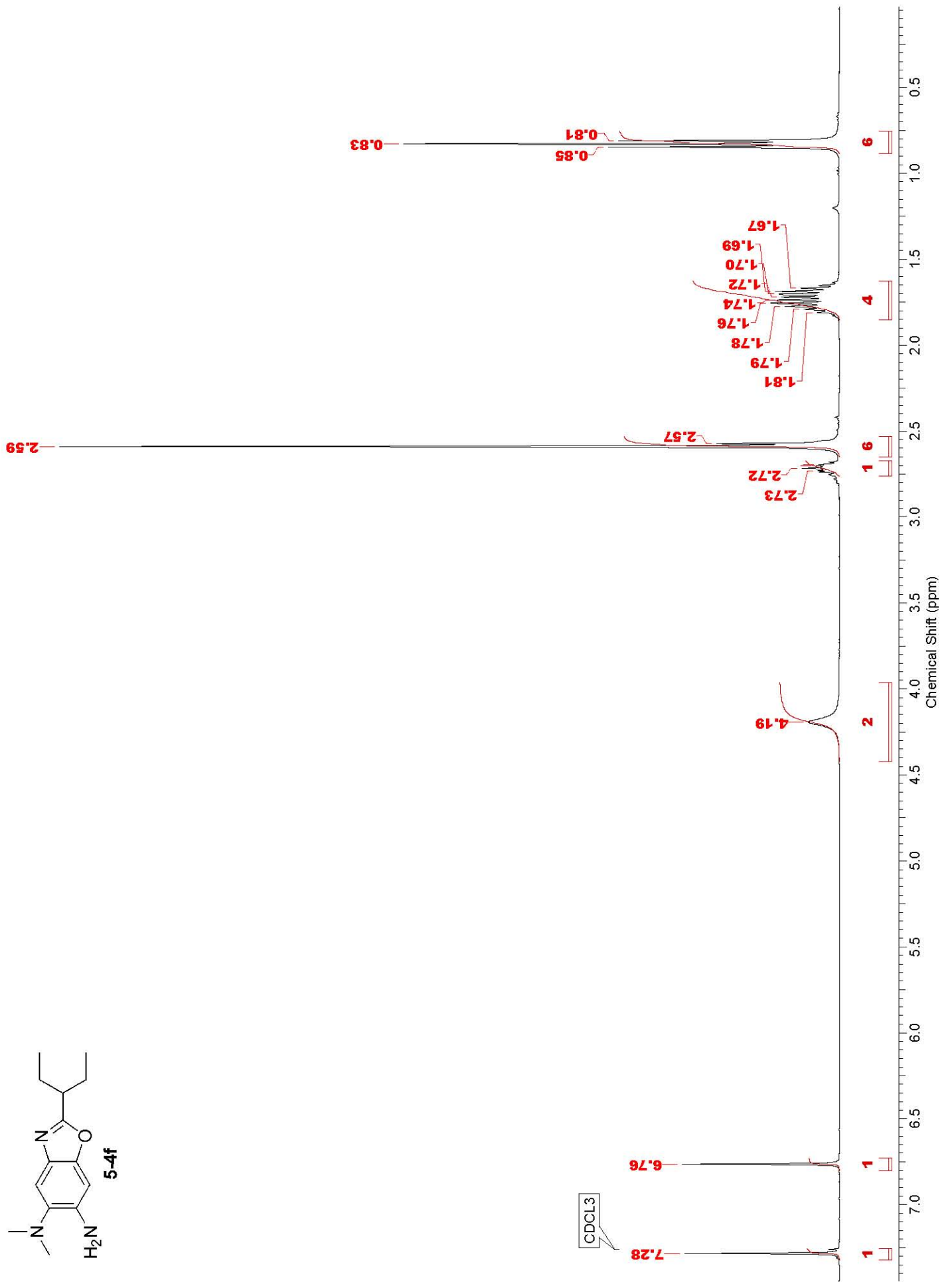
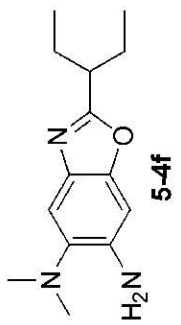


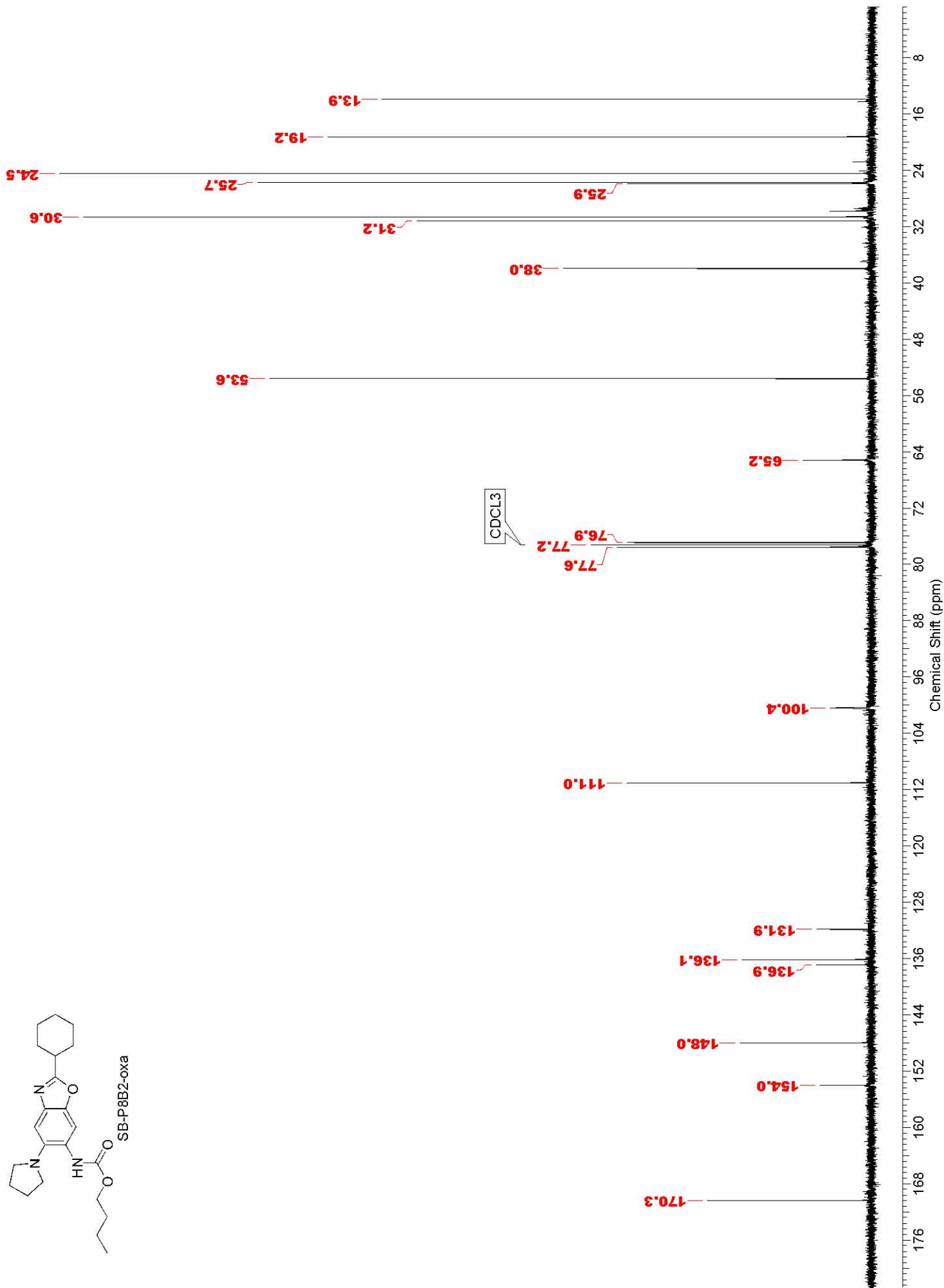
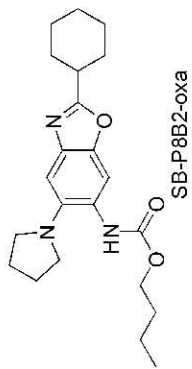


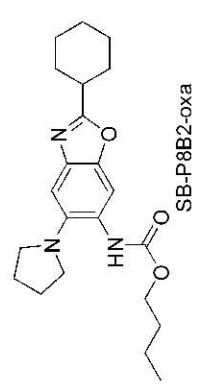
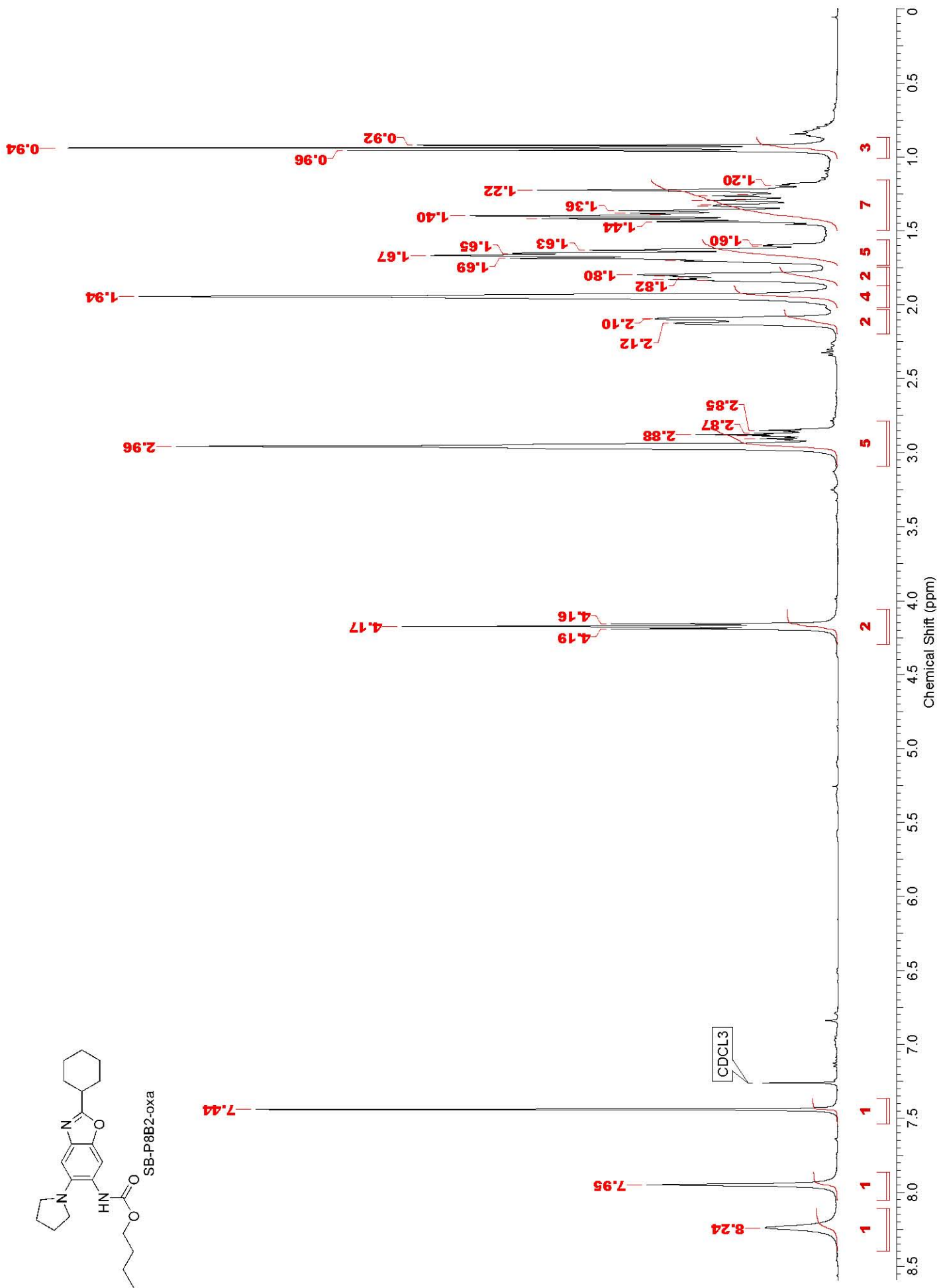


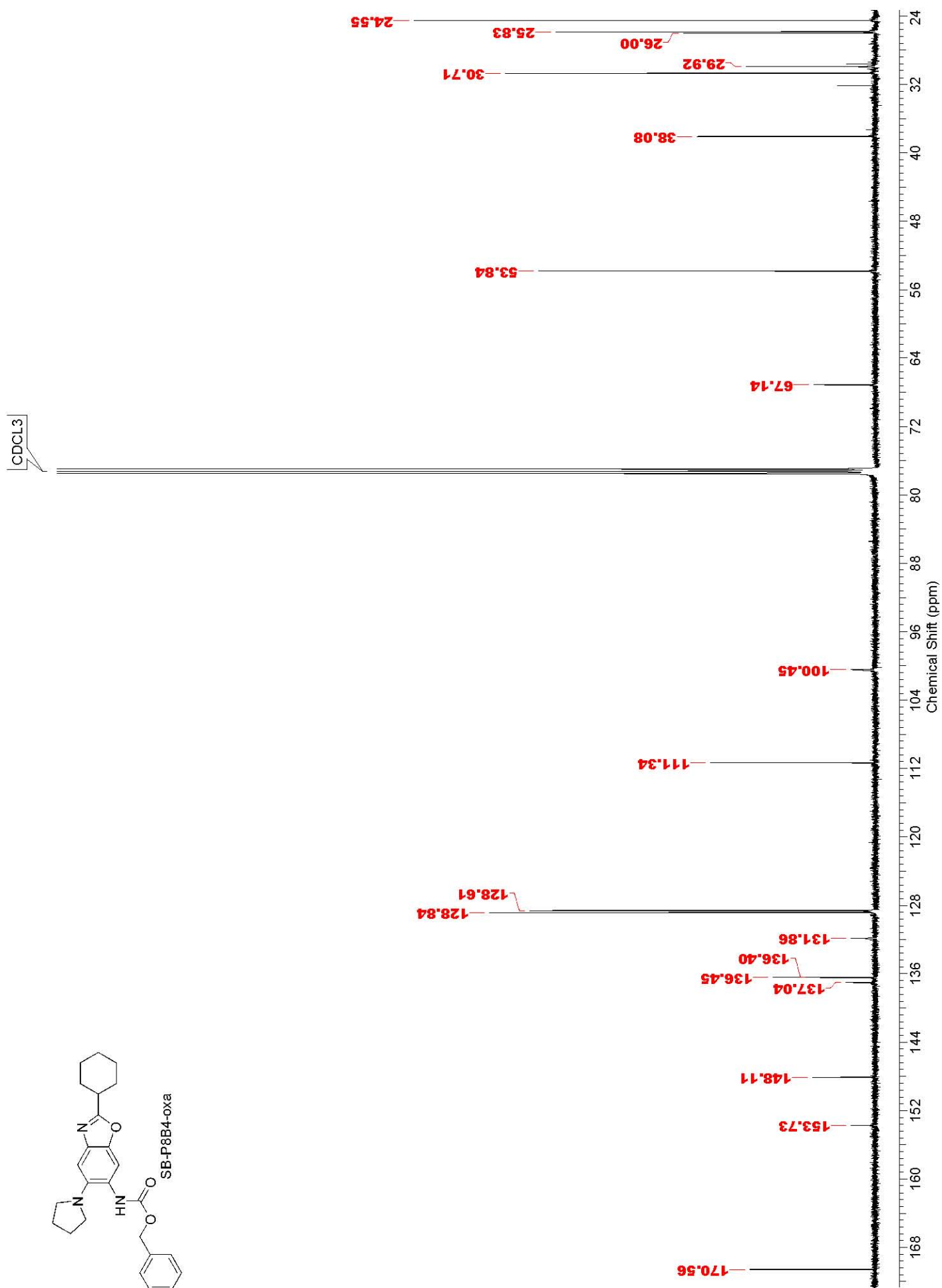
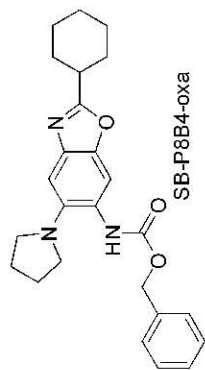


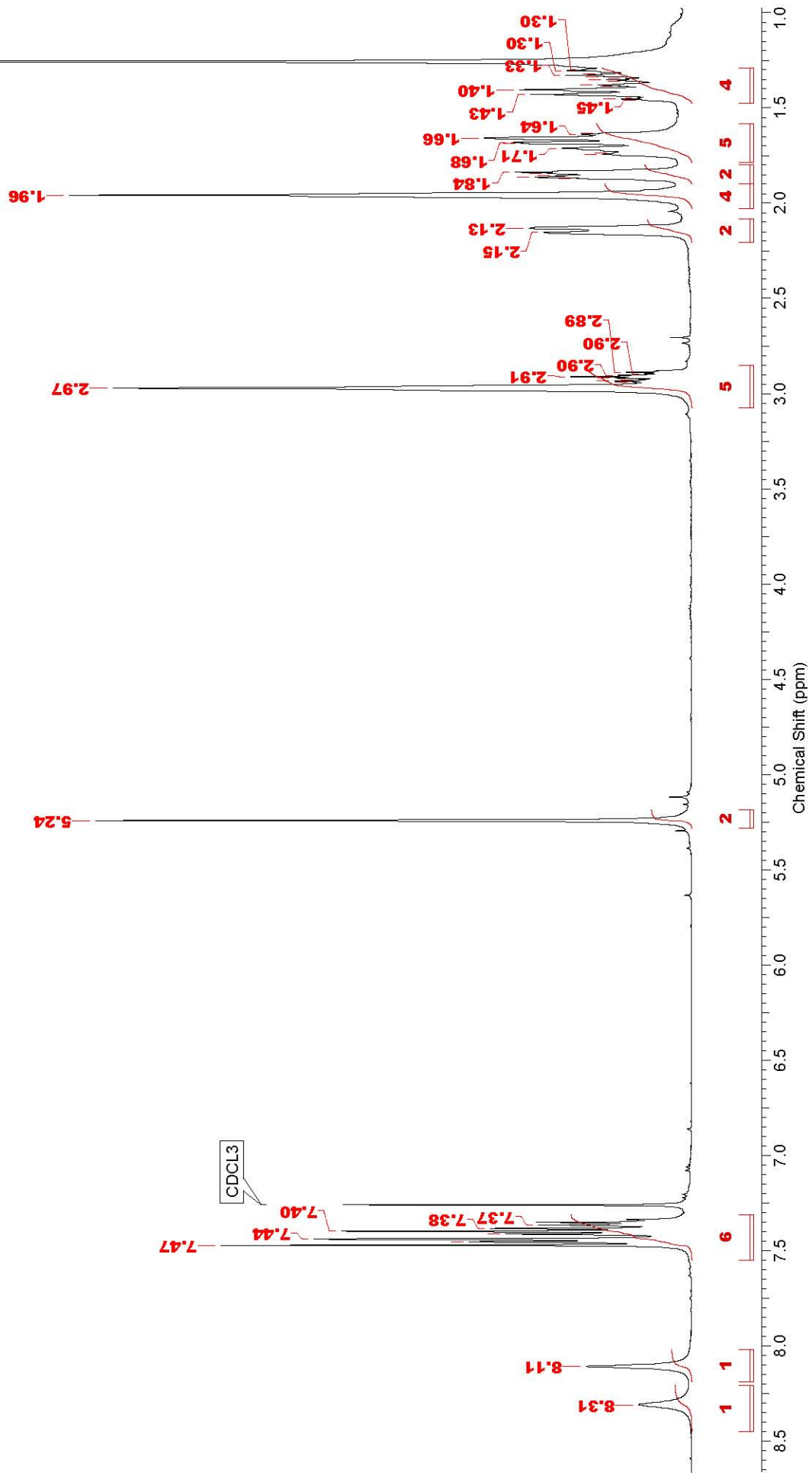
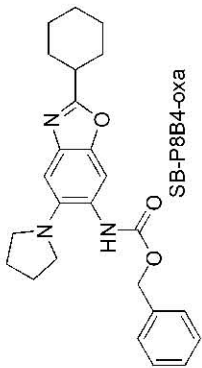


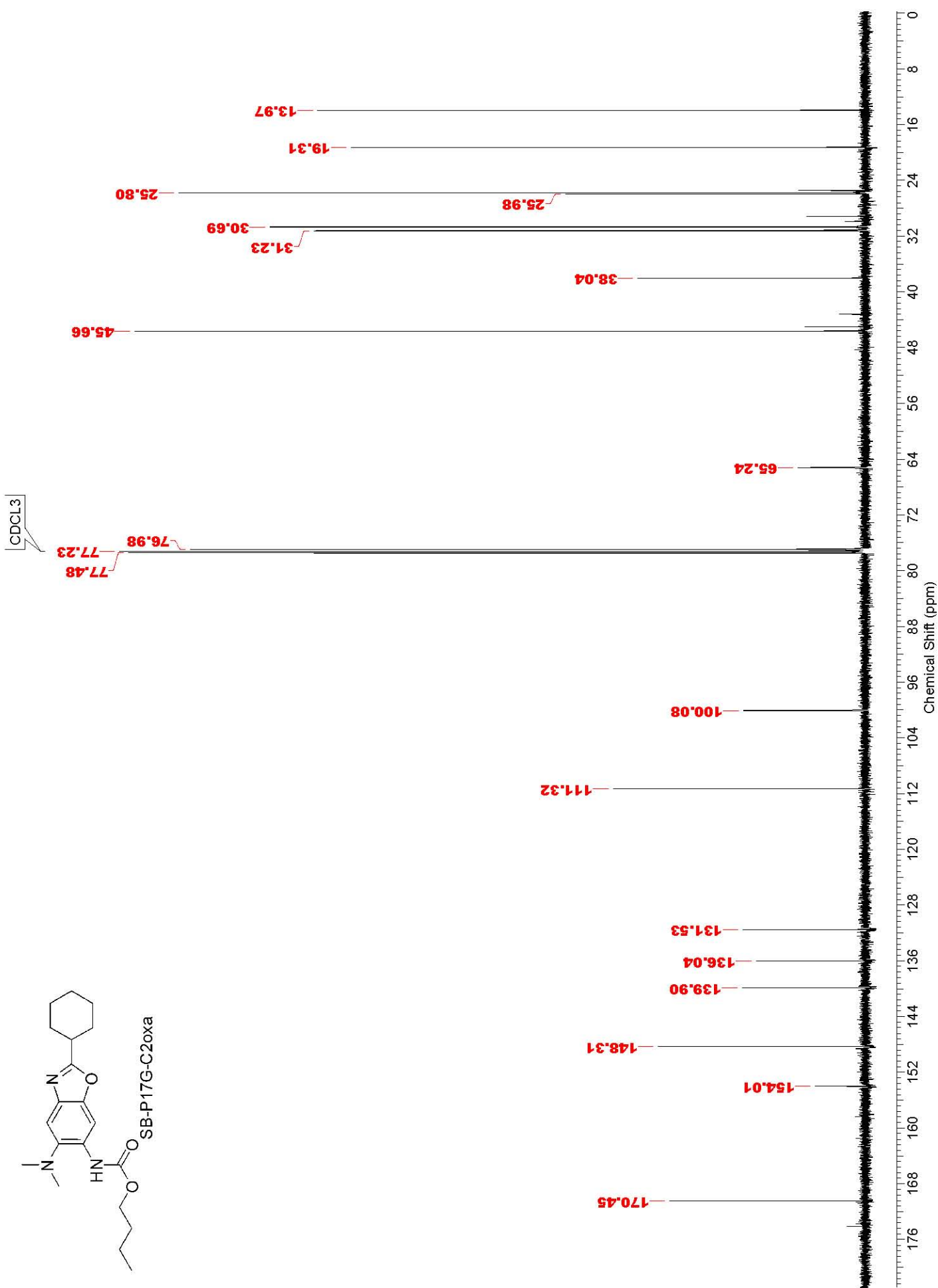
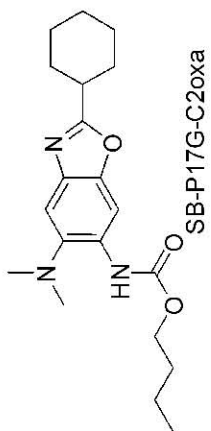


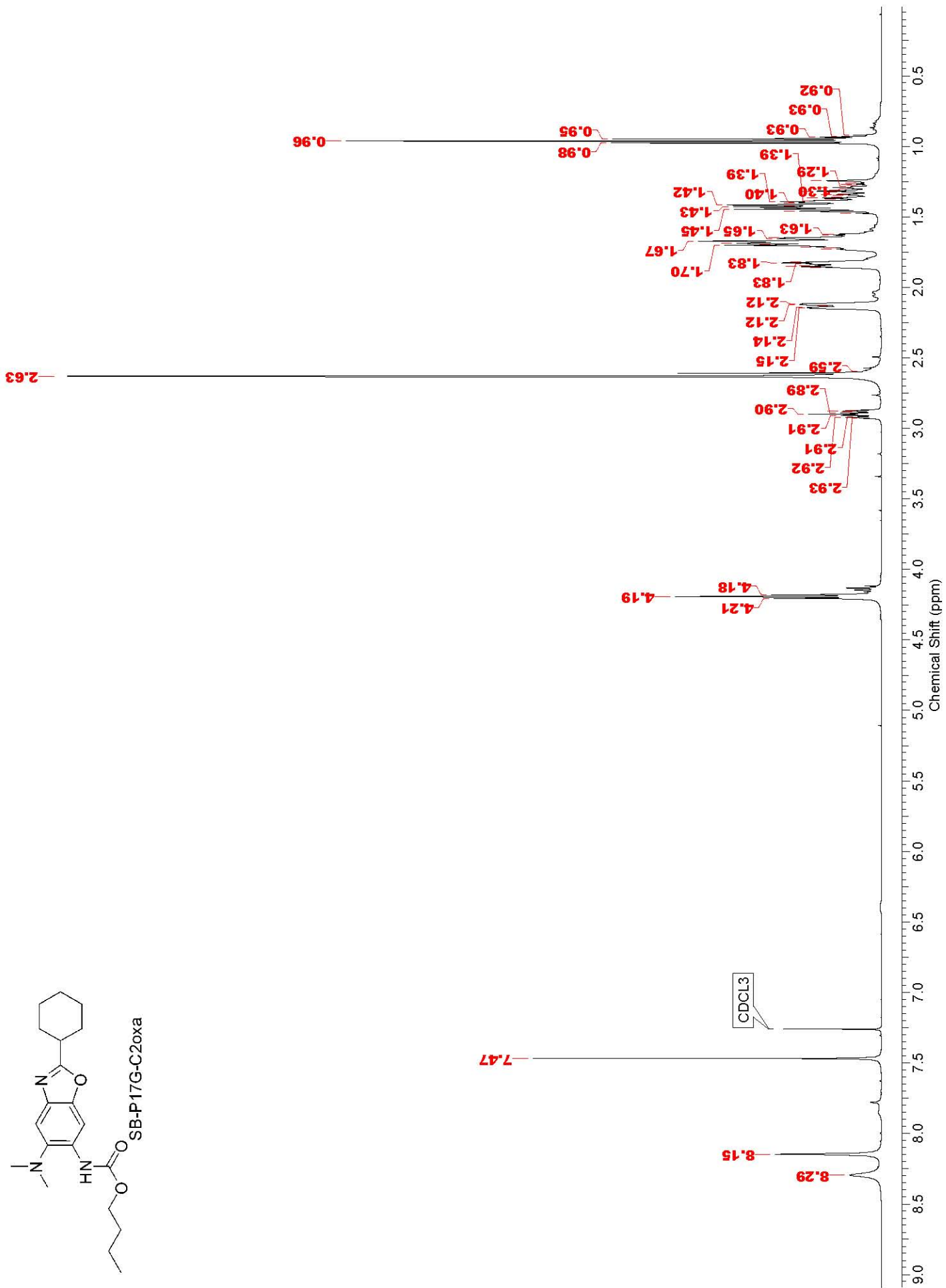
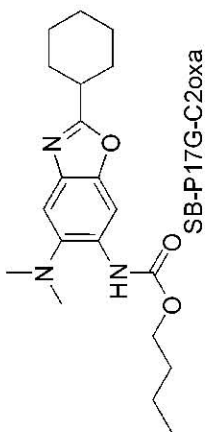


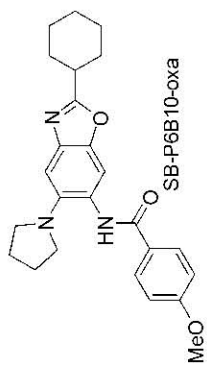




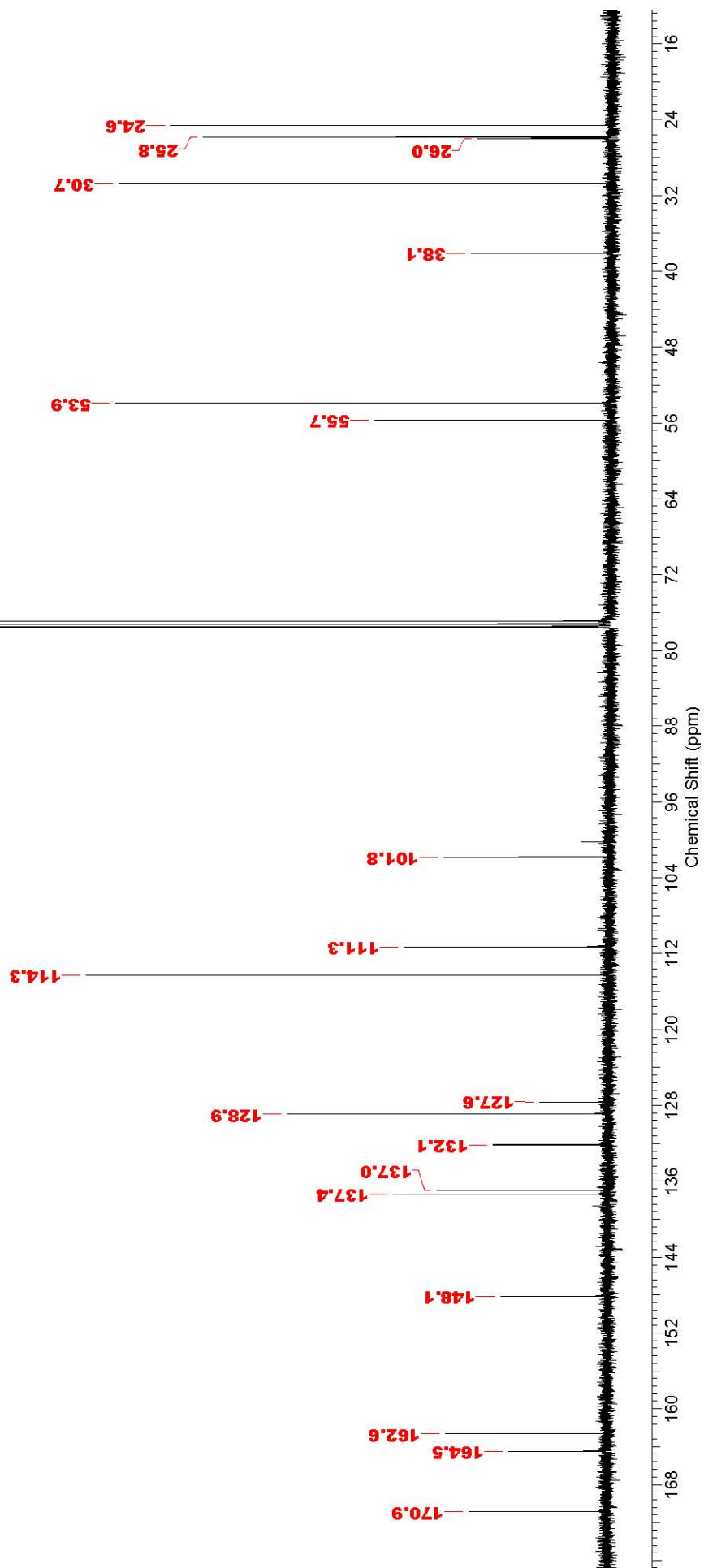


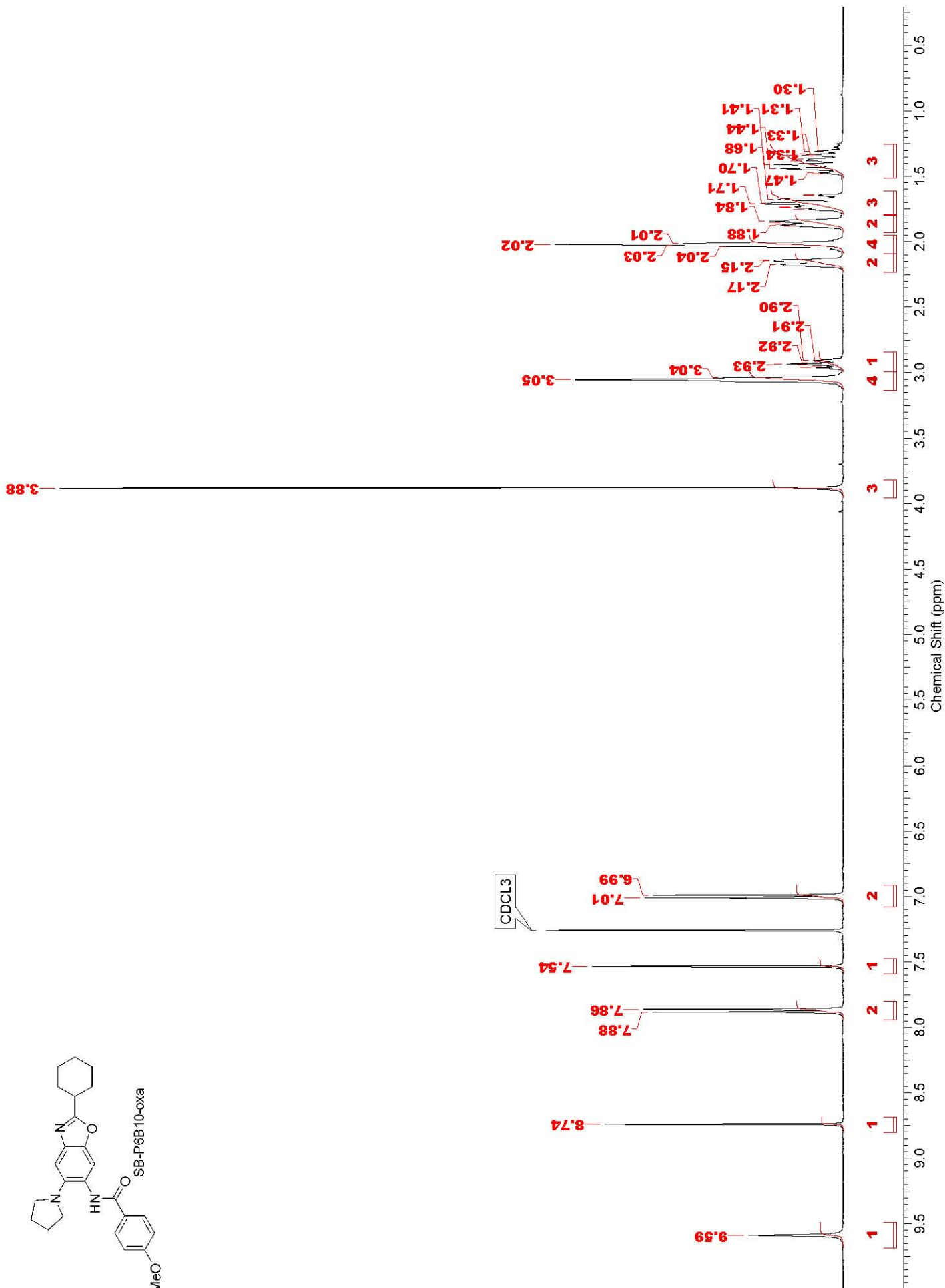
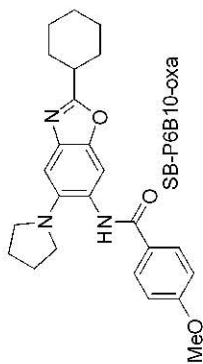


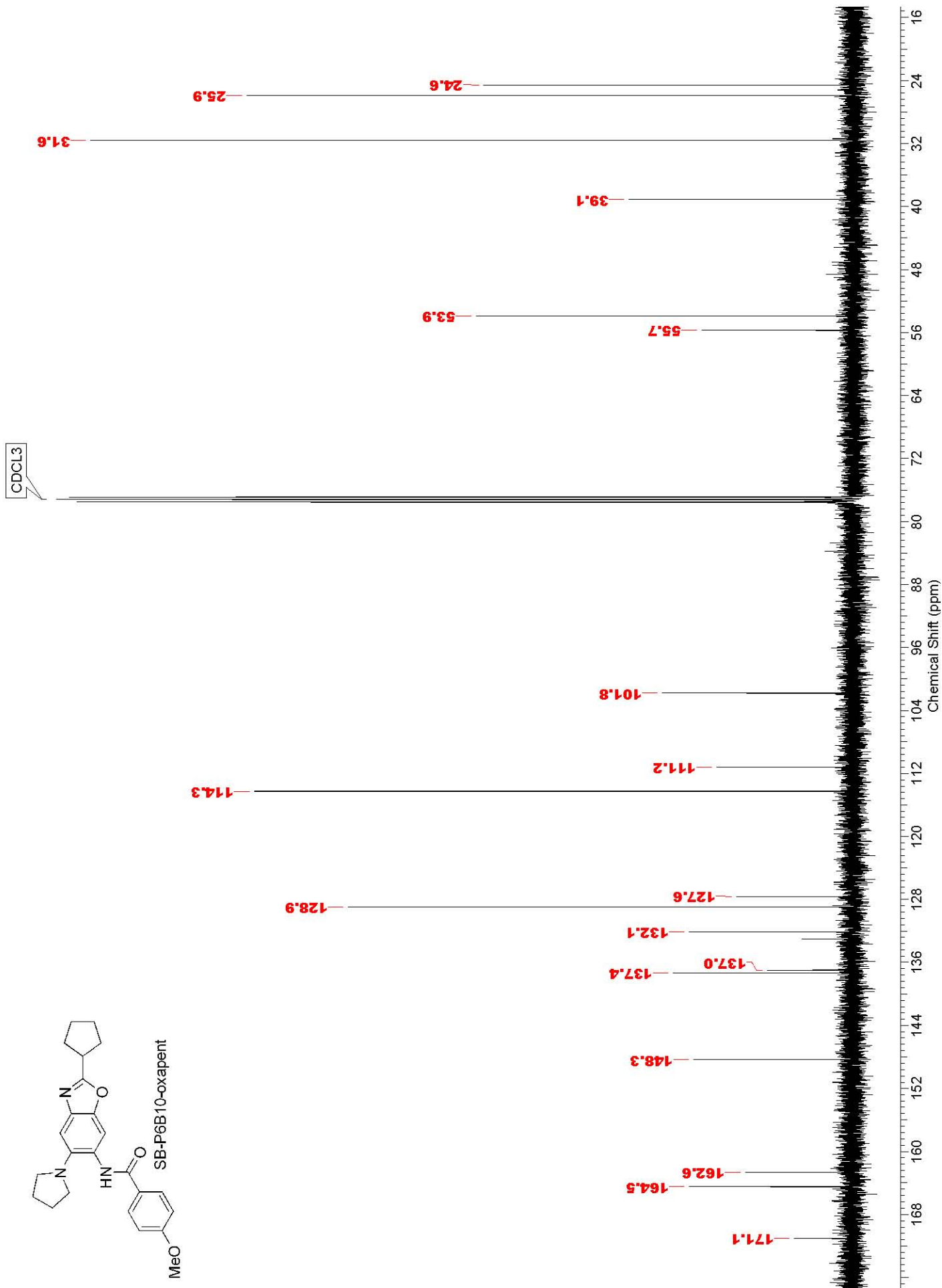
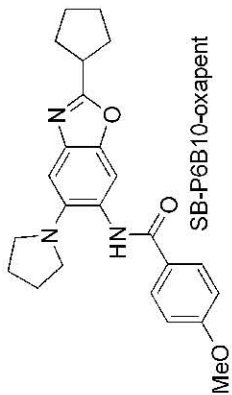


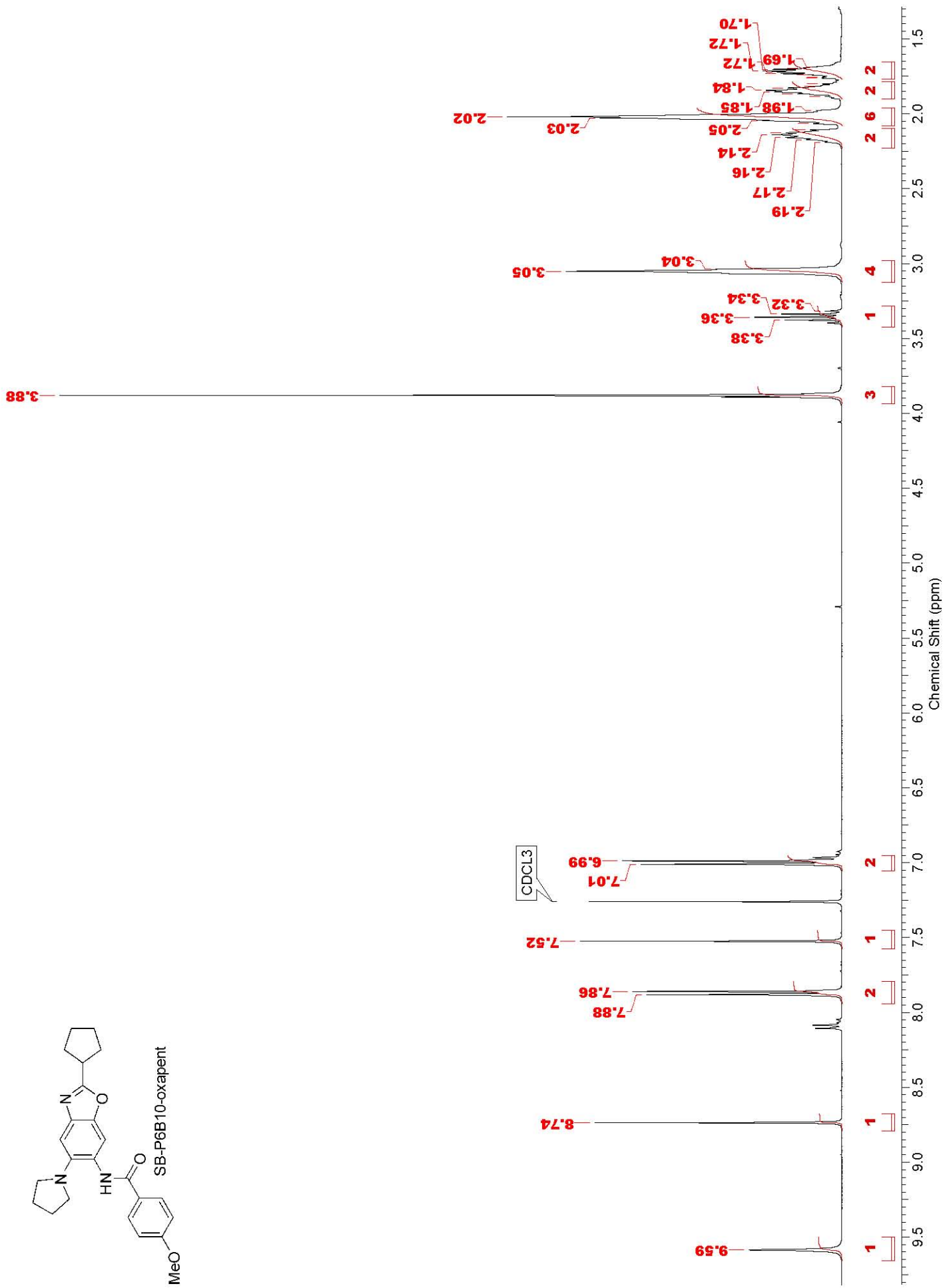
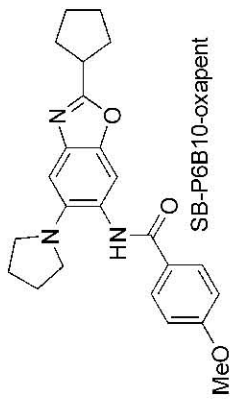


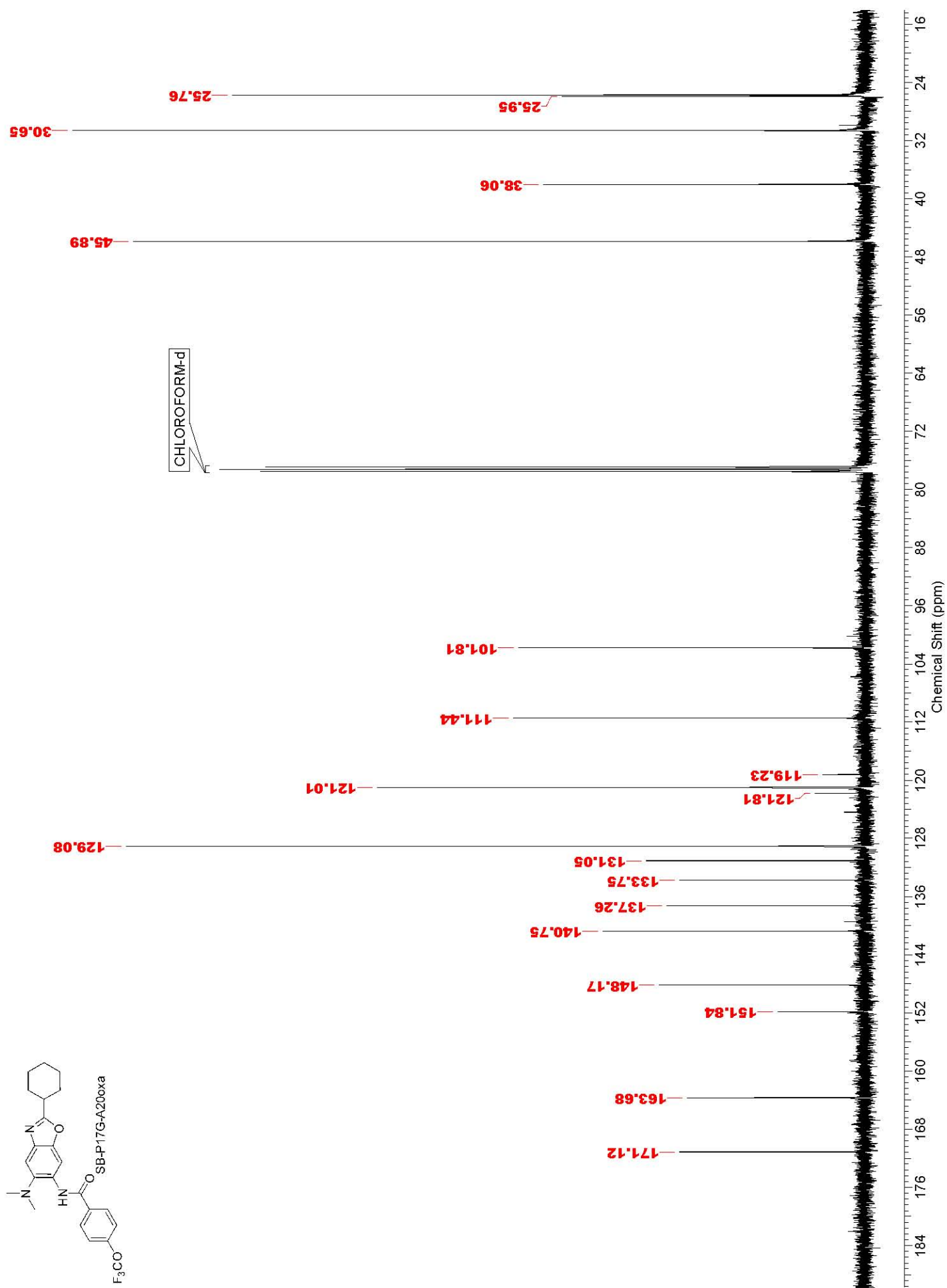
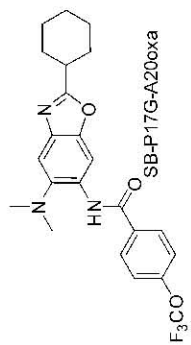
CDCl₃

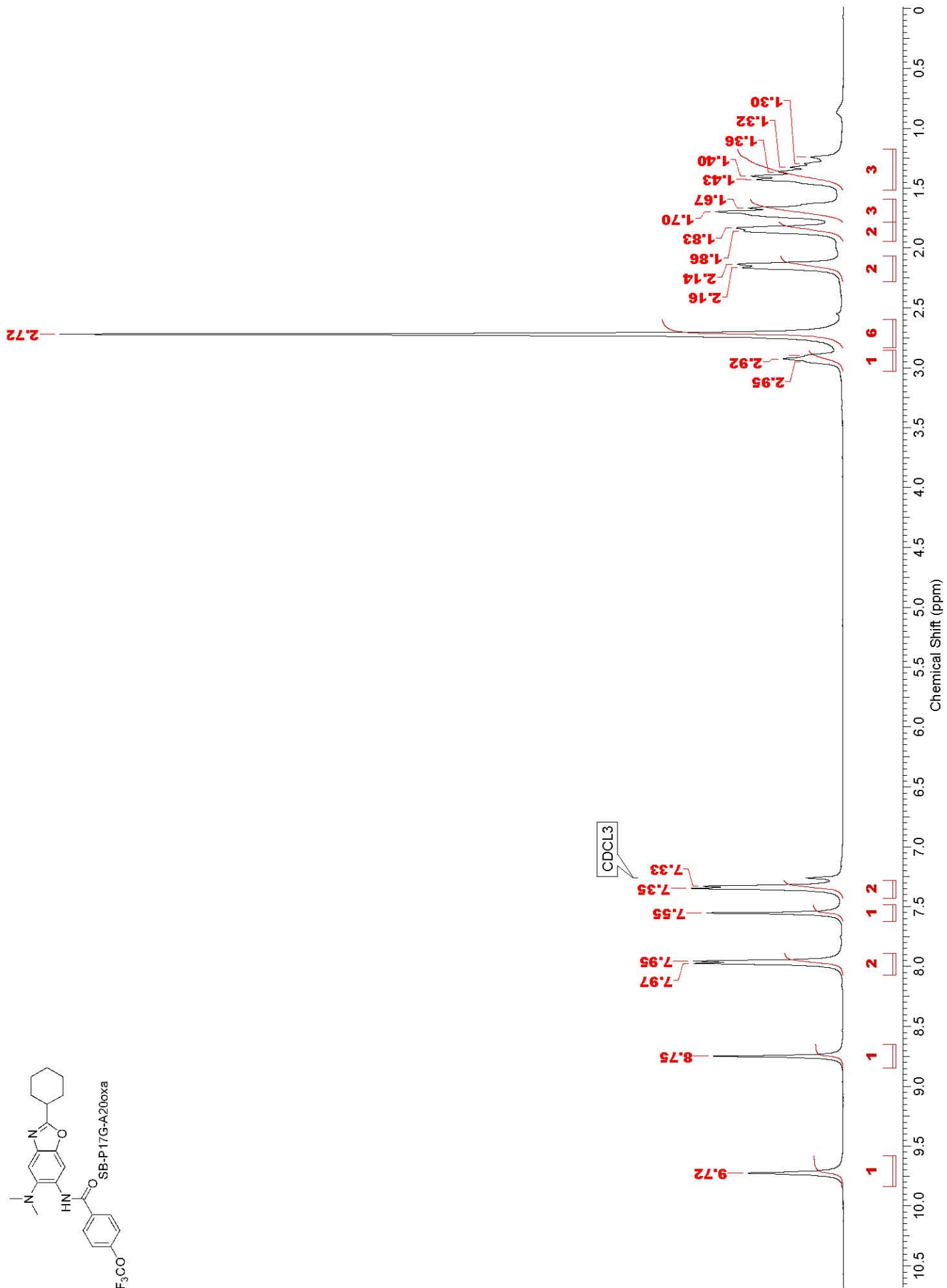
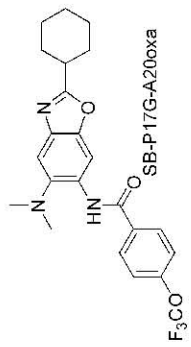


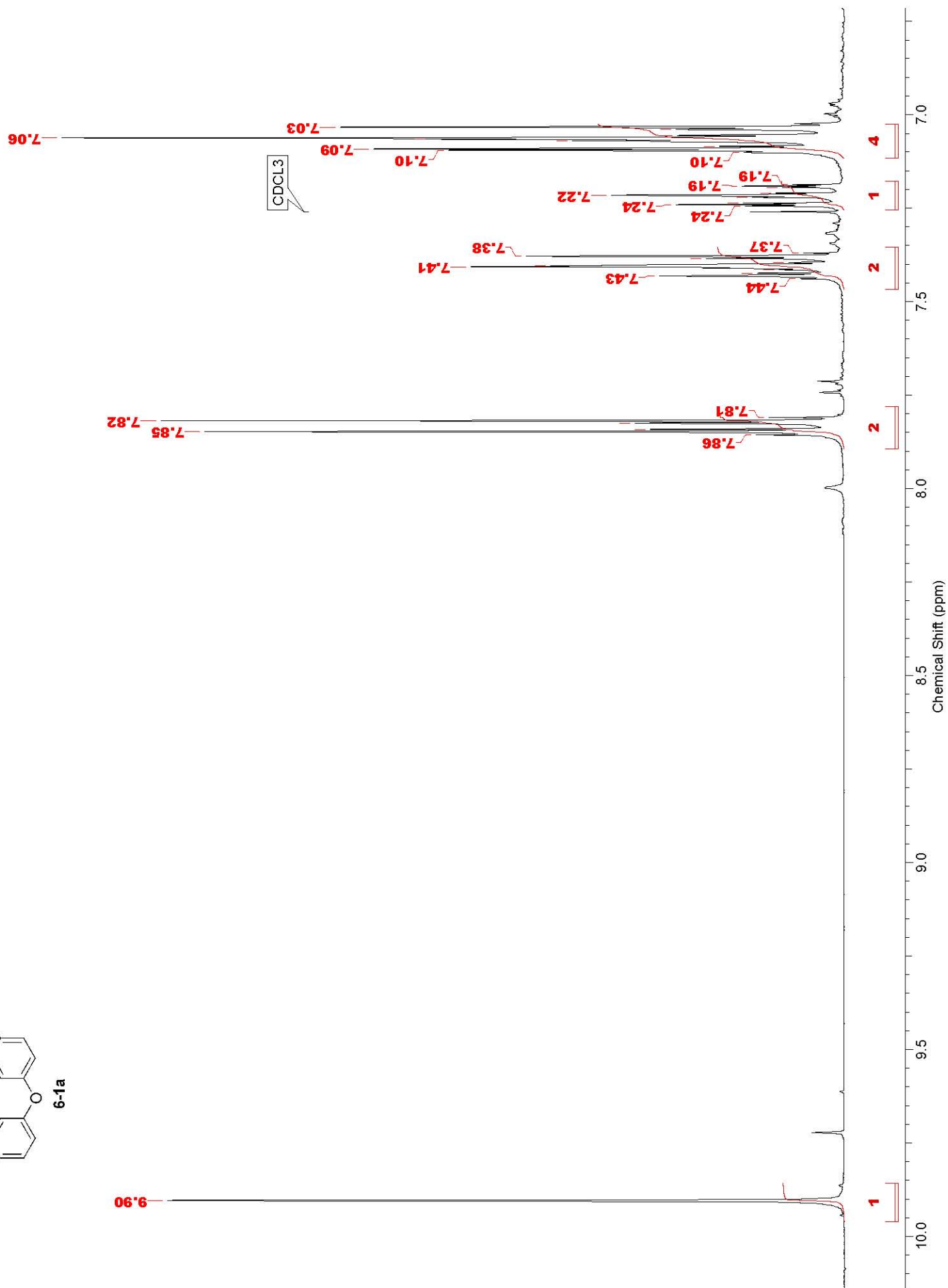
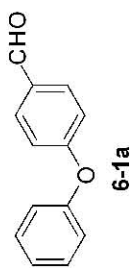


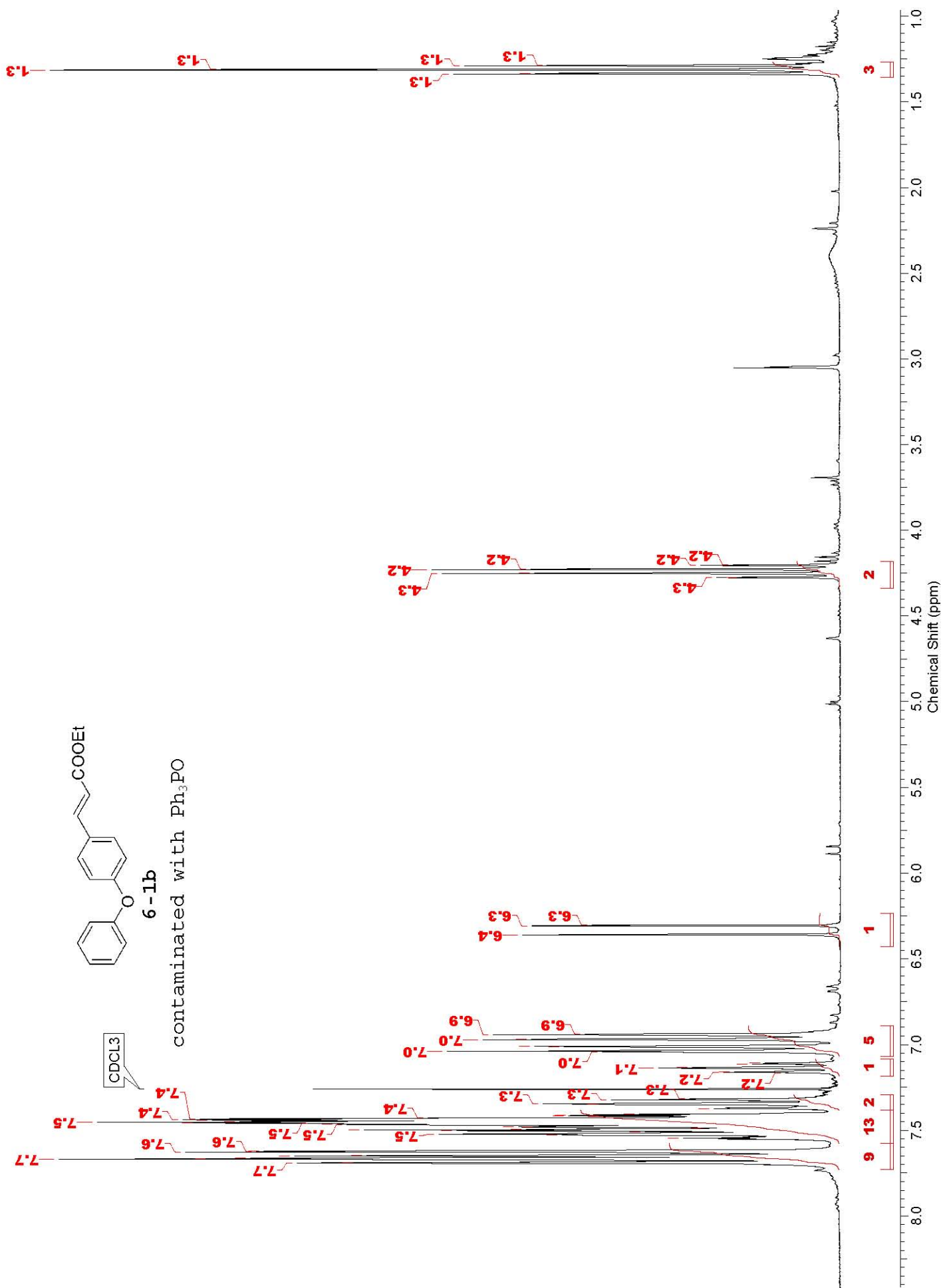


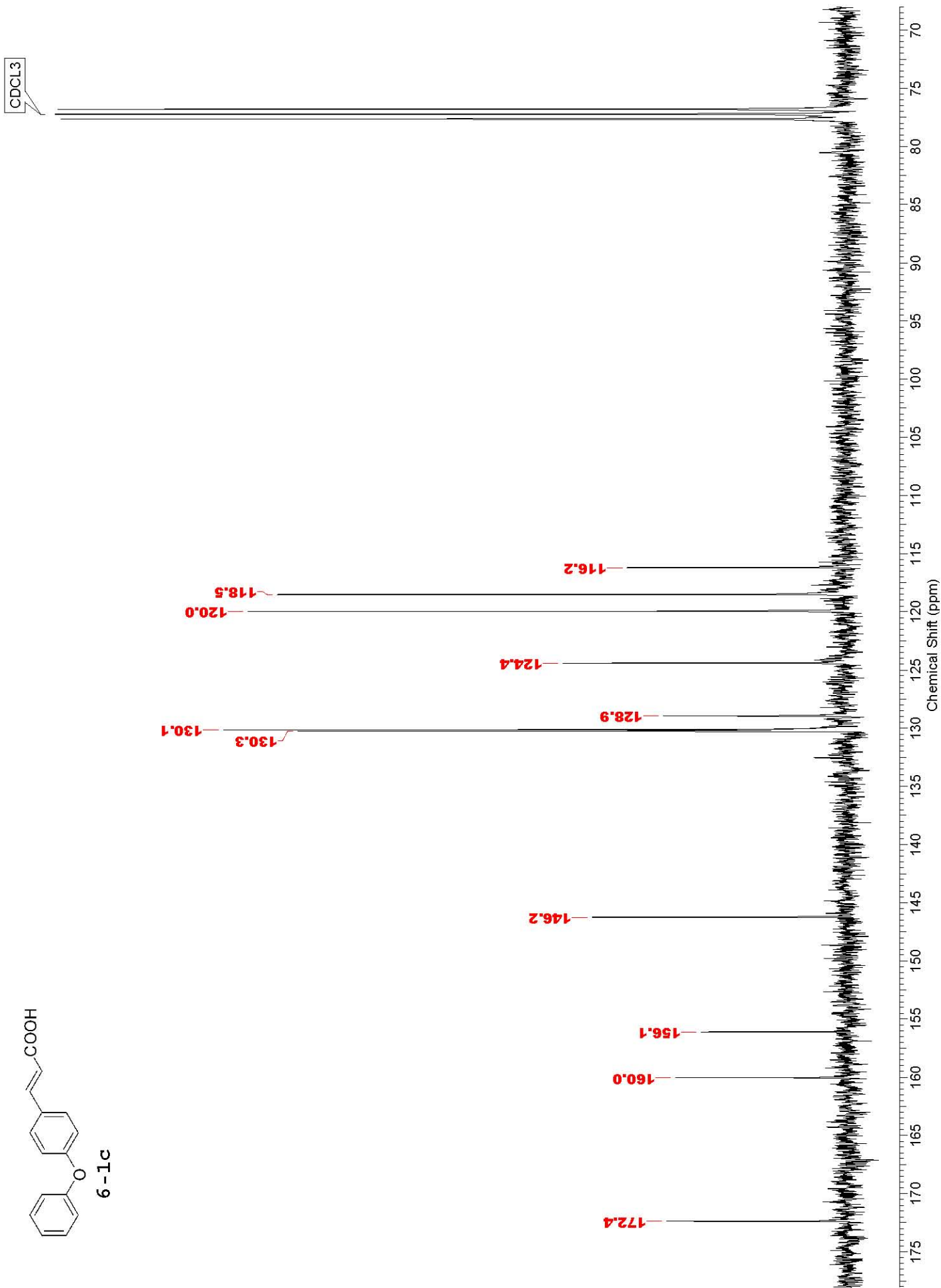
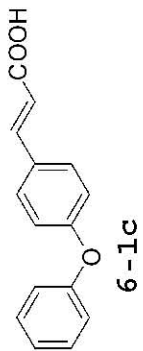


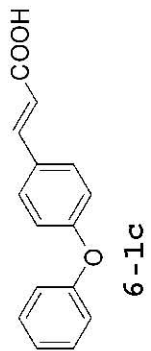




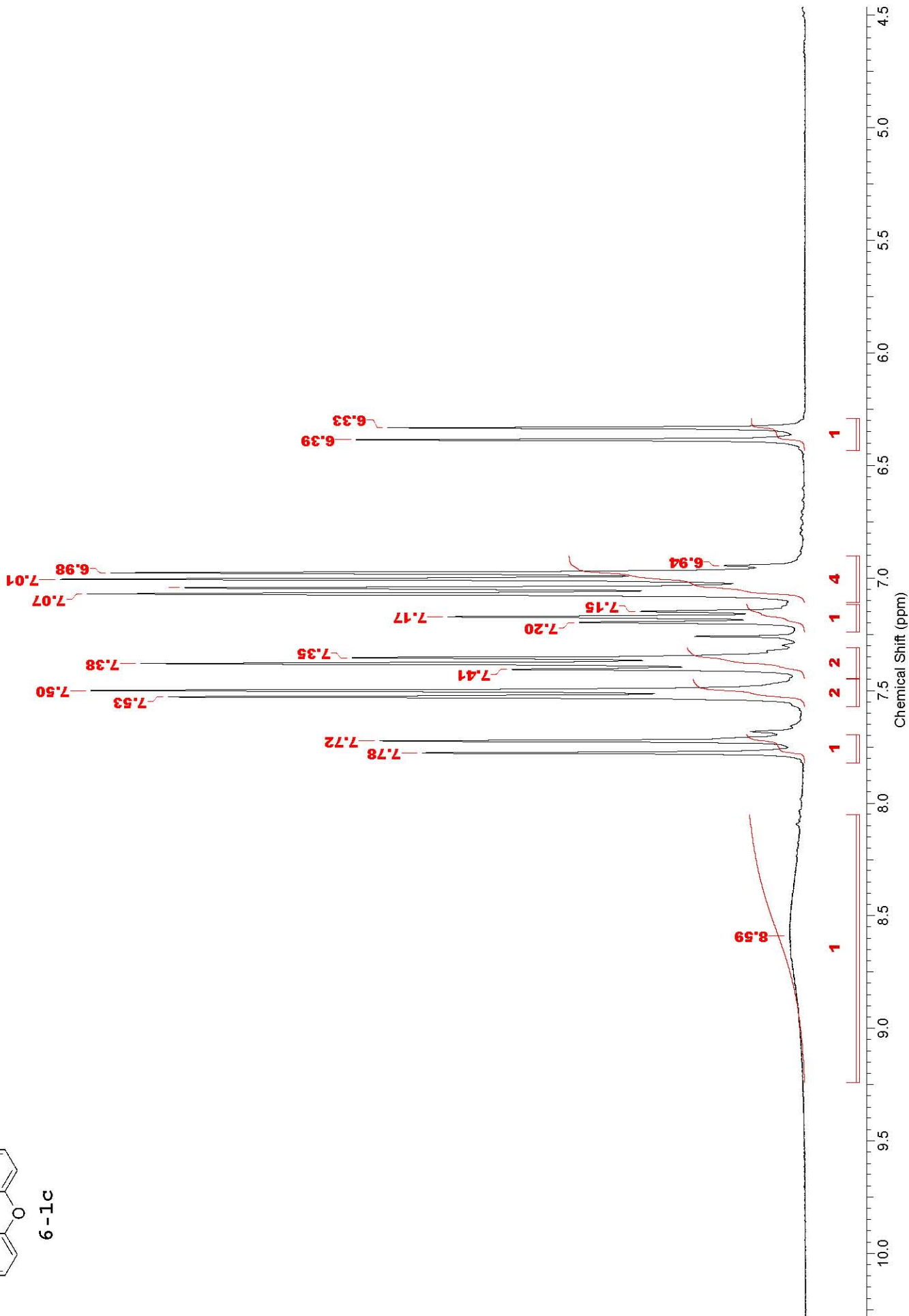


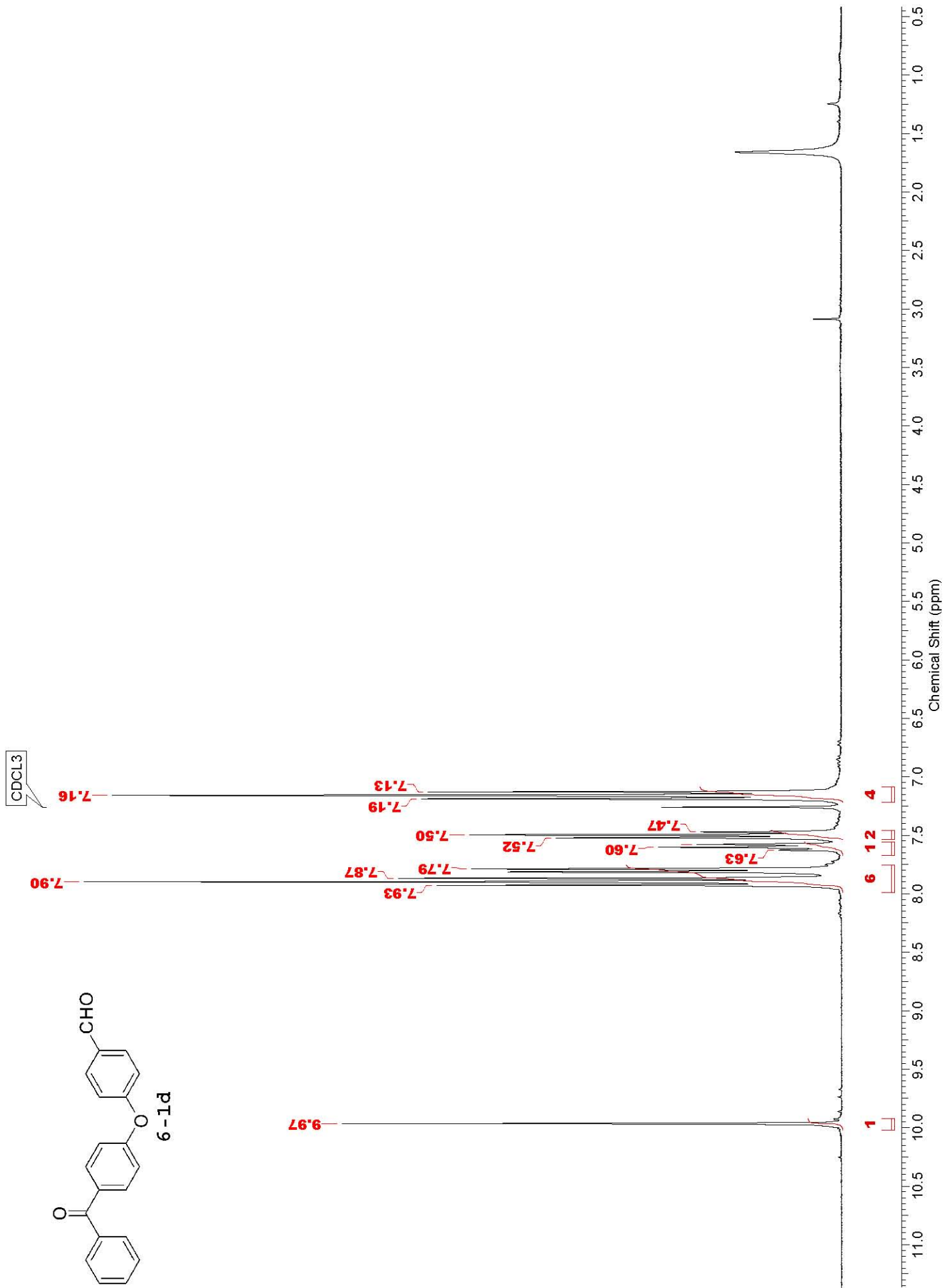
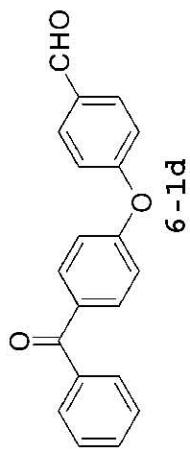


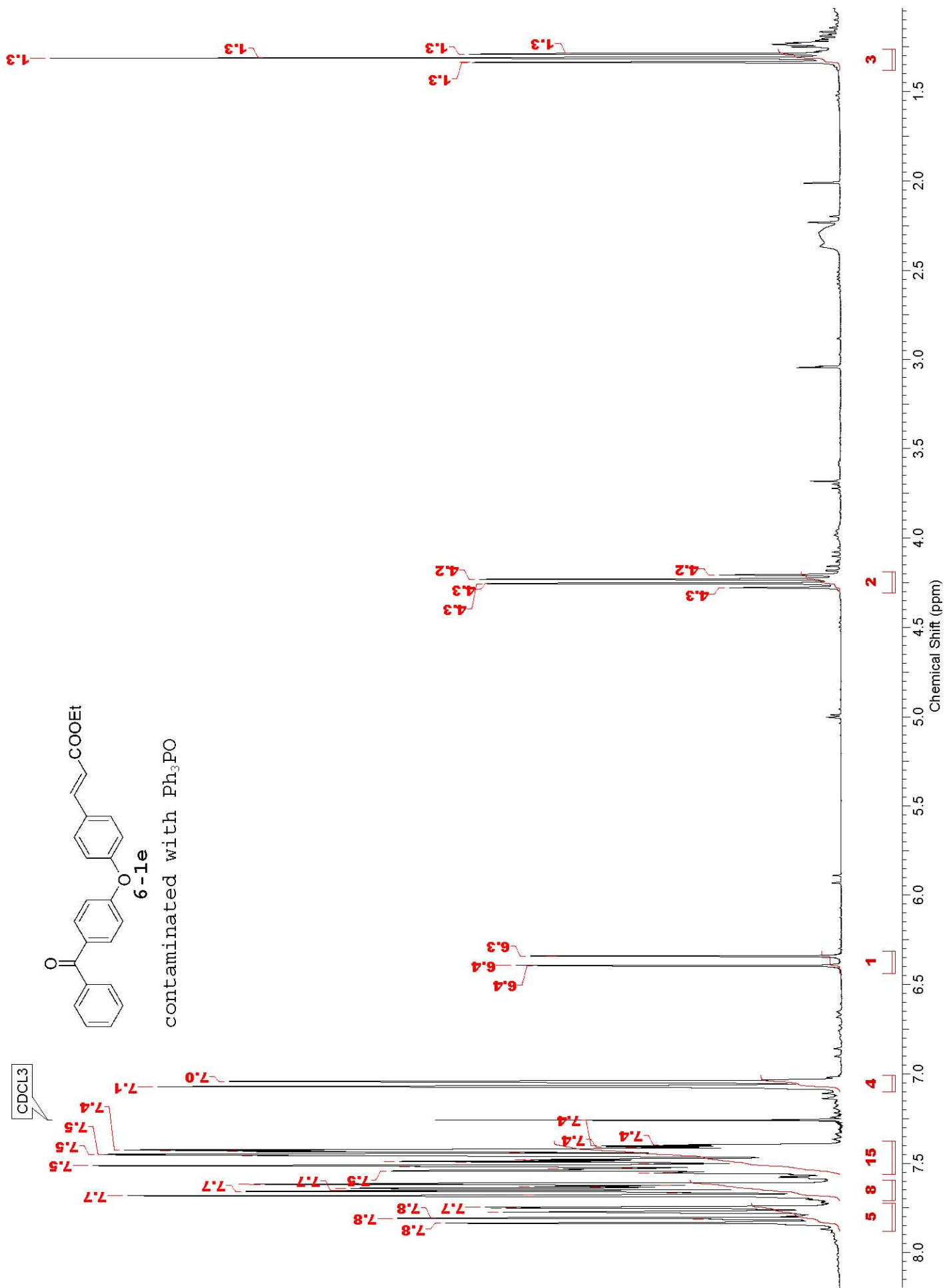


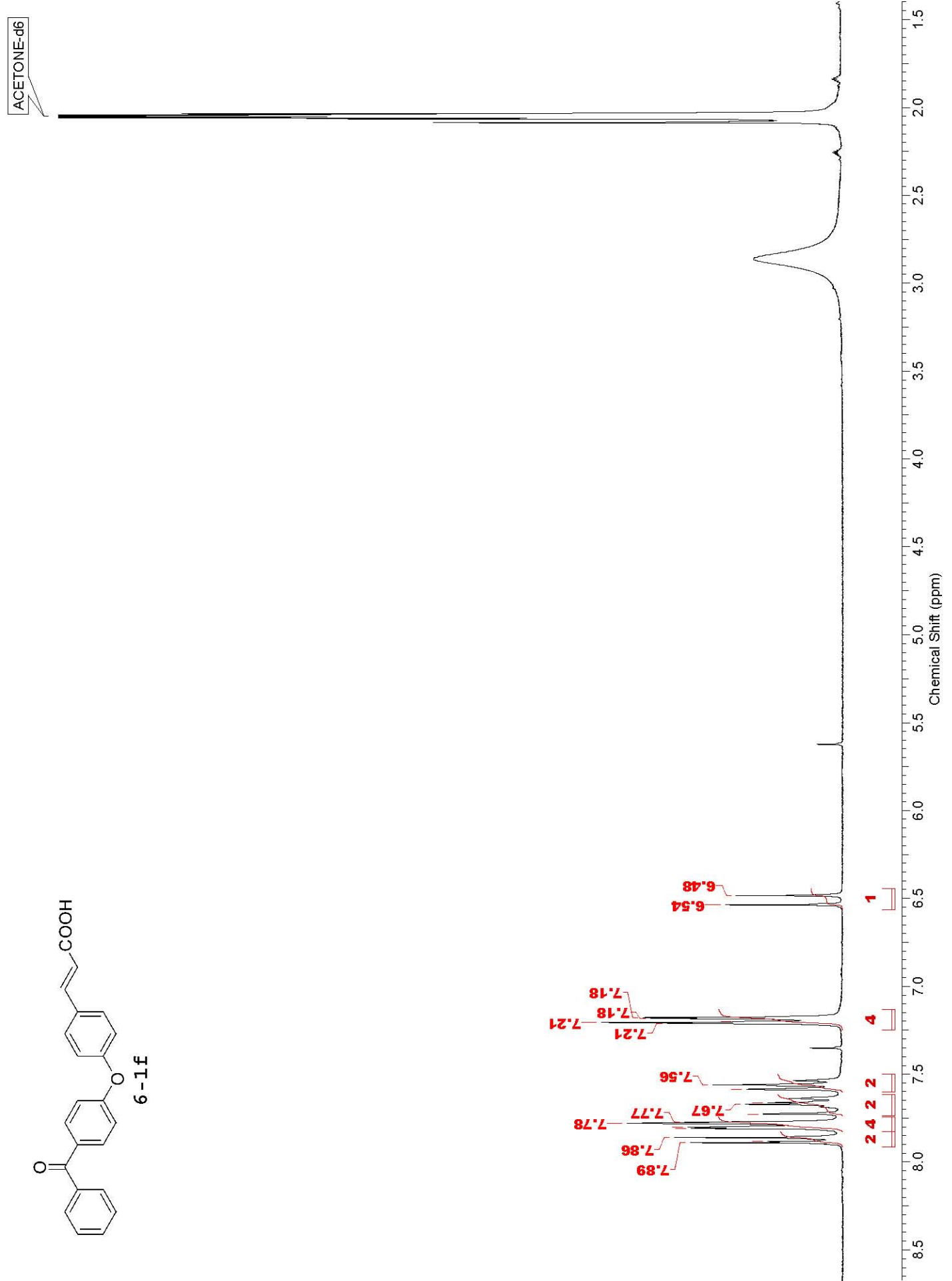
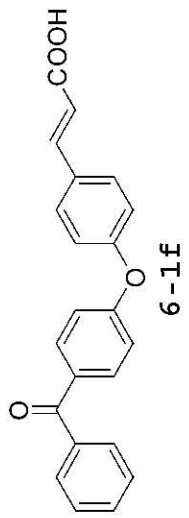


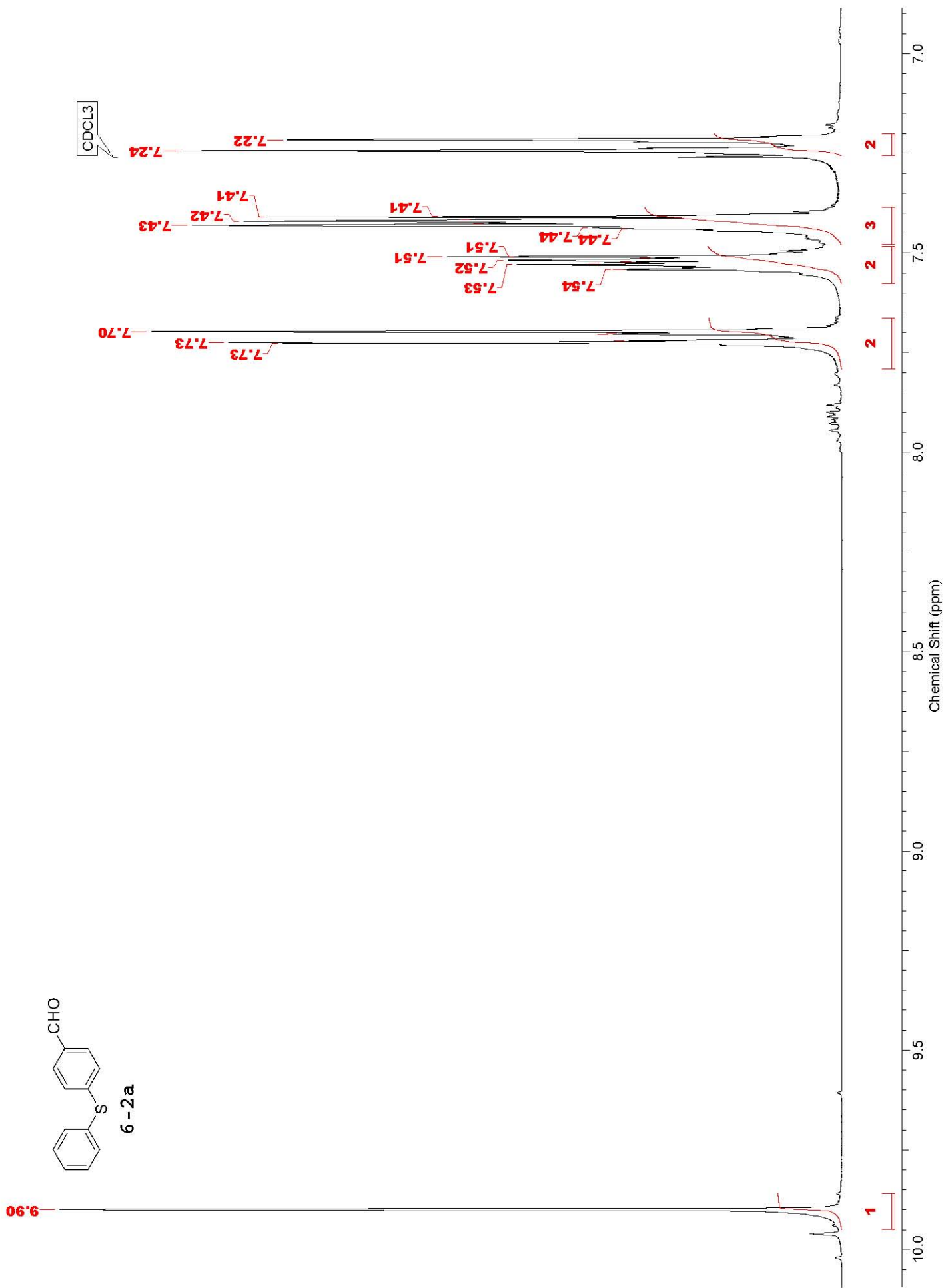
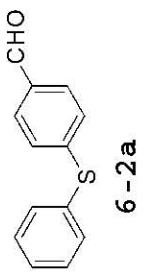
CDCl₃

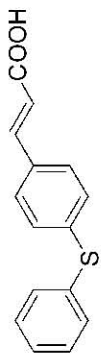




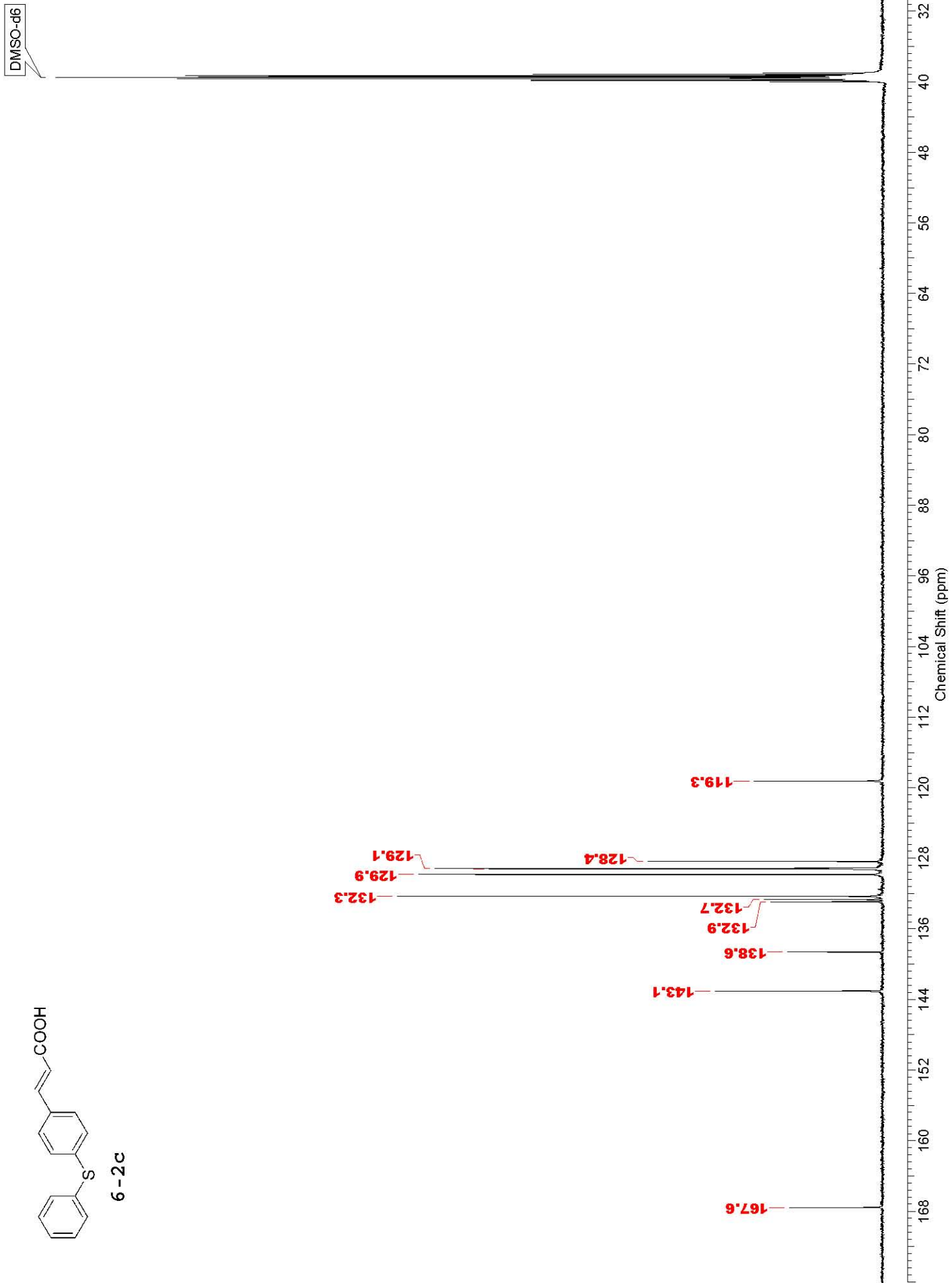


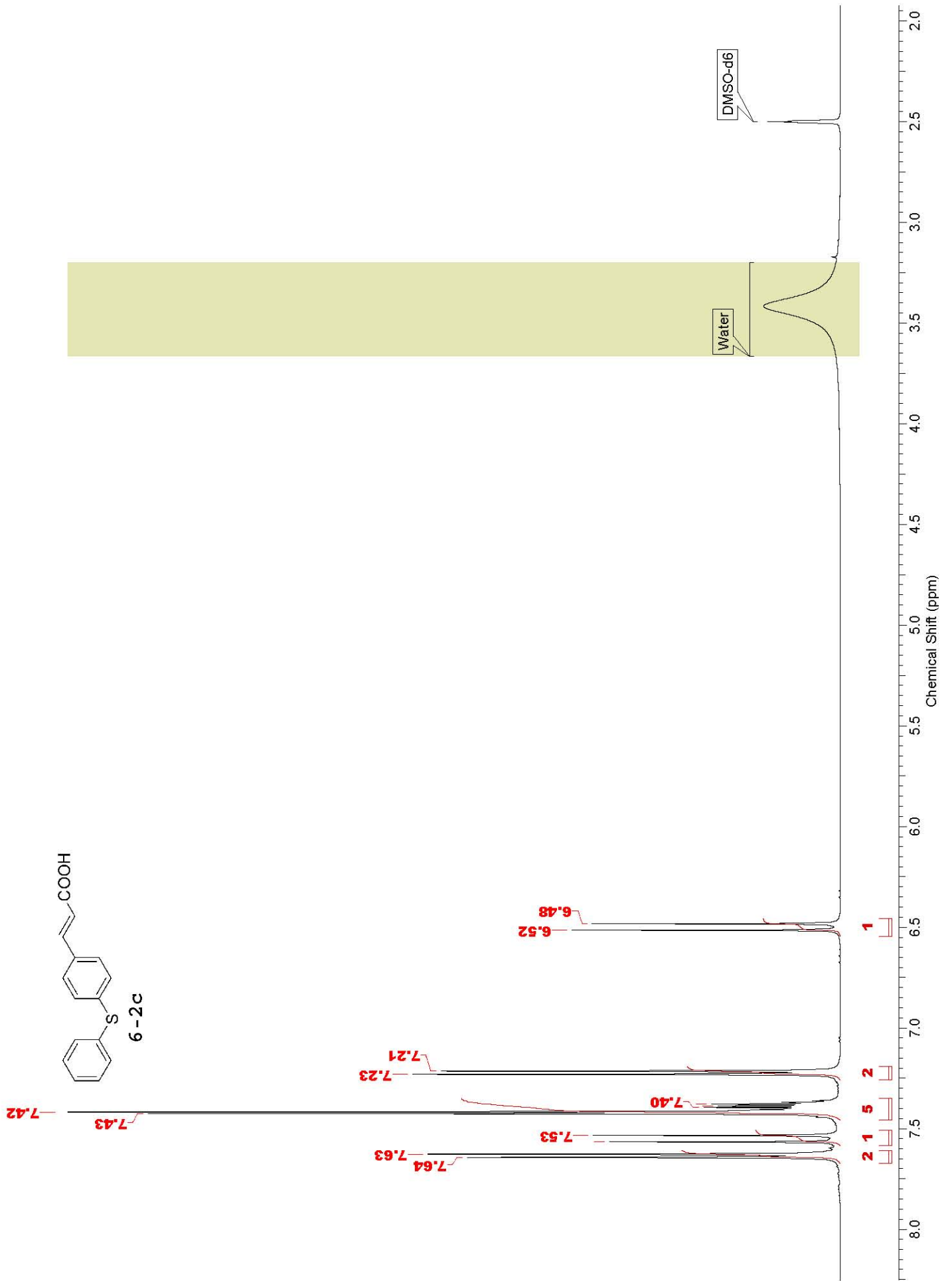


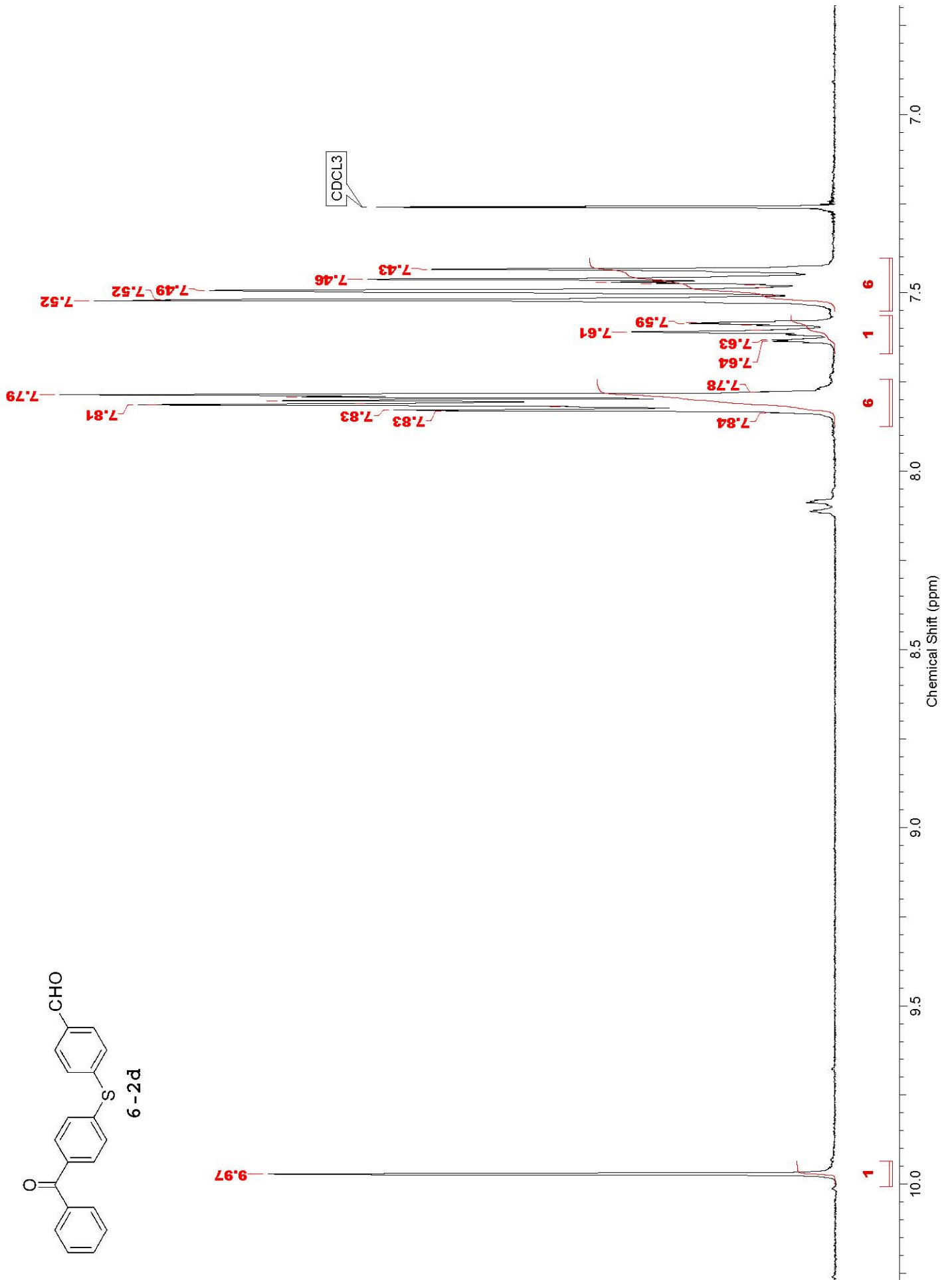
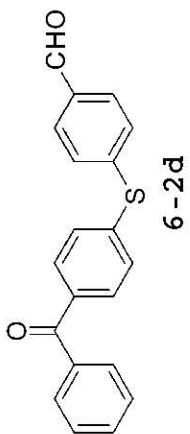


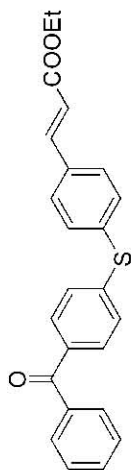


6-2c



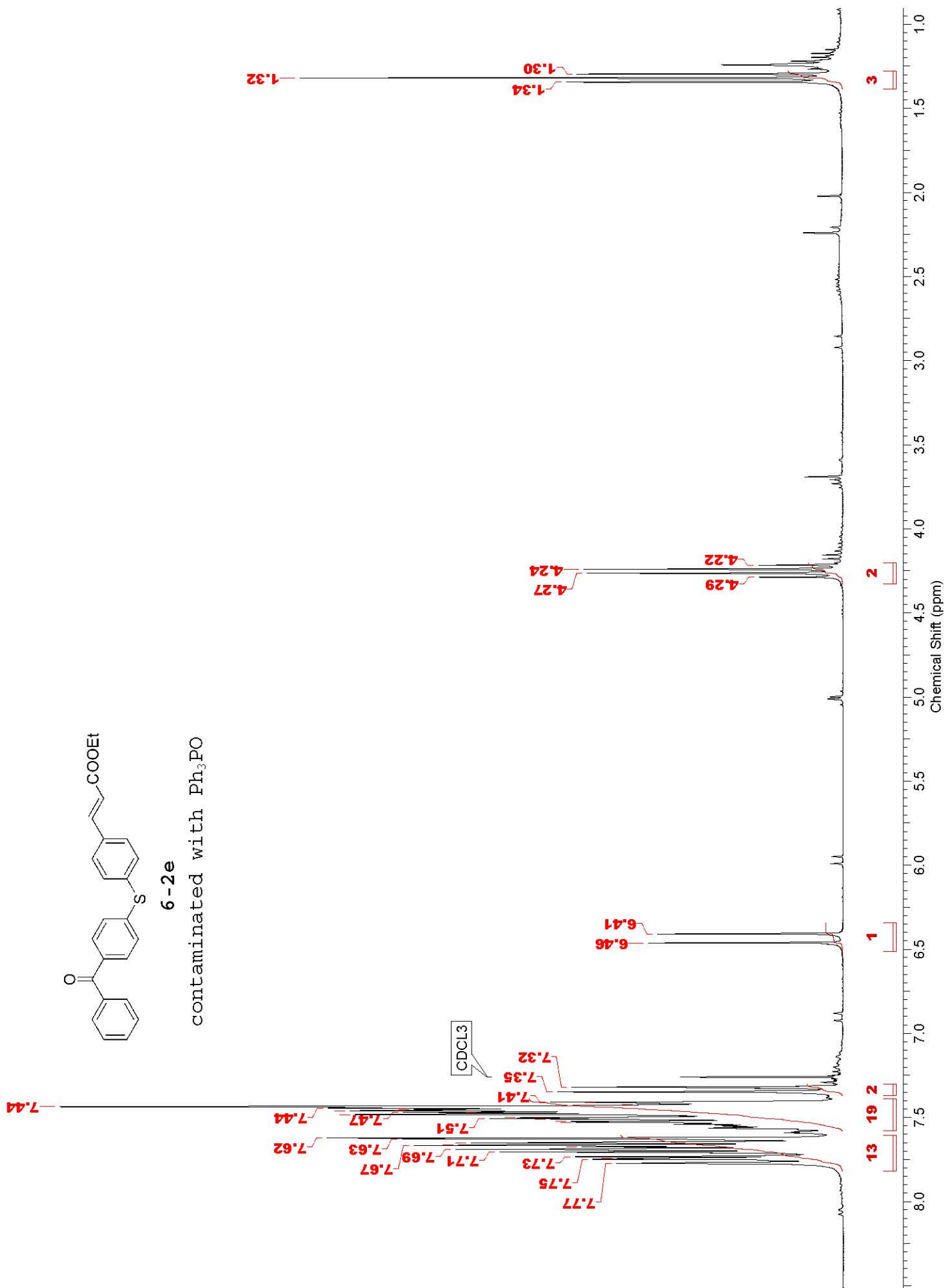


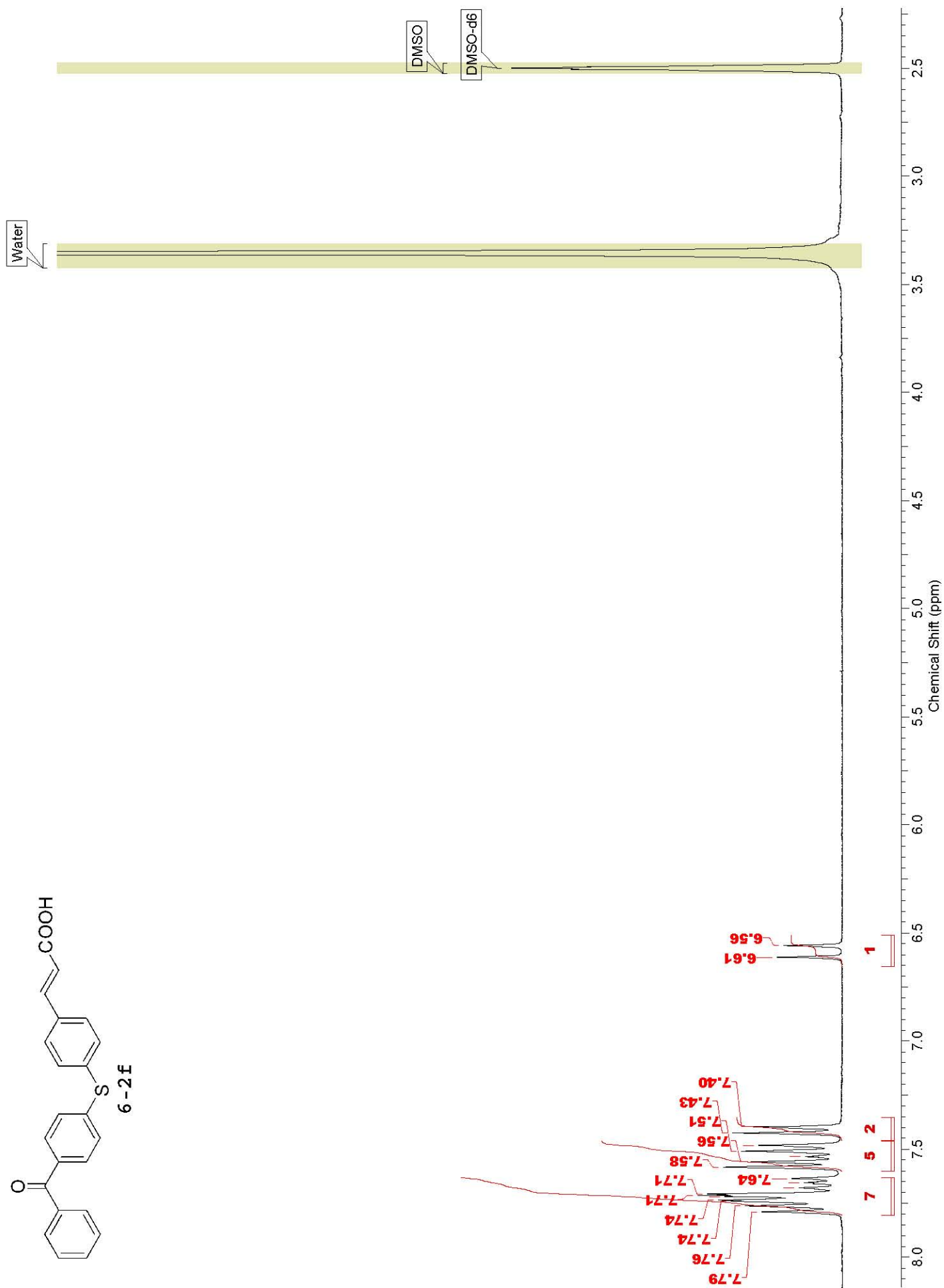
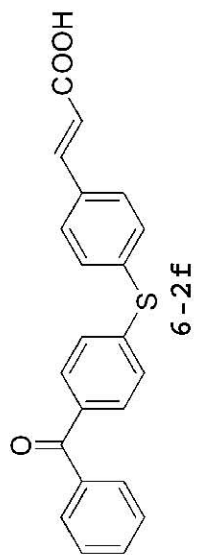


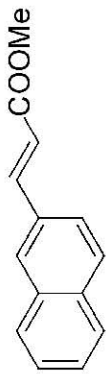


6-2e

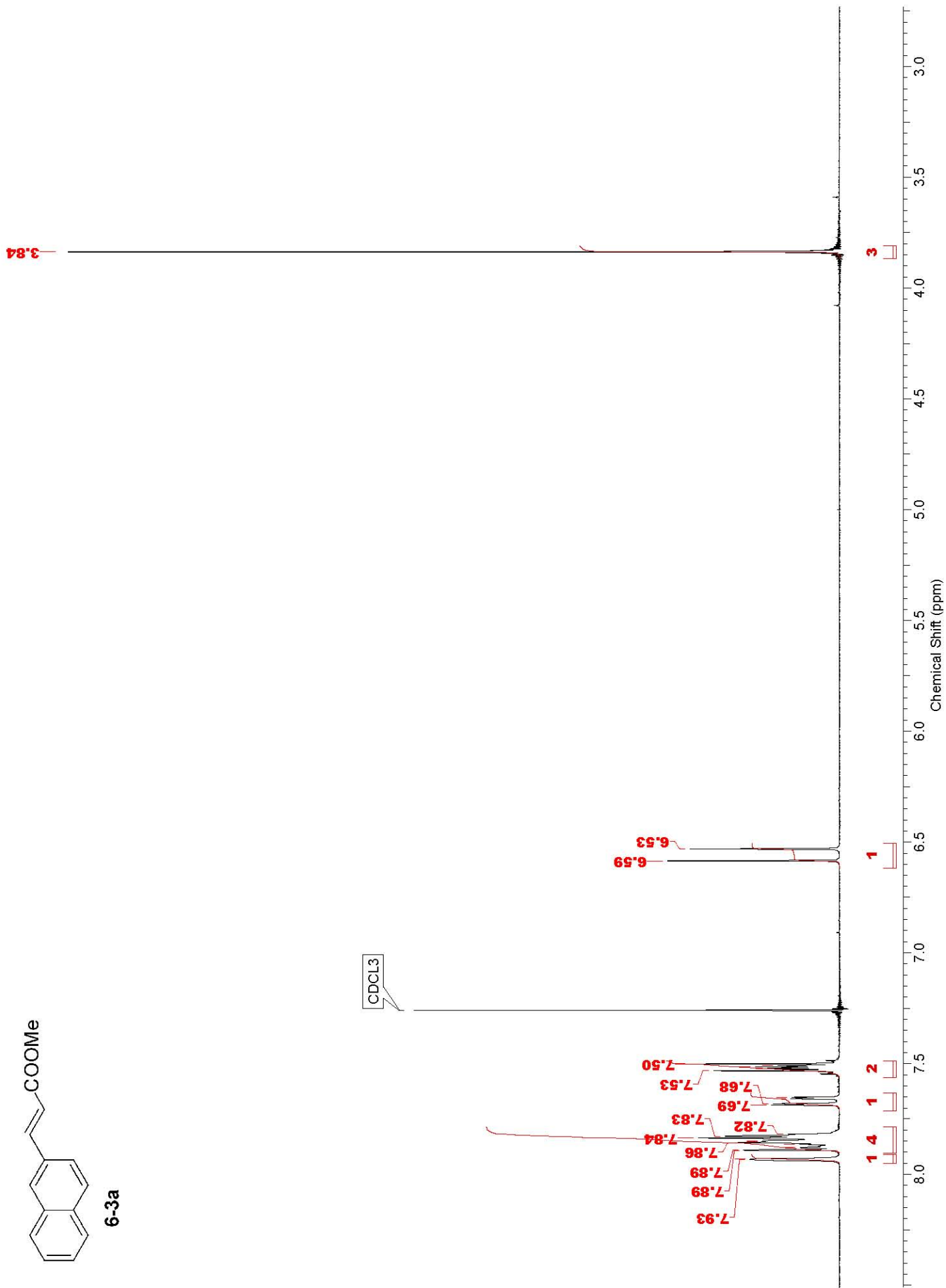
contaminated with Ph_3PO

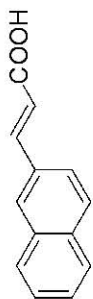






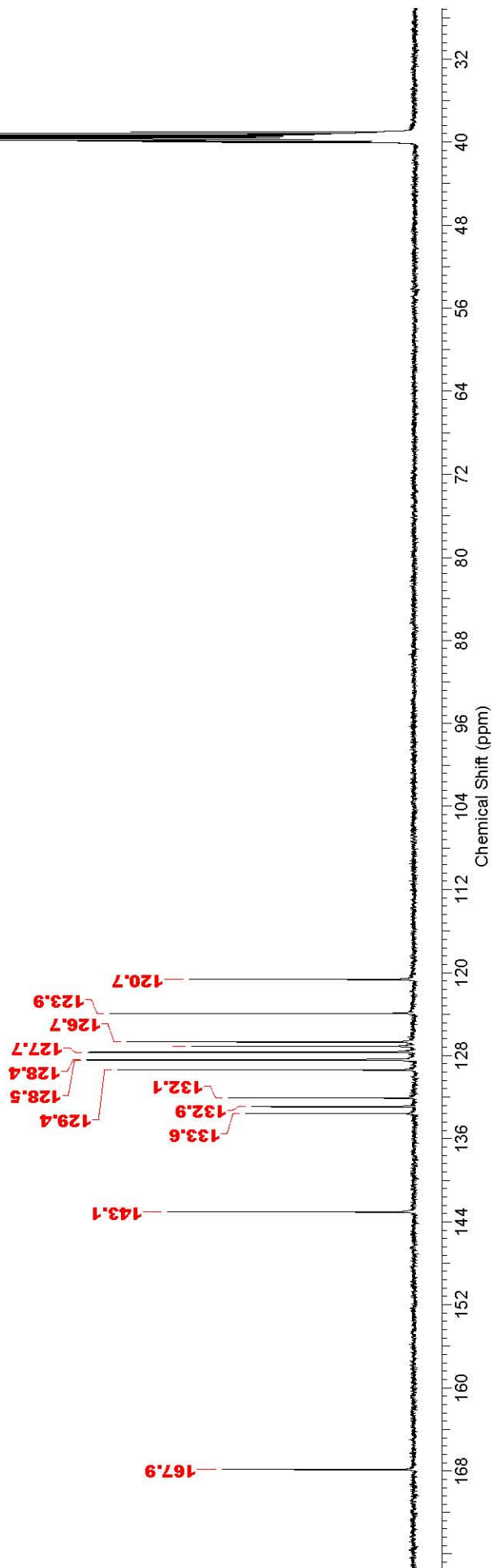
6-3a

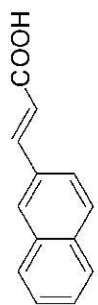




6-3b

DMSO-d6





6-3b

